HIGH-THROUGHPUT PHENOTYPING IN THE GENOMIC IMPROVEMENT OF LIVESTOCK

EDITED BY: Fabyano Fonseca Silva, Guilherme J. M. Rosa and Gota Morota

PUBLISHED IN: Frontiers in Genetics and Frontiers in Veterinary Science

frontiers Research Topics

frontiers

ISSN 1664-8714
ISBN 978-2-88971-145-1
DOI 10.3389/978-2-88971-145-1

About Frontiers

Frontiers is more than just an open-access publisher of scholarly articles: it is a pioneering approach to the world of academia, radically improving the way scholarly research is managed. The grand vision of Frontiers is a world where all people have an equal opportunity to seek, share and generate knowledge. Frontiers provides immediate and permanent online open access to all its publications, but this alone is not enough to realize our grand goals.

Frontiers Journal Series

The Frontiers Journal Series is a multi-tier and interdisciplinary set of open-access, online journals, promising a paradigm shift from the current review, selection and dissemination processes in academic publishing. All Frontiers journals are driven by researchers for researchers; therefore, they constitute a service to the scholarly community. At the same time, the Frontiers Journal Series operates on a revolutionary invention, the tiered publishing system, initially addressing specific communities of scholars, and gradually climbing up to broader public understanding, thus serving the interests of the lay society, too.

Dedication to Quality

Each Frontiers article is a landmark of the highest quality, thanks to genuinely collaborative interactions between authors and review editors, who include some of the world's best academicians. Research must be certified by peers before entering a stream of knowledge that may eventually reach the public - and shape society; therefore, Frontiers only applies the most rigorous and unbiased reviews.
Frontiers revolutionizes research publishing by freely delivering the most outstanding research, evaluated with no bias from both the academic and social point of view. By applying the most advanced information technologies, Frontiers is catapulting scholarly publishing into a new generation.

What are Frontiers Research Topics?

Frontiers Research Topics are very popular trademarks of the Frontiers Journals Series: they are collections of at least ten articles, all centered on a particular subject. With their unique mix of varied contributions from Original Research to Review Articles, Frontiers Research Topics unify the most influential researchers, the latest key findings and historical advances in a hot research area! Find out more on how to host your own Frontiers Research Topic or contribute to one as an author by contacting the Frontiers Editorial Office: frontiersin.org/about/contact

HIGH-THROUGHPUT PHENOTYPING IN THE GENOMIC IMPROVEMENT OF LIVESTOCK

Topic Editors:
Fabyano Fonseca Silva, Universidade Federal de Viçosa, Brazil
Guilherme J. M. Rosa, University of Wisconsin-Madison, United States
Gota Morota, Virginia Tech, United States

Citation: Silva, F. F., Rosa, G. J. M., Morota, G., eds. (2021). High-Throughput Phenotyping in the Genomic Improvement of Livestock. Lausanne: Frontiers Media SA. doi: 10.3389/978-2-88971-145-1

Table of Contents

frontiers in Genetics

EDITORIAL
published: 18 June 2021
doi: 10.3389/fgene.2021.707343

Editorial: High-Throughput Phenotyping in the Genomic Improvement of Livestock

Fabyano Fonseca Silva[1]*, *Gota Morota*[2,3] and *Guilherme Jordão de Magalhães Rosa*[4,5]

[1] Department of Animal Science, Federal University of Viçosa, Viçosa, Brazil, [2] Department of Animal and Poultry Sciences, Virginia Polytechnic Institute and State University, Blacksburg, VA, United States, [3] Center for Advanced Innovation in Agriculture, Virginia Polytechnic Institute and State University, Blacksburg, VA, United States, [4] Department of Animal and Dairy Sciences, University of Wisconsin-Madison, Madison, WI, United States, [5] Department of Biostatistics and Medical Informatics, University of Wisconsin-Madison, Madison, WI, United States

Keywords: automated phenotyping, computer vision, genome-enabled analysis, phenomics, precision livestock farming, animal breeding

Editorial on the Research Topic

High-Throughput Phenotyping in the Genomic Improvement of Livestock

Developments in the area of precision livestock farming (PLF) have promoted the use of high-throughput phenotyping or monitoring in animal breeding and genetics research and applications. For example, genome-enabled prediction, genome-wide association studies, and gene expression analysis have been revisited to accommodate a new opportunity introduced by high-throughput phenotyping (HTP) technologies. One of the most relevant challenges in this context is the handling of large-scale data provided by automated processes such as images collection, continuous real-time sensor-based measurements, and spectroscopy reports, among others. Genomic data analysis has been becoming more complex due to increasing phenotypic records from different data sources, as well as data structures and formats. The current Research Topic addresses this specific topic and includes studies on generating high-throughput phenotypes that were previously difficult or impossible to be measured manually, as well as on statistical or computational methodologies for integrating emerging types of phenotypes in breeding strategies. Such phenotypic traits can be used as indicator or novel traits for the genetic improvement of livestock populations for contemporary and pressing phenotypes or economic and societal importance such as animal health and welfare, environmental footprint, product quality, among others. The insights collected in this Research Topic offer new approaches for collecting, storing, and processing such HTP data.

Successful livestock breeding programs require large-scale and accurate phenotypic data, which are also critical for genomic dissection of complex traits. Digital image analysis, which represents the process of extracting meaningful information from images, can be used as input for imaging processing techniques with direct application for livestock phenotyping. Other technologies, such as activity monitor sensors, automatic feeding systems, and indirect biomarkers at the cellular and physiological levels can be used to provide a wide variety of novel phenotypes. Additionally, the infrared spectrometry has been gaining attention in PLF as a non-destructive measurement tool and a great resource for on-line analysis.

Automated image processing is critical in any application of computer vision to HTP as the size of generated image databases is often huge. Nye et al. proposed the Deep Automatic Phenotyping Segmentation (DeepAPS) framework to show how automatically parsed bull images from web-based sire catalogs together with pedigree data can be converted into useful information by

OPEN ACCESS

Edited and reviewed by:
Johann Sölkner,
University of Natural Resources and Life Sciences Vienna, Austria

***Correspondence:**
Fabyano Fonseca Silva
fabyanofonseca@ufv.br

Specialty section:
This article was submitted to Livestock Genomics, a section of the journal Frontiers in Genetics

Received: *09 May 2021*
Accepted: *19 May 2021*
Published: *18 June 2021*

Citation:
Silva FF, Morota G and Rosa GJM (2021) Editorial: High-Throughput Phenotyping in the Genomic Improvement of Livestock. Front. Genet. 12:707343. doi: 10.3389/fgene.2021.707343

inferring genetic parameters of several morphological measurements in dairy cattle. DeepAPS is based on deep learning, and represents a highly precise and automatic image processing algorithm to generate several phenotypic measures, including coat color and body conformational in dairy cattle.

Although image analysis and computer vision currently represent one of the most promising technologies to provide next-generation phenotypes for animal breeding purposes, there is a need to understand peculiarities behind them. Based on this issue, Fernandes et al. presented a detailed review focusing on a variety of computer vison technologies available as well as their applications to animal breeding programs. After a discussion on different strategies to process digital images, they review the main technologies available for imaging in animal and veterinary sciences, and present a number of applications of computer vision systems, including carcass and meat traits, behavior, health, among others.

According to Brito et al., genomic evaluation for animal welfare related traits using large-scale phenotyping is a suitable alternative for reliable selection under a commercial production system. The authors described the primary statistical and bioinformatic methods available for this aim, focusing on strategies for development of novel welfare indicator traits based on HTP, such as recording of movements based on wearable sensors and accelerometers. Sensor-based phenotypes such as movement capture based on IMU (Inertial Measurement Unit), sound analysis, and infrared thermography coupled with data science are paramount to translate animal welfare indicators into accurate genomic breeding values to be used in selective breeding to improve animal resilience at a commercial level. Bouwman et al. compared change point detection, local extreme approach, and gradient boosting machine for signal segmentation of turkey gait sequences collected from inertial measurement unit sensors. They reported gradient boosting machine was the most accurate method for signal segmentation to describe turkey gait. Temperament is a behavioral trait that is underutilized in animal breeding, mostly because the difficulties with systematic data collection. As reported by Yu et al., temperament could be considered as an indicator of production and efficiency in genetic selection. The authors developed a four-platform standing scale to objectively collect temperament data and proposed factor analytic modeling to investigate the underlying genetic interrelationships among temperament measures.

Infrared spectrometry has been also used to generate novel complex traits in livestock. Bresolin and Dórea presented a comprehensive review on mid- (MIR) and near-infrared (NIR) spectrometry for prediction of complex dairy and beef phenotypes, such as milk composition, feed efficiency, methane emission, fertility, energy balance, health status, and meat quality traits. The authors recommended the use of data mining tools to predict such phenotypes based on MIR and NIR. Additionally, Cecchinato et al. integrated experimental-lab measures, milk infrared spectra, and genomics to improve difficult-to-measure traits in dairy cattle populations. The authors concluded that Fourier-transformed infrared spectroscopy provided acceptable values of accuracy, making possible also the prediction for bulls without phenotyped progeny.

High-throughput phenotyping techniques offer a new opportunity to enhance genomic improvement of livestock, especially for novel phenotypes. The studies published in this Research Topic discuss excellent examples of their potential applications, and also point out for challenges and possible solutions. We encourage the scientific community and industry to read these interesting manuscripts and dive into this extremely exciting field of HTP and its applications in PLF and genetic improvement of livestock populations.

AUTHOR CONTRIBUTIONS

FFS, GM, and GJMR: conceptualization, writing, and review and editing. All authors contributed to the article and approved the submitted version.

Conflict of Interest: The authors declare that the manuscript was written in the absence of any commercial or financial relationships that could be construed as a potential conflict of interest.

frontiers in Genetics

ORIGINAL RESEARCH
published: 28 January 2020
doi: 10.3389/fgene.2019.01391

Genome-Wide Association Analysis Reveals Key Genes Responsible for Egg Production of Lion Head Goose

Qiqi Zhao[1,2], *Junpeng Chen*[3], *Xinheng Zhang*[1,2], *Zhouyi Xu*[1,2], *Zhenping Lin*[3], *Hongxin Li*[1,2], *Wencheng Lin*[1,2] *and Qingmei Xie*[1,2]*

[1] College of Animal Science, South China Agricultural University and Guangdong Provincial Key Lab of Agro-Animal Genomics and Molecular Breeding, Guangzhou, China, [2] Key Laboratory of Animal Health Aquaculture and Environmental Control, Guangzhou, China, [3] Shantou Baisha Research Institute of Original Species of Poultry and Stock, Shantou, China

The lion head goose is one of the most important agricultural resources in China; however, its breeding process is relatively slow. In the present study, a genome-wide association study was performed for the genetic selection of egg production characters in lion head geese. We detected 30 single-nucleotide polymorphisms located in or near 30 genes that might be associated with egg production character, and quantitative real-time polymerase chain reaction was used to verify their expression level in lion head geese. The results showed that the expression levels of *CRTC1* (encoding *CREB*-regulated transcription coactivator 1), *FAAH2* (encoding fatty acid amide hydrolase 2), *GPC3* (encoding glypican 3), and *SERPINC1* (encoding serpin family C member 1) in high egg production population were significantly lower than those in the low egg production populations ($^{*}P < 0.05$). The expression levels of *CLPB* (encoding caseinolytic peptidase B protein homolog), *GNA12* (encoding guanine nucleotide-binding protein subunit alpha-12), and *ZMAT5* (encoding zinc finger, matrin type 5) in the high egg production population were significantly higher than those in the low egg production populations ($^{*}P < 0.05$). The expression of *BMP4* (encoding bone morphogenetic protein 4), *FRMPD3* (encoding *FERM* and *PDZ* domain containing 3), *LIF* (encoding leukemia inhibitory factor), and *NFYC* (encoding nuclear transcription factor Y subunit gamma) in the high egg production population were very significantly lower than those in the low egg production population ($^{**}P < 0.01$). Our findings provide an insight into the economic traits of lion head goose. These candidate genes might be valuable for future breeding improvement.

Keywords: lion head goose, genome wide association study, egg production, candidate genes, quantitative real-time polymerase chain reaction

OPEN ACCESS

Edited by:
Guilherme J. M. Rosa, University of Wisconsin-Madison, United States

Reviewed by:
Eduardo Casas, National Animal Disease Center (USDA ARS), United States
Filippo Biscarini, Italian National Research Council (CNR), Italy

***Correspondence:**
Qingmei Xie
qmx@scau.edu.cn

Specialty section:
This article was submitted to Livestock Genomics, a section of the journal Frontiers in Genetics

Received: *02 August 2019*
Accepted: *19 December 2019*
Published: *28 January 2020*

Citation:
Zhao Q, Chen J, Zhang X, Xu Z, Lin Z, Li H, Lin W and Xie Q (2020) Genome-Wide Association Analysis Reveals Key Genes Responsible for Egg Production of Lion Head Goose. Front. Genet. 10:1391. doi: 10.3389/fgene.2019.01391

INTRODUCTION

The lion head goose is named for the sarcoma that makes it resemble a lion's head from the front. Lion head geese provide great economic benefits via the widespread consumption of their meat as stewed products (Zhuang and Lin, 2006). Lion head geese, originating from Shantou Raoping in Guangdong province, are the only large and major goose species in China, and are the germplasm

resources under special state protection (Chen et al., 2011). Lion head geese, whose ancestors are anser cygnoides, are herbivorous animals showing fast growth and large body size; as such, their feeding is relatively environment-friendly (Huang, 2009; He et al., 2012). However, they show low fertility with an average of 20–25 eggs per year (Zhang, 1991). The egg-laying period is not continuous but is divided into three parts caused by its strong broodiness (Wang, 2007). A lower laying rate may hinder the development of the lion head goose industry. Therefore, based on maintaining the characteristics of its original breeds, improving the low fecundity has become an important breeding objective of lion head goose, among which the egg laying characteristics are one of the most significant aspects (Wang et al., 2008). It is believed that egg production could be improved by adopting a modern genome-enhanced breeding scheme.

Genome-wide association studies (GWASs), which were proposed first by Risch in 1996, are powerful and effective tools to identify genetic markers associated with the trait of interest (Risch and Merikangas, 1996). In recent years, a large number of GWASs on human diseases have been published, such as for vitiligo (Shen et al., 2016) and for livestock animals such as pigs (Luo et al., 2012). Since the development of the HapMap Project, a number of high-density single-nucleotide polymorphism (SNP) chips for plant and animal species like chicken, swine, cattle, sheep, and the like have been developed as well (Gibbs et al., 2003). Hoglund et al. found that a total of 17,388 significant SNP markers and candidate genes associated with female fertility were distributed on 25 chromosomes in the Nordic Red cattle group (Hoglund et al., 2015). Shen *et al.* carried out GWAS on Ningdu Sanhuang chickens with Chicken chip and found the candidate gene, *GARNL1*, which was related to reproductive traits (Shen et al., 2012). Xie used the Illumina Porcine SNP60K chip to screen the potential candidate genes that may be associated with the litter size of the Xiang Pig (Xie, 2016). The production of SNP chips and the appearance of high-throughput sequencing technology have made GWAS an important research strategy in some fields. GWAS is widely accepted as a primary method for gene detection (Jiang et al., 2010).

In the present study, we performed GWAS to identify SNPs and potential genetic variants that may be associated with egg laying character of the lion head geese. Then we attempted to verify their functionality. As a result, we have identified certain genes that might play important roles in the egg laying process.

MATERIALS AND METHODS

Animals Resources and Sample Collection

Lion head geese are the largest goose breed in China and are the one of the world's big goose species. In the past 2 years, we have bred a batch of lion head geese with high and low egg production in the Shantou Baisha Research Institute of Original Species of Poultry and Stock, Guangdong Province. These geese have the same growth environment and nutritional supplements, and they have free access to food and water.

A total of 217 geese blood samples were collected at the Shantou Baisha Research Institute of Original Species of Poultry and Stock, including 136 high egg-production geese (more than 35 eggs per year) and 81 low egg-production geese (less than 25 eggs per year). Blood samples were stored at an ACD anticoagulant tube at −80°C cryogenic refrigerator for further experiments.

DNA Extraction and Whole Genome Sequencing

Genomic DNA was extracted from peripheral blood cells of the high and low egg production groups using a HiPure Blood DNA Mini Kit (Magenbio, Guangzhou, China). After passing the quality inspection of NanoDrop 2000 Spectrophotometer (Thermo, America), the DNA samples were sent to Beijing Genomics Institute (Shenzhen, China) for whole genome resequencing. An Easy DNA Library Prep Kit (MGI, Shenzhen, China) was used to carry out the double-enzyme digestion to construct six libraries, re-sequenced using the BGISEQ-500RS platform with an average 12× sequencing depth and coverage of 8%.

Data Preparation and Statistical Analysis

Genotyping Data

To obtain better quality sequencing data, the raw data was filtered using the software SOAPnuke (Chen et al., 2018). The clean reads were then aligned with the *Anser cygnoides domesticus* genome data (https://www.ncbi.nlm.nih.gov/genome/31397?genome_assembly_id=229313) using BWA (Li and Durbin, 2010; Lu et al., 2015). The software SAMtools and GATK4 (https://software.broadinstitute.org/gatk/download/) then were used to detect variations and SNPs (Li, 2011). To limit the number of false positives and low confidence variants, all called variants were filtered using hard filters set according to the Broad Institute's hard filtering recommendations: quality by depth (QD) 2.0, read position rank sum −8.0, Fisher strand (FS) 60.0, root mean square (RMS) mapping quality (MQ) 40.0, strand odds ratio (SOR) 3.0, mapping quality rank sum test (MQ Rank Sum) −12.5, quality 30, minimum allele frequency 5%, call rate 70%, and Hardy–Weinberg equilibrium (HWE) $P > 1e^{-6}$.

Then, Vcftools was used as a secondary filter, according to the following criteria: minor allele frequency (MAF) 0.05, HWE $P = 1e^{-6}$, and max-missing 0.7 (Danecek et al., 2011).

Given the large number of scaffolds, scaffolds were combined into 21 chromosomes. The ordered SNP loci were separated into the 21 artificial chromosomes per 50 million base pairs (i.e. 1–50 Mbps, 51–100 Mbps etc.). Principal component analysis (PCA) was performed to identify genetic variation and the population structure.

Phenotypic Data

Descriptive statistics of phenotypic data were carried out by SPSS 22 software (IBM Corp., Armonk, NY, USA), and the sample

size, maximum, minimum, average and standard deviation of high and low egg production samples were calculated.

Statistical Analysis

Genome wide association studies was performed using the EMMAX software with egg production character classified by dichotomies, i.e., the data was divided into high and low egg production (Kang et al., 2010). The analysis model was as follows:

$$P = \mu + Z\alpha + SNP + e$$

where P is the vector of phenotypes of the individuals, μ is the intercept of a straight line, Z is the incidence matrix of random polygenic effects, α is the random polygenic effects, SNP is the effect of a single nucleotide polymorphism, and e is the vector of residual errors with $e \sim N(0, I\sigma_e)$, where I is the identity of matrix and σ_e is the residual variance.

Multiple Hypothesis Testing and Correction

The tested SNP markers could be used to make a Bonferroni adjustment with the 5% GWAS-wide significance level:

$$\alpha = \frac{0.05}{n}$$

where α is the GWAS-wide significance level, n is the number of all tested SNP sites. In order to reduce false negative, and then extending the threshold 20 times as the suggestive value.

Population Stratification

Population stratification refers to the existence of subpopulations with different allele frequencies, which may pose a great threat to the validity of GWAS results, and even leads to false-positive results. The quantile–quantile plot (Q-Q plot) was used to assess the GWAS results, to judge whether the *P*-value calculated by SNP correlation analysis deviated from the hypothesis test on the whole overall.

Detection of Candidate Genes

Based on the NCBI database (http://www.ncbi.nlm.nih.gov/) and Ensemble (http://www.ensemblgenomes.org), these SNPs identified by GATK4 were located in or near 30 genes.

Quantification of Candidate Genes

To observe whether the candidate genes were differentially expressed in the high egg production group compared with the low group, we performed quantitative real-time polymerase chain reaction (RT-qPCR) for these genes. Total RNA was extracted from PBCs using the TRIzol reagent, and synthesized into cDNA using a Reverse Transcription Kit (Takara, Shiga, Japan). The cDNA was then used as a template for RT-qPCR using the CFX96 Touch (Bio-Rad, Hercules, CA, USA). The RT-qPCR primer sequences were synthesized by Sangon Biotech (Guangzhou, China) and were stored at −20°C for later use. According to the instructions of 2× SYBR Green qPCR Master Mix kit (Bimake, Houston, TX, USA), the RT-qPCR reaction was performed in triplicate and uses comprises 20 μl, containing 10 μl of 2× SYBR Green qPCR Master Mix, 0.4 μl of ROX Reference Dye, 1 μl of cDNA template, and a 0.5 mM concentration of specific primers. Thermal cycling parameters were as follows: 95°C for 5 min; 40 cycles of 95°C for 15 s, 60°C for 30 s, and 72°C for 30 s and 1 cycle of 95°C for 15 s, 60°C for 60 s, and 95°C for 15 s. Relative mRNA expression levels were calculated using the $2^{-\Delta\Delta Ct}$ method and normalized using the expression of GAPDH [encoding glyceraldehyde-3-phosphate dehydrogenase, (Livak and Schmittgen, 2001)]. All the primers for RT-qPCR are shown in **Table S1**.

RESULTS

Sample Phenotypic Data Statistics

The egg production performance of lion head goose was divided into a high production group (>35 eggs per year) and a low production group (<25 eggs per year).

The phenotypic data of low egg production was graphically recorded in **Figure 1A** and high egg production was in **Figure 1B**. The sample size, maximum, minimum, average and standard deviation of the trait measured in the current experiment were presented in **Table 1** and the boxplot is shown in **Figure 1C**. The sample size, maximum, minimum, average and standard deviation of the high egg production group were 136, 63, 35, 46, 54, while that in the low egg production group were 81, 25, 8, 17, 21, respectively. The annual egg production records for each individual are shown in **Table S2**.

Sequencing Data Statistics

Aligning the clean reads to the reference sequence allowed us to statistically analyze the sequencing depth, coverage rate, mapping rate, and mismatch rate, as shown in **Table 2**. Based on 217 original high egg production and low egg production samples, 8 were excluded because of mismatch, leaving 209 samples (131 high egg production, 78 low egg production). And the average of sequencing depth, coverage rate, mapping rate, and mismatch rate are 12.05%, 7.56%, 91.31%, and 1.48%, respectively.

Genetic Variation and Population Structure

To determine data validity and population structure, PCA was performed based on the variation of the sequence data, taking principal component 1 as the horizontal and principal component 2 as the ordinate (**Figure 2**). The differences among individuals in each group were small, having high similarity. However, the dispersion between the high and low egg production groups was large, showing obvious population differentiation and indicating that there was a great difference between the two groups.

Significant Single-Nucleotide Polymorphisms and Population Stratification Assessment

The PCA results were used as covariates and EMMAX was used for the GWAS analysis. In **Figure 3**, chromosomes 1–21 are

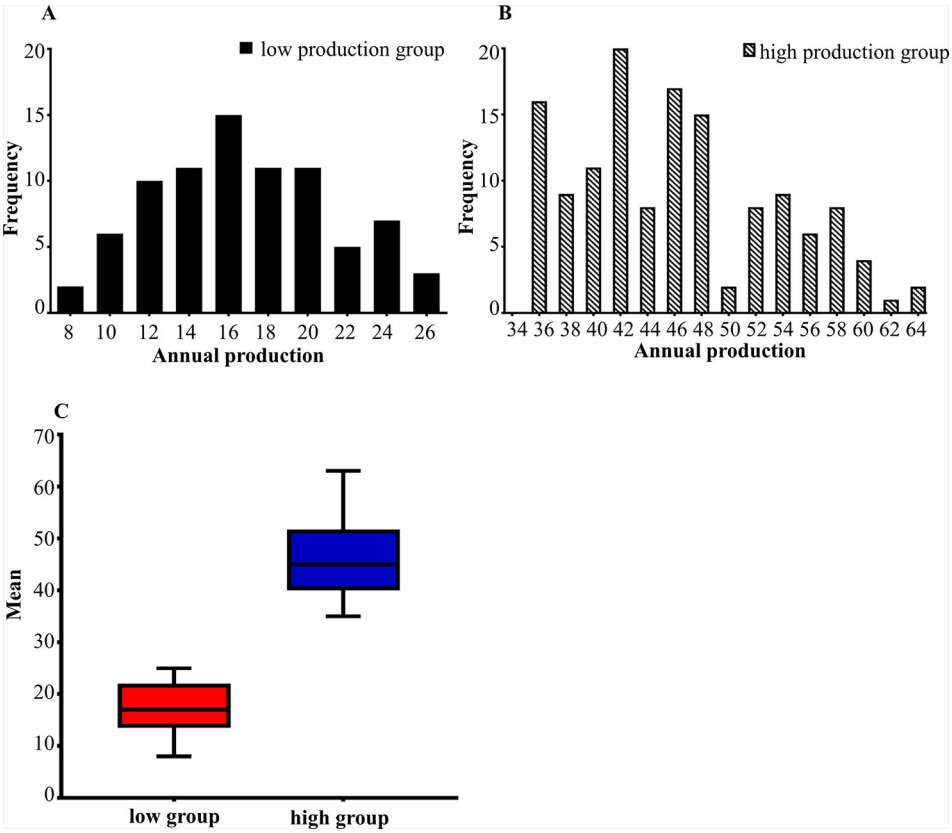

FIGURE 1 | (A, B) The distribution of egg production in two groups. The horizontal axis shows the annual egg production and the vertical axis shows the frequency. **(A)** is the distribution of low egg production group. **(B)** is the distribution of high egg production group. **(C)** is the boxplot of the average between the high and low egg production groups.

TABLE 1 | Phenotypic statistics.

Group	Sample size	Maximum	Minimum	Average	Standard deviation
Low group	81	25	8	17	21
High group	136	63	35	46	54

TABLE 2 | Sequencing statistics.

	Depth	Coverage (%)	Mapping rate (%)	Mismatch (%)
Min	1.26	0.95	88.10	1.20
Max	35.64	16.85	93.06	1.79
Mean	12.05	7.56	91.31	1.48

shown separately with different colors. The corresponding horizontal lines indicated the 5% GWAS-wide significance levels and the threshold was expanded 20 times as a second suggested value. The results are shown in **Figure 3**.

With the conditions of QD 2.0, Read Pos Rank Sum −8.0, FS 60.0, MQ 40.0, SOR 3.0, MQ Rank Sum −12.5, quality 30, minimum allele frequency 5%, call rate 70%, and HWE $P > 1e^{-6}$, we finally identified 30 significant SNPs and the genes located on or near them, as shown in **Table 3**.

The Q-Q plot showed that the screened SNPs were located above the diagonal line, indicating that the analytical model is reasonable. And the significantly higher points located at the top right corner of the graph represented potential candidate molecular markers associated with the trait (**Figure 4**).

Candidate Genes Analysis

To determine whether the candidate genes were differentially expressed in the high and the low egg production group, we performed RT-qPCR on these genes. The expression levels of *BMP4* (encoding bone morphogenetic protein 4), *FRMPD3* (encoding *FERM* and *PDZ* domain containing 3), *LIF* (encoding Leukemia inhibitory factor), and *NFYC* (nuclear transcription factor Y subunit gamma) in the high egg production population were significantly lower than those in the low egg production population ($^{**}P < 0.01$). The expression levels of *CRTC1* (encoding *CREB*-regulated transcription coactivator 1), *FAAH2* (encoding fatty acid amide hydrolase 2), *GPC3* (encoding glypican 3), and *SERPINC1* (encoding serpin

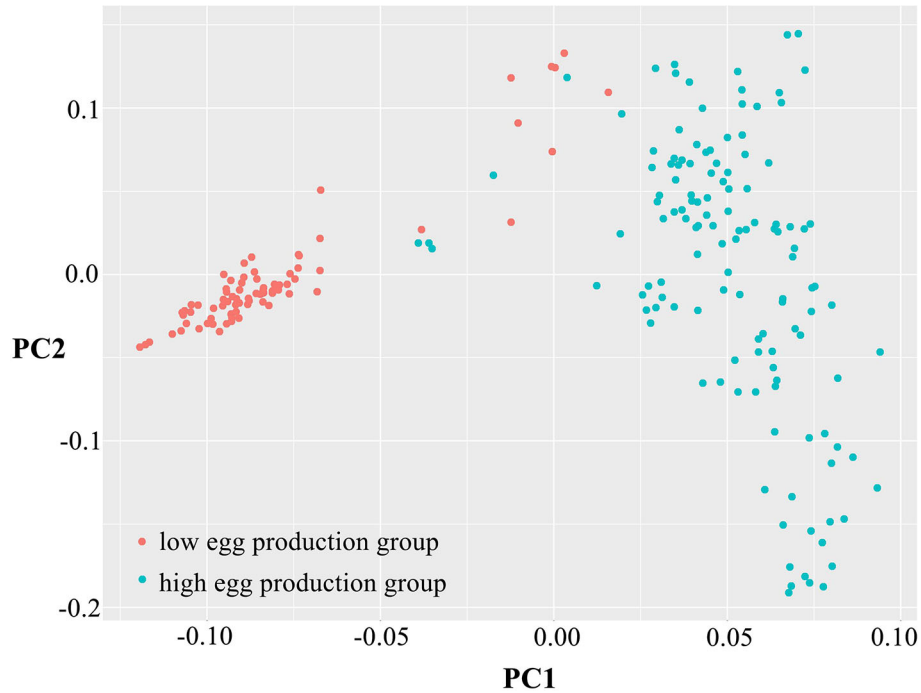

FIGURE 2 | Principal component analysis of egg production. Principal component 1 (PC1) and principal component 2 (PC2) values comprised the X-axis and the Y-axis and were used to draw the scatter gram, and each dot represents one sample. Red points represent low-yield samples and blue points represent high-yield samples.

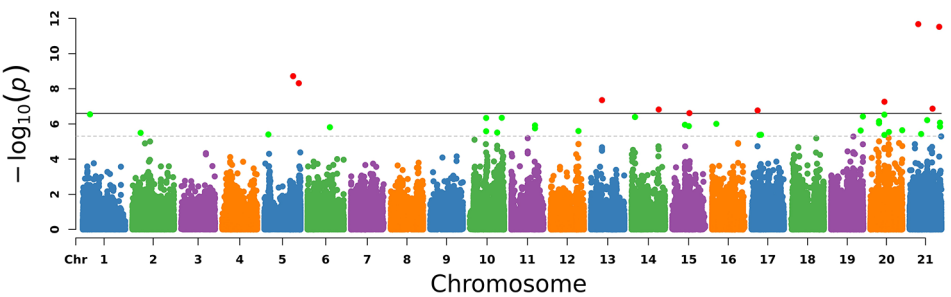

FIGURE 3 | Manhattan plot of –log10 (*P*-values) for the egg laying traits in chromosome order. Each simulated chromosome contains 50 million bases. The solid line indicates the 5% significance level and the dotted line indicates the suggested level that extended the threshold to 20 times. The red points and green points are the significant SNPs.

family C member 1) in the high egg production population were significantly lower than those in the low egg production population (*$P < 0.05$). The expression levels of *CLPB* (encoding caseinolytic peptidase B protein homolog), *GNA12* (encoding guanine nucleotide-binding protein subunit alpha-12), and *ZMAT5* (encoding zinc finger, matrin type 5) in the high egg production population were significantly higher than those in the low egg production population (*$P < 0.05$, **Figure 5A**). The expression levels of the remaining genes (see **Figure 5B** for their symbols) were not significantly different between the two groups (**Figure 5B**).

DISCUSSION

The Significance of Studying the Lion Head Goose

The lion head goose is the largest meat goose currently bred in China. It is characterized by a large size, crude feed tolerance, fast growth, high forage reward, strong stress resistance, and has a delicious meat that has extremely high economic value and is deeply favored by consumers (Zhuang and Lin, 2006). Therefore, an in-depth study of the breeding problem of lion head geese will help to modernize the industry to meet market demand.

TABLE 3 | The SNPs related to egg laying trait was detected by GWAS.

Number	SNP	Position	Gene	*P* value
1	NW_013185654	11050658	*CDH23*	2.84E–07
2	NW_013185657	12830867	*HSD17B12*	3.21E–06
3	NW_013185670	6211741	*EPHB3*	3.95E–06
4	NW_013185674	6277159	*GM2A*	1.92E–09
5	NW_013185675	5989069	*GNA12*	4.83E–09
6	NW_013185680	1530955	*NEXN*	1.54E–06
7	NW_013185711	3613832	*GPC4*	4.56E–07
8	NW_013185714	4862813	*FRMPD3*	3.09E–06
9	NW_013185716	1472974	*NFYC*	4.45E–07
10	NW_013185724	1493289	*GPC3*	1.77E–06
11	NW_013185736	3684650	*HTF3A*	2.53E–06
12	NW_013185743	1607400	*FGF9*	4.42E–08
13	NW_013185754	2051719	*FRY*	4E–07
14	NW_013185766	1522744	*ANTXR*	1.51E–07
15	NW_013185777	85282	*CLPB*	1.12E–06
16	NW_013185779	779290	*SMG7*	1.30E–06
17	NW_013185791	1229858	*SERPINC1*	9.85E–07
18	NW_013185814	703561	*SLITRK6*	1.71E–07
19	NW_013185815	1430965	*BMP4*	4.21E–06
20	NW_013185816	1738455	*RXRA*	4.12E–06
21	NW_013185899	252542	*CRTC1*	2.37E–06
22	NW_013185902	401032	*KCNAB2*	3.75E–07
23	NW_013185915	928804	*TMLHE*	9.1E–07
24	NW_013185925	301227	*LIMA1*	5.46E–08
25	NW_013185930	275521	*DDX49*	2.86E–06
26	NW_013185967	383783	*ELOVL4*	2.28E–06
27	NW_013186001	299910	*ZMAT5*	2.11E–12
28	NW_013186015	302128	*LIF*	3.73E–06
29	NW_013186054	67611	*FAAH2*	6.08E–07
30	NW_013186105	38036	*FBXL20*	1.35E–07

GWAS, genome-wide association studies; SNPs, single-nucleotide polymorphisms.

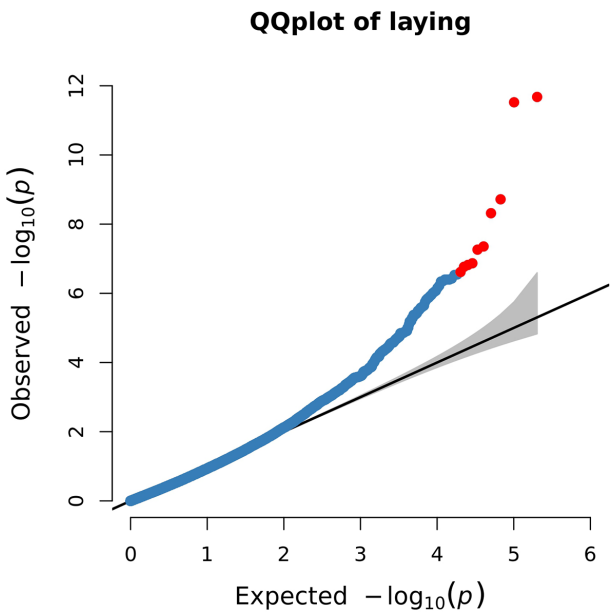

FIGURE 4 | Quantile–quantile (Q-Q) plot of genome-wide association results for egg production. The blue points represent SNPs, and the red points represent the most significant SNPs.

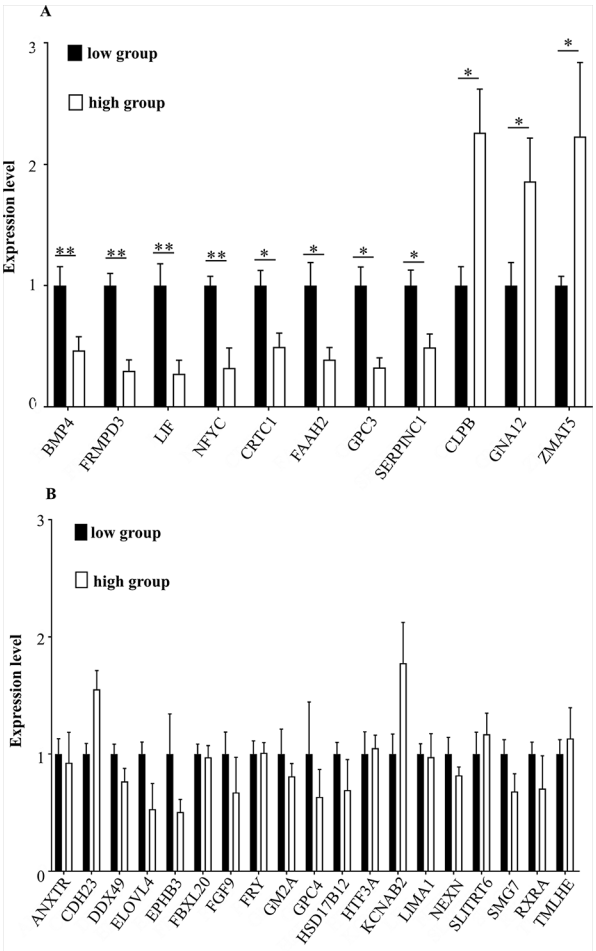

FIGURE 5 | (A, B) The mRNA expression levels of key genes in different groups. The horizontal axis shows the different genes, and mRNA expression levels are on the vertical axis. Sign ** indicates extreme significance ($P < 0.01$). Sign * indicates significance ($P < 0.05$). No marker means no difference.

In this study, the high and low egg production populations selected in a previous study were analyzed, and the number of eggs per year was used as the parameter to carry out GWAS. The phenotypic records of the egg laying character in this research were normally distributed, which was consistent with the separation characteristics and population separation characteristics.

Application of Genome-Wide Association Study

In this study, we performed a GWAS for the egg production trait of a lion head geese population. Genomic studies have been carried out for many agricultural animals, such as chickens, swine, sheep, cattle, and geese, however, few of them have studied regionally important economic species such as lion head geese in China. To the best of our knowledge, this is the first GWA studies for the egg production character of lion head geese. Currently, database such as NCBI and Ensembl contain few reported goose sequences, which need to be further verification.

The research on the breeding of lion head geese has lagged behind that for other economically important species, which has led to many problems in the lion head goose breeding industry, such as backward breeding, and low productivity. With the development of genome-enhanced breeding and the improved the efficiency of genomic selection, it will be possible to protect and develop the breeding resources of the lion head goose, thus promoting the modernization and industrialization of the lion head goose industry.

Significance of This Research

Next generation sequencing technology based on high-throughput sequencing and molecular marker technology, enables the fine mapping of functional genes. Genome selection technology represents a new generation of molecular breeding technology for livestock and poultry. This technique has been successfully applied to the cultivation of sheep (Zhao and Zhang, 2019). The high egg production traits of the lion head goose breeding population, the identification of the SNPs, and the selection of functional genes for economic traits will lay the foundation for the development of genotyping technology for lion head goose breeding.

Detection and Verification of Key Genes

Bioinformatic analyses at the Ensembl and NCBI databases were used to identify the genomic location of SNPs that are significantly associated with the selected trait. Subsequently, bioinformatics and comparative genomics analysis were used to select key genes and make preliminary annotations on related gene functions.

In this study, a GWAS was conducted on the egg production trait of lion head geese, which detected 30 SNPs that were significantly associated with the high egg-production characteristic of lion head geese. We then screened the 30 genes that contained or were near, the SNPs.

Genes *BMP4*, *FRMPD3*, *LIF*, *NFYC*, *CRTC1*, *FAAH2*, *GPC3*, *SERPINC1*, *CLPB*, *GNA12*, and *ZMAT5* showed differential expression in between the high and low egg production populations of lion head geese.

In the present study, the expression levels of the *BMP4*, *LIF*, *NFYC* and *FRMPD3* genes in the low egg production population of the lion head goose were significantly higher than those in the high egg production population.

BMP4 (bone morphogenetic protein 4), a member of the transforming growth factor beta (TGFβ) superfamily of growth factors, was first characterized for its role in bone metabolism (Nilsson and Skinner, 2003). It was subsequently reported to be involved in the regulation of embryonic mesoderm formation, and the formation of primordial germ cells (Nilsson and Skinner, 2003). *BMP4* mediates the formation of the mesoderm in mouse embryos, in which knockdown of *BMP4* leads to death and neonatal malformation (Zhu et al., 2002). It was reported that *BMP4* inhibits secretion of progesterone by granulosa cells and the expression of follicles in sheep and cattle (Monget et al., 2002; Da et al., 2018). Our results were consistent with these reports, i.e., *BMP4* might negatively affect the egg production character of the lion head geese.

FRMPD3 (*FERM* and *PDZ* domain containing 3), located on the human X chromosome, is homologous to *FRMPD4*, which indicated that *FRMPD3* might mediate significant functions related to excitability associated with neuronal migration abnormality; however, the functions of *FRMPD3* have not been reported to be associated with poultry laying performance (Mardinly, 2013).

LIF (leukemia inhibitory factor), a secretory glycoprotein, is essential for the embryo implantation process in mice and humans (Aghajanova, 2004). Females lacking *LIF* are infertile, because their blastocysts cannot be implanted in the uterus, resulting in no clinical pregnancy (Steck et al., 2004). Our results would seem to conflict with those of previous reports, might reflect species inconsistency, or other, as yet unidentified factors. This result requires further verification and testing (Schofield and Kimber, 2005).

NFYC (nuclear transcription factor Y subunit gamma), a histone-fold domain-containing transcription factor, was identified in mice and humans as an oncogene required for the initiation and progression of tumors, and it engaged in chromatin remodeling (Tong et al., 2015). As far as we know, it has never been linked to reproductive function in any species.

The expression levels of the *CRTC1*, *FAAH2*, *GPC3*, and *SERPINC1* genes in the high egg production goose population were significantly lower than those in the low egg production population.

CRTC1 (*CREB*-regulated transcription coactivator 1) is a transcriptional coactivator that has a biological function that affects energy balance and reproduction. Overexpression of *CRTC1* in mice led to obesity and infertility (Altarejos et al., 2008). Breuillaud *et al.* showed that the *CREB* coactivator *CRTC1* is indispensable for mouse fertility (Breuillaud et al., 2009). Our results were consistent with these reports, suggesting that *CRTC1* plays a negative role in the laying trait of the lion head goose.

FAAH2 (fatty acid amide hydrolase 2), a member of the serine hydrolase family of enzymes, regulates several physiological processes, including appetite, inflammation, and various reproductive processes like secretion of gonadotropin-releasing hormone from the hypothalamus (Lunetta et al., 2015). *FAAH2* may participate in negative regulation of egg laying.

GPC3 (glypican 3), a member of the heparan sulfate proteoglycans, has been widely studied as a target in human cancer, such as ovarian carcinoma. *GPC3* mediates the synthesis of integral membrane proteins that interact directly with insulin like growth factor 2 (*IGF2*), which is considered to be an important growth factor in ovarian cancer (Ofuji et al., 2014; Wu et al., 2016). *GPC3* induces apoptosis in ovarian cells, suggesting that it plays an important role in the development of ovarian cancer (Gonzalez et al., 1998). According to comprehensive research reports, we believe that low expression of *GPC3* may promote egg laying in the lion head goose.

SERPINC1 (serpin family C member 1), is the main endogenous anticoagulant. Its mutations cause hereditary

antithrombin deficiency and are associated with increased risk for all forms of pregnancy-related complications, which cause adverse pregnancy reaction (De la Morena-Barrio et al., 2012; Rogenhofer et al., 2014). Thus, *SERPINC1* may encourage low egg production; however, its specific effects require to be further verified.

The expression levels of *CLPB*, *GNA12*, and *ZMAT5* in the high egg production population were significantly increased compared with those in the low egg production population.

CLPB (caseinolytic peptidase B protein homolog) encodes an ATP-dependent chaperone. Disruption of *CLPB* is related to human congenital microcephaly and small birth weight (Capo-Chichi et al., 2015). Our results hint at a similar effect in geese. An increase in *CLPB* might lead to an increase in egg laying.

GNA12 (guanine nucleotide-binding protein subunit alpha-12), the α subunit of a heterotrimeric G protein, participates in cell transformation and embryonic development; is expressed in the cytoplasm of Leydig cells; and has the biological function of promoting the differentiation of cells and elongated sperm cells into mature sperm (Hu et al., 2008, Udayappan and Casey, 2017). Shen et al. showed that preeclampsia is associated with decreased methylation of GNA12 promoters (Shen et al., 2015). Thus, the expression of *GNA12* might promote high egg production in the lion head goose.

For *ZMAT5* (zinc finger, matrin type 5), there have been no reports of its effects on animal reproduction.

CONCLUSIONS

In this study, based on the breeding group of lion head goose, the blood DNA samples were collected to conduct a genome-wide association study on egg production traits. Thirty SNPs related to egg-producing traits were identified, and thirty genes located in or near SNPs were screened. The selected key genes were verified using RT-qPCR. The *BMP4*, CRTC1, *FAAH2*, *FRMPD3*, *GPC3*, *LIF*, *NFYC*, and *SERPINC1* genes might play a negative role in the egg production character of the lion head Goose. The *CLPB*, *GNA12*, and *ZMAT5* genes might play a positive role in egg production character in the laying trait of the lion head goose. The *ANTXR*, *CDH23*, *DDX49*, *ELOVL4*, *EPHB3*, *FBXL20*, *FGF9*, *FRY*, *GM2A*, *GPC4*, *HSD17B12*, *HTF3A*, *KCNAB2*, *LIMA1*, *NEXN*, *SLITRT6*, *SMG7*, *RXRA*, and *TMLHE* genes might have no significant effect on egg production character of the lion head goose. These results require further verification and confirmation.

In the past few years, GWASs have devoted to the identification of key loci and genes related to the molecular breeding of livestock and poultry. These genes may provide novel target for hereditary approaches to improve breeding. Developments in this area will be exciting and will affect the future of genomic breeding. In view of the fact that most of these genetic connections are limited, a large number of sample studies are required in future investigations in order to detect these subtle variations.

DATA AVAILABILITY STATEMENT

The datasets PRJNA552198 for this study can be found in the NCBI (https://www.ncbi.nlm.nih.gov/bioproject/PRJNA552198).

ETHICS STATEMENT

The use of animals in this study was approved by the South China Agricultural University Committee for Animal Experiments (approval ID: SYXK(Guangdong)2019-0136). All study procedures and animal care activities were conducted in accordance with the national and institutional guidelines for the care and use of laboratory animals. Written informed consent was obtained from the owners for the participation of their animals in this study.

AUTHOR CONTRIBUTIONS

QZ and QX are the principal investigator for this article and contributed to the concept and planning of the article, collection of the data, and reporting of the work described. QZ, JC, XZ, ZL, and QX contributed to the planning of the article, collection of the data, and reporting of the work described. ZX, HL, and WL are the other principal investigators for this article and contributed to the concept of the manuscript, planning of the article, collection of the data, and reporting of the work described. All authors contributed to drafting the article or revising it critically for important intellectual content.

FUNDING

This work was supported by the National Modern Agricultural Industry Science and Technology Innovation Center in Guangzhou (2018kczx01) and the Agricultural Science and Technology Innovation and Promotion Project in Guangdong Province (2018LM1112). The funders had no role in the study design, data collection and analysis, decision to publish, or preparation of the manuscript.

ACKNOWLEDGMENTS

The author would like to thank Dr. Shen from the Beijing Genomics Institute in Shenzhen and Dr. Xie from Ming Lead Gene Technology for helping us analyze the data, revise the manuscript and answer our questions.

SUPPLEMENTARY MATERIAL

The Supplementary Material for this article can be found online at: https://www.frontiersin.org/articles/10.3389/fgene.2019.01391/full#supplementary-material

REFERENCES

Aghajanova, L. (2004). Leukemia inhibitory factor and human embryo implantation. *Ann. N. Y. Acad. Sci.* 1034, 176–183. doi: 10.1196/annals.1335.020

Altarejos, J. Y., Goebel, N., Conkright, M. D., Inoue, H., Xie, J., Arias, C. M., et al. (2008). The Creb1 coactivator Crtc1 is required for energy balance and fertility. *Nat. Med.* 14 (10), 1112–1117. doi: 10.1038/nm.1866

Breuillaud, L., Halfon, O., Magistretti, P. J., Pralong, F. P., and Cardinaux, J. R. (2009). Mouse fertility is not dependent on the CREB coactivator Crtc1. *Nat. Med.* 15 (9), 989–990. doi: 10.1038/nm0909-989

Capo-Chichi, J. M., Boissel, S., Brustein, E., Pickles, S., Fallet-Bianco, C., Nassif, C., et al. (2015). Disruption of CLPB is associated with congenital microcephaly, severe encephalopathy and 3-methylglutaconic aciduria. *J. Med. Genet.* 52 (5), 303–311. doi: 10.1136/jmedgenet-2014-102952

Chen, J., Peng, X., Lu, J., Sun, J., Qiu, J., Tang, X., et al. (2011). Anti-season breeding technology of original lion head goose (in Chinese). *Guangdong Agri. Sci.* 38 (10), 100–101. doi: 10.16768/j.issn.1004-874x.2011.10.067

Chen, Y., Chen, Y., Shi, C., Huang, Z., Zhang, Y., Li, S., et al. (2018). SOAPnuke: a MapReduce acceleration-supported software for integrated quality control and preprocessing of high-throughput sequencing data. *Gigascience* 7 (1), 1–6. doi: 10.1093/gigascience/gix120

Da, C. E., Melo, L., Sousa, G. B., Araujo, V. R., Vasconcelos, G. L., Silva, A., et al. (2018). Effect of bone morphogenetic proteins 2 and 4 on survival and development of bovine secondary follicles cultured in vitro. *Theriogenology* 110, 44–51. doi: 10.1016/j.theriogenology.2017.12.032

Danecek, P., Auton, A., Abecasis, G., Albers, C. A., Banks, E., DePristo, M. A., et al. (2011). The variant call format and VCFtools. *Bioinformatics* 27 (15), 2156–2158. doi: 10.1093/bioinformatics/btr330

De la Morena-Barrio, M. E., Anton, A. I., Martinez-Martinez, I., Padilla, J., Minano, A., Navarro-Fernandez, J., et al. (2012). Regulatory regions of SERPINC1 gene: identification of the first mutation associated with antithrombin deficiency. *Thromb Haemost.* 107 (3), 430–437. doi: 10.1160/TH11-10-0701

Gibbs, R., Belmont, J., Hardenbol, P., Willis, T., Yu, F., Yang, H., et al. (2003). The international hapmap project. *Nature* 426, 789–796. doi: 10.1038/nature02168

Gonzalez, A. D., Kaya, M., Shi, W., Song, H., Testa, J. R., Penn, L. Z., et al. (1998). OCI-5/GPC3, a glypican encoded by a gene that is mutated in the Simpson-Golabi-Behmel overgrowth syndrome, induces apoptosis in a cell line-specific manner. *J. Cell Biol.* 141 (6), 1407–1414. doi: 10.1083/jcb.141.6.1407

He, Z., Du, W., and Wang, W. (2012). Advances in molecular research on the origin and evolution of Chinese Goose (in Chinese). *Contemp. Anim. Husbandry* (03), 35–38.

Hoglund, J. K., Buitenhuis, B., Guldbrandtsen, B., Lund, M. S., and Sahana, G. (2015). Genome-wide association study for female fertility in Nordic Red cattle. *BMC Genet.* 16, 110. doi: 10.1186/s12863-015-0269-x

Hu, Y., Xing, J., Chen, L., Guo, X., Du, Y., Zhao, C., et al. (2008). RGS22, a novel testis-specific regulator of G-protein signaling involved in human and mouse spermiogenesis along with GNA12/13 subunits. *Biol. Reprod.* 79 (6), 1021–1029. doi: 10.1095/biolreprod.107.067504

Huang, S. (2009). Feeding management of meat lion head goose (in Chinese). *China Poult.* 31 (22), 65–66. doi: 10.16372/j.issn.1004-6364.2009.22.021

Jiang, L., Liu, J., Sun, D., Ma, P., Ding, X., Yu, Y., et al. (2010). Genome wide association studies for milk production traits in Chinese Holstein population. *PLoS One* 5 (10), e13661. doi: 10.1371/journal.pone.0013661

Kang, H. M., Sul, J. H., Service, S. K., Zaitlen, N. A., Kong, S. Y., Freimer, N. B., et al. (2010). Variance component model to account for sample structure in genome-wide association studies. *Nat. Genet.* 42, 348–354. doi: 10.1038/ng.548

Li, H., and Durbin, R. (2010). Fast and accurate long-read alignment with Burrows-Wheeler transform. *Bioinformatics* 26 (5), 589–595. doi: 10.1093/bioinformatics/btp698

Li, H. (2011). A statistical framework for SNP calling, mutation discovery, association mapping and population genetical parameter estimation from sequencing data. *Bioinformatics* 27 (21), 2987–2993. doi: 10.1093/bioinformatics/btr509

Livak, K. J., and Schmittgen, T. D. (2001). Analysis of relative gene expression data using real-time quantitative PCR and the 2(-Delta Delta C(T)) Method. *Methods* 25, 402–408. doi: 10.1006/meth.2001.1262

Lu, L., Chen, Y., Wang, Z., Li, X., Chen, W., Tao, Z., et al. (2015). The goose genome sequence leads to insights into the evolution of waterfowl and susceptibility to fatty liver. *Genome Biol.* 16, 89. doi: 10.1186/s13059-015-0652-y

Lunetta, K. L., Day, F. R., Sulem, P., Ruth, K. S., Tung, J. Y., Hinds, D. A., et al. (2015). Rare coding variants and X-linked loci associated with age at menarche. *Nat. Commun.* 6, 7756. doi: 10.1038/ncomms8756

Luo, W., Cheng, D., Chen, S., Wang, L., Li, Y., Ma, X., et al. (2012). Genome-wide association analysis of meat quality traits in a porcine Large White× Minzhu intercross population. *Int. J. Biol. Sci.* 8 (4), 580–595. doi: 10.7150/ijbs.3614

Mardinly, A. R. (2013). *Regulation of Synapse Development by Activity Dependent Transcription in Inhibitory Neurons. Doctoral dissertation* (Harvard University). http://nrs.harvard.edu/urn-3:HUL.InstRepos:11151534.

Monget, P., Fabre, S., Mulsant, P., Lecerf, F., Elsen, J. M., Mazerbourg, S., et al. (2002). Regulation of ovarian folliculogenesis by IGF and BMP system in domestic animals. *Domest. Anim. Endocrinol.* 23 (1-2), 139–154. doi: 10.1016/s0739-7240(02)00152-2

Nilsson, E. E., and Skinner, M. K. (2003). Bone morphogenetic protein-4 acts as an ovarian follicle survival factor and promotes primordial follicle development. *Biol. Reprod.* 69 (4), 1265–1272. doi: 10.1095/biolreprod.103.018671

Ofuji, K., Saito, K., Yoshikawa, T., and Nakatsura, T. (2014). Critical analysis of the potential of targeting GPC3 in hepatocellular carcinoma. *J. Hepatocell Carcinoma* 1, 35–42. doi: 10.2147/JHC.S48517

Risch, N., and Merikangas, K. (1996). The future of genetic studies of complex human diseases. *Science* 273 (5281), 1516–1517. doi: 10.1126/science.273.5281.1516

Rogenhofer, N., Bohlmann, M. K., Beuter-Winkler, P., Wurfel, W., Rank, A., Thaler, C. J., et al. (2014). Prevention, management and extent of adverse pregnancy outcomes in women with hereditary antithrombin deficiency. *Ann. Hematol.* 93 (3), 385–392. doi: 10.1007/s00277-013-1892-0

Schofield, G., and Kimber, S. J. (2005). Leukocyte subpopulations in the uteri of leukemia inhibitory factor knockout mice during early pregnancy. *Biol. Reprod.* 72 (4), 872–878. doi: 10.1095/biolreprod.104.034876

Shen, X., Zeng, H., Xie, L., He, J., Li, J., Xie, X., et al. (2012). The GTPase activating Rap/RanGAP domain-like 1 gene is associated with chicken reproductive traits. *PLoS One* 7 (4), e33851. doi: 10.1371/journal.pone.0033851

Shen, L., Yang, Z., Ye, W., and Hua, X. (2015). Correlation of methylation of GNA12 and preeclampsia. *J. Shanghai Jiaotong Univ. (Med. Sci.)*. http://xuebao.shsmu.edu.cn/CN/Y2015/V35/I5/698

Shen, C., Gao, J., Sheng, Y., Dou, J., Zhou, F., Zheng, X., et al. (2016). Genetic Susceptibility to Vitiligo: GWAS approaches for identifying vitiligo susceptibility genes and loci. *Front. Genet.* 7, 3. doi: 10.3389/fgene.2016.00003

Steck, T., Giess, R., Suetterlin, M. W., Bolland, M., Wiest, S., Poehls, U. G., et al. (2004). Leukaemia inhibitory factor (LIF) gene mutations in women with unexplained infertility and recurrent failure of implantation after IVF and embryo transfer. *Eur. J. Obstet. Gynecol. Reprod. Biol.* 112 (1), 69–73. doi: 10.1016/s0301-2115(03)00315-4

Tong, Y., Merino, D., Nimmervoll, B., Gupta, K., Wang, Y. D., Finkelstein, D., et al. (2015). Cross-Species Genomics Identifies TAF12, NFYC, and RAD54L as Choroid Plexus Carcinoma Oncogenes. *Cancer Cell.* 27 (5), 712–727. doi: 10.1016/j.ccell.2015.04.005

Udayappan, U. K., and Casey, P. J. (2017). c-Jun Contributes to transcriptional control of GNA12 Expression in prostate cancer cells. *Molecules* 22 (4), 612. doi: 10.3390/molecules22040612

Wang, S., Lin, Q., Lin, Z., Zhang, C., Zhuang, Y., and Du, Y. (2008). The analytical of the lion- head goose's egg production character heredity performance. *Shuiqin Shijie.* (05), 39–41.

Wang, S. (2007). Analysis on the egg laying situation of lion head goose in different laying period (in Chinese). *Guide Chin. Poult.* 24 (14), 30.

Wu, Y., Liu, H., and Ding, H. (2016). GPC-3 in hepatocellular carcinoma: current perspectives. *J. Hepatocell Carcinoma* 3, 63–67. doi: 10.2147/JHC.S116513

Xie, J. (2016). *Screening and Identification of Genes Related with the Litter Size of Xiang Pig Based on SNP Chip. [master"s thesis]* (Guizhou University).

Zhang, C. (1991). Development of lion head goose breeding resources (in Chinese). *Shantou Technol.* (1), 26–33.

Zhao, Z. D., and Zhang, L. (2019). Applications of genome selection in sheep breeding. *Yi Chuan.* 41 (4), 293–303. doi: 10.16288/j.yczz.18-251

Zhu, X., Zhang, S., Zhao, H., and Cooper, R. S. (2002). Association mapping, using a mixture model for complex traits. *Genet. Epidemiol.* 23 (2), 181–196. doi: 10.1002/gepi.210

Zhuang, Y., and Lin, Z. (2006). Industrialization prospects of lion head goose (in Chinese). *Poult. Husbandry Dis. Control.* (02), 36–37. Article ID: 1008-3847 (2006) 02-0036-02.

Conflict of Interest: The authors declare that the research was conducted in the absence of any commercial or financial relationships that could be construed as a potential conflict of interest.

frontiers in Genetics

ORIGINAL RESEARCH
published: 25 February 2020
doi: 10.3389/fgene.2020.00094

Whole Genome Scan and Selection Signatures for Climate Adaption in Yanbian Cattle

Jiafei Shen[1,2†], *Quratulain Hanif*[3,4†], *Yang Cao*[1], *Yongsheng Yu*[1], *Chuzhao Lei*[2], *Guoliang Zhang*[1] *and Yumin Zhao*[1*]

[1] Key Laboratory of Beef Cattle Genetics and Breeding in Ministry of Agriculture and Rural Agriculture, Branch of Animal Husbandry, Jilin Academy of Agricultural Sciences, Changchun, China, [2] College of Animal Science and Technology, Northwest A&F University, Yangling, China, [3] Computational Biology Laboratory, Department of Agricutural Biotechnology, National Institute for Biotechnology and Genetic Engineering, Faisalabad, Pakistan, [4] Pakistan Institute of Engineering and Applied Sciences, Nilore, Pakistan

OPEN ACCESS

Edited by:
Fabyano Fonseca Silva,
Universidade Federal de Viçosa, Brazil

Reviewed by:
Lingyang Xu,
Chinese Academy of Agricultural Sciences, China
Marielle Moura Baena,
Universidade Federal de Lavras, Brazil

***Correspondence:**
Yumin Zhao
yuminzhao@126.com

[†]These authors have contributed equally to this work

Specialty section:
This article was submitted to Livestock Genomics, a section of the journal Frontiers in Genetics

Received: 26 October 2019
Accepted: 28 January 2020
Published: 25 February 2020

Citation:
Shen J, Hanif Q, Cao Y, Yu Y, Lei C, Zhang G and Zhao Y (2020) Whole Genome Scan and Selection Signatures for Climate Adaption in Yanbian Cattle. Front. Genet. 11:94. doi: 10.3389/fgene.2020.00094

Yanbian cattle is inhabitant of North of China, exhibiting many phenotypic features, such as long, dense body hair, and abundant intramuscular fat, designed to combat the extreme cold climate adaption. In the current study, we studied the cold tolerance of nine Yanbian cattle by whole genome resequencing and compared with African tropical cattle, N'Dama, as a control group. Yanbian cattle was aligned to the Bos taurus reference genome (ARS-UCD1.2) yielding an average of 10.8 fold coverage. The positive selective sweep analysis for the cold adaption in Yanbian cattle were analyzed using composite likelihood ratio (CLR) and nucleotide diversity ($\theta\pi$), resulting in 292 overlapped genes. The strongest selective signal was found on BTA16 with potential mutation in CORT gene, a regulatory gene of primary hormone in the hypothalamic-pituitary-adrenal (HPA) axis, is reported to be associated with the cold stress, representedfour missense mutations (c.269C > T, p.Lys90Ile; c.251A > G, p.Glu84Gly; c.112C > T, p.Pro38Ser; c.86G > A, p.Pro29His). Meanwhile another gene on BTA6, showed significantly higher selective sweep signals for a cold adapted trait for hair follicle and length development, *FGF5* (fibroblast growth factor 5) with a missense mutation (c.191C > T, p.Ser64Phe). Moreover, cold adapted Yanbian cattle was statistically compared with the hot adapted N'Dama cattle, a taurine cattle reported to show superior heat tolerance than zebu cattle, making them better adapted to the hot regions of Africa. XP-CLR, Fst, and $\theta\pi$ ratio were used to compare both breeds, yielding 487, 924, and 346 genes respectively. Among the 12 overlapped genes, (*CD36*) (c.638A > G, p.Lys 213Arg) involved in fat digestion and absorption plays an important role in membrane transport of long-chain fatty acid and its expression could increase in cold exposure. Henceforth, our study provides a novel genetic insights into the cold climate adaptation of Yanbian cattle and identified three candidate genes (*CORT*, *FGF5*, *and CD36*), which can add to an understanding of the cold climate adaptation of Yanbian cattle.

Keywords: cold adaptability, positive selective, *CD36*, *CORT*, *FGF5*

INTRODUCTION

Cold climate adaptation is a general term used to describe the physiological functions associated with cold adaptation. Studies show that cold exposure will lead to increase the blood pressure (De Lorenzo et al., 1999). During cold stress, the body tries to save energy by cheap methods (such as standing hair) and by changes posture to reduce surface area (Cannon and Nedergaard, 2004). To protect tissues from cold damage, the body adopts different processes, which increases warm blood flow near the surface of the skin (Cannon and Nedergaard, 2011). Those adaptation mechanisms, as well as biological processes, suggest the complex mechanisms of adaptation to cold.

Yanbian cattle is a taurine breed that living in northeast China (Xin et al., 2010) and belongs to the "yellow" class of Chinese cattle (Ji et al., 2014). Unlike majority of Chinese indigenous breeds, Yanbian cattle have had no ancestral to breed with indicine cattle (Xin et al., 2014). They are mainly used as herbivores, especially in the rice fields but are also increasingly used for the beef purpose. The living environment of Yanbian cattle has long, freezing winters with snow-covered grounds half a year and only brief summers. The temperature drops as low as −37°C at the peak of the winter season (**Figure S1**). Yanbian cattle exhibit unique morphoanatomical adaptations to the cold climate with its long and dense hairs as predicted by Allen's rule (Allen, 1877), compactly built with short limbs. On the other hand, N'Dama has been known for its heat resistance in the harsh climatic conditions in Africa. The temperature rise as high as 50°C in the summers, while the weather remains hotter rest of the year as well. Thus, it is an ideal taurine to be compared with Yanbian cattle to identify the potential temperature regulating genes and pathways.

Along with constant release of whole-genomic sequence data in domesticated cattle (Daetwyler et al., 2014; Stothard et al., 2015; Kim et al., 2017), continuous expansion of directory to genetic variants (Karim et al., 2011), gradual maturity of selective theory and method (Vitti et al., 2013), the genetic basis of phenotypic diversity can be hunted down at the complete genome level. However, to our knowledge, no information has yet been generated regarding the cold climate adaptation based on whole genomes level in Yanbian cattle.

Yanbian cattle living in cold environments can be an excellent model for the identification of genomic loci explaining cold climate adaptation in cattle. Here, we are starting from the whole genome scan of Yanbian and N'Dama cattle, and reported genes that are positively selected in Yanbian cattle associated with cold stress adaptation. We used composite likelihood ratio (CLR) and θπ statistics to study the diverse nature of Yanbian cattle, which can provide genomic materials for genetic improvement of Yanbian cattle adaptive traits. Furthermore, we also employed three different statistical approaches i.e., XP-CLR, Fst, and $\theta\pi$ ratio, in order to detect selection signatures in Yanbian cattle, compared to N'Dama cattle. The high fat content, marbling, and the superior hide of Yanbian cattle needs to be well preserved and further enhanced. However, the genetic predispositions associated with adaption and enhanced cold tolerant parameters remain uncertain. The current study will help us to enunciate the extreme environmental adaptations and the positive selective sweeps in the Yanbian cattle.

MATERIAL AND METHODS

Library Construction and Sequencing

We generated whole-genome resequencing data for nine Yanbian cattle, three of them have been generated from our previous study (Chen et al., 2018). N'Dama cattle (n=10), a natural inhabitant of temporal climate, was included in the study for the genome comparison, in order to understand the heat and cold tolerance in livestock (Kim et al., 2017). The genomic DNA was extracted from the ear tissues using the standard phenol-chloroform protocol (Sterky et al., 2017). In **Supplementary Note 1** we have detailed description about the approaches and tools utilized in the current analysis.

Read Mapping and Single-Nucleotide Polymorphism Calling

The clean reads were aligned to the latest reference genome sequence (GCF_002263795.1) using Burrows-Wheeler Aligner (BWA)-MEM (Li et al., 2009) with default parameters. The Picard tools (version 1.106) were used to generate the quality matrices whereas, the Genome Analysis Toolkit (GATK, version 3.8) was employed for the single-nucleotide polymorphism (SNP) calling for mapping (McKenna et al., 2010). We used "HaplotypeCaller," "GenotypeGVCFs," and "SelectVariants" argument of GATK to call the raw SNP. The filtration of the raw SNPs was conducted by using "variant Filtration" with the following parameters: 1) the depth of base quality to ensure variant confidence (QD) < 2.0; 2) the quality of mapping reads (MQ) > 40.0; 3) also, the Phred-scaled P-value calculating with Fisher`s exact test (FS) < 60.0; 4) ReadPosRankSum < −8.0, 5) MQRankSum < −12.5; 6) mean sequence depth (for all individuals) > 1/3× and < 3×; while, 7) SOR > 3.0.

Variant Functional Annotation and Enrichment Analysis

The SNP were annotated by SnpEff tool using ARS-UCD1.2 database and gene set enrichment analyses were carried out with Gene Ontology (GO) and Kyoto Encyclopedia of Genes and Genomes (KEGG) pathway using KEGG Orthology-Based Annotation System (KOBAS) tool. To provide a preliminary overview of the genomic excess and test its reliability, we performed different GO and KEGG pathway enrichment analyses with KOBAS using different lists of genes located in chromosomal regions from the different selective analysis methods of Yanbian to N'Dama cattle. The enriched pathways and genes were selected stringently with an adjusted probability ($P < 0.05$).

Selective Sweep Identification

The genome and nucleotide diversity were calculated by $\theta\pi$, whereas, allele frequency for the positive selection signals were attained by CLR in Yanbian cattle. To infer the scan in progress, we used a 50 kb window for both statistical parameters. The CLR

test uses information from allele frequencies to detect selective scans and relies on determining skews in the allele spectrum to bias rare and frequent alleles (Nielsen et al., 2005). Whereas, $\theta\pi$ analyzes the complete polymorphism data to compile the nature of diversity of the species.

We also performed XP-CLR (Chen et al., 2010), Fst, and $\theta\pi$ ratio to identify the potential areas differentially, selected between Yanbian and N'Dama cattle. XP-CLR is used for detecting selective sweeps that models the multilocus allele frequency differentiation between the two populations (Chen et al., 2010). We used a 50 kb non-overlapping sliding windows with the number of SNPs less than 600, and the correlation level reduced the contribution of SNPs to the XP-CLR results to 0.95. XP-CLR values in the top 0.5% of the empirical distribution (XP-CLR> 29.49) are designated as candidate selection scans, and genes that in those window region are defined as potential candidate genes (Lee et al., 2014). It will give more evidence to the same gene regions using different methods (Qanbari and Simianer, 2014). Fst can change the degree of differentiation between the different populations of one species. If populations are differentiated, the number of genetic differentiation in the selected locus region increase while the difference in genomic region is greater than the neutral conditions (Oleksyk et al., 2010). VCFtools were used to calculate the Fst values of the candidate gene regions in a 50 kb window size at an interval of 20 kb steps (Danecek et al., 2011). Finally, the identified selective sweeps regions were annotated to the reference genome (ARS-UCD1.2) and were further explored following the functional analysis. Lastly, $\theta\pi$ ratio between Yanbian and N'Dama cattle groups was calculated as ln(θπ, Yanbian/θπ,N'Dama), which reflected the loss of nucleotide diversity in Yanbian cattle relative to N'Dama.

RESULTS

Resequencing of Yanbian Cattle and Single-Nucleotide Polymorphism Call

The re-sequenced Yanbian and the N'Dama cattle were pooled together in a 19 cattle data set, generated to an average of 9.15X coverage. In total, 4.2 billion reads were generated which were aligned against the ARS-UCD1.2 reference genome using BWA MEM algorithm, yielding ~4.1 billion mapping reads, covering 99.16% of the reference sequence across the region (**Table 1**). After the SNP call, 11,331,903 and 5,720,198 SNPs in Yanbian and N'Dama cattle, respectively were identified. The quality of the SNP call was evaluated with the Ts/Tv ratio (**Table 2**). The SNPs count of Yanbian cattle was observed to be larger than N'Dama, which might account for the low coverage and low genetic diversity of N'Dama sequencing. At the same time, the average ratios of homozygous versus heterozygous SNPs of Yanbian and N'Dama cattle are 0.487 and 0.848, respectively,

TABLE 2 | Functional annotation of the identified single-nucleotide polymorphisms (SNPs) in Yanbian and N'Dama cattle.

Fields		Yanbian	N'Dama	Total
Sample counts		9	10	19
[a]SNP counts		11,331,903	5,720,198	12,246,286
[b]Ts/Tv ratio		2.3604	2.3969	***
Hom/Het ratio		0.467871422	0.848630285	***
[c]SNP categories				
[d]Exon	Synonymous variant	186,012	194,636	314,721
	Initiator codon variant	16	13	21
	Start lost	183	97	237
	Stop gained	858	526	1,151
	Stop lost	167	81	182
	Stop retained variant	150	81	165
Splice site	Splice region variant	37,336	21,114	45,471
	Splice acceptor variant	484	359	613
	Splice donor variant	610	311	723
Intron	Intron variant	48,543,638	27,356,467	55,275,820
	Intragenic variant	7,816,671	4,242,273	8,544,070
UTR	5 prime UTR variant	57,009	36,103	72,734
	5 prime UTR premature-start codon gain variant	9,935	6,167	12,529
	3 prime UTR variant	243,890	122,412	279,308
Intergenic	[e]Upstream gene variant	2,709,568	1,467,399	3,120,061
	[e]Downstream gene variant	2,787,820	1,487,654	3,198,705
	Intergenic region	6,128,216	3,047,398	6,503,198
Functional classes				
	Missense	110,574	78,703	151,271
	Nonsense	858	526	1,151
	Silent	186,039	194,657	314,747

[a]SNP count; the overlapped SNP loci between samples were counted as one.
[b]Ts/Tv ratio: transition–transversion ratio (Ts/Tv) is a method to check the quality of the number of SNP calls.
[c]Because the analysis to categorize the SNPs was done non-exclusively, some SNPs were counted at multiple categories.
[d]SNP categories were clustered by six genomic regions: exon, splice site, intron, UTR, flanking region, and intergenic
[e]Upstream/downstream: 5 Kbp regions that are adjacent to the both ends of a gene were defined as upstream and downstream regions respectively.
The regions (***) were not calculated as it is not required.

TABLE 1 | Summary statistics of Yanbian and N'Dama cattle re-sequenced reads.

Sample name	No. sample	Raw reads	Mapped reads	[a]Properly paired reads	[b]Average coverage	[c]Average fold
Yanbian	9	2,722,889,367	2,716,850,732	2,691,580,076	99.78%	10.8X
N'Dama	10	1,474,655,523	1,453,725,812	1,424,295,346	98.54%	7.5X
Total	19	4,197,544,890	4,170,576,544	4,115,875,422	99.16%	9.15X

[a]Properly paired reads, "properly paired" means that both ends of the reads were mapped with correct orientation and their fragment sizes were less than 500 bp.
[b]Average coverage, assembly coverage calculated as the proportion of bases in the genome assembly that were covered by at least one read.
[c]Average fold, average fold that was calculated as the average depth of coverage across the whole genome.

representing the more genetic diversity in North China with its elevated heterozygous.

Biological Process and Pathways of Yanbian Cattle Population

CLR and $\theta\pi$ statistics were calculated for the Yanbian cattle alone, to distinguish the positive selection region. Based on CLR test statistic, we obtained 604 putative genes (**Table S5**) whereas, 680 positively selected genes were detected by $\theta\pi$ test (**Table S6**). Of these, 292 overlapped genes were detected in both statistics (**Figure 1C**). GO and KEGG pathways were employed by KOBAS, whereas, only 34 enriched pathways were retained (correct $p < 0.05$; **Table S7**; **Figure 1D**).

Positive Selective Signature in Yanbian Cattle Related to Cold Climate Adaptation

Among 292 candidate genes detected in both CLR and $\theta\pi$, some positively selected genes were considered to be associated with cold climate adaptation (*CORT* and *FGF5*). The strongest selection signal found on BTA16 (16:43127555-43129154) contains the *CORT* gene (**Figures 1A, B**), which was reported to be related with the cold stress in mouse, chicken, and humans (Dronjak et al., 2004; Hangalapura et al., 2004). In the cold exposure experiment of rats, *CORT* in the blood of rats significantly increased after 2 h of cold exposure (Dronjak et al., 2004). Meanwhile, the regulatory mechanism of cold stress and stress was studied in chickens, and it was found that *CORT* in plasma was considerably different under variable cold stress levels (Hangalapura et al., 2004). To identify the potential causal mutation around *CORT* locus, we checked all of mutations of Yanbian cattle, and four missense mutations in *CORT* (c.269C > T, p.Lys90Ile; c.251A > G, p.Glu84Gly; c.112C > T, p.Pro38Ser; c.86G > A, p.Pro29His) were found.

Interestingly, we found a gene, fibroblast growth factor 5 (*FGF5*) on BTA6 from CLR test (**Figure 1A**), which has been reported to be related to the development of hair follicles and hair length in cat, dog and human (Drögemüller et al., 2007; Dierks et al., 2013; Higgins et al., 2014). Meanwhile, we also found that *FGF5* was located in a significant region on chromosome from $\theta\pi$ test (**Figure 1B**). Under cold stress conditions, long and dense hairs are very important in order to keep the body warm against the cold environment, a distinctive feature of Yanbian cattle.

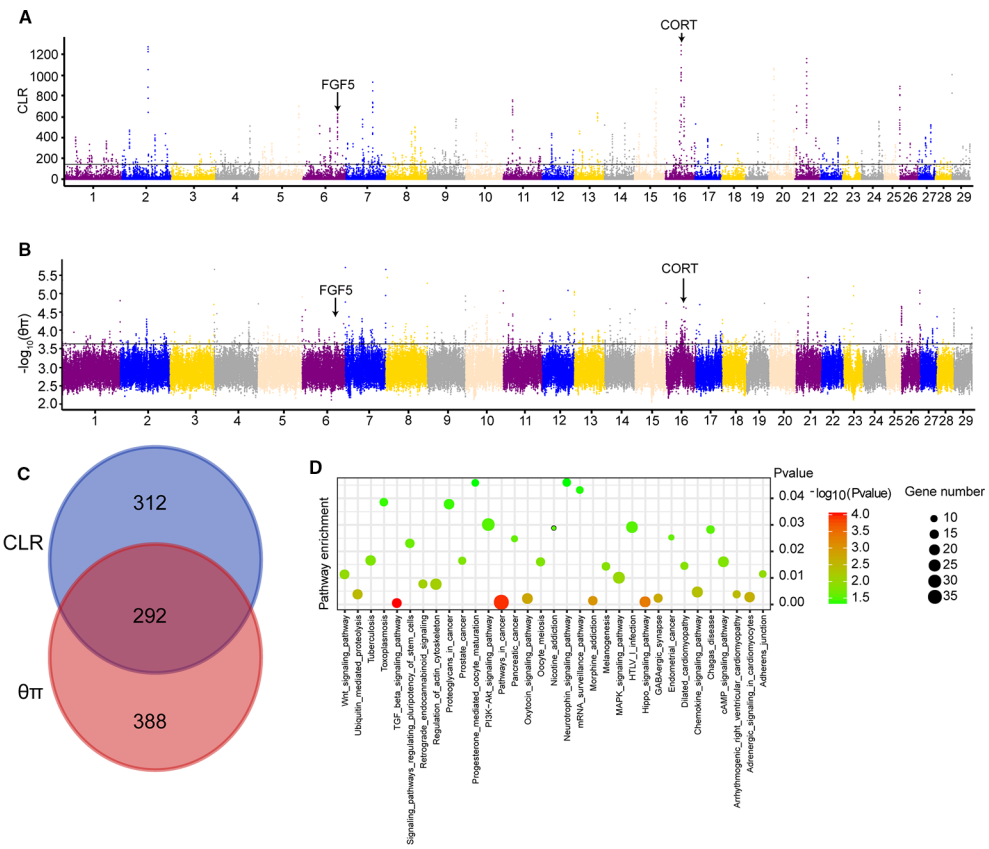

FIGURE 1 | Genome-wide selection scan in Yanbian cattle. **(A, B)** Manhattan plot of the genome-wide distribution of composite likelihood ratio (CLR) and qp in Yanbian cattle using 50 kb windows size and 20 kb step size, respectively. **(C)** Venn diagram showing the genes overlap among CLR and qp significant selection region. **(D)** Kyoto Encyclopedia of Genes and Genomes (KEGG) pathway analysis of differentially expressed genes. Advanced bubble chart shows enrichment of differentially expressed genes in signaling pathways. Y-axis label represents pathway, and X-axis label represents rich factor (rich factor = amount of differentially expressed genes enriched in the pathway/amount of all genes in background gene set). Size and color of the bubble represent amount of differentially expressed genes enriched in pathway and enrichment significance, respectively.

Biological Process and Pathway Between Yanbian and N'Dama Cattle

Moreover, XP-CLR test was performed to distinguish the positive selection region between Yanbian and N'Dama cattle. Based on the analysis, we obtained 487 putative genes (**Table S1**). Whereas, 924 and 346 candidate genes were identified using Fst and $\theta\pi$ ratio between the two populations, respectively. (**Tables S2** and **S3**). In addition, 12 overlapping genes from the three tests were detected and evaluated for the functional studies (**Figure 2D**). GO and KEGG pathways with KOBAS were used to build on biological modules consisting of clusters of functional terms. After wiping out duplicates, 1,375 genes were retained from XP-CLR, Fst, and $\theta\pi$ ratio for the analysis. KEGG pathway analysis resulted in 98 significantly enriched pathways (correct $p < 0.05$; **Table S4**). Vascular smooth muscle contraction, circadian entrainment, hypertrophic cardiomyopathy (HCM), fatty acid metabolism, and fat digestion and absorption were involved as major enrichment pathway, which may play an important role in the cold adaptation of Yanbian cattle.

Candidate Regions and Genes Under Positive Selection in Yanbian and N'Dama Cattle

Here, we compared the genomes of Yanbian and N'Dama cattle to identify signatures of positive selection within each subspecies following environmental and artificial selection pressures. Twelve genes were overlapped in XPCLR, Fst, and $\theta\pi$ ratio methods including fatty acid synthase (*CD36*; **Figures 2A–C**), which plays main role in membrane transport in the heart and adipose tissue. The expression of *CD36* is increased in cold exposure, which enhances brown adipose tissue (BAT) uptake of TG-rich lipoprotein (*TRL*) and of albumin bound FA. Previous studies have shown that *CD36* gene in Hanwoo and Yanbian cattle affects the intramuscular fat deposition. Compared with N'Dama, Yanbian cattle have excellent meat quality. Yanbian cattle have been in the cold environment for a long time, and have a lot of fat deposits in their bodies, which is helpful to resist the cold. The divergent mutations of *CD36* gene were checked between Yanbian and N'Dama cattle, and one missense mutations (c.638A > G, p.Lys 213Arg) was found.

DISCUSSION

We herein carefully examined the whole genome resequencing of Yanbian and N'Dama cattle. The Ts/Tv ratio indicate the quality of resequencing, which was calculated to be 2.36 and 2.39 in Yanbian and N'Dama cattle respectively, comparable with the previous studies (**Tables 1** and **2**) (Choi et al., 2013; Choi et al., 2015). As for the heterozygous and homozygous ratio were concerned in the detected SNPs, the higher ratio of Yanbian cattle suggests that it's population structure maybe normal and have a high heterozygosity rate.

Our study used resequencing data from Yanbian and N'Dama cattle to reveal a detailed genomic information along with

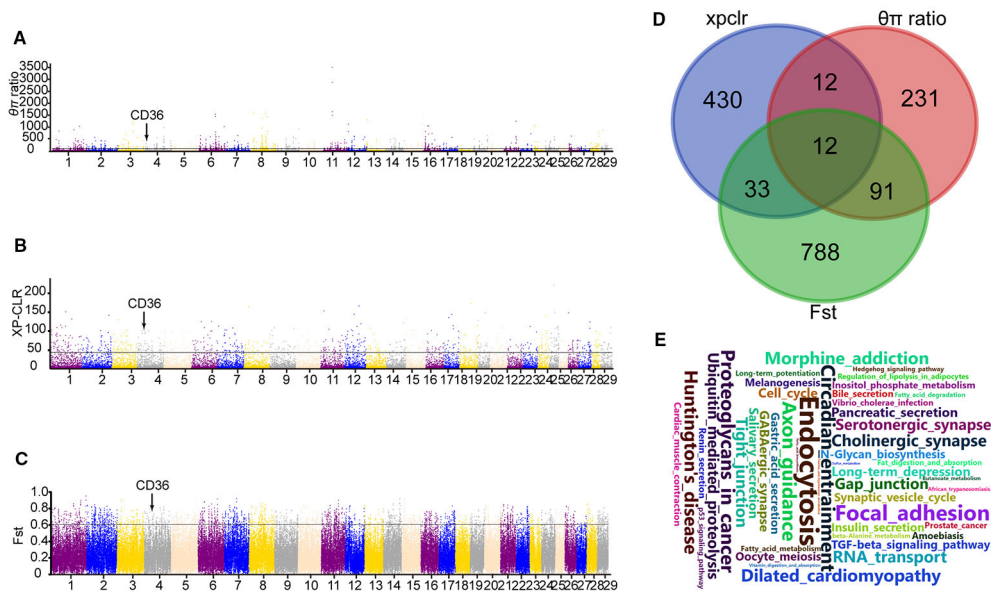

FIGURE 2 | Genome-wide selection scan between Yanbian and N'Dama cattle. **(A–C)** Manhattan plot of the genome-wide distribution of qp ratio, XP-CLR, and Fst between Yanbian and N'Dama cattle using 50 kb windows size and 20 kb step size, respectively. The threshold corresponding to the top 0.5% of qp ratio, XP-CLR, and Fst are marked with a horizontal line, respectively. **(D)** Venn diagram showing the genes overlap among qp ratio, XP-CLR, and Fst significant selection region. **(E)** Word cloud illustrating major enrichment pathway of these genes in qp ratio, XP-CLR, and Fst significant selection region.

candidate genes associated to the cold climate adaptation in Yanbian cattle. Yanbian cattle live in cold north China for a long time. Many biological traits in Yanbian cattle have adapted to the local cold environment, such as long and dense body hairs and increased muscular fat. In order to study the cold-adaptive mechanism of Yanbian cattle, N'Dama cattle was selected, a *Bos taurus* cattle living in the hot areas of Africa, as the reference. Cold adaptation research indicate that more than one mechanism involved in the biological response to cold stress. And it is a multi-factor complex trait that be affected by different factors at different levels in molecular and mechanical aspects. Consistent with the expectations of biological complexity of cold adaptation, our selection test highlights several different processes that are coherently responsible.

We calculated the CLR and $\theta\pi$ to analyze the positive selection of Yanbian cattle. The strongest selection signal of CLR found on BTA16 (16: 43127555-43129154) contains the *CORT* gene (**Figure 1A**), which was reported to be related with the cold stress in mouse, chicken and humans (Dronjak et al., 2004; Hangalapura et al., 2004). Secretion of *CORT*, a primary hormone in the hypothalamic-pituitary-adrenal (*HPA*) axis, exhibits a circadian rhythm in many species (Mormède et al., 2007). At the same time, *CORT* levels are also used as one of the biochemical parameters used to measure the physiological response of animals to stressful environments. Hence, increased cortisol levels in blood are an important stress indicator (Grandin, 1997; Ndlovu et al., 2008). In the cold exposure experiment of rats, *CORT* in the blood of rats significantly increased after 2 h of cold exposure (Dronjak et al., 2004). Meanwhile, the regulatory mechanism of cold stress and stress was studied in chickens, and it was found that *CORT* in plasma was considerably different under variable cold stress levels (Hangalapura et al., 2004). At the same time, we found four missense mutations in *CORT* (c.269C > T, p.Lys90Ile; c.251A > G, p.Glu84Gly; c.112C > T, p.Pro38Ser; c.86G > A, p.Pro29His). Also, *CORT* is one of the biochemical parameters used to measure the physiological response of animals to stressful environments. Under different cold stress levels, the study on the regulation mechanism of cold stress and stress in chickens found that *CORT* levels in plasma were significantly different (Hangalapura et al., 2004). Meanwhile, we also identified another gene *FGF5* that may influence the hair length and density in Yanbian cattle, which is very important for keeping the body warm against the cold environment. *FGF5* has been reported to be related to the development of hair follicles and hair length in cat, dog and human (Drögemüller et al., 2007; Dierks et al., 2013; Higgins et al., 2014). Though, analyzing the selection region of CLR test, *FGF5* was found to be on top prominent point on BTA6 (**Figure 1A**), and also was located in a significant region on BTA6 from $\theta\pi$ test (**Figure 1B**).

Three methods (XP-CLR, Fst and $\theta\pi$ ratio) were used to analysis the whole genome data and choose the significant signals between Yanbian and N'Dama cattle. Twelve genes (*RBFOX1*, *CD36*, *GRXCR2*, *KCNB2*, *NSG2*, *ROBO1*, *NRXN1*, *LINGO2*, *GRM5*, and *AMOTL1*) were overlapped among XP-CLR, Fst, and $\theta\pi$ ratio. Among all, *CD36* plays an important role in membrane transport of long-chain fatty acid (FA) in the heart, skeletal muscle, and adipose tissue (Glatz et al., 2010). The expression of *CD36* is increased in cold exposure, which enhances BAT uptake of TG-rich lipoprotein (TRL) and of albumin bound FA (Bartelt et al., 2011). Previous studies have shown that *CD36* gene in Hanwoo and Yanbian cattle affects the intramuscular fat deposition (Jeong et al., 2012). Also, the expression of *CD36* has been proven to be positively correlated with obesity in dairy cows (Prodanović et al., 2016). Compared with N'Dama, Yanbian cattle have excellent meat quality. Yanbian cattle have been in the cold environment for a long time, and have a lot of fat deposits in their bodies, which is helpful to resist the cold. There are some pathways [fat digestion and absorption, AMPK signaling pathway, phagosome, extracellular matrix receptors (ECM)-receptor interaction] represented in Yanbian and N'Dama cattle include *CD36* genes (**Figures 2A–C**). Studies have shown that fat digestion and absorption pathway affects the heat production of animals, *CD36* gene plays an indispensable role in the heat production (Putri et al., 2015). Also, the expression of *CD36* has been reported to be positively correlated with obesity in dairy cows (Prodanović et al., 2016).

As far as we know, Yanbian cattle as beef cattle is rich in muscle fat. The phenomenon of fat abundance in muscle of Yanbian cattle may be one of the mechanisms for resisting cold climate. A missense mutation (c.638A > G, p.Lys 213Arg) was been found between Yanbian and N'Dama cattle, we speculate that this may be one of the causes of Yanbian cattle cold tolerance.

DATA AVAILABILITY STATEMENT

The bioproject number of the sequencing data information about Yanbian cattle is PRJNA565271 in the NCBI Sequence Read Archive. The sequenced N'Dama cattle genomes in this study are publicly available from GenBank with the Bioproject accession number PRJNA312138.

ETHICS STATEMENT

The animal study was reviewed and approved by Institutional Animal Care and Use Committee of Northwest A&F University following the recommendation of the Regulations for the Administration of Affairs Concerning Experimental Animals of China.

AUTHOR CONTRIBUTIONS

JS and QH contributed equally towards the construction and execution of this manuscript. YC and YY helped in sample collection, CL revised the manuscript and provided with the valuable suggestion. GZ and YZ contributed in the funding for the research.

FUNDING

This work was supported by Natural Science Foundation of China (No. 31872317), the Program of National Beef Cattle and Yak Industrial Technology System (No. CARS-37).

SUPPLEMENTARY MATERIAL

The Supplementary Material for this article can be found online at: https://www.frontiersin.org/articles/10.3389/fgene.2020.00094/full#supplementary-material

REFERENCES

Allen, J. A. (1877). The influence of physical conditions in the genesis of species. *Rad. Rev.* 1, 108–140.

Bartelt, A., Bruns, O. T., Reimer, R., Hohenberg, H., Ittrich, H., Peldschus, K., et al. (2011). Brown adipose tissue activity controls triglyceride clearance. *Nat. Med.* 17, 200–205. doi: 10.1038/nm.2297

Cannon, B., and Nedergaard, J. (2004). Brown adipose tissue: function and physiological significance.*Physiol. Rev.* 84, 277–359. doi: 10.1152/physrev.00015.2003

Cannon, B., and Nedergaard, J. (2011). Nonshivering thermogenesis and its adequate measurement in metabolic studies. *J. Exp. Biol.* 214, 242–253. doi: 10.1242/jeb.050989

Chen, H., Patterson, N., and Reich, D. (2010). Population differentiation as a test for selective sweeps.*Genome Res.* 20, 393–402. doi: 10.1101/gr.100545.109

Chen, N., Cai, Y., Chen, Q., Li, R., Wang, K., Huang, Y., et al. (2018). Whole-genome resequencing reveals world-wide ancestry and adaptive introgression events of domesticated cattle in East Asia. *Nat. Commun.* 9, 2337. doi: 10.1038/s41467-018-04737-0

Choi, J.-W., Liao, X., Park, S., Jeon, H.-J., Chung, W.-H., Stothard, P., et al. (2013). Massively parallel sequencing of Chikso (Korean brindle cattle) to discover genome-wide SNPs and In Dels. *Mol. Cells* 36, 203–211. doi: 10.1007/s10059-013-2347-0

Choi, J., Choi, B., Lee, S., Lee, S., Kim, H., Yu, D., et al. (2015). Whole-genome resequencing analysis of hanwoo and yanbian cattle to identify genome-wide SNPs and signatures of selection. *Mol. Cells* 38, 466–473. doi: 10.14348/molcells.2015.0019

Daetwyler, H. D., Capitan, A., Pausch, H., Stothard, P., Binsbergen, R. V., Brøndum, R. F., et al. (2014). Whole-genome sequencing of 234 bulls facilitates mapping of monogenic and complex traits in cattle. *Nat. Genet.* 46, 858–865. doi: 10.1038/ng.3034

Danecek, P., Auton, A., Abecasis, G., Albers, C. A., Banks, E., DePristo, M. A., et al. (2011). The variant call format and VCFtools. *Bioinformatics* 27, 2156–2158. doi: 10.1093/bioinformatics/btr330

De Lorenzo, F., Sharma, V., Scully, M., and Kakkar, V. V. (1999). Cold adaptation and the seasonal distribution of acute myocardial infarction. *Int. J. Med.* 92, 747–751. doi: 10.1093/qjmed/92.12.747

Dierks, C., Mömke, S., Philipp, U., and Distl, O. (2013). Allelic heterogeneity of FGF 5 mutations causes the long-hair phenotype in dogs. *Anim. Genet.* 44, 425–431. doi: 10.1111/age.12010

Drögemüller, C., Rüfenacht, S., Wichert, B., and Leeb, T. (2007). Mutations within the FGF5 gene are associated with hair length in cats. *Anim. Genet.* 38, 218–221. doi: 10.1111/j.1365-2052.2007.01590.x

Dronjak, S., Gavrilović, L., Filipović, D., Radojčić, M. Bbehavior (2004). Immobilization and cold stress affect sympatho–adrenomedullary system and pituitary–adrenocortical axis of rats exposed to long-term isolation and crowding. *Physiol. Behav.* 81, 409–415. doi: 10.1016/j.physbeh.2004.01.011

Glatz, J. F., Luiken, J. J., and Bonen, A. (2010). Membrane fatty acid transporters as regulators of lipid metabolism: implications for metabolic disease. *Physiol. Behav.* 90, 367–417. doi: 10.1152/physrev.00003.2009

Grandin, T. (1997). Assessment of stress during handling and transport. *J. Anim. Sci.*75, 249–257. doi: 10.2527/1997.751249x

Hangalapura, B. N., Nieuwland, M. G. B., Buyse, J., Kemp, B., and Parmentier, H. K. (2004). Effect of duration of cold stress on plasma adrenal and thyroid hormone levels and immune responses in chicken lines divergently selected for antibody responses. *Poult. Sci.* 83, 1644–1649. doi: 10.1093/ps/83.10.1644

Higgins, C. A., Petukhova, L., Harel, S., Ho, Y. Y., Drill, E., Shapiro, L., et al. (2014). FGF5 is a crucial regulator of hair length in humans. *PNAS* 111, 10648–10653. doi: 10.1073/pnas.1402862111

Jeong, J., Kwon, E., Im, S., Seo, K., and Baik, M. (2012). Expression of fat deposition and fat removal genes is associated with intramuscular fat content in longissimus dorsi muscle of Korean cattle steers. *J. Anim. Sci.* 90, 2044–2053. doi: 10.2527/jas.2011-4753

Ji, S., Yang, R., Lu, C., Qiu, Z., Yan, C., and Zhao, Z. (2014). Differential expression of PPARγ, FASN, and ACADM genes in various adipose tissues and longissimus dorsi muscle from yanbian yellow cattle and yan yellow cattle. *J. Anim. Sci.* 27, 10–18. doi: 10.5713/ajas.2013.13422

Karim, L., Takeda, H., Lin, L., Druet, T., Arias, J. A., Baurain, D., et al. (2011). Variants modulating the expression of a chromosome domain encompassing PLAG1 influence bovine stature. *Nat. Genet.* 43, 405–413. doi: 10.1038/ng.814

Kim, J., Hanotte, O., Mwai, O. A., Dessie, T., Bashir, S., Diallo, B., et al. (2017). The genome landscape of indigenous African cattle. *Genome Biol.* 18, 34. doi: 10.1186/s13059-017-1153-y

Lee, H.-J., Kim, J., Lee, T., Son, J. K., Yoon, H.-B., Baek, K.-S., et al. (2014). Deciphering the genetic blueprint behind Holstein milk proteins and production.*Genome Biol. Evol.* 6, 1366–1374. doi: 10.1093/gbe/evu102

Li, H., Handsaker, B., Wysoker, A., Fennell, T., Ruan, J., Homer, N., et al. (2009). The sequence alignment/map format and SAMtools. *Bioinformatics* 25, 2078–2079. doi: 10.1093/bioinformatics/btp352

McKenna, A., Hanna, M., Banks, E., Sivachenko, A., Cibulskis, K., Kernytsky, A., et al. (2010). The genome analysis toolkit: a MapReduce framework for analyzing next-generation DNA sequencing data.*Genome Res.* 20, 1297–1303. doi: 10.1101/gr.107524.110

Mormède, P., Andanson, S., Aupérin, B., Beerda, B., Guémené, D., Malmkvist, J., et al. (2007). Exploration of the hypothalamic–pituitary–adrenal function as a tool to evaluate animal welfare.*Physiol. Behav.* 92, 317–339. doi: 10.1016/j.physbeh.2006.12.003

Ndlovu, T., Chimonyo, M., Okoh, A. I., and Muchenje, V. (2008). A comparison of stress hormone concentrations at slaughter in Nguni, Bonsmara and Angus steers.*African J. Agric. Res.* 3, 096–100.

Nielsen, R., Williamson, S., Kim, Y., Hubisz, M. J., Clark, A. G., and Bustamante, C. (2005). Genomic scans for selective sweeps using SNP data.*Genome Res.* 15, 1566–1575. doi: 10.1101/gr.4252305

Oleksyk, T. K., Smith, M. W., and O'Brien, S. J. (2010). Genome-wide scans for footprints of natural selection. *Physiol. Trans. R. Soc. B.*365, 185–205. doi: 10.1098/rstb.2009.0219

Prodanović, R., Korićanac, G., Vujanac, I., Djordjević, A., Pantelić, M., Romić, S., et al. (2016). Obesity-driven prepartal hepatic lipid accumulation in dairy cows is associated with increased CD36 and SREBP-1 expression. *Res. Vet. Sci.* 107, 16–19. doi: 10.1016/j.rvsc.2016.04.007

Putri, M., Syamsunarno, M. R. A., Iso, T., Yamaguchi, A., Hanaoka, H., Sunaga, H., et al. (2015). CD36 is indispensable for thermogenesis under conditions of fasting and cold stress. *Biochem. Biophys. Res. Commun.* 457, 520–525. doi: 10.1016/j.bbrc.2014.12.124

Qanbari, S., and Simianer, H. (2014). Mapping signatures of positive selection in the genome of livestock. *Livestock Sci.* 166, 133–143. doi: 10.1016/j.livsci.2014.05.003

Sterky, F. H., Trotter, J. H., Lee, S., Recktenwald, C. V., Du, X., Zhou, B., et al. (2017). Carbonic anhydrase-related protein CA10 is an evolutionarily conserved pan-neurexin ligand. *PNAS* 114, 201621321. doi: 10.1073/pnas.1621321114

Stothard, P., Liao, X., Arantes, A. S., De Pauw, M., Coros, C., Plastow, G., et al. (2015). A large and diverse collection of bovine genome sequences from the

Canadian Cattle Genome Project. *GigaScience* 4, 49–49. doi: 10.1186/s13742-015-0090-5

Vitti, J. J., Grossman, S. R., and Sabeti, P. C. (2013). Detecting natural selection in genomic data. *Annu. Rev. Genet.* 47, 97. doi: 10.1146/annurev-genet-111212-133526

Xin, J., Zhang, L., Li, Z., Liu, X., Jin, H., and Yan, C. (2010). Association of polymorphisms in the calpain I gene with meat quality traits in yanbian yellow cattle of china. *Asian-Australasian J. Anim. Sci.* 24, 9–16. doi: 10.5713/ajas.2011.90407

Xin, Y. P., Zan, L., Liu, Y. F., Tian, W. Q., Wang, H., Cheng, G., et al. (2014). Genetic diversity of Y-short tandem repeats in chinese native cattle breeds. *Asian-Australasian J. Anim. Sci.* 13, 9578–9587. doi: 10.4238/2014.November.14.1

Conflict of Interest: The authors declare that the research was conducted in the absence of any commercial or financial relationships that could be construed as a potential conflict of interest.

frontiers in Genetics

BRIEF RESEARCH REPORT
published: 19 March 2020
doi: 10.3389/fgene.2020.00207

Automated Step Detection in Inertial Measurement Unit Data From Turkeys

Aniek Bouwman[1†], Anatolii Savchuk[2,3†], Abouzar Abbaspourghomi[2] and Bram Visser[3]*

[1] Animal Breeding and Genomics, Wageningen University & Research, Wageningen, Netherlands, [2] Jheronimus Academy of Data Science (JADS), 's-Hertogenbosch, Netherlands, [3] Hendrix Genetics, Boxmeer, Netherlands

Locomotion is an important welfare and health trait in turkey production. Current breeding values for locomotion are often based on subjective scoring. Sensor technologies could be applied to obtain objective evaluation of turkey gait. Inertial measurement units (IMUs) measure acceleration and rotational velocity, which makes them attractive devices for gait analysis. The aim of this study was to compare three different methods for step detection from IMU data from turkeys. This is an essential step for future feature extraction for the evaluation of turkey locomotion. Data from turkeys walking through a corridor with IMUs attached to each upper leg were annotated manually. We evaluated change point detection, local extrema approach, and gradient boosting machine in terms of step detection and precision of start and end point of the steps. All three methods were successful in step detection, but local extrema approach showed more false detections. In terms of precision of start and end point of steps, change point detection performed poorly due to significant irregular delay, while gradient boosting machine was most precise. For the allowed distance to the annotated steps of 0.2 s, the precision of gradient boosting machine was 0.81 and the recall was 0.84, which is much better in comparison to the other two methods (<0.61). At an allowed distance of 1 s, performance of the three models was similar. Gradient boosting machine was identified as the most accurate for signal segmentation with a final goal to extract information about turkey gait; however, it requires an annotated training dataset.

Keywords: inertial measurement unit, step detection, gait analysis, segmentation, accelerometer

OPEN ACCESS

Edited by:
Gota Morota,
Virginia Polytechnic Institute and State University, United States

Reviewed by:
Luiz Brito,
Purdue University, United States
James E. Koltes,
Iowa State University, United States

***Correspondence:**
Aniek Bouwman
aniek.bouwman@wur.nl

† These authors have contributed equally to this work

Specialty section:
This article was submitted to Livestock Genomics, a section of the journal Frontiers in Genetics

Received: *31 October 2019*
Accepted: *21 February 2020*
Published: *19 March 2020*

Citation:
Bouwman A, Savchuk A, Abbaspourghomi A and Visser B (2020) Automated Step Detection in Inertial Measurement Unit Data From Turkeys. Front. Genet. 11:207. doi: 10.3389/fgene.2020.00207

INTRODUCTION

Locomotion is an important welfare and health trait in turkey production. Impaired locomotion compromises growth and (re)production. Breeding programs tend to record locomotion of selection candidates by scoring the conformation or walking ability by a human expert (Quinton et al., 2011). These scores are repeatable, heritable, and valuable to the breeding program. However, these scores are subjective and labor intensive and require animal handling. Therefore, an objective automated locomotion score would be preferred. Sensor technology seems a promising tool for this task. Additionally, it provides opportunities for repeated measurements of individuals, which could lead to more accurate breeding values.

In recent years, sensor technologies have been introduced in livestock production, and some of them are well suited for objective locomotion scoring like force platforms, cameras,

and accelerometers. Force platform systems have been used for locomotion phenotyping in experimental setups (Pastell et al., 2006; Nääs et al., 2010; Maertens et al., 2011; Pluym et al., 2013), but applications on farms are limited because they are expensive and require frequent maintenance. Cameras are upcoming tools in cattle and pigs, with the advantage that they do not disturb the animal (Kashiha et al., 2014; Viazzi et al., 2014; Kuan et al., 2019). However, adding individual animal identification to the image data is a challenge. Accelerometers are widely applied to individual cows and pigs for detecting behavioral changes over time that can indicate signs of estrus and health or welfare impairment, including lameness (e.g., Pastell et al., 2009; Escalante et al., 2013; Tamura et al., 2019). Inertial measurement units (IMUs) are a combination of accelerometer, gyroscope, and sometimes a magnetometer. Besides acceleration, they also measure rotational velocity; together, they can indicate orientation. Human locomotion has been well studied using IMUs, where they are considered as a cost-effective alternative to optical motion systems, which are the golden standard in kinematic analysis in laboratory settings (e.g., Seel et al., 2014; Kluge et al., 2017).

In order to use IMUs for objective evaluation of turkey locomotion, it is essential to describe individual steps by extracting its features. Hence, accurate automated step segmentation of the IMU profile, i.e., defining the start and end point of a single step, is an essential first challenge. Therefore, the aim of this study was to compare different methods for automated step detection from IMU data from turkeys.

MATERIALS AND METHODS

IMU Data

The IMUs used for this study were wireless inertial-magnetic motion trackers (MTw Awinda, XSens Technologies B.V., Enschede, Netherlands). Each IMU contains a triaxial accelerometer, triaxial gyroscope, and triaxial magnetometer. An IMU weighs 16 g and its dimensions are 47 mm × 30 mm × 13 mm. The IMU data were logged to a computer in real time via a receiver.

Data were collected during the standard walkway test applied in the turkey breeding program of Hybrid Turkeys (Hendrix Genetics, Kitchener, Canada). In total, 85 animals were recorded during 1 day. The animals were 20 weeks of age. Two IMUs were attached using Velcro straps, one on each upper leg. Then, the animal was placed in a corridor (∼1.5 m wide) and stimulated to walk in one direction for approximately 5 m. The floor was covered with bedding the animals were familiar with. Because these data were recorded during routine processes, there was little time for the animals to get used to the IMUs around their legs. Occasionally, the animals needed stimulation to start walking or during walking. A person walked along with the animal and waved his hand if needed; when waving was not effective, the animals were tapped on the back or finally pushed.

The recording of the IMU was at 100 Hz and was manually started and stopped; on average, there was 20 s recording material per animal. The IMU output consisted of calibrated time series data for triaxial acceleration, triaxial free acceleration, triaxial angular velocity, and triaxial magnetic field. In addition, orientation data are provided in Euler representation (pitch, roll, yaw), as well as unit quarternions represented by a normalized quaternion q = [W X Y Z], with W being the real component and X, Y, Z being the imaginary parts. More information about the output data can be found in Paulich et al. (2018).

Annotation

The annotation was based on the knowledge that a complete single step can be divided into two stages: (1) from the foot separating from the ground to the foot reaching the highest point, the acceleration at this stage starts to increase until it reaches a maximum value; (2) from the highest point of the foot to the foot hitting the ground, at this stage, the acceleration drops from the maximum value to the minimum value (Wang et al., 2017). In the IMU profile, clear indications of movement can be seen. Knowing that the main actual movement of the animals is walking through the corridor, it is safe to assume these are steps. The location of the steps was annotated by hand for 20 IMU profiles: both leg IMUs of 10 different animals. Plots of acceleration magnitude against time were used to define start and end position of the step. Acceleration magnitude was calculated as $\sqrt{Acc\_X^2 + Acc\_Y^2 + Acc\_Z^2}$ where Acc_X, Acc_Y, and Acc_Z are the output of the triaxial accelerometer in X, Y, and Z direction, respectively (Wang et al., 2017). Half steps at the beginning or end of a profile were not annotated, as well as insignificant movements (acceleration magnitude <20 m/s^2). The number of annotated steps per profile ranged between 7 and 15 with an average of 9.9. These ranges were within expectation from turkeys this age walking ∼5 m. In total, 198 steps (sum of annotated steps over 20 profiles) were annotated and available for further analysis. Although more IMU profiles were available, they were not manually annotated, because the manual annotation was too time-consuming. In addition, the 20 IMU profiles resulted in sufficient steps (198) for model development and performance testing (shown below).

Although we use this manual step annotation for model training and performance evaluation, we do not consider it as the truth. The start and end position of the annotated steps are not perfectly accurate, but this was the best we could do with the data at hand. The step annotation allows us to compare performance of the different methods applied and what may cause the observed differences.

Change Point Detection

Change point is used to denote a significant variation in the probability distribution of time series. Detection of such variations and exact moments when they occurred may be accomplished with the broad family of supervised and unsupervised methods, the extensive overview of which can be found in Aminikhanghahi and Cook (2017). An application of change point detection (CPD) approaches to step segmentation were demonstrated, for example, by Martinez and De Leon (2016). In our study, we applied an unsupervised version of CPD that is called a singular spectrum

transformation (SST). The basic idea of SST is that, for each time point, it compares distribution in the interval before the time point and an interval of the same length after the time point and, based on this, assigns a change point score. Comparison of distributions is made by comparing singular spectrums of two trajectory matrices for these consecutive intervals (Aminikhanghahi and Cook, 2017).

We developed the following algorithm based on the SST that was applied to three acceleration signals Acc_X, Acc_Y, Acc_Z:

(a) To each signal, we applied a low-pass filter to reduce the presence of noise. This step was required because SST does not consider the effect of noise on the system (Aminikhanghahi and Cook, 2017).
(b) For each de-noised signal, we applied SST with windows equal to 10 time points and calculated a change point score.
(c) When the change point score was above 5% of the maximum for a given signal, we declared the step; when it was lower, we declared no step.
(d) Final decision was made by majority: if at least two of the three acceleration signals indicated the step, we declared step at that moment.

Local Extrema Approach

The local extrema approach (LEA) was inspired by the idea that the significant local extrema in a signal should be associated with the changes in the leg movements. Assuming that we have a set of signals, the method can be described by the following procedure:

(a) To each signal (we used Acc_X, Acc_Y, Acc_Z, Gyr_X, Gyr_Y, Gyr_Z, Roll, Pitch, and Yaw here), we applied a low-pass filter to reduce the presence of noise.
(b) With a sliding window equal to 140 time points, we found local minima and local maxima for each signal. Based on the training data, a window of 140 time points ensures there is at least one step in the sliding window, making it the most optimal window to detect local extrema.
(c) From the set of all extrema discovered in step (b), we filtered out those that were within less than 0.5 standard deviations from the surrounding 10 measurements. This step helped us, for example, to get rid of extrema found in the regions where an animal was not moving and no step had occurred.
(d) We combined significant local extrema from all the considered signals into one set. Then, we kept only those significant extrema that were found in more than one signal or those for which there exists at least one other extrema within 0.1 s (10 measurement to the right or 10 to the left). We will refer to such extrema as important extrema.
(e) Based on the detected important extrema and density of their distribution, we created a list of potential intervals that contain steps. For the first local extrema, we formed an interval that starts in that point and has a length of 0.6 s. Then, for the first extrema that has not ended up in that interval, we checked whether it is within 0.12 s to the end of the created interval, and if so, we added it to the interval, consequently updating the interval's length. We continued this procedure until we could not find a new extrema within 0.12 s to the interval. Then, we recorded the detected interval as potential step interval and repeated the procedure for the next important extrema. The time thresholds of 0.6 and 0.12 s were chosen based on the data to assure that only one step was occurring within an interval. From the annotated data, the average step length was 0.6 s, and there was at least 0.12 s in between two steps.
(f) If, in some potential step, interval distance between the first important extrema to the second important extrema was higher than 0.12 s, we removed the first important extrema from the interval and proceed the check for the next element of the interval.
(g) We filtered out intervals that have duration shorter than 0.2 s, because that is too short to be an actual step. We also filtered out intervals that have two consecutive important extrema that were located more than 0.25 s from each other, to assure a dense set of important extrema that support the evidence of a step. These thresholds were based on the annotation of the steps.
(h) Finally, to avoid false-positive indications, we filtered out intervals within which acceleration magnitude was lower than 11 m/s^2. Real steps always showed an acceleration magnitude peak higher than 11 m/s^2; below this value, it may be noise or tremor in the legs.

The obvious drawback of the LEA method is that it depends on a high number of parameters that probably will be different for other species or even another age group of turkeys. While some parameters allow slight deviation from the given numbers, the set of measured signals does not. We found that it is impossible to build successful LEA for step segmentation based only on acceleration signals. The density of received important extrema does not allow to distinguish between parts of the signals that correspond to the step and no step periods.

Gradient Boosting Machine

We used a gradient boosting machine (GBM) implemented in R version of H2O 3.20.0.8 (Landry, 2018) to predict the time points that are part of steps in IMU profiles. The GBM method is a supervised learning task with the advantage of high performance and interpretable models (Elith et al., 2008). Each individual time point within an annotated step was classified as step and each individual time point outside an annotated step was classified as non-step for model training. To build the GBM model, 60% of the 198 manually annotated steps were used for training (125 steps from 12 IMU profiles), 20% for validation (36 steps from 4 profiles), and 20% as an independent test set (37 steps from four profiles).

Except for magnetic field data, all standard IMU output parameters as described above were used for step prediction, as well as magnitude of acceleration. Each of the 20 parameters were transformed by taking the difference between the actual time point measure and a lag or lead measure. Each time series was lagged by 5 to 10 time points, and led by 5 to 10 time points. The lag/lead was applied to detect significant changes in the profiles, the 5 to 10 time points relates to 0.05 to 0.1 s,

which seemed reasonable for significant changes in movement during walking. This resulted in 12 different time series per parameter (e.g., Acc_X_lag5-Acc_X_lag10, Acc_X_lead5-Acc_X_lead10), and a total of 240 predictor variables for the GMB prediction of steps. We ran the GBM model with default settings. The model parameters were as follows: number_of_trees was 50, number_of_internal_trees was 50, model_size_in_bytes was 21040, min_depth was 5, max_depth was 5, mean_depth was 5, min_leaves was 24, max_leaves was 32, and mean_leaves was 28.48. Performance results of the selected GBM model can be found in the **Supplementary Material**.

The prediction of the step per time point is not very helpful in defining features from a step; hence, step start and end needed to be defined. Based on the predictions per time point, we defined the start and end moment of the steps. Starting from the first time point predicted to be a step, if it had at least 10 consecutive step predictions, it was the starting point of that particular step. The end point of that step was the last time point in the row that was predicted a step. This resulted in some steps being very close to each other, so close that they are likely part of the same (annotated) step. Hence, steps within 10 time points were merged together into one step.

Performance Assessment

The main goal of step segmentation is to provide subsequences of a signal for the following feature extraction. Therefore, we have two obvious requirements for segmentation methods: (i) to maximize the number of recognized steps; and (ii) precise start and end moments of the recognized steps. To evaluate performance of proposed methods, we applied techniques used in Haji Ghassemi et al. (2018) and Šprager and Jurič (2018). First, we calculated the numbers of true-positive (TP), false-negative (FN), and false-positive (FP) steps for the 198 annotated steps, where TP are steps detected by the method and also labeled manually in the annotation step; FN are steps that were annotated but not detected by the method; FP are steps detected by the method but which were not annotated.

Based on these numbers, we calculated three metrics: precision $= TP/(TP + FP)$ recall $= TP/(TP + FN)$, and F-score $= 2(Precision \times Recall)/(Precision + Recall)$ (Rijsbergen, 1975). Precision provides punishment for the detected steps that were not annotated; it is equal to one if there are no FP steps. Similarly, recall provides punishment for the annotated steps that were not detected by a method, and is equal to one if there are no FN steps. The F-score is the harmonic mean of precision and recall, and is equal to one if there are no FN or FP steps but decreases with higher number of FP and FN steps (Hand and Christen, 2018).

To be considered as a TP, both the start and end points of detected steps should be within the allowed distance from the corresponding start and end points of the annotated steps. We compared the performance of the different step detection methods at an allowed distance from 0.1 s to 0.5 s and 1 s.

In addition, the average delay per detected start and end point of the corresponding annotated step was calculated for each method. The delay was negative if the detected start or end point was located before the annotated start or end point.

RESULTS

Change Point Detection

The proposed approach based on SST method for CPD detected all steps for animal 010 (no FN) and the only FP detection was actually a true step not annotated because its start point might have been before recording (**Figure 1**). It revealed itself as a quite robust method for step detection. When it comes to the preciseness of the detection of start and end moments, we observed significant delay. The peak of acceleration magnitude is, in some cases, located outside the found interval because of this delay in detection.

Local Extrema Approach

Results of LEA demonstrate less robustness in terms of step detection in comparison to CPD. **Figure 2** shows FP detection, like second detected step for leg 1 of turkey 010, as well as FN steps, like sixth annotated step for leg 2. Based on video material, we confirmed that these were truly FP and FN detections.

Gradient Boosting Machine

Results of the GBM method are plotted in **Figure 3** and demonstrate that all annotated steps for animal 010 were detected (no FN) and the only FP detection was actually a true step not annotated because its start point might have been before recording. The position of the steps detected using the GBM model is acceptable, given that the annotation is not perfect either.

Performance Assessment

Table 1 provides precision, recall, and F-score for the considered methods. All these metrics were calculated based on annotated steps of both legs of four turkeys that were left out of the training of the GBM model. Based on the F-score, GBM performed best at any of the evaluated allowed distances from the annotated start and end points. Somewhat worse result was shown by LEA. For small allowed distances, the performance of CPD was very low. For an allowed distance of 0.1 s, the steps detected by CPD were more than 0.1 s from the start and end point of all annotated steps; hence, none of the steps were declared as TP and precision and recall were zero. However, the performance of CPD considerably increased with an increase of allowed distance.

Unsatisfying performance of CPD for small values of allowed deviation can be explained by the delay in step detection. There was an average delay for start points of the steps of 0.27 s with a standard deviation of 0.15 s. The average delay for the end points was even higher: 0.47 s with a standard deviation of 0.11 s. This indicated that the delays were not constant; therefore, it is not possible to correct for the delay.

As to delays for LEA and GBM, the corresponding values are much smaller in comparison to CPD. For LEA, average delay in start points was 0.14 s ($\pm$ 0.15 s), and 0.15 s ($\pm$ 0.12 s) for end points. For GBM, average delay in start points was 0.09 s ($\pm$ 0.14 s), and 0.05 s ($\pm$ 0.05 s) for end points.

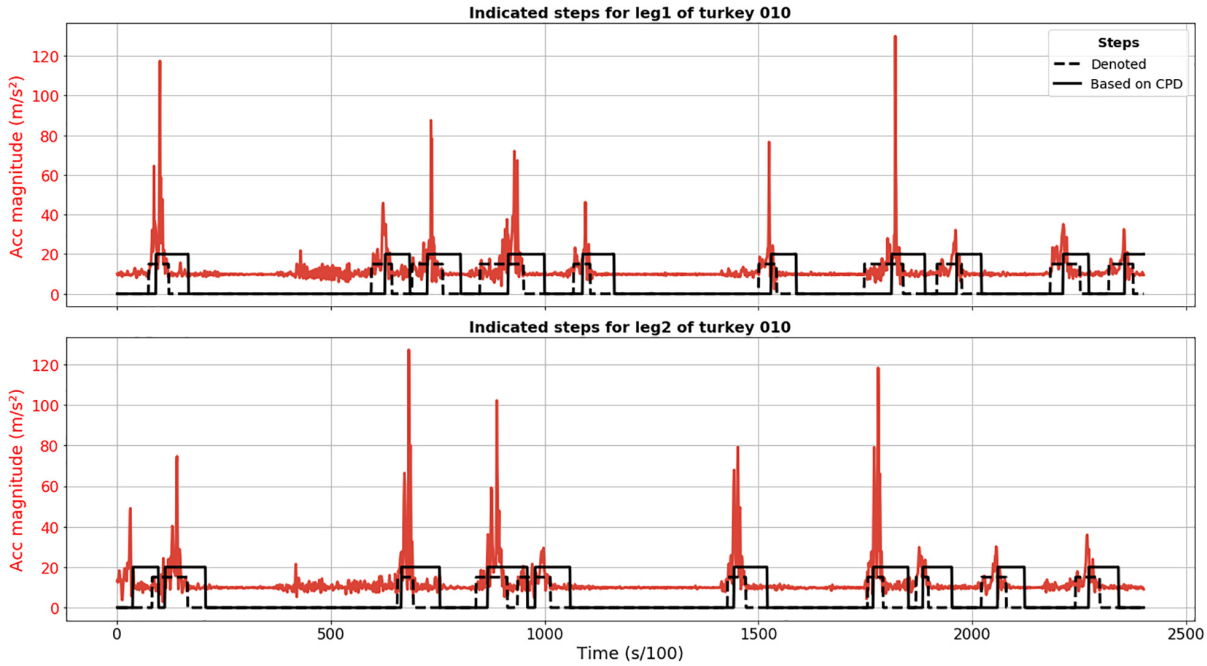

FIGURE 1 | Results of CPD step segmentation for turkey 010 (solid black line) for leg 1 (upper plot) and 2 (lower plot). Acceleration magnitude is plotted in red; dashed black line depicts manually labeled steps.

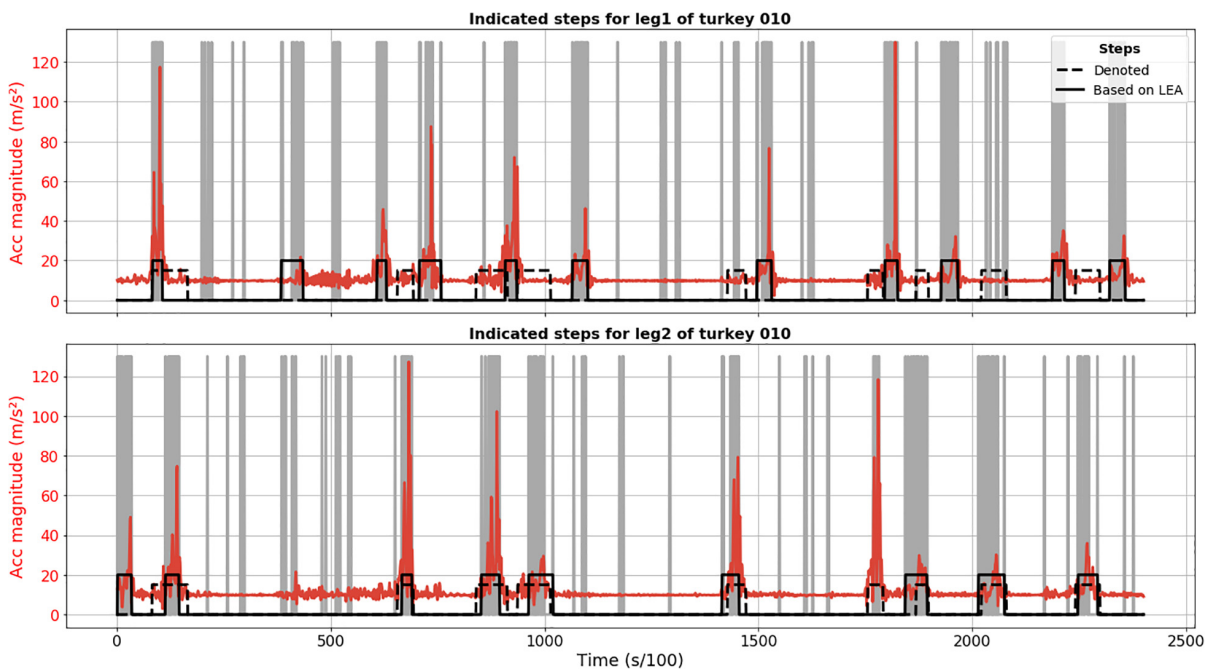

FIGURE 2 | Step segmentation results of LEA for turkey 010 (solid black line) for leg 1 (upper plot) and 2 (lower plot). Acceleration magnitude is plotted in red; dashed black line shows manually labeled steps. Vertical gray lines corresponded to important extrema.

DISCUSSION

The aim of this study was to get accurate start and end position of turkey steps based on IMU data. In terms of step detection in general, all three compared methods were successful, although LEA showed more false detections than CPD and GBM. In terms of precision of start and end point of steps, CPD performed poorly, while GBM was most precise.

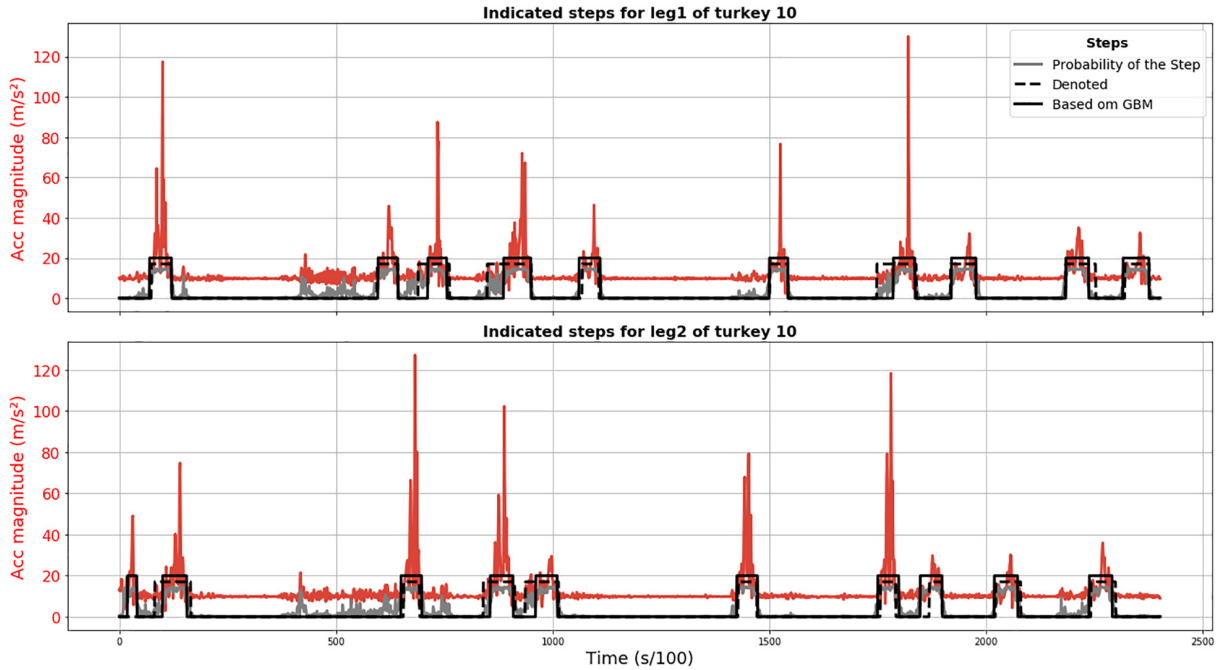

FIGURE 3 | Results of GBM step segmentation for turkey 010 (solid black line) for leg 1 (upper plot) and 2 (lower plot). Acceleration magnitude is plotted in red; dashed black line shows manually labeled steps. The gray line represents the chance of being a step according to the GBM model (×15 for visualization).

Although the data collection was done in a controlled walking test setup, the data are not as clean as experimental setups with humans or trained animals like horses (Pfau et al., 2005). For example, some animals were hesitating and needed stimulation, after which they took a number of short fast steps before continuing at a steady pace. This imposed some difficulties in the annotation of the data, and also hampers accurate step segmentation. It is, however, realistic data, and therefore more diverse and comprehensive compared to experimental setups. This will aid in the development of an algorithm applicable to data retrieved in, for instance, group housing. In addition, it also implicates that the detected steps may need further filtering (e.g., based on standard deviation of certain step features within an individual) depending on the purpose of using the automatically detected steps.

TABLE 1 | Performance results of the step detection methods for different allowed distances (in seconds) from the annotated steps.

Method	Metric	0.1 s	0.2 s	0.3 s	0.4 s	0.5 s	1.0 s
CPD	Precision	0.00	0.01	0.07	0.15	0.49	0.97
	Recall	0.00	0.01	0.07	0.14	0.47	0.91
	F-score	NA[1]	0.01	0.07	0.14	0.48	0.94
LEA	Precision	0.25	0.61	0.74	0.85	0.90	0.95
	Recall	0.23	0.56	0.69	0.78	0.82	0.88
	F-score	0.24	0.58	0.71	0.81	0.86	0.92
GBM	Precision	0.65	0.81	0.87	0.92	0.93	0.97
	Recall	0.67	0.84	0.89	0.95	0.96	1.00
	F-score	0.66	0.82	0.88	0.93	0.95	0.99

[1]*NA = not applicable (due to division by zero).*

There was no golden standard system applied next to the IMU sensor. In experimental settings, optical motion tracking systems are often used as golden standard to test the IMU performance (e.g., Seel et al., 2014; Kluge et al., 2017; Bosch et al., 2018). Here, we used subjective annotation by a person to define the step start and end positions in the IMU profiles knowing that the animals underwent a walking test. In general, we trust that the annotated steps are true steps and were able to check doubtful cases with video material. However, the exact start and end point are debatable, and might be somewhat different if annotated again or by a different person. Therefore, we showed performance results of the methods for different allowed distances to the annotated steps. Also, steps at the beginning or end of the profile were not annotated because the start or end point was unclear. All three methods detected such steps, but because they were not annotated, they showed up as FP steps in the performance assessment. Although the annotation was suboptimal for evaluation of accurate step segmentation, the results show the potential of each method applied along with their drawbacks.

The main problem of CPD was the inconsistency in delayed detection of start and end point of steps. The delay inhibits accurate extraction of step features describing the locomotion. For example, the maximum acceleration magnitude that might be an important feature is often outside the detected steps. Such results make this method inappropriate for step segmentation with the final goal to extract features that thoroughly describe the turkey gait. However, in general, all annotated steps were

detected; therefore, CPD is an appropriate method if exact position is not relevant, for instance for step counting.

As it was demonstrated, LEA does not have problems with the delay. However, it is outperformed by GBM. One possible reason might be that LEA is an unsupervised method and was not trained on the annotated steps that have somewhat subjective nature as they are only an approximation of the truth. LEA has the advantage that it does not need pre-annotation and we believe that with some optimization of parameters, it can be applied for other species as well.

In contrast to the LEA and CPD, the GBM method is a supervised learning method that requires an annotated dataset to train the model. Annotating a dataset is very time-consuming; however, our results showed that the GBM model can be trained on limited annotated data (i.e., 198 steps) with good results for our specific problem. This makes it worthwhile to invest in annotation. We used the GBM as it is state-of-the-art implementation of a powerful classification algorithm, but that does not reject the possibility that some other methods of classification may work with similar level of performance. It would be interesting to see how the trained GMB model performs on IMU data from other species. For optimal performance, it might require a species-specific annotated dataset to build a species-specific GBM model.

We should admit that methods for step detection and segmentation of gait signals are not limited to those evaluated here. There exists a vast number of approaches that use local structure similarly to LEA and, if possible, cyclicity in gait sequences (Derawi et al., 2010; Hundza et al., 2014). The most advanced, for example, presented in Derawi et al. (2010), apply such techniques like dynamic time warping. Another interesting possibility might be represented by clustering. While it does not require pre-annotations, it needs a carefully prepared set of features.

CONCLUSION

In this paper, we compared three approaches for segmentation of turkey gait sequences obtained with IMU sensors. CPD is commonly used for this purpose; the LEA was newly developed based on characteristics of the data, while the GBM is an advanced machine learning classification algorithm. We have found that the GBM shows the best performance even for little allowed deviation for the annotated steps. Performance of LEA is somewhat worse. Significant inconsistent delay for start and end point detection makes CPD inappropriate for detailed gait analyses. GBM can be applied for signal segmentation with the final goal to extract information about turkey gait; however, it requires an annotated training dataset.

DATA AVAILABILITY STATEMENT

The datasets for this article are not publicly available because data is intellectual property of Hendrix Genetics. Requests to access the datasets should be directed to BV, bram.visser@hendrix-genetics.com.

ETHICS STATEMENT

Ethical review and approval was not required for the animal study because The Animal Welfare Body (AWB) of Wageningen Research decided ethical review was not necessary because the applied units were low in weight (<1% of body weight), the units were attached for less than one hour, the animal is not isolated in the corridor and more or less familiar with the corridor.

AUTHOR CONTRIBUTIONS

All authors contributed to conception and design of the study, and read and approved the submitted version of manuscript. AB, AS, and AA performed the statistical analysis. AB and AS wrote the manuscript.

FUNDING

This study was financially supported by the Dutch Ministry of Economic Affairs (TKI Agri & Food project 16022) and the Breed4Food partners Cobb Europe, CRV, Hendrix Genetics and Topigs Norsvin. The funders Cobb Europe, CRV, Hendrix Genetics and Topigs Norsvin were involved in the study design. In addition, Hendrix Genetics was involved in collection, analysis, interpretation of data, the writing of this article and the decision to submit it for publication.

ACKNOWLEDGMENTS

We would like to acknowledge the team at Hybrid Turkeys (Kitchener, Canada) for collection of the data.

SUPPLEMENTARY MATERIAL

The Supplementary Material for this article can be found online at: https://www.frontiersin.org/articles/10.3389/fgene.2020.00207/full#supplementary-material

REFERENCES

Aminikhanghahi, S., and Cook, D. J. (2017). A survey of methods for time series change point detection. *Knowl. Inform. Syst.* 51, 339–367. doi: 10.1007/s10115-016-0987-z

Bosch, S., Serra Bragança, F., Marin-Perianu, M., Marin-Perianu, R., Van der Zwaag, B. J., Voskamp, J., et al. (2018). EquiMoves: a wireless networked inertial measurement system for objective examination of horse gait. *Sensors* 18:850. doi: 10.3390/s18030850

Derawi, M. O., Bours, P., and Holien, K. (eds) (2010). "Improved cycle detection for accelerometer based gait authentication," in *Proceedings of the 2010 Sixth International Conference on Intelligent Information Hiding and Multimedia Signal Processing*, Washington, DC.

Elith, J., Leathwick, J. R., and Hastie, T. (2008). A working guide to boosted regression trees. *J. Anim. Ecol.* 77, 802–813. doi: 10.1111/j.1365-2656.2008.01390.x

Escalante, H. J., Rodriguez, S. V., Cordero, J., Kristensen, A. R., and Cornou, C. (2013). Sow-activity classification from acceleration patterns: a machine learning approach. *Comput. Electr. Agricult.* 93, 17–26. doi: 10.1016/j.compag.2013.01.003

Haji Ghassemi, N., Hannink, J., Martindale, C. F., Gaßner, H., Müller, M., Klucken, J., et al. (2018). Segmentation of gait sequences in sensor-based movement analysis: a comparison of methods in Parkinson's Disease. *Sensors* 18:145. doi: 10.3390/s18010145

Hand, D., and Christen, P. (2018). A note on using the F-measure for evaluating record linkage algorithms. *Stat. Comput.* 28, 539–547. doi: 10.1007/s11222-017-9746-6

Hundza, S. R., Hook, W. R., Harris, C. R., Mahajan, S. V., Leslie, P. A., Spani, C. A., et al. (2014). Accurate and reliable gait cycle detection in Parkinson's Disease. *IEEE Trans. Neural Syst. Rehabil. Eng.* 22, 127–137. doi: 10.1109/TNSRE.2013.2282080

Kashiha, M. A., Bahr, C., Ott, S., Moons, C. P. H., Niewold, T. A., Tuyttens, F., et al. (2014). Automatic monitoring of pig locomotion using image analysis. *Livestock Sci.* 159, 141–148. doi: 10.1016/j.livsci.2013.11.007

Kluge, F., Gaßner, H., Hannink, J., Pasluosta, C., Klucken, J., and Eskofier, B. M. (2017). Towards mobile gait analysis: concurrent validity and test-retest reliability of an inertial measurement system for the assessment of spatio-temporal gait parameters. *Sensors* 17:1522. doi: 10.3390/s17071522

Kuan, C. Y., Tsai, Y. C., Hsu, J. T., Ding, S. T., and Lin, T. T. (2019). "An imaging system based on deep learning for monitoring the feeding behavior of dairy cows," in *Proceedings of the 2019 ASABE Annual International Meeting* (St. Joseph, MI: ASABE).

Landry, M. (2018). *Machine Learning With R and H2O*, 7th Edn. Mountain View, CA: H2O.ai, Inc. Available at: https://www.h2o.ai/wp-content/uploads/2018/01/RBooklet.pdf (accessed March 9, 2020).

Maertens, W., Vangeyte, J., Baert, J., Jantuan, A., Mertens, K. C., De Campeneere, S., et al. (2011). Development of a real time cow gait tracking and analysing tool to assess lameness using a pressure sensitive walkway: the GAITWISE system. *Biosyst. Eng.* 110, 29–39. doi: 10.1016/j.biosystemseng.2011.06.003

Martinez, M., and De Leon, P. L. (2016). *Unsupervised Segmentation and Labeling for Smartphone Acquired Gait Data*. Arizona: International Foundation for Telemetering.

Nääs, I. A., Paz, I. C. D. L. A., Baracho, M., Menezes, A. G., Lima, K. A. O., Bueno, L. G. F., et al. (2010). Assessing locomotion deficiency in broiler chicken. *Sci. Agricola* 67, 129–135. doi: 10.1590/s0103-90162010000200001

Pastell, M., Aisla, A.-M., Hautala, M., Poikalainen, V., Praks, J., Veermäe, I., et al. (2006). Contactless measurement of cow behavior in a milking robot. *Behav. Res. Methods* 38, 479–486. doi: 10.3758/bf03192802

Pastell, M., Tiusanen, J., Hakojärvi, M., and Hänninen, L. (2009). A wireless accelerometer system with wavelet analysis for assessing lameness in cattle. *Biosyst. Eng.* 104, 545–551. doi: 10.1016/j.biosystemseng.2009.09.007

Paulich, M., Schepers, M., Rudigkeit, N., and Bellusci, G. (2018). *Xsens MTw Awinda: Miniature Wireless Inertial-Magnetic Motion Tracker for Highly Accurate 3D Kinematic Applications*. Available at: https://www.xsens.com/hubfs/3446270/Downloads/Manuals/MTwAwinda_WhitePaper.pdf (accessed September 26, 2019).

Pfau, T., Witte, T. H., and Wilson, A. M. (2005). A method for deriving displacement data during cyclical movement using an inertial sensor. *J. Exp. Biol.* 208:2503. doi: 10.1242/jeb.01658

Pluym, L. M., Maes, D., Vangeyte, J., Mertens, K., Baert, J., Van Weyenberg, S., et al. (2013). Development of a system for automatic measurements of force and visual stance variables for objective lameness detection in sows: SowSIS. *Biosyst. Eng.* 116, 64–74. doi: 10.1016/j.biosystemseng.2013.06.009

Quinton, C. D., Wood, B. J., and Miller, S. P. (2011). Genetic analysis of survival and fitness in turkeys with multiple-trait animal models 1. *Poult. Sci.* 90, 2479–2486. doi: 10.3382/ps.2011-01604

Rijsbergen, C. J. V. (1975). *Information Retrieval*. London: Butterworths.

Seel, T., Raisch, J., and Schauer, T. (2014). IMU-Based joint angle measurement for gait analysis. *Sensors* 14, 6891–6909. doi: 10.3390/s140406891

Šprager, S., and Juriè, M. B. (2018). Robust stride segmentation of inertial signals based on local cyclicity estimation. *Sensors* 18:1091. doi: 10.3390/s18041091

Tamura, T., Okubo, Y., Deguchi, Y., Koshikawa, S., Takahashi, M., Chida, Y., et al. (2019). Dairy cattle behavior classifications based on decision tree learning using 3-axis neck-mounted accelerometers. *Anim. Sci. J.* 90, 589–596. doi: 10.1111/asj.13184

Viazzi, S., Bahr, C., Van Hertem, T., Schlageter-Tello, A., Romanini, C. E. B., Halachmi, I., et al. (2014). Comparison of a three-dimensional and two-dimensional camera system for automated measurement of back posture in dairy cows. *Comput. Electr. Agricult.* 100, 139–147. doi: 10.1016/j.compag.2013.11.005

Wang, Y., Vasilakos, A. V., Jin, Q., and Zhu, H. (2017). *Device-to-Device based Proximity Service: Architecture, Issues, and Applications*. Boca Raton, CA: CRC Press.

Conflict of Interest: BV and AS were employed by the company Hendrix Genetics.

The remaining authors declare that the research was conducted in the absence of any commercial or financial relationships that could be construed as a potential conflict of interest.

frontiers in Genetics

ORIGINAL RESEARCH
published: 27 March 2020
doi: 10.3389/fgene.2020.00139

Genome-Wide Association Study Identifies Genomic Loci Associated With Neurotransmitter Concentration in Cattle

Qiuming Chen[1†], Kaixing Qu[2†], Zhijie Ma[3], Jingxi Zhan[2], Fengwei Zhang[1], Jiafei Shen[1], Qingqing Ning[1], Peng Jia[1], Jicai Zhang[2], Ningbo Chen[1], Hong Chen[1], Bizhi Huang[2] and Chuzhao Lei[1]**

[1] Key Laboratory of Animal Genetics, Breeding and Reproduction of Shaanxi Province, College of Animal Science and Technology, Northwest A&F University, Yangling, China, [2] Yunnan Academy of Grassland and Animal Science, Kunming, China, [3] Academy of Animal Science and Veterinary Medicine, Qinghai University, Xining, China

OPEN ACCESS

Edited by:
Guilherme J. M. Rosa, University of Wisconsin–Madison, United States

Reviewed by:
Lingyang Xu, Chinese Academy of Agricultural Sciences, China
Yali Hou, Beijing Institute of Genomics (CAS), China

***Correspondence:**
Bizhi Huang
hbz@ynbp.cn
Chuzhao Lei
leichuzhao1118@126.com

[†]These authors have contributed equally to this work

Specialty section:
This article was submitted to Livestock Genomics, a section of the journal Frontiers in Genetics

Received: *13 October 2019*
Accepted: *06 February 2020*
Published: *27 March 2020*

Citation:
Chen Q, Qu K, Ma Z, Zhan J, Zhang F, Shen J, Ning Q, Jia P, Zhang J, Chen N, Chen H, Huang B and Lei C (2020) Genome-Wide Association Study Identifies Genomic Loci Associated With Neurotransmitter Concentration in Cattle. Front. Genet. 11:139. doi: 10.3389/fgene.2020.00139

Abnormal neurotransmitter concentration is one of the factors that affect the health status, behavioral personality, and welfare level of animals, but the genetic basis of the abnormality is still largely unknown. The objective of this study is to identify putative genomic loci associated with neurotransmitter concentration in cattle. We measured serotonin (5HT), dopamine (DA), cortisol, glutamate (Glu), and ACTH concentrations in blood serum using double-antibody sandwich ELISA in 30 Brahman cattle and 127 Yunling cattle. Interestingly, we found that ACTH concentration was positively correlated with body weight, cannon circumference, and hip width ($P < 0.05$). Genome-wide association study (GWAS) was performed with mixed linear models using autosomal SNPs derived from the whole-genome sequence. We identified five, five, two, three, and five suggestive loci associated with 5HT, DA, cortisol, Glu, and ACTH concentration, respectively. These 20 associated loci implicated 18 candidate genes. For Glu concentration, the most significant association locus was assigned to *MCHR1*, a G-coupled receptor that could modulate glutamate release. For dopamine concentration, a very strong association locus was located in the intron of *SLC18A2*, which is a critical mediator of dopamine dynamics. However, for ACTH concentration, a very strong association locus was assigned to *HTR1F*, a G protein-coupled receptor that can influence the release of ACTH. Other candidate genes of interest identified for neurotransmitter concentration were *PRMT6*, *GADD45A*, *PCCA*, *ANGPT1*, *ACCS*, *LOC100336971*, *TNR*, *GSDMA*, *CNTN3*, *CARMIL1*, *CDKAL1*, *RBFOX1*, *PCDH15*, and *LGALS12*. Our findings will provide targets for the genetic improvement of neurotransmitter-related traits in domestic cattle and basic materials for studying the mechanism of neurotransmitter synthesis, release, and transport in human and animals.

Keywords: neurotransmitter concentration, genome-wide association study, candidate genes, *Bos taurus*, *Bos indicus*

INTRODUCTION

Neurotransmitters are endogenous chemical substances that act as chemical messengers during synaptic transmission. Abnormal of neurotransmitter concentration predisposes to psychiatric and neurodegenerative disease in human. For example, after treatment with clomipramine, the whole-blood serotonin (5HT) content decreased in patients with obsessive-compulsive disorder (Hanna et al., 1993). In the early stages of Parkinson's disease, the dopamine content was reduced in peripheral blood lymphocytes (Caronti et al., 1999). Therefore, investigation of neurotransmitter content in blood is helpful for understanding the mechanism of psychiatric and neurodegenerative disease in human.

In farm animals, neurotransmitter content in blood was often acted as an indicator correlating with physiological state, temperamental difference, and welfare level. In adult cow, the cortisol concentration in plasma increased after machine milking (Negrao et al., 2004). Previous behavioral experiments have demonstrated that excitable cattle exhibited higher cortisol concentration in plasma than moderate cattle (Curley et al., 2006; Cooke et al., 2019). In animal welfare, previous study has proved that minor corral changes and the adoption of good handling practices in Nellore cows can reduce the cortisol release of individuals (Lima et al., 2018). Experiments on slaughter and transportation have also demonstrated that the elevation of ACTH concentration in plasma is a response to physiological stress in cattle (Knights and Smith, 2007; Zulkifli et al., 2014). Although the revelation of genetic mechanisms underlying plasma neurotransmitter concentration will provide a genetic method to select individuals with a stable physiological state and moderate temperament to raise the welfare level and improve production efficiency in cattle, there are few studies that establish the links between neurotransmitter concentration and genetic variants.

Currently, with the decrease of sequencing cost, tens or hundreds of thousands of SNPs can be used to identify the relationship between important differential traits and genetic variants. In milk traits, a genome-wide association study (GWAS) proved that *DGAT1* and *SCD1* could affect fatty acid synthesis (Li et al., 2015). In temperament traits related to neurotransmitter concentration, previous studies have identified numerous QTLs explaining phenotypic difference (Valente et al., 2016; dos Santos et al., 2017). In fact, the number of SNPs for GWAS has risen to tens of millions. For example, based on 25.4 million imputed whole-genome sequence (WGS) variants, a meta-analysis of GWAS identified 163 genomic regions significantly associated with stature (Bouwman et al., 2018). However, no attempts have been made to identify the genomic loci associated with neurotransmitter concentrations.

The Yunling cattle breed considered in this study is a composite of 1/2 Brahman cattle (*Bos indicus*), 1/4 Murray Grey cattle (*Bos taurus*), and 1/4 Yunnan indigenous cattle (*Bos taurus* × *Bos indicus*), respectively. Therefore, it is an excellent model for the identification of genomic loci explaining important differential phenotypic traits in domestic cattle. Here, we detected five neurotransmitter concentrations in blood serum using double-antibody sandwich ELISA in 29 Brahman cattle and 128 Yunling cattle and evaluated the effect of neurotransmitter concentrations on body measurement traits. We uncovered the genetic architecture for neurotransmitter concentration by performing GWAS using the whole-genome sequence. The findings provide genomic material for genetic improvement of neurotransmitter-related traits in domestic cattle and basic materials for exploring the mechanism of neurotransmitter synthesis, release, and transport in mammals.

MATERIALS AND METHODS

Animals

The dataset came from Brahman cattle and Yunling cattle. All test individuals are multiparous cows. To ensure the consistency of reproductive status, the subjects were not within 2 weeks pre-calving, calving, or within 2 weeks post-calving. In terms of feeding management, the experimental animals consist of 36 pen-feeding individuals (five Brahman cattle and 31 Yunling cattle) and 121 free-grazing individuals (25 Brahman cattle and 96 Yunling cattle). All pen-feeding individuals are fed a total mixed ratio (TMR) of 65% coarse and 35% concentrated fodder. From June to November every year, the free-grazing individuals eat grass in the meadow, and from December to May every year, this is supplemented with proper TMR.

Phenotypic Analysis

We encouraged the test individuals into a squeeze crush to perform body measurement and to collect blood and tissue samples. First, we determined 15 body measurement traits using a measuring tape and a measuring stick. These 15 body measurement traits comprised the withers height, hip cross height, body length, chest circumference, abdominal circumference, cannon circumference, chest width, chest depth, hip circumference, hip width, ischium width, head length, forehead size, rump length, and body length. Next, the whole blood was collected from a jugular vein to detect neurotransmitter concentration. Finally, ear tissue was collected to extract genomic DNA using an ear punch.

Serum was harvested from centrifuged whole blood samples (2000 g centrifugation for 20 min) and then stored at −80°C prior to neurotransmitter concentration determination. Neurotransmitter concentrations were determined by the double-antibody sandwich ELISA method according to the manufacturer's manuals (MMBio, Jiangsu, China) by comparison of samples with standard curves generated with known concentrations. The absorbance was originally obtained from a Multiskan MS Primary EIA V. 1.5-0 reader at a wavelength of 450 nm. In addition, we checked for the effect of breed and feeding regime on neurotransmitter concentration using the general linear model in R software ("lm" function).

Genome Sequencing, Alignment, and SNP Detection

DNA extracted from ear tissues taken from Brahman cattle and Yunling cattle was used for this analysis. The standard

phenol-chloroform protocol was used to isolate DNA (Green and Sambrook, 2012). Whole-genome sequencing was performed using the Illumina NovaSeq platform. The size of the insert fragment was 500 bp. Finally, ∼16.51 billion reads were generated. Pair-end sequence reads were mapped to the reference *Bos taurus* genome (ARS-UCD1.2) using BWA-MEM (Li and Durbin, 2009) with default parameters. Picard was used to exclude potential duplicate reads ("REMOVE_DUPLICATES = true"). We used the Genome Analysis Toolkit 3.8 (GATK) (Nekrutenko and Taylor, 2012) ("HaplotypeCaller," "GenotypeGVCFs," and "SelectVariants" modules) to call candidate SNPs. To filter SNPs and avoid possible false positives, the "VariantFiltration" module of GATK was adopted with the following options: (1) SNPs with QD (variant confidence/quality by depth) < 2 were filtered; (2) SNPs with FS (Phred-scaled *P*-value using Fisher's exact test) > 60 were filtered; (3) SNPs with Mapping Quality Rank Sum < -12.5 were filtered; (4) SNPs with Read Pos RankSum < -8.0 were filtered; (5) SNPs with sequence depth (for all individuals) $<$ 1/3x or $>$3x were filtered. Inference of haplotype phase and imputing of missing alleles were performed using Beagle (Browning and Browning, 2007). In addition, we performed principal component analysis using smartPCA in the EIGENSOFT v5.0 package (Patterson et al., 2006) to adjust population stratification.

Partial Correlation Analysis

To investigate the relationship between neurotransmitter concentrations and body measurement traits, partial Pearson's correlation adjusting for ancestry (principal component 1), feeding regime, and breed was computed using the ppcor package (Kim, 2015) in R.

GWAS Analysis

After filtering the SNPs with MAF > 0.1 or missing rate > 0.1, a total of 12983056 SNPs remained and were used to carry out GWAS analysis for neurotransmitter concentrations. The association analysis was carried out using the Genome-Wide Efficient Mixed-Model Association (GEMMA) software package (Zhou and Stephens, 2012). The mixed linear model assumed the following model:

$$y = X\alpha + S\beta + K\mu + \varepsilon$$

where y is a vector of phenotypes, α is a vector of fixed effects representing marker effects, β is a vector of fixed effects representing non-marker effects, and μ is a vector of unknown random effect. X, S, and K represent the incidence matrices related to α, β, and μ, respectively, and ε represents a vector of random residual effects. The principal component 1 was defined as the S matrix. The kinship matrix calculated from nucleotide polymorphism was defined as the K matrix.

To estimate the correction required for multiple testing, the SNP data was subsequently pruned for linkage disequilibrium in PLINK (Purcell et al., 2007), using a 50 SNP sliding window with a five SNP increment between windows, retaining only SNPs with a pairwise $r^2 < 0.2$. The number of LD-pruned SNPs (747,835) was defined as the effective number of independent SNPs. Therefore, the *P*-value thresholds were set at 6.7×10^{-8} (significant, 0.05/747835) and 1.3×10^{-6} (suggestive, 1/747835).

After completing GWAS, we further narrowed down our findings to obtain corresponding candidate genes. Firstly, we calculated the pairwise linkage disequilibrium among SNPs associated with neurotransmitter concentration. The borders of associated loci were defined according to the LD value ($r^2 > 0.6$). False-positive signals were filtered for by retaining the associated loci with $\geq$2 suggestive SNPs. The LD plots of suggestive SNPs for associated loci were visualized using the Haploview program (Barrett et al., 2005). Secondly, the SNP with the smallest P_{wald} value in an association locus with neurotransmitter concentrations was defined as the leading SNP. Finally, we performed functional annotation for suggestive SNPs associated with neurotransmitter concentrations using ANNOVAR (Wang et al., 2010) according to the *Bos taurus* reference genome (ARS-UCD1.2).

RESULTS

Effect of Neurotransmitter Concentration on Body Measurement Traits

We measured five neurotransmitter concentrations, including serotonin (5HT), dopamine (DA), cortisol, glutamate (Glu), and ACTH in blood serum of Brahman cattle and Yunling cattle using the double-antibody sandwich ELISA method. The descriptive statistics of the five neurotransmitter concentrations are summarized in **Table 1**. The coefficients of variation of 5HT, DA, cortisol, Glu, and ACTH concentrations were 19.81, 18.42, 17.45, 17.23, and 18.87%, respectively.

We used a general linear model to test the influence of breed and feeding regime on the five neurotransmitter concentrations. The result showed that there was no significant difference between Brahman cattle and Yunling cattle or between free grazing and pen feeding. We also calculated the pairwise partial correlations among neurotransmitter concentrations (**Figure 1**). The result showed that there was no significant correlation among neurotransmitter concentrations. Meanwhile, the association between neurotransmitter concentrations and the 15 body measurement traits was also assessed using the above approach (**Figure 1**). It is remarkable that only ACTH concentration was positively correlated with body weight ($r_s = 0.251$, $P = 3.31 \times 10^{-3}$), cannon circumference ($r_s = 0.163$, $P = 0.043$), and hip width ($r_s = 0.168$, $P = 0.038$).

Whole-Genome Data Description

Genomic DNA samples from 157 individuals were sequenced to ∼5.60 × genome coverage each. About 16.51 billion reads were aligned to the *Bos taurus* reference genome sequence ARS-UCD1.2, and the average alignment rate was 99.55% (**Supplementary Table S1**). After filtering raw SNPs, a total of ∼40.98 million SNPs were retained. In principal component analysis, principal component 1 explained 3.5% of

TABLE 1 | Descriptive statistics of five neurotransmitter concentrations.

Trait	Maximum	Minimum	Mean	*SD*	CV (%)	Skewness	Kurtosis
5HT (ng/L)	3786	1948	2844	563.53	19.81	0.067	1.63
DA (ng/L)	228.4	112.6	168.3	31.01	18.42	0.164	1.89
Glu (μmol/L)	43.95	24.08	33.76	5.89	17.45	0.070	1.70
Cortisol (μg/L)	228.2	116.7	172.0	29.63	17.23	−0.001	1.86
ACTH (μg/L)	55.90	28.49	41.60	7.85	18.87	0.200	1.87

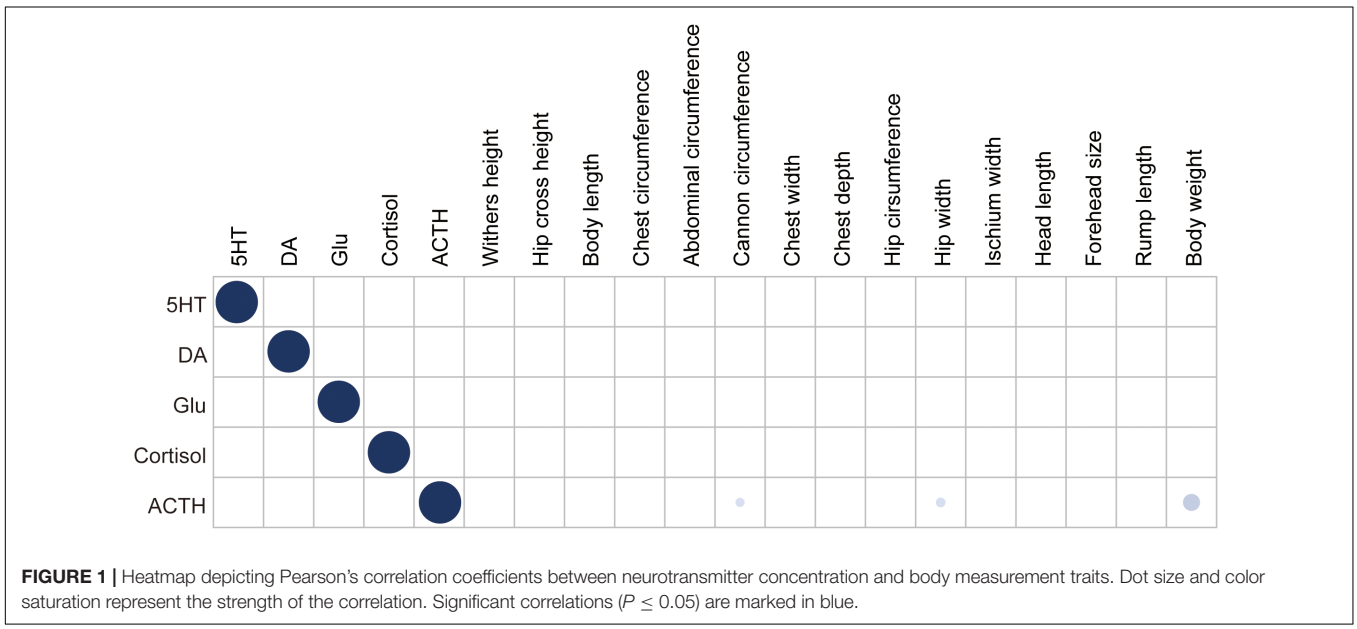

FIGURE 1 | Heatmap depicting Pearson's correlation coefficients between neurotransmitter concentration and body measurement traits. Dot size and color saturation represent the strength of the correlation. Significant correlations ($P \leq 0.05$) are marked in blue.

the total variation and separated Brahman cattle from Yunling cattle (**Figure 2**).

Genome-Wide Association Studies for Five Neurotransmitter Concentrations

The GWAS Manhattan plot for 5HT concentration in blood serum is shown in **Figure 3A**. In total, 36 SNPs were found to be suggestively associated with variation in 5HT concentration (**Supplementary Table S2**). After detecting the linkage disequilibrium of these SNPs, we identified five suggestive association loci for 5HT concentration in blood serum (**Table 2**). According to the annotation of ANNOVAR software, the most significant locus was observed on BTA15 and was located in gene desert (regions over 500 kb that are devoid of protein-coding genes). The second-ranked locus was observed on BTA4 and was also located in gene desert. The third-ranked locus was observed on BTA15, and its leading SNP was located in the intron of *ACCS*. The remaining association loci were observed on BTA19 and BTA22, and their candidate genes embodied *SLC39A11* and *CNTN3*, respectively.

In **Figure 3B**, the GWAS for DA concentration shows that 25 SNPs were found to be suggestively associated with the variation of DA concentration (**Supplementary Table S3**). After detecting the linkage disequilibrium of these SNPs, we identified five suggestive association loci for DA concentration (**Table 2**). Based on the annotation of ANNOVAR software, the most significant locus was observed on BTA23 and was located in the intron of *CDKAL1*. The second-ranked locus, which was located in the intron of *PCCA*, was observed on BTA12. The third-ranked locus was observed on BTA19, and its leading SNP was located in the intron of *GSDMA*. The remaining association loci were observed on BTA25 and BTA26, and their candidate genes included *RBFOX1* and *SLC18A2*, respectively.

Figure 3C shows the GWAS Manhattan plot for cortisol concentration in blood serum. In total, 12 SNPs were found to be suggestively associated with variation in cortisol concentration (**Supplementary Table S4**). After detecting the linkage disequilibrium of these SNPs, we identified two suggestive association loci for cortisol concentration (**Table 2**). After annotation using ANNOVAR, the most significant locus was observed on BTA16, and its nearest gene was *LOC100336971*. Another associated locus was observed on BTA8 and was located in gene desert.

The GWAS Manhattan plot for Glu concentration in blood serum is shown in **Figure 3D**. In total, 11 SNPs were found to be suggestively associated with variation of Glu concentration (**Supplementary Table S5**). After detecting the linkage disequilibrium of these SNPs, we identified three suggestive association loci with Glu concentration (**Table 2**). By means of ANNOVAR annotation, we found that the most significant locus was observed on BTA5 and

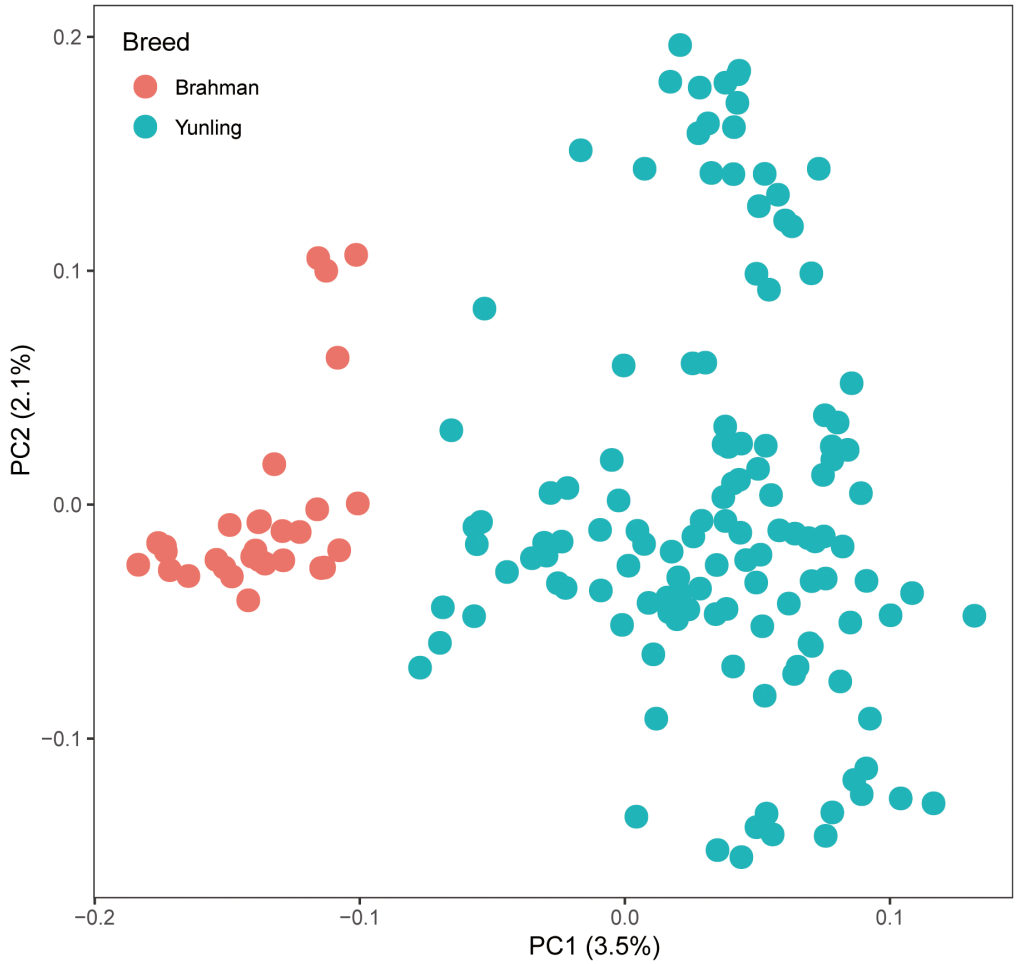

FIGURE 2 | PC plot (PC1 against PC2) using autosomal SNP markers.

was located ∼8 Kb upstream of *MCHR1*. The second-ranked locus was observed on BTA3, and its leading SNP was located upstream of *KLF17*. The third-ranked locus was observed on BTA26 and located in the intron of *PCDH15*.

In **Figure 3E**, our result shows that 34 SNPs were found to be suggestively associated with the variation in ACTH concentration in blood serum (**Supplementary Table S6**). After detecting the linkage disequilibrium of these SNPs, we identified five suggestive association loci for ACTH concentration (**Table 2**). The most significant locus was observed on BTA3 and was located downstream of *PRMT6*. The second-ranked locus was observed on BTA23 and was located in the intron of *CARMIL1*. The third-ranked locus was observed on BTA1, and its leading SNP was located upstream of *HTR1F*. The remaining associated loci were observed on BTA3 and BTA29, and their candidate gene contained *GADD45A* and *LGALS12*, respectively.

The LD plots of 12 loci at which the number of suggestive SNPs associated with neurotransmitter concentration in blood serum was above 3 are presented in **Figure 4**. The results show that four loci had LD blocks (the 1:35945547-35945584 locus, 3:36525172-36526078 locus, 15:68085551-69989675 locus, and 16:28978311-28979773 locus) with a length of less than 1 kb. There were no LD blocks at the remaining eight loci.

DISCUSSION

Previous studies on neurotransmitter concentration in blood have primarily focused on physiological difference under different conditions (Knights and Smith, 2007; Zulkifli et al., 2014; Lima et al., 2018) or analysis of its correlation with temperament in cattle (Curley et al., 2006; Cooke et al., 2019). In our present study, cattle with a higher ACTH concentration in blood serum tended to have better stature for production (i.e., higher body weight, higher cannon circumference, higher hip width). To our knowledge, this is the first correlative identification between ACTH concentration and body measurement traits. Although the correlation is only phenotypic, the positive correlation between ACTH

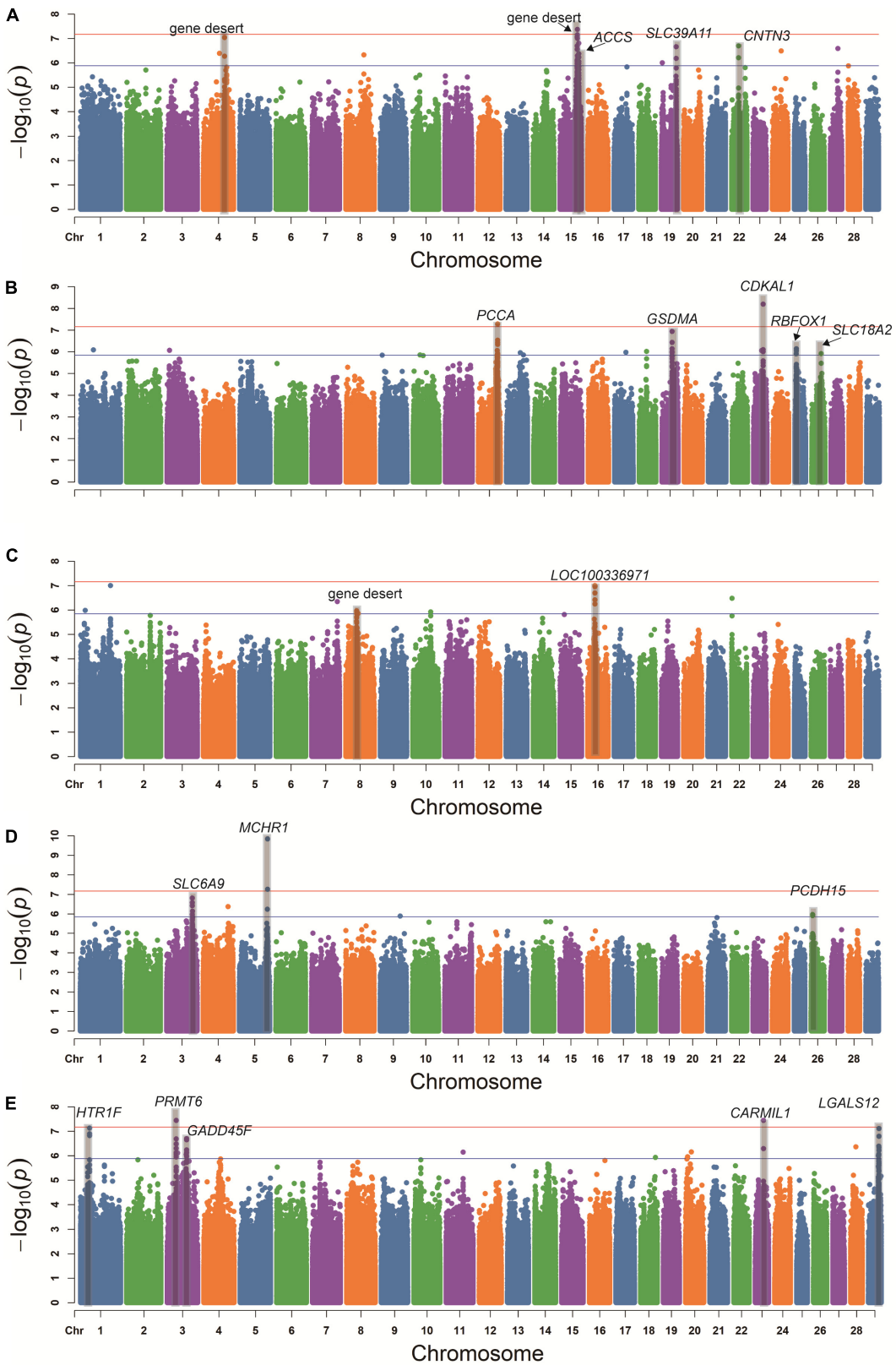

FIGURE 3 | Genome-wide association study of the concentrations of 5HT **(A)**, DA **(B)**, cortisol **(C)**, Glu **(D),** and ACTH **(E)** in blood serum using the mixed linear model. Red line and blue line indicate the significant threshold and suggestive threshold, respectively.

TABLE 2 | Descriptive summary of GWAS for five neurotransmitter concentrations.

Associated locus	Leading variant	MAF	$-\log_{10}P_{wald}$	Trait	Candidate gene
1:35945547–35945584	1:35945558	0.236	7.13	ACTH	*HTR1F*
3:36525172–36526078	3:36526016	0.229	7.45	ACTH	*PRMT6*
3:77705305–77728559	3:77728559	0.398	6.70	ACTH	*GADD45A*
3:101918733–102495677	3:101918733	0.382	6.80	Glu	*SLC6A9*
4:84001170–84005564	4:84005564	0.490	7.04	5HT	Gene desert
5:111980228–111980732	5:111980732	0.242	9.84	Glu	*MCHR1*
8:42958091–42963716	8:42963716	0.481	5.97	Cortisol	Gene desert
12:76815037–76912606	12:76859881	0.223	7.28	DA	*PCCA*
15:68085551–69989675	15:69208676	0.277	7.37	5HT	Gene desert
15:74154782–74195072	15:74186549	0.143	6.80	5HT	*ACCS*
16:28978311–28979773	16:28978311	0.299	7.01	Cortisol	*LOC100336971*
19:40301775–40310333	19:40301775	0.484	6.93	DA	*GSDMA*
19:58424044–58426162	19:58424061	0.487	6.66	5HT	*SLC39A11*
22:27517768–27527029	22:27517768	0.347	6.69	5HT	*CNTN3*
23:32343204–32343711	23:32343711	0.178	7.45	ACTH	*CARMIL1*
23:37336886–37344450	23:37344450	0.255	8.19	DA	*CDKAL1*
25:5800850–5848346	25:5800850	0.169	6.13	DA	*RBFOX1*
26:5310758–5310786	26:5310758	0.223	5.96	Glu	*PCDH15*
26:37563598–37563603	26:37563603	0.182	5.92	DA	*SLC18A2*
29:41276440–41791032	29:41791032	0.172	7.11	ACTH	*LGALS12*

concentration and body measurement traits suggests that improvement of ACTH concentration will have a positive impact on cattle production.

Subsequently, we implemented GWAS to identify the genomic loci explaining the phenotypic variance in neurotransmitter concentrations in blood serum using the whole-genome sequence. We identified five, five, two, three, and five suggestive loci associated with 5HT, DA, cortisol, Glu, and ACTH, respectively, suggesting that neurotransmitter concentration in blood serum is polygenetically controlled. To our knowledge, this is the first identification of genomic loci associated with neurotransmitter concentration in blood serum in cattle using GWAS. Moreover, we found that the LD level for the suggestive loci was very low, suggesting that the loci associated with neurotransmitter concentration were not the target of phenotypic selection or did not experience bottlenecks or gene drift. Although our sample size was smaller for GWAS, the variants with high frequency and large effect have been identified, and further GWAS with a larger sample size will result in the identification of additional variants with low frequency and small effect in future. In addition, our genome coverage was very low (∼5.60×), but a previous study has shown that very low-depth whole-genome sequencing is an efficient alternative to complex trait association studies (Schwartzentruber et al., 2018).

Among 20 suggestive loci, the most significant locus was associated with glutamate concentration in blood serum and was located 8 kb upstream of *MCHR1*, a G-coupled receptor for the neuropeptide melanin-concentrating hormone, which modulates glutamate release from presynaptic terminal (Gao and van den Pol, 2001). Knockout *MCHR1* mice exhibited reduced anxiety-like behavior (Roy et al., 2006). Another strong locus associated with glutamate concentration was assigned to *SLC6A9*, encoding a glycine transporter. In previous studies, glycine has been found to act as an inhibitory neurotransmitter in the central nervous system (Alfadhel et al., 2016) and an obligatory co-agonist of glutamate involved in the regulation of glutamatergic neurotransmission (Johnson and Ascher, 1987), which suggested that *SLC6A9* may participate in the glutamate transporter. For dopamine concentration in blood serum, a strong locus was located in the intron of *SLC18A2*, which is a critical mediator of dopamine dynamics in neuronal terminal (Lohr et al., 2015). Another strong locus associated with dopamine concentration was located in the intron of *PCCA*, which is the alpha subunit of the heterodimeric mitochondrial enzyme Propionyl-CoA carboxylase (Stankovics and Ledley, 1993). It has been demonstrated that dopa decarboxylase is involved in dopamine synthesis (Seifert et al., 1980), suggesting that *PCCA* may participate in the dopamine synthesis. In terms of ACTH concentration, the nearest gene of a leading SNP was *HTR1F*, a G protein-coupled receptor for 5HT, which can regulate the HPA axis by moderating the output of corticotropin-releasing hormone in the hypothalamus and further influence release of ACTH (Falkenberg and Rajeevan, 2010). The identification of these candidate genes may provide better opportunities for investigating the molecular mechanism of neurotransmitter synthesis, release, and transport in mammals.

In conclusion, our study revealed that ACTH concentration in blood serum was significantly related to body measurement traits (body weight, cannon circumference, hip cross height, and hip width). We performed GWAS for neurotransmitter concentration in blood serum using autosomal SNPs derived

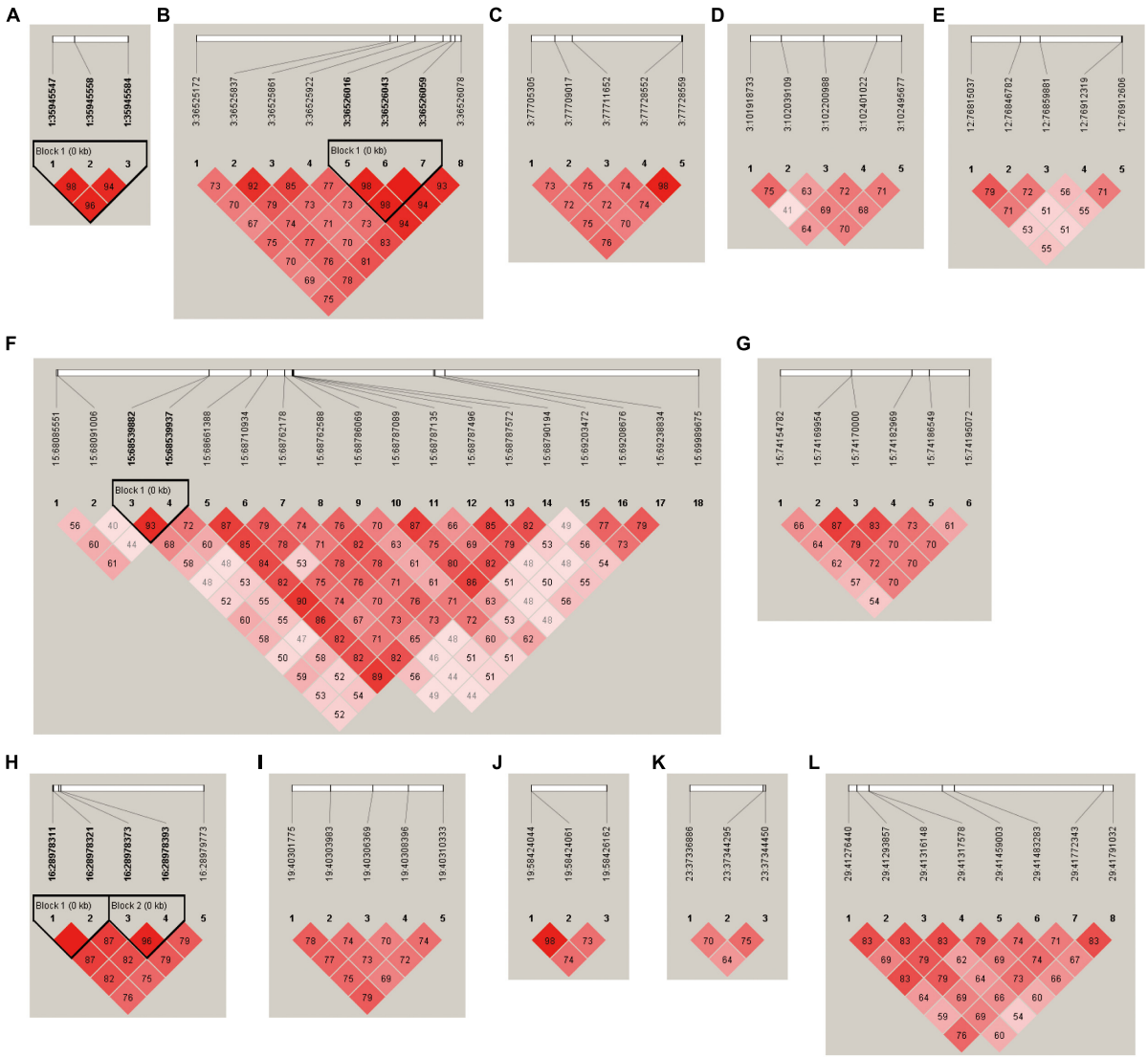

FIGURE 4 | LD plots of suggestive SNPs on neurotransmitter concentration at the **(A)** 1:35945547–35945584 locus, **(B)** 3:36525172–36526078 locus, **(C)** 3:77705305–77728559 locus, **(D)** 3:101918733–102495677 locus, **(E)** 12:76815037–76912606 locus, **(F)** 15:68085551–69989675 locus, **(G)** 15:74154782–74195072 locus, **(H)** 16:28978311–28979773 locus, **(I)** 19:40301775–40310333 locus, **(J)** 19:58424044–58426162 locus, **(K)** 23:37336886–37344450 locus, and **(L)** 29:41276440–41791032 locus.

from WGS and then identified five, five, two, three, and five suggestive loci associated with 5HT, DA, cortisol, Glu, and ACTH, respectively. These 20 loci implicated 17 candidate genes, including *MCHR1* (a G-coupled receptor involved in glutamate release), *SLC18A2* (a critical mediator of dopamine dynamics), and *HTR1F* (a G protein-coupled receptor involved in release of ACTH). The revelation of the genetic underpinnings of neurotransmitter concentration will provide theoretical guidance for the improvement of neurotransmitter concentration by genetic manipulation to reduce stress, elevate welfare level, and boost productivity in cattle. In addition, our findings are helpful for follow-up studies to identify causal variants of difference in neurotransmitter concentration in blood serum and investigate the molecular mechanism of neurotransmitter synthesis, release, and transport in mammals.

DATA AVAILABILITY STATEMENT

Sequences are available from GenBank with the BioProject accession number PRJNA555741.

ETHICS STATEMENT

This study was approved by the Institutional Animal Care and Use Committee of Northwest A&F University (Permit Number: NWAFAC1019).

AUTHOR CONTRIBUTIONS

CL and BH conceived and designed the project. QC, KQ, JZ, QN, PJ, JZ, NC, and HC carried out sampling. QC, FZ, and JS performed the analyses. QC wrote the manuscript. ZM revised the manuscript. All authors reviewed and approved the final manuscript.

FUNDING

This work was supported by the Program of National Beef Cattle and Yak Industrial Technology system (Grant No. CARS-37), the Program of Yunling Scholar, the Young and Middle-aged Academic Technology Leader Backup Talent Cultivation Program in Yunnan Province, China (No. 2018HB045), and Yunnan Provincial Major S&T Project (2019ZG007 and 2019ZG011).

SUPPLEMENTARY MATERIAL

The Supplementary Material for this article can be found online at: https://www.frontiersin.org/articles/10.3389/fgene.2020.00139/full#supplementary-material

TABLE S1 | Summary of sequencing data.

TABLE S2 | The suggestive SNPs associated with 5HT concentration in blood serum.

TABLE S3 | The suggestive SNPs associated with DA concentration in blood serum.

TABLE S4 | The suggestive SNPs associated with cortisol concentration in blood serum.

TABLE S5 | The suggestive SNPs associated with Glu concentration in blood serum.

TABLE S6 | The suggestive SNPs associated with ACTH concentration in blood serum.

REFERENCES

Alfadhel, M., Nashabat, M., Al Qahtani, H., Alfares, A., Al Mutairi, F., Al Shaalan, H., et al. (2016). Mutation in SLC6A9 encoding a glycine transporter causes a novel form of non-ketotic hyperglycinemia in humans. *Hum. Genet.* 135, 1263–1268. doi: 10.1007/s00439-016-1719-x

Barrett, J. C., Fry, B., Maller, J., and Daly, M. J. (2005). Haploview: analysis and visualization of LD and haplotype maps. *Bioinformatics* 21, 263–265. doi: 10.1093/bioinformatics/bth457

Bouwman, A. C., Daetwyler, H. D., Chamberlain, A. J., Ponce, C. H., Sargolzaei, M., Schenkel, F. S., et al. (2018). Meta-analysis of genome-wide association studies for cattle stature identifies common genes that regulate body size in mammals. *Nat. Genet.* 50:362. doi: 10.1038/s41588-018-0056-5

Browning, S. R., and Browning, B. L. (2007). Rapid and accurate haplotype phasing and missing-data inference for whole-genome association studies by use of localized haplotype clustering. *Am. J. Hum. Genet.* 81, 1084–1097. doi: 10.1086/521987

Caronti, B., Tanda, G., Colosimo, C., Ruggieri, S., Calderaro, C., Palladini, G., et al. (1999). Reduced dopamine in peripheral blood lymphocytes in Parkinson's disease. *Neuroreport* 10, 2907–2910. doi: 10.1097/00001756-199909290-00006

Cooke, R. F., Moriel, P., Cappellozza, B. I., Miranda, V. F. B., Batista, L. F. D., Colombo, E. A., et al. (2019). Effects of temperament on growth, plasma cortisol concentrations and puberty attainment in Nelore beef heifers. *Animal* 13, 1208–1213. doi: 10.1017/s1751731118002628

Curley, K. Jr., Paschal, J., Welsh, T. Jr., and Randel, R. (2006). Exit velocity as a measure of cattle temperament is repeatable and associated with serum concentration of cortisol in Brahman bulls. *J. Anim. Sci.* 84, 3100–3103. doi: 10.2527/jas.2006-055

dos Santos, F. C, Peixoto, M. G. C. D., de Souza Fonseca, P. A., Pires Md, F. Á, Ventura, R. V., Rosse , C., et al. (2017). Identification of candidate genes for reactivity in Guzerat (Bos indicus) cattle: a genome-wide association Study. *PloS One* 12:e0169163. doi: 10.1371/journal.pone.0169163

Falkenberg, V. R., and Rajeevan, M. S. (2010). Identification of a potential molecular link between the glucocorticoid and serotonergic signaling systems. *J., Mol. Neurosci.* 41, 322–327. doi: 10.1007/s12031-009-9320-6

Gao, X. B., and van den Pol, A. N. (2001). Melanin concentrating hormone depresses synaptic activity of glutamate and GABA neurons from rat lateral hypothalamus. *J. Physiol.* 533, 237–252. doi: 10.1111/j.1469-7793.2001.0237b.x

Green, M. R., and Sambrook, J. (2012). *Molecular Cloning. A Laboratory Manual 4th*. Cold Spring Harbor, N.Y: Cold Spring Harbor Laboratory Press.

Hanna, G. L., Yuwiler, A., and Cantwell, D. P. (1993). Whole-blood serotonin during clomipramine treatment of juvenile obsessive—compulsive disorder. *J. Child Adoles. Psychopharmacol.* 3, 223–229. doi: 10.1089/cap.1993.3.223

Johnson, J., and Ascher, P. (1987). Glycine potentiates the NMDA response in cultured mouse brain neurons. *Nature* 325, 529. doi: 10.1038/325529a0

Kim, S. (2015). ppcor: an R package for a fast calculation to semi-partial correlation coefficients. *Commun. Statist. Appl. Methods* 22:665. doi: 10.5351/CSAM.2015.22.6.665

Knights, M., and Smith, G. W. (2007). Decreased ACTH secretion during prolonged transportation stress is associated with reduced pituitary responsiveness to tropic hormone stimulation in cattle. *Domest. Anim. Endocrinol.* 33, 442–450. doi: 10.1016/j.domaniend.2006.09.001

Li, H., and Durbin, R. (2009). Fast and accurate short read alignment with Burrows–Wheeler transform. *Bioinformatics* 25, 1754–1760. doi: 10.1093/bioinformatics/btp324

Li, X., Buitenhuis, A. J., Lund, M. S., Li, C., Sun, D., Zhang, Q., et al. (2015). Joint genome-wide association study for milk fatty acid traits in Chinese and Danish Holstein populations. *J. Dairy Sci.* 98, 8152–8163. doi: 10.3168/jds.2015-9383

Lima, M. L. P., Negrão, J. A., de Paz, C. C. P., and Grandin, T. (2018). Minor corral changes and adoption of good handling practices can improve the behavior and reduce cortisol release in Nellore cows. *Trop. Health Prod.* 50, 525–530. doi: 10.1007/s11250-017-1463-9

Lohr, K. M., Stout, K. A., Dunn, A. R., Wang, M., Salahpour, A., Guillot, T. S., et al. (2015). Increased vesicular monoamine transporter 2 (VMAT2; Slc18a2) protects against methamphetamine toxicity. *ACS Chem. Neurosci.* 6, 790–799. doi: 10.1021/acschemneuro.5b00010

Negrao, J., Porcionato, M., De Passille, A., and Rushen, J. (2004). Cortisol in saliva and plasma of cattle after ACTH administration and milking. *J. Dairy Sci.* 87, 1713–1718. doi: 10.3168/jds.S0022-0302(04)73324-X

Nekrutenko, A., and Taylor, J. (2012). Next-generation sequencing data interpretation: enhancing reproducibility and accessibility. *Nat. Rev. Genet.* 13:667. doi: 10.1038/nrg3305

Patterson, N., Price, A. L., and Reich, D. (2006). Population structure and eigenanalysis. *PLoS Genet.* 2:e190. doi: 10.1371/journal.pgen.0020190

Purcell, S., Neale, B., Todd-Brown, K., Thomas, L., Ferreira, M. A., Bender, D., et al. (2007). PLINK: a tool set for whole-genome association and population-based linkage analyses. *Am. J. Huma. Genet.* 81, 559–575. doi: 10.1086/519795

Roy, M., David, N. K., Danao, J. V., Baribault, H., Tian, H., and Giorgetti, M. (2006). Genetic inactivation of melanin-concentrating hormone receptor subtype 1 (MCHR1) in mice exerts anxiolytic-like behavioral effects. *Neuropsychopharmacology* 31:112. doi: 10.1038/sj.npp.1300805

Schwartzentruber, P. D., Kilian, B., Pollard, M. O., Ge, X., Tsafantakis, E., Dedoussis, G., et al. (2018). Very low depth whole genome sequencing in complex trait association studies. *Bioinformatics* 35, 2555–2561. doi: 10.1093/bioinformatics/bty1032

Seifert, W. E. Jr., Foxx, J. L., and Butler, J. I (1980). Age effect on dopamine and serotonin metabolite levels in cerebrospinal fluid. *Ann. Neurol.* 8, 38–42. doi: 10.1002/ana.410080106

Stankovics, J., and Ledley, F. D. (1993). Cloning of functional alpha propionyl CoA carboxylase and correction of enzyme deficiency in pccA fibroblasts. *Am. J. Hum. Genet.* 52, 144.

Valente, T. S., Baldi, F., Sant'Anna, A. C., Albuquerque, L. G., and da Costa, M. J. R. P. (2016). Genome-Wide Association Study between single nucleotide polymorphisms and flight speed in Nellore cattle. *PloS One* 11:e0156956. doi: 10.1371/journal.pone.0156956

Wang, K., Li, M., and Hakonarson, H. (2010). ANNOVAR: functional annotation of genetic variants from high-throughput sequencing data. *Nucleic Acids Res.* 38, e164–e164. doi: 10.1093/nar/gkq603

Zhou, X., and Stephens, M. (2012). Genome-wide efficient mixed-model analysis for association studies. *Nat. Genet.* 44, 821. doi: 10.1038/ng.2310

Zulkifli, I., Goh, Y., Norbaiyah, B., Sazili, A., Lotfi, M., Soleimani, A., et al. (2014). Changes in blood parameters and electroencephalogram of cattle as affected by different stunning and slaughter methods in cattle. *Anim. Prod. Sci.* 54, 187–193. doi: 10.1071/AN12128

Conflict of Interest: The authors declare that the research was conducted in the absence of any commercial or financial relationships that could be construed as a potential conflict of interest.

frontiers in Genetics

ORIGINAL RESEARCH
published: 15 May 2020
doi: 10.3389/fgene.2020.00481

Incorporating Genome Annotation Into Genomic Prediction for Carcass Traits in Chinese Simmental Beef Cattle

Ling Xu[1], Ning Gao[2], Zezhao Wang[1], Lei Xu[1], Ying Liu[1], Yan Chen[1], Lingyang Xu[1], Xue Gao[1], Lupei Zhang[1], Huijiang Gao[1,3], Bo Zhu[1,3] and Junya Li[1,3]**

[1] *Laboratory of Molecular Biology and Bovine Breeding, Institute of Animal Sciences, Chinese Academy of Agricultural Sciences, Beijing, China,* [2] *State Key Laboratory of Biocontrol, School of Life Sciences, Sun Yat-sen University, Guangzhou, China,* [3] *National Centre of Beef Cattle Genetic Evaluation, Beijing, China*

Various methods have been proposed for genomic prediction (GP) in livestock. These methods have mainly focused on statistical considerations and did not include genome annotation information. In this study, to improve the predictive performance of carcass traits in Chinese Simmental beef cattle, we incorporated the genome annotation information into GP. Single nucleotide polymorphisms (SNPs) were annotated to five genomic classes: intergenic, gene, exon, protein coding sequences, and 3′/5′ untranslated region. Haploblocks were constructed for all markers and these five genomic classes by defining a biologically functional unit, and haplotype effects were modeled in both numerical dosage and categorical coding strategies. The first-order epistatic effects among SNPs and haplotypes were modeled using a categorical epistasis model. For all makers, the extension from the SNP-based model to a haplotype-based model improved the accuracy by 5.4–9.8% for carcass weight (CW), live weight (LW), and striploin (SI). For the five genomic classes using the haplotype-based prediction model, the incorporation of gene class information into the model improved the accuracies by an average of 1.4, 2.1, and 1.3% for CW, LW, and SI, respectively, compared with their corresponding results for all markers. Including the first-order epistatic effects into the prediction models improved the accuracies in some traits and genomic classes. Therefore, for traits with moderate-to-high heritability, incorporating genome annotation information of gene class into haplotype-based prediction models could be considered as a promising tool for GP in Chinese Simmental beef cattle, and modeling epistasis in prediction can further increase the accuracy to some degree.

Keywords: genomic prediction, genome annotation, haplotype, Chinese Simmental beef cattle, prediction accuracy

OPEN ACCESS

Edited by:
Guilherme J. M. Rosa, University of Wisconsin–Madison, United States

Reviewed by:
Matthew L. Spangler, University of Nebraska–Lincoln, United States
Fernando Baldi, São Paulo State University, Brazil

****Correspondence:***
Bo Zhu
zhubo@caas.cn
Junya Li
lijunya@caas.cn

Specialty section:
This article was submitted to Livestock Genomics, a section of the journal Frontiers in Genetics

Received: *12 December 2019*
Accepted: *17 April 2020*
Published: *15 May 2020*

Citation:
Xu L, Gao N, Wang Z, Xu L, Liu Y, Chen Y, Xu L, Gao X, Zhang L, Gao H, Zhu B and Li J (2020) Incorporating Genome Annotation Into Genomic Prediction for Carcass Traits in Chinese Simmental Beef Cattle. Front. Genet. 11:481. doi: 10.3389/fgene.2020.00481

INTRODUCTION

Genomic prediction (GP), which uses whole-genome markers to predict genomic breeding value, has been widely used in breeding programs of plants (Heffner et al., 2009; Riedelsheimer et al., 2012; de los Campos et al., 2013; Hayes et al., 2013) and domestic animals (Sonesson and Meuwissen, 2009; Hayes et al., 2010; Erbe et al., 2012; de los Campos et al., 2013), disease risk prediction for

humans (Vazquez et al., 2012; Akey et al., 2014; Abraham et al., 2016), and phenotype prediction of model organisms (Ober et al., 2012; Kooke et al., 2016). Accompanied by the fast development of genotyping and sequencing technologies, various methods with different underlying statistical assumptions have been proposed for GP, including penalized and Bayesian regression methods (Whittaker et al., 2000; Meuwissen et al., 2001; Gianola et al., 2006; VanRaden, 2008; Bennewitz et al., 2009; Habier et al., 2011; Gianola, 2013; Morota and Gianola, 2014). These methods have been applied in cattle populations to improve the prediction accuracy of direct genomic estimated breeding values (DGVs) to some degree (Luan et al., 2009; Hayes et al., 2010; Bolormaa et al., 2013; Fernandes Júnior et al., 2016; Mehrban et al., 2017; Toghiani et al., 2017). However, these established prediction methods have mainly focused on statistical considerations and did not consider the abundantly available biological information. Incorporating biological knowledge, like annotation information (Gao et al., 2017) and gene expression (Li et al., 2019), into GP using an appropriate method may bridge the gap between mathematical models and the underlying biological processes; thus, this information has the potential to improve the prediction accuracy under certain circumstances (Edwards et al., 2016).

Given the availability of genome annotation information, some studies have tried to integrate this information into prediction models to improve the predictive accuracies (Morota et al., 2014; Do et al., 2015; Abdollahi-Arpanahi et al., 2016; Gao et al., 2017; Nani et al., 2019). Single nucleotide polymorphisms (SNPs) were divided into different genomic classes based on the genome annotation information, and GP was conducted for genomic classes using two strategies. The first strategy was to assess the prediction accuracy for each genomic class, and then the genomic class that give the best prediction accuracy was further used for GP (Morota et al., 2014; Do et al., 2015; Abdollahi-Arpanahi et al., 2016). Another strategy was to assign different prior distributions for the different genomic classes, and then all genomic classes were used for prediction (MacLeod et al., 2016). These approaches for incorporating annotation information into GP slightly improved the prediction accuracy in some cases. For instance, Erbe et al. (2012) found that SNPs in the transcribed class produce better predictive performance than other classes in dairy cattle, with a slight increase in prediction accuracy of 0.03 for milk yield, fat yield, and protein yield traits on average. However, others discovered that the prediction accuracy of genomic classes was trait-dependent in the commercial chicken population, and the predictive performance of the whole-genome region remained more accurate (Morota et al., 2014). Generally, these studies have not achieved significant improvements over their corresponding predictions without annotation information. Most studies simply applied standard prediction models for genomic classes based on individual SNPs, with the basic underlying assumption is that at least one marker is in linkage disequilibrium (LD) with each quantitative trait locus (QTL) under high-density markers. The marker density of genomic classes declined after the partitioning, which caused fewer bi-allelic SNPs in LD with a QTL.

An alternative is treating haplotypes that are on tuples of SNPs as predictor variables in GP to compensate for the imperfect LD between SNPs and QTLs (Cuyabano et al., 2015; Da, 2015). The main benefit of using haplotypes for GP is that a haplotype is expected to have a higher LD with a QTL than an individual marker (Calus et al., 2008), and has better ability to identify mutations than a single SNP (Cuyabano et al., 2014). For a trait controlled by rare QTLs, the fitting haplotype could yield a higher accuracy, regardless of the minor allele frequency (MAF) of the QTL (de los Campos et al., 2013). When a high-density SNPs chip was annotated into different genomic classes, at least two SNPs may be included in a genome feature; thus, multi-allelic haplotype-based prediction models are expected to capture the state of a QTL better than single-SNP-based prediction models for genomic classes (Calus et al., 2008; Meuwissen et al., 2014).

In this study, we used annotation information of the cattle genome to divide Illumina BovineHD BeadChip into five genomic classes, including intergenic regions (IGR), gene, exon, protein coding sequences (CDS), and 3′/5′ untranslated regions (UTR) classes. Then, haploblocks were created (Meuwissen et al., 2014) and haplotype effects were modeled using both numerical dosage and categorical coding strategies (Martini et al., 2017) for each genomic class. Although an additive model may explain a major part of the genetic variance in different datasets (Hill et al., 2008), this model does not explicitly capture any kind of interaction that may be present in biochemical pathways that connect gene expression with the ultimate target phenotype. Therefore, statistical models that incorporate interactions between loci are considered as potentially beneficial for GP (Palucci et al., 2007; Pettersson et al., 2011; Su et al., 2012; Mackay, 2014). Epistasis resulting from interactions between genes at different loci was recognized as an important component in dissecting genetic pathways and understanding the evolution of complex genetic systems (Phillips, 2008; Jiang and Reif, 2015). Overall, the objectives of this study were (1) to compare the predictive accuracies of haplotype-based prediction models with SNP-based prediction models, (2) to characterize the predictive performance when genome annotation information was incorporated into haplotype-based prediction model, and (3) to investigate the contribution of epistasis for the accuracy of GP for carcass traits in Chinese Simmental beef cattle.

MATERIALS AND METHODS

Data

Our dataset includes 1346 Simmental cattle born between 2008 and 2015 from Ulgai, Xilingol League, and Inner Mongolia, China. After weaning, cattle were moved to Jinweifuren Co., Ltd. (Beijing, China) for fattening under the same feeding and management conditions. A more detailed description of the management processes was reported in previous studies (Zhu et al., 2016, 2017). All individuals were slaughtered at an average age of 20 months, and carcass and meat quality traits were measured in accordance with the guidelines proposed by the Institutional of Meat Purchase Specifications. All animals used in

the study were treated following the guidelines established by the Council of China Animal Welfare. Protocols of the experiments were approved by the Science Research Department of the Institute of Animal Sciences, Chinese Academy of Agricultural Sciences (CAAS) (Beijing, China). The approval ID/permit numbers are SYXK (Beijing) 2008-007 and SYXK (Beijing) 2008-008. In our study, carcass weight (CW), live weight (LW), and striploin (SI) were analyzed, and their statistical description was summarized in **Table 1**.

Genotyping and Quality Control

The DNA for each animal was obtained from blood using routine procedures. Samples were genotyped with Illumina BovineHD BeadChip. This array contains 777,962 SNPs with an average probe spacing of 3.43 kb and a median spacing of 2.68 kb. Before statistical analysis, the original SNP dataset was filtered using PLINK (v1.90) (Purcell et al., 2007; Chang et al., 2015). Individuals and autosomal SNPs that failed in any of the following criteria were removed, SNPs call rate (>0.90) (MAF > 0.01), Hardy–Weinberg Equilibrium ($p > 10^{-6}$) and individual call rate (>0.90). Missing genotypes were imputed using BEAGLE (v4.1) (Browning and Browning, 2016). Consequently, 1331 individuals and 671,204 SNPs remained. SNPs were coded as the number of copies of the minor allele, i.e., 0, 1, and 2 for the first homozygote, the heterozygote, and the second homozygote, respectively. About population structure, like principal component analysis (PCA) and linkage disequilibrium (LD) were performed in previous studies, which have shown that this population could be separated into five clusters, and the LD (r^2) dropped below 0.2 at distances of 34 kb, indicating that the implementation of GS in this population requires at least 77,941 markers (Niu et al., 2016; Xia et al., 2016).

Heritability Estimation

Phenotypes were adjusted for the environmental fixed effects, including sex, year, and the covariates of body weight upon entering the fattening farm, and the number of fattening days. Subsequently, the adjusted phenotypes were used for further analysis. Variance components were estimated using the following univariate animal model in ASREML (v4.1) (Gilmour et al., 2015):

$$y = 1_n\mu + Za + e \quad (1)$$

where y is the vector of the adjusted phenotypes, $1_n$is an $n \times 1$ vector with entries equal to 1; μ is the overall mean; $a \sim N(0, \sigma_a^2 G)$ is a vector of random additive genetic effect, where G is the additive genetic relationship matrix constructed using all SNPs and σ_a^2 is the additive genetic variance, Z is incidence matrix associating a; and $e \sim N(0, \sigma_e^2 I)$ is a vector of random residuals, where I is the identity matrix and σ_e^2 is the residual variance. The heritability of each trait was estimated using $h^2 = \sigma_a^2/(\sigma_a^2 + \sigma_e^2)$.

SNP Annotation

The latest bovine genome annotation (Bos_taurus.ARS-UCD1.2) was downloaded from Ensemble[1]. According to genome annotation information, the bovine genome was partitioned into five genomic classes: (1) intergenic regions (IGR), (2) gene, (3) exon, (4) protein coding sequences (CDS), and (5) 3′/5′ untranslated regions (UTR) classes. Gene class contained the exon class, and exon class represented a combination of CDS and UTR classes. Thus, overlapping existed among different genomic classes. Then, the SNPs of BovineHD Beadchip were annotated into the corresponding genomic class based on their physical position.

[1]http://asia.ensembl.org/index.html

Haplotype Derivation and Encoding

For the gene, exon, CDS, and UTR classes, a genome feature refers to a single gene, exon, CDS, and UTR, respectively; for the IGR class, a genome feature refers to an interval between two adjacent genes. A group of SNPs that were annotated in a certain genome feature of the five genomic classes was called an SNP set. The phased consecutive SNPs were used for haploblock construction via the approach described by Meuwissen et al. (2014) for each SNP set. The number of SNPs contained in each haploblock depends on the predefined number of types for haplotype allele configurations; here, we used 10 as the maximum number of types (Meuwissen et al., 2014). For SNP sets containing only one SNP, the 0-, 1-, or 2-encoded genotypes were retained for further analysis. Subsequently, haploblocks with at least two haplotype alleles were generated for each SNP set of different genomic classes.

Haplotype effects were then modeled using both numerical dosage (Calus et al., 2008; Cuyabano et al., 2014; Meuwissen et al., 2014) and categorical (Martini et al., 2017) coding strategies. In the numerical dosage model, pseudo-markers were generated for haploblocks by counting the number of copies of the respective allele carried by a certain individual, where the intra-locus additive effects were assumed. The additivity assumption was not necessary in the categorical coding, where the pseudo-markers of haploblocks were coded according to the haplotype allele configurations (genotypes), and each haplotype allele had its own independent effect. **Table 2** shows the coding of a haplotype formed by two consecutive SNPs. Thus, for the five genomic classes, the pseudo-marker matrixes with entries 0, 1, and 2 were reconstructed in both numerical dosage and categorical models (CMs). For all markers, haploblocks were constructed for each chromosome separately using the same approach described above, and the process started from the first marker and followed by their physical order, whereas the genome annotation information was not used to define a biologically functional unit.

Prediction Models

The prediction model used in this study was basically the same as in Eq. (1), except for the different genomic relatedness matrices **G**, which were constructed based on respective prediction approaches (**Table 3**). In our study, the predictive accuracies of using all markers were considered as a benchmark.

In numerical dosage models, GBLUP (VanRaden, 2008) was performed for all markers, and the genomic relatedness matrix was calculated as $G = \frac{(M-P)(M-P)'}{2\sum_{i-1}^{m} p_i(1-p_i)}$, where **M** denotes the (0,

TABLE 1 | Statistical description and heritability estimation of three traits in Chinese Simmental beef cattle.

Traits[1]	The number of phenotype	Mean (SD)	Maximum	Minimum	h^2(SE)
CW	1346	270.67 ± 45.20	486.00	162.60	0.42 ± 0.05
LW	1342	504.95 ± 70.22	776.00	318.00	0.38 ± 0.07
SI	1342	8.55 ± 1.99	15.90	3.21	0.40 ± 0.05

[1] *Carcass weight (CW), live weight (LW), and striploin (SI).*

TABLE 2 | Numerical and categorical coding of a haploblock formed by two consecutive single nucleotide polymorphisms (SNPs).

Haplotype allele 1	Haplotype allele 2	Categorical coding of haploblock[1]	Numerical coding of haploblock			
			AB	Ab	aB	ab
AB	AB	AB|AB	2	0	0	0
AB	Ab	AB|Ab	1	1	0	0
AB	aB	AB|aB	1	0	1	0
AB	ab	AB|ab	1	0	0	1
Ab	Ab	Ab|Ab	0	2	0	0
Ab	aB	Ab|aB	0	1	1	0
Ab	ab	Ab|ab	0	1	0	1
aB	aB	aB|aB	0	0	2	0
aB	ab	aB|ab	0	0	1	1
ab	ab	ab|ab	0	0	0	2

[1] *separates the strands of DNA. Considering this haploblock (let {A, a} and {B, b} denote alleles harbored by the two SNPs, respectively), four possible types of gametes—AB, Ab, aB, and ab—could be generated and 10 types of genotypes are possibly formed in a large population (imprinting is not considered).*

TABLE 3 | Genomic relatedness matrices for different genomic prediction models for all markers or haplotypes.

Models	Description	Relatedness matrices	Use[1]
GBLUP	Genomic best linear unbiased prediction	$G = \frac{(M-P)(M-P)'}{2\sum_{i-1}^{m} p_i(1-p_i)}$	All markers
G_H*BLUP*	Haplotype based GBLUP	$G_H = \frac{M_H M_H'}{Q_H}$	All markers
G_H*BLUP|GA*	Haplotype based *GBLUP* given genome annotation	$G_{H_{GA}} = \frac{M_{H_{GA}} M_{H_{GA}}'}{Q_{H_{GA}}}$	Genomic classes
CM	Categorical marker effect model	$S = (\frac{\sum_{q-1}^{Q} \varphi_{jik}}{m})_{ij}$	All markers
CE	Categorical epistasis model	$E = 0.5 \times mS\#(mS + 1_{n\times n})/m^2$	All markers
C_H*M*	Haplotype based CM	$S_H = (\frac{\sum_{q-1}^{Q} \varphi_{jiq}}{Q_H})_{ij}$	All markers
C_H*E*	Haplotype based CE	$E_H = \frac{0.5 \times Q_H S_H \# (Q_H S_H + 1_{n\times n})}{Q_H^2}$	All markers
C_H*M|GA*	C_H*M* given genome annotation	$\tilde{S} = (\frac{\sum_{q-1}^{Q} \varphi_{jiq}}{Q_{H_{GA}}})_{ij}$	Genomic classes
C_H*E|GA*	C_H*E* given genome annotation	$\tilde{E} = 0.5 \times Q\tilde{S}\#(Q\tilde{S} + 1_{n\times n})/Q_{H_{GA}}^2$	Genomic classes

[1] *Refers to the whole genome-wide SNP; genomic classes refer to IGR, gene, exon, CDS, and UTR class.*

1, and 2) encoded genotype matrix, p_i is the MAF of marker i, m is the number of markers, and P is a matrix with columns equal to $2p_i$. The haplotype-based genomic best linear unbiased prediction (G_H*BLUP*) was performed for all markers. The haplotype-based genomic relatedness matrix in G_H*BLUP* was constructed as the dot product of the haplotype allele matrix (M_H) and expressed as $G_H = \frac{M_H M_H'}{Q_H}$, where M_H is the pseudo-markers matrix with entries 0, 1, and 2 representing the number of copies of each haplotype allele in a haploblock, and Q_H is the total number of haploblocks of whole genome.

For the five genomic classes, haplotype-based genomic best linear unbiased prediction given genome annotation (G_H*BLUP|GA*) was implemented. Similarly, the haplotype-based genomic relatedness matrix in G_H*BLUP|GA* was constructed as $G_{H_{GA}} = \frac{M_{H_{GA}} M_{H_{GA}}'}{Q_{H_{GA}}}$, where $M_{H_{GA}}$ is the haplotype allele matrix with pseudo-markers encoded with (0, 1, and 2), and $Q_{H_{GA}}$ is the total number of haploblocks in the corresponding genomic class.

In CMs, the SNP-based CM (Martini et al., 2017) was applied for all markers, and the genomic relatedness matrix in CM is

expressed as S with entries $S_{ij} = \frac{\sum_{q-1}^{Q} \varphi_{jik}}{m}$, in which φ_{jik} was scored 1 if individual j and i shared the same genotype on marker k; otherwise, $\varphi_{jik}$was scored 0, and m was the number of markers. The haplotype-based CM (C_HM) was applied for all markers as well, in which the number of haploblocks that were in the same state between pairs of individuals were counted. The genomic relatedness matrix in C_HM is expressed as $S_H$with entries $S_{Hji} = (\frac{\sum_{q-1}^{Q} \varphi_{jiq}}{Q_H})$, where φ_{jiq} was scored 1 if individual i and j share the same haplotype allele configuration on haploblock q; otherwise, φ_{jiq} was scored 0; Q_H was the total number of haploblocks, which is the same with that in G_H. Therefore, the entries of S_H represented the proportion of haploblocks with an identical state between pairs of individuals. For the five genomic classes, the haplotype-based CM assigned the genome annotation $C_HM|GA$ was applied. Similarly, the genomic relatedness matrix was built by counting the number of haploblocks that were in an identical state between pairs of individuals (Gao et al., 2017) and expressed as $\tilde{S}$ with entries $\tilde{S}_{ji} = (\frac{\sum_{q-1}^{Q} \varphi_{jiq}}{Q_{H_{GA}}})$, where$\varphi_{jiq}$ is the same as in C_HM, but $Q_{H_{GA}}$ is the total number of haploblocks in certain genomic class, which is the same with that in $G_{H_{GA}}$.

To capture the first-order epistasis among SNPs, the CM model can be extended to categorical epistasis (CE) model (Martini et al., 2017). In the CE model, the genotype combinations of each pair of loci were treated as categorical variables, and the relatedness of two individuals was measured by counting the number of pairs of markers in the same state. The genomic relatedness matrix in the CE model was be deduced from S via the formula$E = 0.5 \times mS\#(mS + 1_{n\times n})/m^2$, where # denotes the Hadamard product. The first-order epistasis between pairs of haploblocks was modeled by extending C_HM to the haplotype-based categorical epistasis model (C_HE) (Gao et al., 2017), where the genotype combinations of each pair of haploblocks were treated as a new categorical variable, and the genomic relatedness matrix was calculated as $E_H = 0.5 \times Q_H S_H\#(Q_H S_H + 1_{n\times n})/Q_H^2$. The corresponding epistatic model that included the first-order epistasis among haploblocks was developed for the five genomic classes and was denoted as $C_HE|GA$ (Gao et al., 2017), where the genomic relatedness matrix was constructed as $\tilde{E} = 0.5 \times Q\tilde{S}\#(Q\tilde{S} + 1_{n\times n})/Q_{H_{GA}}^2$.

Assessment of Prediction Accuracy

The accuracy of GP was assessed using fivefold cross-validation (CV), which assigns animals randomly into five separate subsets with near-equal size. Each subset was used as the validation set only once, with phenotype masked, and the remaining four subsets were treated as a training set. In order to reduce random sampling effects, the CV layout described above was replicated twenty times, where a new randomization was implemented for each replicate so that the each of the subset contains different individuals. DGVs were calculated for each validation subset based on the genomic relatedness matrix. For each replicate, the prediction accuracies were assessed by the correlation between the DGVs and the pre-adjusted phenotypes in the validation set divided by square root of heritability. In addition, in order to assess the extent of bias on GP, linear regression coefficients [b (y, DGV)] of the pre-adjusted phenotypes (y) on the DGVs was calculated for individuals in the validation set. Unbiased models are expected to do not significantly different from 1, whereas values greater than 1 indicate a biased deflation prediction of DGVs and values smaller than 1 indicate a biased inflation prediction of DGVs.

RESULTS

SNP Annotation and Heritability Estimation

We annotated 671,204 filtered SNPs into five genomic classes based on their physical positions. The annotation results and descriptive statistics of each genomic class are displayed in **Table 4**. Overall, 67.03 and 32.97% of the total SNPs were annotated into the IGR and gene classes, respectively. Only 1.46, 1.05, and 0.39% of the total SNPs were annotated into the exon, CDS, and UTR class, respectively. The average MAF among these five genomic classes was in the range of 0.25 to 0.26. The number of haploblocks of gene, exon, CDS, and UTR classes were 87,407, 45,748, 9287, 6799, and 2409, respectively. We counted the number of genome features that were annotated by SNPs for each genomic class (**Table 4**). For instance, 16,286 genes were annotated by SNPs in the gene class, representing 66.30% of the total genes in the bovine genome. Based on the GREML method, the heritability estimates of CW, LW, and SI, were 0.42, 0.38, and 0.40 respectively.

Prediction Accuracy of Haplotype-Based Prediction Model

We first compared the prediction accuracies of all markers between haplotype-based prediction models ($G_HBLUP$and C_HM) and the SNP-based prediction models (*GBLUP* and CM). The results showed that the predictive performances of G_HBLUP andC_HM were more accurate than *GBLUP* and CM in CW, LW, and SI (**Figure 1**). In the numerical dosage models, the accuracy of G_HBLUP was 5.4, 9.8, and 7.1% higher than *GBLUP* in CW, LW, and SI, respectively (**Table 5**). In the CMs, C_HM improved the accuracies by 7.8, 9.5, and 9.4% in CW, LW, and SI, respectively, compared with the CM results. Generally, the numerical dosage models performed better than CMs for most traits. For all markers, *GBLUP* slightly outperformed CM with 3.0, 0.7, and 1.2% higher accuracy in CW, LW, and SI, respectively (**Table 5**). The predictive performance of G_HBLUP was 1% more accurate than C_H M only in LW.

Prediction Accuracy of Haplotype-Based Prediction Model Given Genome Annotation

Under the haplotyped-based model, we further compared the prediction accuracies for the genomic classes with all markers to characterize the benefits of usage genome annotation information in GP. We found that the accuracy of using gene annotation to define haploblocks was consistently higher than that of

TABLE 4 | Mapping results and statistical descriptions of each genomic classes.

Genomic class	# of SNPs[1]	MAF	Mean MAF (SD)	# of haploblocks	# of represented genome feature[2]
IGR class	449,918 (67.03%)	0.009–0.5	0.26 (0.15)	87,407	
Gene class	221,286 (32.97%)	0.009–0.5	0.26 (0.15)	45,748	16,286 (66.30%)
Exon class	9814 (1.46%)	0.010–0.5	0.25 (0.15)	9287	9287 (4.08%)
CDS class	7024 (1.05%)	0.010–0.5	0.25 (0.14)	6799	6799 (3.17%)
UTR class	2614 (0.39%)	0.010–0.5	0.25 (0.15)	2409	2409 (7.26%)
All markers	671,204	0.009–0.5	0.26 (0.15)	115,005	

[1]The number of SNPs annotated in five genomic classes, and their percentage of the whole genome-wide markers is indicated in parentheses. [2]The number of genomic features represented by SNPs in the corresponding genomic class, and their percentage of the total genome features of the reference genome in parentheses. The bovine reference genome contains 24,559 genes, 227,610 exons, 214,584 CDS, and 33,137 UTR. # means "the number."

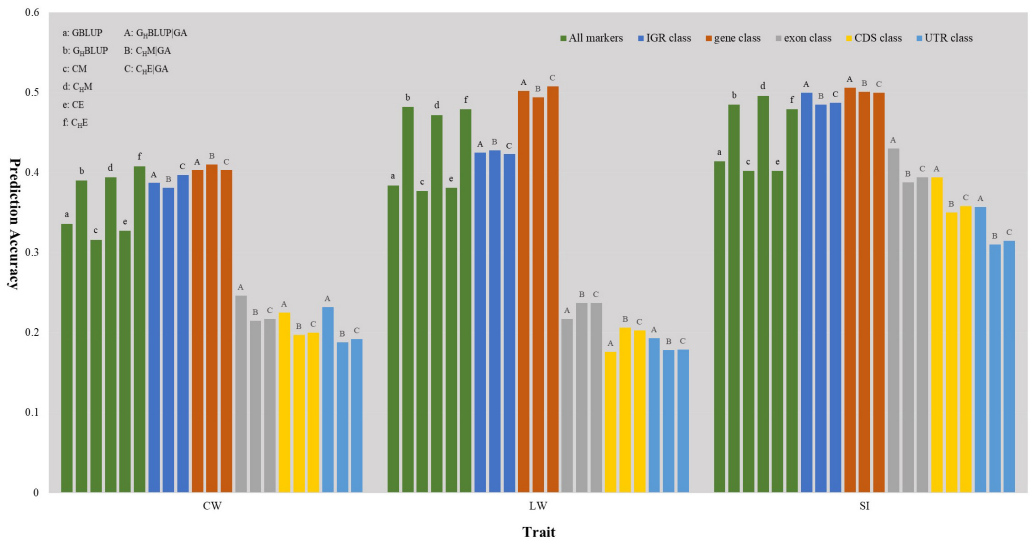

FIGURE 1 | The prediction accuracies of different genomic classes in three traits of Chinese Simmental beef cattle.

all markers across all traits (**Figure 1**). In $G_H BLUP|GA$, the prediction accuracy of gene class was 0.403, 0.502, and 0.506 for CW, LW, and SI, which were 1.3, 2.0, and 2.1% higher than using $G_H BLUP$, respectively. In the CM, $C_H M|GA$ outperformed $C_H M$ in gene class, with accuracy improvements of 1.6, 2.2, and 0.5% in CW, LW, and SI, respectively. For IGR, exon, CDS, and UTR genomic classes, the accuracies using the two haplotype-based prediction models were not improved. In $G_H BLUP|GA$, gene class had 0.6–7.9, 7.6–28.5, 11.2–32.6, and 14.9–30.9% higher accuracies than IGR, exon, CDS, and UTR classes for the three traits, respectively. Analogously, in $C_H M|GA$, the accuracies of the three traits using gene class were 0.1–6.9, 11.3–25.7, 15.1–28.8, and 19.1–31.6% higher than that of IGR, exon, CDS, and UTR classes, respectively (**Table 5**). Comparing the prediction accuracy of numerical dosage with the CM, we found that $G_H BLUP|GA$ maintained more accurate predictive performance than $C_H M|GA$ in most genomic classes (**Table 5**).

Prediction Accuracy of Epistasis Model

Considering the prediction model including epistatic effects may increase the accuracy and reduce the bias of DGVs. The results showed that incorporation of first-order epistatic effects into prediction model can slightly improve the prediction accuracies for most traits and genomic classes (**Figure 1**). When including the epistatic effects amongst SNPs into the CE model for all markers, prediction accuracy increased by 1.1 and 0.4% in CW and LW, respectively (**Table 5**). Similarly, the extension of $C_H M$ to $C_H E$ for all markers improved the prediction accuracies by 1.4 and 0.7% in CW and LW, respectively. For the five genomic classes, compared with $C_H M|GA$, $C_H E|GA$ also had higher prediction accuracies in the IGR class of LW (0.3%), gene class of LW (1.4%), exon class of CW (0.2%) and SI (0.6%), CDS class of CW (0.3%) and SI (0.8%), and UTR class of CW (0.4%) and SI (0.5%).

Regression Coefficient

Table 6 displayed the slope of the regression of the adjusted phenotype on DGVs. For numerical dosage models, the regression coefficients of all marker, IGR, and gene classes were not significantly different from 1 in all traits, indicating the predictions were not significantly biased. For CMs, the regression coefficients of gene, exon, CDS, and UTR classes were significantly different from 1 in CW and LW. However, the regression coefficients for the predictions using the CMs that

TABLE 5 | The prediction accuracies (SD) of different genomic classes in three traits of Chinese Simmental beef cattle.

Trait[1]		Numerical dosage model		Categorical model		Categorical epistasis model	
CW	All maker	GBLUP	0.336 (0.05)	CM	0.316 (0.06)	CE	0.327 (0.06)
	All maker	G_HBLUP	0.390 (0.06)	C_HM	0.394 (0.06)	C_HE	0.408 (0.06)
	IGR class	G_HBLUP|GA	0.397 (0.06)	C_HM|GA	0.387 (0.06	C_HE|GA	0.381 (0.06)
	Gene class	G_HBLUP|GA	0.403 (0.05)	C_HM|GA	0.410 (0.06)	C_HE|GA	0.403 (0.06)
	Exon class	G_HBLUP|GA	0.246 (0.06)	C_HM|GA	0.215 (0.05)	C_HE|GA	0.217 (0.05)
	CDS class	G_HBLUP|GA	0.225 (0.06)	C_HM|GA	0.197 (0.05)	C_HE|GA	0.200 (0.05)
	UTR class	G_HBLUP|GA	0.232 (0.06)	C_HM|GA	0.188 (0.05)	C_HE|GA	0.192 (0.05)
LW	All maker	GBLUP	0.384 (0.05)	CM	0.377 (0.06)	CE	0.381 (0.06)
	All maker	G_HBLUP	0.482 (0.06)	C_HM	0.472 (0.06)	C_HE	0.479 (0.05)
	IGR class	G_HBLUP|GA	0.423 (0.06)	C_HM|GA	0.425 (0.06)	C_HE|GA	0.428 (0.06)
	Gene class	G_HBLUP|GA	0.502 (0.07)	C_HM|GA	0.494 (0.07)	C_HE|GA	0.508 (0.07)
	Exon class	G_HBLUP|GA	0.217 (0.06)	C_HM|GA	0.237 (0.06)	C_HE|GA	0.237 (0.06)
	CDS class	G_HBLUP|GA	0.176 (0.06)	C_HM|GA	0.206 (0.06)	C_HE|GA	0.203 (0.06)
	UTR class	G_HBLUP|GA	0.193 (0.06)	C_HM|GA	0.178 (0.05)	C_HE|GA	0.179 (0.05)
SI	All maker	GBLUP	0.414 (0.07)	CM	0.402 (0.07))	CE	0.402 (0.07)
	All maker	G_HBLUP	0.485 (0.06)	C_HM	0.496 (0.06)	C_HE	0.479 (0.06)
	IGR class	G_HBLUP|GA	0.487 (0.06)	C_HM|GA	0.500 (0.06)	C_HE|GA	0.485 (0.06)
	Gene class	G_HBLUP|GA	0.506 (0.06)	C_HM|GA	0.501 (0.06)	C_HE|GA	0.500 (0.06)
	Exon class	G_HBLUP|GA	0.430 (0.06)	C_HM|GA	0.388 (0.06)	C_HE|GA	0.394 (0.06)
	CDS class	G_HBLUP|GA	0.394 (0.06)	C_HM|GA	0.350 (0.05)	C_HE|GA	0.358 (0.05)
	UTR class	G_HBLUP|GA	0.357 (0.06)	C_HM|GA	0.310 (0.06)	C_HE|GA	0.315 (0.06)

[1] *Carcass weight (CW), live weight (LW), and striploin (SI); prediction accuracies are averaged over the fivefold cross-validation (CV) and then over the 20 replicates.*

TABLE 6 | Regression coefficients (SD) of pre-adjusted phenotypes on DGVs for three traits of Chinese Simmental beef cattle.

Trait[1]		Numerical dosage model		Categorical model		Categorical epistasis model	
CW	All maker	GBLUP	1.102 (0.08)	CM	**1.097** (0.05)	CE	1.087 (0.05)
	All maker	G_HBLUP	1.062 (0.06)	C_HM	1.079 (0.06)	C_HE	**1.388** (0.08)
	IGR class	G_HBLUP|GA	1.064 (0.06)	C_HM|GA	**1.080** (0.07)	C_HE|GA	**1.318** (0.07)
	Gene class	G_HBLUP|GA	1.071 (0.06)	C_HM|GA	**1.090** (0.06)	C_HE|GA	**1.300** (0.07)
	Exon class	G_HBLUP|GA	**1.131** (0.16)	C_HM|GA	**1.143** (0.18)	C_HE|GA	**1.135** (0.18)
	CDS class	G_HBLUP|GA	**1.173** (0.18)	C_HM|GA	**1.169** (0.23)	C_HE|GA	**1.156** (0.21)
	UTR class	G_HBLUP|GA	**1.165** (0.16)	C_HM|GA	**1.232** (0.16)	C_HE|GA	**1.218** (0.16)
LW	All maker	GBLUP	0.984 (0.10)	CM	1.062 (0.09)	CE	**1.094** (0.09)
	All maker	G_HBLUP	1.009 (0.07)	C_HM	1.023 (0.08)	C_HE	**1.546** (0.10)
	IGR class	G_HBLUP|GA	1.051 (0.07)	C_HM|GA	1.073 (0.08)	C_HE|GA	**1.311** (0.08)
	Gene class	G_HBLUP|GA	1.051 (0.04)	C_HM|GA	1.088 (0.04)	C_HE|GA	**1.629** (0.04)
	Exon class	G_HBLUP|GA	**1.187** (0.30)	C_HM|GA	**1.159** (0.22)	C_HE|GA	**1.165** (0.22)
	CDS class	G_HBLUP|GA	**1.386** (0.31)	C_HM|GA	**1.285** (0.25)	C_HE|GA	**1.294** (0.25)
	UTR class	G_HBLUP|GA	**1.197** (0.29)	C_HM|GA	**1.282** (0.33)	C_HE|GA C_HE|GA	**1.278** (0.32)
SI	All maker	GBLUP	1.079 (0.03)	CM	1.076 (0.05)	CE	**1.083** (0.05)
	All maker	G_HBLUP	1.038 (0.05)	C_HM	1.046 (0.04)	C_HE	**1.414** (0.07)
	IGR class	G_HBLUP|GA	1.038 (0.05)	C_HM|GA	1.049 (0.04)	C_HE|GA	**1.338** (0.07)
	Gene class	G_HBLUP|GA	1.050 (0.05)	C_HM|GA	1.050 (0.05)	C_HE|GA	**1.643** (0.06)
	Exon class	G_HBLUP|GA	1.055 (0.03)	C_HM|GA	1.048 (0.05)	C_HE|GA	1.052 (0.05)
	CDS class	G_HBLUP|GA	1.058 (0.05)	C_HM|GA	1.046 (0.07)	C_HE|GA	1.049 (0.08)
	UTR class	G_HBLUP|GA	1.064 (0.07)	C_HM|GA	1.081 (0.10)	C_HE|GA	1.080 (0.10)

[1] *Carcass weight (CW), live weight (LW), and striploin (SI); for each trait (row), the values in bold face indicate the coefficient are significantly different from 1 ($p < 0.05$); regression coefficients are averaged over the fivefold cross-validation (CV) and then over the 20 replicates.*

included the first-order epistasis were significantly different from 1 in all markers and genomic classes, suggesting that these models increased the biasedness of GPs. Generally, among five genomic classes, the regression coefficients of IGR and gene classes were similar to those of all markers, and they contribute to less bias prediction than exon, CDS, and UTR classes. When compared haplotype-based prediction models without including epistasis to the corresponding SNP-based prediction models, we found that the formers' regression coefficients were closer to one, with less biasedness prediction.

DISCUSSION

Advances in high-throughput genotyping technology and the availability of genome annotation information have contributed to the improvement of the predictive performance of complex quantitative traits in livestock species (Morota et al., 2014; Do et al., 2015; Edwards et al., 2016; Nani et al., 2019). To bridge the gap between mathematical models and underlying biological processes, we combined bovine genome annotation information with haplotype-based prediction models to improve the predictive accuracies in Chinese Simmental beef cattle. In this study, whole genome-wide SNPs of BovineHD Beadchip were annotated to five genomic classes. The predictive performance of five genomic classes and all markers was assessed using both numerical and CMs, and the contribution of first-order epistatic effects among SNPs and haploblocks were modeled using categorical coding strategy.

Predictive Performance of Haplotype-Based Prediction Model

Haplotypes have been used widely in human genetics research (Curtis et al., 2001; Chapman et al., 2003; Curtis, 2007); in animal breeding studies, haplotypes have been used for the GP of breeding values with the use of high density SNP chips (Calus et al., 2008; Boichard et al., 2012; Cuyabano et al., 2014; Mucha et al., 2019). In this study, haplotype-based prediction models (G_HBLUP and C_HM) were applied to the whole genome-wide markers, and the result of this scenario was treated as a benchmark. We found that the predictive performance of haplotype-based prediction models was superior to corresponding SNP-based prediction models in the three traits (**Figure 1**), with higher accuracy and less bias. This was consistent with previously reported results in simulated datasets (Calus et al., 2008; Villumsen et al., 2009), dairy cattle (Cuyabano et al., 2014; Hess et al., 2017; Karimi et al., 2018) and beef cattle (Hayes et al., 2007). This may be attributable to haplotypes better capturing LDs with causative mutation or QTLs than single SNPs.

In livestock, SNPs are commonly bi-allelic. When mutations occur, the allele frequencies may remain (almost) unaltered. However, mutations in different loci tend to cause major changes in the haplotype frequencies (Curtis et al., 2001). Thus, when haplotypes were analyzed, a QTL that was not in complete LD with any individual bi-allelic SNP marker may be in complete LD with a multi-marker haplotype. To use a haplotype as an indicator variable in GP, previous studies defined haploblocks by setting windows with a fixed number of SNPs to be placed together as a haploblock (Boichard et al., 2012; Schrooten et al., 2013; Hess et al., 2017), or by considering only the first locus out of 10 consecutive loci in genomic evaluation (Schrooten et al., 2013; Meuwissen et al., 2014). Although their prediction accuracies were improved in GP, the number of SNPs used to outline haploblocks was arbitrarily defined.

To efficiently use the genome properties to define haploblocks and reduce the number of variables for the GP models, several researchers used only haplotypes with a high frequency in the population (Mucha et al., 2019) or based on LD threshold to define haploblocks (Cuyabano et al., 2015). For instance, Cuyabano et al. (2014) used an average LD threshold ($\geq$0.45) to construct haploblocks and found that prediction accuracies increased for the three traits compared with the commonly-used individual SNP. Similarly, we used the cattle genome annotation information to define a biologically functional unit and constructed a haploblock for each unit. This strategy may reflect underlying biological processes and avoid haploblocks being arbitrarily defined. Our study contributes to the improvement of prediction accuracy using a haplotype-based model, since the functional unit contains the combined effects of tightly linked *cis*-acting causal variants (Garnier et al., 2013; Da, 2015), and the number of haplotypes having effects was significantly larger than that for SNP models (Calus et al., 2008). Jiang et al. (2018) indicated that the increase in accuracy bringing by haplotype-based prediction models may be explained by this model capitalizing on local epistatic effects among markers.

Predictive Performance Among Five Genomic Classes

In our study, we applied | GA approaches based on the concept of defining biologically functional units as predictor variables. The results showed that the accuracies and biasedness of prediction for gene and IGR classes were consistently better than those for the exon, CDS, and UTR classes, regardless of which | GA prediction models were used. Firstly, this finding may be attributed to the number of SNPs annotated in its corresponding genomic class, which decreased from the IGR to UTR classes. As previously suggested, the number of markers plays an important role in affecting the GP performance (Zhong et al., 2009; Daetwyler et al., 2010). With decreasing number of markers, the physical distance increased between the markers and QTLs and reduced the LD between markers and QTLs, which would lead to poor predictive power (Yang et al., 2010; Zhang et al., 2011; de los Campos et al., 2013). Yang et al. (2010) found that when the causative mutation loci had a lower MAF, a decrease in marker density would result in an incomplete linkage between the SNP and causative mutation loci; thus, these markers only explained a limited genetic variance.

In our study, 67.03 and 32.97% of the total SNPs were located within the IGR class and gene class, respectively, whereas only 0.39% of total SNPs was annotated in the UTR class, which had the lowest predictive accuracy. Secondly, the average number of SNPs in a haploblock may affect the prediction accuracy of genomic classes as well. It is clear that if each haploblock

consisted of only one marker, the haplotype-based prediction models were exactly identical to the corresponding SNP-based prediction models (Gao et al., 2017). In the IGR and gene classes, 87,407 and 45,748 haploblocks were constructed (**Table 4**), respectively, and 96.82 and 94.21% of the total haploblocks consisted of more than one SNP, which resulted in 5.15 and 4.84 SNPs per haploblock on average, respectively. However, only 9287, 6799, and 2409 haploblocks were constructed in the exon, CDS, and UTR classes. The average number of SNPs per haploblock was 1.06, 1.03, and 1.08, respectively, which indicated haplotype-based prediction models for these genomic classes were similar to SNP-based prediction models. Finally, the number of biological functional units that was used to construct the statistical framework in the | GA approaches could also be a key factor in affecting the predictive accuracies, since the biological functional units may reflect the underlying biological process.

According to the bovine genome annotation information, the bovine reference genome contained 24,559 genes, 227,610 exons, 214,584 CDS, and 33,137 UTR. In this study, gene class represented 66.3% (16,286 out of 24,559 genes) of the total genes of the reference genome, whereas 4.08% (9287 out of 227,610 exons), 3.17% (6799 out of 214,584 CDS), and 7.26% (2409 out of 33,137 UTR) of the total exons, CDS, and UTR of reference genome were respectively represented by exon, CDS, and UTR classes. Consequently, the high proportion of biological-functional-unit-like genes may contribute to stronger predictive power. Taken together, these factors may explain the outstanding predictive performance displayed in gene class compared with the other classes.

Benefits of Using Genome Annotation Information in GP

When the genome annotation information was incorporated into the haplotype-based prediction models, we also observed a slight or moderate improvement in prediction accuracies for the three traits. This can be explained by the traits having different genetic architectures (Daetwyler et al., 2010). The number of QTLs and the distribution of their effects may influence the prediction accuracies of genomic classes. For three traits, the gene class improved the prediction accuracy in comparison with the result of all markers using the haplotype-based prediction model, which was consistent with reported results in mouse and drosophila populations (Gao et al., 2017). This may reflect that genetic signals of the gene class are well tagged in these traits, despite more haploblocks being constructed in the scenario of all markers. The method of defining a biological unit through haplotypes might have increased the linkage of markers and QTLs, which not only allowed the effects of QTL to be better captured but also reduced the density of unrelated markers. Studies have reported that gene class has the most potential to be enriched for trait-associated variants and was more likely to explain a large proportion of the total additive variance (Kamanu et al., 2012; Kindt et al., 2013; Koufariotis et al., 2014). However, Morota et al. (2014) and Abdollahi-Arpanahi et al. (2016) found that the gene class did not lead to an improvement in predictive ability, and the whole genome-wide SNP-based prediction model remained the most efficient method for GP in chicken. These studies only annotated SNPs to the corresponding genomic class and applied the routine GP process for genomic classes. In this case, the genome annotation information cannot be comprehensively used in the SNP-based model because the biologically functional units were not defined as predictor variables in the model.

The usage of genome annotation information of the IGR class also led to a slight improvement in prediction accuracy in CW and SI. Studies have suggested that the IGR class, such as non-coding conserved regions, miRNA, and regulatory regions, might harbor important genetic variants associated with complex traits in crops (Hindorff et al., 2009; Schaub et al., 2012) and humans (Gusev et al., 2014; Finucane et al., 2015). For instance, a study suggested that more than 75% of identified SNPs are embedded in regulatory genome segments in common human diseases (Maurano et al., 2012). Therefore, the IGR class may contribute to a large phenotypic variation. Overall, combining the genome annotation information of the gene class with the haplotype-based prediction models can improve the prediction accuracies, and this can be considered as a promising tool of GP for economically important traits in Chinese Simmental beef cattle.

Effects of Numerical and Categorical Model on Prediction Accuracy

When comparing the predictive performance of the numerical model with the CM, we found that *GBLUP* slightly outperformed the SNP-based CM in three traits. Martini et al. (2017) compared the predictive performance of *CM* with *GBLUP*, and found only slight differences in predictive ability between *CM*and *GBLUP* among 13 traits in mouse. The *CM* does not use the assumption of constant allele substitution effects like *GBLUP*; instead, it models the independent effect of each genotype at a locus, which enables the modeling of dominance (Martini et al., 2017). The advantages of *CM* depend on the population structure and the influence of the dominance effects on a particular trait. One reason to use *CM* instead of *GBLUP* might be the population having prevalent heterosis, since heterosis creates a deviation from the linear dosage model. When most loci are mainly present in only two of the three possible SNP genotypes, the CM cannot substantially outperform *GBLUP* (Martini et al., 2017). Gao et al. (2017) found that $G_H BLUP$ outperformed $C_H M$ in eight traits, and $C_H M$ outperformed $G_H BLUP$ in three traits. Analogously, in our study, $G_H BLUP|GA$ displayed better predictive performance than $C_H M|GA$ in most of the genomic classes among three traits. However, a similar pattern was not observed by Gao et al. (2017), who found that $C_H M|GA$ performed better than $G_H BLUP|GA$in the gene class among most traits.

Contribution of First-Order Epistasis to Prediction Accuracy

Epistasis has long been recognized as a biologically influential component contributing to the genetic architecture of

quantitative traits (Mackay, 2014). Several genomic selection approaches have been developed to model both additive and epistatic effects (Xu, 2007; Cai et al., 2011; Wittenburg et al., 2011; Wang et al., 2012). To minimize the inherently high computational costs of those methods, EGBLUP (Jiang and Reif, 2015) and kernel Hilbert space regression accommodating epistasis within the GP models were proposed (Morota and Gianola, 2014). Generally, the influence of epistasis on GP ranges from positive to negative. In some studies, prediction accuracies increased (Hayes et al., 2009; Su et al., 2012; Jiang and Reif, 2015; He et al., 2016), whereas in others, modeling epistasis adversely affected prediction accuracies (Lorenzana and Bernardo, 2009). For instance, Su et al. (2012) extended GBLUP to EGBLUP to estimate both additive and additive by additive epistatic genetic effects. They found that the epistatic variance accounted for 9.5% of the total phenotypic variance, and the predictive reliabilities of genomic predicted breeding values increased by 0.3%, which was consistent with the results reported by Muñoz et al. (2014). These discrepancies can be explained by the complexities of the studied traits, which are controlled by many loci exhibiting small effects entailing a low QTL detection power.

In this study, the first-order epistatic effects were captured by the categorical epistasis model, which can eliminate the undesired coding-dependent properties of EGBLUP (He et al., 2015; Martini et al., 2017). Although EGBLUP has been applied in other studies (Jiang and Reif, 2015), Martini et al. (2017) suggested that both EGBLUP and the Gaussian kernel in an RKHS approach respond differently to a change in marker coding: a translation of the coding impacts the predictive ability of EGBLUP, but not that of the Gaussian kernel. The difference of coding strategy in the CM with the traditional encoding (0, 1, 2) in EGBLUP meant that the additivity assumption was not necessary in the categorical coding and the encoding of SNPs or haploblocks corresponded to the allele configurations, which enables the modeling of dominance (Martini et al., 2017). In CMs, for all markers, the first-order epistasis of pairs of SNPs were modeled by the CE model, and we found an increase in predictive accuracies from step CM to the CE model in all traits except SI. Martini et al. (2017) also found that CE was slightly better than CM in the simulated and mouse datasets.C_HE modeling of the first-order epistasis between pairs of haploblocks also increased the predictive accuracies of all makers of CW and LW. Similarly, Gao et al. (2017) found an improvement in predictive ability from CM to CE, and from C_HM to C_HE. For genomic classes, we observed a slight increase in accuracy in the gene class of LW and the CDS class of SI from $C_HM|GA$ to $C_HE|GA$. These findings suggest that the first-order epistatic effects captured by markers was likely to contribute to some of the phenotypic variations of the traits observed in this study.

CONCLUSION

In our study, genome annotation information was incorporated into the haplotype-based prediction model for GP of three carcass traits in Chinese Simmental beef cattle. To enable comparison, the SNP-based and haplotype-based prediction methods were applied for all markers, and their results were treated as a benchmark. We found that when the haplotype was treated as a predictor variable, the prediction accuracy improved in most traits. After combining the genome annotation information of the gene class with the haplotype-based prediction model, a further increase in accuracy was observed in most traits compared with the results of all markers obtained by haplotype-based prediction models without genome annotation. The first-order epistatic effects among SNPs and haplotypes slightly improved the prediction accuracy of all markers in LW and CW. In conclusion, incorporating genome annotation information of gene classes into GP models through haplotype-based models could be considered as a promising tool for the GP of carcass traits in Chinese Simmental beef cattle.

DATA AVAILABILITY STATEMENT

Genotype data have been submitted to Dryad: doi: 10.5061/dryad.4qc06. Bovine genome annotation (Bos_taurus.ARS-UCD1.2) was downloaded from Ensemble (http://asia.ensembl.org/index.html).

ETHICS STATEMENT

The animal study was reviewed and approved by Science Research Department of the Institute of Animal Sciences, Chinese Academy of Agricultural Sciences (CAAS) (Beijing, China).

AUTHOR CONTRIBUTIONS

LX simulated and analyzed the data and wrote the manuscript. ZW, LX, and YL collected the data. NG, YC, XG, HG, LYX, LZ, BZ, and JL discussed and improved the manuscript. All authors read and approved the final manuscript.

FUNDING

This work was supported by National Natural Science Foundation of China (31802049, 31372294, and 31201782), Chinese Academy of Agricultural Sciences of Technology Innovation Project (CAAS-XTCX2016010, CAAS-ZDXT2018006, and ASTIP-IAS03), Program of National Beef Cattle and Yak Industrial Technology System (CARS-37), Cattle Breeding Innovative Research Team of Chinese Academy of Agricultural Sciences (cxgc-ias-03, Y2016PT17, and 2019-YWF-YTS-11), Beijing Natural Science Foundation (6154032).

REFERENCES

Abdollahi-Arpanahi, R., Morota, G., Valente, B. D., Kranis, A., Rosa, G. J., and Gianola, D. (2016). Differential contribution of genomic regions to marked genetic variation and prediction of quantitative traits in broiler chickens. *Genet. Sel. Evol.* 48:10. doi: 10.1186/s12711-12016-10187-z

Abraham, G., Havulinna, A. S., Bhalala, O. G., Byars, S. G., De Livera, A. M., Yetukuri, L., et al. (2016). Genomic prediction of coronary heart disease. *Eur. Heart J.* 37, 3267–3278. doi: 10.1093/eurheartj/ehw450

Akey, J. M., Abraham, G., Tye-Din, J. A., Bhalala, O. G., Kowalczyk, A., Zobel, J., et al. (2014). Accurate and robust genomic prediction of celiac disease using statistical learning. *PLoS Genet.* 10:e1004137. doi: 10.1001371/journal.pgen.1004137

Bennewitz, J., Solberg, T., and Meuwissen, T. (2009). Genomic breeding value estimation using nonparametric additive regression models. *Genet. Sel. Evol.* 41:20. doi: 10.1186/1297-9686-1141-1120

Boichard, D., Guillaume, F., Baur, A., Croiseau, P., Rossignol, M.-N., Boscher, M. Y., et al. (2012). Genomic selection in French dairy cattle. *Anim. Prod. Sci.* 52, 115–120. doi: 10.1186/s12711-019-0495-1

Bolormaa, S., Pryce, J. E., Kemper, K., Savin, K., Hayes, B. J., Barendse, W., et al. (2013). Accuracy of prediction of genomic breeding values for residual feed intake and carcass and meat quality traits in *Bos taurus*, *Bos indicus*, and composite beef cattle1. *J. Anim. Sci.* 91, 3088–3104. doi: 10.2527/jas.2012-5827

Browning, B. L., and Browning, S. R. (2016). Genotype imputation with millions of reference samples. *Am. J. Hum. Genet.* 98, 116–126. doi: 10.1016/j.ajhg.2015.11.020

Cai, X., Huang, A., and Xu, S. (2011). Fast empirical Bayesian LASSO for multiple quantitative trait locus mapping. *BMC Bioinformatics* 12:211. doi: 10.1186/1471-2105-12-211

Calus, M. P., Meuwissen, T. H., de Roos, A. P., and Veerkamp, R. F. (2008). Accuracy of genomic selection using different methods to define haplotypes. *Genetics* 178, 553–561. doi: 10.1534/genetics.107.080838

Chang, C. C., Chow, C. C., Tellier, L. C. A. M., Vattikuti, S., Purcell, S. M., and Lee, J. J. (2015). Second-generation PLINK: rising to the challenge of larger and richer datasets. *Gigascience* 4:7. doi: 10.1186/s13742-015-0047-8

Chapman, J. M., Cooper, J. D., Todd, J. A., and Clayton, D. G. (2003). Detecting disease associations due to linkage disequilibrium using haplotype tags: a class of tests and the determinants of statistical power. *Hum. Heredity* 56, 18–31. doi: 10.1159/000073729

Curtis, D. (2007). Comparison of artificial neural network analysis with other multimarker methods for detecting genetic association. *BMC Genet.* 8:49. doi: 10.1186/1471-2156-8-49

Curtis, D., North, B., and Sham, P. (2001). Use of an artificial neural network to detect association between a disease and multiple marker genotypes. *Ann. Hum. Genet.* 65, 95–107. doi: 10.1046/j.1469-1809.2001.6510095.x

Cuyabano, B. C. D., Su, G., and Lund, M. S. (2014). Genomic prediction of genetic merit using LD-based haplotypes in the Nordic Holstein population. *BMC Genomics* 15:1171. doi: 10.1186/1471-2164-1115-1171

Cuyabano, B. C. D., Su, G., and Lund, M. S. (2015). Selection of haplotype variables from a high-density marker map for genomic prediction. *Genet. Sel. Evol.* 47:61. doi: 10.1186/s12711-015-0143-3

Da, Y. (2015). Multi-allelic haplotype model based on genetic partition for genomic prediction and variance component estimation using SNP markers. *BMC Genet.* 16:144. doi: 10.1186/s12863-015-0301-1

Daetwyler, H. D., Pong-Wong, R., Villanueva, B., and Woolliams, J. A. (2010). The impact of genetic architecture on genome-wide evaluation methods. *Genetics* 185, 1021–1031. doi: 10.1534/genetics.110.116855

de los Campos, G., Hickey, J. M., Pong-Wong, R., Daetwyler, H. D., and Calus, M. P. L. (2013). Whole-genome regression and prediction methods applied to plant and animal breeding. *Genetics* 193, 327–345. doi: 10.1534/genetics.112.143313

Do, D. N., Janss, L. L., Jensen, J., and Kadarmideen, H. N. (2015). SNP annotation-based whole genomic prediction and selection: an application to feed efficiency and its component traits in pigs. *J. Anim. Sci.* 93, 2056–2063. doi: 10.2527/jas.2014-8640

Edwards, S. M., Sorensen, I. F., Sarup, P., Mackay, T. F., and Sorensen, P. (2016). Genomic prediction for quantitative traits is improved by mapping variants to gene ontology categories in *Drosophila melanogaster*. *Genetics* 203, 1871–1883. doi: 10.1534/genetics.116.187161

Erbe, M., Hayes, B. J., Matukumalli, L. K., Goswami, S., Bowman, P. J., Reich, C. M., et al. (2012). Improving accuracy of genomic predictions within and between dairy cattle breeds with imputed high-density single nucleotide polymorphism panels. *J. Dairy Sci.* 95, 4114–4129. doi: 10.3168/jds.2011-5019

Fernandes Júnior, G. A., Rosa, G. J. M., Valente, B. D., Carvalheiro, R., Baldi, F., Garcia, D. A., et al. (2016). Genomic prediction of breeding values for carcass traits in Nellore cattle. *Genet. Sel. Evol.* 48:7. doi: 10.1186/s12711-016-0188-y

Finucane, H. K., Bulik-Sullivan, B., Gusev, A., Trynka, G., Reshef, Y., Loh, P.-R., et al. (2015). Partitioning heritability by functional annotation using genome-wide association summary statistics. *Nat. Genet.* 47:1228. doi: 10.1038/ng.3404

Gao, N., Martini, J. W. R., Zhang, Z., Yuan, X., Zhang, H., Simianer, H., et al. (2017). Incorporating gene annotation into genomic prediction of complex phenotypes. *Genetics* 207, 489–501. doi: 10.1534/genetics.117.300198

Garnier, S., Truong, V., Brocheton, J., Zeller, T., Rovital, M., Wild, P. S., et al. (2013). Genome-wide haplotype analysis of cis expression quantitative trait loci in monocytes. *PLoS Genet.* 9:e1003240. doi: 10.1371/journal.pgen.1003240

Gianola, D. (2013). Priors in whole-genome regression: the bayesian alphabet returns. *Genetics* 194, 573–596. doi: 10.1534/genetics.113.151753

Gianola, D., Fernando, R. L., and Stella, A. (2006). Genomic-assisted prediction of genetic value with semiparametric procedures. *Genetics* 173, 1761–1776. doi: 10.1534/genetics.105.049510

Gilmour, A., Gogel, B., Cullis, B., Welham, S., and Thompson, R. (2015). *ASReml User Guide Release 4.1 Structural Specification*. Hemel Hempstead: VSN International Ltd,

Gusev, A., Lee, S. H., Trynka, G., Finucane, H., Vilhjálmsson, B. J., Xu, H., et al. (2014). Partitioning heritability of regulatory and cell-type-specific variants across 11 common diseases. *Am. J. Hum. Genet.* 95, 535–552. doi: 10.1016/j.ajhg.2014.10.004

Habier, D., Fernando, R. L., Kizilkaya, K., and Garrick, D. J. (2011). Extension of the bayesian alphabet for genomic selection. *BMC Bioinformatics* 12:186. doi: 10.1186/1471-2105-1112-1186

Hayes, B. J., Bowman, P. J., Chamberlain, A. J., and Goddard, M. E. (2009). Invited review: genomic selection in dairy cattle: progress and challenges. *J. Dairy Sci.* 92, 433–443. doi: 10.3168/jds.2008-1646

Hayes, B. J., Chamberlain, A. J., McPartlan, H., Macleod, I., Sethuraman, L., and Goddard, M. E. (2007). Accuracy of marker-assisted selection with single markers and marker haplotypes in cattle. *Genet. Res.* 89, 215–220. doi: 10.1017/S0016672307008865

Hayes, B. J., Cogan, N. O., Pembleton, L. W., Goddard, M. E., Wang, J., Spangenberg, G. C., et al. (2013). Prospects for genomic selection in forage plant species. *Plant Breed.* 132, 133–143. doi: 10.1371/journal.pone.0059668

Hayes, B. J., Pryce, J., Chamberlain, A. J., Bowman, P. J., and Goddard, M. E. (2010). Genetic architecture of complex traits and accuracy of genomic prediction: coat colour, milk-fat percentage, and type in Holstein cattle as contrasting model traits. *PLoS Genet.* 6:e1001139. doi: 10.1001371/journal.pgen.1001139

He, D., Wang, Z., and Parida, L. (2015). Data-driven encoding for quantitative genetic trait prediction. *BMC Bioinformatics* 16:S10. doi: 10.1186/1471-2105-16-S1-S10

He, S., Schulthess, A. W., Mirdita, V., Zhao, Y., Korzun, V., Bothe, R., et al. (2016). Genomic selection in a commercial winter wheat population. *Theor. Appl. Genet.* 129, 641–651. doi: 10.1007/s00122-015-2655-1

Heffner, E. L., Sorrells, M. E., and Jannink, J.-L. (2009). Genomic selection for crop improvement. *Crop Sci.* 49, 1–12. doi: 10.3389/fpls.2013.00023

Hess, M., Druet, T., Hess, A., and Garrick, D. (2017). Fixed-length haplotypes can improve genomic prediction accuracy in an admixed dairy cattle population. *Genet. Sel. Evol.* 49:54. doi: 10.1186/s12711-017-0329-y

Hill, W. G., Goddard, M. E., and Visscher, P. M. (2008). Data and theory point to mainly additive genetic variance for complex traits. *PLoS Genet.* 4:e1000008. doi: 10.1371/journal.pgen.1000008

Hindorff, L. A., Sethupathy, P., Junkins, H. A., Ramos, E. M., Mehta, J. P., Collins, F. S., et al. (2009). Potential etiologic and functional implications of genome-wide association loci for human diseases and traits. *Proc. Natl. Acad. Sci. U.S.A.* 106, 9362–9367. doi: 10.1073/pnas.0903103106

Jiang, Y., and Reif, J. C. (2015). Modeling epistasis in genomic selection. *Genetics* 201, 759–768.

Jiang, Y., Schmidt, R. H., and Reif, J. C. (2018). Haplotype-based genome-wide prediction models exploit local epistatic interactions among markers. *G3 (Bethesda)* 8, 1687–1699. doi: 10.1534/g3.117.300548

Kamanu, F. K., Medvedeva, Y. A., Schaefer, U., Jankovic, B. R., Archer, J. A., and Bajic, V. B. (2012). Mutations and binding sites of human transcription factors. *Front. Genet.* 3:100. doi: 10.1371/journal.pgen.1006207

Karimi, Z., Sargolzaei, M., Robinson, J. A. B., and Schenkel, F. S. (2018). Assessing haplotype-based models for genomic evaluation in Holstein cattle. *Can. J. Anim. Sci.* 98, 750–759.

Kindt, A. S. D., Navarro, P., Semple, C. A. M., and Haley, C. S. (2013). The genomic signature of trait-associated variants. *BMC Genomics* 14:108. doi: 10.1186/1471-2164-1114-1108

Kooke, R., Kruijer, W., Bours, R., Becker, F., Kuhn, A., van de Geest, H., et al. (2016). Genome-wide association mapping and genomic prediction elucidate the genetic architecture of morphological traits in *Arabidopsis*. *Plant Physiol.* 170, 2187–2203. doi: 10.1104/pp.15.00997

Koufariotis, L., Chen, Y.-P. P., Bolormaa, S., and Hayes, B. J. (2014). Regulatory and coding genome regions are enriched for trait associated variants in dairy and beef cattle. *BMC Genomics* 15:436. doi: 10.1186/1471-2164-1115-1436

Li, Z., Gao, N., Martini, J. W. R., and Simianer, H. (2019). Integrating gene expression data into genomic prediction. *Front. Genet.* 10:126. doi: 10.3389/fgene.2019.00126

Lorenzana, R. E., and Bernardo, R. (2009). Accuracy of genotypic value predictions for marker-based selection in biparental plant populations. *Theor. Appl. Genet.* 120, 151–161. doi: 10.1007/s00122-009-1166-3

Luan, T., Woolliams, J. A., Lien, S., Kent, M., Svendsen, M., and Meuwissen, T. H. E. (2009). The accuracy of genomic selection in Norwegian red cattle assessed by cross-validation. *Genetics* 183, 1119–1126. doi: 10.1534/genetics.109.107391

Mackay, T. F. (2014). Epistasis and quantitative traits: using model organisms to study gene–gene interactions. *Nat. Rev. Genet.* 15:22. doi: 10.1038/nrg3627

MacLeod, I. M., Bowman, P. J., Vander Jagt, C. J., Haile-Mariam, M., Kemper, K. E., Chamberlain, A. J., et al. (2016). Exploiting biological priors and sequence variants enhances QTL discovery and genomic prediction of complex traits. *BMC Genomics* 17:144. doi: 10.1186/s12864-016-2443-6

Martini, J. W., Gao, N., Cardoso, D. F., Wimmer, V., Erbe, M., Cantet, R. J., et al. (2017). Genomic prediction with epistasis models: on the marker-coding-dependent performance of the extended GBLUP and properties of the categorical epistasis model (CE). *BMC Bioinformatics* 18:3. doi: 10.1186/s12859-12016-11439-12851

Maurano, M. T., Humbert, R., Rynes, E., Thurman, R. E., Haugen, E., Wang, H., et al. (2012). Systematic localization of common disease-associated variation in regulatory DNA. *Science* 337, 1190–1195. doi: 10.1126/science.1222794

Mehrban, H., Lee, D. H., Moradi, M. H., IlCho, C., Naserkheil, M., and Ibáñez-Escriche, N. (2017). Predictive performance of genomic selection methods for carcass traits in Hanwoo beef cattle: impacts of the genetic architecture. *Genet. Sel. Evol.* 49:1. doi: 10.1186/s12711-016-0283-0

Meuwissen, T. H., Hayes, B. J., and Goddard, M. E. (2001). Prediction of total genetic value using genome-wide dense marker maps. *Genetics* 157, 1819–1829.

Meuwissen, T. H., Odegard, J., Andersen-Ranberg, I., and Grindflek, E. (2014). On the distance of genetic relationships and the accuracy of genomic prediction in pig breeding. *Genet. Sel. Evol.* 46:49. doi: 10.1186/1297-9686-1146-1149

Morota, G., Abdollahi-Arpanahi, R., Kranis, A., and Gianola, D. (2014). Genome-enabled prediction of quantitative traits in chickens using genomic annotation. *BMC Genomics* 15:109. doi: 10.1186/1471-2164-15-109

Morota, G., and Gianola, D. (2014). Kernel-based whole-genome prediction of complex traits: a review. *Front. Genet.* 5:363. doi: 10.3389/fgene.2014.00363

Mucha, A., Wierzbicki, H., Kamiński, S., Oleński, K., and Hering, D. (2019). High-frequency marker haplotypes in the genomic selection of dairy cattle. *J. Appl. Genet.* 60, 179–186. doi: 10.1007/s13353-019-00489-9

Muñoz, P. R., Resende, M. F., Gezan, S. A., Resende, M. D. V., de los Campos, G., Kirst, M., et al. (2014). Unraveling additive from nonadditive effects using genomic relationship matrices. *Genetics* 198, 1759–1768. doi: 10.1534/genetics.114.171322

Nani, J. P., Rezende, F. M., and Peñagaricano, F. (2019). Predicting male fertility in dairy cattle using markers with large effect and functional annotation data. *BMC Genomics* 20:258. doi: 10.1186/s12864-019-5644-y

Niu, H., Zhu, B., Guo, P., Zhang, W. G., Xue, J. L., Chen, Y., et al. (2016). Estimation of linkage disequilibrium levels and haplotype block structure in Chinese Simmental and Wagyu beef cattle using high-density genotypes. *Livest. Sci.* 190, 1–9.

Ober, U., Ayroles, J. F., Stone, E. A., Richards, S., Zhu, D., Gibbs, R. A., et al. (2012). Using whole-genome sequence data to predict quantitative trait phenotypes in *Drosophila melanogaster*. *PLoS Genet.* 8:e1002685. doi: 10.1001371/journal.pgen.1002685

Palucci, V., Schaeffer, L. R., Miglior, F., and Osborne, V. (2007). Non-additive genetic effects for fertility traits in Canadian holstein cattle (open access publication). *Genet. Sel. Evol.* 39:181. doi: 10.1186/1297-9686-39-2-181

Pettersson, M., Besnier, F., Siegel, P. B., and Carlborg, Ö (2011). Replication and explorations of high-order epistasis using a large advanced intercross line pedigree. *PLoS Genet.* 7:e1002180. doi: 10.1371/journal.pgen.1002180

Phillips, P. C. (2008). Epistasis — the essential role of gene interactions in the structure and evolution of genetic systems. *Nat. Rev. Genet.* 9:855. doi: 10.1038/nrg2452

Purcell, S., Neale, B., Todd-Brown, K., Thomas, L., Ferreira, M. A. R., Bender, D., et al. (2007). PLINK: a tool set for whole-genome association and population-based linkage analyses. *Am. J. Hum. Genet.* 81, 559–575.

Riedelsheimer, C., Czedik-Eysenberg, A., Grieder, C., Lisec, J., Technow, F., Sulpice, R., et al. (2012). Genomic and metabolic prediction of complex heterotic traits in hybrid maize. *Nat. Genet.* 44, 217–220.

Schaub, M. A., Boyle, A. P., Kundaje, A., Batzoglou, S., and Snyder, M. (2012). Linking disease associations with regulatory information in the human genome. *Genome Res.* 22, 1748–1759.

Schrooten, C., Schopen, G., Parker, A., Medley, A., and Beatson, P. (2013). Across-breed genomic evaluation based on bovine high density genotypes and phenotypes of bulls and cows. *Proc. Assoc. Advmt. Anim. Breed. Genet.* 20, 138–141.

Sonesson, A. K., and Meuwissen, T. H. (2009). Testing strategies for genomic selection in aquaculture breeding programs. *Genet. Sel. Evol.* 41:37. doi: 10.1186/s12864-12017-13557-12861

Su, G., Christensen, O. F., Ostersen, T., Henryon, M., and Lund, M. S. (2012). Estimating additive and non-additive genetic variances and predicting genetic merits using genome-wide dense single nucleotide polymorphism markers. *PLoS One* 7:e45293. doi: 10.1371/journal.pone.0045293

Toghiani, S., Hay, E., Sumreddee, P., Geary, T. W., Rekaya, R., and Roberts, A. J. (2017). Genomic prediction of continuous and binary fertility traits of females in a composite beef cattle breed. *J. Anim. Sci.* 95, 4787–4795.

VanRaden, P. M. (2008). Efficient methods to compute genomic predictions. *J. Dairy Sci.* 91, 4414–4423.

Vazquez, I., de los Campos, G., Klimentidis, Y. C., Rosa, G. J., Gianola, D., Yi, N., et al. (2012). A comprehensive genetic approach for improving prediction of skin cancer risk in humans. *Genetics* 192, 1493–1502.

Villumsen, T. M., Janss, L., and Lund, M. S. (2009). The importance of haplotype length and heritability using genomic selection in dairy cattle. *J. Anim. Breed. Genet.* 126, 3–13.

Wang, D., El-Basyoni, I. S., Baenziger, P. S., Crossa, J., Eskridge, K. M., and Dweikat, I. (2012). Prediction of genetic values of quantitative traits with epistatic effects in plant breeding populations. *Heredity* 109:313.

Whittaker, J. C., Thompson, R., and Denham, M. C. (2000). Marker-assisted selection using ridge regression. *Genet Res.* 75, 249–252.

Wittenburg, D., Melzer, N., and Reinsch, N. (2011). Including non-additive genetic effects in Bayesian methods for the prediction of genetic values based on genome-wide markers. *BMC Genet.* 12:74. doi: 10.1186/1471-2156-12-74

Xia, J., Qi, X., Wu, Y., Zhu, B., Xu, L. Y., Gao, H. J., et al. (2016). Genome-wide association study identifies loci and candidate genes for meat quality traits in Simmental beef cattle. *Mamm. Genome* 27, 246–255.

Xu, S. (2007). An empirical Bayes method for estimating epistatic effects of quantitative trait loci. *Biometrics* 63, 513–521.

Yang, J., Benyamin, B., McEvoy, B. P., Gordon, S., Henders, A. K., Nyholt, D. R., et al. (2010). Common SNPs explain a large proportion of the heritability for human height. *Nat. Genet.* 42, 565–569.

Zhang, Z., Ding, X., Liu, J., Zhang, Q., and de Koning, D. J. (2011). Accuracy of genomic prediction using low-density marker panels. *J. Dairy Sci.* 94, 3642–3650.

Zhong, S., Dekkers, J. C., Fernando, R. L., and Jannink, J.-L. (2009). Factors affecting accuracy from genomic selection in populations derived from multiple inbred lines: a barley case study. *Genetics* 182, 355–364.

Zhu, B., Niu, H., Zhang, W., Wang, Z., Liang, Y., Guan, L., et al. (2017). Genome wide association study and genomic prediction for fatty acid composition in Chinese Simmental beef cattle using high density SNP array. *BMC Genomics* 18:464. doi: 10.1186/s12864-017-3847-7

Zhu, B., Zhu, M., Jiang, J., Niu, H., Wang, Y., Wu, Y., et al. (2016). The impact of variable degrees of freedom and scale parameters in Bayesian methods for genomic prediction in Chinese Simmental beef cattle. *PLoS One* 11:e0154118. doi: 10.1371/journal.pone.0154118

Conflict of Interest: The authors declare that the research was conducted in the absence of any commercial or financial relationships that could be construed as a potential conflict of interest.

frontiers in Genetics

ORIGINAL RESEARCH
published: 21 May 2020
doi: 10.3389/fgene.2020.00513

Estimating Conformational Traits in Dairy Cattle With DeepAPS: A Two-Step Deep Learning Automated Phenotyping and Segmentation Approach

Jessica Nye[1†], Laura M. Zingaretti[1*†] and Miguel Pérez-Enciso[1,2*]*

[1] Centre for Research in Agricultural Genomics (CRAG), CSIC-IRTA-UAB-UB Consortium, Barcelona, Spain, [2] ICREA, Barcelona, Spain

OPEN ACCESS

Edited by:
Guilherme J. M. Rosa,
University of Wisconsin-Madison,
United States

Reviewed by:
Shogo Tsuruta,
University of Georgia, United States
Christian Maltecca,
North Carolina State University,
United States

***Correspondence:**
Jessica Nye
Jessica.Nye@gmail.com
Laura M. Zingaretti
m.lau.zingaretti@gmail.com
Miguel Pérez-Enciso
miguel.perez@uab.es

[†] These authors have contributed equally to this work

Specialty section:
This article was submitted to Livestock Genomics, a section of the journal Frontiers in Genetics

Received: 05 December 2019
Accepted: 27 April 2020
Published: 21 May 2020

Citation:
Nye J, Zingaretti LM and Pérez-Enciso M (2020) Estimating Conformational Traits in Dairy Cattle With DeepAPS: A Two-Step Deep Learning Automated Phenotyping and Segmentation Approach. Front. Genet. 11:513. doi: 10.3389/fgene.2020.00513

Assessing conformation features in an accurate and rapid manner remains a challenge in the dairy industry. While recent developments in computer vision has greatly improved automated background removal, these methods have not been fully translated to biological studies. Here, we present a composite method (DeepAPS) that combines two readily available algorithms in order to create a precise mask for an animal image. This method performs accurately when compared with manual classification of proportion of coat color with an adjusted R^2 = 0.926. Using the output mask, we are able to automatically extract useful phenotypic information for 14 additional morphological features. Using pedigree and image information from a web catalog (www.semex.com), we estimated high heritabilities (ranging from h^2 = 0.18–0.82), indicating that meaningful biological information has been extracted automatically from imaging data. This method can be applied to other datasets and requires only a minimal number of image annotations (∼50) to train this partially supervised machine-learning approach. DeepAPS allows for the rapid and accurate quantification of multiple phenotypic measurements while minimizing study cost. The pipeline is available at https://github.com/lauzingaretti/deepaps.

Keywords: image analysis, morphology, phenomics, image mask, deep learning, dairy cattle

INTRODUCTION

Breeding programs depend on large-scale, accurate phenotyping, which is also critical for genomic dissection of complex traits. While the genome of an organism can be characterized, e.g., with high density genotyping arrays, the "phenome" is much more complex and can never be fully described, as it varies over time and changes with the environment (Houle et al., 2010). The cost of genotyping continues to drop, but there is still a need for improvements in obtaining high-performance phenotypes at a lower cost (Tardieu et al., 2017). In cattle, the number of phenotypes recorded in traditional breeding schemes is relatively small, because its recording is expensive. For instance, yearly milk yield is usually inferred by extrapolation using a few lactation measurements, whereas actual milk production can now be measured individually and daily using automated milking robots.

In addition to milk yield, dairy cattle breeders are interested in conformational traits. These metrics are not only relevant aesthetically but can also have an important influence on an animal's breeding value. Body conformation is associated with dairy performance (Guliński et al., 2005) and longevity, which strongly contributes to lifetime milk production (Sawa et al., 2013). Milk production is positively correlated with udder size (Mingoas et al., 2017). The highest negative economic impact for dairy farmers is caused by lameness either due to leg malformations or injury (Sogstad et al., 2006; Green et al., 2010). Extracting the detailed conformational phenotypes which may impact progeny success are likewise time consuming and costly to collect, and in the absence of quantitative tools, farmers often evaluate morphometric measurements qualitatively.

The emergence of modern sensor technologies, such as Unmanned Aerial Vehicles (UAV) combined with simple digital cameras (Kefauver et al., 2017), mass spectroscopy, robotics, and hyper-spectral images (Fahlgren et al., 2015), among others, have revolutionized breeding programs, mainly in plants, allowing for non-invasive evaluation of multiple complex traits. Although in animal breeding their application is more scarce, modern livestock farming is beginning to benefit from access to these inexpensive sensor tools. Now, it is possible to remotely monitor behavior (Guzhva et al., 2016; Foris et al., 2019; Zehner et al., 2019) and animal welfare (Beer et al., 2016), assess movement (Chapinal et al., 2011), measure body confirmation (Van Hertem et al., 2013; Song et al., 2018), quantify individual food intake (Braun et al., 2014; Beer et al., 2016; Foris et al., 2019), maintain an optimum environment (Chen and Chen, 2019), or decrease instances of stillbirths (Palombi et al., 2013; Ouellet et al., 2016). These automated measurements rely on temperature (Palombi et al., 2013; Ouellet et al., 2016; Chen and Chen, 2019), pressure (Braun et al., 2014; Beer et al., 2016), movement (Chapinal et al., 2011), and visual (Van Hertem et al., 2013; Guzhva et al., 2016; Song et al., 2018; Foris et al., 2019; Zehner et al., 2019) sensors.

As several remote monitoring schemes are based on digital images or video, automated image analysis techniques are urgently needed to quantify traits of interest (Zhang et al., 2018). Applying image analysis to breeding programs is not new, however many of these methods largely depend on time consuming image-by-image processing facilitated by the researcher (as in Hayes et al., 2010; Cortes et al., 2017; Rosero et al., 2019). The few automated resources currently implemented for cattle analyses require complicated set-ups and costly equipment (Chapinal et al., 2011; Song et al., 2018). This is not surprising as accurately quantifying phenotypic information is one of the most challenging aspects in biology (Houle et al., 2011; Boggess et al., 2013; Rahaman et al., 2015).

The availability of new algorithms based on machine learning has revolutionized computer vision, impacting a wide range of fields that rely on computers to analyze images, with the potential to optimize herd care and improve animal and plant breeding program outcomes (Song et al., 2018; Foris et al., 2019; Zehner et al., 2019). These recent advances have led to precise object detection and semantic segmentation in complex images (Girshick et al., 2014; Han et al., 2018; Gu et al., 2018).

Here, we show how automatically parsed web-based catalog datasets can be converted into useful information by automatically inferring genetic parameters of several morphological measurements in dairy cattle. We combined web scraping, deep learning, and statistical techniques in order to achieve our objective. The proposed methodology is a mixture between a supervised deep learning approach, Mask R-CNN (He et al., 2017) and an unsupervised algorithm (Kanezaki, 2018) which can achieve highly precise automatic image segmentation. After removing the background, phenotypic information, including coat color and body conformational traits can be easily quantified. Lastly, we demonstrate the potential applications of this method in other datasets. We assert that our work could constitute a good proxy for using inexpensive and non-invasive computer vision techniques into the dairy cattle breeding programs.

MATERIALS AND METHODS

Image Collection

Images of bulls were collected through web-scraping using the python library Beautiful Soup (Richardson, 2007). Images from sire catalogs of six Artificial Insemination companies were collected. We additionally automatically collected bull images from one semen provider[1] and those of identified familial relationships (daughters, dams, granddams, and great granddams) where possible. We downloaded a total of 1,819 images. These images ranged in size between 339–879 pixels and 257–672 pixels for width and height, respectively. The animals are Holstein with patched black and white bodies, but some images are red Holstein. Individuals ranged in color from all white, all black, all brown, to a mixture of the colors. The images were flipped so that all animals faced the right side of the image using ImageMagick version 7.0.9-0 convert -flop function. The animals are standing in front of dynamic backgrounds including forest, field, snow, water, and straw. All images contained only one animal, and sometimes contained a person or an arm.

Automated Segmentation

One of the most challenging tasks in computer vision is instance segmentation, i.e., the identification of boundaries of objects at the pixel level (Kanezaki, 2018), whereas object classification, i.e., to determine if an object belongs to certain class is relatively simpler. R-CNN (Girshick et al., 2014), a deep learning approach, as well as Fast R-CNN (Girshick, 2015), Faster R-CNN (Ren et al., 2015), or Mask R-CNN (He et al., 2017) are widely used to solve this task. Although these methods are efficient, they are not accurate enough for some purposes since the obtained segmentation often removes parts of the object of interest or contains parts of the background.

We applied a two-step procedure to automatically segment the animal's profile as accurately as possible. The composite method begins by using Mask R-CNN (He et al., 2017), which has three outputs for each candidate object in an input image (**Figure 1A**):

[1] www.semex.com

a class label (say "cow"), bounding box offset or region of interest (RoI), and the object mask consisting of an approximate layout of a spatial object. As in the original Mask R-CNN, we used the annotated image database common objects in context (COCO; Lin et al., 2014)[2] to train the algorithm, and select the class codes for cow. In short, Mask R-CNN is a deep learning algorithm that consists of two steps: first, it proposes regions within the image that may contain objects of interest and, second, generates a mask for every detected object. The latter step consists of a binary classification of pixels, either a pixel belongs to the object or to the background. For more details about this method readers can consult, e.g., https://towardsdatascience.com/computer-vision-instance-segmentation-with-mask-r-cnn-7983502fcad1, https://engineering.matterport.com/splash-of-color-instance-segmentation-with-mask-r-cnn-and-tensorflow-7c761e238b46 or should refer to He et al. (2017). **Figure 1B** shows the applied mask predicted by Mask R-CNN, this mask removes the majority of the background, but also removes parts of the cow's body making it necessary for the development of our two-step composite method. We used the implementation of Mask R-CNN in https://github.com/matterport/Mask_RCNN.

After the RoI and class labels are extracted, we select only the RoI for our desired object (i.e., the bull or cow). This allows us to remove some of the background and obtain a smaller, less noisy image. As explained above, the Mask R-CNN segmentation was not accurate enough for our purposes (**Figure 1B**). Therefore, we passed the RoI and predicted mask to a modified version of the unsupervised image segmentation algorithm from Kanezaki (2018). We used the code available at https://github.com/kanezaki/pytorch-unsupervised-segmentation. The original algorithm relies on separating pixels from each other and grouping them into distinct clusters based on color and texture. The underlying assumptions of this model are that: (1) pixels of similar features should be clustered together, (2) spatially continuous pixels should be clustered together, and (3) the number of clusters should be large. This is achieved by applying a linear classifier which groups pixels into different clusters based on their features. The difference between the original algorithm and ours is we do not try to maximize the total number of clusters, but instead we merely improve upon the mask generated by Mask R-CNN based on pixel identity. This makes more effective the algorithm to run, since the algorithm applied to the whole original image was not completely satisfactory. This proceeds by self-training the network through back propagation, by alternating between two stages: (1) forward super pixel refinement, and (2) backward gradient descent. Much like any supervised approach this is achieved by calculating the cross-entropy loss between network and cluster labels, then back propagating the error rates used to update the convolutional filter parameters. Backpropagation is a popular and clever method used in deep learning. It allows computing the gradient of the loss function very efficiently by using the chain rule for derivatives, which greatly simplifies optimization in complex models.

After refinement through the unsupervised algorithm, we obtained a relatively precise mask for our input image (**Figure 1C**). However, the unsupervised clustering still can confound the foreground and the background. We then apply an additional filter to the mask, median blur function from OpenCV (Bradski, 2000), removing small islands that have been mislabeled during the clustering step (**Figure 1D**). We lastly apply the mask by coloring all pixels predicted to be in the background by a solid color (**Figure 1E**).

To extract the proportion of and average color(s) from each cluster, we apply k-means using the scikit-learn library (Pedregosa et al., 2011). To measure anatomical features, we extract only the outline of the desired object from the mask (**Figure 1F**) using the edge detection algorithm developed by Canny (1986) and implemented in OpenCV (Bradski, 2000). After extracting the edge, we apply one more filter to remove any islands that may remain using the remove_small_objects function from the morphology package available from scikit-learn (Pedregosa et al., 2011). Now that the input image has been reduced down to just the object outline, we can take advantage of common conformational

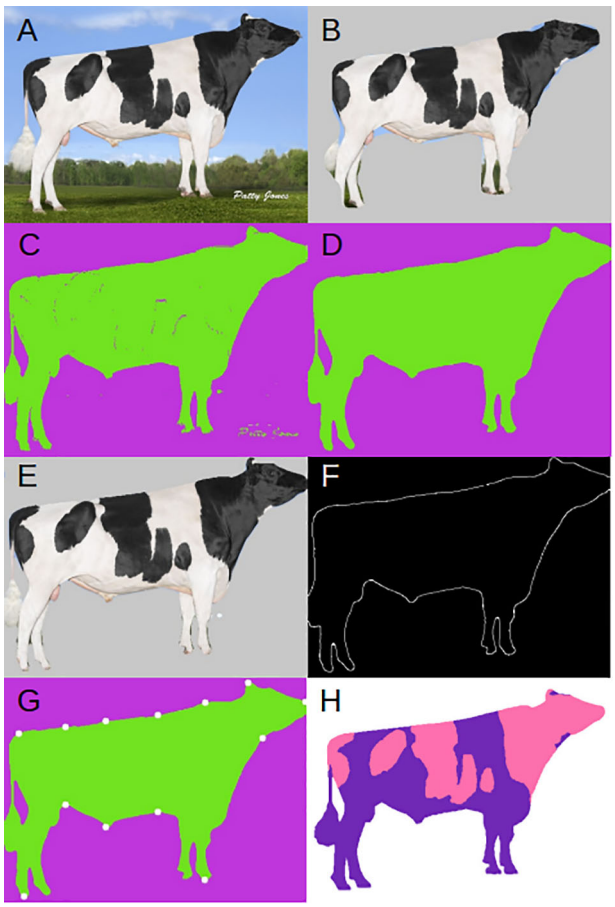

FIGURE 1 | Example input and outputs. **(A)** Original input image. **(B)** Mask R-CNN applied mask. **(C)** DeepAPS raw output. **(D)** Final output of DeepAPS after all applied filters. **(E)** Final DeepAPS mask applied to input image. **(F)** Outline extraction of original input image. **(G)** Extracted landmark coordinates. **(H)** Manual color segmentation. Image from Semex.

[2]http://cocodataset.org

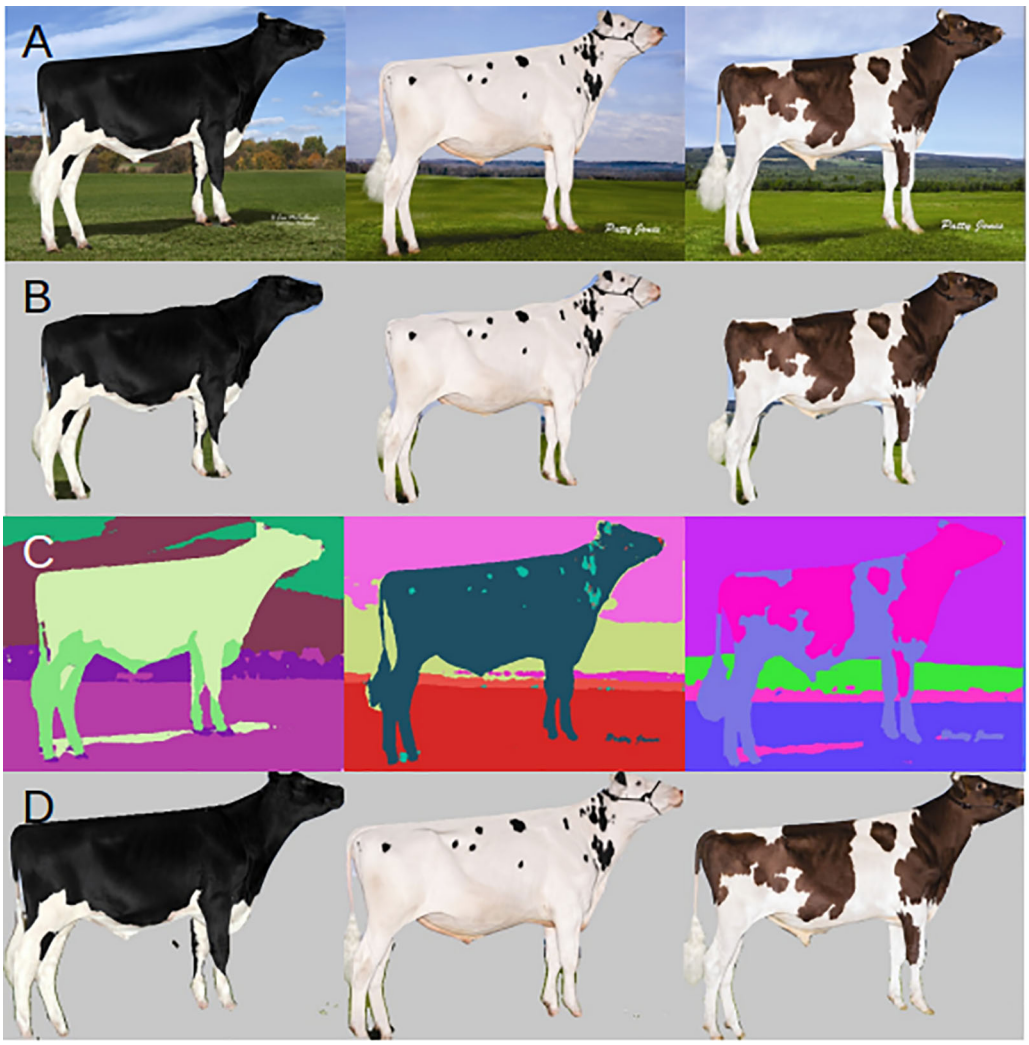

FIGURE 2 | Example input and outputs. **(A)** Original input image. **(B)** Mask R-CNN applied mask. **(C)** DeepAPS raw output. **(D)** Final output of DeepAPS after all applied filters.

features of the underlying data, and extract pixel coordinates. For example, we extracted the coordinate of the pixel closest to the bottom left corner which corresponds to the back foot of the cow. We proceeded in this way to extract 13 coordinates from each animal (**Figure 1G**). We then calculate the distance in pixels between various points, effectively extracting body confirmations automatically. The 14 conformational traits are described in **Supplementary Figure S1**. Code for the whole pipeline is available at https://github.com/lauzingaretti/deepaps.

Manual Segmentation

To check how accurate the automated segmentation was, we manually segmented N = 481 images that were not of Semex origin. We used Kanezaki's demo.py program (2018) in python3.6 (van Rossum, 1995) using default parameters. The output images were opened in the image processing software GIMP[3], and the background was manually changed from the colored cluster to white (**Figure 1H**). To extract the color clusters, we calculated the proportion of color clusters in each image by using k-means as above, and manually matched each color cluster to the original picture and removed the proportion of background.

Genetic Parameters

To calculate heritabilities for the measured phenotypes, we extracted pedigree information and constructed a relationship matrix for each bull whenever possible. This was done by automatic web scraping in the sire catalog website, where we identified bull id, any relative type (i.e., daughter, dam, granddam, and great granddam), and their images. From the list of bull and

[3]https://www.gimp.org/

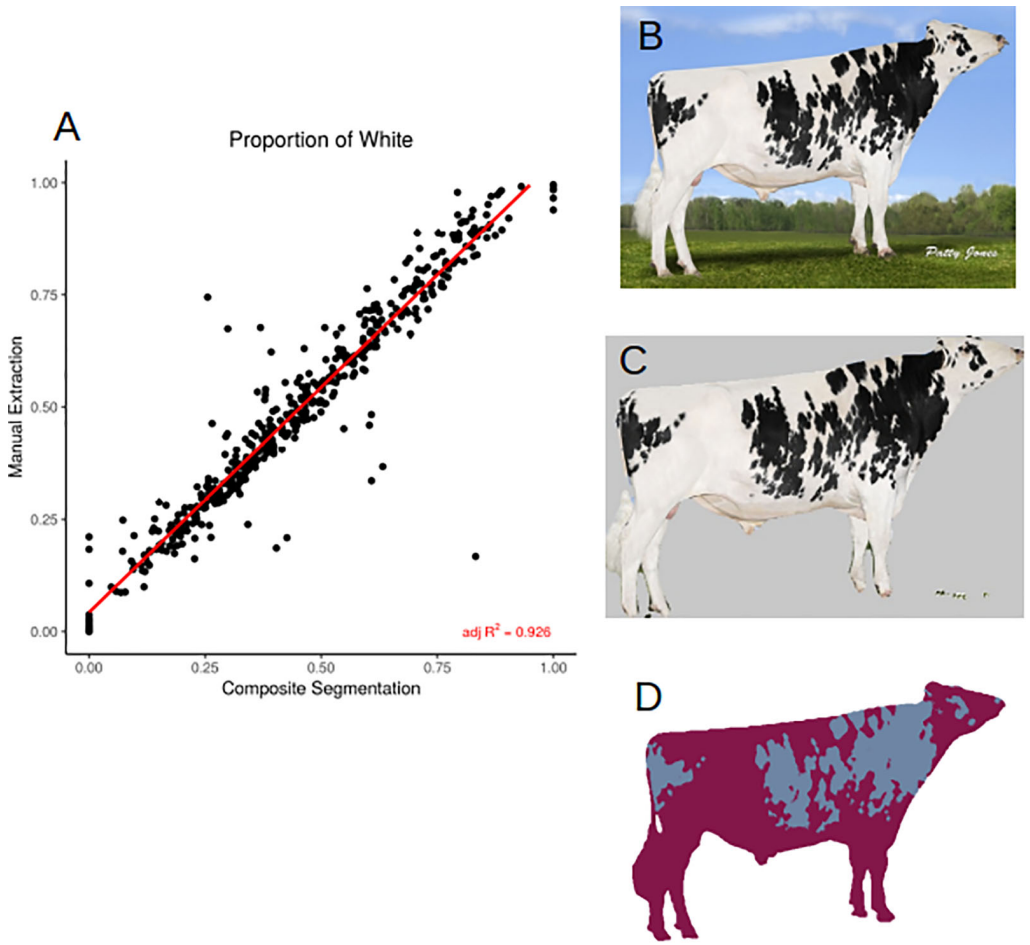

FIGURE 3 | (A) Correlation (adjusted R^2 = 0.926) between manual and automated color segmentation of 481 images. **(B)** Example input image. **(C)** Applied DeepAPS output mask. **(D)** Manual color segmentation. Image from Semex.

relatives' ids, we computed the standard numerator relationship matrix, which contains the genetic relationships assuming an infinitesimal model. Bayesian estimates of heritability were calculated with the R 3.5.2. (R Core Team, 2013) package BGLR (Perez and de los Campos, 2014) using default priors. One thousand Gibbs iterations were performed. Our sample sizes were N = 1,338 for proportion of white and N = 1,062 for morphological characteristics. The difference in sample size is due to removing any image with a missing coordinate.

Application to Other Datasets

To assess the applicability to other datasets, we chose two other objects that had been annotated in the COCO database (Lin et al., 2014), horse and giraffe, as well as two objects that had not been annotated, butterfly and duck. We downloaded 50 images from the internet that had the license set to "labeled for non-commercial reuse" for horse and giraffe and 100 images for butterfly and duck. For the unannotated objects we annotated 50 of the images using VGG Image Annotator (VIA; Dutta and Zissermann, 2019). These annotations were used to train a model in Mask R-CNN using the starting weights of the COCO database (Lin et al., 2014). The model was trained for 20 epochs and default parameters. Using either the COCO or custom model, DeepAPS was applied and the composite mask was visually assessed for accuracy.

RESULTS

We first visually compared the masks generated by the three methods that were applied to our entire dataset of 1,819 images (**Figure 2A**). When we used the supervised algorithm Mask R-CNN and applied the mask to the input images (**Figure 2B**), we observed in all cases parts of the cow body were removed along with the background (i.e., tail, nose, ear, and hoof). These masks are not satisfactorily precise to extract morphological measurements. The unsupervised segmentation by back propagation (**Figure 2C**) often separates the precise border between cow and background, but that this method on its own is not automated. Each output image would still need to be processed separately

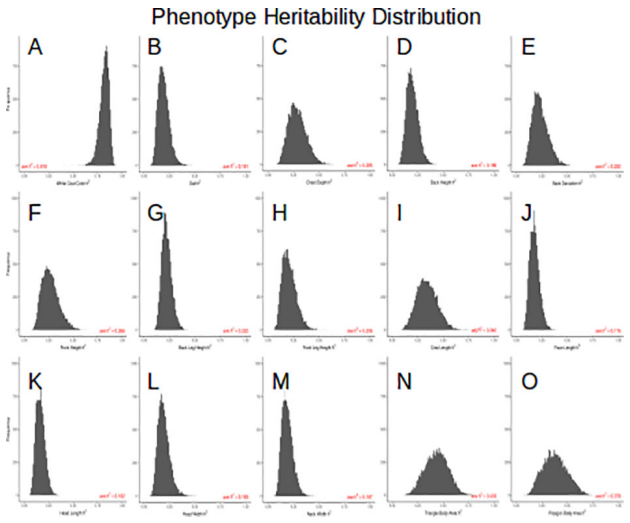

FIGURE 4 | (A) posterior h^2 distribution of the white coat color, **(B)** posterior h^2 distribution of the gait, **(C)** posterior h^2 distribution of the chest depth, **(D)** posterior h^2 distribution of the back height, **(E)** posterior h^2 distribution of the back deviation, **(F)** posterior h^2 distribution of the front height, **(G)** posterior h^2 distribution of the back leg height, **(H)** posterior h^2 distribution of the front leg height, **(I)** posterior h^2 distribution of the cow length, **(J)** posterior h^2 distribution of the face length, **(K)** posterior h^2 distribution of the head length, **(L)** posterior h^2 distribution of the head width, **(M)** posterior h^2 distribution of the neck width, **(N)** posterior h^2 distribution of the triangle body area, **(O)** posterior h^2 distribution of the polygon body area.

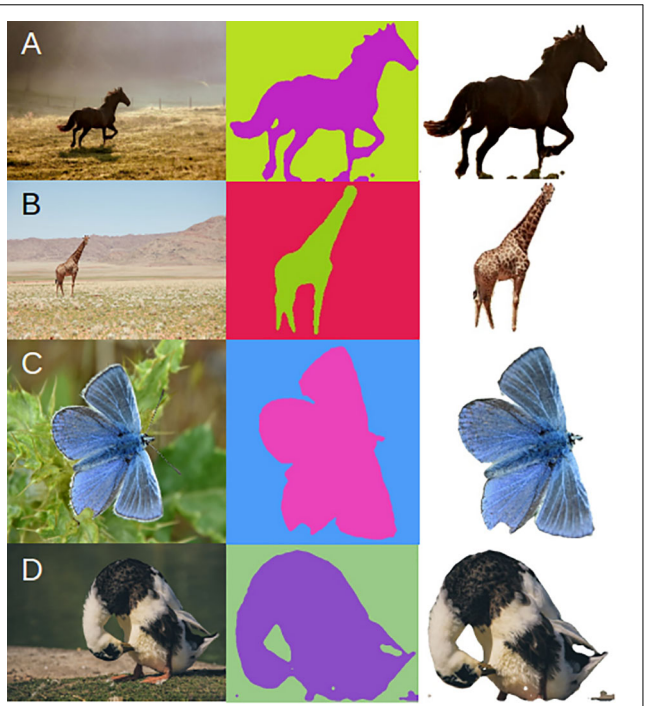

FIGURE 5 | Application of DeepAPS method to four additional datasets. **(A)** Horses and **(B)** Giraffes trained using the COCO database. **(C)** Butterflies and **(D)** Ducks trained using 50 custom annotations.

in order to match which body parts were grouped into each color cluster. DeepAPS (**Figure 2D**) across our input dataset produces a more accurate mask than Mask R-CNN and a fully automated mask, which the unsupervised approach fails to do.

In order to assess how accurately we were able to extract the true coat color percentage from each image, we compared manual and automated color segmentation. Our test set consists of 481 manually annotated images. After removing the background, we clustered each bull into one- or two-color components and extracted the percentage of dark and light colors in the coats. The automated method reports a highly accurate color segmentation with an adjusted R^2 = 0.926 (**Figure 3A**) when compared to manual segmentation (**Figures 3B–D**). The images that fall out as outliers belong to one of two groups, the majority of the outliers have small image sizes (less than 400 × 400 pixels), and therefore the quality was not sufficient to accurately separate the body into two color classes, the second group were bulls with a two-toned body color, in which the legs were of a different color than the body. In these cases, the algorithm has difficulty in separating the dark-colored legs from the dark background.

Because the mask recovered after using this composite method is so precise, we could extract coordinates of 13 points located around the outline of the cow body (**Figure 1G** and **Supplementary Figure S1**) which allowed for measurements of 14 body conformation distances (see **Supplementary Figure S2** for phenotypic distributions). Next, we estimated heritability using 1,338 images of related animals, in which we had partial information about great granddam, granddam, dam, bull, and daughter relationships. Our relationship matrix consists of 689 families, with an average of 2.6 individuals per family. **Figure 4** shows the 15 posterior distributions of the heritability calculations and lists average values. Coat color proportion has the highest calculated heritability h^2 = 0.82, followed by body area (triangle) h^2 = 0.43, body area (polygon) h^2 = 0.38, and cow body length h^2 = 0.34. These values are similar to previously published results (Hayes et al., 2010; Pritchard et al., 2013). These high heritability measurements indicate foremost that the meaningful genetic information can be quickly and easily extracted from imaging and pedigree data available online.

To assess whether this method is robust to the type and quality of the underlying data, we downloaded images from the internet of horse, giraffe, butterfly, and duck. These images were randomly collected, and we had no control over quality, size, lighting, or background. We also wanted to test how many input annotations are required to produce a robust mask using DeepAPS. Because the two-step method uses back propagation in order to refine the predicted mask generated from the machine learning algorithm, we hypothesized that fewer annotations would be needed. Therefore, we annotated 50 images for the butterfly and duck datasets, as they were not pre-annotated in the COCO database. We found that overall, our composite method preforms accurately (**Figure 5**). The masks generated from the thousands of annotations from the COCO dataset were precise

(**Figures 5A,B**), while those based on only 50 annotations were still far more accurate than using any currently available method (**Figures 5C,D**). These results together indicate this method is robust to input data and can still preform reliably despite being trained by few instances, making it a promising tool for automatic morphological analyses.

DISCUSSION

In recent decades, there have been vast improvements in molecular and statistical methods applied to animal and plant breeding. While modern livestock studies typically involve the analysis of entire genomes and/or vast number of polymorphic sites (Börner et al., 2012; Wiggans et al., 2017; Yin and König, 2019), high throughput phenotyping is lagging, especially in animal breeding. Often, phenotypic variation is explored today in the same manner as it was done decades ago, using simple quantifications such as length, number, categorical classifications, etc (Houle et al., 2010, 2011; Cole et al., 2011). Phenomics is extremely important in breeding programs in particular, as the desired outcome is a change in a phenotype. As phenotypes are formed by a complex process involving multiple genes, is dependent on the environment, and dynamic overtime, collecting multiple descriptive statistics can make relating genotype to phenotype more feasible and, importantly, more meaningful.

Images are among the easiest to collect data and are underutilized. Here we combine two of the state-of-the-art image analysis tools, the supervised Mask R-CNN (He et al., 2017) and unsupervised segmentation (Kanezaki, 2018) in order to automatically extract phenotypic measurements accurately. Not only can we create a precision mask but can cluster and segment the underlying colors and automatically measure body confirmation. Accurate image segmentation remains the most challenging part of computer vision. The ability of DeepAPS to separate the animal from multiple background types at the pixel level out preforms, for our purposes, the available algorithms currently published (Kanezaki, 2018; He et al., 2017).

The validity and speed of this method allows for multiple quantitative morphological traits to be implemented in breeding programs. Despite the success of ongoing dairy breeding programs (Wiggans et al., 2017), including more and accurately quantified measurements has the potential to result in further improvements (Goddard, 2009; Gonzalez-Recio et al., 2014). Furthermore, this method uses standard side-view stud images which are inexpensive to generate and store. Our presented method eliminates the high cost of phenotype collection while maintaining quality and can contribute to lowering the cost of conformational measurement collections.

Our analyses were performed on images scrubbed from the internet. As such, we had no control over backgrounds, lighting, image size, or quality. Despite the dynamic input data on which we tested DeepAPS, we were able to produce high quality masks and phenotypic measurements in most cases (**Figure 4**). Furthermore, the heritability rates we calculated from over 1,000 images of related individuals broadly agree with published results, indicating that our method accurately captures underlying information. Hayes et al., 2010) estimated heritability of coat color percentage by manual quantification and reported a heritability of $h^2 = 0.74$ in $N = 327$ bulls; remarkably, we found similar estimates ($h^2 = 0.81$), even if our pedigree information was quite incomplete. The reported heritability of back leg height is nearly identical to previous reports ($h^2 = 0.22$ vs. 0.21; Pritchard et al., 2013). Nevertheless, estimates of two other reported conformational heritabilities were somewhat lower: chest depth $h^2 = 0.28$ vs. 0.37 and height $h^2 = 0.27$ vs. 0.42 (Pritchard et al., 2013); perhaps because actual metrics analyzed here are not exactly those used in previous studies and because we cannot obtain absolute values (e.g., height in meters), since there is not a common scale across images. In all, this proof of concept shows how genetic parameters could be estimated using solely data that are already available on the web. For practical applications, more accurate estimates suitable for breeding programs could be obtained, e.g., combining SNP genotyping data with automatic image analyses from larger datasets.

While imaging data is fast and simple to collect as well as inexpensive to store, the most burdensome stage of image analysis is the generation of image annotations. We found that this method is able to leverage the publicly available COCO database and apply it to new and different problem sets. Allowing for the creation of an accurate object mask based only on a training set of 50 instances (**Figure 5**), which is remarkably low for any machine learning approach.

This method has the potential to allow for imaging data to be easily and quickly applied to high-throughput studies, which can be highly useful and improve extant breeding programs. We provide a combined deep learning algorithm that results in highly accurate segmentation of animal profiles, which is necessary for further processing in applications related to conformational measurements. Nevertheless, we are well aware that much work remains to be done in the area. For instance, software to accurately quantify a number of additional conformational features, such as udder metrics or movement, using different angle pictures or videos should be developed. Software should also be optimized for speed and be able to analyze high-resolution pictures.

DATA AVAILABILITY STATEMENT

The datasets generated for this study are available on request to the corresponding author.

AUTHOR CONTRIBUTIONS

MP-E conceived and supervised the research. JN and LZ performed the research and wrote the code. JN drafted the manuscript with contributions from the other authors.

FUNDING

LZ was supported by a Ph.D. grant from the Ministry of Economy and Science (MINECO, Spain), by the MINECO

grant AGL2016-78709-R to MP-E and from the EU through the BFU2016-77236-P (MINECO/AEI/FEDER, EU) and the "Centro de Excelencia Severo Ochoa 2016-2019" award SEV-2015-0533.

ACKNOWLEDGMENTS

We thank comments and suggestions from José Antonio Jiménez (CONAFE, Valdemoro, Spain) and Michael Louis from Semex.

SUPPLEMENTARY MATERIAL

The Supplementary Material for this article can be found online at: https://www.frontiersin.org/articles/10.3389/fgene.2020.00513/full#supplementary-material

FIGURE S1 | Description of the 14 extracted conformational traits.

FIGURE S2 | Phenotypic distributions for the 14 measured anatomical features (*N* = 1,062).

REFERENCES

Beer, G., Alsaaod, M., Starke, M., Schuepbach-Regula, G., Müller, H., Kohler, P., et al. (2016). Use of extended characteristics of locomotion and feeding behavior for automated identification of lame dairy cows. *PLoS One* 11:e0155796. doi: 10.1371/journal.pone.0155796

Boggess, M. V., Lippolis, J. D., Hurkman, W. J., Fagerquist, C. K., Briggs, S. P., Gomes, A. V., et al. (2013). The need for agriculture phenotyping: "Moving from genotype to phenotype". *J. Proteo.* 93, 20–39. doi: 10.1016/j.jprot.2013.03.021

Börner, V., Teuscher, F., and Reinsch, N. (2012). Optimum multistage genomic selection in dairy cattle. *J. Dairy Sci.* 95, 2097–2107. doi: 10.3168/jds.2011-4381

Bradski, G. (2000). The OpenCV library. *Dr. Dobbs J.* 120, 122–125.

Braun, U., Tschoner, T., and Hässig, M. (2014). Evaluation of eating and rumination behavior using a noseband pressure sensor in cows during the peripartum period. *BMC Vet. Res.* 10:195. doi: 10.1186/s12917-014-0195-6

Canny, J. (1986). A computational approach to edge detection. *IEEE T. Pattern Anal.* 8, 679–698.

Chapinal, N., de Passillé, A. M., Pastell, M., Hänninen, L., Munksgaard, L., and Rushen, J. (2011). Measurement of acceleration while walking as an automated method for gait assessment in dairy cattle. *J. Dairy Sci.* 94, 2895–2901. doi: 10.3168/jds.2010-3882

Chen, C. S., and Chen, W. C. (2019). Research and development of automatic monitoring system for livestock farms. *Appl. Sci.* 9:1132.

Cole, J. B., Wiggans, G. R., Ma, L., Sonstegard, T. S., Lawlor, T. J. Jr., Crooker, B. A., et al. (2011). Genome-wide association analysis of thirty-one production, health, reproduction and body conformation traits in contemporary U.S. Holstein cows. *BMC Genomics* 12:408. doi: 10.1186/1471-2164-12-408

Cortes, D. F. M., Catarina, R. S., Barros, G. B. D. A., Arêdes, F. A. S., da Silveira, S. F., Ferreguetti, G. A., et al. (2017). Model-assisted phenotyping by digital images in papaya breeding programs. *Sci. Agric.* 74, 294–302.

Dutta, A., and Zissermann, A. (2019). *The VIA Annotation Software for Images, Audio, and Video*. New York, NY: ACM.

Fahlgren, N., Gehan, M. A., and Baxter, I. (2015). Lights, camera, action: high-throughput plant phenotyping is ready for a close-up. *Curr. Opin. Plant Biol.* 24, 93–99. doi: 10.1016/j.pbi.2015.02.006

Foris, B., Thompson, A. J., von Keyserlingk, M. A. G., Melzer, N., and Weary, D. M. (2019). Automatic detection of feeding- and drinking-related agonistic behavior and dominance in dairy cows. *J. Dairy Sci.* 102, 9176–9186. doi: 10.3168/jds.2019-16697

Girshick, R. G. (2015). Fast R-CNN. *IEEE Comput. Soc. Conf. Comput. Vis.* 2015, 1440–1448.

Girshick, R. G., Donahue, J., Darrell, T., and Malik, J. (2014). "Rich feature hierarchies for accurate object detection and semantic segmentation," in *Proceedings of the 2014 IEEE Conference on Computer Vision and Pattern Recognition*, Columbus, OH, 580–587.

Goddard, M. (2009). Genomic selection: prediction of accuracy and maximization of long-term response. *Genetica* 136, 245–257. doi: 10.1007/s10709-008-9308-0

Gonzalez-Recio, O., Coffey, M. P., and Pryce, J. E. (2014). On the value of the phenotypes in the genomic era. *J. Dairy Sci.* 97, 7905–7915. doi: 10.3168/jds.2019-102-6-5764

Green, L. E., Borkert, J., Monti, G., and Tadich, N. (2010). Assocications between lesion-specific lameness and the milk yield of 1,635 dairy cows from seven herds in the Xth region of Chile and implications for management of lame dairy cows worldwide. *Anim. Welfare* 19, 419–427.

Gu, J., Wang, Z., Kuen, J., Ma, L., Shahroudy, A., Shuai, B., et al. (2018). Recent advances in convolutional neural networks. *Pat. Recognit.* 77, 354–377.

Guliński, P., Młynek, K., Litwińczuk, Z., and Dobrogowska, E. (2005). Heritabilities of genetic and phenotypic correlations between condition score and production and conformation traits in Black-and-White cows. *Anim. Sci. Pap. Rep.* 23, 33–41.

Guzhva, O., Ardö, H., Herlin, A., Nilsson, M., Åström, K., and Bergsten, C. (2016). Feasibility study for the implementation of an automatic system for the detection of social interactions in the waiting area of automatic milking stations by using a video surveillance system. *Comput. Elect. Agric.* 127, 506–509.

Han, J., Zhang, D., Cheng, G., Liu, N., and Xu, D. (2018). Advanced Deep-Learning techniques for salient and category-specific object detection: a survey. *IEEE Signal Process.* 35, 84–100.

Hayes, B. J., Pryce, J., Chamerlain, A. J., Bowman, P. J., and Goddard, M. E. (2010). Genetic architecture of complex traits and accuracy of genomic prediction: coat colour, milk-fat percentage, and type in Holstein Cattle as contrasting model traits. *PLoS Genet.* 6:e1001139. doi: 10.1371/journal.pgen.1001139

He, K., Gkioxari, G., Dollár, P., and Girshick, R. (2017). Mask R-CNN. *IEEE Int. Conf. Comput. Vis.* 2017, 2980–2988.

Houle, D., Govindaraju, D. R., and Omholt, S. (2010). Phenomics: the next challenge. *Nat. Rev. Genet.* 11, 855–866.

Houle, D., Pélabon, C., and Wagner, G. P. (2011). Measurement and meaning in biology. *Q. Rev. Biol.* 86, 3–34.

Kanezaki, A. (2018). Unsupervised image segmentation by backpropagation. *IEEE Int. Conf. Comput. Vis.* 1543–1547.

Kefauver, S. C., Vincente, R., Vergara-Díaz, O., Fernandez-Gallego, J. A., Kerfal, S., Lopez, A., et al. (2017). Comparative UAV and field phenotyping to assess yield and nitrogen use efficiency in hybrid and conventional barley. *Front. Plant Sci.* 8:1733. doi: 10.3389/fpls.2017.01733

Lin, T. Y., Maire, M., Belongie, S., Bourdev, L., Girshick, R., Hays, J., et al. (2014). "Microsoft COCO: common objects in context," *Computer Vision – ECCV 2014*, eds D. Fleet, T. Pajdla, B. Schiele, and T. Tuytelaars (Cham: Springer), 740–755.

Mingoas, K. J. P., Awah-Ndukum, J., Dakyang, H., and Zoli, P. A. (2017). Effects of body conformation and udder morphology on milk yield of zebu cows in North region of Cameroon. *Vet. World* 10, 901–905. doi: 10.14202/vetworld.2017.901-905

Ouellet, V., Vasseur, E., Heuwieser, W., Burfeind, O., Maldague, X., and Charbonneau, É (2016). Evaluation of calving indicators measured by automated monitoring devices to predict the onset of calving in Holstein dairy cows. *J. Dairy Sci.* 99, 1539–1548. doi: 10.3168/jds.2015-10057

Palombi, C., Paolucci, M., Stradaioli, G., Corubolo, M., Pascolo, P. B., and Monaci, M. (2013). Evaluation of remote monitoring of parturition in dairy cattle as a new tool for calving management. *BMC Vet. Res.* 9:191. doi: 10.1186/1746-6148-9-191

Pedregosa, F., Varoquaux, G., Gramfort, A., Michel, V., Thirion, B., Grisel, O., et al. (2011). Scikit-learn: machine learning in python. *J. Mach. Learn. Res.* 12, 2825–2830.

Perez, P., and de los Campos, G. (2014). Genome-wide regression and prediction with the BGLR statistical package. *Genetics* 198, 483–495. doi: 10.1534/genetics.114.164442

Pritchard, T., Coffey, M., Mrode, R., and Wall, E. (2013). Genetic parameters for production, health, fertility and longevity traits in dairy cows. *Animal* 7, 34–46. doi: 10.1017/S1751731112001401

R Core Team (2013). *R: A Language and Environment for Statistical Computing*. Vienna: R Foundation for Statistical Computing.

Rahaman, M. M., Chen, D., Gillani, Z., Klukas, C., and Chen, M. (2015). Advanced phenotyping and phenotype data analysis for the study of plant growth and development. *Front. Plant Sci.* 6:619. doi: 10.3389/fpls.2015.00619

Ren, S., He, K., Girshick, R., and Sun, J. (2015). Faster R-CNN: towards real-time object detection with region proposal networks. *NeuralPS* 39, 91–99. doi: 10.1109/TPAMI.2016.2577031

Richardson, L. (2007). *Beautiful Soup Documentation*. Available online at: http://citebay.com/how-to-cite/beautiful-soup/

Rosero, A., Granada, L., Pérez, J. L., Rosero, D., Burgos-Paz, W., Martínez, R., et al. (2019). Morphometric and colurimetric tools to dissect morphological diversity: an application in sweet potato. *Genet. Resour. Crop Evol.* 66, 1257–1278.

Sawa, A., Bogucki, M., Krêñel-Czopek, S., and Neja, W. (2013). Relationship between conformational traits and lifetime production efficiency of cows. *ISRN Vet. Sci.* 2013:124690.

Sogstad, ÅM., Østerås, O., and Fjeldaas, T. (2006). Bovine claw and limb disorders related to reproductive performance and production diseases. *J. Dairy Sci.* 89, 2519–2528. doi: 10.3168/jds.S0022-0302(06)72327-X

Song, X., Bokkers, E. A. M., van der Tol, P. P. J., Groot Koerkamp, P. W. G., and van Mourik, S. (2018). Automated body weight prediction of dairy cows using 3-dimensional vision. *J. Dairy Sci.* 101, 4448–4459. doi: 10.3168/jds.2017-13094

Tardieu, F., Cabrera-Bosquet, L., Pridmore, T., and Bennett, M. (2017). Plant phenomics, from sensors to knowledge. *Curr. Biol.* 27, R770–R783. doi: 10.1016/j.cub.2017.05.055

Van Hertem, T., Alchanatis, V., Antler, A., Maltz, E., Halachmi, I., Schlageter-Tello, A., et al. (2013). Comparison of segmentation algorithms for cow contour extraction from natural barn background in side-view images. *Comput. Electron. Agr.* 91, 65–74.

van Rossum, G. (1995). *Centrum voor Wiskunde en Informatica*. Python tutorial, technical report CS-R9526. Amsterdam: University of Amsterdam.

Wiggans, G. R., Cole, J. B., Hubbard, S. M., and Sonstegard, T. S. (2017). Genomic selection in dairy cattle: the USDA experience. *Annu. Rev. Anim. Biosci.* 5, 309–327. doi: 10.1146/annurev-animal-021815-111422

Yin, T., and König, S. (2019). Genome-wide associations and detection of potential candidate genes for direct genetic and maternal genetic effects influencing dairy cattle body weight at different ages. *Genet. Select. Evol.* 51:4. doi: 10.1186/s12711-018-0444-4

Zehner, N., Niederhauser, J. J., Schick, M., and Umstatter, C. (2019). Development and validation of a predictive model for calving time based on sensor measurements of ingestive behavior in dairy cows. *Comput. Electron. Agric.* 161, 62–71.

Zhang, S., Huang, W., and Zhang, C. (2018). Three-channel convolutional neural networks for vegetable leaf disease recognition. *Cogn. Syst. Res.* 53, 31–41.

Conflict of Interest: The authors declare that the research was conducted in the absence of any commercial or financial relationships that could be construed as a potential conflict of interest.

frontiers in Veterinary Science

ORIGINAL RESEARCH
published: 02 June 2020
doi: 10.3389/fvets.2020.00251

Rumen Microbiota Distribution Analyzed by High-Throughput Sequencing After Oral Doxycycline Administration in Beef Cattle

Fengmei Chen[1], *Guangmin Cheng*[1], *Yulin Xu*[2,3,4,5], *Yunzhou Wang*[1], *Qingxiang Xia*[1] and *Shilin Hu*[1]*

[1] Shandong Research Center for Technology of Reduction of Antibiotics Administered to Animal and Poultry, Shandong Vocational Animal Science and Veterinary College, Weifang, China, [2] Comparative Medicine Research Institute, Yangzhou University, Yangzhou, China, [3] College Veterinary Medicine, Yangzhou University, Yangzhou, China, [4] Jiangsu Co-innovation Center for Prevention and Control of Important Animal Infectious Diseases and Zoonoses, Yangzhou, China, [5] Joint International Research Laboratory of Agriculture and Agri-Product Safety, Yangzhou University, Yangzhou, China

OPEN ACCESS

Edited by:
Guilherme J. M. Rosa, University of Wisconsin-Madison, United States

Reviewed by:
Chunping Zhao, Northwest A&F University, China
Filippo Biscarini, National Research Council (CNR), Italy

***Correspondence:**
Shilin Hu
sdmxhsl@163.com;
13563600485@163.com

Specialty section:
This article was submitted to Livestock Genomics, a section of the journal Frontiers in Veterinary Science

Received: *16 October 2019*
Accepted: *16 April 2020*
Published: *02 June 2020*

Citation:
Chen F, Cheng G, Xu Y, Wang Y, Xia Q and Hu S (2020) Rumen Microbiota Distribution Analyzed by High-Throughput Sequencing After Oral Doxycycline Administration in Beef Cattle. Front. Vet. Sci. 7:251. doi: 10.3389/fvets.2020.00251

The beef cattle rumen is a heterogenous microbial ecosystem that is necessary for the host to digest food and support growth. The importance of the rumen microbiota (RM) is also widely recognized for its critical roles in metabolism and immunity. The level of health is indicated by a dynamic RM distribution. We performed high-throughput sequencing of the bacterial 16S rRNA gene to compare microbial populations between rumens in beef cattle with or without doxycycline treatment to assess dynamic microbiotic shifts following antibiotic administration. The results of the operational taxonomic unit analysis and alpha and beta diversity calculations showed that doxycycline-treated beef cattle had lower species richness and bacterial diversity than those without doxycycline. Bacteroidetes was the predominant phylum in rumen samples without doxycycline, while Proteobacteria was the governing phylum in the presence of doxycycline. On the family level, the top three predominant populations in group qlqlwy (not treated with doxycycline) were Prevotellaceae, Lachnospiraceae, and Ruminococcaceae, compared to Xanthomonadaceae, Prevotellaceae, and Rikenellaceae in group qlhlwy (treated with doxycycline). At the genus level, the top predominant population in group qlqlwy was unidentified_Prevotellaceae. However, in group qlhlwy, the top predominant population was Stenotrophomonas. The results revealed significant RM differences in beef cattle with or without doxycycline. Oral doxycycline may induce RM composition differences, and bacterial richness may also influence corresponding changes that could guide antibiotic use in adult ruminants. This study is the first to assess microbiota distribution in beef cattle rumen after doxycycline administration.

Keywords: beef cattle, rumen microbiota, doxycycline, MiSeq sequencing, dysbacteriosis, oral antibiotics, bacterial richness

HIGHLIGHTS

- This is the first study of cattle rumen microbiota after doxycycline treatment.
- Doxycycline-treated beef cattle have lower species richness and diversity.
- Bacteroidetes was the most dominant phylum in untreated rumen samples.
- Proteobacteria was the governing phylum in the presence of doxycycline.

INTRODUCTION

Ruminants convert human-inedible plant biomass into meat and dairy products with high nutritional value. However, recent studies reported that the gastrointestinal tract (GIT) microbiome plays a major role in the health, physiology, and production traits of ruminants. The rumen is an important digestive organ in ruminants and home to one of the most complex microbial communities, which has long attracted the interest of microbiologists. This organ is rich in bacteria, fungi, and ciliates that ferment forage grass to form volatile fatty acids (VFAs) and microbial proteins (MPs) that provide nutrients for the growth, development, and production of ruminants. The main members of the rumen microbiota (RM) are now well understood. Bacteria account for most species and are geographically widespread in many ruminants and individual animals (1). Ciliate protozoa, which account for up to half of the biomass, are composed of species unique to the rumen (2). The number of anaerobic fungi is relatively small but seems to play an important role in digesting the cell walls of plants that are difficult to break down (3). Archaea are major contributors to methane emissions (4). The RM enhances fiber digestibility, decreases methane emissions, improves the efficiency of nitrogen usage, and also helps explain differences in nutrient digestibility or feed efficiency among animals fed with the same diet. Physiologists and nutritionists have described the rumen's key role in digesting fiber feed and providing nutrition to host animals (5). The intestinal microbiota of beef cattle is also a complex microecosystem. It plays important roles in host material metabolism, immune regulation, biology barriers, and host defense. The number of bacteria in the hindgut system is similar to that in the rumen, and the dominant bacteria in several RM also appear in the normal microbiota of the ruminant large intestine. Characterizing, quantifying, and understanding the role of the RM therefore have significant scientific, economic, and environmental significance. Recent investigations using omics-based approaches reported that RM differences in cattle are associated with production efficacy and health traits. Most RM studies have focused on the microecosystem (6–8). Some have shown that season, animal species, age, diet structure, and other factors can all affect RM (9, 10). However, there are fewer studies on the effect of antibiotics on RM.

16S rRNA sequencing is a quick and easy way to explore the relationship between RM characteristics and animal health (11, 12). It is a validated, rapid, cost-effective approach for analyzing microbial communities and their relevance to environmental factors (13, 14). This technology has been successfully applied to analyze complex bacterial ecosystems in the gut (15).

The discovery and subsequent widespread use of antibiotics controlled infection, saving countless lives, and it played an important role in the prevention and treatment of animal infectious diseases. However, the harm caused by abuse and overuse has attracted wide concern. An imbalance between RM and intestinal microbiota is one of the main adverse reactions, with physiological bacteria greatly reduced and pathogenic bacteria multiplying. Studies have shown that dysbacteriosis (changes in bacterial composition) can lead to the development of digestive, endocrine, psychiatric, systemic, autoimmune, and some infectious diseases (16–20). Ruminants have been recognized as a potential reservoir of antibiotic-resistance genes (21). In addition, including antimicrobials in ruminant diets can select for resistant organisms, potentially modifying the autochthonous RM (22). Doxycycline is a member of the tetracycline class with improved stability and pharmacological efficacy compared to traditional tetracycline (23). This highly effective antibacterial drug has a wide range of applications, good bioavailability, and a few serious adverse events (24). It is mainly used to treat respiratory, urinary, and biliary tract infections caused by sensitive bacteria. Doxycycline is commonly employed in dairy farming and has been used in human and veterinary medicine to fight bacterial infections and promote the growth of food-producing animals, improving feed efficiency and animal performance (25).

Some farmers in China inappropriately give antibiotics to ruminants by oral administration, which can lead to adverse events such as anorexia, belching, regurgitation, severe diarrhea, and even death. This study was conducted to explore the effects of oral antibiotics on the RM. It was designed to assess the distribution and richness of bacterial microbiota in the rumen of beef cattle before and after taking doxycycline. The results show significant RM differences in beef cattle depending on doxycycline administration. Oral doxycycline may alter the RM composition, and bacterial richness may influence corresponding changes that could provide a theoretical basis for the rational and correct use of antibiotics in adult ruminants.

METHODS

Ethics Statement

All the cows used in this study were treated according to relevant national and international guidelines, and all efforts were made to minimize suffering. The study protocol was approved by the Animal Ethics Committee of Shandong Vocational Animal Science and Veterinary College. No endangered or protected species were involved.

Animals and Sample Collection

Six healthy, 20-month-old, male Simmental cattle were randomly selected from a beef cattle farm in Shandong province. Animals were kept according to standard beef cattle management methods and fed under standard livestock management practices. The diet feed formulations are shown in **Table 1**. Three heads were in the experimental group, and three heads served as the control

TABLE 1 | Beef cattle diet feed formulations.

Raw material	Ratio (%)
Corn	25.6
Soybean meal	7.15
Bran	6.25
Palm meal	8.25
Corn husk	5.5
Vinasse	5.5
Hay meal	8.7
Silage from whole plants	30.5
Premix	1.25
Salt	0.6
Calcium carbonate	0.7
Total	100
Dietary nutrient content	
Dry matter %	70.26
RND/kg	6.32
Crude protein %	12.27
Calcium %	0.67
Phosphorus %	0.34

RND (beef cattle energy unit) is the calculated value, other components are measured values.

group. The experimental group was fed with doxycycline 20 mg/kg dissolved in 500 ml of 0.9% sodium chloride solution every morning for 6 days. The control group was given 0.9% sodium chloride solution daily. Data show that the feed stays in the rumen for 20–48 h, and the entire digestive process is 40–70 h. After continuous ingestion for 6 days and 2 h after feeding, the rumen contents had undergone at least two cycles. Samples were collected on the seventh day to better assess the effect of doxycycline on multi-rumen microorganisms. On the seventh day, 50-ml rumen fluid samples were collected by inserting a gastric catheter orally after feeding 2 h; they were transported to the laboratory on ice within 2 h and stored at −80°C.

DNA Extraction, Amplification, and Sequencing

Genomic DNA was extracted with a TIANamp Genomic DNA Kit (TIANGEN Bio-Tek Co. Ltd., Beijing, China) according to the manufacturer's instructions, and each sample extract was purified with a GeneJET^{TM} Gel Extraction Kit (Thermo Fisher Scientific, Waltham, MA, USA). Generation sequencing library preparation and Illumina MiSeq sequencing were subsequently conducted at Novogene, Inc. (Beijing, China). The 16S rRNA genes of distinct regions (16S V4/16S V3/16S V3-V4/16S V4-V5) were amplified using a specific primer (16S V4: 515F-806R) with the barcode. All polymerase chain reaction (PCR) experiments were performed in 30-μl volumes: 15 μl of Phusion® High-Fidelity PCR Master Mix (New England Biolabs, Ipswich, MA, USA), 0.2 μM of forward and reverse primers, and 10-ng template DNA. Initial denaturation was performed for 1 min at 98°C followed by 30 denaturation cycles at 98°C for 10 s, annealing at 50°C for 30 s, and elongation at 72°C for 30 s. Then samples were held at 72°C for 5 min. In addition to the 16S target-specific sequence, we generated sequencing libraries with Ion Plus Fragment Library Kit 48 rxns (Thermo Fisher Scientific) following the manufacturer's protocol. Library quality was assessed with a Qubit@ 2.0 Fluorometer (Thermo Fisher Scientific). The library was sequenced on an Ion S5 TM XL platform that generated 400-/600-bp single-end reads. The V3, V4, and V5 sequences were processed, spliced, and analyzed by Novogene, Inc.

Bioinformatics and Statistical Analysis

Single-end reads were assigned based on their unique barcode and truncated by removing the barcode and primer sequence. Quality filtering on raw reads was done under specific filtering conditions to generate high-quality clean reads according to the Cutadapt (26) (V1.9.1, http://cutadapt.readthedocs.io/en/stable/) quality-controlled process. The sample data were separated from the reads obtained according to Barcode, and the Barcode and primer sequences were cut to obtain the original data (raw reads). The reads obtained with the above process still contained chimera sequences. The reads sequence was compared with the species annotation database (https://github.com/torognes/vsearch/) (27) to detect the chimera sequence, which was then removed to obtain the final valid data (clean reads) (28). These were compared with the Silva reference database (https://www.arb-silva.de/) (29) using the UCHIME algorithm (http://www.drive5.com/usearch/manual/uchime_algo.html) (30) to detect chimeric sequences, which were removed (31) to produce clean reads. High-quality sequences were binned into operational taxonomic units (OTUs) with Uparse software (Uparse v7.0.1001, http://drive5.com/uparse/) (32) at a 97% sequence identity threshold. The SSUrRNA of the Silva132 database (https://www.arb-silva.de/) (29, 32) was used based on the Mothur algorithm to annotate taxonomic information for each representative sequence. To study phylogenetic relationships of different OTUs and identify dominant species in samples (groups), we conducted multiple sequence alignment with MUSCLE software (Version 3.8.31, http://www.drive5.com/muscle/) (33). Finally, the data of each sample were homogenized, and those with the least amount of data in the sample were homogenized using a process provided in a script from Novogene, Inc. (there is no specific software). The homogenization process is necessary due to the inconsistency of sequencing depth and the number of sequences between samples. To minimize experimental and human statistical error, we need to set the sequence number of each sample at the same depth level, especially for the comparative analysis between samples. The homogenization method is to set a threshold value (sample with the lowest sequence number), then randomly selected sequence bars set by the threshold value are chosen from the sample for further analysis.

The total number of sequences used to compare each sample is the same, so the relative abundances of species in each sample can be compared. For example, in the following table in the text, the total number of sequences Total_tag minus Uniq_tag

is the final number of sequences used for species annotation (Tax_tag+Unclassified_tag). Among them, sampled B1 had the lowest number of sequences at 40,518.

#OTU_num	qlqlwy1	qlqlwy2	qlqlwy3	qlhlwy1	qlhlwy2	qlhlwy3
#Total_tag	71551	80159	62353	70003	65758	66571
#Uniq_tag	28559	39641	21461	18986	16687	20805
#Tax_tag	42992	40518	40892	51017	49071	45766
#Unclassified_tag	0	0	0	0	0	0
#Tax_tag + #Unclassified_tag	42992	40518	40892	51017	49071	45766

Subsequent analyses of alpha and beta diversity were performed based on these normalized output data. Alpha diversity analysis included the Shannon index, the abundance-based coverage estimator (ACE), and Chao1. Good's coverage index is obtained by adding the number of OTUs with only one sequence and the total number of sequences appearing in the sample in the calculation, so it relatively reflects the sequencing depth of the sample. Beta diversity included both the weighted and unweighted UniFrac values as calculated with QIIME software (Version 1.7.0). Principal component analysis (PCA) was applied to reduce the dimensions of the OTU counts original variables using the FactoMineR and ggplot2 packages in R software (Version 2.15.3). The difference matrixes of OTU abundance of both groups of samples were visualized by principal coordinate analysis (PCoA) to identify principal coordinates and visualize complex, multidimensional data. The distance matrixes of weighted or unweighted UniFrac values were transformed to a new set of orthogonal axes, by which the maximum variation factor is demonstrated by first principal coordinate, the second maximum factor by the second principal coordinate, etc. The PCoA results were displayed with the WGCNA, stat, and ggplot2 packages in R software (Version 2.15.3). To assess similarity between two groups of samples, a tree was constructed by clustering. In environmental biology, UPGMA (Unweighted Pair-group Method with Arithmetic Mean) is a commonly used cluster analysis method that was first used to solve the classification problem. The basic concept of UPGMA is as follows. Identify the two samples with the smallest distance and form a new node (new sample) with a branch point located at half the distance between the two samples; then calculate the new average distance between the "sample" and other samples, and then find the smallest two samples for clustering. This process is repeated until all the samples come together in a complete clustering tree. UPGMA cluster analysis is performed using weighted and unweighted UniFrac distance matrixes, and the clustering results are integrated with the relative abundance of species at the gate level for each sample. UPGMA clustering was carried out as a form of hierarchical clustering to interpret the distance matrix using average linkage in QIIME software (Version 1.7.0). ANOSIM is the analysis of similarity; this nonparametric test is used to examine whether the difference between groups is significantly greater than the difference within groups to determine if there is clear clustering from the analysis of the distance matrix (34).

The size of the intragroup differences can be used to determine whether the grouping is meaningful and to test inter- and intragroup differences between two groups or among more groups. ANOSIM uses the R vegan package (ANOSIM function) based on the Bray–Curtis distance value. The ANOSIM results showed that the R-value was between −1 and 1.

$$R = \frac{r_b - r_w}{\frac{1}{4}[n(n-1)]}$$

where r_b is the mean rank of between group dissimilarities, r_w is the mean rank of within group dissimilarities, and n is the number of samples.

An $R > 0$ indicates that the similarity within groups is lower than the similarity between groups. An $R < 0$ indicates that the similarity between groups is lower than that within groups. Significance testing was performed to identify differences between groups, which were considered significant at $P < 0.05$. Data are given as mean ± standard deviation (SD) and were analyzed with SPSS 17.0 software (SPSS Inc., Chicago, IL, USA).

RESULTS AND DISCUSSION

Microbial Diversity Index Analysis of Rumens With or Without Doxycycline

Rumen contents were collected for high-throughput sequencing to assess bacterial community composition in rumens of beef cattle with or without oral doxycycline. To study the species composition of each sample, we included OTUs with 97% identity on the valid labels of all samples, clustered the OTUs, and then annotated the OTU sequences. The 97% identity value refers to the comparison between the read and reference sequences. An OTU is defined as a read with 97% nucleotide sequence identity. Based on 97% species similarity, 1,047 and 590 OTUs were obtained from samples from the qlqlwy and qlhlwy groups, respectively. Among all samples, there were 1,073 OTUs, of which 564 in both groups were defined as core OTUs (52.56% of all OTUs, **Figure 1G**). The representative sequence was selected by removing the effective tags, and the singletons were arranged according to the abundance and clustered according to 97% similarity. The representative sequence is the one with the highest frequency. In addition, 26 OTUs were uniquely identified only in group qlhlwy.

Bacterial diversity and richness (alpha diversity measurements) were assessed with the Shannon index, Chao1, ACE, and Good's coverage. Good's coverage for each sample was >99.75% (**Figure 1B**), demonstrating that the 16SrDNA sequences in these samples represent most bacteria present. The highest microbial richness was in the rumens without doxycycline; the average Chao1 index was 899.17 (**Figure 1D**), and the average ACE index was 862.011 (**Figure 1A**). The richness of rumens from cattle treated with doxycycline was lower than in those without doxycycline, and the average Chao1

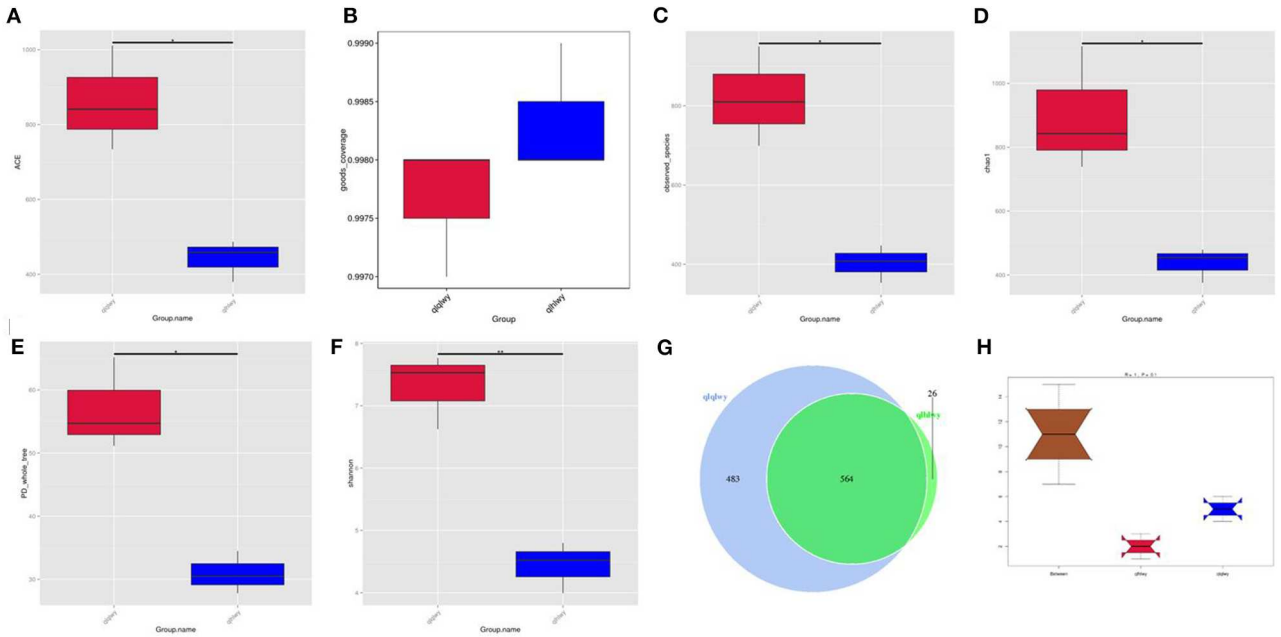

FIGURE 1 | Collation results of DNA sequence data and microbial diversity index analyses. **(A)** ACE index, **(B)** Good's coverage index, **(C)** observed species index, **(D)** PD whole tree, **(E)** Chao1 index, **(F)** Shannon index, **(G)** Venn diagram. The numbers represent the unique or common OTUs of each group. **(H)** ANOSIM analysis. "Between" represents the difference between groups; an R-value closer to 1 indicates greater difference. "qlqlwy" and "qlhlwy" represent the two groups.

and ACE indexes were 436.38 and 441.65 (**Figures 1A,D**), respectively. Similarly, the Shannon indexes in rumen samples from untreated and treated cattle were 7.312 and 4.437, respectively (**Figure 1F**). Moreover, the observed species and phylogenetic diversity (PD) whole tree of rumens were more abundant in the untreated group (**Figures 1C,E**). Consistently, the rumen of doxycycline-treated cattle had lower Simpson diversity index values. Furthermore, ANOSIM results showed that between-group differences were greater than those within groups ($R = 1$, $P = 0.1$; **Figure 1H**). For community richness comparisons, both ACE and Chao1 showed that the rumens of untreated cattle contained significantly more observed and estimated OTUs than doxycycline-treated cows. This result demonstrates that doxycycline reduces bacterial diversity and abundance in the rumen of beef cattle.

Beta-Diversity Analysis of the Microbial Communities of Rumens With or Without Doxycycline

The relationships between the community structures of beef cattle RM were examined using PCoA. The UniFrac distance matrix revealed clear differences among all individual samples and groups. The microbiota in each group were clustered. **Figures 2A,B** depict the weighted and unweighted UniFrac distances of PCoA analyses, respectively, and show that the RM of doxycycline-treated cattle were distinct from untreated samples. The relationships among community structures as revealed by PCoA were further examined by assessing between-group weighted UniFrac distances and the UPGMA tree. Consistent with the PCoA plot, the UPGMA tree showed significantly different microbial community structures between groups qlqlwy and qlhlwy for weighted UniFrac distance (**Figure 2C**) but not unweighted Unifrac distance (**Figure 2D**).

A rank abundance curve was generated to further demonstrate species abundance and evenness. In group qlqlwy RM samples, the OTU ranks were ∼800 more than those of group qlhlwy, which were close to 400 (**Figure 3B**), indicating less abundant species compositions in group qlhlwy samples. All curves were relatively flat, indicating relative uniform species compositions for all samples (**Figure 3A**). These curves tend to be flat when the number of effective sequences reaches 30,000. The number of valid sequences of each sample was >40,000, which indicated sufficient sequencing data.

Bacterial Community Composition at Different Taxonomical Levels

We next analyzed rumen bacterial community composition and structure by taxonomical level. According to the phylum assignment result, Bacteroidetes was the predominant phylum in group qlqlwy samples, whereas Proteobacteria was the governing phylum in group qlhlwy. Firmicutes and Bacteroidetes were the secondary phyla for groups qlqlwy and qlhlwy, respectively (**Figure 4A**). Bacterial abundance was also analyzed for family (**Figure 4B**) and genus (**Figure 4C**). On the family level, there were significant between-group differences. The

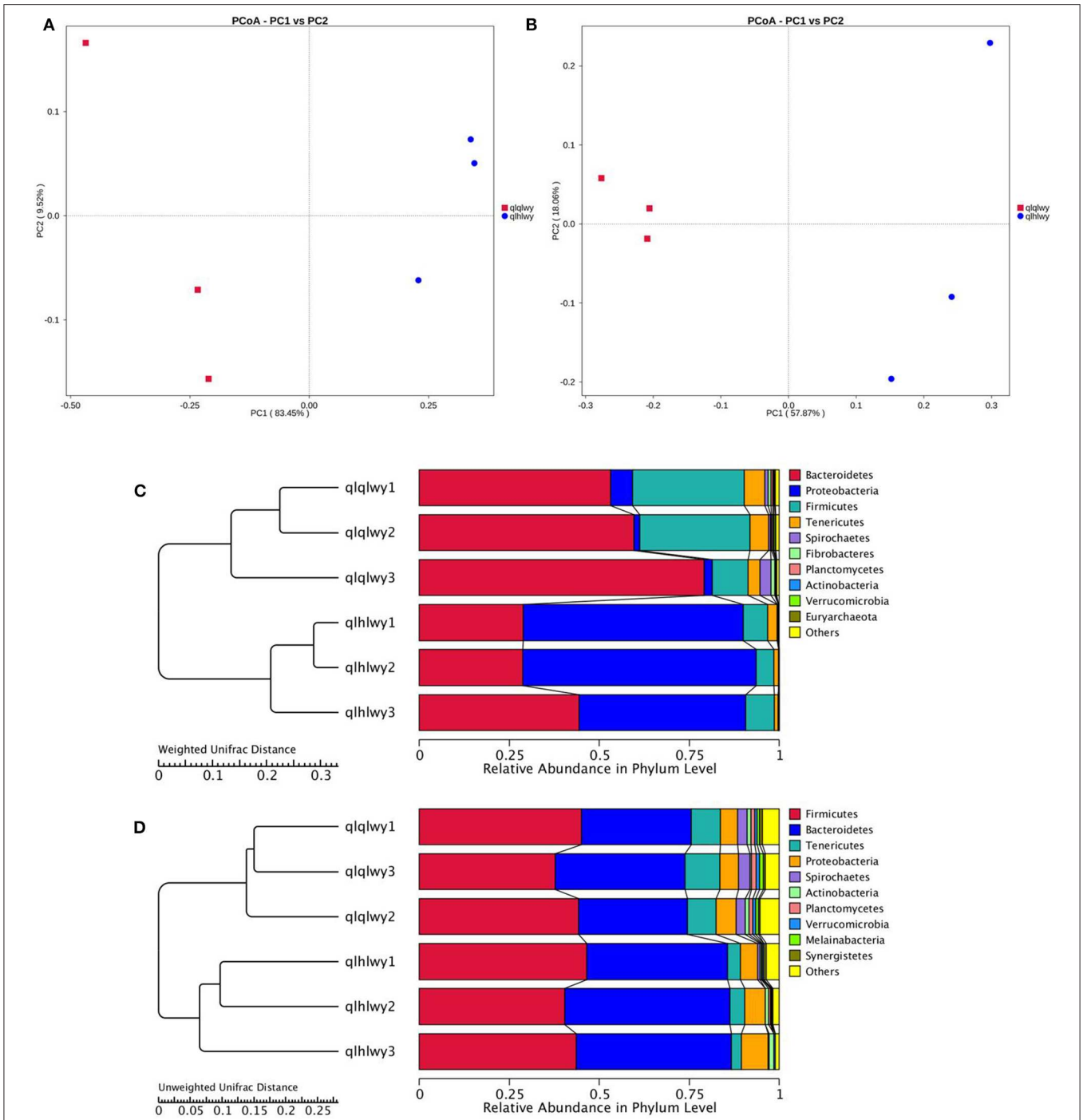

FIGURE 2 | Differences in bacterial community structures and relationships among all samples. **(A,B)** PCoA of bacterial community structures of the RM in the three sample groups. Each blue point represents a sample. The distance between two points represents the difference of RM. PCoA shows distinct bacterial communities between different samples. **(C)** The UPGMA tree analysis of samples in evolution in weighted unifrac distance. **(D)** The UPGMA tree analysis of samples in evolution in unweighted unifrac distance.

top three predominant populations in group qlqlwy were Prevotellaceae, Lachnospiraceae, and Ruminococcaceae, compared to Xanthomonadaceae, Prevotellaceae, and Rikenellaceae for group qlhlwy (**Figure 4B**). At the genus level, there were also significant differences among three samples from two groups. The top predominant population in group qlqlwy was unidentified_Prevotellaceae. However, in group qlhlwy, the most common genus was Stenotrophomonas

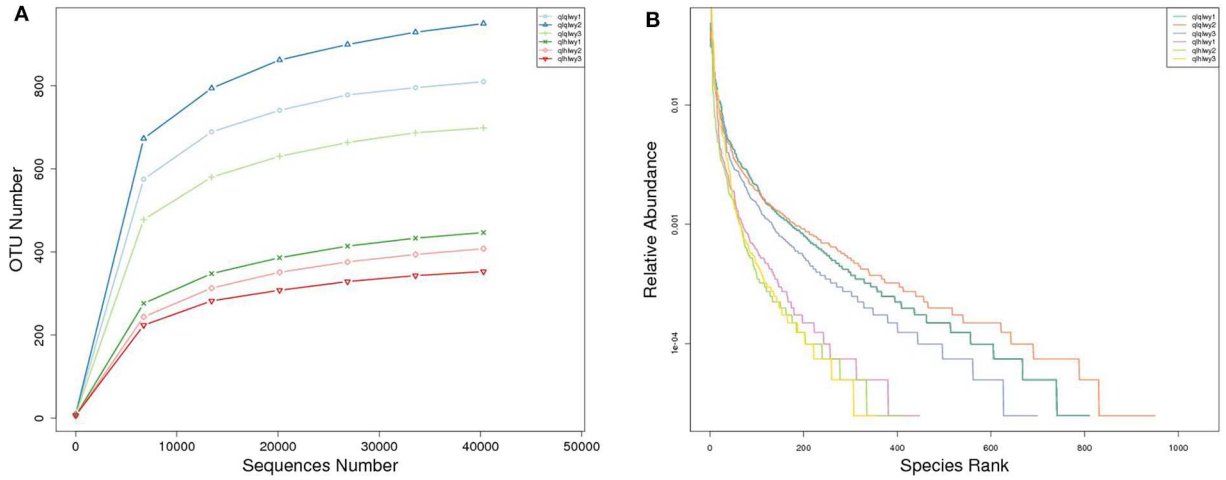

FIGURE 3 | Sample feasibility analysis. Each curve represents a sample. **(A)** Rarefaction curves depicting the effect of sequences on the number of identified OTUs in the rank abundance curve. **(B)** The abscissa indicates the OTU (species) abundance order, and the ordinate corresponds to the relative abundance ratio of OTU (species).

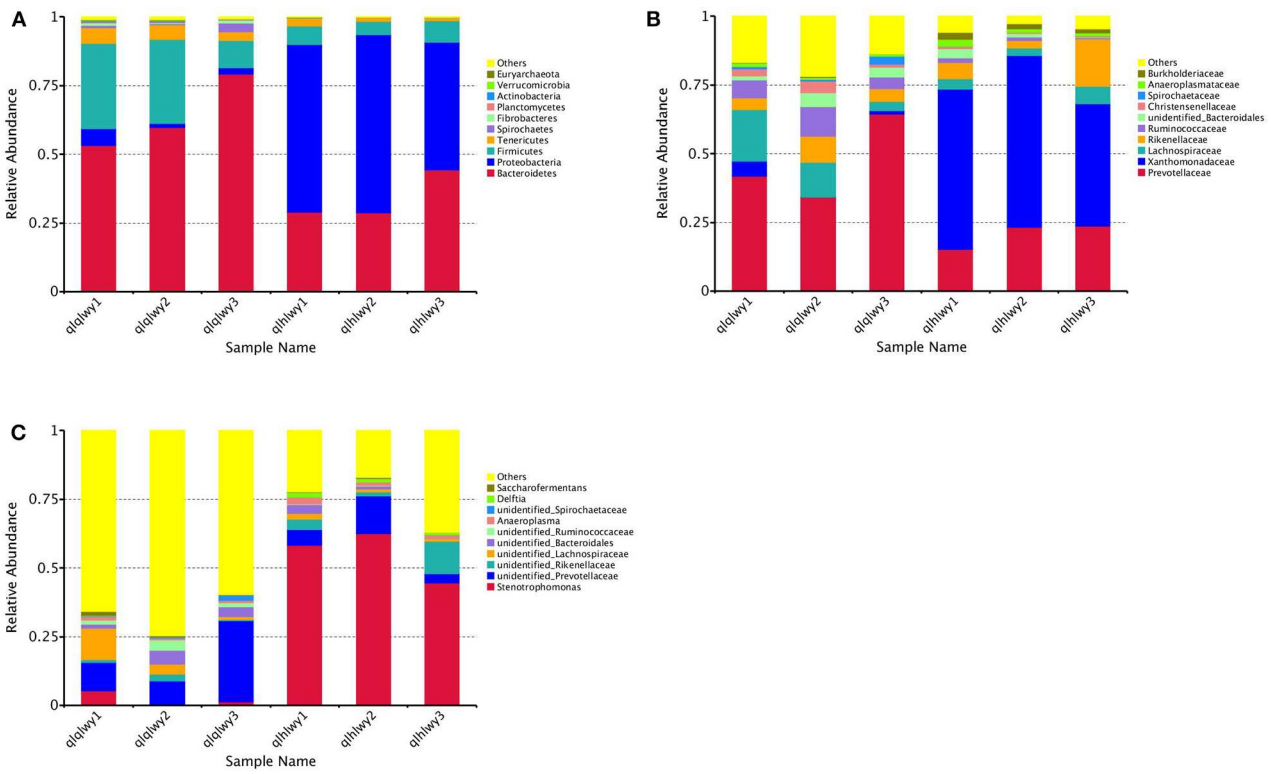

FIGURE 4 | Microbial composition of different samples. Each bar represents the average relative abundance of each bacterial taxon within a group. The top 11 abundant taxa are shown. **(A)** Taxa assignments at Phylum level. **(B)** Taxa assignments at Family level. **(C)** Taxa assignments at Genus level.

(**Figure 4C**). The most important factor is that there were obvious changes between unidentified_Prevotellaceae and Stenotrophomonas with treatment. The proportion of unidentified_Prevotellaceae gradually decreased with doxycycline, while Stenotrophomonas increased (**Figure 4C**). This finding demonstrates that doxycycline treatment clearly affects the bacterial community composition of the rumen in beef cattle.

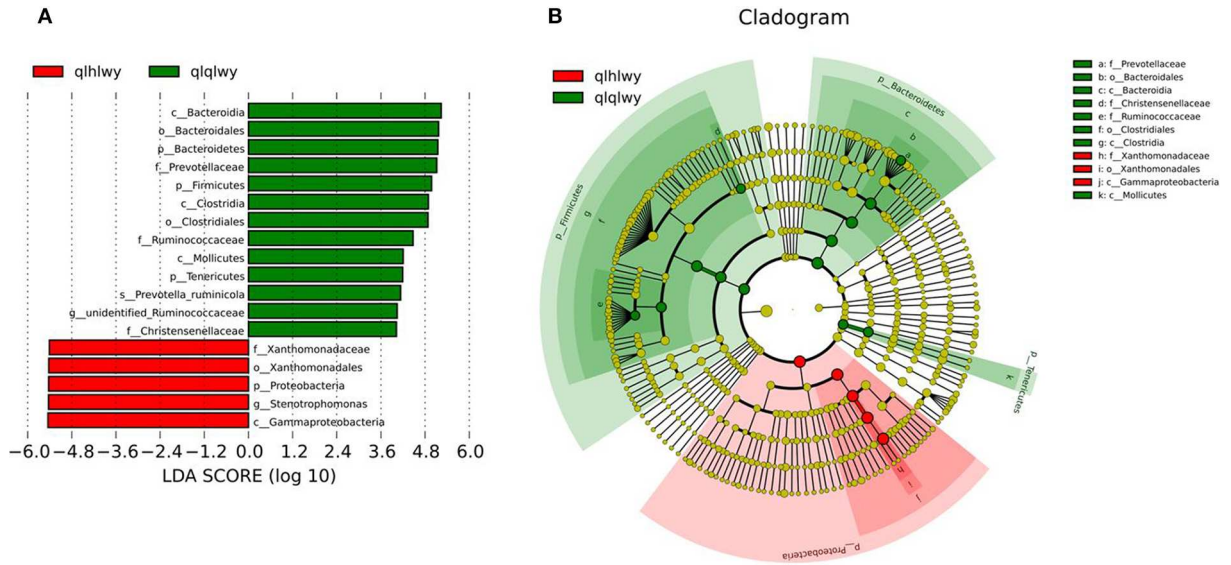

FIGURE 5 | Bacterial taxa significantly differentiated rumens samples of cows with or without doxycycline identified by LEfSe using the default parameters. **(A)** Histogram of LDA scores computed for bacterial taxa differentially abundant between groups. **(B)** Bacterial taxa that were differentially abundant visualized using a cladogram.

Differences in Bacterial Communities Between Rumens With or Without Doxycycline

Linear discriminant analysis (LDA) effect size (LEfSe) was applied to the top 18 taxa (average relative abundance >0.00001) to determine which were significantly different between groups (**Figure 5A**). The bacterial taxa of rumens differentially represented the groups qlqlwy and qlhlwy. Eight and three bacterial taxa were significantly more abundant in qlqlwy and qlhlwy, respectively (**Figure 5B**). The RM in group qlqlwy was significantly more diverse in both species and relative abundance. Bacteroides was the most abundant taxa in group qlqlwy, whereas Xanthomonadaceae was the most common in group qlhlwy. These are consistent with the bacterial community compositions of the rumen samples described above.

Correlation of RM in Beef Cattle With or Without Doxycycline

There were significant differences in the diversity and abundance of intestinal microbiota following doxycycline treatment. To investigate the effect of doxycycline on RM, we performed a statistical analysis of metagenomic profiles (STAMP, **Figure 6**). There were no significant differences in other RM between the two groups except for Bacteroidetes ($P = 0.04$) and Proteobacteria ($P = 0.008$). Bacteroidetes was previously determined to have a high abundance in beef cattle without doxycycline, indicating that these are necessary for normal animals (**Figure 4A**). In addition, Proteobacteria had high abundance in doxycycline-treated animals, but the proportion of Bacteroidetes decreased, suggesting that doxycycline can promote Proteobacteria growth, and inhibit Bacteroidetes survival. Tenericutes, Planctomycetes, and Melainabacteria in group qlhwly also showed decreasing trends. Despite their low abundance, these changes should not be ignored.

The gastrointestinal microbiota is called the "second genome" and plays an important role in animal growth and health, especially in ruminants. Previous studies have shown that gastrointestinal microbes can influence body weight and digestion and decrease the risks of infection and autoimmune diseases. The intestinal microbiota has been linked to several conditions including diabetes and inflammatory bowel disease (35, 36). It was also reported that there was a significant difference in the bacterial composition of BALBc mice receiving comparable immune programs in specific pathogen-free units of different centers, which supported the role of intestinal microbiota in regulating the induction response (37). Over time, the RM has been investigated in sheep, cattle, and other ruminants. Mammalian gastrointestinal studies have examined the effects of the microbiota on metabolism, physiology, and immunology (38, 39), but there are a few reports of RM differences in cattle following antibiotic administration. Here, we analyzed bacterial diversity and abundance in the contents of cattle RM after doxycycline treatment. The results showed that the abundance and diversity of bacteria in the RM of cattle on doxycycline were lower than in untreated cattle.

The RM of dairy beef cattle is not present at birth, but as the animals are in constant contact with the external environment, it gradually colonizes, survives, and reproduces after adapting to the environment. Cattle RM reportedly increase in diversity and tend to be composed of mature bacteria as animals age (40).

The present results demonstrate significant differences in the RM after doxycycline treatment. Prior to antibiotic

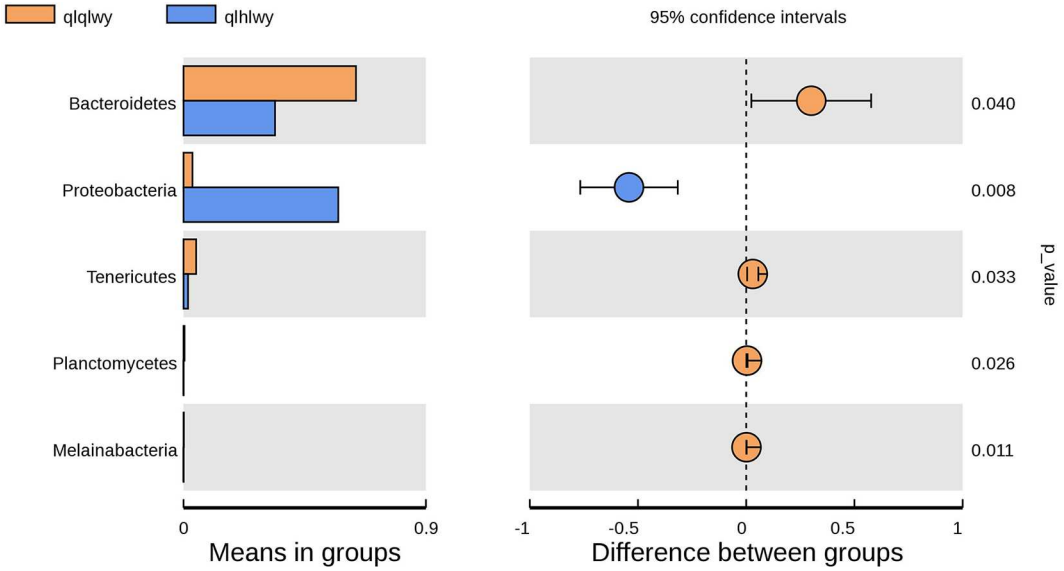

FIGURE 6 | Differences in bacterial abundance between the groups qlqlwy and qlhlwy. Left, abundance ratios of different strains in two samples. Middle, difference in bacterial abundance within the 95% confidence interval. Right, *P*-values of significance testing.

administration, Bacteroidetes and Firmicutes were the most common phyla in the rumen samples of group qlqlwy, which is consistent with a previous report (40). After doxycycline administration, Proteobacteria became the most abundant phylum in group qlhlwy. The proportion of Bacteroides was small. The dominant bacteria in the RM are mainly composed of Bacteroides, Proteobacteria, and Firmicutes, but their proportions vary greatly.

Gene functions in the intestinal microbiota of healthy humans may be more diverse than previously hypothesized, and the main axis of taxonomic variation in the microbiome may not capture the largest functional variation (41). Bacteroides are beneficial intestinal microbiota because they break down polysaccharides and improve nutrient utilization (42), degrade carbohydrates and proteins, and promote the development of the gastrointestinal immune system (43). All these events strengthen the host's immune system (44). In ruminants, Firmicutes is involved in degrading fiber and cellulose (45) and maintaining an appropriate intestinal micro-ecological balance (46).

Since intestinal microbiota imbalance is usually caused by a continuously increased abundance of Proteobacteria, the physiological human intestinal microbiota contains only a small proportion of that phylum. Increased prevalence of Proteus could be a useful diagnostic marker for dysbiosis and disease risk (47). In support of the proposed relationship between metabolic disorder and Proteobacteria expansion, a mono-association study of germ-free mice revealed an obesogenic potential of Proteobacteria (48). In fact, a growing body of evidence suggests that an abundance of Proteobacteria members may be a pathogenetic feature. This feature has known associations with metabolic disorders and inflammatory bowel diseases, but it may also play a role in lung diseases including asthma and chronic obstructive pulmonary disease. All of these conditions have varying degrees of inflammation.

Many studies have confirmed that the use of antibiotics and some drugs can alter the RM of dairy beef cattle. Li et al. (49) fed pasteurized antibiotic milk, antibiotic milk, or fresh milk to 2-, 3-, and 6-month-old calves. Antibiotic milk gradually increased Firmicutes abundance, while Bacteroides gradually decreased. There were also significant proteobacteria differences in each group. Shen et al. (50) demonstrated that monensin and nisin both reduced the numbers of bacteria, fungi, and methanogens. It is undeniable that antibiotics have strong effects against dangerous pathogens, but they also damage the beneficial bacteria colonized in the rumen and change the steady state of rumen microorganisms, especially when taken orally. Therefore, it is necessary to judiciously use antibiotics in dairy cow production. When there is no choice, injection is preferred over oral administration to minimize damage to the RM.

The number of animals selected for this study was limited due to the research cost. Our results should therefore be confirmed in a larger sample of animals.

DATA AVAILABILITY STATEMENT

The datasets generated for this study can be found in NCBI SRA, NCBI Accession Nos. PRJNA624243 and PRJNA624271.

ETHICS STATEMENT

The animal study was reviewed and approved by Shandong Vocational Animal Science and Veterinary College. Written informed consent was obtained from the owners for the participation of their animals in this study.

AUTHOR CONTRIBUTIONS

All authors designed the subject, collected the sample, analysed, and wrote the manuscript.

FUNDING

This work was financially supported by the Shandong modern agricultural industry technology system cattle industry innovation team construction project (SDAIT-09-05).

REFERENCES

1. Flint HJ. The rumen microbial ecosystem–some recent developments. Trends Microbiol. (1997) 5:483–8. doi: 10.1016/S0966-842X(97)01159-1
2. Henderson G, Cox F, Ganesh S, Jonker A, Young W, Global Rumen Census Collaborators, et al. Rumen microbial community composition varies with diet and host, but a core microbiome is found across a wide geographical range. *Sci Rep*. (2015) 5:14567. doi: 10.1038/srep14567
3. Gruninger RJ, Puniya AK, Callaghan TM, Edwards JE, Youssef N, Dagar SS, et al. Anaerobic fungi (phylum *Neocallimastigomycota*): advances in understanding their taxonomy, life cycle, ecology, role and biotechnological potential. *FEMS Microbiol Ecol.* (2014) 90:1–17. doi: 10.1111/1574-6941.12383
4. Janssen PH, Kirs M. Structure of the archaeal community of the rumen. *Appl Environ Microbiol.* (2008) 74:3619–25. doi: 10.1128/AEM.02812-07
5. Wallace RJ, Sasson G, Garnsworthy PC, Tapio I, Gregson EM, Bani P, et al. A heritable subset of the core rumen microbiome dictates dairy cow productivity and emissions. *Sci Adv*. (2019) 5:eaav8391. doi: 10.1126/sciadv.aav8391
6. Firkins JL, Yu Z. RUMINANT NUTRITION SYMPOSIUM: How to use data on the rumen microbiome to improve our understanding of ruminant nutrition. *J Anim Sci.* (2015) 93:1450–70. doi: 10.2527/jas.2014-8754
7. Li F, Guan LL. Metatranscriptomic profiling reveals linkages between the active rumen microbiome and feed efficiency in beef cattle. *Appl Environ Microbiol.* (2017) 83:e00061–17. doi: 10.1128/AEM.00061-17
8. Shabat SK, Sasson G, Doron-Faigenboim A, Durman T, Yaacoby S, Berg Miller ME, et al. Specific microbiome-dependent mechanisms underlie the energy harvest efficiency of ruminants. *ISME J.* (2016) 10:2958–72. doi: 10.1038/ismej.2016.62
9. Dan R, Zhang H, Long R, Ding X, Zhang X. Seasonal shift of rumen bacteria quantity of grazing tibetan sheep and forage nutrition by grazing sheep. *Acta Prataculturae Sinica*. (2009) 18:100–4.
10. Xu Q. (2015). *The Impact of Ration and Goat Breeds on the Composition and the Relative Abundance of Microbial Species in Goat Rumen*. (Master's Thesis), Sichuan Agricultural University, Ya 'an. p. 19–48.
11. Marx V. Next-generation sequencing: the genome jigsaw. *Nature.* (2013) 501:263–8. doi: 10.1038/501261a
12. Shendure J, Lieberman Aiden E. The expanding scope of DNA sequencing. *Nat Biotechnol.* (2012) 30:1084–94. doi: 10.1038/nbt.2421
13. McGovern E, Waters SM, Blackshields G, McCabe MS. Evaluating established methods for rumen 16S rRNA amplicon sequencing with mock microbial populations. *Front Microbiol.* (2018) 9:1365. doi: 10.3389/fmicb.2018.01365
14. Paz HA, Anderson CL, Muller MJ, Kononoff PJ, Fernando SC. Rumen bacterial community composition in holstein and jersey cows is different under same dietary condition and is not affected by sampling method. *Front Microbiol.* (2016) 7:1206. doi: 10.3389/fmicb.2016.01206
15. Kim HB, Isaacson RE. The pig gut microbial diversity: understanding the pig gut microbial ecology through the next generation high throughput sequencing. *Vet Microbiol.* (2015) 177:242–51. doi: 10.1016/j.vetmic.2015.03.014
16. De Palma G, Lynch MD, Lu J, Dang VT, Deng Y, Jury J, et al. (2017). Transplantation of fecal microbiota from patients with irritable bowel syndrome alters gut function and behavior in recipient mice. *Sci Transl Med*. 9:eaaf6397. doi: 10.1126/scitranslmed.aaf6397
17. Pushalkar S, Hundeyin M, Daley D, Zambirinis CP, Kurz E, Mishra A, et al. (2018). The pancreatic cancer microbiome promotes oncogenesis by induction of innate and adaptive immune suppression. *Cancer Discov*. 8:403–16. doi: 10.1158/2159-8290.CD-17-1134
18. Livanos AE, Greiner TU, Vangay P, Pathmasiri W, Stewart D, McRitchie S, et al. Antibiotic mediated gut microbiome perturbation accelerates development of type 1 diabetes in mice. *Nat Microbiol*. (2016) 11:16140. doi: 10.1038/nmicrobiol.2016.140
19. Cani PD. Microbiota and metabolites in metabolic diseases. *Nat Rev Endocrinology*. (2019) 15:69–70. doi: 10.1038/s41574-018-0143-9
20. Zhang Y, Luo Y. Research progress on the mechanism of intestinal mucosal damage and protection. *Chin J Microecol*. (2010) 22: 85–7. doi: 10.13381/j.cnki.cjm.2010.01.012
21. Hitch TCA, Thomas BJ, Friedersdorff JCA, Ougham H, Creevey CJ. Deep sequence analysis reveals the ovine rumen as a reservoir of antibiotic resistance genes. *Environ Pollut*. (2018) 235:571–5. doi: 10.1016/j.envpol.2017.12.067
22. Cameron A, McAllister TA. Antimicrobial usage and resistance in beef production. *J Anim Sci Biotechnol.* (2016) 7:68. doi: 10.1186/s40104-016-0127-3
23. Ben Saad H, Kharrat N, Krayem N, Boudawara O, Boudawara T, Zeghal N, et al. Biological properties of *Alsidium* corallinum and its potential protective effects against damage caused by potassium bromate in the mouse liver. *Environ Sci Pollut Res Int.* (2016) 23:3809–23. doi: 10.1007/s11356-015-5620-2
24. Cross R, Ling C, Day NP, McGready R, Paris DH. Revisiting doxycycline in pregnancy and early childhood–time to rebuild its reputation? *Expert Opin Drug Saf.* (2016) 15:367–82. doi: 10.1517/14740338.2016.1133584
25. Daghrir R, Drogui P. Tetracycline antibiotics in the environment: a review. *Environ Chem Lett.* (2013) 11:209–27. doi: 10.1007/s10311-013-0404-8
26. Martin M. Cutadapt removes adapter sequences from high-throughput sequencing reads. *Embnet J.* (2011) 17:10–12. doi: 10.14806/ej.17.1.200
27. Kechin A, Boyarskikh U, Kel A, Filipenko M. cutPrimers: a new tool for accurate cutting of primers from reads of targeted next generation sequencing. *J Comput Biol.* (2017) 24:1138–43. doi: 10.1089/cmb.2017.0096
28. Rognes T, Flouri T, Nichols B, Quince C, Mahe F. VSEARCH: a versatile open source tool for metagenomics. *PeerJ.* (2016) 4:e2584. doi: 10.7717/peerj.2584
29. Quast C, Pruesse E, Yilmaz P, Gerken J, Schweer T, Yarza P, et al. The SILVA ribosomal RNA gene database project: improved data processing and web-based tools. *Nucleic Acids Res.* (2013) 41:D590–6. doi: 10.1093/nar/gks1219
30. Edgar RC, Haas BJ, Clemente JC, Quince C, Knight R. UCHIME improves sensitivity and speed of chimera detection. *Bioinformatics.* (2011) 27:2194–200. doi: 10.1093/bioinformatics/btr381
31. Haas BJ, Gevers D, Earl AM, Feldgarden M, Ward DV, Giannoukos G, et al. Chimeric 16S rRNA sequence formation and detection in Sanger and 454-pyrosequenced PCR amplicons. *Genome Res.* (2011) 21:494–504. doi: 10.1101/gr.112730.110
32. Edgar RC. UPARSE: highly accurate OTU sequences from microbial amplicon reads. *Nat Methods.* (2013) 10:996–8. doi: 10.1038/nmeth.2604
33. Edgar RC. MUSCLE: multiple sequence alignment with high accuracy and high throughput. *Nucleic Acids Res.* (2004) 32:1792–7. doi: 10.1093/nar/gkh340
34. Chapman MG, Underwood AJ. Ecological patterns in multivariate assemblages: information and interpretation of negative values in ANOSIM tests. *Mar Ecol Prog Ser.* (1999) 180:257–65. doi: 10.3354/meps180257
35. Brown CT, Davis-Richardson AG, Giongo A, Gano KA, Crabb DB, Mukherjee N, et al. Gut microbiome metagenomics analysis suggests a functional model for the development of autoimmunity for type 1 diabetes. *PLoS ONE.* (2011) 6:e25792. doi: 10.1371/journal.pone.0025792
36. Frank DN, St Amand AL, Feldman RA, Boedeker EC, Harpaz N, Pace NR. Molecular-phylogenetic characterization of microbial community imbalances in human inflammatory bowel diseases. *Proc Natl Acad Sci USA*. (2007) 104:13780–5. doi: 10.1073/pnas.0706625104
37. Masetti G, Moshkelgosha S, Kohling HL, Covelli D, Banga JP, Berchner-Pfannschmidt U, et al. Gut microbiota in experimental murine model of Graves' orbitopathy established in d rent environments may

modulate clinical presentation of disease. *Microbiome.* (2018) 6:97. doi: 10.1186/s40168-018-0478-4
38. Wang J, Fan H, Han Y, Zhao J, Zhou Z. Characterization of the microbial communities along the gastrointestinal tract of sheep by 454 pyrosequencing analysis. *Asian-Australas J Anim Sci.* (2017) 30:100–10. doi: 10.5713/ajas.16.0166
39. Zeng Y, Zeng D, Zhang Y, Ni X, Tang Y, Zhu H, et al. Characterization of the cellulolytic bacteria communities along the gastrointestinal tract of Chinese mongolian sheep by using PCR-DGGE and real-time PCR analysis. *World J Microbiol Biotechnol.* (2015) 31:1103–13. doi: 10.1007/s11274-015-1860-z
40. Jami E, Israel A, Kotser A, Mizrahi I. Exploring the bovine rumen bacterial community from birth to adulthood. *ISME J.* (2013) 7:1069–79. doi: 10.1038/ismej.2013.2
41. Bradley PH, Pollard KS. Proteobacteria explain significant functional variability in the human gut microbiome. *Microbiome.* (2017) 5:36. doi: 10.1186/s40168-017-0244-z
42. Backhed F, Ding H, Wang T, Hooper LV, Koh GY, Nagy A, et al. The gut microbiota as an environmental factor that regulates fat storage. *Proc Natl Acad Sci USA.* (2004) 101:15718–23. doi: 10.1073/pnas.0407076101
43. Spence C, Wells WG, Smith CJ. Characterization of the primary starch utilization operon in the obligate anaerobe *Bacteroides Fragilis*: regulation by carbon source and oxygen. *J Bacteriol.* (2006) 188:4663–72. doi: 10.1128/JB.00125-06
44. Hooper LV. Bacterial contributions to mammalian gut development. *Trends Microbiol.* (2004) 12:129–34. doi: 10.1016/j.tim.2004.01.001
45. Thoetkiattikul H, Mhuantong W, Laothanachareon T, Tangphatsornruang S, Pattarajinda V, Eurwilaichitr L, et al. Comparative analysis of microbial profiles in cow rumen fed with different dietary fiber by tagged 16S rRNA gene pyrosequencing. *Curr Microbiol.* (2013) 67:130–7. doi: 10.1007/s00284-013-0336-3
46. Sears CL. A dynamic partnership: celebrating our gut flora. *Anaerobe.* (2005) 11:247–51. doi: 10.1016/j.anaerobe.2005.05.001
47. Shin NR, Whon TW, Bae JW. Proteobacteria: microbial signature of dysbiosis in gut microbiota. *Trends Biotechnol.* (2015) 33:496–503. doi: 10.1016/j.tibtech.2015.06.011
48. Fei N, Zhao L. An opportunistic pathogen isolated from the gut of an obese human causes obesity in germfree mice. *ISME J.* (2013) 7:880–4. doi: 10.1038/ismej.2012.153
49. Li W, Han Y, Yuan X, Wang G, Wang Z, Pan Q, et al. Metagenomic analysis reveals the influences of milk containing antibiotics on the rumen microbes of calves. *Arch Microbiol.* (2017) 199:433–43. doi: 10.1007/s00203-016-1311-8
50. Shen J, Liu Z, Yu Z, Zhu W. Monensin and nisin affect rumen fermentation and microbiota differently *in vitro*. *Front Microbiol.* (2017) 8:1111. doi: 10.3389/fmicb.2017.01111

Conflict of Interest: The authors declare that the research was conducted in the absence of any commercial or financial relationships that could be construed as a potential conflict of interest.

frontiers in Genetics

ORIGINAL RESEARCH
published: 12 June 2020
doi: 10.3389/fgene.2020.00599

Deciphering Cattle Temperament Measures Derived From a Four-Platform Standing Scale Using Genetic Factor Analytic Modeling

Haipeng Yu[1†], Gota Morota[1†], Elfren F. Celestino Jr.[2†], Carl R. Dahlen[2], Sarah A. Wagner[2†], David G. Riley[3] and Lauren L. Hulsman Hanna[2*†]*

[1] Department of Animal and Poultry Sciences, Virginia Polytechnic Institute and State University, Blacksburg, VA, United States, [2] Department of Animal Sciences, North Dakota State University, Fargo, ND, United States, [3] Department of Animal Science, Texas A&M University, College Station, TX, United States

OPEN ACCESS

Edited by:
Jiuzhou Song,
University of Maryland, College Park, United States

Reviewed by:
Eduardo Casas,
National Animal Disease Center (USDA ARS), United States
Elisabeth Jonas,
Swedish University of Agricultural Sciences, Sweden

***Correspondence:**
Gota Morota
morota@vt.edu
Lauren L. Hulsman Hanna
lauren.hanna@ndsu.edu

†ORCID:
Haipeng Yu
orcid.org/0000-0002-8923-9733
Gota Morota
orcid.org/0000-0002-3567-6911
Elfren F. Celestino Jr.
orcid.org/0000-0002-1713-2961
Sarah A. Wagner
orcid.org/0000-0002-4046-7583
Lauren L. Hulsman Hanna
orcid.org/0000-0002-8392-887X

Specialty section:
This article was submitted to Livestock Genomics, a section of the journal Frontiers in Genetics

Received: 05 February 2020
Accepted: 18 May 2020
Published: 12 June 2020

Citation:
Yu H, Morota G, Celestino EF Jr, Dahlen CR, Wagner SA, Riley DG and Hulsman Hanna LL (2020) Deciphering Cattle Temperament Measures Derived From a Four-Platform Standing Scale Using Genetic Factor Analytic Modeling. Front. Genet. 11:599. doi: 10.3389/fgene.2020.00599

The animal's reaction to human handling (i.e., temperament) is critical for work safety, productivity, and welfare. Subjective phenotyping methods have been traditionally used in beef cattle production. Even so, subjective scales rely on the evaluator's knowledge and interpretation of temperament, which may require substantial experience. Selection based on such subjective scores may not precisely change temperament preferences in cattle. The objectives of this study were to investigate the underlying genetic interrelationships among temperament measurements using genetic factor analytic modeling and validate a movement-based objective method (four-platform standing scale, FPSS) as a measure of temperament. Relationships among subjective methods of docility score (DS), temperament score (TS), 12 qualitative behavior assessment (QBA) attributes and objective FPSS including the standard deviation of total weight on FPSS over time (SSD) and coefficient of variation of SSD (CVSSD) were investigated using 1,528 calves at weaning age. An exploratory factor analysis (EFA) identified two latent variables account for TS and 12 QBA attributes, termed *difficult* and *easy* from their characteristics. Inclusion of DS in EFA was not a good fit because it was evaluated under restraint and other measures were not. A Bayesian confirmatory factor analysis inferred the *difficult* and *easy* scores discovered in EFA. This was followed by fitting a pedigree-based Bayesian multi-trait model to characterize the genetic interrelationships among *difficult*, *easy*, DS, SSD, and CVSSD. Estimates of heritability ranged from 0.18 to 0.4 with the posterior standard deviation averaging 0.06. The factors of *difficult* and *easy* exhibited a large negative genetic correlation of −0.92. Moderate genetic correlation was found between DS and *difficult* (0.36), *easy* (−0.31), SSD (0.42), and CVSSD (0.34) as well as FPSS with *difficult* (CVSSD: 0.35; SSD: 0.42) and *easy* (CVSSD: −0.35; SSD: −0.4). Correlation coefficients indicate selection could be performed with either and have similar outcomes. We contend that genetic factor analytic modeling provided a new approach to unravel the complexity of animal behaviors and FPSS-like measures could increase the efficiency of genetic selection by providing automatic, objective, and consistent phenotyping measures that could be an alternative of DS, which has been widely used in beef production.

Keywords: beef cattle, factor analysis, four-platform standing scale, precision agriculture, temperament

1. INTRODUCTION

Temperament in cattle traditionally refers to the animal's behavior in the bail (Tulloh, 1961) or the reaction of animal to human handling (Burrow and Dillon, 1997). Previous studies have revealed cattle temperament has a significant relationship with production, reproduction, immunity, and carcass traits (King et al., 2006; Burdick et al., 2011; Haskell et al., 2014). Additionally, temperament is usually evaluated at an earlier stage of cattle than some production traits. Therefore, temperament could be considered as an indicator of production traits in genetic selection, where selection on temperament can provide an opportunity to improve production and efficiency in the beef industry. Temperament is a complex trait that comprises various behavioral characteristics such as shyness-boldness, exploration avoidance, activity, sociability, and aggressiveness (Réale et al., 2007). Several subjective methods were proposed to score temperament, including temperament scoring of cattle handled in a crush with head bail (Tulloh, 1961), flight distance (Fordyce et al., 1982), docility test (Le Neindre et al., 1995), chute test (Tier et al., 2001), race score (Turner et al., 2011), and qualitative behavior assessment (QBA) (Sant-Anna and da Costa, 2013). These subjective methods are able to integrate various levels of temperament attributes (e.g., calmness, agitation, flightiness, aggressiveness) into a single score and create a standardized test by taking advantage of the experience and interpretation of the human evaluator on cattle. This is advantageous for typical production operations due to ease of capturing data compared to objective methods that require specialized equipment (e.g., exit velocity). Even so, closely working with cattle may cause potential danger for evaluators during scoring. Furthermore, there is a concern with evaluation bias in subjective methods, which makes comparison of temperament scoring methods across experiments difficult. Due to this, measurements without human interpretation, such as exit velocity (Burrow et al., 1988), movement-measuring-devices (Stookey et al., 1994; Sebastian et al., 2011), strain gauges (Schwartzkopf-Genswein et al., 1997), and objective chute score (Bruno et al., 2018), have been tested to provide objective and quantifiable temperament measurements. Understanding how these objective measures relate to behavioral attributes is of interest, where most studies have only compared a few common subjective methods with objective methods using a standard multi-trait model (Burrow et al., 1988; Stookey et al., 1994; Sebastian et al., 2011; Bruno et al., 2018). Computational limitations have also hindered further research in understanding relationship between objective and subjective methods of temperament. Therefore, this study introduces a novel, potentially cost effective objective method using a four-platform standing scale (FPSS) and investigates its relationship with subjective methods of docility score (DS), temperament score (TS), and qualitative behavior assessment (QBA) attributes. The objectives of this study were to apply genetic factor analytic modeling to characterize the underlying genetic interrelationships among temperament measures and validate FPSS as an objective measurement of cattle temperament. We employed new statistical approaches, explanatory factor analysis (EFA) and confirmatory factor analysis (CFA), to overcome the computational challenges due to a large number of correlated subjective measurements. To our knowledge, this is the first study to investigate the novel objective measurement FPSS using EFA and CFA for the genetic analysis of cattle temperament.

2. MATERIALS AND METHODS

2.1. Animals

From 2014 to 2017, data were collected at weaning time (late September to late October) at North Dakota State University Central Grasslands Research Extension Center (CGREC) near Streeter, North Dakota. Calves ($n = 1,528$), including 749 heifers and 779 steers, were scored at the weaning age (average age was 161.0 ± 17.0 d) and included for analysis. Calves were either sired by Angus bulls (all 4 yr) or by Hereford bulls (3 yr) and were from Angus-influenced (all 4 yr) or Hereford by Angus-influenced (2 yr) dams. Calves were assigned to one of two primary breeds (50% or greater) based on known breed percentages, which resulted in 1,340 Angus- (666 heifers, 674 steers) and 188 Hereford-based (83 heifers, 105 steers) calves. A pedigree including 109,703 animals was formed using the information of dams and records of complete ancestry for registered bulls provided by the American Angus Association and American Hereford Association. All procedures involved in data collection were reviewed and approved by the Institutional Animal Care and Use Committee of North Dakota State University.

2.2. Experiment Procedure

The details of temperament evaluation procedure during the first year of data collection was previously described by Hulsman Hanna et al. (2019) and was repeated the remaining 3 years of the study except for collection of the blood draw effect. Briefly, calves were moved through the working pens to the evaluation areas and then sorted to different holding pens for management. In a given year, four evaluators were randomly assigned two of three subjective scoring methods (DS, TS, and QBA) prior to evaluation. A total of 11 evaluators were presented over the 4 yr period as some evaluators were not able to return for all years of the study. Averages per animal for each subjective method that had at least three evaluator scores were used in this study since the focus of this study was not evaluator variation. Basic means and standard deviations are presented in **Table S1**. The first method scored was DS, which is a six point scale where one and six refer to calm and aggressive, respectively (Beef Improvement Federation, 2018). The evaluation of DS was done at the silencer chute with the head of the calf caught and each calf was evaluated <1 min. Following the evaluation of DS, weaning weight of the calf was recorded when its body was squeezed. Upon released from silencer chute, the calf then entered the FPSS (Pacific Industrial Scale, British Columbia, Canada) to collect the weight shifts on each quadrant (see next section for further details). Following FPSS, TS and 12 QBA attributes were evaluated in the outside testing area, while a single human handler calmly interacted with the calf. The presence of this human handler was intended to facilitate evaluation of the

different aspects of these subjective methods. Following Sant-Anna and da Costa (2013), TS is a five point scale, with the neutral value (3) removed, where one indicates calm and five indicates wild or aggressive. The 12 attributes of QBA consist of active, agitated, apathetic, attentive, calm, curious, distressed, fearful, happy, irritated, positively occupied, and relaxed (Sant-Anna and da Costa, 2013), which can be grouped into positive and negative behaviors. Each attribute was scored on a 136 mm line indicating the extent of expression, where the far left and far right refer to no expression and complete expression of the attribute, respectively. Evaluators were given a list of QBA in a specific order, however evaluators scored calves as the attributes were able to be assessed (i.e., based on calf behaviors), therefore a specific order of scoring QBA was never consistent across calves or evaluators. Each calf was measured < 3 min and then sorted into a holding pen for management purposes.

2.3. FPSS Measurements

The FPSS provides a novel method of quantifying cattle temperament while also weighing the animal (**Figure S1**). The FPSS has scales in each quadrant and connects to a computer controlled by a worker. Prior to the calf entering the scale, the worker first enters the tag number of the calf. Once the calf is on the scale, the worker starts recording weights on the four-platform for at least 45 s by starting the recording software. The FPSS computer software is able to record approximately 15 records per second. The worker also keeps a log of any issues encountered with the calf, large movements, and where those issues fall in the records, however these do not influence the selection of records used. Following data collection, FPSS records of each animal were reviewed for quality before used in subsequent analyses. To do this, the ideal start point for a given animal's scale records (i.e., when the animal is considered as completely standing on the scale) was identified following the protocol in **Figure 1**. Once the start point was identified, that point and 499 subsequent records were used to calculate the mean and standard deviation of the total weight. The standard deviation of FPSS measurements (SSD) and the coefficient of variation of the SSD (CVSSD = SSD divided by mean) were used as temperament scores for subsequent analyses. The basis of SSD is that animals that are more temperamental will move more often and have larger standard deviations. The CVSSD was calculated as there was concern the actual weight of the animal would bias the SSD as larger animals may naturally have larger standard deviations in records.

2.4. Exploratory Factor Analysis

We fitted EFA using subjective measurements including TS and 12 QBA attributes ($t = 13$). The logic of using EFA is to discover the underlying latent variables or factors (q) to represent observed measurements. Thereby, a network structure between latent variables and phenotypes was first explored and further used for downstream analysis. An EFA model is given as a function of latent factor scores

$$\mathbf{T} = \mathbf{\Lambda F} + \boldsymbol{\epsilon}, \tag{1}$$

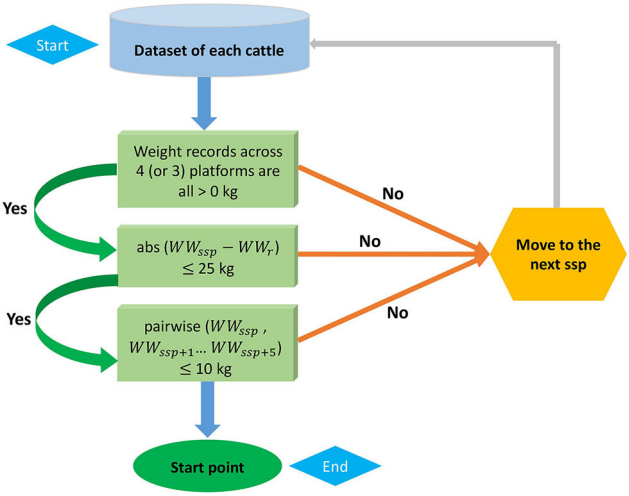

FIGURE 1 | A flow of criteria to identify the start point of four-platform standing scale measurement. The abs and pairwise refer to the absolute difference and pairwise absolute difference, respectively. WW_{ssp} denotes the weaning weight at current suspected start point (ssp) and WW_{ssp+i} is the weaning weight at the following *i*th point of ssp, where $i = 1$ to 5. WW_r is weaning weight recorded in chute system.

where $\mathbf{T}$ is a $t \times n$ phenotypic matrix, $\mathbf{\Lambda}$ is the $t \times q$ factor loading matrix, $\mathbf{F}$ is the $q \times n$ latent factor scores, and $\boldsymbol{\epsilon}$ is the $t \times n$ matrix of specific effects. The matrix $\mathbf{\Lambda}$ includes the factor loading coefficients, which can be considered as regression coefficients reflecting the relationships between observed phenotypes and underlying latent variables. The variance-covariance structure of $\mathbf{T}$ is

$$var(\mathbf{T}) = \mathbf{\Lambda \Phi \Lambda}' + \mathbf{\Psi}, \tag{2}$$

where $\mathbf{\Phi}$ is the variance of factor scores and $\mathbf{\Psi}$ is the variance of specific effects. With the assumption of $\mathbf{F} \sim \mathcal{N}(\mathbf{0}, \mathbf{I})$, a vector of phenotypes follows a multivariate Gaussian distribution $\mathbf{t}_i \overset{iid}{\sim} \mathcal{N}(\mathbf{0}, \mathbf{\Sigma})$, where *i* refers to *i*th individual and $\mathbf{\Sigma} = \mathbf{\Lambda \Lambda}' + \mathbf{\Psi}$. The log-likelihood of the factor analysis model is

$$\mathcal{L}(\mathbf{\Lambda}, \mathbf{\Psi}|\mathbf{T}) = -\frac{nq}{2} log 2\pi - \frac{n}{2} log(\mathbf{\Sigma}) - \frac{n}{2} log(\mathbf{T}' \mathbf{\Sigma^{-1}} \mathbf{T}).$$

The number of underlying latent variables q was determined using a parallel analysis (Horn, 1965). In brief, the eigenvalues of the observed data and simulated data conditioned on the observed data were computed to extract latent variables until the observed data had a smaller eigenvalue than the simulated data. Parameters $\mathbf{\Lambda}$ and $\mathbf{\Psi}$ were estimated by maximizing the log-likelihood of $\mathcal{L}(\mathbf{\Lambda}, \mathbf{\Psi}|\mathbf{T})$ using an iteration method. We used the R package psych (Revelle, 2018) to fit EFA. We posited that DS may not align with other subjective measures since it is collected in a confined setting, whereas other subjective measures used in this study were in a pen with free movement. An additional EFA was fitted including DS to confirm this assumption.

2.5. Bayesian Confirmatory Factor Analysis

Using results from the EFA as a prior, a confirmatory factor analysis (CFA) under the Bayesian framework was fitted following the procedure described in Yu et al. (2019) to obtain factor scores. We assigned the following priors for Equations (1) and (2).

$$\begin{aligned}\boldsymbol{\Lambda} &\sim \mathcal{N}(0, 0.01)\\ \boldsymbol{\Phi} &\sim \mathcal{W}^{-1}(\mathbf{I_{22}}, 3)\\ \boldsymbol{\Psi} &\sim \Gamma^{-1}(1, 0.5).\end{aligned}$$

The blavaan R package (Merkle and Rosseel, 2018) coupled with the rstan R package (Carpenter et al., 2017) were applied to solve the Bayesian CFA model. A Markov chain Monte Carlo (MCMC) with 6,000 samples and 3,000 burn-in was adapted to infer the model parameters and in total three MCMC chains were sampled. The model convergence was validated using the combination of trace plots and a potential scale reduction factor (PSRF) less than 1.2 (Brooks and Gelman, 1998). A PSRF compares the estimated variances across chains and within the chain, where a large difference indicates additional Gibbs samplings may be required. This was followed by calculating the factor scores (**F**) of latent variables using the Gibbs samples. When factor scores are considered missing, the **F** is sampled from a conditional distribution of $p(\mathbf{F}|\boldsymbol{\theta}, \mathbf{T})$ (Lee and Song, 2012) using a data augmentation (Tanner and Wong, 1987), where $\boldsymbol{\theta}$ refers to the unknown parameters $\boldsymbol{\Lambda}$, $\boldsymbol{\Phi}$, and $\boldsymbol{\Psi}$. The factor scores of latent variables were summarized from the posterior mean of **F** and considered as new phenotypes in the downstream analysis.

2.6. Bayesian Multivariate Best Linear Unbiased Prediction

We used a pedigree-based Bayesian multivariate best linear unbiased prediction model to perform genetic analysis of SSD, CVSSD, DS, and latent variables.

$$\mathbf{Y} = \boldsymbol{\mu} + \mathbf{Xb} + \mathbf{Zu} + \boldsymbol{\epsilon},$$

where **Y** is a vector of factor scores with individuals ordered within traits, **X** is the incidence matrix of fixed effects, **Z** is the incidence matrix relating individuals with additive genetic effects, $\boldsymbol{\mu}$ is the vector of intercept, **b** is the vector of fixed effects, **u** is the vector of additive genetic effects, and $\boldsymbol{\epsilon}$ is the vector of residuals. The incidence matrix **X** included birth year by date of collection ($n = 2$ per year), primary breed, and sex following recommendations by (Burrow, 2001; Hulsman Hanna et al., 2019). The joint distribution of **u** and $\boldsymbol{\epsilon}$ follows a multivariate normal

$$\begin{pmatrix}\mathbf{u}\\ \boldsymbol{\epsilon}\end{pmatrix} \sim \mathcal{N}\left[\begin{pmatrix}\mathbf{0}\\ \mathbf{0}\end{pmatrix}, \begin{pmatrix}\boldsymbol{\Sigma}_u \otimes \mathbf{A} & \mathbf{0}\\ \mathbf{0} & \boldsymbol{\Sigma}_\epsilon \otimes \mathbf{I}\end{pmatrix}\right],$$

where **A** refers to the numerator relationship matrix, **I** is an identity matrix, $\boldsymbol{\Sigma}_u$ and $\boldsymbol{\Sigma}_\epsilon$ are genetic and residual variance-covariance matrices, respectively. Flat priors were assigned to $\boldsymbol{\mu}$ and **b**. Inverse Wishart distributions with identity scale matrix and 5 degrees of freedom were assigned for $\boldsymbol{\Sigma}_u$ and $\boldsymbol{\Sigma}_e$. The MTM R package (https://github.com/QuantGen/MTM) was employed to infer the parameters in the Bayesian multi-trait linear mixed model and obtain the posterior distribution of these parameters. This was followed by estimating genetic correlations and heritabilities using posterior mean estimates from 10,000 Gibbs samples with 3,000 burn-in and a thinning rate of 5. The model convergence was checked using the trace plots.

3. RESULTS

3.1. Phenotypic Correlation

The phenotypic correlations between all subjective and objective measurements are displayed in **Figure 2**. The subjective measurement TS showed a positive correlation with active, fearful, agitated, irritated, and distressed, whereas, a negative correlation with relaxed, calm, and apathetic was found. Among 12 QBA attributes, we observed positive correlations between similar attributes of temperament (e.g., relaxed and calm) and negative correlations for opposite aspects of temperament (e.g., fearful and calm), which supports the use of EFA for this dataset.

3.2. Latent Structure

The parallel analysis scree plot discovered the first two factors as latent groups (**Figure S2**). The EFA loadings in **Figure 3** further identified these two latent groups can be interpreted as *difficult* (factor 1) and *easy* (factor 2) due to loading values. According to **Figure 4**, the descriptors *difficult* and *easy* were identified because we observed factor 1 has higher loadings for negative temperament attributes (i.e., TS, active, fearful, agitated, irritated, and distressed) and factor 2 has higher loadings for positive temperament attributes (i.e., relaxed, calm, attentive, positively occupied, curious, apathetic, and happy). The EFA factor loadings including DS is displayed in **Figure S3**. As expected, we found that both factors 1 and 2 have low loadings for DS.

The standardized factor loading coefficients and their posterior standard deviations from CFA assuming latent structure shown in **Figure 4** are presented in **Table 1**. The standardized factor loading coefficients can be interpreted as regression coefficients. Overall, we found two factors have strong contributions to 13 subjective measurements. The factor *difficult* presented a strong positive loading to TS (0.861), active (0.820), fearful (0.840), agitated (0.937), irritated (0.844), and distressed (0.607), suggesting difficult is a comprehensive representation of undesirable aspects of temperament. The factor *easy* showed a positive strong loading to relaxed (0.968), calm (0.982), positively occupied (0.636), curious (0.514), apathetic (0.761), and happy (0.730), indicating an increase of *easy* can result in more desirable temperament.

3.3. Genetic Relationships Among Temperament Measurements

The inclusion of birth year by date of collection, breed, and sex fixed effects in multivariate analyses of this study follow previous literature. In this study, birth year by date of collection was significant, breed was not significant, and sex was only significant for CVSSD and *easy* based on 95%

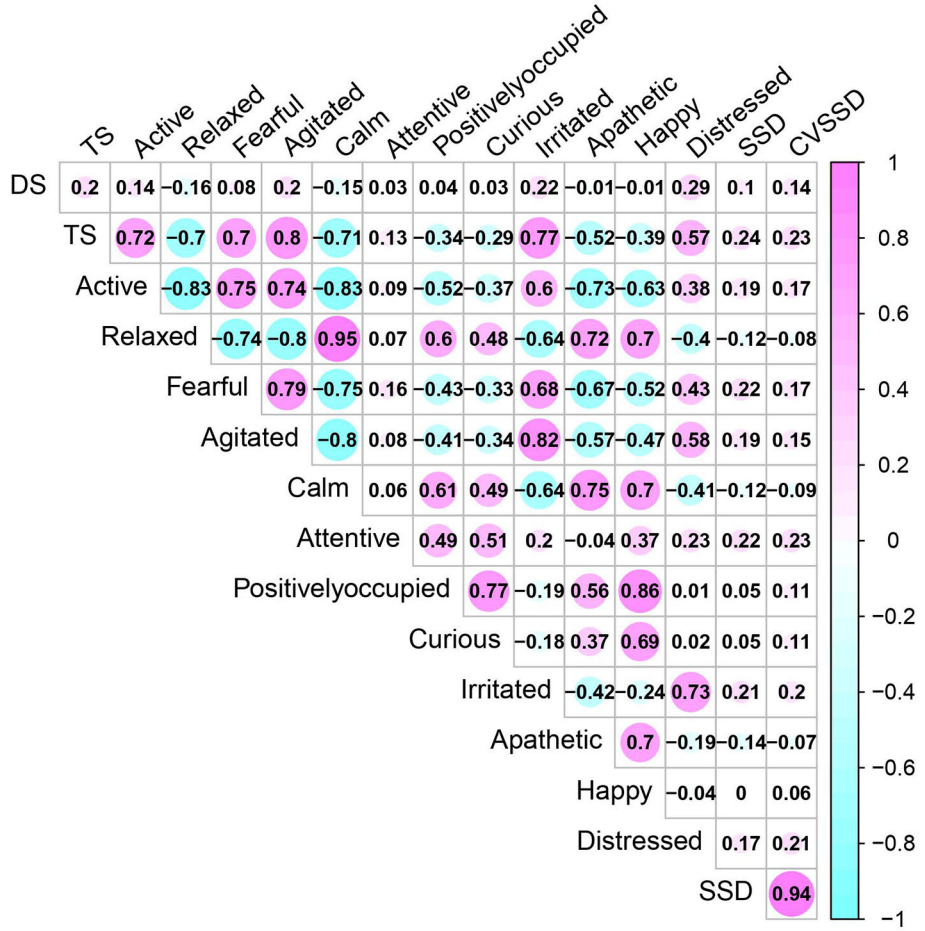

FIGURE 2 | Phenotypic Pearson correlation coefficients between temperament measurements including temperament score (TS), docility score (DS), 12 qualitative behavior assessment attributes, and movement-based scores using four-platform standing scale standard deviation (SSD) and its coefficient of variation (CVSSD).

highest posterior density intervals. The heifers were found to act more temperamental than steers. Effect of sex for these two traits follow trends seen in other literature (Gauly et al., 2001). The estimates of heritability (diagonals) and genetic correlation coefficients (off-diagonals) among SSD, CVSSD, DS, and *easy* and *difficult* factors are shown in **Figure 5**. The largest negative genetic correlation was observed between *difficult* and *easy* with a posterior standard deviation of 0.02. In reference to DS, SSD, and CVSSD, *difficult* and *easy* had moderate genetic correlations with a posterior standard deviation of 0.16. Intuitively, *difficult* had positive genetic correlations (**Figure 5**) with DS, SSD, and CVSSD indicating difficulty of handling increased with increasing values of those variables, respectively. Likewise, *easy* had negative genetic correlations with all three variables. The subjective measure of DS showed a positive genetic correlation with objective measures SSD and CVSSD, along with a posterior standard deviation of 0.16 and 0.17, respectively. Thus, a selection on cattle with lower DS measurement may also result in lower SSD and CVSSD measurements. The two objective measurements SSD and CVSSD showed the largest positive genetic correlation with a posterior standard deviation of 0.06. Among all five measurements, we found *difficult* and *easy* showed the largest heritability estimates. The subjective measure DS showed larger heritability estimates than SSD and CVSSD. Heritability estimates of SSD and CVSSD were similar. All heritability estimates had a posterior standard deviation of about 0.06.

4. DISCUSSION

4.1. Factor Analytic Model

Phenotypes are often correlated at the genetic level due to the pleiotropic effect or the linkage disequilibrium among quantitative trait loci. The multivariate modeling has been widely used to model correlated structure by taking the advantage of the genetic or environmental covariance between phenotypes (Henderson and Quaas, 1976; Campbell et al., 2019). The standard multi-trait approach has been proven to be useful for a trait with low heritability or having scarce records (Mrode, 2014). However, it faces a computational challenge when the number of phenotypes included is large. Thus, dimensional

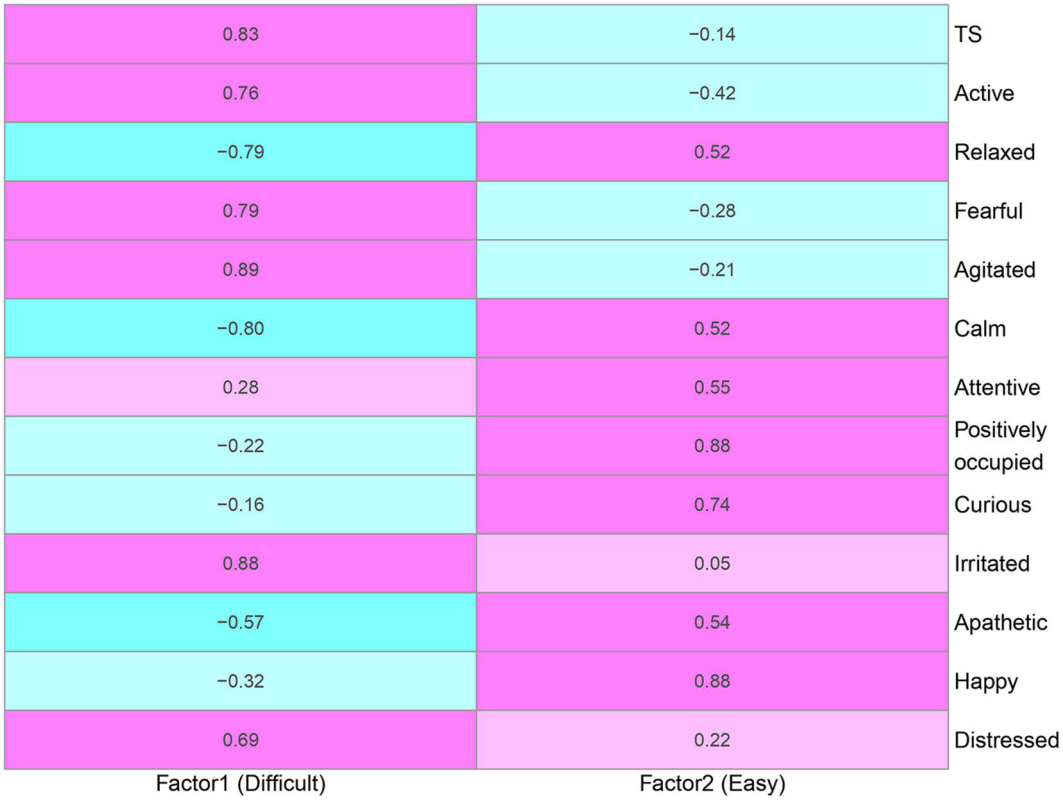

FIGURE 3 | Factor loadings between factors and phenotypes derived from the explanatory factor analysis using temperament score (TS) and 12 qualitative behavior assessment attributes. Positive and negative relationships are denoted as pink and blue, respectively. Factors 1 and 2 are labeled as *Difficult* and *Easy* because of positive loadings on negative and positive temperament attributes, respectively. The degree of shading corresponds to the intensity of the relationships.

reduction methods play an important role in handling high-dimensional phenotypes.

One commonly used approach to study temperament measures is principal component analysis (PCA). This approach calculates principal components (PCs) from a linear combination of observed phenotypes by maximizing the total variance. Napolitano et al. (2012) and Fleming et al. (2013) applied PCA to analyze QBA with the aim of studying dairy buffalo behavior and horse behavior during endurance ride, respectively. Sant-Anna and da Costa (2013) extracted the first principal component from QBA and used it as a new phenotype to study cattle temperament. These studies all suggested traits associated with calm and agitated have a large contribution to the first principal component, which are two extreme characteristics of temperament. The validity of PCs derived from PCA in capturing animal behaviors of both calm and agitated have been supported by the significant correlations with other temperament methods in several studies (Petherick et al., 2002; Sant-Anna and da Costa, 2013). One of the favorable features of QBA is its comprehensive description of temperament by measuring different behaviors. However, the integration of all QBA attributes using PCs with extremely opposite measures (e.g., calm and agitated) may not be desirable because PCA maximizes the total variance, not the variance due to the common signal among measurements. Consequently, selection for temperament based on PCs may be accompanied by substantial risk. Thus, we employed factor analytic modeling for the first time to study temperament measures, which provides a novel approach to investigate multi-phenotypes. The idea behind factor analytic modeling is to represent the observed phenotypes using the unobserved latent variables or factors by maximizing the common variance between correlated phenotypes. When the number of underlying factors are unknown, it is possible to estimate from the data. For instance, de Los Campos and Gianola (2007) performed multi-trait analysis using a factor structure under the Bayesian framework. Alternatively, we can apply a CFA model, when the latent structure is assumed to be known. Peñagaricano et al. (2015) investigated the interrelationships of five latent variables extracted from 19 traits in swine using CFA. Similarly, a Bayesian CFA combined with Bayesian Network was employed to characterize the wide spectrum of 48 rice phenotypes in Yu et al. (2019). These studies determined the latent structure by leveraging the prior biological knowledge between factors and phenotypes. Although the factor analytic model has been applied in animal and plant breeding, there is still paucity of its application to a temperament research.

In this study, we leveraged the combination of EFA and CFA models to identify the mapping between underlying factors

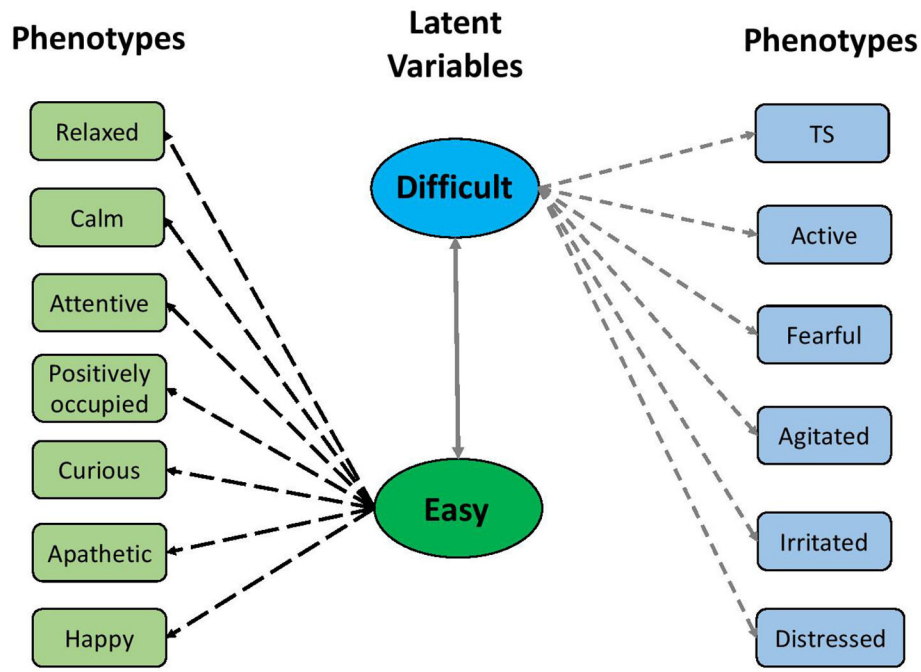

FIGURE 4 | The latent structure between two factors and 12 qualitative behavior assessment attributes. The two factors were defined based on their relationships with negative and positive temperament attributes, respectively.

TABLE 1 | Standardized factor loading and corresponding posterior standard deviation from the Bayesian confirmatory factor analysis.

Latent variable	Observed phenotype	Loading	Posterior standard deviation
Difficult	TS	0.861	0.007
Difficult	Active	0.820	0.010
Difficult	Fearful	0.840	0.008
Difficult	Agitated	0.937	0.004
Difficult	Irritated	0.844	0.009
Difficult	Distressed	0.607	0.016
Easy	Relaxed	0.968	0.002
Easy	Calm	0.982	0.002
Easy	Attentive	0.079	0.025
Easy	Positively occupied	0.636	0.015
Easy	Curious	0.514	0.019
Easy	Apathetic	0.761	0.011
Easy	Happy	0.730	0.012

FIGURE 5 | Genetic correlation estimates between latent variables (*Difficult* and *Easy*) and temperament measurements including docility score (DS), standard deviation of total weight on scale over time (SSD), and coefficient of variation of SSD (CVSSD). *Difficult* and *Easy* were defined based on their relationships with negative and positive temperament attributes, respectively. The diagonal elements are the heritability estimates.

and temperament measures, and performed genetic analysis of inferred factors scores. The EFA model aims at estimating the degree of the contributions of factor to phenotypes, while cross-loading (multiple factors contribute to the same phenotype) is allowed. Using the factor loading coefficients, we inferred the latent structure by removing cross-loading. The combination of EFA and CFA modeling relied on a data-driven method to detect the mapping between factors and phenotypes, which is a common case in practice when prior biological knowledge is not available. In this study, we identified two factors *difficult* and *easy* from TS and 12 QBA. This corroborates the findings from

previous studies using PCA, where the first principal component has been heavily influenced by both calm and agitated related traits (Napolitano et al., 2012; Fleming et al., 2013; Sant-Anna and da Costa, 2013).

4.2. Temperament Measurements

Previous studies reported the estimate of chute score heritability, similar with DS in this study, ranged from 0.11 to 0.34 (Le Neindre et al., 1995; Kadel et al., 2006; Beckman et al., 2007; Hoppe et al., 2010). Burrow and Corbet (2000) suggested objective methods have higher heritabilities than subjective methods of scoring temperament. However, our findings show FPSS measures have slightly lower heritabilities than subjective methods (**Figure 5**). Haskell et al. (2014) reviewed studies using the objective method of flight speed (exit velocity) and found heritability ranged from 0.05 to 0.70. As suggested by many previous studies, heritability estimates vary in studies based on the population's phenotypic variation. For temperament studies, this is typically due to differences in experimental design across experiments (e.g., how evaluators interpret and score the animal behavior), different measurement protocols (e.g., the coding of temperament measurements), and breed differences.

Most subjective measures have positive genetic correlations to other subjective measures in previous studies. For example, Grandin (1993) reported a positive correlation between docility test and chute test using Limousin cattle. A positive genetic correlation between race score and crush score (0.530) was detected by Turner et al. (2011) in *Bos taurus* cattle. Sant-Anna and da Costa (2013) discovered a positive genetic correlation between flight speed and temperament index (0.49), which is the first principal component derived from QBA attributes in principal component analysis. An analogous correlation has been detected in this study, where DS showed a positive genetic correlation with *difficult* (0.36), and a negative genetic correlation with *easy* (−0.31) as shown in **Figure 5**. *Difficult* and *easy* exhibited a large negative genetic correlation (−0.92) which is expected based on the pattern of the temperament measures they loaded to. In this study, subjective methods of DS and *difficult* displayed a moderate positive genetic correlation with objective measurements of SSD (0.42 and 0.42) and CVSSD (0.34 and 0.35). Turner et al. (2011) reported the flight speed has a positive genetic correlation with race score (0.210) and crush score (0.321). Parham et al. (2019) found the exit score and exit velocity capture the same temperament behavior based on a high genetic correlation (0.81). A moderate genetic correlation between flight speed and chute test score has been reported by previous studies (Hoppe et al., 2010; Cafe et al., 2011). These genetic correlations may vary with the differences in breeds, beef production system, evaluator design (e.g., the number of evaluator presented in the study and how evaluator was selected), and/or the number of traits included in a multi-trait analysis. However, genetic correlations found in this study are consistent with previous studies.

DS used in this study, which is also known as chute score (Grandin, 1993), has been widely used in the cattle industry due to its convenience. However, the application of DS is still relying on the human evaluator, which suggests a lack of automation and consistency across populations evaluated (Hieber, 2016; Celestino et al., 2019). Furthermore, DS is the only measurement of temperament with the animal under a restrained condition in contrast with other measurements, which is supported by poor factor loading scores relative to other measures in **Figure S3**. Therefore, we did not combine DS with other subjective methods for EFA. Furthermore, because DS and the two FPSS measures showed similar correlations with *difficult* and *easy* latent variables, the use of FPSS over DS is preferred. This is because the FPSS measures provide automatic, objective, accurate, and consistent measures of temperament rather than relying on evaluator experience and reporting that is needed for DS. It is unlikely, however, that replacement of current scales in cattle production will occur soon due to this. However, the theory of using movement-based scores for temperament has been supported by Sebastian et al. (2011) and Bruno et al. (2018), indicating that replacement of DS with a cost-effective movement-based measure is feasible for genetic selection purposes. Even though DS and FPSS measures identify similar selection on *difficult* and *easy* attributes based on pedigree and correlation coefficients, it is unclear if similar biological pathways or systems are being selected on. Expanding this work to include molecular data to identify genomic relationships among animals and their temperament scores is needed to clarify if selection using movement-based methods can really replace the use of DS in the cattle industry.

5. CONCLUSIONS

Temperament in cattle is a complex trait that is currently being collected in the cattle industry using the subjective DS method. Our study proves that (1) DS (a restrained score) does not align with temperament attributes that are not restrained and (2) measures captured using the FPSS (objectives measures) have similar genetic correlations to DS. This provides support that movement-measuring devices such as the FPSS can be a feasible replacement for DS and mirror more non-restrained attributes of cattle temperament. Furthermore, our study is the first to implement EFA, Bayesian CFA, and multivariate factor analytic modeling approaches to identify and confirm suspected relationships among multiple traits captured on the same set of animals. We contend that the multivariate factor analytic model applied to the current cattle temperament study provides a new avenue to unravel the complexity of animal behaviors.

DATA AVAILABILITY STATEMENT

The datasets used in the current study are available from the corresponding author Lauren L. Hulsman Hanna: lauren.hanna@ndsu.edu.

ETHICS STATEMENT

The animal study was reviewed and approved by Institutional Animal Care and Use Committee of North Dakota State University (protocols A15015 and A18005).

AUTHOR CONTRIBUTIONS

This temperament study was conceived and implemented by LH, CD, SW, and DR. EC performed data entry and audit of raw temperament data and pedigree. HY and GM conceptualized applying factor analytic modeling. HY performed the statistical analysis, initial interpretations of results, and drafted the manuscript. HY, GM, EC, CD, SW, DR, and LH revised the manuscript. All authors read and approved the final manuscript.

FUNDING

This work was supported by the North Dakota Agricultural Experiment Station funds to LH.

ACKNOWLEDGMENTS

The authors wish to express their gratitude to the Central Grasslands Research Extension Center director and staff for their assistance with this project, specifically Bryan Neville, Kevin Sedivec, Stephanie Becker, Jessalyn Bachler, Cody Molle, and Rodney Schmidt. Additionally, data collection for this manuscript would not have been possible without the assistance of Kelsey Amborn, Friederike Baumgaertner, Nayan Bhowmik, Dani Black, Justin Crosswhite, Mellissa Crosswhite, Sarah Cushing, Erin Gaugler, Ashley Giedd, Michael Gonda, Lauren Goetze, Jordan Hieber, Alexis Hoelmer, Logan Hulst, Leah Maertens, Kacie McCarthy, Mikayla Miller, Nicolas Negrin, Blaine Novack, William Ogdahl, Nathan Olson, Felipe da Silva, Andrea Strong, Xin Sun, and Sarah Underdahl. This manuscript has been released as a pre-print at bioRxiv (Yu et al., 2020).

SUPPLEMENTARY MATERIAL

The Supplementary Material for this article can be found online at: https://www.frontiersin.org/articles/10.3389/fgene.2020.00599/full#supplementary-material

REFERENCES

Beckman, D., Enns, R., Speidel, S., Brigham, B., and Garrick, D. (2007). Maternal effects on docility in Limousin cattle. *J. Anim. Sci.* 85, 650–657. doi: 10.2527/jas.2006-450

Beef Improvement Federation (2018). *Uniform Guidelines for Beef Improvement Programs, 9th Edn.* Beef Improvement Federation.

Brooks, S. P., and Gelman, A. (1998). General methods for monitoring convergence of iterative simulations. *J. Comput. Graph. Stat.* 7, 434–455. doi: 10.1080/10618600.1998.10474787

Bruno, K., Vanzant, E., Vanzant, K., Altman, A., Kudupoje, M., and McLeod, K. (2018). Relationship between quantitative measures of temperament and other observed behaviors in growing cattle. *Appl. Anim. Behav. Sci.* 199, 59–66. doi: 10.1016/j.applanim.2017.10.009

Burdick, N., Randel, R., Carroll, J., and Welsh, T. (2011). Interactions between temperament, stress, and immune function in cattle. *Int. J. Zool.* 2011:373197. doi: 10.1155/2011/373197

Burrow, H. (2001). Variances and covariances between productive and adaptive traits and temperament in a composite breed of tropical beef cattle. *Livestock Product. Sci.* 70, 213–233. doi: 10.1016/S0301-6226(01)00178-6

Burrow, H., and Corbet, N. (2000). Genetic and environmental factors affecting temperament of zebu and zebu-derived beef cattle grazed at pasture in the tropics. *Austral. J. Agric. Res.* 51, 155–162. doi: 10.1071/AR99053

Burrow, H., and Dillon, R. (1997). Relationships between temperament and growth in a feedlot and commercial carcass traits of Bos indicus crossbreds. *Austral. J. Exp. Agric.* 37, 407–411. doi: 10.1071/EA96148

Burrow, H., Seifert, G., and Corbet, N. (1988). "A new technique for measuring temperament in cattle," in *Proceedings of the Australian Society of Animal Production* (Sydney, NSW), 154–157.

Cafe, L., Robinson, D. L., Ferguson, D., McIntyre, B. L., Geesink, G., and Greenwood, P. (2011). Cattle temperament: persistence of assessments and associations with productivity, efficiency, carcass and meat quality traits. *J. Anim. Sci.* 89, 1452–1465. doi: 10.2527/jas.2010-3304

Campbell, M. T., Yu, H., Momen, M., and Morota, G. (2019). Examining the relationships between phenotypic plasticity and local environments with genomic structural equation models. *bioRxiv [preprint]*. doi: 10.1101/2019.12.11.873257

Carpenter, B., Gelman, A., Hoffman, M. D., Lee, D., Goodrich, B., Betancourt, M., et al. (2017). Stan: A probabilistic programming language. *J. Stat. Softw.* 76, 1–29. doi: 10.18637/jss.v076.i01

Celestino, E. F. Jr., Hieber, J. K., Dahlen, C. R., Riley, D. G., Wagner, S. A., and Hulsman Hanna, L. L. (2019). Differences in evaluators and genetic parameter estimations using subjective measurements of beef cattle temperament. *Transl. Anim. Sci.* 3(Suppl_1):1769–1773. doi: 10.1093/tas/txz084

de Los Campos, G., and Gianola, D. (2007). Factor analysis models for structuring covariance matrices of additive genetic effects: a bayesian implementation. *Genet. Select. Evol.* 39:481. doi: 10.1186/1297-9686-39-5-481

Fleming, P. A., Paisley, C. L., Barnes, A. L., and Wemelsfelder, F. (2013). Application of qualitative behavioural assessment to horses during an endurance ride. *Appl. Anim. Behav. Sci.* 144, 80–88. doi: 10.1016/j.applanim.2012.12.001

Fordyce, G., Goddard, M., and Seifert, G. (1982). "The measurement of temperament in cattle and the effect of experience and genotype," in *Proceedings of the Australian Society of Animal Production* (Sydney, NSW), 329–32.

Gauly, M., Mathiak, H., Hoffmann, K., Kraus, M., and Erhardt, G. (2001). Estimating genetic variability in temperamental traits in German angus and simmental cattle. *Appl. Anim. Behav. Sci.* 74, 109–119. doi: 10.1016/S0168-1591(01)00151-4

Grandin, T. (1993). Behavioral agitation during handling of cattle is persistent over time. *Appl. Anim. Behav. Sci.* 36, 1–9. doi: 10.1016/0168-1591(93)90094-6

Haskell, M. J., Simm, G., and Turner, S. P. (2014). Genetic selection for temperament traits in dairy and beef cattle. *Front. Genet.* 5:368. doi: 10.3389/fgene.2014.00368

Henderson, C., and Quaas, R. (1976). Multiple trait evaluation using relatives' records. *J. Anim. Sci.* 43, 1188–1197. doi: 10.2527/jas1976.4361188x

Hieber, J. (2016). Temperament evaluation in beef cattle: understanding evaluator bias within subjective measurements of docility score, temperament score, and qualitative behavior assessment (Ph.D. thesis). North Dakota State University, Fargo, ND.

Hoppe, S., Brandt, H., König, S., Erhardt, G., and Gauly, M. (2010). Temperament traits of beef calves measured under field conditions and their relationships to performance. *J. Anim. Sci.* 88, 1982–1989. doi: 10.2527/jas.2008-1557

Horn, J. L. (1965). A rationale and test for the number of factors in factor analysis. *Psychometrika* 30, 179–185. doi: 10.1007/BF02289447

Hulsman Hanna, L. L., Hieber, J. K., Yu, H., Celestino, E. F. Jr., Dahlen, C. R., Wagner, S. A., et al. (2019). Blood collection has negligible impact on scoring temperament in angus-based weaned calves. *Livestock Sci.* 230:103835. doi: 10.1016/j.livsci.2019.103835

Kadel, M. J., Johnston, D. J., Burrow, H. M., Graser, H.-U., and Ferguson, D. M. (2006). Genetics of flight time and other measures of temperament and their

value as selection criteria for improving meat quality traits in tropically adapted breeds of beef cattle. *Austral. J. Agric. Res.* 57, 1029–1035. doi: 10.1071/AR05082

King, D., Pfeiffer, C. S., Randel, R., Welsh, T. Jr., Oliphint, R., Baird, B., et al. (2006). Influence of animal temperament and stress responsiveness on the carcass quality and beef tenderness of feedlot cattle. *Meat Sci.* 74, 546–556. doi: 10.1016/j.meatsci.2006.05.004

Le Neindre, P., Trillat, G., Sapa, J., Ménissier, F., Bonnet, J., and Chupin, J. (1995). Individual differences in docility in limousin cattle. *J. Anim. Sci.* 73, 2249–2253. doi: 10.2527/1995.7382249x

Lee, S.-Y., and Song, X.-Y. (2012). *Basic and Advanced Bayesian Structural Equation Modeling: With Applications in the Medical and Behavioral Sciences*. Hoboken, NJ: John Wiley & Sons.

Merkle, E., and Rosseel, Y. (2018). blavaan: Bayesian structural equation models via parameter expansion. *J. Stat. Softw.* 85, 1–30. doi: 10.18637/jss.v085.i04

Mrode, R. A. (2014). *Linear Models for the Prediction of Animal Breeding Values*. Wallingford; Oxfordshire: CABI. doi: 10.1079/9781780643915.0000

Napolitano, F., De Rosa, G., Grasso, F., and Wemelsfelder, F. (2012). Qualitative behaviour assessment of dairy buffaloes (*Bubalus bubalis*). *Appl. Anim. Behav. Sci.* 141, 91–100. doi: 10.1016/j.applanim.2012.08.002

Parham, J. T., Tanner, A. E., Barkley, K., Pullen, L., Wahlberg, M. L., Swecker, W. S. Jr., et al. (2019). Temperamental cattle acclimate more substantially to repeated handling. *Appl. Anim. Behav. Sci.* 212, 36–43. doi: 10.1016/j.applanim.2019.01.001

Peñagaricano, F., Valente, B., Steibel, J., Bates, R., Ernst, C., Khatib, H., et al. (2015). Searching for causal networks involving latent variables in complex traits: application to growth, carcass, and meat quality traits in pigs. *J. Anim. Sci.* 93, 4617–4623. doi: 10.2527/jas.2015-9213

Petherick, J. C., Holroyd, R., Doogan, V., and Venus, B. (2002). Productivity, carcass and meat quality of lot-fed Bos indicus cross steers grouped according to temperament. *Austral. J. Exp. Agric.* 42, 389–398. doi: 10.1071/EA01084

Réale, D., Reader, S. M., Sol, D., McDougall, P. T., and Dingemanse, N. J. (2007). Integrating animal temperament within ecology and evolution. *Biol. Rev.* 82, 291–318. doi: 10.1111/j.1469-185X.2007.00010.x

Revelle, W. (2018). *psych: Procedures for Psychological, Psychometric, and Personality Research*. R package version 1.8.12. Northwestern University, Evanston, IL.

Sant-Anna, A. C., and da Costa, M. J. P. (2013). Validity and feasibility of qualitative behavior assessment for the evaluation of Nellore cattle temperament. *Livestock Sci.* 157, 254–262. doi: 10.1016/j.livsci.2013.08.004

Schwartzkopf-Genswein, K., Stookey, J., and Welford, R. (1997). Behavior of cattle during hot-iron and freeze branding and the effects on subsequent handling ease. *J. Anim. Sci.* 75, 2064–2072. doi: 10.2527/1997.7582064x

Sebastian, T., Watts, J., Stookey, J., Buchanan, F., and Waldner, C. (2011). Temperament in beef cattle: methods of measurement and their relationship to production. *Can. J. Anim. Sci.* 91, 557–565. doi: 10.4141/cjas 2010-041

Stookey, J., Nickel, T., Hanson, J., and Vandenbosch, S. (1994). A movement-measuring-device for objectively measuring temperament in beef cattle and for use in determining factors that influence handling. *J. Anim. Sci.* 72(Suppl 1):207.

Tanner, M. A., and Wong, W. H. (1987). The calculation of posterior distributions by data augmentation. *J. Am. Stat. Assoc.* 82, 528–540. doi: 10.1080/01621459.1987.10478458

Tier, B., Henshall, J., and McSweeny, J. (2001). "Potential for improving the docility of Limousin cattle in Australia," in *Proceedings of the Association for the Advancement of Animal Breeding and Genetics* (Queenstown, TAS), 345–347.

Tulloh, N. (1961). Behaviour of cattle in yards. II. A study of temperament. *Anim. Behav.* 9, 25–30. doi: 10.1016/0003-3472(61)90046-X

Turner, S., Navajas, E., Hyslop, J., Ross, D., Richardson, R., Prieto, N., et al. (2011). Associations between response to handling and growth and meat quality in frequently handled *Bos taurus* beef cattle. *J. Anim. Sci.* 89, 4239–4248. doi: 10.2527/jas.2010-3790

Yu, H., Campbell, M. T., Zhang, Q., Walia, H., and Morota, G. (2019). Genomic bayesian confirmatory factor analysis and bayesian network to characterize a wide spectrum of rice phenotypes. *Genes Genomes Genet.* 9, 1975–1986. doi: 10.1534/g3.119.400154

Yu, H., Morota, G., Celestino, E. F., Dahlen, C. R., Wagner, S. A., Riley, D. G., et al. (2020). Deciphering cattle temperament measures derived from a four-platform standing scale using genetic factor analytic modeling. *bioRxiv [preprint]*. doi: 10.1101/2020.01.20.913343

Conflict of Interest: The authors declare that the research was conducted in the absence of any commercial or financial relationships that could be construed as a potential conflict of interest.

frontiers in Genetics

ORIGINAL RESEARCH
published: 03 July 2020
doi: 10.3389/fgene.2020.00692

A Genome-Wide Association Study on Feed Efficiency Related Traits in Landrace Pigs

Lu Fu[1†], Yao Jiang[1†], Chonglong Wang[2], Mengran Mei[1], Ziwen Zhou[1], Yifan Jiang[1], Hailiang Song[1] and Xiangdong Ding[1]*

[1] National Engineering Laboratory for Animal Breeding, Laboratory of Animal Genetics, Breeding and Reproduction, Ministry of Agriculture, College of Animal Science and Technology, China Agricultural University, Beijing, China, [2] Institute of Animal Husbandry and Veterinary Medicine, Anhui Academy of Agricultural Sciences, Hefei, China

Feed efficiency (FE) traits in pigs are of utmost economic importance. Genetic improvement of FE related traits in pigs might significantly reduce production cost and energy consumption. Hence, our study aimed at identifying SNPs and candidate genes associated with FE related traits, including feed conversion ratio (FCR), average daily gain (ADG), average daily feed intake (ADFI), and residual feed intake (RFI). A genome-wide association study (GWAS) was performed for the four FE related traits in 296 Landrace pigs genotyped with PorcineSNP50 BeadChip. Two different single-trait methods, single SNP linear model GWAS (LM-GWAS) and single-step GWAS (ssGWAS), were implemented. Our results showed that the two methods showed high consistency with respect to SNP identification. A total of 32 common significant SNPs associated with the four FE related traits were identified. Bioinformatics analysis revealed eight common QTL regions, of which three QTL regions related to ADFI and RFI traits were overlapped. Gene ontology analysis revealed six common candidate genes (*PRELID2, GPER1, PDX1, TEX2, PLCL2, ICAM2*) relevant for the four FE related traits. These genes are involved in the processes of fat synthesis and decomposition, lipid transport process, insulin metabolism, among others. Our results provide, new insights into the genetic mechanisms and candidate function genes of FE related traits in pigs. However, further investigations to validate these results are warranted.

Keywords: genome-wide association study, feed efficiency, feed conversion ratio, average daily gain, average daily feed intake, residual feed intake

OPEN ACCESS

Edited by:
Fabyano Fonseca Silva, Universidade Federal de Viçosa, Brazil

Reviewed by:
Rodrigo Reis Mota, Gembloux Agro-Bio Tech - University of Liège, Belgium
Rodrigo Mezêncio Godinho, Topigs Norsvin Research Center, Netherlands

****Correspondence:***
Xiangdong Ding
xding@cau.edu.cn

[†] These authors have contributed equally to this work

Specialty section:
This article was submitted to Livestock Genomics, a section of the journal Frontiers in Genetics

Received: *03 December 2019*
Accepted: *05 June 2020*
Published: *03 July 2020*

Citation:
Fu L, Jiang Y, Wang C, Mei M, Zhou Z, Jiang Y, Song H and Ding X (2020) A Genome-Wide Association Study on Feed Efficiency Related Traits in Landrace Pigs. Front. Genet. 11:692. doi: 10.3389/fgene.2020.00692

INTRODUCTION

Feed accounts for about 65% of the total cost in modern pig production and feed efficiency (FE) traits in pigs are critical (Sanchez et al., 2017). Better FE dramatically reduces production costs, thus contributes to a reduction of the final cost of products and decreases farming expenses and energy consumption (Ding et al., 2018). Breeding programs to improve FE have been undertaken for many years, but FE related traits, such as average daily feed intake (ADFI) and residual feed intake (RFI), are still difficult to be improved because they can neither be selected nor directly

measured (Silva et al., 2019). Usually, FE is evaluated by four traits: feed conversion ratio (FCR), average daily gain (ADG), ADFI, and RFI (Onteru et al., 2013). The phenotypic measurements of FCR, ADFI, and RFI are difficult and costly which need an automatic feeding system. Besides, the selection of single FE related traits may affect other traits that are valuable for pig production, such as growth rate (Horodyska et al., 2017). This conundrum makes the genetic investigation of FE very important.

Therefore, it is essential to understand the molecular mechanism and genetic basis underlying FE related traits for the improvement of FE. In past decades, hundreds of quantitative trait loci (QTLs) affecting complex traits in pigs, including FE related traits, have been detected. Among these, 346, 618, 96, and 96 QTLs for FCR, ADG, ADFI, and RFI have been identified in different pig populations,[1] respectively. However, their molecular regulation mechanism remains largely unknown.

In recent years, with the development of dense genomic markers and significant reduction in cost, genome-wide association study (GWAS) has become increasingly popular for detecting genetic variants associated with economic traits (Do et al., 2014b; Ding et al., 2018). Studies have revealed many potential candidate genes for FE related traits in pigs. For FCR, several researchers reported that significant SNPs and QTLs were mainly located on chromosomes (SSC) 4, 6, 7, 8, 17, and 18 (Sahana et al., 2013; Horodyska et al., 2017). Another study identified three QTLs for ADG, which were located on SSC 4, 14, and 15 (Ji et al., 2019). Compared to FCR and ADG, only few studies on RFI were carried out in pigs. Onteru et al. (2013) reported several QTLs on chromosomes 7 and 14 that are related to RFI in Yorkshire pigs. Recently, Silva et al. (2019) identified three QTL regions located on SSC1 that are associated with ADFI. Although high density chips and GWAS had detected more and more genetic variants in pig economic traits, FE related traits (ADFI and RFI) still progress slowly because of the difficultly in phenotype measuring and recording. In addition, most of these studies, mainly focus on Duroc and Yorkshire breeds, and FE related traits studies on Landrace have been rarely reported. So far, according to PigQTLdb,[1] four FE related traits (FCR, ADG, ADFI, and RFI) have been reported 371 QTLs in Duroc, 185 in Yorkshire and only 46 in Landrace pigs. Therefore, further investigation is needed to better understand FE related traits in Landrace population.

In this study, we performed a GWAS in a Landrace population to identify genomic regions and genes associated with four FE related traits: FCR, ADG, ADFI, and RFI.

MATERIALS AND METHODS

Ethics Statement

The whole recording procedure of ear tissue samples was carried out in strict accordance with the protocol approved by the Institutional Animal Care and Use Committee (IACUC) at the China Agricultural University. The IACUC of the China Agricultural University approved this study (permit number DK996).

Animals and Phenotypes

In this study 296 Landrace pigs were sampled. Phenotypic information of two batches comprising 156 and 140 pigs was recorded from April to July, and July to August in 2018, respectively. The first batch of 156 pigs was obtained from 46 litters born in April (one to nine individuals from each litter with an average of three), and the 140 pigs in the second batch born in July were obtained from 41 L (one to eight individuals from each litter with an average of three). The original feeding records were automatically generated by the pig automatic feeding system (ACEMO128 Feeding station, France). The phenotypic data comprised individual ID, starting weight, daily feed intake, daily weight gain, final weight, feeding period, and feed conversion rate. Data were collected from each pig during the feeding period (approximately 11 weeks old), from 25 to 100 kg body weight (BW). The piglets were group-housed in half-open cement-floor pens (10–12 animals in each pen, with an average space of two m^2 per pig). Each animal was labeled with a unique electronic identification tag on the ear and detected by the automatic feeding system. Once a pig visited the feeder, the date and exact start and stop feeding time, the animal number, and feed consumption of each visit were recorded.

The traits (ADFI, FCR, and ADG) for each pig were calculated throughout the testing periods according to the information provided by the automatic feeding system. ADFI was calculated by the total amount of recorded feed intake divided by the length of the fattening period. ADG was calculated by total weight gain (final weight minus initial weight) during measure periods divided by the corresponding feeding days. FCR was calculated as the ratio of total feed intake to total weight gain. Finally, RFI was calculated following the formula (Do et al., 2013).

$$\mathrm{RFI} = \mathrm{ADFI} - (\beta_0 + \beta_1 \mathrm{BW} + \beta_2 * \mathrm{ADG} + \mathrm{e})$$

where β_0 is the intercept, β_1 represents the partial regression coefficient of ADFI on BW, β_2 is the partial regression coefficient of ADFI on ADG, and e is the residual error.

The phenotype values of four FE related traits were calculated, and their corresponding descriptive statistics were performed (**Table 1**). The average FCR was 2.47 with a standard deviation of 0.52, whereas ADG and ADFI were 0.79 and 1.93 kg per day on

TABLE 1 | The descriptive statistics of four feed efficiency traits.

Trait[a]	N-1[b]	N-2[c]	Mean	SD[d]	Min	Max	p_value[e]
FCR	156	140	2.47	0.52	1.05	4.75	1.02E-09
ADG (kg/day)	156	140	0.79	0.12	0.38	1.18	0.89
ADFI (kg/day)	156	140	1.93	0.38	0.68	2.91	2.63E-10
RFI (kg)	156	140	0.01	0.32	−1.00	0.83	1.76E-14

[a]FCR, feed conversion ratio; ADG, average daily gain; ADFI, average daily feed intake; RFI, residual feed intake. [b]N-1 = number of individuals for each trait in the first batch. [c]N-2 = number of individuals for each trait in the second batch. [d]SD = standard deviation. [e]p_value = p-value of Student's test for two batches data at significance level 0.05.

[1]http://www.animalgenome.org/cgi-bin/QTLdb/SS/index

average with a standard deviation of 0.12 and 0.38, respectively. RFI ranged from -1.00 to 0.83 kg with an average of 0.01 and a standard deviation of 0.32. The Student's *t*-test showed that the data from the two batches of pigs were significantly different for FCR, ADFI, and RFI. The genetic correlations of FE related traits were calculated using ASREML software (Gilmour et al., 2015) four traits were analyzed together. The model fitted for FCR, ADG, ADFI, and RFI was:

$$y = \mu + Xb + Z_1a + Z_2t + e$$

with

$$E\begin{Bmatrix} y \\ a \\ t \\ e \end{Bmatrix} = \begin{Bmatrix} Xb \\ 0 \\ 0 \\ 0 \end{Bmatrix}, \ Var\begin{Bmatrix} a \\ t \\ e \end{Bmatrix} = \begin{Bmatrix} A\sigma_a^2 & 0 & 0 \\ 0 & I\sigma_t^2 & 0 \\ 0 & 0 & I\sigma_e^2 \end{Bmatrix}$$

where, **y** is the vector of phenotypic values of four trait; μ is the population mean; **b** is the fixed effect of the batch; **a** is the vector of additive genetic effects; **t** is the vector of litter effects; **e** is a vector of residual error effects. **X**, $\mathbf{Z}_1$, and $\mathbf{Z}_2$ are incidence matrices of **y** related to **b**, **a,** and **t**, respectively. **A** is the genetic relationship matrix, five generations of pedigree were traced back to construct A, and $\sigma_a{}^2$ is the additive genetic variance. **I** is the identity matrix of appropriate dimension, $\sigma_t{}^2$ is the variance of litter effect and $\sigma_e{}^2$ is the residual variance.

Subsequently, genetic correlations were calculated based on the variance components as follows:

$$r_A = \frac{cov(a_1, a_2)}{\sigma_{a_1}\sigma_{a_2}}$$

where, r_A is the genetic correlation between trait 1 and trait 2, a_1 and a_2 represent the additive genetic values of trait 1 and trait 2 for same individuals, $cov(a_1,a_2)$ and σ_{a1}, σ_{a2} refer to the genetic covariance of two traits and genetic standard deviation of trait 1 and trait 2, respectively.

Genotyping and Quality Control

Genomic DNA was extracted from ear samples using a TIANamp Blood DNA Kit (catalog number DP348; Tiangen, Beijing). Genotyping was performed on 50697 SNPs across the entire pig genome using a PorcineSNP50 BeadChip (Illumina, San Diego, CA, United States). Quality control was performed using PLINK 1.9 software (Chang et al., 2015). Individuals with call rates (CR) less than 95% were removed and then SNP with CR less than 95%, minor allele frequencies (MAF) < 5%, or significant deviation from the Hardy–Weinberg equilibrium (HWE; $P < 10 \times 10^{-6}$) were removed. After genotype quality control, no individuals were removed, and 41272 SNPs remained for further analysis.

Genome-Wide Association Study

In this study, two different single-trait methods, single SNP linear model GWAS (LM-GWAS) and single-step GWAS (ssGWAS) were implemented to identify significant SNPs associated with FE related traits.

Linear Model GWAS (LM-GWAS)

A single SNP marker linear regression model was performed using the following single-trait animal model to detect the association of SNP with the four FE related traits, respectively. In order to control population stratification and to account for shared genetic effects of related individuals, a random polygenic effect was included in this model (Sanchez et al., 2014):

$$y = \mu + batch + bx + g + e$$

where, **batch** is the fixed effect of the batch; **b** is the average effect of the gene substitution of a particular SNP; **x** is a vector of the SNP genotype (coded as 0, 1, or 2); **g** is a vector of random polygenic effects with a normal distribution $\mathbf{g}\sim N(0, \mathbf{G}\sigma^2)$, in which σ^2 is the additive polygenic variance, and **G** is the genomic relationship matrix constructed using all markers following Yang et al. (2011) **e** is a vector of residual effects with a normal distribution $e\sim N(0, \mathbf{I}\sigma_e{}^2)$, where **I** is the identity matrix of appropriate dimension and $\sigma_e{}^2$ is the residual variance. For each SNP marker, the estimation of b and its sampling variance $\sigma_b{}^2$ can be obtained through the mixed model equations.

Single-Step GWAS (ssGWAS)

Compared to LM-GWAS, the following single-trait animal model in ssGWAS proposed by Wang et al. (2012) can simultaneously use all the SNP information:

$$y = Xb + Zu + e$$

where **b** is the fixed effect of batch; **u** is the vector of additive genetic effects with a normal distribution $\mu\sim N(0, \mathbf{G}\sigma_\mu{}^2)$, $\sigma_u{}^2$ is the additive genetic variance, and **G** is same as in LM-GWAS. **X** and **Z** are incidence matrices of **y** related to **b** and **u**, respectively.

The effect of each SNP can be estimated by ssGWAS, following Aguilar et al. (2019) the *P*-value of each SNP was calculated:

$$p_i = P_t\left(\frac{\hat{u}_i}{\sqrt{\hat{\sigma}_i^2/n}}, n-1\right)$$

where P_t is the distribution function of t distribution, $\frac{u}{i}$ is ith SNP effect, $\widehat{\sigma}_i{}^2$ is the genetic variance of ith SNP, n is the number of animals with ith SNP.

The software GCTA (Yang et al., 2011) was used for the LM-GWAS method. The genetic variance of each SNP was also provided. For ssGWAS, blupf90 was to estimate genomic breeding values that were used to further estimate SNP effects and *P*-values via postGSf90 (Aguilar et al., 2018).

In order to control false positives, the False Discovery Rate (FDR) method for multiple testing was used (Benjamin and Hochberg, 1995; Weller et al., 1998). FDR was calculated as:

$$FDR = \frac{m \times P_{Max}}{n}$$

where **m** is the number of times to be tested, **n** is the number of significant SNPs at assigned FDR level, e.g., 0.01. $\mathbf{P}_{Max}$ is the genome-wide significance level empirical *P*-value of FDR adjusted. Based on the *P*-values of SNPs obtained by two different

methods, the empirical *P*-value of FDR adjusted at the genome-wide significance level of 0.01 was calculated on each trait for two methods in this study.

Population Stratification

In order to assess the influence of population stratification on the GWAS, A quantile-quantile (Q-Q) plot was generated using PLINK 1.9 software.

Identification of Candidate Genes

After identifying significant SNPs by GWAS, the genes located in or overlapping between the 0.25 Mb downstream and 0.25 Mb upstream region of the significant SNPs were determined using the Ensembl (Sus scrofa 11.1 genome version).[2] QTLdb[3] was used to annotate significant SNPs located in previously mapped QTLs in pigs. To identify the related pathways and function annotation, KEGG[4] and Gene Ontology analyses[5] were performed.

RESULTS

Genetic Correlations of FE Related Traits

The genetic correlations of FE related traits ranged from 0.12 to 0.90, while the standard errors of all genetic correlations were high. Among the four FE related traits, FCR had the highest genetic correlations of 0.90 with ADFI, while it had the lowest genetic correlation of 0.12 with ADG. The corresponding standard errors were 0.17 and 0.59. The genetic correlation between FCR and RFI was 0.72 with standard error of 0.18. Similarly, the genetic correlation of RFI with ADFI was 0.71 with standard error of 0.14. The genetic correlations of ADG with ADFI and RFI were 0.51 and 0.38 with standard errors of 0.34 and 0.44, respectively.

Population Stratification

False-positive results for significant SNPs are the most critical problem in GWAS. Therefore, it is essential to control population stratification and reduce the occurrence of false-positive results. The quantile-quantile plots (Q-Q plots) show that the influence of population stratification was negligible (**Figure 1**). Moreover, the average genomic inflation factors (λ) for the four FE related traits were close to 1 (range 1.02–1.09). The QQ plots and λ suggest that there were little or no residual population structure effects on the test statistic inflation. Despite the small sample size, the results of GWAS were reasonable and worth further investigation.

Identification of Significant SNPs and QTL Regions Associated With FE Related Traits

All significant SNPs associated with the four FE related traits (FCR, ADG, ADFI, and RFI) identified by GWAS are illustrated in **Supplementary Tables 1, 2** and **Figures 2**, **3**. In LM-GWAS and ssGWAS methods, the empirical *P*-values of a multiple testing based on FDR adjusted at the genome-wide significance level of 0.01 for FCR were 7.48×10^{-4} and 7.17×10^{-4}, respectively. For ADG, ADFI and RFI, the genome-wide empirical *P*-values obtained by LM-GWAS were 5.64×10^{-4}, 6.53×10^{-4} and 7.58×10^{-4}, and ssGWAS were 5.24×10^{-4}, 6.16×10^{-4} and 5.89×10^{-4}, respectively. A total of 55 and 50 genome-wide significant SNPs were found by LM-GWAS and ssGWAS methods, 32 SNPs out of them were common (**Figure 4**). Among the 55 significant SNPs identified by the LM-GWAS method, 15, 11, 13, and 16 SNPs were related to FCR, ADG, ADFI, and RFI, and correspondingly explained 2.66, 1.33, 1.64, and 1.80% additive genetic variance, respectively. These SNPs were mainly located on all autosomes except SSC15 (**Supplementary Table 1**). Among them, two significant SNPs (WU_10.2_6_122065838, WU_10.2_4_116973174) were associated with both ADFI and RFI. The ssGWAS method identified 9, 13, 17, and 11 significant SNPs associated with FCR, ADG, ADFI and RFI, which were mainly located on SSC3, 4, 8, 9, and 17, respectively (**Supplementary Table 2**), and explained 1.20, 1.79, 2.07, and 1.29% additive genetic variance. Among the 50 SNPs, three common SNPs (WU_10.2_6_122065838, ALGA0049005 and ALGA0019602) were all significant in both ADFI and RFI. In addition, the SNP WU_10.2_6_122065838 was also identified in the LM-GWAS method.

Meanwhile, 13 regions were identified by two methods, as shown in **Table 2**. Among them, eight common regions were found by two different methods. Three regions for FCR were found located on SSC7, SSC17, and SSC18, respectively. Four regions for ADG were identified on SSC2, SSC3, SSC4, and SSC5. Four regions for ADFI and five regions for RFI were also identified. Among them, one region for ADG and ADFI, and two regions for ADFI and RFI overlapped. According to Pig QTLdb,[1] eight regions identified in our study overlapped or were close to the reported QTLs related to FCR, ADG, ADFI, and RFI. Among them, four regions overlapped and four regions were nearby the reported QTLs.

Identification of Candidate Genes

All the significant SNPs identified by the two methods were annotated within the 0.25 Mb downstream and upstream region with reference to the Sus scrofa 11.1 genome assembly. GO analysis separately revealed 12 candidate genes for LM-GWAS and 7 candidate genes for ssGWAS (**Table 3**). Combined these two methods, 13 positional candidate genes were detected for the four FE related traits. Among them, six genes had function related to FCR, two genes for ADG, four genes for ADFI, and two for RFI. These 13 candidate genes have a highlight biology function with FE, which involved in biological processes such as lipid metabolism, carbohydrate metabolism, lipid transport, and regulation of insulin secretion. Among them, six genes were identified in both LM-GWAS and ssGWAS methods.

[2]http://www.ensembl.org/Sus_scrofa/Info/Index/

[3]http://www.animalgenome.org/cgi-bin/QTLdb/SS/download?file=gbpSS_11.1

[4]http://www.kegg.jp/kegg/pathway.html/

[5]http://www.pantherdb.org/

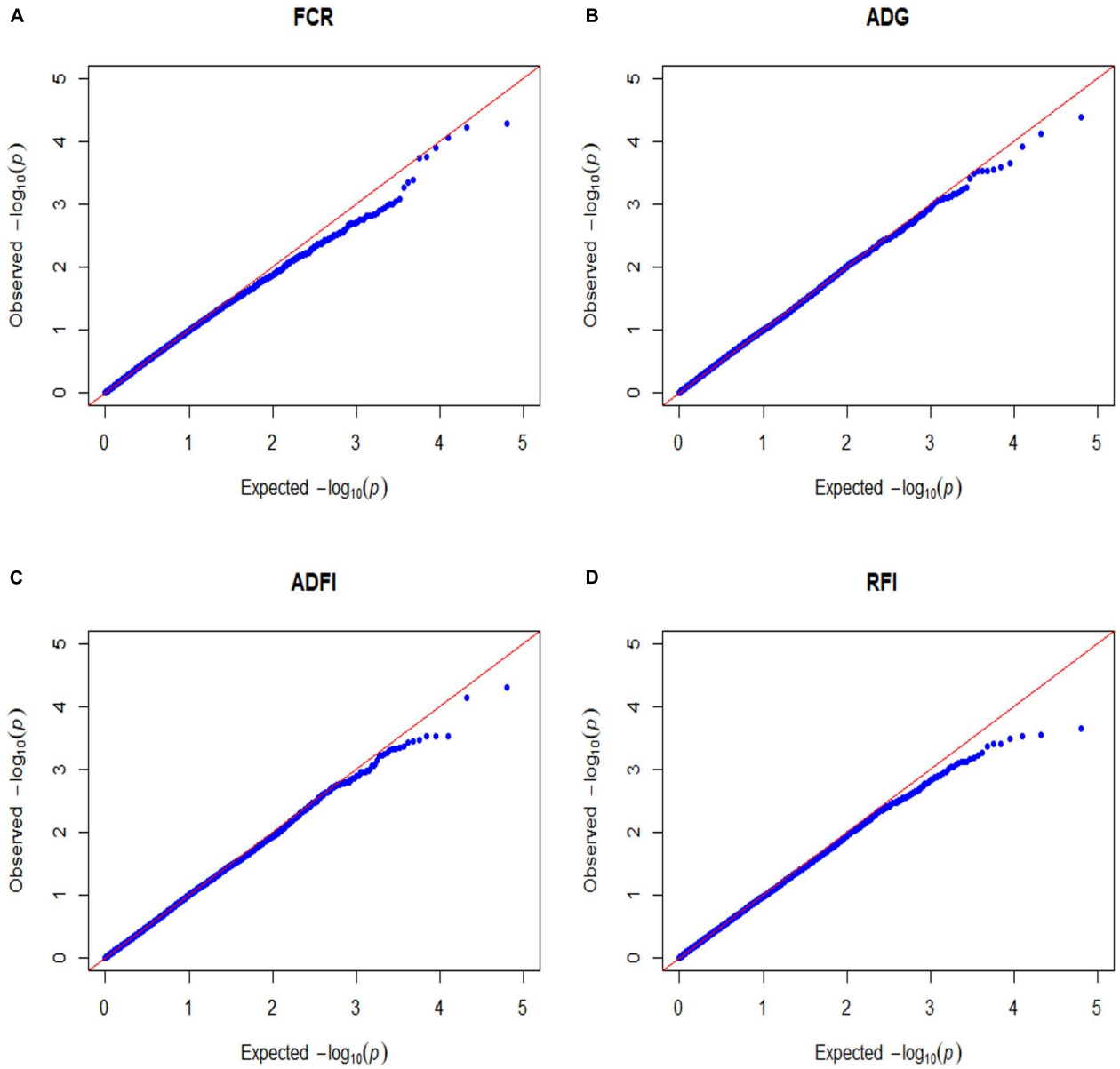

FIGURE 1 | Quantile–quantile plots of GWAS for four feed efficiency traits in a Landrace population. FCR, Feed conversion ratio; ADG, Average daily gain; ADFI, Average daily feed intake; RFI, Residual feed intake. The *x*-axis and the *y*-axis represent the expected and observed -$\log_{10}$(*P*-value). **(A)** FCR. **(B)** ADG. **(C)** ADFI. **(D)** RFI.

DISCUSSION

Sample Size for GWAS

Sample size is a key factor for the efficiency of GWAS; one drawback of this study is that only 296 Landrace pigs were used to detect the genetic variants related to FE related traits. Compared to other traits, the measurements of FE related traits are usually difficult. Besides, it is not easy to acquire a large sample size. For instance, Ding et al. (2017) used a comparable population size of 338 Duroc boars to detect feeding behavior and eating efficiency by GWAS. Ramayo-Caldas et al. (2019) integrated GWAS and gene expression to identify putative regulators and predictors of FE using 350 Duroc pigs. To minimize the effect of the small sample size on GWAS, the phenotypes were strictly measured in this study, and two different methods were implemented, which adopted a single-marker only or multiple SNPs simultaneously to take into account the genetic correlations among relevant traits.

Genetic Correlations and Significant SNPs With Pleiotropy

GWAS performed in pigs revealed significant associations for economically-relevant traits. In recent years, researches

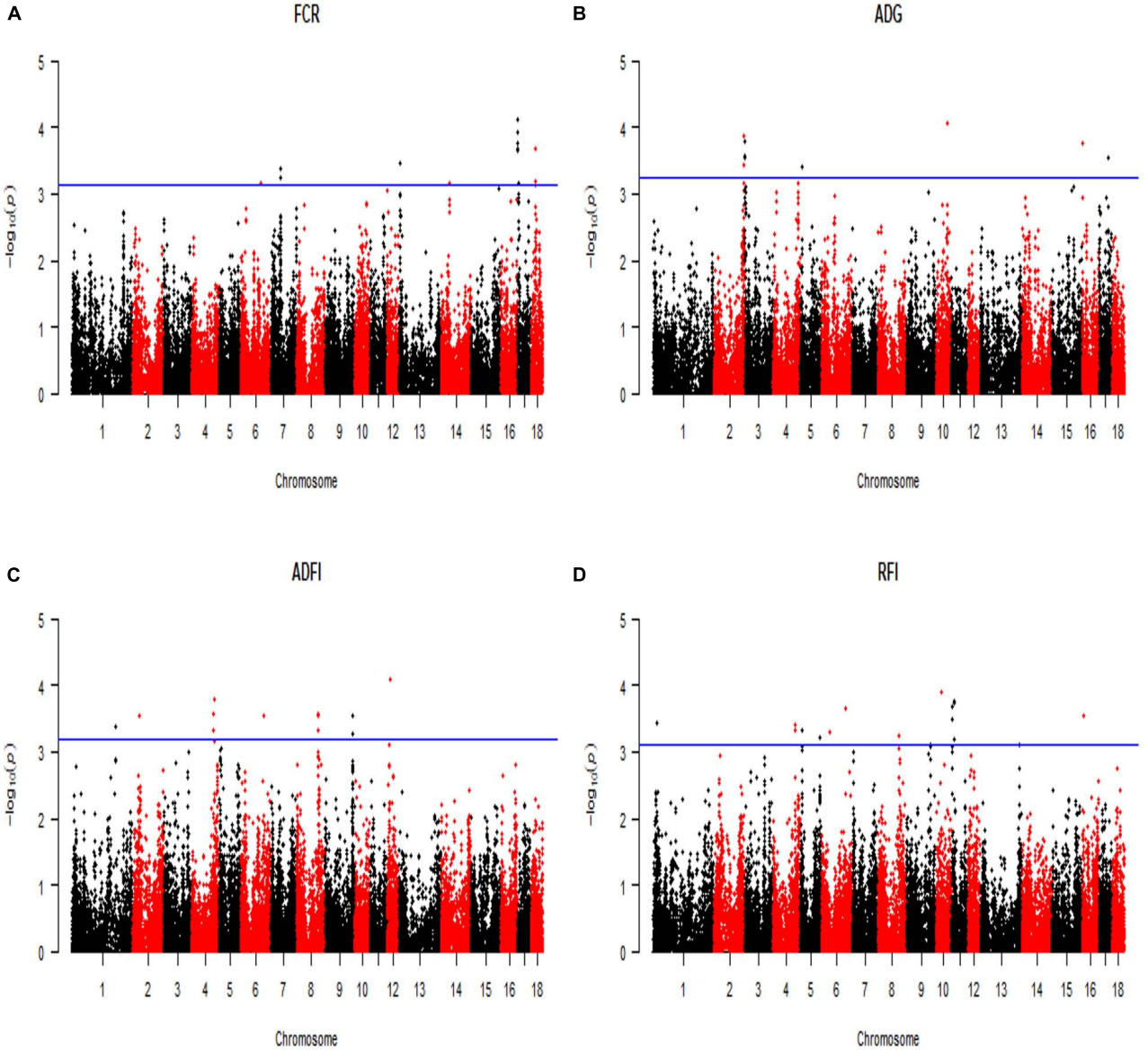

FIGURE 2 | Manhattan plot of the genome-wide association analysis on four feed efficiency traits by using linear model GWAS (LM-GWAS) method. FCR, Feed conversion ratio; ADG, Average daily gain; ADFI, Average daily feed intake; RFI, Residual feed intake. In the Manhattan plots, negative log10 *P*-values of the quantified SNPs were plotted against their genomic positions. The *x*-axis and the *y*-axis represent the number of chromosome and the observed -$\log_{10}$(*P*-value), respectively. Different colors indicate various chromosomes. The blue lines indicate the genome-wide significant thresholds of FDR adjusted, respectively. For **(A)** FCR, it was 7.48×10^{-4}. Similarly, **(B)** ADG was 5.64×10^{-4}, **(C)** ADFI was 6.53×10^{-4}, and **(D)** RFI was 7.58×10^{-4}.

performed GWAS on FE related traits, unveiling high genetic correlations. For instance, Godinho et al. (2018) found that in purebred pig ADFI highly genetically correlates with FCR (0.71) and RFI (0.73), respectively. FCR had a high correlation with RFI (0.82). Do et al. (2013) also found high genetic correlations between FE related traits in Landrace. They found the genetic correlation of ADG and ADFI was 0.72. RFI had highly genetic correlations with FCR (0.91) and ADFI (0.84). Similar results were also found in our study (**Table 2**). Furthermore, our results showed that some significant SNPs with pleiotropic effects were identified. Four SNPs were significantly associated with both ADFI and RFI. Moreover, significant SNPs identified in GWAS overlap between some extent for these two traits. Based on the regions of merging neighbored significant SNPs, significant SNPs for ADFI (4 SNPs) and RFI (2 SNPs) were located in a region of 105.57–106.83 Mb on SSC4. Similarly, the regions of 102.88–105.56 Mb on SSC8 correlated with both RFI and ADFI. We speculate that due to the pleiotropy of the SNPs associated with one trait (ADFI/ RFI), these traits tend to affect multiple additional phenotypes. Likewise, in cattle, many concordant QTLs between RFIp (calculated from linear phenotypic regression) and RFIg (calculated from linear genetic

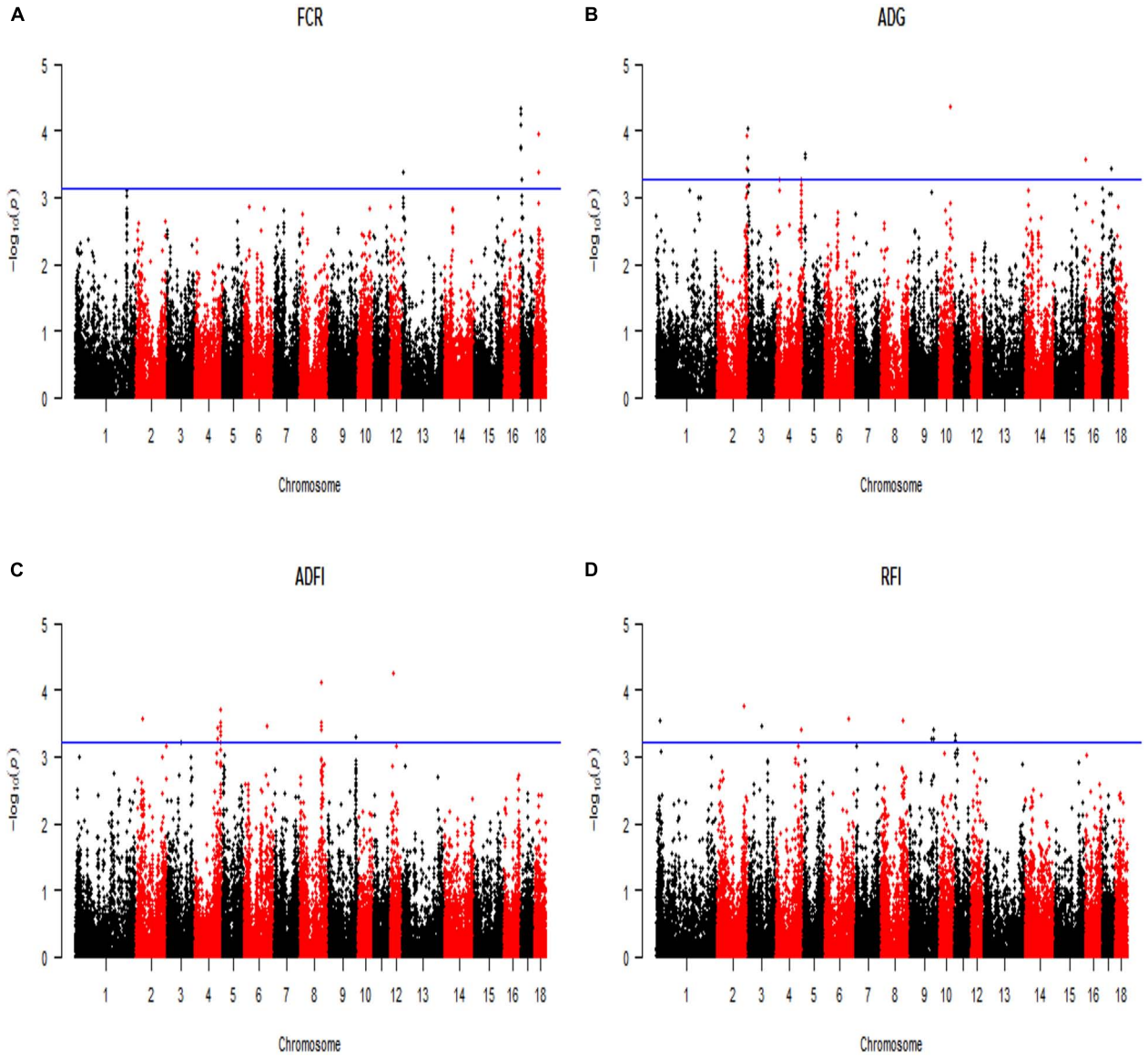

FIGURE 3 | Manhattan plot of the genome-wide association analysis on four feed efficiency traits by using single-step GWAS (ssGWAS) method. FCR, Feed conversion ratio; ADG, Average daily gain; ADFI, Average daily feed intake; RFI, Residual feed intake. In the Manhattan plots, negative log10 *P*-values of the quantified SNPs were plotted against their genomic positions. The *x*-axis and the *y*-axis represent the number of chromosome and the observed -$\log_{10}$(*P*-value), respectively. Different colors indicate various chromosomes. The blue lines indicate the genome-wide significant thresholds of FDR adjusted, respectively. For **(A)** FCR, it was 7.17×10^{-4}. Similarly, **(B)** ADG was 5.52×10^{-4}, **(C)** ADFI was 6.16×10^{-4}, and **(D)** RFI was 5.89×10^{-4}.

regression) were reported by Nkrumah et al. (2007) 14 common and 3 distinct QTLs were identified for the two RFI measures.

The Comparison of Different Methods

Single SNP regression model is widely used in GWAS to identify the association of SNP with traits of interest, whereas it usually yields a high false-positive rate due to ignoring the linkage disequilibrium between adjacent SNPs. Some researchers investigated a haplotype-based sliding window strategy to reduce the false-positive by using multiple SNPs simultaneously. Some studies indicated that sliding window could result in different QTL regions, genes and SNPs with a single SNP method (Guo Y. et al., 2008; Braz et al., 2019) while some results showed that sliding window for GWAS could be complementary to single SNP analysis (Lorenz et al., 2010; Guerra et al., 2019). The controversy may perhaps depend on the different genetic architecture of the target trait. Recently, ssGWAS, which enables simultaneous analysis of an extensive array of SNPs, demonstrated its superiority in the reduction of false-positive rates (Wang et al., 2012). Therefore, ssGWAS and LM-GWAS were both used in our study to reduce false-positive rates and identified the correctness of our results. Our results reinforce the

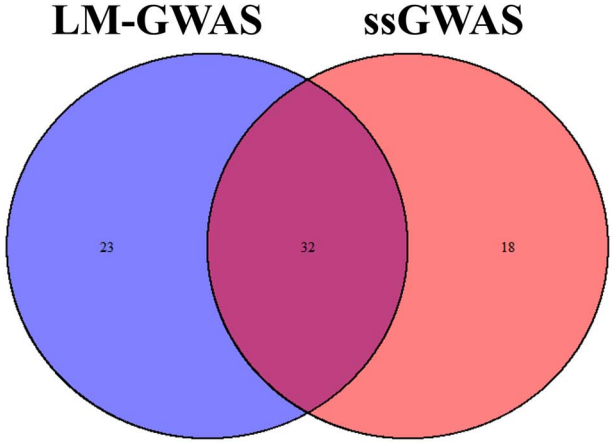

FIGURE 4 | Venn plot of significant SNPs in two methods. Significant SNPs by linear model GWAS (LM-GWAS) and single-step GWAS (ssGWAS) for four traits.

high consistency of these two methods, in which 32 common significant SNPs were identified by both methods (**Figure 4**). Meanwhile, Wang et al. (2014) reported that ssGWAS and a single-marker model had similar results in broiler chickens. So all these two methods could improve the power of GWAS and the accuracy of significant SNPs selected.

QTLs Related to FE Related Traits

Alignment of the genetic and physical maps on the Sus scrofa 11.1 genome assembly (Pig QTLdatabase) enabled comparison of the QTLs detected in our study with previously described QTL regions, and several of QTLs were selected for further analysis. The most prominent common regions for FCR were identified on SSC17, and 18. A QTL from this study located at 20.48–20.96 Mb on SSC18 coincides with a QTL identified for ADG in a Duroc sire population mapped across the region of 21.47–21.47 Mb (Wang et al., 2015). For ADFI, the most promising QTLs were detected on porcine SSC9. A QTL located at 128.77–129.09 Mb on SSC9 overlapped with a QTL for ADFI in a pig line (Reyer et al., 2017). In addition, other QTLs located in 1.15–2.69 Mb (SSC17) for FCR and 0.35–0.54 Mb (SSC3) for ADG were all also consistent with QTLs for BW (Guo Y. M. et al., 2008; Fan et al., 2009). Two interesting regions containing all 6 significant SNPs for both ADFI and RFI were detected in the regions of 105.57–106.83 Mb on SSC4 and 102.88–105.56 Mb on SSC8. Among them, the QTL located in 105.57–106.83 Mb overlapped with two identified QTLs for FCR in the regions of 105.64–105.64 Mb and 106.51–124.31 Mb (Wang et al., 2015). Thus, this QTL has been independently discovered in different populations for ADFI/RFI and FCR, which further supports the biological relevance of common genetic variation on FE related traits (Becker et al., 2013). Another QTL for ADFI/RFI traits located at 102.88–105.56 Mb on SSC8 found in this study was in close proximity to a QTL (107.04–113.33 Mb) for ADG reported by Haggman and Uimari (2017). The remaining QTL regions for ADG identified in this study on SSC2 and 5 were close to regions affecting FE related traits and growth rate according to literature reports (Fan et al., 2009; Rothammer et al., 2014). Gregersen et al. (2012) reported a limited overlap of QTL for a particular trait between breeds. Although the sample size was limited, our result also had a large number of overlapping and coinciding QTL regions is in accordance with others' GWAS results, and it suggests that our present study is reliable and accurate in a certain extent, and worth of further research for verifying candidate genes.

Potential Candidate Genes

Potential Candidate Genes for FCR

Growth rate and feed intake were major influencing factors of FCR. One candidate gene Phospholipase A2 Group IB (*PLA2G1B*), which can encode a secreted member of the phospholipase A2 (*PLA2*), is crucial for the biological functions of lipid metabolic and catabolic processes. Hollie and Hui (2011) found that *PLA2G1B* affects the inhibition of lysophospholipid absorption, and limits lipid catabolic process. Additionally, *PLA2G1B* also produces lysophospholipids that limit hepatic fat catabolism and reduce energy consumption (Labonte et al., 2010). In previous studies on pigs, lipid metabolism pathway and energy pathway closely associated with RFI in muscle and adipose tissues (Lkhagvadorj et al., 2010; Vincent et al., 2015; Gondret et al., 2016). The *PLA2G1B* gene can have an effect on lipid metabolism in pigs and thus, on FCR, the ratio between feed intake and BW gain. Another candidate gene, Sirtuin 4 (*SIRT4*), has a vital role in glutamine metabolism and negative regulation of insulin secretion. Some researchers found that this gene is a regulator of insulin secretion, and it can reduce pancreatic insulin secretion (Anderson et al., 2017; Zaganjor et al., 2017; Huynh et al., 2018). Insulin sensitivity modulation and glucose handling influence energy metabolism and FE related traits (Fontanesi et al., 2012). Moreover, Do et al. (2014b) reported that insulin secretion affects the metabolic process of carbonization, which drives feed intake and FCR. In a previous study, lower insulin secretion led to a decrease in RFI, which triggered fat deposition (Hoque et al., 2009). The other four candidate genes (*PLCL2, phospholipase C like 2; SPAM1, Sus scrofa sperm adhesion molecule 1; HYAL4, hyaluronidase 4; ENSSSCG00000016602*) which were reportedly related to FE traits in pigs, are similarly involved in fat synthesis and decomposition processes, as well as insulin and lipid metabolism, and lipid transport.

Potential Candidate Genes for ADG

An important FE related trait is ADG, and many animal nutritionists consider this trait to be a major ethological concern. The most significant locus, *ASGA0036538*, was closest to the G Protein-coupled Estrogen Receptor 1 (*GPER1*) gene. *GPER1* is associated with positive regulation of insulin secretion, inhibition of fat cell differentiation (Williams, 2012) and insulin signal pathway (Kumar et al., 2011). Hayes et al. (2011) reported that the *GPER1* gene could stimulate the release of insulin and prevent the apoptosis of pancreatic beta cells. Although GPER1 has not been reported in pigs, it was associated with activate estrogen receptors involved in the hypothalamic control of multiple homeostatic functions in mice, such as energy metabolism (Hadjimarkou and Vasudevan, 2018). Do et al. (2014a) found that genes

TABLE 2 | Quantitative traits loci (QTLs) related to four feed efficiency traits.

Trait[a]	Method[b]	Chromosome	Region (Mb)[c]	N[d]	QTL region (Mb)[e]	Traits related with QTL
FCR	a	7	**45.83–45.86**	2	45.10–53.98	Average daily gain (Quintanilla et al., 2002)
	a&b	17	1.15–2.69	7	0.44–20.053	Body weight (Guo Y. M. et al., 2008b)
	a&b	18	20.48–20.96	2	21.47–21.47	Average daily gain (Wang et al., 2015)
ADG	a&b	2	147.07–147.11	2	148.27–148.27	Body depth/width (Fan et al., 2009)
	a&b	3	0.35–0.54	3	1.79–4.20	Body weight (Fan et al., 2009)
	a&b	5	8.85–8.87	3	9.29–9.29	Average daily gain (Rothammer et al., 2014)
ADG\ADFI	b	4	120.99–121.96	5	120.51–134.90	Body weight (Bartenschlager and Geldermann, 2003)
ADFI	a&b	9	**128.77–129.09**	2	128.00–128.99	Daily feed intake (Reyer et al., 2017)
					128.99–147.51	Body weight (10 weeks) (Yoo et al., 2014)
ADFI\RFI	a&b	4	**105.57–106.83**	6	105.64–105.64	Feed conversion ratio (Wang et al., 2015)
					106.51–124.31	Average daily gain (Malek et al., 2001)
	a&b	8	102.88–105.56	6	107.04–113.33	Feed intake per feeding (Ding et al., 2017)
RFI	b	9	112.25–112.31	3	114.32–123.52	Lipid accretion rate (Duthie et al., 2008)
	a	11	**5.38–6.37**	2	6.01–6.99	Residual feed intake (Jiao et al., 2014)
			16.03–16.08	3	15.85–15.85	Feed conversion ratio (Horodyska et al., 2017)

[a]FCR, Feed conversion ratio; ADG, Average daily gain; ADFI, Average daily feed intake; RFI, Residual feed intake. [b]a = linear model GWAS (LM-GWAS), b = single-step GWAS (ssGWAS). [c]Region (Mb) = the merging of neighbored significant SNPs. [d]N = Number of significant SNPs in the region. [e]QTL region (Mb) = The QTL regions reported in Pig QTLdb. Values in bold had an overlap region with QTLs for FE related traits in Pig QTLdb.

TABLE 3 | Significant SNPs and related genes for four feed efficiency traits.

Trait[a]	Method[b]	SNP name	Chromosome	Position (bp)	Gene[c]	Distance[d]	Gene function
FCR	a&b	WU_10.2_13_3842462	13	3,655,526	*PLCL2*	-150,373	Lipid catabolic process
	a	ASGA0062927	14	40,507,969	*SIRT4*	+204,081	Negative regulation of insulin secretion
					PLA2G1B	+185,650	Lipid metabolic process
	a	ASGA0062929	14	40,548,521	*PLA2G1B*	+226,202	Lipid metabolic process
	a	ALGA0097485	18	23,538,749	*SPAM1*	-51,203	Carbohydrate metabolic process
					HYAL4	-85,477	
					ENSSSCG00000016602	-88,233	
ADG	a&b	ASGA0100941	2	147,068,762	*PRELID2*	-40,819	Phospholipid transport process
	a&b	WU_10.2_2_153522747	2	147,112,980	*PRELID2*	Within	Phospholipid transport process
	a&b	WU_10.2_3_329436	3	537,968	*GPER1*	-174,192	Positive regulation of insulin secretion; negative regulation of lipid biosynthetic process
ADFI	a	ASGA0005581	1	203,367,107	*ACER2*	-19,714	Lipid metabolic process
	b	ALGA0019602	3	68,298,863	*HK2*	+67,248	Glucose metabolic process; glycolytic process
	a&b	ALGA0065251	12	14,839,808	*TEX2*	Within	Lipid transport process
					ICAM2	-42115	Insulin metabolic process
RFI	b	ALGA0019602	3	68,298,863	*HK2*	+67,248	Glucose metabolic process; glycolytic process
	b	WU_10.2_11_4727497	11	50,92,611	*PDX1*	-211,028	Glucose metabolic process; insulin secretion
	a&b	ALGA0060467	11	53,79,554	*PDX1*	+68,711	Glucose metabolic process; insulin secretion

[a]FCR, Feed conversion ratio; ADG, Average daily gain; ADFI, Average daily feed intake; RFI, Residual feed intake. [b]a , linear model GWAS (LM-GWAS); b, single-step GWAS (ssGWAS). [c]PLCL2, Phospholipase C Like 2; SIRT4, Sirtuin 4; PLA2G1B, Phospholipase A2 Group IB; SPAM1, Sperm Adhesion Molecule 1; HYAL4, Hyaluronidase 4; PRELID2, PRELI Domain Containing 2; GPER1, G Protein-coupled Estrogen Receptor 1; ACER2, Alkaline Ceramidase 2; HK2, Hexokinase 2; TEX2, Testis Expressed 2; ICAM2, Hexokinase 2; PDX1, Pancreatic and Duodenal Homeobox 1. [d]+/-: The SNP located in the upstream/downstream region of the nearest gene.

which are involved in insulin signaling and energy metabolism pathway played an important function in the regulation of FE related traits, such as RFI. Our study confirmed previous investigations. As to PRELI Domain Containing 2 (*PRELID2*), which is associated with phospholipid transport process and related pathway. In previous GWAS studies on pigs, the *PRELID2* gene has been reported to be associated with reproduction traits in Yorkshire pigs (Wang et al., 2018). Its relation to ADG, to

the best of our knowledge, this genetic association was reported in pigs for the first time. Auqui et al. (2019) found that fatter pigs had higher cholesterol levels, suggesting a link between cholesterol levels and body weight. Their results demonstrated that *PRELID2* could significantly regulate body weight through cholesterol levels. The three genes above were found by both LM-GWAS and ssGWAS methods.

Potential Candidate Genes for ADFI

Some breeders are concerned about ADFI because this trait is highly associated with FE and growth rate (Do et al., 2013). Both LM-GWAS and ssGWAS methods identified a significant locus, ALGA0065251. According to the annotation, Intercellular adhesion molecule 2 (*ICAM2*) and Testis expressed 2 (*TEX2*) are associated with ADFI. *ICAM2* has a key function in glucose stimulus and insulin metabolic process (Qiu et al., 2008). The relation between insulin signaling pathway and RFI has been shown in pigs (Do et al., 2014b) and cattle (Chen et al., 2012; Rolf et al., 2012). In pigs, *ICAM2* gene is reported a meat quality traits involved in lipid metabolism and intramuscular fat deposition (Jeong et al., 2015). Researchers suggested that *ICAM2* was closely related to glucose stimulus and insulin metabolic processes, which are important for FE. Grefhorst et al. (2019) reported that *TEX2* promotes the transfer of cholesterol and other lipids in different cyclic lipoprotein. Our results show that *TEX2* is associated with the ADFI trait in Landrace pigs for the first time. Of note, a strong association between *TEX2* and FE, and growth rate in broilers was reported (Willson et al., 2017). Another candidate gene Alkaline Ceramidase 2 (*ACER2*), is closely associated with lipid metabolism (Zhang et al., 2019). This gene was identified by the LM-GWAS method. Several studies also support the notion that lipid metabolism is associated with RFI in pigs (Lkhagvadorj et al., 2010) and cattle (Herd and Arthur, 2009). Lkhagvadorj et al. (2010) found many genes in fat and liver that were differently expressed in low and high RFI pigs in response to caloric restriction and indicated that lipid metabolic pathways were important for regulation of RFI. Nevertheless, the lipid metabolic process is a very broad term, and therefore it might be worthy of further investigation to identify the exact sub-process that are involved in ADFI metabolism. Besides, one candidate gene (*HK2, Hexokinase 2*) was identified by the ssGWAS method. This gene was reportedly associated with glucose metabolism, insulin secretion, and glycolytic regulation (Wei et al., 2016; Miller et al., 2019). Our findings support a better understanding of the ADFI trait in pig lipid metabolism.

Potential Candidate Genes for RFI

RFI is an essential trait for animal husbandry and many studies have been conducted to investigate the genetic architecture underlying this trait. A variety of pathways may mediate RFI, such as hormones and growth factors that act through receptor tyrosine kinases [e.g., epidermal growth factor (EGF), insulin] (Hayes et al., 2011). Only one common locus *ALGA0060467* was found significantly associated with RFI in the current study and it is located the upstream of the Pancreatic Duodenal Homeobox 1 (*PDX1*). SNP, WU_10.2_11_4727497, associated with RFI was identified by ssGWAS method, it is also close to PDX1. Notably, the direct link between *PDX1* and FE related traits has not been reported previously in pigs. Interestingly, *PDX1* is associated with some classical pathways such as glucose/energy metabolism and insulin secretion pathway. In the adult endocrine pancreas, *PDX1* is a pivotal factor for the up-regulation of insulin gene transcription that, in turn, regulates somatostatin, the expression of glucokinase, glucose transporter protein-2, and islet amyloid peptide (Park et al., 2008). Do et al. (2014b) reported that insulin signaling pathway plays important roles in controlling RFI in Duroc pigs, and it has been shown that insulin also affects feed intake and feed behavior in chickens (Shiraishi et al., 2008, 2011). Moreover, many reports showed that *PDX1* was closely related to porcine pancreas development (Choi et al., 2009) and diabetes (Matsunari et al., 2014). Pancreas and diabetes are closely related to feed intake, digestion, absorption, and metabolism. Hence, *PDX1* might exert a vital function on feed intake and feed behavior. Another gene *HK2*, was found significantly associated with both RFI and ADFI by using the ssGWAS method as mentioned before.

CONCLUSION

In summary, the present study indicated that the result of LM-GWAS and ssGWAS methods are highly consistent. Combining LM-GWAS and ssGWAS improved not only the power of GWAS in a small population but also allowed screening of candidate genes with high reliability (such as *PLA2G1B* and *PRELID2)*. This study provides a better understanding of the genetic mechanisms underlying feed efficiency related traits, which offers an opportunity for increased feed efficiency using marker-assisted selection or genomic selection in pigs.

DATA AVAILABILITY STATEMENT

The SNP array dataset generated for this study can be found in Figshare https://figshare.com/articles/GWAS/12431975.

ETHICS STATEMENT

The animal study was reviewed and approved by the Institutional Animal Care and Use Committee (IACUC) at the China Agricultural University (permit number DK996). Written informed consent was obtained from the owners for the participation of their animals in this study.

AUTHOR CONTRIBUTIONS

XD designed and supervised the study. LF and YaJ conducted the statistical analyses and interpretation of results. MM, ZZ, and WC conceived the experimental traits. YiJ and HS prepared the samples for DNA genotyping. LF and YaJ wrote the manuscript, which was critically remarked by XD. All authors contributed to the article and approved the submitted version.

FUNDING

This work was supported by grants from the earmarked fund for the National Key Research and Development Project (2019YFE0106800), the China Agriculture Research System (CARS-35), Modern Agriculture Science and Technology Key Project of Hebei Province (19226376D), the National Natural Science Foundation of China (31671327), Major Project of Selection for New Livestock and Poultry Breeds of Zhejiang Province (2016C02054-5), Anhui Academy of Agricultural Sciences Key Laboratory Project (No. 2019YL021).

ACKNOWLEDGMENTS

We gratefully acknowledge the constructive comments from the reviewers.

SUPPLEMENTARY MATERIAL

The Supplementary Material for this article can be found online at: https://www.frontiersin.org/articles/10.3389/fgene.2020.00692/full#supplementary-material

REFERENCES

Aguilar, I., Legarra, A., Cardoso, F., Masuda, Y., Lourenco, D., and Misztal, I. (2019). Frequentist p-values for large-scale-single step genome-wide association, with an application to birth weight in American Angus cattle. *Genet. Select. Evol.* 51:28.

Aguilar, I., Tsuruta, S., Masuda, Y., Lourenco, D., Legarra, A., and Misztal, I. (2018). "BLUPF90 suite of programs for animal breeding with focus on genomics," in *Proceedings of the 11th World Congress on Genetics Applied To Livestock Production*, New Zealand.

Anderson, K. A., Huynh, F. K., Fisher-Wellman, K., Stuart, J. D., Peterson, B. S., Douros, J. D., et al. (2017). SIRT4 Is a lysine deacylase that controls leucine metabolism and insulin secretion. *Cell Metab.* 25, 838–855.e15. doi: 10.1016/j.cmet.2017.03.003

Auqui, S. M., Egea, M., Penaranda, I., Garrido, M. D., and Linares, M. B. (2019). Rustic chato murciano pig breed: effect of the weight on carcass and meat quality. *Meat Sci.* 156, 105–110. doi: 10.1016/j.meatsci.2019.05.022

Bartenschlager, S. S., and Geldermann, G. M. H. (2003). Linkage and QTL mapping for *Sus scrofa* chromosom. *J. Anim. Breed. Genet.* 120, 11–19.

Becker, D., Wimmers, K., Luther, H., Hofer, A., and Leeb, T. (2013). A genome-wide association study to detect QTL for commercially important traits in swiss large white boars. *PLoS One* 8:e55951. doi: 10.1371/journal.pone.0055951

Benjamin, Y., and Hochberg, Y. (1995). Controlling the false discovery rate: a practical and powerful approach to multiple testing. *J. R. Statist. Soc. B* 57, 289–300. doi: 10.1111/j.2517-6161.1995.tb02031.x

Braz, C. U., Taylor, J. F., Bresolin, T., Espigolan, R., Feitosa, F. L. B., Carvalheiro, R., et al. (2019). Sliding window haplotype approaches overcome single SNP analysis limitations in identifying genes for meat tenderness in Nelore cattle. *BMC Genet.* 20:8. doi: 10.1186/s12863-019-0713-4

Chang, C. C., Chow, C. C., Tellier, L. C., Vattikuti, S., Purcell, S. M., and Lee, J. J. (2015). Second-generation PLINK: rising to the challenge of larger and richer datasets. *Gigascience* 4:7.

Chen, Y., Arthur, P. F., Barchia, I. M., Quinn, K., Parnell, P. F., and Herd, R. M. (2012). Using gene expression information obtained by quantitative real-time PCR to evaluate Angus bulls divergently selected for feed efficiency. *Anim. Product. Sci.* 52:1058. doi: 10.1071/an12098

Choi, J.-S., Cho, Y.-K., Yoon, S.-H., Kwon, S. O., Koo, D.-B., and Yu, K. (2009). Proteomic analysis of porcine pancreas development. *BMB Rep.* 42, 661–666. doi: 10.5483/bmbrep.2009.42.10.661

Ding, R., Quan, J., Yang, M., Wang, X., Zheng, E., Yang, H., et al. (2017). Genome-wide association analysis reveals genetic loci and candidate genes for feeding behavior and eating efficiency in Duroc boars. *PLoS One* 12:e0183244. doi: 10.1371/journal.pone.0183244

Ding, R., Yang, M., Wang, X., Quan, J., Zhuang, Z., Zhou, S., et al. (2018). Genetic architecture of feeding behavior and feed efficiency in a duroc pig population. *Front. Genet.* 9:220. doi: 10.3389/fgene.2018.00220

Do, D. N., Ostersen, T., Strathe, A. B., Mark, T., Jensen, J., and Kadarmideen, H. N. (2014a). Genome-wide association and systems genetic analyses of residual feed intake, daily feed consumption, backfat and weight gain in pigs. *BMC Genet.* 15:27. doi: 10.1186/s12863-019-0713-27

Do, D. N., Strathe, A. B., Ostersen, T., Pant, S. D., and Kadarmideen, H. N. (2014b). Genome-wide association and pathway analysis of feed efficiency in pigs reveal candidate genes and pathways for residual feed intake. *Front. Genet.* 5:307. doi: 10.3389/fgene.2018.00307

Do, D. N., Strathe, A. B., Jensen, J., Mark, T., and Kadarmideen, H. N. (2013). Genetic parameters for different measures of feed efficiency and related traits in boars of three pig breeds. *J. Anim. Sci.* 91, 4069–4079. doi: 10.2527/jas.2012-6197

Duthie, C., Simm, G., Doeschl-Wilson, A., Kalm, E., Knap, P. W., and Roehe, R. (2008). Quantitative trait loci for chemical body composition traits in pigs and their positional associations with body tissues, growth and feed intake. *Anim. Genet.* 39, 130–140. doi: 10.1111/j.1365-2052.2007.01689.x

Fan, B., Onteru, S. K., Mote, B. E., Serenius, T., Stalder, K. J., and Rothschild, M. F. (2009). Large-scale association study for structural soundness and leg locomotion traits in the pig. *Genet. Sel. Evol.* 41:14. doi: 10.1186/1297-9686-41-14

Fontanesi, L., Schiavo, G., Galimberti, G., Calò, D. G., Scotti, E., Martelli, P. L., et al. (2012). A genome wide association study for backfat thickness in Italian Large white pigs highlights new regions affecting fat deposition including neuronal genes. *BMC Genomics* 13:583. doi: 10.1186/s12863-019-0713-583

Gilmour, A., Gogel, B., Cullis, B., Welham, S., and Thompson, R. (2015). *ASReml Userguide Release 4.1*. Hemel Hempstead: VSN International.

Godinho, R. M., Bergsma, R., Silva, F. F., Sevillano, C. A., Knol, E. F., Lopes, M. S., et al. (2018). Genetic correlations between feed efficiency traits, and growth performance and carcass traits in purebred and crossbred pigs. *J. Anim. Sci.* 96, 817–829. doi: 10.1093/jas/skx011

Gondret, F., Vincent, A., Houee-Bigot, M., Siegel, A., Lagarrigue, S., Louveau, I., et al. (2016). Molecular alterations induced by a high-fat high-fiber diet in porcine adipose tissues: variations according to the anatomical fat location. *BMC Genomics* 17:120. doi: 10.1186/s12863-019-0713-120

Grefhorst, A., Verkad, H. J., and Groen, A. K. (2019). The TICE pathway: mechanisms and lipid-lowering therapies. *Method. Debakey Cardiovasc. J.* 15, 70–76.

Gregersen, V. R., Conley, L. N., Sorensen, K. K., Guldbrandtsen, B., Velander, I. H., and Bendixen, C. (2012). Genome-wide association scan and phased haplotype construction for quantitative trait loci affecting boar taint in three pig breeds. *BMC Genomics* 13:22. doi: 10.1186/s12863-019-0713-22

Guerra, F. P., Suren, H., Holliday, J., Richards, J. H., Fiehn, O., Famula, R., et al. (2019). Exome resequencing and GWAS for growth, ecophysiology, and chemical and metabolomic composition of wood of *Populus trichocarpa*. *BMC Genomics* 20:875. doi: 10.1186/s12863-019-0713-875

Guo, Y., Li, J., Bonham, A. J., Wang, Y., and Deng, H. (2008). Gains in power for exhaustive analyses of haplotypes using variable-sized sliding window strategy: a comparison of association-mapping strategies. *Eur. J. Hum. Genet.* 17, 785–792. doi: 10.1038/ejhg.2008.244

Guo, Y. M., Lee, G. J., Archibald, A. L., and Haley, C. S. (2008). Quantitative trait loci for production traits in pigs: a combined analysis of two Meishan x large white populations. *Anim. Genet.* 39, 486–495. doi: 10.1111/j.1365-2052.2008.01756.x

Hadjimarkou, M. M., and Vasudevan, N. (2018). GPER1/GPR30 in the brain: crosstalk with classical estrogen receptors and implications for behavior. *J. Steroid Biochem. Mol. Biol.* 176, 57–64. doi: 10.1016/j.jsbmb.2017.04.012

Haggman, J., and Uimari, P. (2017). Novel harmful recessive haplotypes for reproductive traits in pigs. *J. Anim. Breed. Genet.* 134, 129–135. doi: 10.1111/jbg.12240

Hayes, M. R., Leichner, T. M., Zhao, S., Lee, G. S., Chowansky, A., Zimmer, D., et al. (2011). Intracellular signals mediating the food intake-suppressive effects of hindbrain glucagon-like peptide-1 receptor activation. *Cell Metab.* 13, 320–330. doi: 10.1016/j.cmet.2011.02.001

Herd, R. M., and Arthur, P. F. (2009). Physiological basis for residual feed intake. *J. Anim. Sci.* 87, E64–E71.

Hollie, N. I., and Hui, D. Y. (2011). Group 1B phospholipase A(2) deficiency protects against diet-induced hyperlipidemia in mice. *J. Lipid Res.* 52, 2005–2011. doi: 10.1194/jlr.m019463

Hoque, M. A., Katoh, K., and Suzuki, K. (2009). Genetic associations of residual feed intake with serum insulin-like growth factor-I and leptin concentrations, meat quality, and carcass cross sectional fat area ratios in Duroc pigs. *J. Anim. Sci.* 87, 3069–3075. doi: 10.2527/jas.2008-1268

Horodyska, J., Hamill, R. M., Varley, P. F., Reyer, H., and Wimmers, K. (2017). Genome-wide association analysis and functional annotation of positional candidate genes for feed conversion efficiency and growth rate in pigs. *PLoS One* 12:e0173482. doi: 10.1371/journal.pone.00173482

Huynh, F. K., Hu, X., Lin, Z., Johnson, J. D., and Hirschey, M. D. (2018). Loss of sirtuin 4 leads to elevated glucose- and leucine-stimulated insulin levels and accelerated age-induced insulin resistance in multiple murine genetic backgrounds. *J. Inherit. Metab. Dis.* 41, 59–72. doi: 10.1007/s10545-017-0069-8

Jeong, H., Song, K. D., Seo, M., Caetano-Anolles, K., Kim, J., Kwak, W., et al. (2015). Exploring evidence of positive selection reveals genetic basis of meat quality traits in Berkshire pigs through whole genome sequencing. *BMC Genet.* 16:104. doi: 10.1186/s12863-019-0713-104

Ji, J., Yan, G., Chen, D., Xiao, S., Gao, J., and Zhang, Z. (2019). An association study using imputed whole-genome sequence data identifies novel significant loci for growth-related traits in a Duroc x Erhualian F2 population. *J. Anim. Breed. Genet.* 136, 217–228. doi: 10.1111/jbg.12389

Jiao, S., Maltecca, C., Gray, F., and Cassady, J. P. (2014). Feed intake, average daily gain, feed efficiency, and real-time ultrasound traits in Du roc pigs: II. Genomewide association. *J. Anim. Sci.* 92, 2846–2860. doi: 10.2527/jas.2014-7337

Kumar, R., Balhuizen, A., Amisten, S., Lundquist, I., and Salehi, A. (2011). Insulinotropic and antidiabetic effects of 17beta-estradiol and the GPR30 agonist G-1 on human pancreatic islets. *Endocrinology* 152, 2568–2579. doi: 10.1210/en.2010-1361

Labonte, E. D., Pfluger, P. T., Cash, J. G., Kuhel, D. G., Roja, J. C., Magness, D. P., et al. (2010). Postprandial lysophospholipid suppresses hepatic fatty acid oxidation: the molecular link between group 1B phospholipase A2 and diet-induced obesity. *FASEB J.* 24, 2516–2524. doi: 10.1096/fj.09-144436

Lkhagvadorj, S., Qu, L., Cai, W., Couture, O. P., Barb, C. R., Hausman, G. J., et al. (2010). Gene expression profiling of the short-term adaptive response to acute caloric restriction in liver and adipose tissues of pigs differing in feed efficienc. *Am. J. Physiol. Regul. Integr. Comp. Physiol.* 298, 494–507.

Lorenz, A. J., Hamblin, M. T., and Jannink, J.-L. (2010). Performance of single nucleotide polymorphisms versus haplotypes for genome-wide association analysis in barley. *PLoS One* 5:e14079. doi: 10.1371/journal.pone.014079

Malek, M., Dekkers, J. C., Lee, H. K., Baas, T. J., and Rothschild, M. F. (2001). A molecular genome scan analysis to identify chromosomal regions influencing economic traits in the pig. I. Growth and body composition. *Mamm. Genome* 12, 630–636. doi: 10.1007/s003350020018

Matsunari, H., Kobayashi, T., Watanabe, M., Umeyama, K., Nakano, K., Kanai, T., et al. (2014). Transgenic pigs with pancreas-specific expression of green fluorescent protein. *J. Reprod. Dev.* 60, 230–237. doi: 10.1262/jrd.2014-006

Miller, E. G., Huber, L. A., Cant, J. P., Levesque, C. L., and de Lange, C. F. M. (2019). The effect of pregnancy on nitrogen retention, maternal insulin sensitivity, and mRNA abundance of genes involved in energy and amino acid metabolism in gilts. *J. Anim. Sci.* 97, 4912–4921. doi: 10.1093/jas/skz355

Nkrumah, J. D., Sherman, E. L., Li, C., Marques, E., Crews, D. H., Bartusiak, R., et al. (2007). Primary genome scan to identify putative quantitative trait loci for feedlot growth rate, feed intake, and feed efficiency of beef cattle. *J. Anim. Sci.* 85, 3170–3181. doi: 10.2527/jas.2007-0234

Onteru, S. K., Gorbach, D. M., Young, J. M., Garrick, D. J., Dekkers, J. C. M., and Rothschild, M. F. (2013). Whole genome association studies of residual feed intake and related traits in the pig. *PLoS One* 8:e61756. doi: 10.1371/journal.pone.0061756

Park, J. H., Stoffers, D. A., Nicholls, R. D., and Simmons, R. A. (2008). Development of type 2 diabetes following intrauterine growth retardation in rats is associated with progressive epigenetic silencing of Pdx1. *J. Clin. Invest.* 118, 2316–2324.

Qiu, J., Ni, Y. H., Chen, R. H., Ji, C. B., Liu, F., Zhang, C. M., et al. (2008). Gene expression profiles of adipose tissue of obese rats after central administration of neuropeptide Y-Y5 receptor antisense oligodeoxynucleotides by cDNA microarrays. *Peptides* 29, 2052–2060. doi: 10.1016/j.peptides.2008.06.024

Quintanilla, R., Milan, D., and Bidanel, J. P. (2002). A further look at quantitative trait loci affecting growth and fatness in a cross between Meishan and Large White pig populations. *Genet. Sel. Evol.* 34, 193–210.

Ramayo-Caldas, Y., Marmol-Sanchez, E., Ballester, M., Sanchez, J. P., Gonzalez-Prendes, R., Amills, M., et al. (2019). Integrating genome-wide co-association and gene expression to identify putative regulators and predictors of feed efficiency in pigs. *Genet. Sel. Evol.* 51:48.

Reyer, H., Shirali, M., Ponsuksili, S., Murani, E., Varley, P. F., Jensen, J., et al. (2017). Exploring the genetics of feed efficiency and feeding behaviour traits in a pig line highly selected for performance characteristics. *Mol. Genet. Genomics* 292, 1001–1011. doi: 10.1007/s00438-017-1325-1

Rolf, M. M., Taylor, J. F., Schnabel, R. D., McKay, S. D., McClure, M. C., Northcutt, S. L., et al. (2012). Genome-wide association analysis for feed efficiency in Angus cattle. *Anim. Genet.* 43, 367–374. doi: 10.1111/j.1365-2052.2011.02273.x

Rothammer, S., Kremer, P. V., Bernau, M., Fernandez-Figares, I., Pfister-Schär, J., Medugorac, I., et al. (2014). Genome-wide QTL mapping of nine body composition and bone mineral density traits in pigs. *Genet. Select. Evol.* 46, 1–11.

Sahana, G., Kadlecová, V., Hornsh, H., Nielsen, B., and Christensen, O. F. (2013). A genome-wide association scan in pig identifi es novel regions associated with feed effi ciency trait. *J. Anim. Sci.* 91, 1041–1050. doi: 10.2527/jas.2012-5643

Sanchez, J. P., Ragab, M., Quintanilla, R., Rothschild, M. F., and Piles, M. (2017). Genetic parameters and expected responses to selection for components of feed efficiency in a Duroc pig line. *Genet. Sel. Evol.* 49, 86.

Sanchez, M.-P., Tribout, T., Iannuccelli, N., Bouffaud, M., Servin, B., Dehais, P., et al. (2014). A genome-wide association study of production traits in a commercial population of Large White pigs: evidence of haplotypes affecting meat quality. *Genet. Select. Evol.* 46:12. doi: 10.1186/1297-9686-46-12

Shiraishi, J., Tanizawa, H., Fujita, M., Kawakami, S., and Bungo, T. (2011). Localization of hypothalamic insulin receptor in neonatal chicks: evidence for insulinergic system control of feeding behavior. *Neurosci. Lett.* 491, 177–180. doi: 10.1016/j.neulet.2011.01.031

Shiraishi, J., Yanagita, K., Fujita, M., and Bungo, T. (2008). Central insulin suppresses feeding behavior via melanocortins in chicks. *Domest. Anim. Endocrinol.* 34, 223–228. doi: 10.1016/j.domaniend.2007.05.002

Silva, E. F., Lopes, M. S., Lopes, P. S., and Gasparino, E. (2019). A genome-wide association study for feed efficiency-related traits in a crossbred pig population. *Animal* 13, 2447–2456. doi: 10.1017/s1751731119000910

Vincent, A., Louveau, I., Gondre, F., Tréfeu, C., Gilbert, H., and Lefaucheur, L. (2015). Divergent selection for residual feed intake affects the transcriptomic and proteomic profiles of pig skeletal muscle1. *J. Anim. Sci.* 93, 2745–2758. doi: 10.2527/jas.2015-8928

Wang, H., Misztal, I., Aguilar, I., Legarra, A., Fernando, R. L., Vitezica, Z., et al. (2014). Genome-wide association mapping including phenotypes from relatives without genotypes in a single-step (ssGWAS) for 6-week body weight in broiler chickens. *Front. Genet.* 5:134. doi: 10.3389/fgene.2018.00134

Wang, H., Misztal, I., Aguilar, I., Legarra, A., and Muir, W. M. (2012). Genome-wide association mapping including phenotypes from relatives without genotypes. *Genet. Res.* 94, 73–83. doi: 10.1017/s0016672312000274

Wang, K., Liu, D., Hernandez-Sanchez, J., Chen, J., Liu, C., Wu, Z., et al. (2015). Genome wide association analysis reveals new production trait genes in a male duroc population. *PLoS One* 10:e0139207. doi: 10.1371/journal.pone.00139207

Wang, Y., Ding, X., Tan, Z., Xing, K., Yang, T., Wang, Y., et al. (2018). Genome-wide association study for reproductive traits in a Large White pig population. *Anim. Genet.* 49, 127–131. doi: 10.1111/age.12638

Wei, H., Zhou, Y., Jiang, S., Huang, F., Peng, J., and Jiang, S. (2016). Transcriptional response of porcine skeletal muscle to feeding a linseed-enriched diet to growing pigs. *J. Anim. Sci. Biotechnol.* 7:6.

Weller, J. I., Song, J. Z., Heyen, D. W., Lewin, H. A., and Ron, M. (1998). A new approach to the problem of multiple comparisons in the genetic dissection of complex traits. *Genetics* 150, 1699–1706.

Williams, G. (2012). Aromatase up-regulation, insulin and raised intracellular oestrogens in men, induce adiposity, metabolic syndrome and prostate disease, via aberrant ER-alpha and GPER signalling. *Mol. Cell. Endocrinol.* 351, 269–278. doi: 10.1016/j.mce.2011.12.017

Willson, N. L., Forder, R. E. A., Tearle, R. G., Nattrass, G. S., Hughes, R. J., and Hynd, P. I. (2017). Evaluation of fatty acid metabolism and innate immunity interactions between commercial broiler, F1 layer x broiler cross and commercial layer strains selected for different growth potentials. *J. Anim. Sci. Biotechnol.* 8:70.

Yang, J., Lee, S. H., Goddard, M. E., and Visscher, P. M. (2011). GCTA: a tool for genome-wide complex trait analysis. *Am. J. Hum. Genet.* 88, 76–82. doi: 10.1016/j.ajhg.2010.11.011

Yoo, C. K., Park, H. B., Lee, J. B., Jung, E. J., Kim, B. M., Kim, H. I., et al. (2014). QTL analysis of body weight and carcass body length traits in an F2 intercross between landrace and korean native pigs. *Anim. Genet.* 45, 589–592. doi: 10.1111/age.12166

Zaganjor, E., Vyas, S., and Haigis, M. C. (2017). SIRT4 is a regulator of insulin secretion. *Cell Chem. Biol.* 24, 656–658. doi: 10.1016/j.chembiol.2017.06.002

Zhang, T., Zhao, Q., Xiao, X., Yang, R., Hu, D., Zhu, X., et al. (2019). Modulation of lipid metabolism by celastrol. *J. Proteome Res.* 18, 1133–1144. doi: 10.1021/acs.jproteome.8b00797

Conflict of Interest: The authors declare that the research was conducted in the absence of any commercial or financial relationships that could be construed as a potential conflict of interest.

frontiers in Genetics

ORIGINAL RESEARCH
published: 30 July 2020
doi: 10.3389/fgene.2020.00797

Development of Genomic Resources and Identification of Genetic Diversity and Genetic Structure of the Domestic Bactrian Camel in China by RAD Sequencing

Chenmiao Liu, Huiling Chen, Zhanjun Ren, Xuejiao Yang and Chengdong Zhang*

College of Animal Science and Technology, Northwest A&F University, Xianyang, China

The domestic Bactrian camel is indispensable to agricultural production in the desertification area of China owning to its endurance to hunger and thirst, cold resistance, drought resistance, and good long-distance transportation. Therefore, it is necessary to investigate the genetic diversity, genetic structure, and genes with important roles in the evolution of this species. In this study, 1,568,087 SNPs were identified in 47 domestic Bactrian camels inhabiting four regions of China, namely Inner Mongolia, Gansu, Qinghai, and Xinjiang, by restriction site associated DNA sequencing (RAD-seq). The SNP data were used for nucleotide diversity analysis (π) and linkage disequilibrium (LD) attenuation analysis to elucidate the genetic diversity of the domestic Bactrian camel in the four regions studied. Results showed that Xinjiang camels had the highest nucleotide diversity and the fastest decay rate of the LD coefficient; therefore, Xinjiang camels had the highest genetic diversity. Structure analysis, principal component analysis (PCA), and phylogenetic tree construction by the neighbor-joining (NJ) method showed that Qinghai camels clustered separately, at a larger phylogenetic distance from camels in the other regions. Through analyses of selection signals, it was found that the number of selected genes shared by Inner Mongolia camels, Qinghai camels, Xinjiang camels, and Gansu camels was 7, 24, 25, and 113, respectively. The shared selected genes of the domestic Bactrian camel in the four regions were further analyzed, and three shared genes (GRIA3, XIAP, and THOC2) of the domestic Bactrian camel in China were identified. Gene Ontology (GO) classification and Kyoto Encyclopedia of Genes and Genomes (KEGG) enrichment analysis were performed on the shared selected genes of the domestic Bactrian camel in all four regions studied. Across all regions, genes involved in the cellular process were the most abundant subcategory under biological process. Cell and cell part represented the main proportion of genes under cellular component. Binding represented the main molecular function. In addition, the shared selected genes of the domestic Bactrian camel in the four regions of China were significantly enriched in the long-term depression pathway. The research should enable further study of the genetic resources of the domestic Bactrian camel, as well as the conservation of these resources.

Keywords: RAD sequencing, Bactrian camel, single nucleotide polymorphisms, genomic resource, genetic analysis

OPEN ACCESS

Edited by:
Guilherme J. M. Rosa, University of Wisconsin-Madison, United States

Reviewed by:
Derek M. Bickhart, United States Department of Agriculture (USDA), United States
Albano Beja-Pereira, University of Porto, Portugal

****Correspondence:***
Zhanjun Ren
Renzhanjun@nwsuaf.edu.cn

Specialty section:
This article was submitted to Livestock Genomics, a section of the journal Frontiers in Genetics

Received: *23 December 2019*
Accepted: *03 July 2020*
Published: *30 July 2020*

Citation:
Liu C, Chen H, Ren Z, Yang X and Zhang C (2020) Development of Genomic Resources and Identification of Genetic Diversity and Genetic Structure of the Domestic Bactrian Camel in China by RAD Sequencing. Front. Genet. 11:797. doi: 10.3389/fgene.2020.00797

INTRODUCTION

The domestic Bactrian camel plays an important role in economic activities and trade, as well as in national defense, and has cultural significance; therefore, this animal represents one of the most valuable livestock resources in China (Chen et al., 2018). With the impact of modern civilization, such as the growth of the automobile transportation industry and the destruction of the natural environment, the number of domestic Bactrian camels has been greatly reduced, from 618,600 in 1981 to 380,000 in present-day China. Therefore, it is essential to study the genetic diversity of the domestic Bactrian camel and conserve its germplasm resources (Ming et al., 2017). To date, a variety of studies have been conducted on the origin, domestication, and genetic diversity of the domestic Bactrian camel worldwide. Molecular clock analysis based on the complete mitochondrial genome sequences shows that the wild camel was not the direct ancestor of the domestic Bactrian camel. The domestic Bactrian camel is considered to be monophyletic in terms of its evolutionary origin, and to originate from a single wild population (Ji et al., 2009). The earliest evidence on the domestication of Bactrian camels is mainly derived from the northeast of Ilang and the south of neighboring Turkmenistan, especially in the Kopet Daghmountain region. Bactrian camel skeletons were found in the second cultural layer of the Anau ruins on the northern edge of the mountain range, dating back to 3500–3000 BC (Meadow and Zeder, 1978). Studies of the genetic diversity of the domestic Bactrian camel through analysis of mitochondrial sequence variation found that there were no significant genetic differences between populations in China, Russia, and Mongolia, indicating that a strong gene flow occurred due to the extensive movement of the domestic Bactrian camel (Ming et al., 2017). However, the use of RAD-seq to identify whole-genome single nucleotide polymorphisms (SNPs) for genetic analysis of the domestic Bactrian camel in the four regions of China has not been reported to date.

In the past few decades, the use of SNPs for studying species genetic diversity and population structure has become widespread (Ren et al., 2019). The rapid development of high-throughput sequencing technology has led to the use of restriction site-associated DNA sequencing (RAD-seq) as a relatively cost-effective way to identify a large number of SNPs throughout the genome (Miller et al., 2007; Davey et al., 2011). So far, RAD-seq has been widely applied to population genetics studies of a variety of species (Zhang et al., 2016). For instance, Díaz-Arce et al. (2016) used RAD-seq data to infer the phylogeny of tuna based on whole-genome nuclear markers. Ren et al. (2019) used the RAD-seq method to identify genome-wide SNPs, and studied the genetic diversity and population structure of four Chinese rabbit breeds.

In this study, we discovered genome-wide SNPs in the domestic Bactrian camel using the RAD-seq method. We then investigated the genetic diversity, genetic structure, and genes with important roles in the evolution of this species in four regions of China (Inner Mongolia, Gansu, Qinghai, and Xinjiang). The study clarified the phylogenetic relationship of the domestic Bactrian camel in China and explored the genomic resources of this species. And the SNP resources generated in this study offer a valuable tool for future genetics and genomics research of the domestic Bactrian camel.

MATERIALS AND METHODS

Sample Collection and DNA Extraction

Forty-seven venous blood samples were obtained from seven populations of domestic Bactrian agricultural camels from four regions of China (Inner Mongolia, Gansu, Qinghai, and Xinjiang) (**Table 1**) to ensure that each sample was derived from a different family, and there was no kinship between individuals. All methods and experimental protocols of this study were performed in accordance with guidelines and regulations of the animal ethics committee of Northwest A and F University (China) and the National Natural Science Foundation of China (31172178) Animal Care and Use Committee. DNA samples were extracted following a standard phenol-chloroform extraction procedure (Sambrook and Russell, 2002) and were diluted to 20 ng/μ L.

Construction and Sequencing of RAD Libraries

RAD-seq libraries were constructed in accordance with the modified protocol (Baird et al., 2008). In short, EcoRI (New England Biolabs) was used to digest genomic DNA (0.1–1 μg; from a single sample or pooled samples), and P1 adaptors were connected at the cutting site. Then, the samples were pooled, randomly sheared, and size-selected in sequential steps. After the second adaptors (P2) were added, the sequencing libraries were constructed using DNA fragments of 300–700 bp in length. Finally, the constructed libraries were sequenced using the Illumina HiSeq3000 platform, and 100 bp paired-end reads were generated.

Quality Control, Read Mapping, and SNP Calling

Quality trimming generated using fastp is an indispensable step to ensure high confidence of variant calling (Chen et al., 2018). Applying three strict filtering criteria, raw reads were processed to obtain high-quality clean reads: (i) removing reads with $\geq$10% unidentified nucleotides (N); (ii) removing reads with $>$50% bases having phred quality scores of $\leq$20; and (iii) removing reads aligned to the barcode adapter.

The Burrows-Wheeler Aligner (BWA) was used to align the clean reads of each sample with the reference genome[1] with the settings "mem 4 -k 32 -M", where -k is the minimum seed length, and -M being an option used to mark shorter split alignment hits as secondary alignments (Li and Durbin, 2009). GATK's Unified Genotyper was used to conduct variant calling on all samples

[1]https://www.ncbi.nlm.nih.gov/genome/10741

TABLE 1 | Information for domestic Bactrian camels in the four sampled regions of China.

Number	Group	Population	Sampling site	Sample size
1	Xinjiang camel	Nanjiang camel	Wensu county, Xinjiang	7
		Beijiang camel	Qinghe county, Xinjiang	7
		Dongjiang camel	Mulei county, Xinjiang	7
2	Gansu camel	Hexi camel	Yongchang county, Gansu	5
3	Qinghai camel	Qinghai camel	Mohe, Qinghai	7
4	Inner Mongolia camel	Alashan camel	Alashan Left Banner, Inner Mongolia	7
		Sunite camel	Sunite Right Banner, Inner Mongolia	7
Total				47

(DePristo et al., 2011). GATK's Variant Filtration with proper standards was used to filter SNPs (-Window 4, -filter "QD < 2.0 || FS > 60.0 || MQ < 40.0",-G_filter "GQ < 20").

Genetics Analyses

First, we used the VCFtools software suite to study the overall read depth and chromosome distribution of all SNPs (Danecek et al., 2011). The minimum read coverage for a SNP to be called is 3×, and all non-completely missing polymorphic loci (-max-missing 1e-06-non-ref-af 1e-06) were used for counting. The nucleotide diversity (π) of the domestic Bactrian camel in four regions of China was calculated using the PopGenome software package[2] (Pfeifer et al., 2014). In addition, we used the 1,568,087 identified SNPs to estimate the linkage disequilibrium (LD) attenuation trend by calculating the LD coefficient (r^2) between two points in a range of sequence (typically <5 Mb). The more rapid the decay of r^2, the higher the genetic diversity of population is; r^2 values in the range of 0,1 represent the correlation between two points: if r^2 is 0, there is no correlation between the two loci, whereas if r^2 is 1, the two loci are completely correlated. "LD attenuation distance" was used to evaluate the speed of LD attenuation (Guo, 2012).

Analyses of Population Structure

The genetic structure was studied by phylogenetic tree construction, principal component analysis, and analysis of population structure. Following the identification of SNPs, 1,568,087 SNPs were used to calculate the phylogenetic distance between populations. The phylogenetic tree was constructed using a neighbor-joining (NJ) method with the software Treebest (version 1.9.2) to determine the evolutionary relationship between populations. Bootstrap values were generated from 1,000 replications. After removing sites with a missing rate of 50% or more, the remaining 865,774 loci were used for PCA, which was carried out using the GCTA software in R to further study the population genetic structure between regions (Yang et al., 2011). The STRUCTURE program[3] (in order to ensure the independence of SNP marks, we used PLINK software to filter 865,774 SNPs according to LD intensity, the remaining 12,046 loci were used for structure analysis, -indep-pairwise 250 10 0.1, 250 kb window, the step size of 10 SNPs, r^2 is <1) was used for analysis of population structure. We predefined the number of genetic clusters from $K = 2$ to $K = 6$ (BURNIN = 5,000 times, NUMREPS = 100,000), and repeated each K-value three times (Liu et al., 2019). Next, we used the POPHELPER software[4] to calculate the value of ΔK; then, we used the CLUMPP software[5] to combine the results of three repetitions (Schraiber and Akey, 2015). The fixation index (Fst) was calculated according to the statistical function of Fst in the PopGenome software package to study the genetic diversity between different regions (Pfeifer et al., 2014). Fst can also be used to infer the genetic distance between different regions. After removing the site with a missing rate of 50% or more, the remaining 865,774 loci were used for Fst analysis. PLINK 1.9 was used to calculate the inbreeding coefficient (Fis) of the domestic Bactrian camel in four regions[6]. After obtaining the Fis value for each sample, the average value in the region was determined.

Analyses of Selection Signals

The top 5% region was selected based on the interception of two different parameters, namely nucleotide diversity (π) (Nei and Li, 1979) and population differentiation index (F_{ST}) (Danecek et al., 2011). Using the 50 kb sliding window method with a step size of 25 kb, the −log10 transform of Nei's π was used to select the lower end of diversity windows, and these parameters were quantified by internal PERL Scripts. All related graphs were drawn using R scripts (R Core Team, 2013). With Gansu camels as the control group and Inner Mongolia camels as the selection group, the genes of Inner Mongolia camels under selection pressure were identified. With Qinghai camels as the control group and Inner Mongolia camels as the selection group, the genes of Inner Mongolia camels under selection pressure were identified. With Xinjiang camels as the control group and Inner Mongolia camels as the selection group, the genes of Inner Mongolia camels under selection pressure were identified. Venn diagrams were then used to determine the common genes under selection pressure in Inner Mongolia camels; these genes played a crucial role in the evolution of this group. Using the same comparison method, the common genes under selection pressure were identified in Gansu camels, Qinghai camels, and Xinjiang camels.

[2]https://cran.r-project.org/web/packages/PopGenome/vignettes/Whole_genome_analyses_using_VCF_files.pdf?tdsourcetag=s_pctim_aiomsg

[3]http://web.stanford.edu/group/pritchardlab/structure.html

[4]https://www.ncbi.nlm.nih.gov/pubmed/26850166

[5]https://www.ncbi.nlm.nih.gov/pubmed/17485429

[6]http://zzz.bwh.harvard.edu/plink/

Sequence Annotation and Enrichment Analyses

In order to further systematically elucidate the complex biological functions of the genes, the common genes of the domestic Bactrian camel under selection pressure, in the four regions of China investigated in this study, were mapped against both GO and KEGG databases. GO enrichment analysis was performed with WEGO software, and gene numbers were calculated for every term (Ye et al., 2006). KEGG enrichment analysis using the KEGG database[7] and KOBAS software were performed to determine the statistical enrichment in KEGG pathways of the common genes of the domestic Bactrian camel under selection pressure in the four regions (Mao et al., 2005). The calculated *p*-value was subject to false discovery rate (FDR) correction, applying FDR $\leq$ 0.05 as the threshold. Pathways meeting this condition were defined as significantly enriched pathways in the abovementioned genes.

RESULTS

RAD-Tag Sequencing and Data Filtering

RAD sequencing produced a total of 131.13G of raw data for 47 normal sequenced individuals prior to quality filtering, with an average of 2.79G per sample, ranging from 1.36 to 4.57G. After quality filtering of the sequence data, 129.24G of clean data (1.34G to 4.30G for each sample, with an average of 2.75G) were retained, representing an average effective mapping rate of 98.57%. We mapped 1,568,087 regions, and the average spacing of RAD regions on the draft camel genome assembly was 1201.39 bp. The percentage of high-quality clean reads was above 97.73%, and the number of reads on the alignment was mostly above 97.39%. Of the clean reads retained, an average of 19.01 million reads were retained for each sample. In short, our sequencing data showed a high phred quality (Q20 > 94%, Q30 > 87%), and the GC content was stable, at between 40.71 and 45.13% (**Supplementary Tables S1–S4**).

Genetics Analyses

In this study, 1,568,087 SNPs were generated by RAD-seq. There were 548,830 loci (35%) in the transversion and 1,019,257 loci (65%) in the transition. The ratio of transition to transversion was close to 2:1. There were differences in the number of SNPs of the domestic Bactrian camel between the four regions, and the number of SNPs was in the following order: Xinjiang camels > Inner Mongolia camels > Qinghai camels > Gansu camels. The LD attenuation analysis of the domestic Bactrian camels from the four regions showed that the attenuation rate of the LD coefficient differed between the four regions, and that the attenuation rate was Xinjiang camels > Inner Mongolia camels > Qinghai camels > Gansu camels (**Figure 1**). Genome-wide nucleotide diversity was estimated from the SNP data. Because nucleotide diversity represents genetic diversity to an extent, it can be concluded from the data in **Table 2** that the nucleotide diversity (π) of Xinjiang camels was the highest.

[7]http://www.genome.jp/kegg/

Population Structure Analyses

Genetic analysis of population structure using STRUCTURE software and PCA showed similar patterns. Cross-validation with $K = 5$ was the most suitable for the true differentiation history of the domestic Bactrian camel. At $K = 5$, the ancestral background of Qinghai camels was relatively pure, with a major genetic ancestor. Although the Inner Mongolia camels, Xinjiang camels, and Gansu camels had multiple genetic ancestors, a major genetic ancestor was evident. At $K = 2$, Qinghai camels were obviously separated from the camels in other regions, indicating that this group was phylogenetically distant from the camels in other regions. The PCA map showed that the Qinghai camels clustered together separately, and were phylogenetically distant from the camels in other regions. Inner Mongolia camels and Xinjiang camels gathered together, indicating that their genetic relationship was relatively close. The phylogenetic tree constructed by the NJ method showed that the domestic Bactrian camels of the four regions gathered together, and the branches of the tree were obvious. Xinjiang camels and Inner Mongolia camels gathered together (**Figure 1**). The Fst values were calculated to study the genetic distance between different regions. As shown in **Table 2**, it can be concluded that the average Fst between the Qinghai camels and the domestic Bactrian camels in other regions was 0.1185, second only to Gansu camels (0.1201), indicating a large genetic distance between Qinghai camels and other domestic Bactrian camels. It should be noted that the farther the kinship, the smaller the inbreeding coefficient. The average Fis between Qinghai camels and domestic Bactrian camels in other regions was the lowest, indicating a large genetic distance from camels in the other regions; these findings were consistent with the results of PCA and structure analysis.

Analyses of Selection Signals

The top 5% regions were selected by combining the π and the F_{ST}. With Gansu camels as the control group and Inner Mongolia camels as the selection group, 238 selected genes were obtained. With Qinghai camels as the control group and Inner Mongolia camels as the selection group, 365 selected genes were obtained. With Xinjiang camels as the control group and Inner Mongolia camels as the selection group, 287 selected genes were obtained. Among them, 7 selected genes shared by Inner Mongolia camels were identified between all three comparisons (**Figure 2** and **Supplementary Tables S5–S7**). Using the same comparison method, it was found that the number of selected genes shared by Qinghai camels, Xinjiang camels, and Gansu camels was 24, 25, and 113, respectively (**Supplementary Figures S1–S3** and **Supplementary Tables S8–S16**). Venn diagrams were used to further analyze the shared selected genes of the domestic Bactrian camel between the four regions in China, and three shared genes (*GRIA3, XIAP, THOC2*) were identified in the domestic Bactrian camel across all four regions (**Figure 7**).

Sequence Annotation and Enrichment Analyses

GO classification was carried out on the shared selected genes of the domestic Bactrian camel in the four regions. For Inner

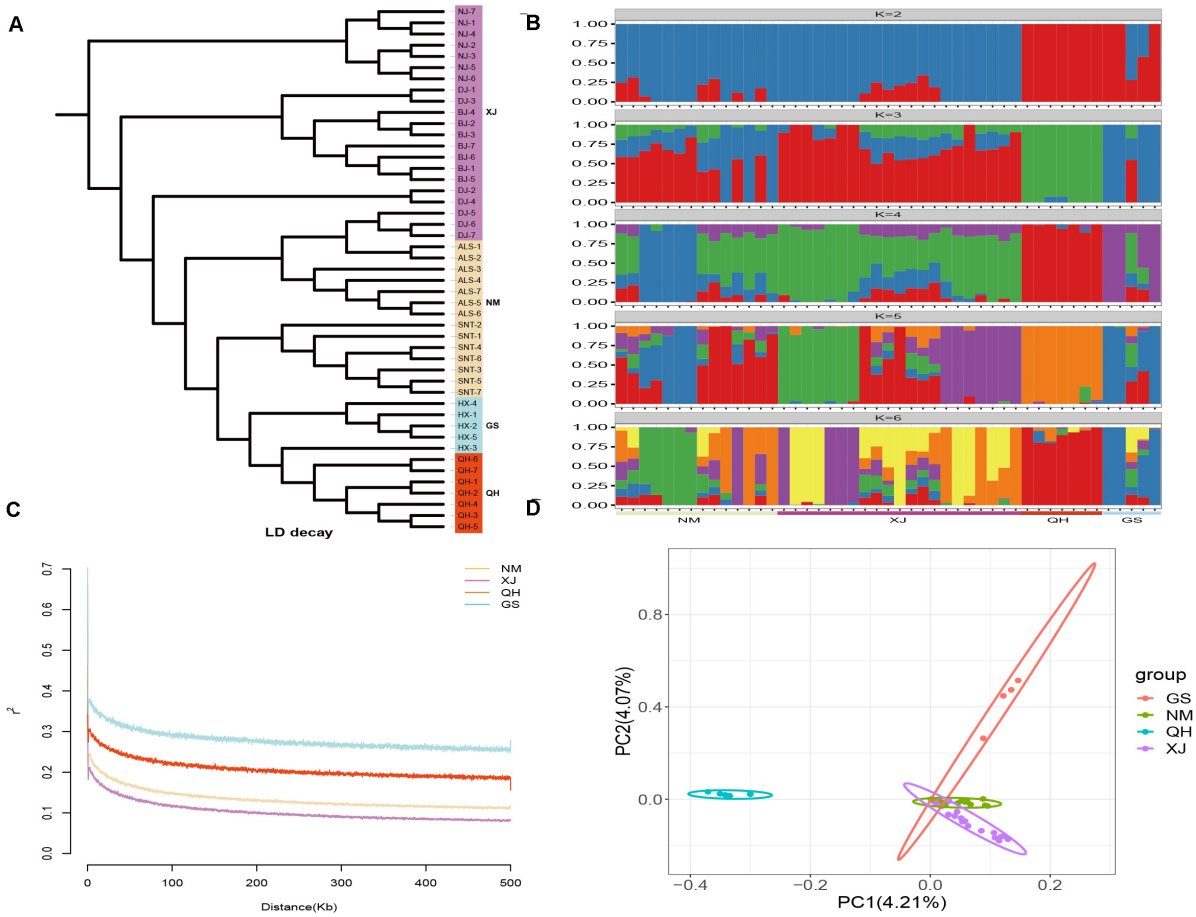

FIGURE 1 | Structure analyses of the domestic Bactrian camel in four regions of China. **(A)** Phylogenetic tree construction with the neighbor-joining (NJ) method. **(B)** Groups structure clustering figure of the domestic Bactrian camel in four regions of China. **(C)** LD attenuation map of the domestic Bactrian camel in four regions of China. **(D)** Principal components analysis of the domestic Bactrian camel in four regions of China.

TABLE 2 | Fst, π, and Fis values for domestic Bactrian camels in the four regions of China.

Number	Group	Average_Fst	π	Average_Fis
1	Xinjiang camel	0.07737	0.0001249	0.4473
2	Gansu camel	0.1201	0.0001091	0.4193
3	Qinghai camel	0.1185	0.0001088	0.3782
4	Inner Mongolia camel	0.08036	0.0001223	0.4434

Mongolia camels, the genes involved in the single-organism process (GO: 0044699) were the most abundant under biological process. Cell (GO: 0005623), cell part (GO: 0044464), and organelle (GO: 0043226) represented the main proportion of the cellular component. Binding (GO: 0005488) accounted for a high proportion of the molecular functional category (**Figure 3** and **Supplementary Table S17**). For Qinghai camels and Gansu camels, the most abundant subcategory under biological process was cellular process (GO: 0009987). Under the category of cellular component, the most abundantly expressed genes were cell (GO: 0005623) and cell part (GO: 0044464). Binding (GO: 0005488) represented the main molecular function (**Figures 4**, **6** and **Supplementary Tables S18**, **S20**). For Xinjiang camels, the genes involved in the cellular process (GO: 0009987) were the most abundant subcategory in biological process. Organelle (GO: 0043226) accounted for a high proportion under cellular component. Binding (GO: 0005488) represented the main molecular function (**Figure 5** and **Supplementary Table S19**).

KEGG enrichment analysis of the shared selected genes of the domestic Bactrian camel in the four regions was performed. Among the Inner Mongolia camels, the shared selected genes were significantly enriched in eight pathways, including long-term depression and circadian entrainment (**Figure 3** and **Supplementary Table S21**). Among the Qinghai camels, the shared selected genes were mainly enriched in focal adhesion pathway (**Figure 4** and **Supplementary Table S22**). Among Xinjiang camels, the shared selected genes were mainly enriched in neuroactive ligand-receptor interaction pathway (**Figure 5** and **Supplementary Table S23**). Among the Gansu camels, the shared selected genes were significantly enriched in ubiquitin mediated proteolysis and renin-angiotensin system pathway (**Figure 6** and **Supplementary Table S24**).

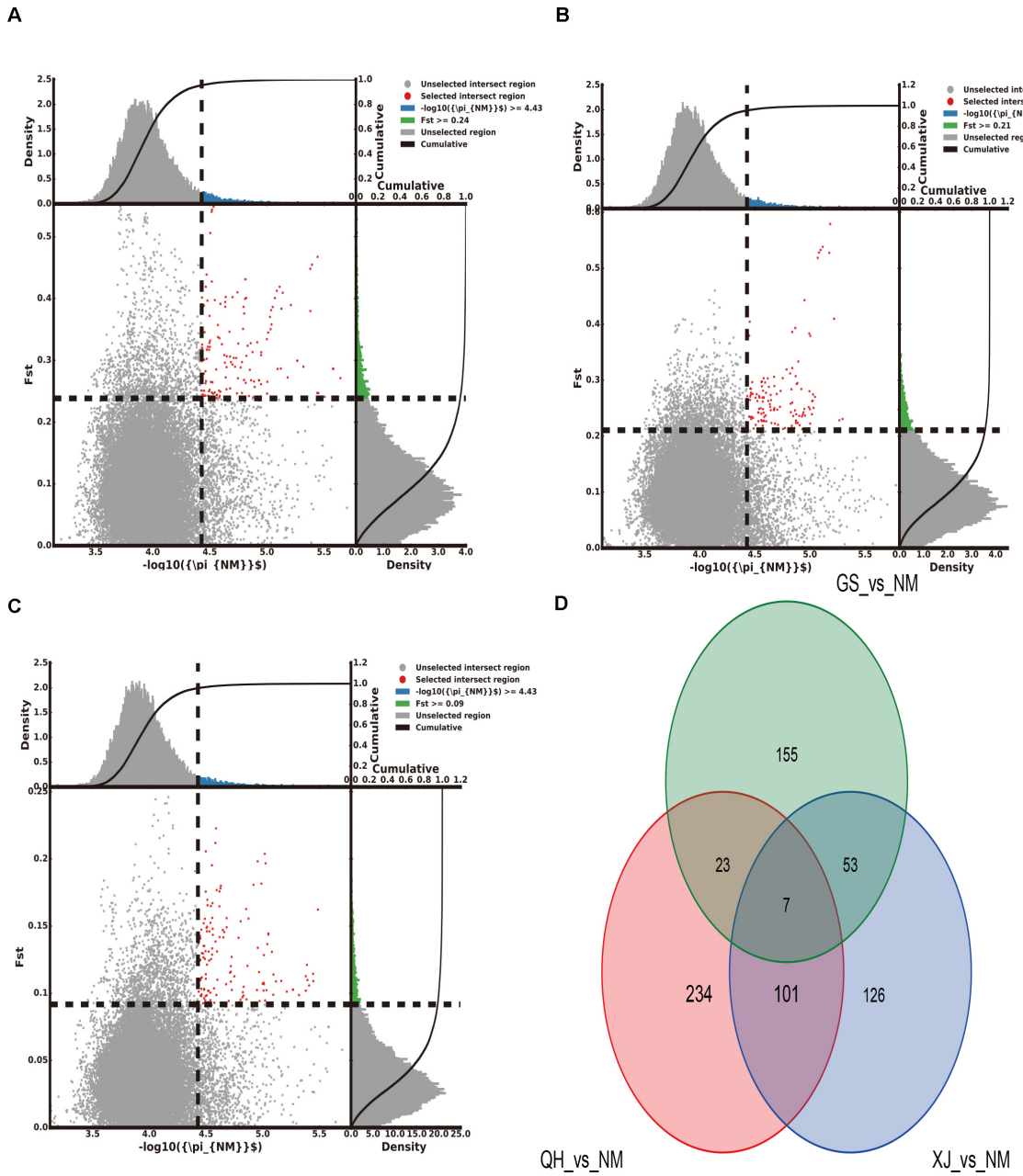

FIGURE 2 | The number of selected genes shared by the Inner Mongolia group of camels. **(A)** Gansu camels were the control group and Inner Mongolia camels were the selection group; 238 selected genes were obtained. **(B)** Qinghai camels were the control group and Inner Mongolia camels were the selection group; 365 selected genes were obtained. **(C)** Xinjiang camels were the control group and Inner Mongolia camels were the selection group; 287 selected genes were obtained. **(D)** Seven selected genes were shared by Inner Mongolia camels.

DISCUSSION

We reported the identification of 1,568,087 SNP loci in the domestic Bactrian camel in four regions of China, using RAD-seq. When read mapping, we used higher "*k*"-values, and the parameter settings are within the reasonable range of the software default (Cao et al., 2019; Shibuya and Comin, 2019; Liu et al., 2020). The filtered SNPs were subjected to LD attenuation analysis and nucleotide diversity analysis (π). The results indicated that Xinjiang camels had the largest number of SNPs, the fastest decay of the LD coefficient, the highest nucleotide diversity, and the highest genetic diversity: these features may be attributable to the preservation of the genetic diversity of this group's ancestors (Abdulla et al., 2009).

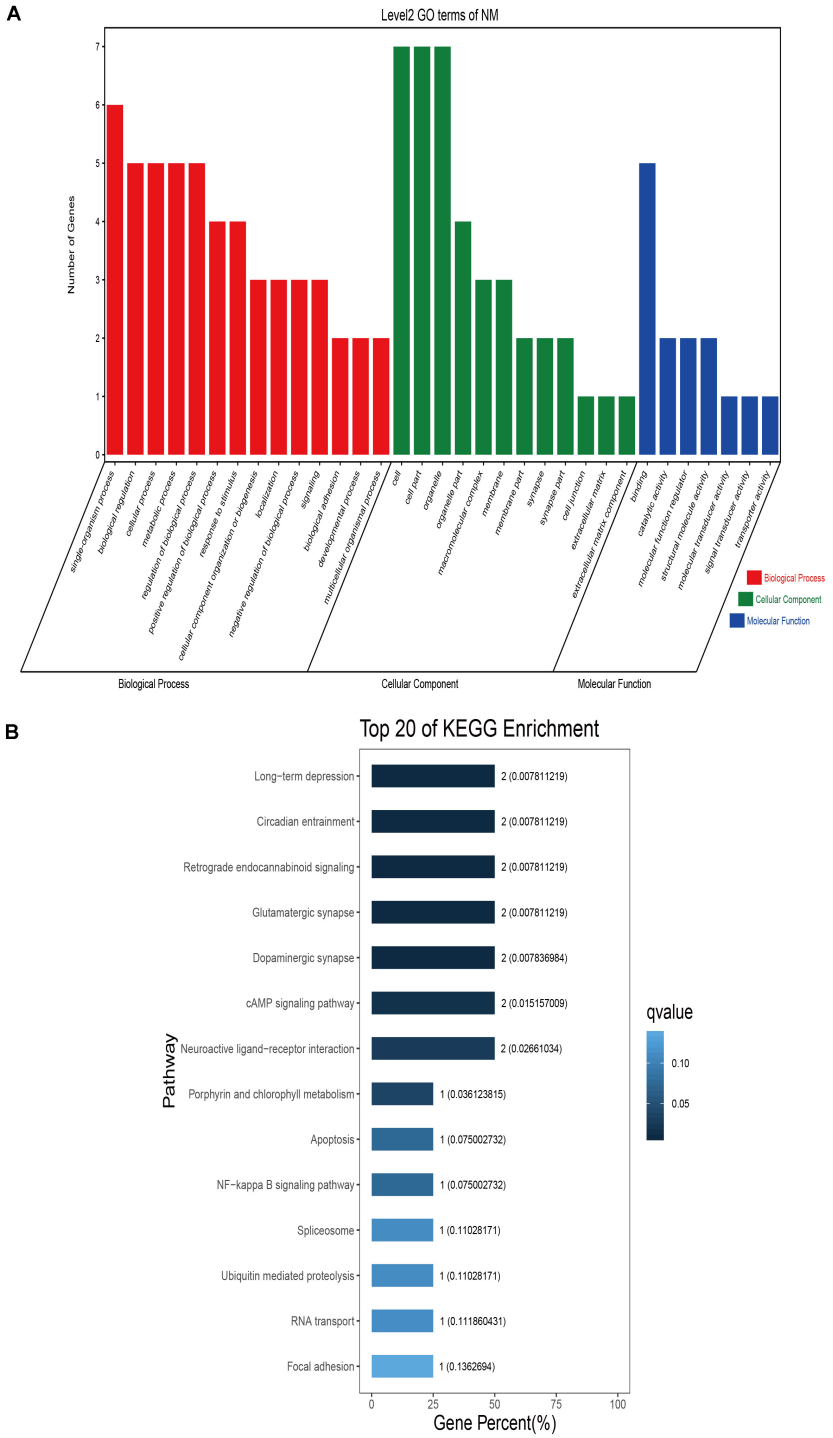

FIGURE 3 | Go classification and KEGG enrichment of the shared selected genes of Inner Mongolia camels. **(A)** Go classification of the shared selected genes of Inner Mongolia camels. **(B)** KEGG enrichment of the shared selected genes of Inner Mongolia camels.

Population structural analysis, PCA, and Fis results suggested that Qinghai camels were phylogenetically distant from camels in other regions; this may be due to the geographical distribution of the Qinghai camels. The Mohe camel farm is located at an altitude of 3000 meters, which is far more elevated than the location of the domestic Bactrian camels in other regions, resulting in less genetic communication between Qinghai camels and domestic Bactrian camels in other regions. Phylogenetic

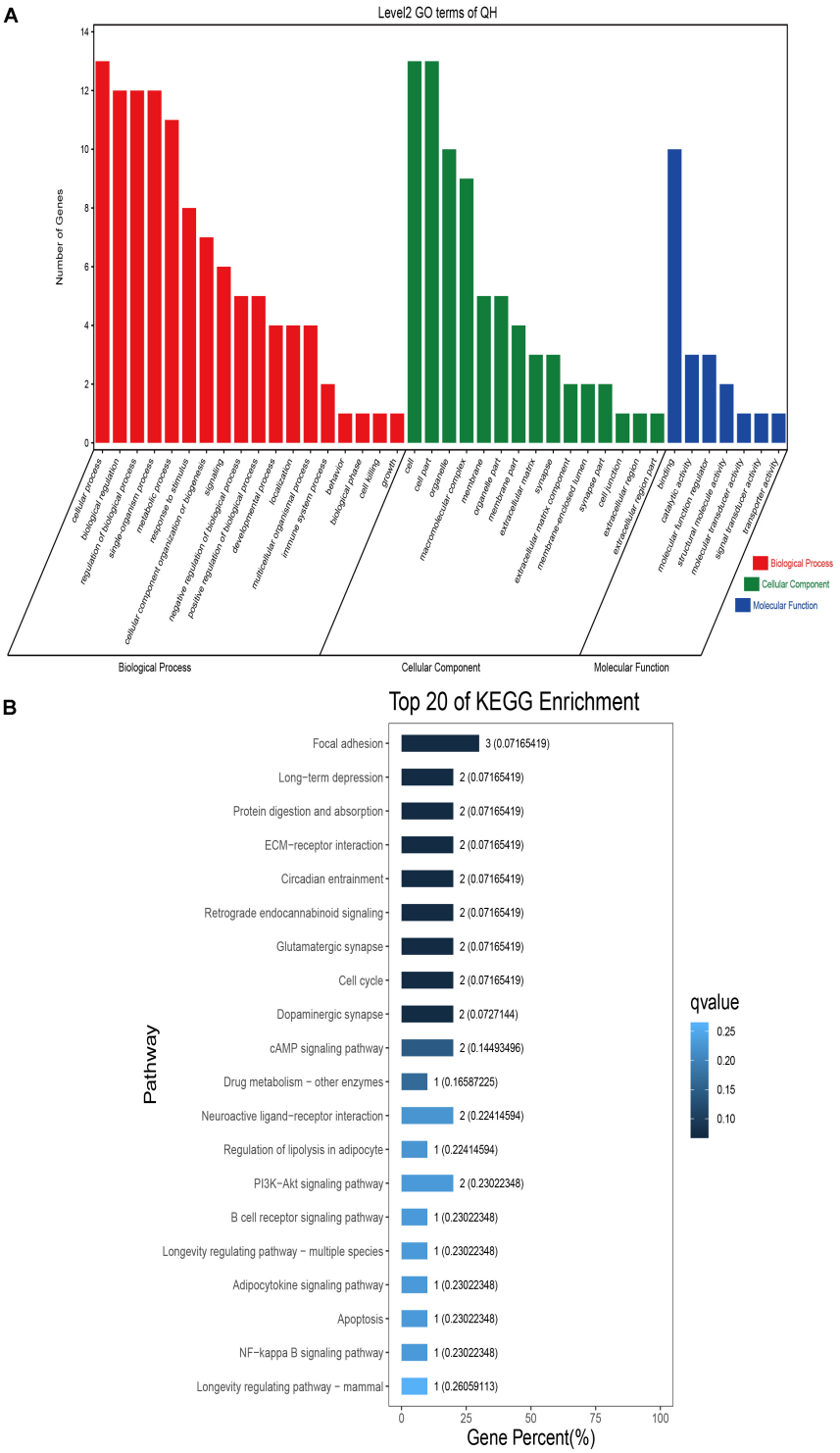

FIGURE 4 | Go classification and KEGG enrichment of the shared selected genes of Qinghai camels. **(A)** Go classification of the shared selected genes of Qinghai camels. **(B)** KEGG enrichment of the shared selected genes of Qinghai camels.

trees constructed using the NJ method as well as PCA data revealed that the genetic relationship between Xinjiang camels and Inner Mongolia camels was relatively close. According to historical records, Inner Mongolia camels were extensively used to transport military supplies to Xinjiang in the Qing Dynasty, which may have promoted the genetic communication between

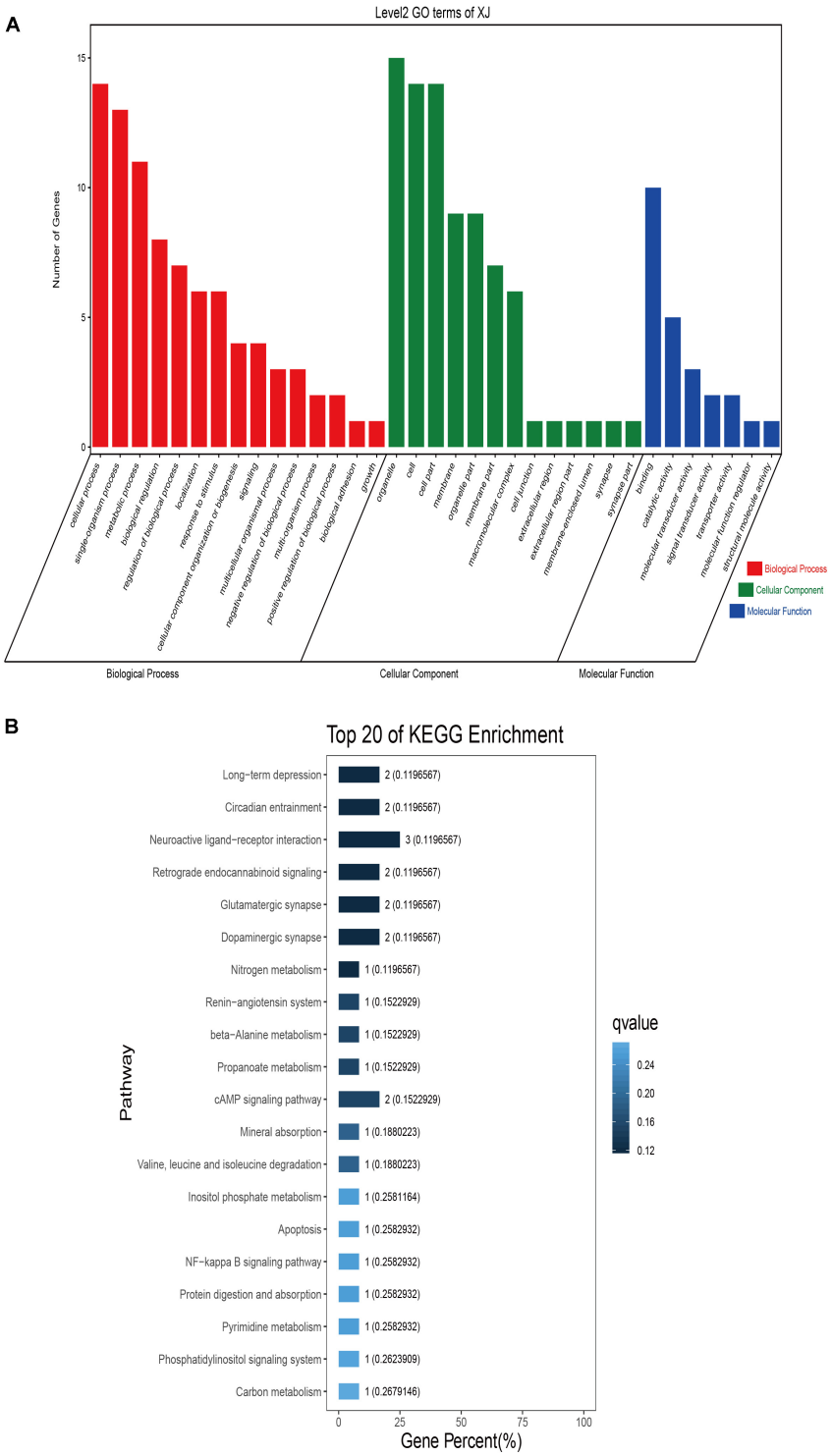

FIGURE 5 | Go classification and KEGG enrichment of the shared selected genes of Xinjiang camels. **(A)** Go classification of the shared selected genes of Xinjiang camels. **(B)** KEGG enrichment of the shared selected genes of Xinjiang camels.

Inner Mongolia camels and Xinjiang camels (Tong, 2018). The average Fst between Gansu camels and domestic Bactrian camels in other regions was the largest, and were phylogenetically distant from the camels in other regions. This may be related to the geographical location of Gansu camels. Yongchang County is located at the northern foot of the Qilian Mountain, close to

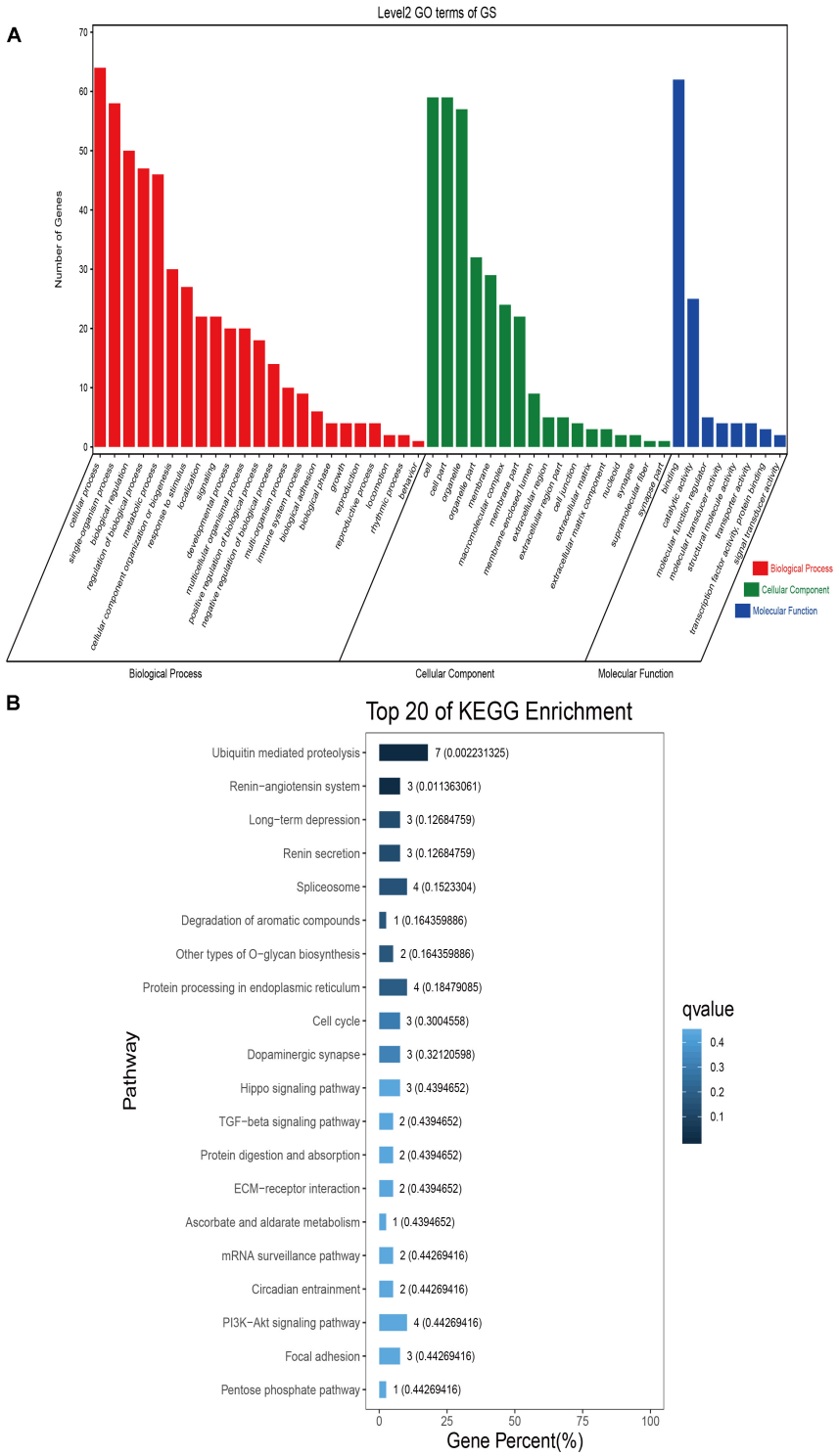

FIGURE 6 | Go classification and KEGG enrichment of the shared selected genes of Gansu camels. **(A)** Go classification of the shared selected genes of Gansu camels. **(B)** KEGG enrichment of the shared selected genes of Gansu camels.

the Badain Jaran desert, resulting in less genetic communication between Gansu camels and other domestic Bactrian camels. Analyses of selection signals showed that the number of selected genes shared by Inner Mongolia camels, Qinghai camels, Xinjiang camels and Gansu camels was 7, 24, 25, and 113, respectively. GO classification and KEGG enrichment analysis

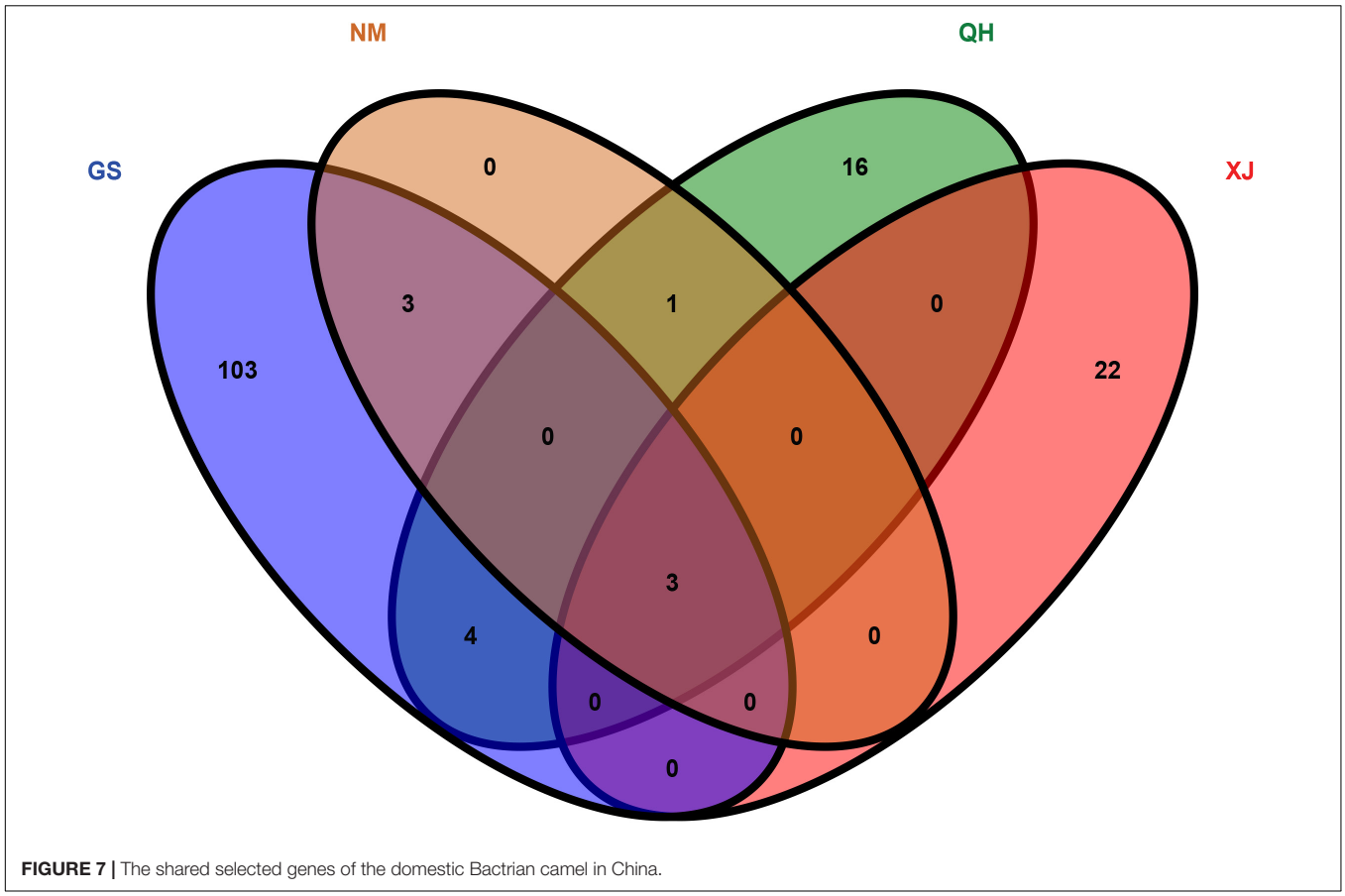

FIGURE 7 | The shared selected genes of the domestic Bactrian camel in China.

were performed on the shared selected genes. The results showed that the most abundant subcategory under biological process was cellular process (GO: 0009987). Cell (GO: 0005623), and cell part (GO: 0044464) accounted for a high proportion of the subcategories under cellular component. Binding (GO: 0005488) represented the main molecular function. The shared selected genes of domestic Bactrian camel populations in the four regions were all significantly enriched in the long-term depression pathway. This finding fills the gap in the genome study of the domestic bactrian camel in China (He et al., 2009; Ming et al., 2019).

The shared selected genes of the domestic Bactrian camel between the four regions in China were further analyzed to identify three shared genes (*GRIA3, XIAP, THOC2*) in the domestic Bactrian camel across all four regions. To our knowledge, this is the first study to identify genes of importance in the evolution of the domestic Bactrian camel in China. *GRIA3* (glutamate receptor 3) is the main excitatory neurotransmitter receptor in the mammalian brain, and is activated in many normal neurophysiologic processes. *GRIA3* regulates the activity of AMPA glutamate receptor and the NMDA receptor (Kato et al., 2010). Both AMPA receptors and NMDA receptors are classes of vital receptors in learning and memory (Brechet et al., 2017; Wang et al., 2018). According to the report of global human geography, the camel's memory is second to none in all animals, and the ability of camels to remember routes gives these animals the capacity to navigate journeys accurately during sandstorms. *GRIA3* is therefore an interesting target for future research on the genome of the domestic bactrian camel in China. *XIAP* (E3 ubiquitin-protein ligase *XIAP*) is a multifunctional protein involved in the cellular response to DNA damage, and can also regulate inflammatory signal transduction and immunity (Deveraux et al., 1997; Damgaard and Gyrd-Hansen, 2011). The harsh environmental conditions of the habitat of the domestic Bactrian camel may promote apoptosis, DNA damage, and inflammatory reactions (Yuan et al., 2017). It can therefore be concluded that *XIAP* is an interesting target for future research on the genome of the domestic bactrian camel in China. *THOC2* (THO complex subunit 2) is a protein-coding gene that is involved in neuronal generation and neuronal development (Straesser et al., 2002). Mutations in this gene can cause hypotonia, gait disturbance, and tremors (Kumar et al., 2015). This gene is also an interesting target for future research on the genome of the domestic bactrian camel in China. A PPI network of the products of the three shared genes, constructed with STRING[8], showed that there was interaction between the three encoded proteins (**Supplementary Figure S4**). Interestingly, the shared selected genes of the domestic Bactrian camel in the four regions were significantly enriched in the long-term depression (LTD) pathway. LTD has previously been

[8]https://string-db.org/

assigned an assistant role in signal-to-noise adjustment or "forgetting". However, LTD also contributes directly to the storage of hippocampal information (Collingridge et al., 2010). Furthermore, LTD plays a dominant role in the processing of precise spatial features. Increasing evidence supports the notion that LTD enables distinct and separate forms of information storage, which together promote the generation of a spatial cognitive map (Kemp and Manahan-Vaughan, 2007).

In brief, we identified the SNPs present in the domestic Bactrian camel genome on a whole-genome basis, and systematically studied the genetic diversity, genetic structure, and genes of importance in the evolution of the domestic Bactrian camel in four regions of China. The results should enable further study of the genetic resources of this mammal, as well as the conservation of these resources. In future studies, we aim to collaborate internationally to collect blood samples from camel populations inhabiting other regions along the Silk Road in order to further explore the available genome resources of this species.

DATA AVAILABILITY STATEMENT

The datasets generated for this study can be found in the NCBI SRA. Bioproject #PRJNA522647 and Biosamples #SAMN10948548–SAMN10948594.

ETHICS STATEMENT

The animal study was reviewed and approved by National Natural Science Foundation of China (31172178). Written informed consent was obtained from the owners for the participation of their animals in this study.

AUTHOR CONTRIBUTIONS

ZR and CL designed the study and wrote the manuscript. HC collected the samples. CZ and XY contributed to the data analysis. All authors read and approved the manuscript.

FUNDING

This study was supported by the National Natural Science Foundation of China, 31172178.

SUPPLEMENTARY MATERIAL

The Supplementary Material for this article can be found online at: https://www.frontiersin.org/articles/10.3389/fgene.2020.00797/full#supplementary-material

REFERENCES

Abdulla, M. A., Ahmed, I., Assawamakin, A., Bhak, J., Brahmachari, S. K., Calacal, G. C., et al. (2009). Mapping human genetic diversity in Asia. *Science* 326, 1541–1545. doi: 10.1126/science.1177074

Baird, N. A., Etter, P. D., Atwood, T. S., Currey, M. C., Shiver, A. L., Lewis, Z. A., et al. (2008). Rapid SNP discovery and genetic mapping using sequenced RAD markers. *PLoS One* 3:e3376. doi: 10.1371/journal.pone.0003376

Brechet, A., Buchert, R., Schwenk, J., Boudkkazi, S., and Fakler, B. (2017). AMPA-receptor specific biogenesis complexes control synaptic transmission and intellectual ability. *Nat. Commun.* 8, 1–14. doi: 10.1038/ncomms15910

Cao, D. N., Wang, M., Ge, Y., and Gong, S. P. (2019). Draft genome of the big-headed turtle Platysternon megacephalum. *Sci. Data* 6:60. doi: 10.1038/s41597-019-0067-9

Chen, H. L., Ren, Z. J., Zhao, J. P., Zhang, C. D., and Yang, X. J. (2018). Y-chromosome polymorphisms of the domestic bactrian camel in China. *J. Genet.* 97, 3–10. doi: 10.1007/s12041-017-0852-1

Collingridge, G. L., Peineau, S., Howland, J. G., and Wang, Y. T. (2010). Long-term depression in the CNS. *Nat. Rev. Neurosci.* 11, 459–473. doi: 10.1038/nrn2867

Damgaard, R. B., and Gyrd-Hansen, M. (2011). Inhibitor of apoptosis (IAP) proteins in regulation of inflammation and innate immunity. *Discov. Med.* 11, 221–231.

Danecek, P., Auton, A., Abecasis, G., Albers, C. A., Banks, E., DePristo, M. A., et al. (2011). The variant call format and VCFtools. *Bioinformatics* 27, 2156–2158. doi: 10.1093/bioinformatics/btr330

Davey, J. W., Hohenlohe, P. A., Etter, P. D., Boone, J. Q., Blaxter, M. L., and Catchen, J. M. (2011). Genome-wide genetic marker discovery and genotyping using next-generation sequencing. *Nat. Rev. Genet.* 12, 499–510. doi: 10.1038/nrg3012

DePristo, M. A., Banks, E., Poplin, R., Garimella, K. V., Maguire, J. R., Hartl, C., et al. (2011). A framework for variation discovery and genotyping using next-generation DNA sequencing data. *Nat. Genet.* 43, 491–498. doi: 10.1038/ng.806

Deveraux, Q. L., Takahashi, R., Salvesen, G. S., and Reed, J. C. (1997). X-linked IAP is a direct inhibitor of cell-death proteases. *Nature* 388, 300–304. doi: 10.1038/40901

Díaz-Arce, N., Arrizabalaga, H., Murua, H., Irigoien, X., and Rodríguez-Ezpeleta, N. (2016). RAD-seq derived genome-wide nuclear markers resolve the phylogeny of tunas. *Mol. Phylogenet. Evol.* 102, 202–207. doi: 10.1016/j.ympev.2016.06.002

Guo, C. Y. (2012). *Association Analysis Of Genetic Diversity Of Jianghuai Soybean Breeding Germplasm and QTL of Breeding Target Traits*. Master's thesis, Nanjing Agriculture University, Nanjing, IL.

He, X. H., Han, X. L., and Ma, Y. H. (2009). Progress in the study of genetic diversity of bactrian camel. *Acta Ecol. Anim. Domast.* 30, 9–13.

Ji, R., Cui, P., Ding, F., Geng, J., and Meng, H. (2009). Monophyletic origin of domestic bactrian camel (*Camelus bactrianus*) and its evolutionary relationship with the extant wild camel (*Camelus bactrianus* ferus). *Anim. Genet.* 40, 377–382. doi: 10.1111/j.1365-2052.2008.01848.x

Kato, A. S., Gill, M. B., Ho, M. T., Yu, H., and Bredt, D. S. (2010). Hippocampal AMPA receptor gating controlled by both TARP and cornichon proteins. *Neuron* 68, 1082–1096. doi: 10.1016/j.neuron.2010.11.026

Kemp, A., and Manahan-Vaughan, D. (2007). Hippocampal long-term depression: master or minion in declarative memory processes? *Trends Neurosci.* 30, 111–118. doi: 10.1016/j.tins.2007.01.002

Kumar, R., Corbett, M. A., van Bon, B. W. M., Woenig, J. A., Douglas, E., Friend, K. L., et al. (2015). THOC2 mutations implicate mRNA-export pathway in X-linked intellectual disability. *Am. J. Hum. Genet.* 97, 302–310. doi: 10.1016/j.ajhg.2015.05.021

Li, H., and Durbin, R. (2009). Fast and accurate short read alignment with burrows-wheeler transform. *Bioinformatics* 25, 1754–1760. doi: 10.1093/bioinformatics/btp324

Liu, C. M., Chen, H. L., Ren, Z. J., Zhang, C. D., and Yang, X. J. (2019). Population genetic analysis of the domestic bactrian camel in China by RAD-seq. *Ecol. Evol.* 9, 11232–11242. doi: 10.1002/ece3.5624

Liu, X., Li, C., Chen, M., Liu, B., Yan, X. J., Ning, J. H., et al. (2020). Draft genomes of two Atlantic bay scallop subspecies *Argopecten irradians* irradians and *A. i. concentricus*. *Sci. Data* 7:99. doi: 10.1038/s41597-020-0441-7

Mao, X., Cai, T., Olyarchuk, J. G., and Wei, L. (2005). Automated genome annotation and pathway identification using the KEGG Orthology (KO) as a controlled vocabulary. *Bioinformatics* 21, 3787–3793. doi: 10.1093/bioinformatics/bti430

Meadow, R. H., and Zeder, M. A. (1978). Approaches to faunal analysis in the Middle East. *Peabody Museum Bull.* 2, 91–103.

Miller, M. R., Dunham, J. P., Amores, A., Cresko, W. A., and Johnson, E. A. (2007). Rapid and cost-effective polymorphism identification and genotyping using restriction site associated DNA (RAD) markers. *Genome Res.* 17, 240–248. doi: 10.1101/gr.5681207

Ming, L., Yi, L., He, J., Hai, L., and Ji, R. M. T. (2019). Identification of microsatellites and parentage testing development of bactrian camel (*Camelus bactrianus*). *J. Camel. Pract. Res.* 26, 133–142.

Ming, L., Yi, L., Sa, R., Wang, Z. X., Wang, Z., and Ji, R. M. T. (2017). Genetic diversity and phylogeographic structure of bactrian camels shown by mitochondrial sequence variations. *Anim. Genet.* 48, 217–220. doi: 10.1111/age.12511

Nei, M., and Li, W. H. (1979). Mathematical model for studying genetic variation in terms of restriction endonucleases. *Proc. Natl. Acad. Sci. U.S.A.* 76, 5269–5273. doi: 10.1073/pnas.76.10.5269

Pfeifer, B., Wittelsbürger, U., Ramos-Onsins, S. E., and Lercher, M. J. (2014). PopGenome: an efficient Swiss army knife for population genomic analyses in R. *Mol. Biol. Evol.* 31, 1929–1936. doi: 10.1093/molbev/msu136

R Core Team (2013). *R: A Language And Environment For Statistical Computing*. Vienna: R Core Team.

Ren, A. Y., Du, K., Jia, X. B., Yang, R., Wang, J., Chen, S. Y., et al. (2019). Genetic diversity and population structure of four Chinese rabbit breeds. *PLoS One* 14:e0222503. doi: 10.1371/journal.pone.0222503

Sambrook, J., and Russell, D. W. (2002). *Translated by Huang, PT 444 Molecular Cloning A Laboratory Manual*. Beijing: Science Press.

Schraiber, J. G., and Akey, J. M. (2015). Methods and models for unravelling human evolutionary history. *Nat. Rev. Genet.* 16, 727–740. doi: 10.1038/nrg4005

Shibuya, Y., and Comin, M. (2019). Better quality score compression through sequence-based quality smoothing. *BMC Bioinform.* 20:302. doi: 10.1186/s12859-019-2883-5

Straesser, K., Masuda, S., Mason, P., Pfannstiel, J., Oppizzi, M., Rodriguez-Navarro, S., et al. (2002). TREX is a conserved complex coupling transcription with messenger RNA export. *Nature* 417, 304–308. doi: 10.1038/nature746

Tong, B. (2018). Study on camel transportation of the inner Mongolian Hui people on "silk tea camel road" in grassland. *Tea in Fujian.* 11:451.

Wang, J., Lv, X., Wu, Y., Xu, T., and Qiu, S. (2018). Postsynaptic RIM1 modulates synaptic function by facilitating membrane delivery of recycling NMDARs in hippocampal neurons. *Nat. Commun.* 9, 1–15. doi: 10.1038/s41467-018-04672-0

Yang, J., Lee, S. H., Goddard, M. E., and Visscher, P. M. (2011). GCTA: a tool for genome-wide complex trait analysis. *Am. J. Hum. Genet.* 88, 76–82. doi: 10.1016/j.ajhg.2010.11.011

Ye, J., Fang, L., Zheng, H. K., Zhang, Y., Chen, J., Zhang, Z. J., et al. (2006). WEGO: a web tool for plotting GO annotations. *Nucleic Acids Res.* 34, 293–297. doi: 10.1093/nar/gkl031

Yuan, S. P., Wen, J., Zheng, R. C., and Qin, S. (2017). Progress in research on squamous cell carcinoma of the skin caused by ultraviolet radiation. *J. Diagn. Ther. Dermato Venereol.* 24, 423–426.

Zhang, B. D., Xue, D. X., Wang, J., Li, Y. L., Liu, B. J., and Liu, J. X. (2016). Development and preliminary evaluation of a genomewide single nucleotide polymorphisms resource generated by RAD-seq for the small yellow croaker (*Larimichthys polyactis*). *Mol. Ecol. Resour.* 16, 755–768. doi: 10.1111/1755-0998.12476

Conflict of Interest: The authors declare that the research was conducted in the absence of any commercial or financial relationships that could be construed as a potential conflict of interest.

frontiers in Genetics

REVIEW
published: 31 July 2020
doi: 10.3389/fgene.2020.00793

Large-Scale Phenotyping of Livestock Welfare in Commercial Production Systems: A New Frontier in Animal Breeding

Luiz F. Brito[1], Hinayah R. Oliveira[1,2], Betty R. McConn[3], Allan P. Schinckel[1], Aitor Arrazola[4], Jeremy N. Marchant-Forde[5] and Jay S. Johnson[5]*

[1] Department of Animal Sciences, Purdue University, West Lafayette, IN, United States, [2] Department of Animal Biosciences, University of Guelph, Guelph, ON, Canada, [3] Oak Ridge Institute for Science and Education, Oak Ridge, TN, United States, [4] Department of Comparative Pathobiology, Purdue University, West Lafayette, IN, United States, [5] USDA-ARS Livestock Behavior Research Unit, West Lafayette, IN, United States

OPEN ACCESS

Edited by:
Guilherme J. M. Rosa, University of Wisconsin–Madison, United States

Reviewed by:
Eveline M. Ibeagha-Awemu, Agriculture and Agri-Food Canada (AAFC), Canada
Jennie Elizabeth Pryce, AgriBio, La Trobe University, Australia
Florence Phocas, INRA Centre Jouy-en-Josas, France

***Correspondence:**
Luiz F. Brito
britol@purdue.edu

Specialty section:
This article was submitted to Livestock Genomics, a section of the journal Frontiers in Genetics

Received: *15 April 2020*
Accepted: *03 July 2020*
Published: *31 July 2020*

Citation:
Brito LF, Oliveira HR, McConn BR, Schinckel AP, Arrazola A, Marchant-Forde JN and Johnson JS (2020) Large-Scale Phenotyping of Livestock Welfare in Commercial Production Systems: A New Frontier in Animal Breeding. Front. Genet. 11:793. doi: 10.3389/fgene.2020.00793

Genomic breeding programs have been paramount in improving the rates of genetic progress of productive efficiency traits in livestock. Such improvement has been accompanied by the intensification of production systems, use of a wider range of precision technologies in routine management practices, and high-throughput phenotyping. Simultaneously, a greater public awareness of animal welfare has influenced livestock producers to place more emphasis on welfare relative to production traits. Therefore, management practices and breeding technologies in livestock have been developed in recent years to enhance animal welfare. In particular, genomic selection can be used to improve livestock social behavior, resilience to disease and other stress factors, and ease habituation to production system changes. The main requirements for including novel behavioral and welfare traits in genomic breeding schemes are: (1) to identify traits that represent the biological mechanisms of the industry breeding goals; (2) the availability of individual phenotypic records measured on a large number of animals (ideally with genomic information); (3) the derived traits are heritable, biologically meaningful, repeatable, and (ideally) not highly correlated with other traits already included in the selection indexes; and (4) genomic information is available for a large number of individuals (or genetically close individuals) with phenotypic records. In this review, we (1) describe a potential route for development of novel welfare indicator traits (using ideal phenotypes) for both genetic and genomic selection schemes; (2) summarize key indicator variables of livestock behavior and welfare, including a detailed assessment of thermal stress in livestock; (3) describe the primary statistical and bioinformatic methods available for large-scale data analyses of animal welfare; and (4) identify major advancements, challenges, and opportunities to generate high-throughput and large-scale datasets to enable genetic and genomic selection for improved welfare in livestock. A wide variety of novel welfare indicator traits can be derived from information captured by modern technology such as sensors, automatic feeding systems, milking robots, activity monitors, video cameras, and

indirect biomarkers at the cellular and physiological levels. The development of novel traits coupled with genomic selection schemes for improved welfare in livestock can be feasible and optimized based on recently developed (or developing) technologies. Efficient implementation of genetic and genomic selection for improved animal welfare also requires the integration of a multitude of scientific fields such as cell and molecular biology, neuroscience, immunology, stress physiology, computer science, engineering, quantitative genomics, and bioinformatics.

Keywords: behavioral genomics, big data, digital agriculture, phenomics, genomic information, genomic selection, novel phenotypes, precision livestock

INTRODUCTION

Animal welfare has increasingly relevant ethical, legal, and economic implications in livestock production around the world (Rushen et al., 2011; Koknaroglu and Akunal, 2013; Marchant-Forde, 2015; Grethe, 2017). Animal product consumers, and public in general, are becoming more interested in ensuring good welfare practices at all stages of the animal production chain, which has direct implications for the whole industry. In addition, poor welfare is associated with reduced animal productivity, longevity, poor meat quality, low reproductive performance, and high prevalence of diseases in herds or flocks (Cockram, 2002; Moberg, 2009; Miranda-de la Lama et al., 2013; Grethe, 2017; Croney et al., 2018a,b; Gonzalez-Rivas et al., 2020). This global importance of animal welfare is indicated by the inclusion of increasing numbers of species-specific and situation-specific animal welfare chapters in the OIE Terrestrial Animal Health Code (World Organization for Animal Health – OIE, 2019).

Historically, animal welfare has been defined under one of three over-arching, and intersecting themes or approaches (Fraser, 2008). These welfare approaches are biological functioning, natural behavior, and affective states. These three approaches overlap to provide a holistic overview of the welfare of the individual, and indicators of the three approaches should be taken into account in welfare assessments (Fraser et al., 1997). Nonetheless, defining measurable parameters that incorporate the underlying processes of all three approaches for multiple individuals under commercial conditions is challenging. This task is particularly difficult due to the context-dependent and conditional nature of the behavioral response and the affective state of the animals. However, the expression of natural behaviors is paramount to improve welfare due to species-specific behavioral needs (Duncan, 1998; Olsson et al., 2011). Specific behaviors (e.g., motivated behaviors) have an intrinsic value for animals, and the performance of these behaviors is necessary to achieve acceptable animal welfare (Duncan, 1998). Non-met behavioral needs and motivated behaviors results in frustration and can develop in distress and other emotional disorders (Mason, 2006; Keeling et al., 2011). Animals are sentience beings, and this implies that livestock can experience positive and negative affective states. For this reason, animal emotions are essential in welfare assessments, and improvements in animal welfare should promote positive affective states and reduce the negative ones (Broom, 2011; Mellor, 2016).

An often used approach in animal welfare assessment is based on the Five Freedoms (Brambell, 1965; McCulloch, 2013), which consists of the absence of negative welfare (thirst, hunger, and malnutrition; physical and thermal discomfort; pain, injury, and disease; fear; and distress) as well as the presence of positive welfare (e.g., freedom to engage in motivated behaviors; Broom, 1991; De Goede et al., 2013). These have been applied mostly in terms of housing and husbandry (Mellor, 2016). However, welfare assessments using the Five Freedoms examine on-farm environment by looking mostly at input or resource-based measures that usually describe the physical environment rather than at outcome or animal-based measures that directly refer to animal status (Butterworth et al., 2017). More recent focus has been on the development of animal-based indicators and expert opinion states that "*animal-based measures are the most appropriate indicators of animal welfare and a carefully selected combination of animal-based measures can be used to assess the welfare of a target population in a valid and robust way*" (European Food Safety Authority [EFSA], 2012).

Despite the fact that various countries have implemented regulations and legislation to ensure ethical animal treatment from birth to slaughter (Rushen et al., 2011), completely eliminating welfare issues (e.g., incidence of diseases, thermal, and metabolic stress) is still very challenging or impossible due to multiple factors, including: climate change, especially in outdoor systems (Cole et al., 2017); growing intensification of commercial production systems; group-housed animals in inadequate systems (negative interactions, e.g., due to aggressive behaviors, feather pecking, and cannibalism); antibiotic resistance (Mathew et al., 2007; Woolhouse et al., 2015); high disease prevalence (Zessin, 2006); and, to a lesser extent, genetic selection based on a limited number of production traits in some breeding programs or indirect genetic responses (Rauw et al., 1998, 2017). In this context, the implementation of selective breeding schemes to genetically modify the animals' biological mechanisms and/or behaviors in ways that improve welfare in commercial systems is a promising route (Jensen et al., 2008; Turner, 2011; Croney et al., 2018b). This is likely to be achieved through selection and breeding of more resilient animals.

Genetic selection for improved welfare has been investigated and implemented in livestock species over the past few decades (Rodenburg and Turner, 2012; Canario et al., 2013). Several traits associated with animal welfare have been shown to be heritable (the majority of the estimates are in the range of 0.15 to 0.40;

TABLE 1 | Heritability estimates for indicators of heat tolerance based on direct or indirect traits in pigs.

Indicator trait	Breed	Heritability	References
Feeding behavior	Crossbred animals (grow-finish)	0.02 to 0.21	Cross et al., 2018
Thermoregulation	Crossbred animals	0.39 to 0.83	Kim K. S. et al., 2018
Lactation performance	Large White (Lactating sows)	0.20 to 0.31	Gourdine et al., 2017
Thermoregulation	Large White (Lactating sows)	0.34 to 0.39	Gourdine et al., 2017
Body weight	Duroc (grow-finish)	0.23 to 0.26	Fragomeni et al., 2016
Hot Carcass weight	Crossbred animals (grow-finish)	0.17 to 0.18	Fragomeni et al., 2016
Farrowing rate	Large White and crossbred sows	0.02 to 0.08	Bloemhof et al., 2012
Carcass weight	Terminal crossbred (grow-finish)	0.14 to 0.51	Zumbach et al., 2008

Tables 1–4), including: feather pecking (Buitenhuis et al., 2004; Muir et al., 2014; Grams et al., 2015), cannibalism (Rodenburg et al., 2008; Bennewitz et al., 2014), animal robustness (Muir et al., 2014; Rauw and Gomez-Raya, 2015; Friggens et al., 2017), overall mortality (Knol et al., 2002; Grandinson, 2005; Bolhuis et al., 2009), leg health (McLaren et al., 2016; Vargas et al., 2017), bone strength (Kapell et al., 2017; Oviedo-Rondón et al., 2017; Siegel et al., 2019), and immune response and disease resistance (Bishop and MacKenzie, 2003; Stear et al., 2012; Mallard et al., 2015; Schultz et al., 2020). Genetic and genomic selection for welfare traits, itself, is unlikely to solve all the welfare issues in commercial livestock operations. However, selective breeding is a complementary approach to other strategies (e.g., management, nutrition, housing, and biosecurity), which should result in permanent and cumulative gains in welfare (resilience) over generations.

In brief, genomic selection (Meuwissen et al., 2001) refers to the use of a large number of markers distributed across the whole genome to estimate the breeding values (and future performance) of breeding individuals for traits of interest (e.g., temperament, feather pecking). Genomics provides a great venue for genetically improving animal welfare, as it permits increasing the accuracy of breeding values for selection candidates or close relatives, even if they are not exposed to additional stressors. In this regard, data collection can be performed in chosen herds or flocks (e.g., nucleus or phenotyping herds) that are genetically connected to the potential breeding animals. This creates an opportunity to measure a large number of traits (deep phenotyping) in the same group of animals and use this information to genetically select non-phenotyped animals in commercial farms. As long as there is a sufficiently large training population (individuals with both phenotypes and genotypes) genetically related to the selection candidates, the accuracy of genomic breeding values can be moderate to high. Therefore, genomic tools facilitates selection for complex behavioral and welfare traits in commercial farms (Rodenburg and Turner, 2012). This is very advantageous, especially in the case of disease resilience, where a disease challenge might be required and cannot be performed in the nucleus farms (Putz et al., 2019).

A limited number of livestock breeding programs have included welfare indicator traits in their selection schemes (Miglior et al., 2017; Preisinger, 2018; Turner et al., 2018; Chang et al., 2020). A major challenge for the implementation of genetic evaluation for welfare traits has been the difficulty in collecting individual measurements on a large number of animals (Houle et al., 2010; Turner et al., 2018). As welfare is a multifactorial state, there is a need for simultaneously measuring multiple variables over time (repeated records). This requirement can be a major constraint in commercial breeding programs due to the infrastructure needed to collect the data, economic feasibility, standardization of data collection protocols, and lack (or reduced availability) of equipment and procedures that maximize the welfare of the animals during the measurements.

More recently, precision livestock farming (PLF) technologies (Friggens and Thorup, 2015; Berckmans, 2017), also termed digital agriculture (Liakos et al., 2018), have been presented as an alternative to individually assessing welfare indicator traits on commercial farms. These technologies rely on continuous automatic real-time monitoring and controlling of animal activities and environmental conditions (Berckmans, 2014). This is usually done using sensors (e.g., accelerometers, ruminal boluses, biosensors, and radio-frequency identification – RFID-enabled ear tags), imaging (e.g., cameras), sounds (e.g., microphones), and recording of movements (Lohölter et al., 2013; Andriamandroso et al., 2016; Terrasson et al., 2016; Neethirajan, 2017; Vranken and Berckmans, 2017; Rufener et al., 2018; Ellen et al., 2019; Halachmi et al., 2019). However, many of these technologies measure phenotypes at flock or herd level, down to pen level, with individual-level data options only more widespread for large livestock species kept in smaller numbers. In addition to PLF technologies, variables based on simpler equipment and protocols can also be collected in large scale and used to assess animal welfare (e.g., lesion scoring, hoof health scoring, docility scoring, and milking temperament assessed by animal handlers). Furthermore, computational and data science fields (e.g., machine learning, computer vision, and cyber-physical systems) are quickly advancing (Nayeri et al., 2019; Tomisław et al., 2019; Verma et al., 2020). Thus, datasets generated from PLF technologies coupled with data science developments are paramount to translate animal welfare indicators into accurate genomic breeding values to be used for selective breeding aiming to enhance animal welfare.

Previous reviews have focused on the use of precision technologies for a variety of purposes, especially on-farm management (Neethirajan, 2017; Neethirajan et al., 2017; Vranken and Berckmans, 2017; Croney et al., 2018b; Benjamin and Yik, 2019; Halachmi et al., 2019). The current review, expands this scope by focusing on the use of precision technologies for selective breeding to enhance animal welfare in commercial livestock production, with a focus on terrestrial species. In this context, our main objectives are to: (1) describe ways to develop novel welfare indicator traits (using ideal phenotypes) for both genetic and genomic selection

schemes; (2) summarize key indicator variables of livestock behavior and welfare, including a detailed assessment of thermal stress in livestock; (3) describe the primary statistical and bioinformatic methods available for large-scale data analyses of animal welfare; and (4) identify major advancements, challenges, and opportunities to generate high-throughput and large-scale datasets to enable genetic or genomic selection for enhanced welfare in livestock.

MAIN REQUIREMENTS FOR IDENTIFYING WELFARE TRAITS FOR SELECTIVE BREEDING PURPOSES

Animal welfare science is a relatively new field that is quickly evolving in an interdisciplinary manner (Carenzi and Verga, 2009; Broom, 2011; Marchant-Forde, 2015). The longitudinal measurement or quantification of multiple welfare indicators is the main requirement for selective breeding to enhance animal welfare. In this section we present some ideas toward the identification and description of ideal phenotypes for selective breeding.

A phenotype, or phenotypic trait, is defined here as a variable that can be measured on a continuous (e.g., cortisol level, body temperature), or categorical (e.g., docility and longevity scores) scale in individual animals and represents a biological mechanism at a certain time point (or life stage). Animal welfare is a multidimensional concept comprising physical, behavioral, physiological, and emotional aspects (Broom, 1991; Rushen et al., 2011), and thus, its objective measurement [automated assessment with no bias or dependence on the device used (or technician doing the assessment)] is a challenging task.

Firstly, continuous monitoring of the animal welfare state from birth to slaughter (or involuntary culling) is needed because animals can be more or less prone to certain welfare issues at specific life stages [e.g., food allergies and gut inflammation after weaning in piglets (Jayaraman and Nyachoti, 2017; Radcliffe et al., 2019), tail biting and aggressive behaviors after mixing pigs in larger groups (Camerlink et al., 2013; Shen et al., 2019), feather pecking in laying hens (Ellen et al., 2019), and age-specific disease occurrences such as mastitis in dairy species (Barkema et al., 2015)]. Therefore, longitudinal phenotypes need to be collected and analyzed (Rauw and Gomez-Raya, 2015; Berghof et al., 2019; Oliveira et al., 2019a). Resilience, defined as the capacity of an animal to be minimally affected by disturbances or to rapidly return to the state attained before exposure to a disturbance (Berghof et al., 2019), can also indicate welfare. Based on longitudinal measurements, resilience indicators may be derived based on deviations from expected production levels over a period of time (Berghof et al., 2019), or variations in automatically recorded feed intake (Putz et al., 2019). For instance, Putz et al. (2019) proposed various novel phenotypes related to disease resilience using daily feed intake data from growing pigs under a multifactorial natural disease challenge that was designed to mimic a commercial environment with high disease burden. The novel resilience phenotypes proposed by the authors were heritable and genetically correlated with mortality and treatment rate (Putz et al., 2019). In the context of longitudinal measurements, it is worth noting that stress responses can be beneficial in helping the animals to cope with their environment and challenging situations. However, overstimulated stress response (too frequent or for too long) can detrimentally affect biological functions such as production, immune response, and coping abilities (Moberg, 2009; Palme, 2012; Rauw et al., 2017).

Secondly, a large number of variables need to be accurately measured in individual animals as biological indicators of the Five Freedoms (Brambell, 1965; McCulloch, 2013), including physiological, behavioral, emotional state, and physical and health characteristics. A single stressor can impact biological functions of the animal in different ways [e.g., feed deprivation can cause weight loss, hunger and frustration, behavioral changes, altered metabolic rate (Ketterson and King, 1977), and immune suppression; thermal stress can cause altered feed intake, digestion, discomfort, uneven growth and body weight, and altered metabolic function leading to distress and increased mortality (Johnson, 2018); and social isolation, group mixing and restraint can result in altered heart rate, elevated cortisol levels, frustration, aggressive behavior, and weaker immune systems (Ruis et al., 2001; Shen et al., 2019)]. Interestingly, the stress response to possible threatening stimuli varies among individuals dependent on how the stress is perceived (i.e., individual susceptibility), resulting in different individual welfare outcomes. Animals are capable of experiencing positive and negative emotions, and welfare indicators should not only focus on physical conditions but on their emotional states as well (Reimert et al., 2013; Wemelsfelder and Mullan, 2014; Jirkof et al., 2019; Lawrence et al., 2019). In addition to physiological indicators of stress, recording the prevalence of behavioral signs associated with negative welfare such as arousal and hyperactivity, frustration, distress, and depression can provide important clues about how animals are coping with their environment as well as their welfare (Keeling et al., 2011).

Thirdly, data collection should be based on non-invasive methods that do not result in additional stress or discomfort to the animals or alter their routine or circadian rhythms. For instance, handling animals for measuring blood parameters could cause stress hormone release (Stewart et al., 2005; Cook, 2012). This could be an issue for assessing the undisturbed welfare status of the animal in commercial production settings. Please note that the effect of handling-induced cortisol release can be minimized by recording the time from start of handling to end of blood collection and including it as a covariate in the models; or alternatively, training the animals to habituate to the blood collection procedure, depending on the study goals. Similarly, phenotyping animals during a stressful event intrinsic to their management environment has been suggested to be preferred than exposing animals to an experimentally imposed stressful situation (Colditz and Hine, 2016).

The derived phenotypes need to be collected at a low cost to enable measurement of a large number of animals, which is a requirement for successful implementation of genetic and genomic evaluations (Goddard et al., 2010), as previously discussed. Obtaining phenotypic measurements that

are accurate, biologically meaningful, repeatable, and comparable among laboratories, countries, or companies, is critical for genomic studies and its applications (Hocquette et al., 2012). Therefore, standardizing measurement protocols or defining phenotypes that can be easily standardized is needed because traits recorded in different ways might reflect different biological mechanisms, which may lead to difficulty in the implementation of genetic and genomic evaluations based on datasets from multiple phenotyping centers (or farms, countries, etc.). This is still challenging as there are not enough welfare studies to support differences in such protocols. The lack of available datasets and optimal protocols indicates a need for worldwide funding agencies (private and public) to increase financial support for phenotyping animal welfare indicators for breeding purposes. This has been recently included as a key priority in some agricultural funding agencies as outlined in the latest USDA Blueprint for Animal Genome Research 2018–2027 (Rexroad et al., 2019).

Lastly and critically important, the phenotypes identified need to be heritable and repeatable. Low heritability might only indicate high phenotypic variability in comparison to the total additive genetic variance. Therefore, when necessary, it is crucial to identify alternative variables that can better capture the genetic variability for the trait(s) of interest (i.e., higher heritability; König and May, 2019). The rate of genetic progress for a certain trait also depends on the generation interval (Falconer and Mackay, 1996), and therefore, traits that are measured earlier in life, but reflect the welfare status of the animal in its whole life (or at a later stage), are desirable. In this context, genomic selection is a very powerful tool, as it enables the calculation of genomic breeding values for young animals with no phenotypic measurements (i.e., reduce generation interval). The genetic correlation between welfare and commonly selected traits also need to be investigated and appropriately weighted in selection indexes to avoid detrimental effects in other important traits (Phocas et al., 2016a,b).

The greater availability of high-throughput phenotyping technologies (e.g., automated monitoring systems) in nucleus and commercial farms, better communication and data sharing among data recording organizations (e.g., Dairy Herd Improvement, breed associations, veterinary clinics, and slaughter facilities), and greater integration of complementary disciplines will contribute to overcoming some of the challenges associated with time and cost of welfare data collection (Wemelsfelder and Mullan, 2014). In addition, PLF tools enable the collection of continuous and real-time phenotypes as well as environmental conditions (e.g., thermal stress, humidity, air quality; Laberge and Rousseau, 2017), that are of great use for assessing animal welfare.

WELFARE ASSESSMENT IN LIVESTOCK PRODUCTION

The welfare of animals is determined by the interaction between intrinsic animal characteristics and the environments in which they are raised. The definition of welfare indicators is largely dependent on a clear understanding of the biological and emotional mechanisms behind the phenotypic variability observed in the animal's response to different stimuli. Novel indicators are being proposed as the animal welfare science moves forward. As discussed by Marchant-Forde (2015), accurate welfare assessment should be comprised of components that describe or quantify cellular, physical, physiological/biochemical, and psychological states, and may include scoring scales for additional health and behavior indicators such as body weight, respiration rate, ocular discharge, feces condition, and provoked behavioral response (Marchant-Forde, 2015). Vertical phenotyping is therefore of great importance because several variables can be related to a family of phenotypic traits (Hocquette et al., 2012).

The aggregation of multiple indicators to produce an overall assessment of animal welfare is of great relevance (Botreau et al., 2007a,b). One can expect that genomic selection for improved welfare will continue to be a very interdisciplinary field, integrating animal welfare, cell and molecular biology, neuroscience, immunology, stress physiology, computer science, engineering, quantitative genomics, and bioinformatics. This section will succinctly review biological mechanisms behind animal welfare and how this knowledge can be used for the identification of novel welfare indicators for breeding purposes.

Biological Mechanisms Related to Animal Welfare

Livestock in commercial production systems are constantly exposed to a variety of environmental stressors or management practices (e.g., human presence, noise, strange objects, restricted space, heat, cold, humidity, and feed restriction). Therefore, the animals' welfare, productivity, and environmental fitness will rely on their ability to cope with and react to these challenges (Broom, 1991; Guy et al., 2012; Colditz and Hine, 2016; Berghof et al., 2019; Hu et al., 2019). At any point in time in which an animal is exposed to a variety of potential challenges or stressors, it will counteract using behavioral and physiological processes or sub-systems, linked through a network of neural and hormonal communication. The stressors may vary in magnitude and duration – being short-term (acute) or longer-term (chronic) – and if the animal's processes counteract and adjust successfully, the animal copes with the stressor and habituates (Moberg and Mench, 2000). This ability to cope and habituate is the cornerstone of resilience – the ability to use these biological sub-systems to bounce back to "normal functioning" after disturbance (Scheffer et al., 2018). An animal with high resilience is able to recover quickly from larger disturbances and there is low temporal autocorrelation in the fluctuations of any given sub-system working to counteract disturbances (Scheffer et al., 2018; Berghof et al., 2019). There is also the ability of the sub-systems to work more independently in animals with high resilience and to return the animal to the baseline state, before its interconnected sub-systems are also activated. With low resilience, the opposite is true. A small disturbance may show a slow recovery, high temporal autocorrelation, and high inter-dependence among

sub-systems, with the worst-case scenario resulting in a cascade of sub-system failure (Scheffer et al., 2018).

Within animal agriculture, the main causes of stress include environmental, immunological, metabolic, and social factors. Some may be acute, for example, a single aggressive interaction after mixing which is quickly resolved; some may be chronic, for example, periods of sustained heat during summer months; and some may even be permanent. A stress response is activated when the central nervous system perceives a potential threat to homeostasis. From the central nervous system, electrochemical impulses are transmitted to the effector organs of the body (muscles and glands) to initiate appropriate responses to the stimuli (Cheng, 2010). The defense response consists of a combination of four general biological responses (Moberg and Mench, 2000): the autonomic nervous system response, the neuroendocrine response, the immune response, and the behavioral responses. Under extensive conditions, behavior can often be adapted to mitigate the stress quickly. If confronted by aggression, an individual can retreat and end the encounter if given enough space. If hot, the animal can seek shade or wallow. In farming systems, the behavioral processes may be more constrained, and lack of space or thermal zones can mean that an immediate behavioral response is not possible, as in these two examples. The individual's response to external stressors can be influenced by numerous factors including prior experience, genetics, age, sex, physiological status, emotional state, and cognitive ability (Colditz and Hine, 2016).

The intricate details of stress system activation are available elsewhere (Godoy et al., 2018), but generally, both physical and psychological stressors interact through different pathways to activate the hypothalamic-pituitary-adrenal (HPA), and sympathetic-adrenal medullary (SAM) systems, which activate together multiple sub-systems to maintain homeostasis. The SAM axis results in the release of catecholamines, such as epinephrine (E) and norepinephrine (NE), from the adrenal medulla. The concentrations of E and NE are increased due to a variety of stressors (Dalin et al., 1993) and activation is rapid, within one to two seconds, since E and NE half-lives are short. Simultaneous to the activation of the SAM axis, the hypothalamus also activates the HPA axis releasing corticotropin-releasing factor from the paraventricular nucleus of the hypothalamus. Corticotropin-releasing factor stimulates the anterior pituitary to release adrenocorticotropic hormone which activates the adrenal gland to secrete glucocorticoids (i.e., cortisol, corticosterone) into the blood. Therefore, cortisol concentrations have been used as an indicator of stress (Ott et al., 2014), but not without debate as to the appropriateness and need for refinement (Ralph and Tilbrook, 2016). Glucocorticoid release is much slower than the release of catecholamines, in most species beginning around 2 min after the stressor. However, there is also a circadian pattern to glucocorticoid release due to their priming effect and thus, there are limitations in relying on single time-point samples. The glucocorticoids act collectively with the catecholamines to increase blood glucose (Dallman and Hellhammer, 2011), thus ensuring that there are enough energy reserves needed to mitigate the stressors. Furthermore, the release of cortisol elicits a negative feedback response to the HPA axis to return to basal levels and homeostasis (Manteuffel, 2002; Stephens and Wand, 2012). There is large variation in the response of the various components of the HPA axis (Mormède et al., 2011), indicating a clear potential to genetically select for biological changes in the stress response.

Indicators of Animal Welfare

There is large variability in animal's response to stress factors (Turner, 2011; Koknaroglu and Akunal, 2013; Turner et al., 2018). Therefore, welfare assessment is needed in order to identify the most resilient and healthiest animals for breeding purposes as well as to develop mitigation strategies to minimize or eliminate welfare issues. The evaluation of animal welfare involves a complete assessment of the animal's physiological, behavioral, physical, and emotional state. Some of these indicators can even be quantified prior to clinical signs of poor welfare (e.g., milk somatic cell count and clinical mastitis). This complete assessment relies on some key principles, such as those developed in the Welfare Quality Project (described in Rushen et al., 2011): good feeding, proper housing, good health conditions, and appropriate behavior. These conditions can be assessed based on various parameters, including aggressive behavior when mixing or regrouping animals [especially in pigs (Wurtz et al., 2017; Shen et al., 2019)], approach or avoidance behaviors (Smulders et al., 2006), blood parameters (König and May, 2019), body condition score (Roche et al., 2009), body mutilations [e.g., tail damage (Keeling et al., 1996; Heinonen et al., 2010)], body temperature (Weschenfelder et al., 2012), cannibalism (Lambton et al., 2015), feather pecking (Buitenhuis et al., 2003), feeding behavior [e.g., active chewing time, rumination time, standing and lying time (Ding et al., 2018)], proportion of time active and its posture (Vasseur et al., 2012), immune response (Kovács et al., 2014), response to infection (Nyman et al., 2014), inflammation (Heinonen et al., 2010), heart and respiration rates (von Borell et al., 2007), glucocorticoids (corticosterone and cortisol; Mormède et al., 2011; König and May, 2019), lameness and gait problems (Chapinal et al., 2013), panting frequency (Sullivan et al., 2011), poor maternal care [e.g., savaging in pigs (Hellbrügge et al., 2008b)], ruminal pH (indicator of digestive issues, such as ruminal acidosis; Abdela, 2016), shivering (Liu et al., 2017), social interactions (Rault et al., 2013), abnormal repetitive behaviors (Mason, 2006; Olsson et al., 2011), frustration behaviors (Duncan, 1998; Keeling et al., 2011), variations in daily feed intake (Putz et al., 2019), and water intake (Kume et al., 2010). As previously mentioned, this large number of variables indicates that overall animal welfare needs to be assessed based on a combination of multiple traits.

An Example of Welfare Assessment: Quantifying Thermal Stress in Livestock

Body temperature measurements facilitate determination of the animal's thermoregulatory ability under varying environmental conditions. These phenotypic records may be valuable in selecting breeding stock with improved welfare under environmental conditions that cause heat stress (Carabaño et al., 2017, 2019). Heat tolerance is heritable (**Table 1**; Ansari-Mahyari et al., 2019; Carabaño et al., 2019;

Osei-Amponsah et al., 2019) and causes major welfare and economic losses to the livestock industry (Mayorga et al., 2020); however, the ability to appropriately analyze and understand phenotypic indicators is necessary for the development of new breeding programs to select for heat tolerant animals. Absolute body temperature (T_B) measures may be used to assess an animal's heat stress response whereby greater T_B can indicate increased heat sensitivity and reduced T_B can indicate greater heat tolerance (Johnson, 2018). For the simplest analyses, either daily average T_B or T_B during certain time periods (e.g., morning, afternoon, and night-time) may be calculated to compare between animals under differing environmental heat loads. As an assessment of T_B responsiveness, the T_B change rate as a function of increasing heat load (**Figure 1A**) can be used to determine heat stress sensitivity. In addition, these data can be used to determine the ability of animals to acclimate or adapt if compared across heat stress exposure days, whereby a greater decrease in T_B responsiveness over exposure days can indicate improved acclimation ability and these data may be important markers for selecting animals with better heat stress coping abilities.

Although these analyses are valuable in initial thermal sensitivity assessments, these data alone cannot explain the underlying cause of thermal sensitivity or tolerance. This is important when trying to balance heat tolerance with maintained productivity because heat tolerance may be an outcome of decreased metabolic rate resulting from decreased performance (Brown-Brandl et al., 2014), which is not a desirable outcome under commercial production conditions. Therefore, understanding how animals dissipate excess body heat and how heat dissipation interacts with heat tolerance and productivity is an important factor to consider in breeding programs. When obtaining phenotypic thermoregulatory data, it is important that measures of heat dissipation (e.g., respiration rate – RR, skin temperature – T_S, and sweating rate – SR) are taken in combination with T_B to ascertain information about an animal's capacity to maintain euthermia as heat dissipation influences T_B, and T_B influences heat dissipation (Blatteis, 1998). Balancing heat production with heat loss is essential under environmental conditions that cause heat stress in animals. Animals with improved performance (e.g., milk production, growth rate, and egg production) generate greater metabolic heat when compared to their lower producing counterparts (Brown-Brandl et al., 2014; Cabezón et al., 2017). In turn, the heat sensitivity of high producing animals may be increased if heat dissipation capacity is not sufficient.

Several analyses may be used to assess relationships between heat dissipation mechanisms and T_B. To determine heat dissipation efficiency through the skin, the relationship between T_S and T_B can be calculated. As heat dissipation through the skin is reliant on core T_B, an increased ratio may indicate greater heat dissipation. However, this ratio may be influenced by the external environment (e.g., cooler temperatures cause vasoconstriction and warmer temperatures cause vasodilation; Blatteis, 1998) and thus ambient temperature can be used in the analysis. In this case, the thermal circulation index may be calculated using T_S, ambient temperature, and T_B as described by Curtis (1983): thermal circulation index = (T_S – ambient temperature)/(T_B – T_S). The thermal circulation index can be used to determine the capacity of an animal to dissipate heat from the core to the skin and subsequently to the surroundings under steady state thermal conditions (Kpodo et al., 2019). In addition to T_S, the assessment of T_B as a function of RR may be used to assess RR efficiency whereby

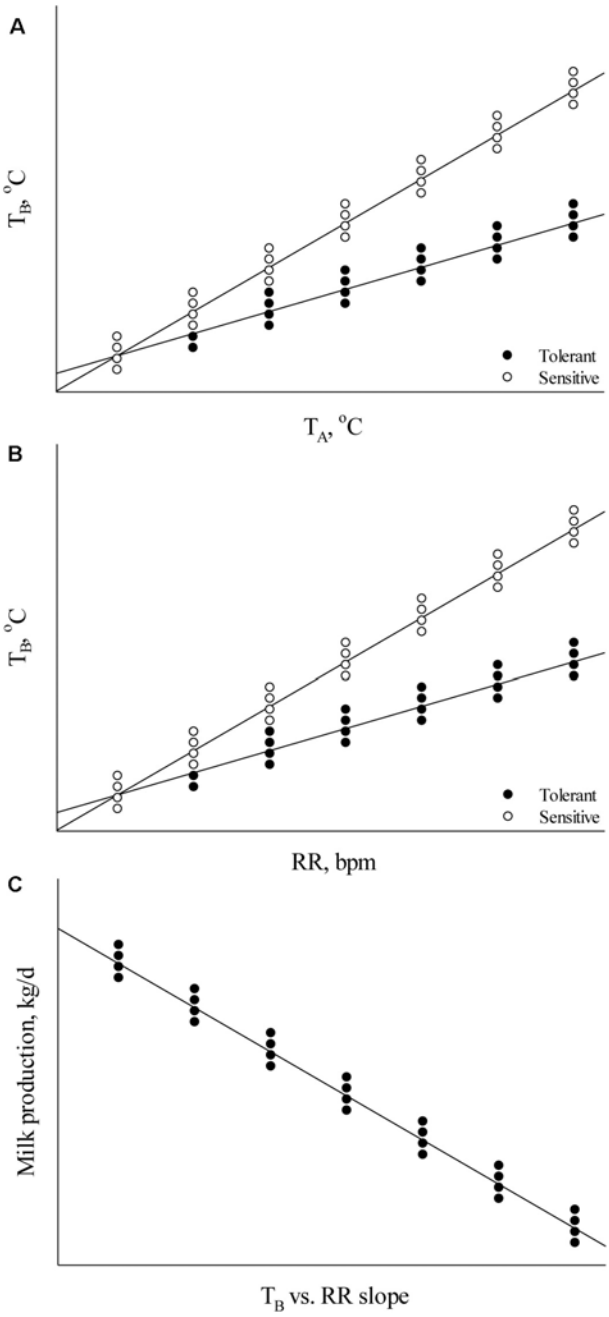

FIGURE 1 | Relationships between **(A)** body temperature (T_B) and ambient temperature (T_A), **(B)** T_B and respiration rate (RR), and **(C)** milk production and the T_B vs. RR slope.

a greater T_B slope with increasing RR indicates reduced RR efficiency and a decreased slope indicates increased efficiency (**Figure 1B**). This is an important factor to consider outside of absolute RR values because an increase in RR may not necessarily indicate greater heat sensitivity if the end result is a euthermic T_B. Alternatively, comparing RR as a function of T_B may explain heat sensitivity in which a lower RR rise with increasing T_B can explain heat sensitivity if the RR increase is not sufficient to dissipate excess body heat. These methods may also be applied to the assessment of SR. Finally, results from these thermoregulation analyses may also be compared with performance parameters to determine their influence on growth rate, reproductive success, milk output, and egg production (**Figure 1C**). These data can enable balancing improved welfare under heat stress conditions with performance measures and evaluate which thermoregulatory measure is most important in a particular system.

There are multiple strategies for increasing heat tolerance, such as within-breed genetic or genomic selection (Nguyen et al., 2017; Carabaño et al., 2019), crossbreeding or the use of more climatic adapted genetic resources such as Zebu cattle (*Bos taurus indicus*), and slow growing or less-feathered birds (Singh et al., 2001; N'dri et al., 2007; Fathi et al., 2013). Furthermore, gene editing might also be an important tool for introgressing certain gene alleles that confer greater heat tolerance (Hansen, 2020), such as the "slick hair" gene in cattle (Littlejohn et al., 2014), and "naked neck" and "frizzle" genes in chicken (Fathi et al., 2013).

Phenotyping Technologies Used to Assess Thermal Stress

Body temperature measures are commonly used to assess the thermoregulatory capacity of animals. These measures often include RR, SR, T_S, and T_B, and these phenotypic traits are most commonly used as a determination of heat stress. Traditionally, these measures were obtained through labor intensive and invasive practices. However, in recent years, several non-invasive and/or automated methods to collect these data have been developed.

Skin temperature

During heat stress, blood flow to the skin increases to facilitate heat dissipation, which may be measured by an increase in T_S (Yahav et al., 2005; Katiyatiya et al., 2017). However, environmental factors such as wind speed, humidity, and direct sunlight exposure (Church et al., 2014), or physical factors such as hair thickness, hair length, and hair and skin color (Gebremedhin et al., 2008) can impact the efficiency of heat loss through the skin or directly alter the T_S independent of changes in T_B (i.e., direct sunlight exposure, exposure to heating elements, etc.). Interpreting T_S values requires additional inputs and considerations. For animals housed outdoors without shade (i.e., cattle on pasture or in feedlots) or under heating elements (i.e., pigs or chickens under heat lamps), it is difficult to separate the effects of the environment on changing T_S compared to the influence of T_B on increasing/decreasing T_S due to heat dissipation through the skin. It is important to consider that T_S measures greater than T_B should not be interpreted as heat dissipation as it is impossible to dissipate a greater amount of heat than is produced within the body and it is likely that these values are indicative of environmental influences on the T_S rather than changing T_B. In cases where radiant heat is not a factor (i.e., environmental chambers, in the shade, etc.) T_S measures (on shaved or hairless skin) may be helpful in the assessment of heat dissipation for the selection of more heat tolerant animals and a common, non-invasive method to assess T_S is through infrared thermography (Ferreira et al., 2011; Nääs et al., 2014; Lees et al., 2018). Taken together, researchers must consider these factors when making determinations about the significance of changing T_S in relation to heat dissipation vs. radiant heat load.

Infrared thermography measures the infrared radiation emitted from an animal and this radiation depends on the temperature, emissivity, and conductivity of the animal (Knízková et al., 2007). There are two types of infrared systems to measure temperature on animals: infrared thermometers and thermal cameras. Infrared cameras are more software intensive than infrared thermometers and can be used for monitoring large areas (Sellier et al., 2014), which allow for a greater representation of the T_S of the entire animal or at specific sites as desired by the researcher. An alternative to infrared technology that may be more invasive are contact sensors affixed to the skin (Teunissen et al., 2011; Mostaço et al., 2015). Contact sensors are more accurate than infrared technology and provide continuous automated measurements, but potential issues precluding their use may include battery life and long-term adhesion to the skin (Mostaço et al., 2015), and destruction or loss of the devices in group-housed animals. Therefore, researchers should assess both types of technology and determine which one best fits their requirements in a particular environment or research setting.

Respiration rate

In general, animals cope with heat stress by increasing RR to reduce the extra heat load via evaporative heat loss. However, it is important to mention that during extreme heat strain when heat loss cannot be balanced with heat gain, animals will switch from increased RR to deep slow respirations (López Armengol et al., 2017). One way to measure RR is visually by counting flank movements at the flank region (Mostaço et al., 2015). While this traditional method is regularly used, it is labor-intensive and time consuming. As an alternative to this method, researchers have developed technologies that assess RR through changes in air temperature near the nostrils of animals using infrared thermography (Lowe et al., 2019), or direct measures of air temperature near the nostrils using a mounted device (Milan et al., 2016). The use of sensors to detect nasal exhalation pressure has been proposed to evaluate RR in cattle (Strutzke et al., 2019). Finally, researchers have also used an externally-mounted bioharness designed for humans, that measures chest expansion (Briefer et al., 2015). Unfortunately, many of the automated methods to assess RR are in development and there are currently no known commercially-available and validated options for

researchers to automatically (and non-invasively) assess RR in livestock animals.

Sweating rate

Cattle increase SR to dissipate excess body heat through evaporative heat loss from the skin surface. Heat loss via sweating may be influenced by wind velocity, air temperature, relative humidity, and thermal and solar radiation (Collier and Gebremedhin, 2015). The SR can be determined using a digital moisture sensor on the dorsal areas of animals to determine *trans*-epidermal water loss (Nuutinen et al., 2003; Gebremedhin et al., 2008). The digital moisture sensor is a closed system, free of ambient airflow, and allows for monitoring of water loss (Scharf et al., 2008). Another method to measure SR is applying a cobalt chloride disk to the skin and recording the length of time the cobalt chloride disk changes color in order to calculate SR (Moser et al., 2012; Nursita and Cholis, 2019). However, a potential drawback to this method in animals is the ability to maintain the disk on the skin for the length of time required for the color change to occur.

Body temperature

Heat stress causes an increase in T_B implying that the animal has lost the ability to maintain homeostasis. In pigs, infrared (Mostaço et al., 2015), and digital clinical thermometers (Gebremedhin et al., 2008; Mostaço et al., 2015) are commonly used to measure T_B rectally. However, when using a clinical thermometer, restraint is often required, which can stress the animal and potentially increase T_B. Other reliable and accurate T_B measurement devices include surgically implanted telemetry devices (Lacey et al., 2000) and intramuscularly implanted microchips (Iyasere et al., 2017). Both devices are good for automatically collecting data at pre-set intervals, but have the risk of infection after surgery and a greater recovery time prior to data collection. In cattle, less invasive studies have used automatic measurements of reticule-rumen boluses (Timsit et al., 2011; Liang et al., 2013), which give continuous rumen temperature measurements in real time (Lohölter et al., 2013; Lees et al., 2018). In pigs, gastrointestinal temperature can be measured using orally administered temperature sensors (or boluses, as commonly defined in similar sensors used in cattle studies) monitored with a wireless core body temperature data recorder (Johnson et al., 2016). Although the boluses allow measurement without disturbing the animal, they have short communication distances between the bolus and reader thus requiring manual data collection, the boluses are costly, and T_B fluctuations may exist depending on the temperature of feed and water consumed (Lee et al., 2016b). Alternatively, vaginal implantation of wireless sensors can accurately determine T_B using a radio-telemetric system (Kyle et al., 1998; Johnson and Shade, 2017) or a temperature logger (Gebremedhin et al., 2008). Specifically, in pigs (Johnson et al., 2016), beef cattle (Burdick et al., 2012), and dairy cattle (Garner et al., 2016), vaginal temperature can be measured with a thermochron temperature recorder attached to a plastic device controlled internal drug releasing device. However, this is only effective in females. Finally, temperature sensing with an ear canal radiotelemetry system can be used on cattle due to its long-distance wireless communication and simple attachment similar to ear tagging (Lee et al., 2016b), which provides temperature stability but has the risk of the tagged device to fall off.

HIGH-THROUGHPUT PHENOTYPING TECHNOLOGIES

The rapid development of integrated biological (e.g., *-omics* technologies) and engineering systems and the Internet of Things (IoT) is enabling the development of affordable monitoring devices and high-throughput technologies (Neethirajan et al., 2017). These tools can be used for individually monitoring large numbers of animals in commercial settings and are advantageous to quantify biological indicators through rapid, repeatable, and automated measurements. This is crucial because the ideal welfare assessment indicators should be as objective as possible, robust (can be applied under a wide range of on- and off-farm situations), relevant and valid (reveal aspects of the animal's affective or physiological state that is important to their welfare), reliable (can be repeated with confidence in the results), cost-effective, and well accepted by all industry's stakeholders (Fleming et al., 2016).

The technological devices used include sensors such as cameras, microphones to capture vocalizations, thermometers, automated feeding and milking systems, automatic scales to measure body weight and lean-fat ratios, milk spectral data, electrodes to detect skin conductivity and heart rate, and accelerometers (Vranken and Berckmans, 2017; Benjamin and Yik, 2019; Halachmi et al., 2019). In this section, we describe phenotyping technologies that can be (or have been) used to assess animal welfare and potentially incorporated in genetic or genomic evaluation schemes in commercial livestock systems. It is important to note that some of these technologies are still under development and validation stages. In some cases, there could exist disagreements on their ability to assess welfare (de Rosa et al., 2019). We have highlighted examples from multiple species, but it is worth noting that the technologies and indicator traits described in this study can be easily translated or extrapolated from one species to another.

Biomarkers

As previously indicated, various endocrine and behavioral mechanisms are involved in coping with stressors (e.g., aggression, hunger, and disease challenge). Glucocorticoids, secreted by the adrenal glands, are the most evident indicators of a stress response (Cook, 2012; Palme, 2012). They are usually measured in plasma samples; however, blood collection itself can cause additional stress as a result of handling and restraint (Cook, 2012). Palme (2012) discussed various non-invasive methods for the determination of glucocorticoids or their metabolites in saliva, urine, excreta, milk, hair/feathers, and eggs. Fecal and hair (or feather) samples are promising alternatives as circulating hormone levels are integrated over a certain period of time and are less affected by short fluctuations (Palme, 2012;

Pawluski et al., 2017). The frequency of sample collection will depend on whether the impact of acute or chronic stress factors is being evaluated.

In addition to cortisol, various blood-based biomarkers have been associated with aggression in pigs, including plasma triiodothyronine (T3), 5-hydroxytryptamine, and tryptophan (Shen et al., 2019). Furthermore, disease challenge is another great welfare impairment. Huzzey et al. (2011) evaluated the potential of using pre-partum analytes associated with stress (cortisol) or inflammation (haptoglobin), and NEFA (non-esterified fatty acids) as indicators of increased risk for health complications after calving. The authors reported that NEFA was a more suitable post-partum health indicator compared to fecal or plasma cortisol metabolites, and plasma haptoglobin.

In some species (e.g., dairy cattle, dairy sheep, and dairy goats), additional biomarkers can be identified in body fluids measured routinely, such as milk. For instance, in milk, mid-infrared spectrometry (MIR) has been used to monitor potential metabolic issues and diseases such as mastitis, ketosis, fat–protein ratio, NEFA or phospholipids, glucose, and insulin growth factor 1 (Egger-Danner et al., 2014; Tetens et al., 2015; König and May, 2019), usually associated with negative welfare implications in production systems. In this regard, fat–protein from routine milk recording data has been indicated as a selection criterion to improve metabolic stability (Koeck et al., 2014). As such, various research projects have investigated the use of milk MIR data for prediction of novel indicator traits for selection purposes [e.g., RobustMilk, Opti-MIR, PhenoFinlait, and GplusE (Egger-Danner et al., 2014)].

Mastitis is a disease with major welfare implications in dairy species (Martin et al., 2018). Test-day somatic cell count (transformed to somatic cell score) is a routinely collected phenotype that has already been included in commercial breeding programs to improve udder health (Miglior et al., 2017; Martin et al., 2018). Minerals (e.g., Ca, K, Mg, Zn, Se, and P) or mineral content measured via milk MIR has also been suggested as potential biomarkers to improve mastitis resistance (Egger-Danner et al., 2014), and milk protein fractions as suitable biomarkers for heat tolerance (Carabaño et al., 2017).

Animals raised in extensive production systems (e.g., beef cattle, sheep) can suffer substantially from endoparasite infections caused by gastrointestinal nematodes (Papadopoulos et al., 2012). Various biomarkers have been proposed to genetically select for host resistance (i.e., ability to control pathogen burden) or tolerance (i.e., ability to limit the impact of a given pathogen burden on performance), but serum or milk antibodies (different isotypes of immunoglobulins), and fecal egg count are the most commonly used indicators (Bishop and Morris, 2007; König and May, 2019).

In ruminant species, measuring rumen pH can indicate metabolic and nutritional dysfunctions associated with negative welfare implications such as acidosis (Leek, 1983; Hamilton et al., 2019). There are various sensors available to measure H-ion concentration in the rumen by electrical means. These sensors (or boluses) are usually coupled with radio-frequency transmitters for continuous real-time data acquisition and there are already various commercially available devices (Mottram et al., 2008; Kim H. et al., 2018; Hamilton et al., 2019). Technology prices are decreasing over time and its quality is improving (e.g., robustness, battery life). Such devices can generate a large amount of data to be used for identifying disease resilient animals for breeding purposes.

There is also a potential to use biosensors for breath analysis aiming to identify disease indicators (bovine respiratory disease, tuberculosis, brucellosis, and ketoacidosis), especially volatile organic compounds (Fend et al., 2005; Burciaga-Robles et al., 2009; Neethirajan et al., 2017). Biosensors to analyze metabolites in sweat [e.g., lactate levels; indicator of physical stress (Jia et al., 2013)] have also been developed and converted to portable formats [e.g., belts, adhesive RFID sensor patch (Neethirajan et al., 2017)]. A large number of alternative compounds have been investigated over time, including adrenaline, noradrenaline, corticotropin-releasing factor, prolactin, glucose, lactic acid, blood leukocyte levels, and cellular immune response (Neethirajan et al., 2017). There are various bioanalytical devices and wearable technologies that can be implanted on the animals to analyze sweat composition [e.g., sodium and lactate content (Garcia et al., 2016; Glennon et al., 2016; Heikenfeld, 2016)], and assess body temperature (Sellier et al., 2014) such as wireless temperature sensor nodes that can be appressed to the base of calf's tail (Nogami et al., 2014), detection of analytes and pathogens (Mungroo and Neethirajan, 2014; Vidic et al., 2017), and many others (Neethirajan, 2017).

The development of biosensors is rapidly advancing in human research (Metkar and Girigoswami, 2019), and one can expect that these technologies will soon be adapted to the livestock industry. High-throughput phenotyping of physiological and metabolic changes combined with large-scale genomic (and other *-omic*) datasets will be paramount on implementing genomic selection for improved animal welfare in commercial farms. It is important to highlight that it is very unlikely that a single or few biomarkers could be used for a holistic assessment of animal welfare. However, welfare biomarkers can be complementary to other data sources.

Machine Vision (Cameras)

Machine vision has been used for several purposes in animal sciences, including determination of body weight (Tscharke and Banhazi, 2013; Kongsro, 2014), body condition score (Azzaro et al., 2011; Halachmi et al., 2013), detection of aggressive behavior (Lee et al., 2016a; Chen et al., 2017; Nasirahmadi et al., 2017), walking patterns and lameness (Stavrakakis et al., 2015), and posture and behavior during lactation (Lao et al., 2016). Often, video recordings are used to manually assess animal behavior (Oczak et al., 2013), but the manual analysis of these videos is time-consuming, and may introduce human error (Catarinucci et al., 2014).

A wide variety of cameras are available (e.g., RGB, infrared thermography cameras, 3D cameras), and more recently, there is an increasing number of research projects investigating the automation of machine vision and data analytics (Ventura et al., 2020). Therefore, machine vision is expected to play an important role in the design of large-scale data collection for breeding schemes to improve animal welfare. For instance,

3D cameras [e.g., Microsoft Kinect (Microsoft, Redmond, and Washington) and Intel RealSense (Intel, Portland, and Oregon)] are usually equipped with a high-definition camera, an infrared illuminator, and time-of-flight (ToF) depth sensor that produces color (Benjamin and Yik, 2019). These cameras are reasonably cost-effective, can handle large amounts of data, have low power requirements, do not require any contact with the animal (remote measuring), and are adaptable to variable light and background conditions (Benjamin and Yik, 2019).

Infrared thermography or thermal imaging is increasingly being used as a non-invasive method to assess animals' physiological and emotional state, including skin temperature, inflammation in certain areas of the body (e.g., udder – mastitis), locomotion disorders, and respiratory diseases (Stewart et al., 2005; Alsaaod et al., 2014; Harris-Bridge et al., 2018; Jorquera-Chavez et al., 2019). Boileau et al. (2019) used infrared thermography taken from pigs in a controlled test environment and indicated that the obtained peripheral temperature provided useful information about the physiological and welfare outcomes of aggressive behavior in pigs. Moreover, image motion feature extraction was used for recognition of aggressive behaviors among group-housed pigs, with an accuracy of 95.82 and 97.04% for medium and high aggression, respectively (Chen et al., 2017). Infrared thermo-imaging has also been investigated as a potential tool to quantify the number of ticks in the body surface of Brangus cattle, which causes major health and welfare issues, especially in tropical countries (Barbedo et al., 2017).

In the swine industry, farrowing is a challenging stage for both the sow (transition from gestation to farrowing and lactation), and the piglets (susceptibility to crushing, chilling, and malnutrition; Marchant et al., 2001; Johnson and Marchant-Forde, 2009). Aiming to identify solutions to these issues, Leonard et al. (2019) monitored behavioral activities of sows and piglets in a commercial setting utilizing an autonomous machine vision system. A digital and ToF depth imaging system was implemented and a process with minimal user input to analyze the collected images was developed to calculate the hourly and daily posture and behavior activities of sows housed in individual farrowing crates. Depth sensors were placed on top of each stall in three farrowing rooms and controlled by mini-computers. Algorithms were able to accurately classify sow behavior (sitting: 99.4%, standing: 99.2%, kneeling: 99.7%, and lying: 99.9%). This autonomous system enables acquisition of a large amount of replicated data, and this research is a great example of integrated technology into on-farm environments that can potentially generate phenotypic records for genomic selection purposes. Lao et al. (2016) also used a machine vision-based system that automatically recognizes sow behavioral activities (e.g., lying, sitting, standing, kneeling, feeding, drinking, and shifting) in farrowing crates. The system consists of a low-cost 3D camera that simultaneously acquires digital and depth images and a software program that detects and identifies sow behaviors. This algorithm achieved an accuracy of 99.9% for lying, 96.4% for sitting, 99.2% for standing, 78.1% for kneeling, 97.4% for feeding, 92.7% for drinking, and 63.9% for transitioning between behaviors. As sows are individually housed in farrowing crates, these systems will likely be very useful for selective breeding for maternal ability [e.g., maternal behavior, piglet survival (Hellbrügge et al., 2008a)], and other alternative breeding goals (Baxter et al., 2011; Muns et al., 2016).

Another use of machine vision is analyzing the overall posture of the animal to detect lameness (and genetically select for improved hoof health). Blackie et al. (2013) evaluated kinematic gait analysis to assess stride characteristics, joint flexion and spine posture in dairy cows with different lameness status. The dairy cows were video-recorded walking along an alley (1.6 m wide), with colorful markers placed in specific parts of their bodies. In this case, the need for markers is a limitation for measuring large numbers of animals. Under farm conditions, body movement pattern recognition was applied to identify lameness in dairy cattle with an accuracy of 76% (Viazzi et al., 2013). Abdul Jabbar et al. (2017) used three-dimensional (3D) video data to analyze gait asymmetry by simultaneously tracking the movements of the spine and hind limbs of dairy cows and precisely identified 95.7% of lame cows. Body condition score is another variable that can be automatically recorded, including through the use of a Kinect camera (Microsoft Corp., Redmond, WA, United States) triggered by passive infrared motion detectors (Spoliansky et al., 2016), or by modeling cow body shape from digital images (Azzaro et al., 2011).

Tail biting is a major welfare issue in the swine industry and is a heritable trait [i.e., can be reduced through selective breeding (Breuer et al., 2005)]. Brünger et al. (2019) used neural networks to identify tail lesions in pictures from 13,124 pig carcasses and was able to correctly identify 74% of tail lesions and 95% of tail losses. Also in pigs, the behavioral and clinical alterations of growing pigs infected with two common strains of *Salmonella* spp. were investigated using a video-recording system (Ahmed et al., 2014). Recordings were able to detect clear changes in pigs' movement, feeding and drinking behavior in response to *Salmonella* spp. infection. Additionally, Porto et al. (2015) used a multi-camera video-recording system to detect cow feeding behavior with an accuracy of 88% for feeding and 86% for standing behavior. Furthermore, Vetters et al. (2013) used an infrared sensor to determine the flight speed, to cross a fixed distance of 1.83 m, when exiting the squeeze chute as an indicator of cattle temperament.

Heart rate and heart rate variability are indicators of cardiovascular system functioning and cardiac autonomic modulation that are used to estimate physiological and psychological stress in animals (von Borell et al., 2007). In recent years, optical methods for measuring heart rate have received increased interest and technical development (Halachmi et al., 2019). Beiderman et al. (2014) proposed a photonic remote sensing system assembled on a robotic platform to measure important biological indicators such as heart beating, breathing and chewing activity. In this research, the algorithm development used image processing and image pattern recognition techniques. This promising technology can be used in livestock breeding farms to generate useful and practical information about animal welfare and stress resilience to incorporate into breeding programs.

Machine vision can generate a large amount of data in individual animals with high precision and through

remote sensing (non-invasive method), but there is still a need to optimize accurate data collection and individual identification/recognition (connecting images to animal ID is still a challenging process). Kashiha et al. (2013) investigated the feasibility of an automated machine vision method to identify marked pigs in a pen and achieved an accuracy of 88.7%. However, more efficient alternatives are still needed. Major and on-going advancements are happening in this area. For instance, facial recognition to identify individual animals is currently being investigated (Hansen et al., 2018).

Wurtz et al. (2019) performed a comprehensive systematic review of studies that used machine vision technology to assess behavior of indoor-housed farm animals. The authors highlighted the need to build upon existing knowledge, instead of developing devices from scratch, and validate these devices under commercial settings (in large scale). Some equipment cannot be used for measuring large numbers of animals, which is a constraint for generation of data for breeding purposes.

Activity Sensors (Accelerometers, Activity Monitors)

Activity sensor or accelerometer devices are becoming popular in commercial livestock operations and, therefore, have great potential to generate large-scale datasets for breeding purposes. In general, accelerometers contain several sensors that record location and transmit velocity and acceleration data in one or all three dimensions (Benjamin and Yik, 2019). This includes static forces (e.g., animal is lying down), as well as movements (e.g., walking; Benjamin and Yik, 2019). These devices can be attached to different parts of the animal body (e.g., ear, neck, back, feet, and legs) and classify a variety of activities such as feeding, gait (and lameness), lying, panting, ruminating, standing, walking, nest-building (pigs), and grazing behavior (Cornou and Lundbye-Christensen, 2008; Escalante et al., 2013; Oczak et al., 2015; Thompson et al., 2016; Traulsen et al., 2018; Alsaaod et al., 2019; Benaissa et al., 2019; Halachmi et al., 2019). These metrics can be used as indicators of welfare (including health status) and for detection of positive or negative welfare status (Alsaaod et al., 2019; Benaissa et al., 2019). For instance, day-to-day variation in activity has been successfully used for lameness detection in dairy cattle (De Mol et al., 2013; Alsaaod et al., 2019), which is a heritable trait (Chapinal et al., 2013). Accelerometers and activity loggers have been also used in poultry to record the development of space use in layers housed in multi-tiers aviaries (Kozak et al., 2016a,b) and gait in grower and finisher turkeys (Dalton et al., 2016). Results reported in de Haas et al. (2017) suggest that activity patterns recorded by accelerometers can help to detect the onset of feather pecking. Therefore, recording devices such as accelerometers and activity monitors are sensitive to detect the development of behavioral and health problems in livestock.

In this section, we describe some studies using activity sensors that generated data feasible for inclusion in selective breeding schemes. The pedometer is a commonly used activity-monitoring device in dairy cattle, and there are multiple types available in the market. For instance, Shepley et al. (2017) and Mattachini et al. (2013) reported the successful application of pedometers for calculating activity and detecting lying behavior in dairy cows, respectively. Oczak et al. (2015) used accelerometer data (ear tag with a 3-axis accelerometer sensor) to determine nest-building behaviors of non-crated farrowing sows with more than 85% accuracy. This could aid in the generation of data to improve genetic selection for maternal behavior and piglet survival. Borchers et al. (2016) evaluated six different triaxial accelerometer technologies that provided accurate assessment of cow behavior, including feeding time, lying time, and rumination pattern. Along the same lines, Benaissa et al. (2019) used leg- and neck-mounted accelerometers combined with machine learning algorithms to automatically record dairy cow behavior (i.e., lying, standing, and feeding behavior) with high precision (80–99%) and sensitivity (87–99%).

Activity sensors can also be useful in outdoor production systems. For instance, González et al. (2015) performed unsupervised behavioral classification of electronic data collected at high frequency from collar-mounted motion and GPS sensors in grazing cattle. The behaviors assessed included foraging, ruminating, walking, resting, and "other active behaviors" (which included scratching against objects, head shaking, and grooming). Similar results have also been presented in other studies (e.g., Williams et al., 2016; Manning et al., 2017). As wireless data transfer in real time from collar transmitters to data analysis stations is possible and feasible, the large datasets generated are another great source of potential welfare indicators to include in pasture-based breeding schemes. In free-stall-housed dairy cattle, Bikker et al. (2014) indicated the potential use of a 3-D accelerometer that can be attached to ear identification tags and used to classify behaviors (e.g., resting, ruminating) based on ear movements.

In summary, accelerometers are small and low-cost devices that can be embedded into wearable sensors used in wireless sensor networks to generate and transfer real-time data to databases (data center stations). They are usually used for tracking animals' positions and recording locomotion and activity/inactivity patterns in general (Benjamin and Yik, 2019), but a large number of traits can be derived from the data collected (Williams et al., 2016). In addition to using all the data generated for management (e.g., reproduction, disease detection) purposes, there is still a greater need to investigate the usefulness of such datasets for breeding more resilient animals with a better welfare. We expect that the recent availability of large-scale datasets generated by such devices in herds/flocks of animals with both pedigree and genomic information has great potential to redirect livestock breeding goals.

Acoustic Sensing (e.g., Vocalization)

Livestock vocalizations can be a good source of information about animal welfare status and social interactions (Exadaktylos et al., 2014; Neethirajan, 2017). Acoustic sensing is a non-invasive method, inexpensive, and less dependent on lighting or the specific position of the animal (Mcloughlin et al., 2019). Some studies have investigated the relationship between vocalization and health (Exadaktylos et al., 2008; Silva et al., 2009; Ferrari et al., 2010), poultry welfare (Zimmerman and Koene, 1998), stress events [e.g., piglet crushing (Manteuffel et al., 2017), pain

during husbandry procedures (Marchant-Forde et al., 2009)], and feeding behavior based on pecking sound (Aydin et al., 2014). Various devices have been developed over time. For instance, a microphone can be installed in rumination neck collars to record rumination time based on sounds of regurgitation (Ambriz-Vilchis et al., 2015).

Despite the wealth of information that can be captured by sounds, acoustic devices are a more challenging source of data collection for livestock breeding purposes. Most commercial breeding programs are of medium to large size and intensive systems (i.e., many animals are housed together at high stocking density). Various sounds are therefore produced at the same time, and sound analysis or sound recognition becomes difficult due to background noise (Du et al., 2018). Identifying the focal animal emitting the vocalization is also challenging, especially under on-farm conditions (e.g., noise background due to feeding and ventilation equipment, other animals). There are automatic measurement techniques and software being developed that could focus on specific vocalizations at specific time points (e.g., transport, handling; Moura et al., 2008; Halachmi et al., 2019). There might also be an opportunity to combine technologies such as machine vision, machine learning, and acoustic sensors.

Automatic Milking Systems (Milking Robots)

With the intensification of dairy cattle production, automated milking systems (AMS; milking robots) are becoming more popular around the world. Labor cost savings in AMS have been estimated to range from 18 to 46% (Rotz et al., 2003; Mathijs, 2004; Bijl et al., 2007). In addition, the benefits of AMS include higher milk production per cow as a result of greater milking frequency (Tremblay et al., 2016; Tse et al., 2017), improved cow welfare (Jacobs and Siegford, 2012), earlier and easier disease detection (Tse et al., 2017), more interesting/fewer routine activities for the dairy producers (Woodford et al., 2015), and more flexible lifestyle to the farmers compared to conventional milking systems. The proportion of dairy farms using AMS is expected to increase substantially over the next years. Moreover, AMS generate a large amount of data that can be used to derive phenotypes that can be helpful for breeding purposes [e.g., disease disorders (King and DeVries, 2018)].

Several variables influence the welfare, performance, and efficiency of milk production in AMS. These traits include: (1) the willingness of the cow to voluntarily enter the milking robots. Therefore, milking interval and frequency are largely influenced by individual cow motivation. In this regard, cow training has been identified as a key challenge by producers (Tse et al., 2018). Thus, genetically selecting cows that are easier to train (or other motivation traits to enter the milking robot, such as low neophobic cows) is highly desirable; (2) cow ability to stay calm during cleaning/disinfection and attachment of milking equipment, especially in the presence of sounds and mechanical movements. Cows with a proactive temperament kick-off the milking equipment and prolong preparation and teat attachment times (Wethal and Heringstad, 2019); (3) inter-milking interval; (4) udder and individual quarter milk production (as more heterogeneous production among quarters will result in longer retention in the milking box); (5) udder conformation and teat size/placement, which is associated with teat cup attachment success rate; (6) milking time and length of the milking procedure (milking box time), which is directly associated with milking speed; (7) milk flow rate (milking speed). It is worth noting that milking speed is unfavorably correlated with udder health, and consequently, both traits need to be considered simultaneously (Sewalen et al., 2011). In addition, (8) cow dominance behavior, as more submissive cows are forced to wait for a longer period of time and forced to adjust their feeding behavior and milking times; and, (9) ability to quickly leave the milking robots after the last teat cup is removed. Despite the importance of all these traits, relatively few studies have investigated how they can be quantified based on data generated in AMS, their genomic predictive ability, and the degree to which these traits are associated with longevity, health (e.g., mastitis), and other economically and welfare important traits. This is a great source of data that can be used to genetically improve various resilience and performance traits in dairy cattle. More recently, some studies have investigated the genetic background of AMS-derived traits, indicating that it generates various variables that are heritable (**Table 2**).

Individual Feed Intake Recording Systems

Individual feed intake recording systems are usually used for collecting data to enable precision management as well as genetic and genomic selection for improved feed efficiency (Hoque and Suzuki, 2009; Egger-Danner et al., 2014; Hadinia et al., 2019). However, there are additional variables that can be used as proxies of animal resilience and feeding behavior (Maselyne et al., 2015; Putz et al., 2019). For instance, voluntary variations in feed intake can indicate disease resilience, feeding competition, or negative agonistic interactions (Ahmed et al., 2014; Munsterhjelm et al., 2015; Matthews et al., 2016; Putz et al., 2019). In some cases these changes might not differ with regards to the total consumption but rather the frequency and duration of feeding activities (Tolkamp et al., 2011).

There is a large number of automated feeding systems commercially available that can be used to measure feed intake, feeding behavior, and other related variables (Hoque and Suzuki, 2009; Chen et al., 2010; Maselyne et al., 2015; Johnston et al., 2016; Matthews et al., 2016). Most systems use specially-designed single-space feeders (Maselyne et al., 2015). In general, there is a RFID (radio-frequency identification) antenna to identify the focal animals feeding and traits of their feeding bout. In addition to consumption rate (i.e., feed intake per unit of time), various other variables can be extracted such as the frequency of meals, meal duration, feeding duration, feeding pattern (e.g., time of the day; Maselyne et al., 2015), agonistic behaviors, and dominance relationships among dairy cows (Foris et al., 2019). Automatically recorded datasets have been used to understand the genomic background (including GWAS) of feeding behavior traits such as daily number of feeder visits, feeding time and duration per visit, and total daily duration at feeder (Do et al., 2013). Predictors or early indicators of tail biting outbreaks have been identified using

TABLE 2 | Heritability estimates for traits derived from Automated Milking Systems (AMS; milking robots) in Holstein (HO), Norwegian Red (NR), and Swedish Red (SR) cattle.

Trait	Measurement protocol or trait definition	Breed	Heritability (SE)	References
Attachment failures (%)	Proportion of milkings with at least one attachment failure	HO, SR	0.21 (0.07)–0.31 (0.07)	Carlström et al., 2016
Average flow rate (kg/min)	Average of the milk flows measured for each quarter within 1 milking	HO, SR	0.37 (0.06)–0.48 (0.08)	Carlström et al., 2013
Average milk flow	Average milk flow in kg/min	HO	0.25 (0.07)	Viviana Santos et al., 2018
Box time	Time from when a cow enters the AMS to when it exits the milking unit	NR	0.27 (0.03)	Wethal and Heringstad, 2019
Box time (min)	Difference between begin and end time	HO, SR	0.21 (0.05)–0.44 (0.07)	Carlström et al., 2013
Distance front-rear (mm)	Average distance between the front and rear teat ends	HO	0.56 (0.02)–0.61 (0.02)	Poppe et al., 2019
Electrical conductivity from all four quarters	Electrical conductivity was used as an indicator reflecting the udder health status	HO	0.53 (0.09)	Viviana Santos et al., 2018
Electrical conductivity	Electrical conductivity (EC) measured as maximum (ECmax) and mean (ECmean)	HO	0.23–0.35 (0.03)	Wethal et al., 2020
Elevated mastitis risk	Please see the formula in the reference	HO	0.09 (0.04)	Wethal et al., 2020
Flow rate	Average kg of milk/min of milking time	NR	0.48 (0.04)	Wethal and Heringstad, 2019
Front teat distance (mm)	Distance between left and right front teat ends	HO	0.53 (0.03)–0.60 (0.02)	Poppe et al., 2019
Handling time	Difference between box time and milking time and sums the time before the milk starts flowing and the time from when the last teat cup was removed to the time the cow leaves the system	NR	0.05 (0.01)	Wethal and Heringstad, 2019
Handling time (min)	Difference between box time and milking time	HO, SR	0.05 (0.02)–0.15 (0.03)	Carlström et al., 2016
Incomplete milking (%)	Proportion of incomplete milkings out of all milkings throughout the lactation	HO, SR	0.02 (0.03)–0.06 (0.05)	Carlström et al., 2016
Incomplete milkings	Number of daily milkings with a minimum of one teat registered as incompletely milked	NR	0.01 (0.01)	Wethal and Heringstad, 2019
Interval between two consecutive milkings	Time span between two consecutive milkings	HO	0.07 (0.03)	Viviana Santos et al., 2018
Kick-offs	Daily number of milkings with at least one teat cup kick-off	NR	0.06 (0.01)	Wethal and Heringstad, 2019
Log-transformed handling time	Log of handling time	NR	0.07 (0.02)	Wethal and Heringstad, 2019
Log-transformed online cell count	Udder health indicator	HO	0.09 (0.03)	Wethal et al., 2020
Milk yield at a quarter basis: front left	Milk yield measured by the AMS	HO	0.19 (0.06)	Viviana Santos et al., 2018
Milk yield at a quarter basis: front right	Milk yield measured by the AMS	HO	0.05 (0.06)	Viviana Santos et al., 2018
Milk yield at a quarter basis: rear left	Milk yield measured by the AMS	HO	0.11 (0.06)	Viviana Santos et al., 2018
Milk yield at a quarter basis: rear right	Milk yield measured by the AMS	HO	0.08 (0.05)	Viviana Santos et al., 2018
Milking efficiency	Ratio of milk yield (kg) and box time (min)	NR	0.22 (0.03)	Wethal and Heringstad, 2019
Milking frequency	Recorded by the AMS	HO	0.14 (0.01)	Nixon et al., 2009
Milking frequency	Number of milkings per day	NR	0.05 (0.01)	Wethal and Heringstad, 2019
Milking interval	Difference between the begin time for the present milking and the begin time for the previous milking	SR	0.09 (0.03)–0.23 (0.05)	Carlström et al., 2013
Milking interval	Time between milking sessions	NR	0.02 (<0.01)	Wethal and Heringstad, 2019
Milking interval (hours)	Difference between the begin time for the present milking and the begin time for the previous milking	HO	0.17 (0.05)–0.26 (0.05)	Carlström et al., 2013
Number of milkings	Number of milkings per cow per 24 h	HO, SR	0.02 (0.01)–0.07 (0.01)	Carlström et al., 2013
Rear teat distance	Distance between left and right rear teat ends in mm	HO	0.37 (0.03)–0.47 (0.02)	Poppe et al., 2019
Rejected milkings	Number of visits for cows in the AMS without being milked	NR	0.02 (<0.01)	Wethal and Heringstad, 2019

(Continued)

TABLE 2 | Continued

Trait	Measurement protocol or trait definition	Breed	Heritability (SE)	References
Teat not found	Defined as the number of daily milkings in which the AMS was unable to find at least one of the teats for milking	NR	0.002 (0.004)	Wethal and Heringstad, 2019
Total milk yield per day	Milk yield measured by the AMS	HO	0.18 (0.06)	Viviana Santos et al., 2018
Udder balance (mm)	Average difference in distance to the floor between the front and rear teat ends	HO	0.38 (0.03)–0.40 (0.02)	Poppe et al., 2019
Udder depth (mm)	Average distance of teat ends to the floor	HO	0.65 (0.02)–0.69 (0.02)	Poppe et al., 2019

data from electronic feeders (Wallenbeck and Keeling, 2013), suggesting another potential source of data for selective breeding against damaging and aggressive behaviors in pigs.

Automated calf feeders are becoming more common as well (Johnston et al., 2016). These systems deliver milk via a nipple at volumes and frequencies that resemble natural calf feeding behavior, support faster growth (De Paula Vieira et al., 2008), and promote calf health such as reduced sickness events (Godden et al., 2005; Barkema et al., 2015). The data generated (e.g., individual milk intake rate, frequency of feeding events) can also be used to derive proxies for genomic selection for improved calf health and overall resilience variables for genomic selection purposes.

In the case of poultry, precision feeding stations in broiler breeders can provide individual information about their performance in terms of growth rate and feed intake during rearing and lay (Hadinia et al., 2019). This information allows individual and automatic management of the feed restriction level and improve body weight uniformity in the flock (Zuidhof, 2018). For breeding selection purposes, individual performance records with precision feeding enable selection for feed efficiency. Feed efficiency in addition to other traits in the pedigree lines facilitates the selection of a parent stock with high welfare and performance that need low feed intake for the same growth rate.

In summary, automated feeding systems are becoming popular in livestock production and the large amount of data generated can also be used to derive welfare and resilience indicators for genetic and genomic selection (Howie et al., 2009, 2011). Studies investigating the genetic background of traits measured by automated feed intake recording systems are shown in **Table 3**.

Microbiota Profiling

The gut microbiome can influence various host biological processes including immunity, growth, metabolism, brain development and functioning, behavioral stress (both acute and chronic), neurophysiological disorders, and emotional well-being such as anxiety and depression (Mu et al., 2016; Karsas et al., 2018; Kraimi et al., 2019). Therefore, an alternative (and complementary route) approach for minimizing welfare issues might be by altering the gut microbiota through selection (i.e., host-microbiome interactions), dietary changes (Parois et al., 2020), and management processes (Kurilshikov et al., 2017; Kraimi et al., 2019). There is evidence of a bidirectional interaction between the host and the gut microbiome in which changes in the microbial community affect host behavior and perturbations in behavior alter the composition of the gut microbiota (Collins and Bercik, 2009; Mu et al., 2016).

In pigs, the interplay between gastrointestinal tract microbiota, host genetics, and complex traits (mainly related to growth and feed efficiency) was investigated using extensive quantitative-genetic methods and they found that the bacteria genera had a significant narrow sense host heritability ranging from 0.32 to 0.57 (Camarinha-Silva et al., 2017). Another study compared the gut microbiota of two chicken lines raised under the same husbandry and dietary conditions and reported that 68 (out of 190) microbiome species were affected by genotype (line), gender and genotype by gender interactions (Zhao et al., 2013). In addition, the genetic relationships between behavior and digestive efficiency was investigated in 860 chickens from a cross between two lines divergently selected on digestive efficiency (Mignon-Grasteau et al., 2017). The authors detected common genomic regions for the presence of bacteria such as *Lactobacillus* and *L. crispatus* and traits such as feeding behavior (Mignon-Grasteau et al., 2017). A pilot study investigated the effects of early-life microbiota transplantation on feather pecking, and behavioral and physiological traits related to feather pecking (van der Eijk et al., 2020). The researchers reported that chicken lines with divergent genetic merit for feather pecking had different microbiota composition. Furthermore, early-life microbiota transplantation had immediate and long-term effects on behavioral responses and long-term effects on immune characteristics and peripheral serotonin; however, the effects were dependent on the host genotype (van der Eijk et al., 2020).

Targeted sequencing and metagenome shotgun sequencing are the two main approaches for generating microbiome profiling. Recently, a low-cost and high-throughput approach based on Restriction-Enzyme Reduced Representation Sequencing (RE-RRS) has been proposed as an alternative to capture the diversity of the rumen microbiome (Hess et al., 2020). As the costs to generate sequencing datasets decrease, microbiome profiling might be an additional relevant phenotype for further investigations and potential applications for selection to improved welfare in livestock species.

Qualitative/Subjective Scores of Behavioral/Welfare Indicator Traits

Qualitative and subjective scoring are additional approaches to assess animal welfare. Many of these indicators can be collected

TABLE 3 | Heritability estimates for traits derived from automated feeding systems in sheep, swine and cattle.

Trait	Measurement protocol or trait definition (general observations)	Species	Heritability (SE)	References
Feed intake at the visit	Feed intake recorded by the automatic feeder	Sheep	0.38 (0.07)	Marie-Etancelin et al., 2019
Feeding duration at the visit	Time recorded by the automatic feeder	Sheep	0.28 (0.06)	Marie-Etancelin et al., 2019
Between−visit time	Between−visit time interval	Sheep	0.38 (0.07)	Marie-Etancelin et al., 2019
Feeding rate	Defined as the ratio between feed intake and feeding duration	Sheep	0.37 (0.06)	Marie-Etancelin et al., 2019
Number of meals per day	A minimum of two consecutive data points were required to constitute a meal	Swine	0.315 (0.075)	Rohrer et al., 2013
Average meal length (s)	Meal length was calculated as number of consecutive data points times 20 s	Swine	0.604 (0.087)	Rohrer et al., 2013
Daily meal time (m)	Recorded by the feeder – no details presented	Swine	0.37 (0.079)	Rohrer et al., 2013
Percentage of meals alone	Recorded by the feeder – no details presented	Swine	0.391 (0.076)	Rohrer et al., 2013
Average number of pigs at feeder	Recorded by the feeder – no details presented	Swine	0.514 (0.081)	Rohrer et al., 2013
Percentage of meals at gate-side	Recorded by the feeder – no details presented	Swine	0.157 (0.056)	Rohrer et al., 2013
Percentage of meals at open-side	Recorded by the feeder – no details presented	Swine	0.213 (0.070)	Rohrer et al., 2013
Feeding duration, min·d-1	Recorded by the feeder – no details presented	Cattle	0.25 (0.16)	Durunna et al., 2011
Head-down time, min·d-1	Recorded by the feeder – no details presented	Cattle	0.14 (0.15)	Durunna et al., 2011
Feeding rate, kg·h-1	Recorded by the feeder – no details presented	Cattle	0.35 (0.16)	Durunna et al., 2011
Feeding frequency, visits·d-1	Recorded by the feeder – no details presented	Cattle	0.56 (0.19)	Durunna et al., 2011
Feeding duration, min·d-1	Recorded by the feeder – no details presented	Cattle	0.14 (0.11)	Durunna et al., 2011
Head-down time, min·d-1	Recorded by the feeder – no details presented	Cattle	0.09 (0.1)	Durunna et al., 2011
Feeding rate, kg·h-1	Recorded by the feeder – no details presented	Cattle	0.67 (0.19)	Durunna et al., 2011
Feeding frequency, visits·d-1	Recorded by the feeder – no details presented	Cattle	0.59 (0.18)	Durunna et al., 2011

on a large scale and incorporated into livestock breeding schemes to enhance animal welfare and overall resilience. For instance, Hessing et al. (1993) suggested using the back-test as a stress indicator in pigs. In brief, pigs are manually restrained on their backs for a certain period of time (e.g., 1 min) and are scored based on their behavioral responses to assess reactivity and proactivity. For example, Rohrer et al. (2013) used the back-test to determine the effects of early-life handling in pigs. In addition to the back-test, Løvendahl et al. (2005) estimated variance components for aggressive behavior of sows at mixing by counting the number of mild or severe aggressive behaviors performed or received during 30 min after grouping and determined maternal ability by recording the sows' responses to piglet vocalization during handling.

Additional subjective scoring systems of temperament include: docility score in cattle (Adamczyk et al., 2013; Haskell et al., 2014; Schmidt et al., 2014), milking temperament in dairy cattle (Chang et al., 2020), maternal behavior and reactivity in mobile chute in Zebu cattle (Peixoto et al., 2011), and tests involving novelty, emotional reactivity, human contact and social isolation (Boissy et al., 2005; Mignon-Grasteau et al., 2017; Larsen et al., 2018). Furthermore, health scoring systems have also been proposed: lung scoring (as an indicator of pneumonia resistance, McRae et al., 2016), FAMACHA eye color chart scoring in sheep and goats [as an indicator of internal parasite resilience (Kaplan et al., 2004)], and body condition scoring (Köck et al., 2018). In addition to the objective indicators of climatic resilience presented before, some examples of qualitative scores of climatic resilience are: hair length in cattle (Piccoli et al., 2020), drooling score, respiration rate, and panting score (Gaughan et al., 2008; Schütz et al., 2014). Lameness scoring systems are widely used across livestock species (Thomsen et al., 2008; Reader et al., 2011; Nalon et al., 2013; Granquist et al., 2019). In cattle raised in extensive production systems, important adaptation traits have been genetically and genomically evaluated, including prepuce (navel) score, hair length score, and ocular pigmentation score, in addition to tick resistance (based on tick count; Piccoli et al., 2020). There are various methods available to aggregate multiple indicators to produce an overall assessment of animal welfare (Botreau et al., 2007a,b).

Despite the usefulness of qualitative scoring systems, it is important to note that observer bias and experience can influence subjective scores of animal behavior and welfare (Tuyttens et al., 2014). Fleming et al. (2016) presents a detailed description on the contributions of qualitative behavioral assessments in livestock welfare.

LARGE-SCALE DATA ANALYSIS: STATISTICAL AND COMPUTATIONAL METHODS

Major technological advancements in large-scale data analyses have been mainly driven by the availability and use of PLF technologies (Rutten et al., 2013). The advancements in data collection have been accompanied by the development and refinement of sophisticated statistical and data analysis methods. In this regard, a plethora of machine learning approaches have been applied (and is currently in expansion) in livestock breeding programs (Nayeri et al., 2019).

TABLE 4 | Heritability estimates for traits derived from various technologies and biomarkers in chicken and cattle.

Technology (summary)	Trait	Measurement protocol or trait definition (general observations)	Species	Heritability (SE)	References
Camera	Frequency of feeding	Determined by the focal sampling on each individual (a meal was defined as a sequence during which birds were continuously feeding and which was separated from another feeding event by more than 3 s)	Chicken	0.06 (0.02)	Mignon-Grasteau et al., 2017
Camera	Frequency of moving	Recorded by camera – no details presented	Chicken	0.09 (0.07)	Mignon-Grasteau et al., 2017
Camera	Frequency of lying	Recorded by camera – no details presented	Chicken	0.10 (0.06)	Mignon-Grasteau et al., 2017
Infrared sensors	Flight speed (m/s)	Infrared sensors were used to trigger the start and stop of the timing system	Cattle	0.49 (0.18)	Nkrumah et al., 2007
Milk infrared spectra	Blood β-hydroxybutyrate at 11 to 30 DIM	Blood BHB was predicted from milk spectra	Cattle	0.248 (0.005)	Belay et al., 2017
Milk infrared spectra	Blood β-hydroxybutyrate at 31 to 60 DIM	Blood BHB was predicted from milk spectra	Cattle	0.274 (0.004)	Belay et al., 2017
Milk infrared spectra	Blood β-hydroxybutyrate at 61 to 90 DIM	Blood BHB was predicted from milk spectra	Cattle	0.322 (0.005)	Belay et al., 2017
Milk infrared spectra	Blood β-hydroxybutyrate at 91 to 120 DIM	Blood BHB was predicted from milk spectra	Cattle	0.360 (0.005)	Belay et al., 2017
Transponder	Daily feeding duration (min/d)	Daily feeding duration was computed as the sum of the difference between feeding event end-times and start times per day for each animal	Cattle	0.28 (0.12)	Nkrumah et al., 2007
Transponder	Daily feeding head down time (min/d)	Sum of the number of times the electronic identification (transponder) of the animal was detected by the Growsafe system during a feeding event multiplied by the scanning time of the system	Cattle	0.33 (0.12)	Nkrumah et al., 2007
Transponder	Daily feeding frequency (events/d)	Number of independent feeding events for a particular animal in a day (recorded by the transponder)	Cattle	0.38 (0.13)	Nkrumah et al., 2007

The development of prediction equations for welfare indicator traits is expected to increase. In the case of dairy species, milk MIR has a great potential to be used as indirect predictor of many traits that are expensive or difficult to measure directly, including health status indicators (De Marchi et al., 2014; Bastin et al., 2016; Dórea et al., 2018).

The wide availability of large-scale and high-throughput phenotypes requires adequate computational capacity and powerful software to store, manage, and rapidly (or real time) transfer data from farms (or other data recording stations) to central databases. High-throughput data extraction can be performed using software such as Pig[1], MapReduce[2], and Hadoop[3] (Koltes et al., 2019). The definition of the methods to convert the stored phenotypes into useful information for real-time management decisions in the farm or breeding purposes is still a challenging task (Koltes et al., 2019). Therefore, the development of statistical methods such as machine learning and neural artificial intelligence are of great relevance.

Phenotypic quality control is one of the first steps in the data analysis process and consists of removing noise and outliers. Data standardization or transformation can also be needed depending on the statistical model assumptions, when merging datasets from different populations, or when using different equipment, calibration methods, or data collection protocols (Norton and Berckmans, 2018). Big data handling and manipulation requires good computational infrastructure and efficient programming methods (Nayeri et al., 2019). Furthermore, most PLF devices generate repeated records for each individual [i.e., longitudinal traits (Oliveira et al., 2019a)], which are highly desirable for monitoring livestock welfare. However, the covariance structure among records needs to be considered in the statistical models (Oliveira et al., 2019a).

Defining the appropriate statistical methods and models to be used for data analyses is paramount for the accuracy of the results obtained. However, this can be challenging when there is a large number of variables extracted from the high-throughput

[1]https://pig.apache.org/

[2]https://en.wikipedia.org/wiki/MapReduce

[3]https://hadoop.apache.org/

phenotypic datasets (Koltes et al., 2019; Nayeri et al., 2019). In the case of predictive modeling, feature selection can improve model performance and avoid or reduce model overfitting (Saeys et al., 2007), as well as improving the model interpretability (Butterworth, 2018).

One approach to analyze high-throughput phenotypic data consists of statistically evaluating differences between the averages of groups (Norton and Berckmans, 2018), considering all together or within specific time points. Thus, the research question needs to be clearly described, which is directly related to the final goal of using the monitoring algorithm (Nayeri et al., 2019). Common examples of welfare-related objectives are recognizing cow gait score or footpad lesion scores in chickens (Norton and Berckmans, 2018). The next step consists of defining the reference points that can be used to draw a conclusion related to the final algorithm-use goal (Butterworth, 2018).

When fitting longitudinal records, many popular statistical methods will frequently overfit the data, due to its high dimensionality and rank deficiency (Butterworth, 2018). In this context, machine learning is viewed as a key method to deal with big data, and it has proven to be useful in classifying individuals through supervised learning algorithms (Nayeri et al., 2019). The classification methods based on supervised learning algorithms can use class labels previously defined by the researcher, or by permitting the unsupervised learning (Saeys et al., 2007). However, other methods such as neural networks, support vector machines, linear and non-linear density based classifiers, decision trees, naive Bayes, wavelet analysis, k-nearest neighbor, and k-means have also being reported in the literature in terms of classification analysis (Butterworth, 2018; Koltes et al., 2019; Nayeri et al., 2019). For instance, Bakoev et al. (2020), evaluated the prediction accuracy of nine machine learning classification algorithms and reported that Random Forest and K-Nearest Neighbors better predicted pig leg weakness based on measurements taken at an early stage of the animal development.

GENETIC AND GENOMIC SELECTION TO ENHANCE ANIMAL WELFARE AND OVERALL RESILIENCE

There are two main options to evaluate animal welfare (based on resilience indicators) in a breeding program (Knap, 2008): (1) using reaction norm analysis, which enable the estimation of breeding values for production performance considering different environmental gradients (indirect approach), or, (2) directly including the measurable welfare traits in the breeding goal and in the selection indexes (direct approach), as mentioned in the previous sections in this review. However, usually reaction norms have been used for genetic evaluations of livestock animals due to the arduousness of using the direct approach and correctly defining the measurable trait (Rauw and Gomez-Raya, 2015).

Reaction norm has been defined as the expression pattern of a trait along a continuous environmental gradient (de Jong, 1995; Knap, 2005). Several variables can be used as environmental gradients in the reaction norms, such as disease exposure, social stress, temperature, and nutrient quality (Rauw and Gomez-Raya, 2015). Thus, animals maintaining production, health, and coping well across the environmental gradient are suggested to be more resilient (Rauw and Gomez-Raya, 2015). Although reaction norms are mostly described as linear relationships, they can take more complex shapes. Thus, the first derivative of the function in that environment is defined as plasticity, i.e., the difference in trait measurements between environments (de Jong, 1995).

Reaction norm models have been mainly applied to beef and dairy cattle, due to the wide use of artificial insemination and consequently dispersion of semen into several different environments. Therefore, this wide range of environments facilitate the investigation of changes in the expression of traits through a continuous descriptor of environments (Rauw and Gomez-Raya, 2015). In this context, Ravagnolo and Misztal (2002) estimated the genetic component of heat tolerance for non-return rate in Holstein cattle using a random regression animal model (Oliveira et al., 2019a) and temperature humidity index (THI). THI was calculated using temperature and humidity data provided by public weather stations, which can be obtained from on-line sources in various countries. For instance, this has been done in beef cattle for birth weight, weaning weight, post-weaning weight gain, and yearling scrotal circumference by using reaction norms and the contemporary groups as the environmental descriptor (Santana et al., 2013).

Another interesting application of reaction norms is for genomic prediction of breeding values. Few studies have reported the estimation of breeding values for animals in different environments using either a multiple-step (Silva et al., 2014) or single-step (Mota et al., 2016; Oliveira et al., 2018) approach. In this context, Silva et al. (2014) concluded that reaction norms should be used for proper genomic evaluation of total number of piglets born. Moreover, Oliveira et al. (2019b) showed that random regression models can be used to estimate Single Nucleotide Polymorphism (SNP) effects over time in genome-wide association studies.

Despite the great potential of reaction norm models for genetic and genomic evaluation of livestock animals, they have not been used to model welfare indicators yet. However, Sih et al. (2004) proposed that behavior can be included in reaction norms models. Similarly, Dingemanse et al. (2010) indicated that animal behavior can be described as a function of environmental variation. In this context, Dingemanse et al. (2012) used reaction norms to estimate genetic parameters for exploration behavior in an open-field test of wild-caught three-spined stickleback fish. Similar analysis can potentially be applied to social interactions, feeding behavior, and activity patterns in livestock production systems (Rauw and Gomez-Raya, 2015). In addition to using climatic variables from public weather stations, there is a growing interest on recording additional and more precise climatic variables within production operations (Laberge and Rousseau, 2017).

As reviewed by Egger-Danner et al. (2014), some countries have well established health recording systems (e.g., Austria, Canada, France, Germany, and Nordic countries), including the use of veterinary diagnoses, whereas others focus on producer-recorded data. Combined use of health data from farmers and

diagnosis documented by veterinarians may be an option to improve coverage of direct health data (Egger-Danner et al., 2014). Data recorded in slaughter facilities (e.g., tail lesions in pigs; skin lesions in poultry) might also be a useful source of data for breeding purposes.

Modifying animals' environments by eliminating all stressors and other causes of poor welfare through management approaches (e.g., housing, management practices, nutrition, biosecurity) can be thought of as the soundest alternative to improve welfare in livestock operations. However, this is very difficult (or impossible) to achieve in commercial farms due to economic and practical constraints and additional factors such as climate change and antibiotic resistance. Therefore, genetically selecting animals that are more resilient to different stressors and better suited for that environment, while also developing strategies to minimize the stress sources and causes of impaired welfare, is likely to be the more successful alternative in the long-term (Rodenburg and Turner, 2012).

There is clear within-population genetic variation to response to stress and overall resilience (**Tables 1–4**), indicating that genetic progress for enhanced animal welfare can be successfully achieved. Direct selection for reduced stress responsiveness can impact other relevant traits (e.g., performance, reproduction) due to pleiotropic or linkage effects. Therefore, the practical application of selective breeding to enhance welfare and overall resilience will require the use of selection indexes to enable simultaneous genetic progress on all relevant traits in individual populations. Ignoring genetic correlations among traits can result in undesirable effects, such as reduced welfare, coping mechanisms, and overall resilience due to primary selection for performance traits (Rauw et al., 1998; Rauw and Gomez-Raya, 2015). Furthermore, ignoring direct selection for welfare indicators could increase competition and agonistic interactions, which would reduce welfare, and consequently, overall productivity (Cheng, 2010; Rodenburg and Turner, 2012; Muir et al., 2014).

Genetic and genomic selection to enhance animal welfare and overall resilience can be achieved through multi-trait selection and selection indexes (Muir et al., 2014), combining various indicators of welfare and resilience, as described in this review. These traits include both direct and indirect indicators of welfare and resilience. Genomic selection has become the gold standard approach for genetically evaluating and selecting breeding animals (Meuwissen et al., 2016). This is especially advantageous for welfare traits because genomic breeding values can be predicted for selection candidates that have not been challenged by a certain stressor (e.g., pathogens, heat stress). This can be done by using data from a large training population (animals with both phenotypes and genotypes) of individuals genetically related that are raised under those stress conditions (e.g., tropical regions in the case of heat stress). Genomics also provides an opportunity to better understand the biological mechanisms associated with each trait through genome-wide association studies and functional analyses. In addition to genomic and phenotypic datasets, alternative "-omic" approaches can be of great value to unravel biological mechanisms underlying animal welfare and to improve the accuracy of genomic predictions. This includes multiple phenotypic layers, such as gene expression (transcriptomics), epigenomics (e.g., DNA methylation), proteins (proteomics), metabolites (metabolomics), lipids (lipidomics), and microbiota (microbiomics). The integration of multi-omic data and joint modeling and analyses are very powerful techniques to understand the systems biology of healthy and sustainable production of animals (Suravajhala et al., 2016). Despite the usefulness of such approaches, there are still many challenges and further developments to be addressed (Suravajhala et al., 2016).

Welfare is predicted to play an important role in livestock breeding goals (Rodenburg and Turner, 2012; Croney et al., 2018a). This is mainly due to the clear benefits of improved welfare in farm production efficiency and sustainability [e.g., reduced mortality, improved animal health, and product quality (Dawkins, 2017)], but in certain cases can have detrimental effects in overall production efficiency. In this context, various livestock breeding programs have started to incorporate welfare and resilience indicators in their breeding programs. Examples of welfare indicators that have been investigated or included in selection schemes in livestock breeding programs around the world are: aggression (Løvendahl et al., 2005); behavior (Rohrer et al., 2013); boar taint (to avoid castration; Tajet et al., 2006; Zadinová et al., 2016), calf wellness (Gonzalez-Peña et al., 2019), calving ease (Jamrozik and Miller, 2014; Vanderick et al., 2014; Li and Brown, 2016), cortisol levels (Mormède et al., 2011); docility (Norris et al., 2014); feather pecking (Dawkins and Layton, 2012), feet and leg health (Kapell et al., 2012, 2017); fertility disorders (Guarini et al., 2018; Fleming et al., 2019), hoof health [in cattle (Chapinal et al., 2013; Häggman and Juga, 2013; Heringstad et al., 2018), sheep (Conington et al., 2008), and pigs (Quintanilla et al., 2006)]; lesion scores (Wurtz et al., 2017; Angarita et al., 2019), longevity (Serenius and Stalder, 2006; Ramos et al., 2020), mastitis (Martin et al., 2018); maternal behavior and progeny survival (Gäde et al., 2008; Hellbrügge et al., 2008a,b), metabolic diseases (Egger-Danner et al., 2014; Jamrozik et al., 2016; Pryce et al., 2016), nematode resistance (Doeschl-Wilson et al., 2008), overall resilience (Berghof et al., 2019), paratuberculosis (Brito et al., 2018; Mallikarjunappa et al., 2020); pre-weaning survival (Su et al., 2007; Nielsen et al., 2013); social dominance (Tong et al., 2020); tail or ear biting (Breuer et al., 2005), and thermal tolerance (Fragomeni et al., 2016; Misztal, 2017; Nguyen et al., 2017; Xu et al., 2017). Genetic selection and modern genomic techniques (e.g., gene editing) might also be an alternative to eliminate the need for stressful procedures in commercial applications such as cattle dehorning (Van Eenennaam and Young, 2018).

Since domestication, artificial selection has altered coping mechanisms of livestock animals. For instance, there is evidence that chronic stressors have made modern laying hens more fearful of humans than their ancestors (Jones et al., 1988; El-Lethey et al., 2000; Jensen et al., 2006), and increased feather pecking and cannibalism in a larger range of environmental conditions (Canario et al., 2013; Decina et al., 2019). Also, pigs selected for high lean growth, show increased anxiety in the presence of humans (Scott et al., 2000) and leaner pigs are more stressed by transport and harder to handle

than fatter pigs (Grandin, 1998). In general, livestock breeding programs focus primarily on direct breeding values (selection for individual production; Rodenburg and Turner, 2012). However, most livestock species are group-housed, and therefore, genetic selection for associative effects (social breeding values) has been proposed (Muir, 2003). Associative effects represent the social impacts of one animal on the performance of another. For instance, genetic selection based on group rather than individual performance can reduce mortality due to aggressive behaviors in poultry and pigs (Muir, 1996, 2005; Rodenburg et al., 2010; Angarita et al., 2019). The incorporation of indirect genetic effects in livestock breeding programs has the potential to substantially increase responses to selection in traits affected by social interactions [e.g., feather pecking, cannibalism; (Rodenburg et al., 2010; Rodenburg and Turner, 2012)]. There are three main methods to improve associative effects (Ellen et al., 2014): (1) direct selection to reduce aggressiveness; (2) multi-level selection (Bijma and Wade, 2008; Muir et al., 2013); and (3) multi-trait selection where the direct and associative effects of each animal are estimated and directly selected for in a selection index (Muir, 2005; Bijma et al., 2007a,b; Muir et al., 2014). Some factors that can impact the estimates of indirect genetic effects are: level of competition for resources (e.g., feed, water), stocking density, age, and body weight variation when animals are mixed.

As previously indicated, selective breeding for enhanced welfare may require breeding animals to be exposed to the stressor on which the animals will be genetically evaluated for (e.g., pathogens, thermal stress). However, breeding nucleus animals are usually raised under high health and biosecurity standards, in low stocking densities, and low level of environmental stressors. Therefore, there might be genotype-by-environment (GxE) interactions if selection is based entirely on phenotypic records obtained in nucleus farms. Genomics can facilitate this process, as a training population can be developed based on animals raised in commercial farms (with all common stressors). Therefore, GxE should be considered when performing genomic selection for improved animal welfare and overall resilience. For example, behavior expression might differ based on animal group size (even at the same stocking density), resource availability, housing system, and use of PLF technologies (e.g., milking robot).

Practical implementation of selection to enhance animal welfare will require the development of appropriate selection indexes for combining indicators of welfare and overall resilience. However, this is challenging due to the difficulty of determining the economic value or importance of each welfare indicator trait (Nielsen et al., 2008; Croney et al., 2018a). In this context, the main challenges associated with the incorporation of animal welfare in livestock breeding goals are (Nielsen et al., 2008): (1) defining the social and economic value of improved animal welfare; (2) the perspectives of all stakeholders (e.g., farmers, consumers, citizens, and governmental authorities) need to be considered when defining the breeding goals, in which a consensus can be difficult to be achieved; and, (3) potential antagonist relationships with performance (or other conventional traits; Nielsen et al., 2008).

The wealth of data generated by PLF, data recording organizations, and genotyping schemes require the availability of good computational infrastructure, efficient software and well-trained professionals (Morota et al., 2018; Koltes et al., 2019). In addition to management practices, using these datasets for breeding purposes is expected to motivate farmers to further invest in phenotyping and genotyping tools. More efficient use of PLF datasets include international modeling and data-sharing initiatives and by adopting a collaboration model between industry, researchers, farmers, and stakeholders (Halachmi et al., 2019).

Most studies and applications of breeding for animal welfare have focused on intensive production systems, whilst extensive conditions (infrequent handling or reduced contact with humans) have largely been ignored (Turner and Dwyer, 2007; Rodenburg and Turner, 2012; Turner et al., 2018). There are welfare issues in extensive production systems (e.g., heat stress; temperament; and disease challenge), and genetic selection for improved welfare under those conditions should also be *a priority* for breeding companies and organizations.

Agroecological and organic production systems are expected to become more common over the next decades (Dumont et al., 2014; Phocas et al., 2016a,b). Therefore, breeding goals will also need to be refined for improved welfare and resilience under those conditions (as reviewed by Phocas et al., 2016a,b). As noted by Phocas et al. (2016a), breeding objectives for smallholder production systems in developing countries tend to differ from those in developed countries, especially due to environmental, economic and socio-cultural differences. Therefore, it is clear that welfare concerns are present across production systems, but in different levels, and alternative approaches will need to be taken to optimize welfare while increasing food production to meet the demands of a growing human population.

FINAL REMARKS

Quantifying welfare is paramount for breeding more resilient animals. Some of the main requirements for defining ideal welfare indicators are: (1) variables should be continuously recorded throughout the animals' life; (2) a large number of variables need to be accurately measured in individual animals as biological indicators of the five freedoms, including physiological, behavioral, and emotional state, and physical and health characteristics; (3) data collection should be based on non-invasive methods that do not result in additional stress or discomfort to the animals or alter their routine or circadian rhythms; (4) the derived phenotypes need to be collected at a low cost to enable measurement of a large number of animals, which is a requirement for successful implementation of genetic and genomic evaluations; (5) phenotypic measurements that are accurate, valid, repeatable, and comparable among laboratories, countries, or companies is critical; and (6) the phenotypes identified need to be heritable and repeatable.

The definition of welfare indicators is largely dependent on a clear understanding of the biological and emotional mechanisms behind the phenotypic variability observed in the

animal's response to different stimuli. Therefore, the evaluation of animal welfare involves a complete assessment of the animal's physiological, behavioral, physical, and emotional state. Some of these indicators can even be quantified prior to clinical signs of poor welfare (e.g., clinical mastitis).

The rapid development of integrated biological (e.g., -*omics* technologies) and engineering systems and the IoT is enabling the development of affordable monitoring devices and high-throughput technologies (Neethirajan et al., 2017). These tools can be used to individually monitor large numbers of animals in commercial settings and are advantageous to quantify biological indicators through rapid, repeatable, and automated measurements. The technological devices used include sensors such as cameras, microphones to capture vocalizations, thermometers, automated feeding and milking systems, automatic scales to measure lean-fat ratios, milk spectral data, electrodes to detect skin conductivity and heart rate, and accelerometers. Qualitative scoring systems can also be used to assess some aspects of animal welfare as well as data routinely collected in commercial farms. As Animal Welfare science evolves, novel indicators will emerge and improve our understanding of animal welfare. Further improvements in precision technologies, integration of data from multiple systems and, in particular, increased training of farmers, their personnel, and advisors to use sensor derived data will play a major role in modern livestock production (Barkema et al., 2015). The greater availability of high-throughput phenotyping technologies (e.g., automated monitoring systems) in nucleus and commercial farms, better communication and data sharing among data recording organizations (e.g., Dairy Herd Improvement, breed associations, veterinary clinics, and slaughter facilities), and greater integration of complementary disciplines will contribute to overcoming some of the challenges associated with time and cost of welfare data collection (Wemelsfelder and Mullan, 2014). In addition, PLF tools enable the collection of continuous and real-time phenotypes as well as environmental conditions (e.g., thermal stress, humidity, and air quality; Laberge and Rousseau, 2017), that are of great use for assessing animal welfare.

Genetic and genomic selection to enhance animal welfare and overall resilience can be achieved through multi-trait selection and selection indexes (Muir et al., 2014), combining various indicators of welfare and resilience. Genomic selection is especially advantageous for welfare traits because genomic breeding values can be predicted for selection candidates that have not been challenged by a certain stressor (e.g., pathogens, heat stress). Genomic selection for welfare traits, itself, is unlikely to solve all the welfare issues in commercial livestock operations. However, selective breeding is a complementary approach to other strategies (e.g., management, nutrition, housing, and biosecurity), which will result in permanent and cumulative gains in welfare (resilience) over generations.

Genetic and genomic selection for improved animal welfare require a multidisciplinary approach, including the integration of a multitude of scientific field such as cell and molecular biology, neuroscience, immunology, stress physiology, computer science, engineering, quantitative genomics, and bioinformatics. In this context, it is paramount to train the next generation of researchers in multi-disciplinary teams and develop collaborative research projects.

High welfare standards will continue to be *a priority* in livestock production systems. We expect that this review provides a comprehensive description of welfare phenotyping techniques coupled with the use of genetic and genomic selection to enhance animal welfare in commercial production systems.

AUTHOR CONTRIBUTIONS

LB conceived the article subject, prepared the review outline, and developed the concepts during the writing process. LB, HO, BM, JJ, and AS wrote the manuscript. LB, HO, BM, JJ, AS, AA, and JM-F edited the manuscript and provided additional comments. All the authors revised and accepted the final version of the manuscript.

FUNDING

This activity was funded by Purdue University as part of AgSEED Crossroads funding to support Indiana's Agriculture and Rural Development. This work was also funded by the Agriculture and Food Research Initiative Competitive Grant number 2020-67015-31575 from the USDA National Institute of Food and Agriculture.

ACKNOWLEDGMENTS

The authors acknowledge Drs. Don Lay (USDA-ARS, United States), Candace Croney (Purdue University, United States), and Sanjay Mallikarjunappa (University of Guelph, Canada) for reading and providing great suggestions in the final version of the manuscript.

REFERENCES

Abdela, N. (2016). Sub-acute ruminal acidosis (SARA) and its consequence in dairy cattle: a review of past and recent research at global prospective. *Achiev. Life Sci.* 10, 187–196. doi: 10.1016/j.als.2016.11.006

Abdul Jabbar, K., Hansen, M. F., Smith, M. L., and Smith, L. N. (2017). Early and non-intrusive lameness detection in dairy cows using 3-dimensional video. *Biosyst. Eng.* 153, 63–69. doi: 10.1016/j.biosystemseng.2016.09.017

Adamczyk, K., Pokorska, J., Makulska, J., Earley, B., and Mazurek, M. (2013). Genetic analysis and evaluation of behavioural traits in cattle. *Livest. Sci.* 154, 1–12. doi: 10.1016/j.livsci.2013.01.016

Ahmed, S. T., Mun, H. S., Yoe, H., and Yang, C. J. (2014). Monitoring of behavior using a video-recording system for recognition of *Salmonella* infection in experimentally infected growing pigs. *Animal* 9, 115–121. doi: 10.1017/S1751731114002213

Alsaaod, M., Fadul, M., and Steiner, A. (2019). Automatic lameness detection in cattle. *Vet. J.* 236, 35–44. doi: 10.1016/j.tvjl.2019.01.005

Alsaaod, M., Syring, C., Dietrich, J., Doherr, M. G., Gujan, T., and Steiner, A. (2014). A field trial of infrared thermography as a non-invasive diagnostic tool for early detection of digital dermatitis in dairy cows. *Vet. J.* 2, 281–285. doi: 10.1016/j.tvjl.2013.11.028

Ambriz-Vilchis, V., Jessop, N. S., Fawcett, R. H., Shaw, D. J., and Macrae, A. I. (2015). Comparison of rumination activity measured using rumination collars against direct visual observations and analysis of video recordings of dairy cows in commercial farm environments. *J. Dairy Sci.* 98, 1750–1758. doi: 10.3168/jds.2014-8565

Andriamandroso, A. L. H., Mercatoris, B., Lebeau, F., and Bindelle, J. (2016). A review on the use of sensors to monitor cattle jaw movements and behavior when grazing. *Biotechnol. Agron. Soc. Environ.* 20, 273–286. doi: 10.25518/1780-4507.13058

Angarita, B. K., Cantet, R. J. C., Wurtz, K. E., O'Malley, C. I., Siegford, J. M., Ernst, C. W., et al. (2019). Estimation of indirect social genetic effects for skin lesion count in group-housed pigs by quantifying behavioral interactions. *J. Anim. Sci.* 97, 3658–3668. doi: 10.1093/jas/skz244

Ansari-Mahyari, S., Ojali, M. R., Forutan, M., Riasi, A., and Brito, L. F. (2019). Investigating the genetic architecture of conception and non-return rates in Holstein cattle under heat stress conditions. *Trop. Animal Heal. Prod.* 51, 1847–1853. doi: 10.1007/s11250-019-01875-5

Aydin, A., Bahr, C., Viazzi, S., Exadaktylos, V., Buyse, J., and Berckmans, D. (2014). A novel method to automatically measure the feed intake of broiler chickens by sound technology. *Comput. Electron. Agric.* 101, 17–23. doi: 10.1016/j.compag.2013.11.012

Azzaro, G., Caccamo, M., Ferguson, J. D., Battiato, S., Farinella, G. M., Guarnera, G. C., et al. (2011). Objective estimation of body condition score by modeling cow body shape from digital images. *J. Dairy Sci.* 94, 2126–2137. doi: 10.3168/jds.2010-3467

Bakoev, S., Getmantseva, L., Kolosova, M., Kostyunina, O., Chartier, D. R., and Tatarinova, T. V. (2020). PigLeg: prediction of swine phenotype using machine learning. *PeerJ* 8:e8764. doi: 10.7717/peerj.8764

Barbedo, J. G. A., Gomes, C. C. G., Cardoso, F. F., Domingues, R., Ramos, J. V., and McManus, C. M. (2017). The use of infrared images to detect ticks in cattle and proposal of an algorithm for quantifying the infestation. *Vet. Parasitol.* 235, 106–112. doi: 10.1016/j.vetpar.2017.01.020

Barkema, H. W., von Keyserlingk, M. A. G., Kastelic, J. P., Lam, T. J. G. M., Luby, C., Roy, J. P., et al. (2015). Invited review: changes in the dairy industry affecting dairy cattle health and welfare. *J. Dairy Sci.* 98, 7426–7445. doi: 10.3168/jds.2015-9377

Bastin, C., Théron, L., Lainé, A., and Gengler, N. (2016). On the role of mid-infrared predicted phenotypes in fertility and health dairy breeding programs. *J. Dairy Sci.* 98, 7426–7445. doi: 10.3168/jds.2015-10087

Baxter, E. M., Jarvis, S., Sherwood, L., Farish, M., Roehe, R., Lawrence, A. B., et al. (2011). Genetic and environmental effects on piglet survival and maternal behaviour of the farrowing sow. *Appl. Anim. Behav. Sci.* 130, 28–41. doi: 10.1016/j.applanim.2010.11.020

Beiderman, Y., Kunin, M., Kolberg, E., Halachmi, I., Abramov, B., Amsalem, R., et al. (2014). Automatic solution for detection, identification and biomedical monitoring of a cow using remote sensing for optimised treatment of cattle. *J. Agric. Eng.* 5, 153–160. doi: 10.4081/jae.2014.418

Belay, T. K., Dagnachew, B. S., Kowalski, Z. M., and Ådnøy, T. (2017). An attempt at predicting blood β-hydroxybutyrate from Fourier-transform mid-infrared spectra of milk using multivariate mixed models in Polish dairy cattle. *J. Dairy Sci.* 100, 6312–6326. doi: 10.3168/jds.2016-12252

Benaissa, S., Tuyttens, F. A. M., Plets, D., de Pessemier, T., Trogh, J., Tanghe, E., et al. (2019). On the use of on-cow accelerometers for the classification of behaviours in dairy barns. *Res. Vet. Sci.* 125, 425–433. doi: 10.1016/j.rvsc.2017.10.005

Benjamin, M., and Yik, S. (2019). Precision livestock farming in swine welfare: a review for swine practitioners. *Animals* 9:133. doi: 10.3390/ani9040133

Bennewitz, J., Bögelein, S., Stratz, P., Rodehutscord, M., Piepho, H. P., Kjaer, J. B., et al. (2014). Genetic parameters for feather pecking and aggressive behavior in a large F2-cross of laying hens using generalized linear mixed models. *Poult. Sci.* 93, 810–817. doi: 10.3382/ps.2013-03638

Berckmans, D. (2014). Precision livestock farming technologies for welfare management in intensive livestock systems. *OIE Rev. Sci. Tech.* 33, 189–196. doi: 10.20506/rst.33.1.2273

Berckmans, D. (2017). General introduction to precision livestock farming. *Anim. Front.* 7, 6–11. doi: 10.2527/af.2017.0102

Berghof, T. V. L., Poppe, M., and Mulder, H. A. (2019). Opportunities to improve resilience in animal breeding programs. *Front. Genet.* 9:692. doi: 10.3389/fgene.2018.00692

Bijl, R., Kooistra, S. R., and Hogeveen, H. (2007). The profitability of automatic milking on Dutch dairy farms. *J. Dairy Sci.* 90, 239–248. doi: 10.3168/jds.S0022-0302(07)72625-5

Bijma, P., Muir, W. M., Ellen, E. D., Wolf, J. B., and Van Arendonk, J. A. M. (2007a). Multilevel selection 2: estimating the genetic parameters determining inheritance and response to selection. *Genetics* 175, 289–299. doi: 10.1534/genetics.106.062729

Bijma, P., Muir, W. M., and Van Arendonk, J. A. M. (2007b). Multilevel selection 1: quantitative genetics of inheritance and response to selection. *Genetics* 175, 277–288. doi: 10.1534/genetics.106.062711

Bijma, P., and Wade, M. J. (2008). The joint effects of kin, multilevel selection and indirect genetic effects on response to genetic selection. *J. Evol. Biol.* 21, 1175–1188. doi: 10.1111/j.1420-9101.2008.01550.x

Bikker, J. P., van Laar, H., Rump, P., Doorenbos, J., van Meurs, K., Griffioen, G. M., et al. (2014). Technical note: evaluation of an ear-attached movement sensor to record cow feeding behavior and activity. *J. Dairy Sci.* 97, 2974–2979. doi: 10.3168/jds.2013-7560

Bishop, S. C., and MacKenzie, K. M. (2003). Genetic management strategies for controlling infectious diseases in livestock populations. *Genet. Sel. Evol.* 35, S3–S17. doi: 10.1017/s1752756200007110

Bishop, S. C., and Morris, C. A. (2007). Genetics of disease resistance in sheep and goats. *Small Rumin. Res.* 70, 48–59. doi: 10.1016/j.smallrumres.2007.01.006

Blackie, N., Bleach, E. C. L., Amory, J. R., and Scaife, J. R. (2013). Associations between locomotion score and kinematic measures in dairy cows with varying hoof lesion types. *J. Dairy Sci.* 96, 3564–3572. doi: 10.3168/jds.2012-5597

Blatteis, C. M. (1998). *Physiology and Pathophysiology of Temperature Regulation*. Singapore: World Scientific.

Bloemhof, S., Kause, A., Knol, E. F., Van Arendonk, J. A. M., and Misztal, I. (2012). Heat stress effects on farrowing rate in sows: genetic parameter estimation using within-line and crossbred models. *J. Anim. Sci.* 90, 2109–2119. doi: 10.2527/jas.2011-4650

Boileau, A., Farish, M., Turner, S. P., and Camerlink, I. (2019). Infrared thermography of agonistic behaviour in pigs. *Physiol. Behav.* 210:112637. doi: 10.1016/j.physbeh.2019.112637

Boissy, A., Bouix, J., Orgeur, P., Poindron, P., Bibé, B., and Le Neindre, P. (2005). Genetic analysis of emotional reactivity in sheep: effects of the genotypes of the lambs and of their dams. *Genet. Sel. Evol.* 37, 381–340. doi: 10.1051/gse:2005007

Bolhuis, J. E., Ellen, E. D., Van Reenen, C. G., De Groot, J., Napel, J., Ten Koopmanschap, R. E., et al. (2009). Effects of genetic group selection against mortality on behavior and peripheral serotonin in domestic laying hens with trimmed and intact beaks. *Physiol. Behav.* 97, 470–475. doi: 10.1016/j.physbeh.2009.03.021

Borchers, M. R., Chang, Y. M., Tsai, I. C., Wadsworth, B. A., and Bewley, J. M. (2016). A validation of technologies monitoring dairy cow feeding, ruminating, and lying behaviors. *J. Dairy Sci.* 99, 7458–7466. doi: 10.3168/jds.2015-10843

Botreau, R., Bonde, M., Butterworth, A., Perny, P., Bracke, M. B. M., Capdeville, J., et al. (2007a). Aggregation of measures to produce an overall assessment of animal welfare. Part 1: a review of existing methods. *Animal* 1, 1179–1187. doi: 10.1017/S1751731107000535

Botreau, R., Bracke, M. B. M., Perny, P., Butterworth, A., Capdeville, J., Van Reenen, C. G., et al. (2007b). Aggregation of measures to produce an overall assessment of animal welfare. Part 2: analysis of constraints. *Animal* 1, 1188–1197. doi: 10.1017/S1751731107000547

Brambell, F. W. R. (1965). *Report of The Technical Committee to Enquire into the Welfare of Animals Kept Under Intensive Livestock Husbandry Systems*. London: her Majesty's Stationery Office.

Breuer, K., Sutcliffe, M. E. M., Mercer, J. T., Rance, K. A., O'Connell, N. E., Sneddon, I. A., et al. (2005). Heritability of clinical tail-biting and its relation to performance traits. *Livest. Prod. Sci.* 93, 87–94. doi: 10.1016/j.livprodsci.2004.11.009

Briefer, E. F., Tettamanti, F., and McElligott, A. G. (2015). Emotions in goats: mapping physiological, behavioural and vocal profiles. *Anim. Behav.* 99, 131–143. doi: 10.1016/j.anbehav.2014.11.002

Brito, L. F., Mallikarjunappa, S., Sargolzaei, M., Koeck, A., Chesnais, J., Schenkel, F. S., et al. (2018). The genetic architecture of milk ELISA scores as an indicator of Johne's disease (paratuberculosis) in dairy cattle. *J. Dairy Sci.* 101, 10062–10075. doi: 10.3168/jds.2017-14250

Broom, D. M. (1991). Animal welfare: concepts and measurement. *J. Anim. Sci.* 9, 4167–4175. doi: 10.2527/1991.69104167x

Broom, D. M. (2011). A history of animal welfare science. *Acta Biotheor.* 59, 121–137. doi: 10.1007/s10441-011-9123-3

Brown-Brandl, T. M., Hayes, M. D., Xin, H., Nienaber, J. A., Li, H., Eigenberg, R. A., et al. (2014). Heat and moisture production of modern swine. *ASHRAE Trans.* 120, 469–489.

Brünger, J., Dippel, S., Koch, R., and Veit, C. (2019). Tailception: using neural networks for assessing tail lesions on pictures of pig carcasses. *Animal* 13, 1030–1036. doi: 10.1017/S1751731118003038

Buitenhuis, A. J., Rodenburg, T. B., Van Hierden, Y. M., Siwek, M., Cornelissen, S. J. B., Nieuwland, M. G. B., et al. (2003). Mapping quantitative trait loci affecting feather pecking behavior and stress response in laying hens. *Poult. Sci.* 2, 1215–1222. doi: 10.1093/ps/82.8.1215

Buitenhuis, A. J., Rodenburg, T. B., Wissink, P. H., Visscher, J., Koene, P., Bovenhuis, H., et al. (2004). Genetic and phenotypic correlations between feather pecking behavior, stress response, immune response, and egg quality traits in laying hens. *Poult. Sci.* 83, 1077–1082. doi: 10.1093/ps/83.7.1077

Burciaga-Robles, L. O., Holland, B. P., Step, D. L., Krehbiel, C. R., McMillen, G. L., Richards, C. J., et al. (2009). Evaluation of breath biomarkers and serum haptoglobin concentration for diagnosis of bovine respiratory disease in heifers newly arrived at a feedlot. *Am. J. Vet. Res.* 70, 1291–1298. doi: 10.2460/ajvr.70.10.1291

Burdick, N. C., Carroll, J. A., Dailey, J. W., Randel, R. D., Falkenberg, S. M., and Schmidt, T. B. (2012). Development of a self-contained, indwelling vaginal temperature probe for use in cattle research. *J. Therm. Biol.* 37, 339–343. doi: 10.1016/j.jtherbio.2011.10.007

Butterworth, A. (2018). *Animal Welfare in a Changing World*. Wallingford: CABI.

Butterworth, A., Mench, J. A., and Wielebnowski, N. (2017). Practical strategies to assess (and improve) welfare. *Anim. Welfare* 37, 339–343. doi: 10.1079/9781845936594.0200

Cabezón, F. A., Schinckel, A. P., Richert, B. T., Peralta, W. A., and Gandarillas, M. (2017). TECHNICAL NOTE: application of models to estimate daily heat production of lactating sows. *Prof. Anim. Sci.* 33, 357–362. doi: 10.15232/pas.2016-1583

Camarinha-Silva, A., Maushammer, M., Wellmann, R., Vital, M., Preuss, S., and Bennewitz, J. (2017). Host genome influence on gut microbial composition and microbial prediction of complex traits in pigs. *Genetics* 206, 1637–1644. doi: 10.1534/genetics.117.200782

Camerlink, I., Turner, S. P., Bijma, P., and Bolhuis, J. E. (2013). Indirect Genetic Effects and housing conditions in relation to aggressive behaviour in pigs. *PLoS One* 8:e65136. doi: 10.1371/journal.pone.0065136

Canario, L., Mignon-Grasteau, S., Dupont-Nivet, M., and Phocas, F. (2013). Genetics of behavioural adaptation of livestock to farming conditions. *Animal* 7, 357–377. doi: 10.1017/S1751731112001978

Carabaño, M. J., Ramón, M., Díaz, C., Molina, A., Pérez-Guzmán, M. D., and Serradilla, J. M. (2017). Breeding and genetics symposium: breeding for resilience to heat stress effects in dairy ruminants. A comprehensive review. *J. Anim. Sci.* 95, 1813–1826. doi: 10.2527/jas.2016.1114

Carabaño, M. J., Ramón, M., Menéndez-Buxadera, A., Molina, A., and Díaz, C. (2019). Selecting for heat tolerance. *Anim. Front.* 9, 62–68. doi: 10.1093/af/vfy033

Carenzi, C., and Verga, M. (2009). Animal welfare: review of the scientific concept and definition. *Ital. J. Anim. Sci.* 8, 21–30. doi: 10.4081/ijas.2009.s1.21

Carlström, C., Pettersson, G., Johansson, K., Strandberg, E., Stålhammar, H., and Philipsson, J. (2013). Feasibility of using automatic milking system data from commercial herds for genetic analysis of milkability. *J. Dairy Sci.* 96, 5324–5332. doi: 10.3168/jds.2012-6221

Carlström, C., Strandberg, E., Pettersson, G., Johansson, K., Stålhammar, H., and Philipsson, J. (2016). Genetic associations of teat cup attachment failures, incomplete milkings, and handling time in automatic milking systems with milkability, temperament, and udder conformation. *Acta Agric. Scand. A Anim. Sci.* 66, 75–83. doi: 10.1080/09064702.2016.1260153

Catarinucci, L., Colella, R., Mainetti, L., Patrono, L., Pieretti, S., Secco, A., et al. (2014). An animal tracking system for behavior analysis using radio frequency identification. *Lab. Anim.* 43, 321–327. doi: 10.1038/laban.547

Chang, Y., Brito, L. F., Alvarenga, A. B., and Wang, Y. (2020). Incorporating temperament traits in dairy cattle breeding programs: challenges and opportunities in the phenomics era. *Anim. Front.* 10, 29–36. doi: 10.1093/af/vfaa006

Chapinal, N., Koeck, A., Sewalem, A., Kelton, D. F., Mason, S., Cramer, G., et al. (2013). Genetic parameters for hoof lesions and their relationship with feet and leg traits in Canadian Holstein cows. *J. Dairy Sci.* 96, 2596–2604. doi: 10.3168/jds.2012-6071

Chen, C., Zhu, W., Ma, C., Guo, Y., Huang, W., and Ruan, C. (2017). Image motion feature extraction for recognition of aggressive behaviors among group-housed pigs. *Comput. Electron. Agric.* 142, 380–387. doi: 10.1016/j.compag.2017.09.013

Chen, C. Y., Misztal, I., Tsuruta, S., Zumbach, B., Herring, W. O., Holl, J., et al. (2010). Estimation of genetic parameters of feed intake and daily gain in Durocs using data from electronic swine feeders. *J. Anim. Breed. Genet.* 127, 230–234. doi: 10.1111/j.1439-0388.2009.00833.x

Cheng, H. W. (2010). Breeding of tomorrow's chickens to improve well-being. *Poult. Sci.* 89, 805–813. doi: 10.3382/ps.2009-00361

Church, J. S., Hegadoren, P. R., Paetkau, M. J., Miller, C. C., Regev-Shoshani, G., Schaefer, A. L., et al. (2014). Influence of environmental factors on infrared eye temperature measurements in cattle. *Res. Vet. Sci.* 96, 220–226. doi: 10.1016/j.rvsc.2013.11.006

Cockram, M. S. (2002). The biology of animal stress: basic principles and implications for animal welfare. *Vet. J.* 1, 77–82. doi: 10.1053/tvjl.2001.0558

Colditz, I. G., and Hine, B. C. (2016). Resilience in farm animals: biology, management, breeding and implications for animal welfare. *Anim. Prod. Sci.* 56, 1961–1983. doi: 10.1071/AN15297

Cole, J. B., Bormann, J. M., Gill, C. A., Khatib, H., Koltes, J. E., Maltecca, C., et al. (2017). Breeding and genetics symposium: resilience of livestock to changing environments. *J. Anim. Sci.* 95, 1777–1779. doi: 10.2527/jas2017.1402

Collier, R. J., and Gebremedhin, K. G. (2015). Thermal biology of domestic animals. *Annu. Rev. Anim. Biosci.* 3, 513–532. doi: 10.1146/annurev-animal-022114-110659

Collins, S. M., and Bercik, P. (2009). The relationship between intestinal microbiota and the central nervous system in normal gastrointestinal function and disease. *Gastroent* 136, 2003–2014. doi: 10.1053/j.gastro.2009.01.075

Conington, J., Hosie, B., Nieuwhof, G. J., Bishop, S. C., and Bünger, L. (2008). Breeding for resistance to footrot - The use of hoof lesion scoring to quantify footrot in sheep. *Vet. Res. Commun.* 32, 583–589. doi: 10.1007/s11259-008-9062-x

Cook, N. J. (2012). Review: minimally invasive sampling media and the measurement of corticosteroids as biomarkers of stress in animals. *Can. J. Anim. Sci.* 92, 227–259. doi: 10.4141/CJAS2012-045

Cornou, C., and Lundbye-Christensen, S. (2008). Classifying sows' activity types from acceleration patterns. An application of the Multi-Process Kalman Filter. *Appl. Anim. Behav. Sci.* 111, 262–273. doi: 10.1016/j.applanim.2007.06.021

Croney, C., Mench, J., Muir, W., Anthony, R., Golab, G., Hofacre, C., et al. (2018a). *Scientific, Ethical, and Economic Aspects of Farm Animal Welfare. CAST Task Force Report- R143*. Available online at: https://www.cast-science:publication/scientific-ethical-and-economic-aspects-of-farm-animal-welfare/ (accessed November 3, 2019).

Croney, C., Muir, W., Ni, J. Q., Widmar, N. O., and Varner, G. (2018b). An overview of engineering approaches to improving agricultural animal welfare. *J. Agric. Environ. Ethics* 2, 143–159. doi: 10.1007/s10806-018-9716-9719

Cross, A. J., Keel, B. N., Brown-Brandl, T. M., Cassady, J. P., and Rohrer, G. A. (2018). Genome-wide association of changes in swine feeding behaviour due to heat stress. *Genet. Sel. Evol.* 50, 1–12. doi: 10.1186/s12711-018-0382-381

Curtis, S. (1983). *Environmental Management in Animal Agriculture*. Ames: Iowa State University Press, 6–96.

Dalin, A. M., Magnusson, U., Häggendal, J., and Nyberg, L. (1993). The effect of thiopentone-sodium anesthesia and surgery, relocation, grouping, and hydrocortisone treatment on the blood levels of cortisol, corticosteroid-binding

globulin, and catecholamines in pigs. *J. Anim. Sci.* 71, 1902–1909. doi: 10.2527/1993.7171902x

Dallman, M. F., and Hellhammer, D. (2011). *Regulation of the Hypothalamo-Pituitary-Adrenal Axis, Chronic Stress, and Energy: The Role of Brain Networks. The Handbook of Stress Science, Biology Psychology and Health*. Cham: Springer.

Dalton, H. A., Wood, B. J., Dickey, J. P., and Torrey, S. (2016). Validation of HOBO Pendant® data loggers for automated step detection in two age classes of male turkeys: growers and finishers. *Appl. Animal Behav. Sci.* 176, 63–69. doi: 10.1016/j.applanim.2015.12.005

Dawkins, M. S. (2017). Animal welfare and efficient farming: is conflict inevitable? *Anim. Prod. Sci.* 57, 201–208. doi: 10.1071/AN15383

Dawkins, M. S., and Layton, R. (2012). Breeding for better welfare: genetic goals for broiler chickens and their parents. *Anim. Welfare* 21, 147–155. doi: 10.7120/09627286.21.2.147

De Goede, D., Gremmen, B., Rodenburg, T. B., Bolhuis, J. E., Bijma, P., Scholten, M., et al. (2013). Reducing damaging behaviour in robust livestock farming. *NJAS Wageningen J. Life Sci.* 66, 49–53. doi: 10.1016/j.njas.2013.05.006

de Haas, E. N., van der Eijk, J. A., and Rodenburg, T. B. (2017). "Automatic ultra-wideband sensor detection shows selection on feather pecking increases activity in laying hens," in *Proceedings of The European Symposium on Poultry Welfare*, (Rueil-Malmaison: World's Poultry Science Association [WPSA]).

de Jong, G. (1995). Phenotypic plasticity as a product of selection in a variable environment. *Am. Nat.* 4, 493–512. doi: 10.1086/285752

De Marchi, M., Toffanin, V., Cassandro, M., and Penasa, M. (2014). Invited review: mid-infrared spectroscopy as phenotyping tool for milk traits. *J. Dairy Sci.* 97, 1171–1186. doi: 10.3168/jds.2013-6799

De Mol, R. M., André, G., Bleumer, E. J. B., van der Werf, J. T. N., de Haas, Y., and van Reenen, C. G. (2013). Applicability of day-to-day variation in behavior for the automated detection of lameness in dairy cows. *J. Dairy Sci.* 96, 3703–3712. doi: 10.3168/jds.2012-6305

De Paula Vieira, A., Guesdon, V., de Passillé, A. M., von Keyserlingk, M. A. G., and Weary, D. M. (2008). Behavioural indicators of hunger in dairy calves. *Appl. Anim. Behav. Sci.* 109, 180–189. doi: 10.1016/j.applanim.2007.03.006

de Rosa, G., Di Palo, R., Serafini, R., Grasso, F., Bragaglio, A., Braghieri, A., et al. (2019). Different assessment systems fail to agree on the evaluation of dairy cattle welfare at farm level. *Livest. Sci.* 229, 145–149. doi: 10.1016/j.livsci.2019.09.024

Decina, C., Berke, O., van Staaveren, N., Baes, C. F., Widowski, T. M., and Harlander-Matauschek, A. (2019). A cross-sectional study on feather cover damage in Canadian laying hens in non-cage housing systems. *BMC Vet. Res.* 15:435. doi: 10.1186/s12917-019-2168-2

Ding, R., Yang, M., Wang, X., Quan, J., Zhuang, Z., Zhou, S., et al. (2018). Genetic architecture of feeding behavior and feed efficiency in a Duroc pig population. *Front. Genet.* 9:220. doi: 10.3389/fgene.2018.00220

Dingemanse, N. J., Barber, I., Wright, J., and Brommer, J. E. (2012). Quantitative genetics of behavioural reaction norms: genetic correlations between personality and behavioural plasticity vary across stickleback populations. *J. Evol. Biol.* 25, 485–496. doi: 10.1111/j.1420-9101.2011.02439.x

Dingemanse, N. J., Kazem, A. J. N., Réale, D., and Wright, J. (2010). Behavioural reaction norms: animal personality meets individual plasticity. *Trends Ecol. Evol.* 25, 81–89. doi: 10.1016/j.tree.2009.07.013

Do, D. N., Strathe, A. B., Ostersen, T., Jensen, J., Mark, T., and Kadarmideen, H. N. (2013). Genome-wide association study reveals genetic architecture of eating behavior in pigs and its implications for humans obesity by comparative mapping. *PLoS One* 8:e71509. doi: 10.1371/journal.pone.0071509

Doeschl-Wilson, A. B., Vagenas, D., Kyriazakis, I., and Bishop, S. C. (2008). Exploring the assumptions underlying genetic variation in host nematode resistance. *Genet. Sel. Evol.* 40, 1–24. doi: 10.1186/1297-9686-40-3-241

Dórea, J. R. R., Rosa, G. J. M., Weld, K. A., and Armentano, L. E. (2018). Mining data from milk infrared spectroscopy to improve feed intake predictions in lactating dairy cows. *J. Dairy Sci.* 101, 5878–5889. doi: 10.3168/jds.2017-13997

Du, X., Lao, F., and Teng, G. (2018). A sound source localisation analytical method for monitoring the abnormal night vocalisations of poultry. *Sensors* 18:2906. doi: 10.3390/s18092906

Dumont, B., González-García, E., Thomas, M., Fortun-Lamothe, L., Ducrot, C., Dourmad, J. Y., et al. (2014). Forty research issues for the redesign of animal production systems in the 21st century. *Animal* 8, 1382–1393. doi: 10.1017/S1751731114001281

Duncan, I. J. H. (1998). Behaviour and behavioural needs. *Poult. Sci.* 77, 1766–1772. doi: 10.1093/ps/77.12.1766

Durunna, O. N., Wang, Z., Basarab, J. A., Okine, E. K., and Moore, S. S. (2011). Phenotypic and genetic relationships among feeding behavior traits, feed intake, and residual feed intake in steers fed grower and finisher diets. *J. Anim. Sci.* 89, 3401–3409. doi: 10.2527/jas.2011-3867

Egger-Danner, C., Cole, J. B., Pryce, J. E., Gengler, N., Heringstad, B., Bradley, A., et al. (2014). Invited review: overview of new traits and phenotyping strategies in dairy cattle with a focus on functional traits. *Animal* 9, 191–207. doi: 10.1017/S1751731114002614

Ellen, E. D., Bas Rodenburg, T., Albers, G. A. A., Elizabeth Bolhuis, J., Camerlink, I., Duijvesteijn, N., et al. (2014). The prospects of selection for social genetic effects to improve welfare and productivity in livestock. *Front. Genet.* 5:377. doi: 10.3389/fgene.2014.00377

Ellen, E. D., Van Der Sluis, M., Siegford, J., Guzhva, O., Toscano, M. J., Bennewitz, J., et al. (2019). Review of sensor technologies in animal breeding: phenotyping behaviors of laying hens to select against feather pecking. *Animals* 9:108. doi: 10.3390/ani9030108

El-Lethey, H., Aerni, V., Jungi, T. W., and Wechsler, B. (2000). Stress and feather pecking in laying hens in relation to housing conditions. *Br. Poult. Sci.* 41, 22–28. doi: 10.1080/00071660086358

Escalante, H. J., Rodriguez, S. V., Cordero, J., Kristensen, A. R., and Cornou, C. (2013). Sow-activity classification from acceleration patterns: a machine learning approach. *Comput. Electron. Agric.* 93, 17–26. doi: 10.1016/j.compag.2013.01.003

European Food Safety Authority [EFSA] (2012). *Panel on Animal Health, Welfare*. Available at: https://www.efsa.europa.eu/en/panels/ahaw (accessed November 07, 2019).

Exadaktylos, V., Silva, M., Aerts, J. M., Taylor, C. J., and Berckmans, D. (2008). Real-time recognition of sick pig cough sounds. *Comput. Electron. Agric.* 63, 207–214. doi: 10.1016/j.compag.2008.02.010

Exadaktylos, V., Silva, M., and Berckmans, D. (2014). Automatic identification and interpretation of animal sounds, application to livestock production optimisation. *Soundsc. Semiot. Localisation Categorisation* 8, 65–81. doi: 10.5772/56040

Falconer, D. S., and Mackay, T. F. C. (1996). *Introduction to Quantitative Genetics*, 4th Edn. Essex: Pearson Education Limited.

Fathi, M. M., Galal, A., El-Safty, S., and Mahrous, M. (2013). Naked neck and frizzle genes for improving chickens raised under high ambient temperature: I. Growth performance and egg production. *Poultry Sci. J.* 69, 813–832. doi: 10.1017/S0043933913000834

Fend, R., Geddes, R., Lesellier, S., Vordermeier, H. M., Corner, L. A. L., Gormley, E., et al. (2005). Use of an electronic nose to diagnose *Mycobacterium bovis* infection in badgers and cattle. *J. Clin. Microbiol.* 43, 1745–1751. doi: 10.1128/JCM.43.4.1745-1751.2005

Ferrari, S., Piccinini, R., Silva, M., Exadaktylos, V., Berckmans, D., and Guarino, M. (2010). Cough sound description in relation to respiratory diseases in dairy calves. *Prev. Vet. Med.* 96, 276–280. doi: 10.1016/j.prevetmed.2010.06.013

Ferreira, V. M. O. S., Francisco, N. S., Belloni, M., Aguirre, G. M. Z., Caldara, F. R., Nääs, I. A., et al. (2011). Infrared thermography applied to the evaluation of metabolic heat loss of chicks fed with different energy densities. *Rev. Bras. Cienc. Avic.* 13, 113–118. doi: 10.1590/S1516-635X2011000200005

Fleming, A., Baes, C. F., Martin, A. A. A., Chud, T. C. S., Malchiodi, F., Brito, L. F., et al. (2019). Symposium review: the choice and collection of new relevant phenotypes for fertility selection. *J. Dairy Sci.* 102, 3772–3734. doi: 10.3168/jds.2018-15470

Fleming, P. A., Clarke, T., Wickham, S. L., Stockman, C. A., Barnes, A. L., Collins, T., et al. (2016). The contribution of qualitative behavioural assessment to appraisal of livestock welfare. *Anim. Prod. Sci.* 56, 1569–1578. doi: 10.1071/AN15101

Foris, B., Thompson, A. J., von Keyserlingk, M. A. G., Melzer, N., and Weary, D. M. (2019). Automatic detection of feeding- and drinking-related agonistic behavior and dominance in dairy cows. *J. Dairy Sci.* 10, 9176–9186. doi: 10.3168/jds.2019-16697

Fragomeni, B. O., Lourenco, D. A. L., Tsuruta, S., Bradford, H. L., Gray, K. A., Huang, Y., et al. (2016). Using single-step genomic best linear unbiased predictor to enhance the mitigation of seasonal losses due to heat stress in pigs. *J. Anim. Sci.* 94, 5004–5013. doi: 10.2527/jas.2016-2820

Fraser, D. (2008). Understanding animal welfare. *Acta Vet. Scand.* 50, 1–7. doi: 10.1186/1751-0147-50-S1-S1

Fraser, D., Weary, D. M., Pajor, E. A., and Milligan, B. N. (1997). A scientific conception of animal welfare that reflects ethical concerns. *Anim. Welfare* 6, 187–205.

Friggens, N. C., Blanc, F., Berry, D. P., and Puillet, L. (2017). Review: deciphering animal robustness. A synthesis to facilitate its use in livestock breeding and management. *Animal* 11, 2237–2251. doi: 10.1017/S175173111700088X

Friggens, N. C., and Thorup, V. M. (2015). From monitoring to precision phenotyping: towards a systemic use of precision livestock measures in dairy herds. *Proc. New Zeal. Soc. Anim. Prod.* 75, 145–148.

Gäde, S., Bennewitz, J., Kirchner, K., Looft, H., Knap, P. W., Thaller, G., et al. (2008). Genetic parameters for maternal behaviour traits in sows. *Livest. Sci.* 114, 31–41. doi: 10.1016/j.livsci.2007.04.006

Garcia, S. O., Ulyanova, Y. V., Figueroa-Teran, R., Bhatt, K. H., Singhal, S., and Atanassov, P. (2016). Wearable sensor system powered by a biofuel cell for detection of lactate levels in sweat. *ECS J. Solid State Sci. Technol.* 5, M3075–M3081. doi: 10.1149/2.0131608jss

Garner, J. B., Douglas, M. L., Williams, S. R. O., Wales, W. J., Marett, L. C., Nguyen, T. T. T., et al. (2016). Genomic selection improves heat tolerance in dairy cattle. *Sci. Rep.* 6:34114. doi: 10.1038/srep34114

Gaughan, J. B., Mader, T. L., Holt, S. M., and Lisle, A. (2008). A new heat load index for feedlot cattle. *J. Anim. Sci.* 86, 226–234. doi: 10.2527/jas.2007-0305

Gebremedhin, K. G., Hillman, P. E., Lee, C. N., Collier, R. J., Willard, S. T., Arthington, J. D., et al. (2008). Sweating rates of dairy cows and beef heifers in hot conditions. *Trans. ASABE* 51, 2167–2178. doi: 10.13031/2013.25397

Glennon, T., O'Quigley, C., McCaul, M., Matzeu, G., Beirne, S., Wallace, G. G., et al. (2016). 'SWEATCH': a wearable platform for harvesting and analysing sweat sodium content. *Electroanalysis* 28, 1283–1289. doi: 10.1002/elan.201600106

Goddard, M. E., Hayes, B. J., and Meuwissen, T. H. E. (2010). Genomic selection in livestock populations. *Genet. Res.* 92, 413–421. doi: 10.1017/S0016672310000613

Godden, S. M., Fetrow, J. P., Feirtag, J. M., Green, L. R., and Wells, S. J. (2005). Economic analysis of feeding pasteurized nonsaleable milk versus conventional milk replacer to dairy calves. *J. Am. Vet. Med. Assoc.* 9, 1547–1554. doi: 10.2460/javma.2005.226.1547

Godoy, L. D., Rossignoli, M. T., Delfino-Pereira, P., Garcia-Cairasco, N., and de Lima Umeoka, E. H. (2018). A comprehensive overview on stress neurobiology: basic concepts and clinical implications. *Front. Behav. Neurosci.* 12:127. doi: 10.3389/fnbeh.2018.00127

González, L. A., Bishop-Hurley, G. J., Handcock, R. N., and Crossman, C. (2015). Behavioral classification of data from collars containing motion sensors in grazing cattle. *Comput. Electron. Agric.* 110, 91–102. doi: 10.1016/j.compag.2014.10.018

Gonzalez-Peña, D., Vukasinovic, N., Brooker, J. J., Przybyla, C. A., and DeNise, S. K. (2019). Genomic evaluation for calf wellness traits in Holstein cattle. *J. Dairy Sci.* 102, 2319–2329. doi: 10.3168/jds.2018-15540

Gonzalez-Rivas, P. A., Chauhan, S. S., Ha, M., Fegan, N., Dunshea, F. R., and Warner, R. D. (2020). Effects of heat stress on animal physiology, metabolism, and meat quality: a review. *Meat Sci.* 162:108025. doi: 10.1016/j.meatsci.2019.108025

Gourdine, J.-L., Mandonnet, N., Giorgi, M., and Renaudeau, D. (2017). Genetic parameters for thermoregulation and production traits in lactating sows reared in tropical climate. *Animal* 11, 365–374. doi: 10.1017/s175173111600135x

Grams, V., Bögelein, S., Grashorn, M. A., Bessei, W., and Bennewitz, J. (2015). Quantitative genetic analysis of traits related to fear and feather pecking in laying hens. *Behav. Genet.* 45, 228–235. doi: 10.1007/s10519-014-9695-1

Grandin, T. (1998). "Genetics and behavior during handling, restraint, and herding," in *Genetics and the Behavior of Domestic Animals*, eds T. Grandin and M. J. Deesing (Cambridge, MA: Academic Press).

Grandinson, K. (2005). Genetic background of maternal behaviour and its relation to offspring survival. *Livest. Prod. Sci.* 93, 43–50. doi: 10.1016/j.livprodsci.2004.11.005

Granquist, E. G., Vasdal, G., De Jong, I. C., and Moe, R. O. (2019). Lameness and its relationship with health and production measures in broiler chickens. *Animal* 13, 2365–2372. doi: 10.1017/S1751731119000466

Grethe, H. (2017). The economics of farm animal welfare. *Annu. Rev. Resour. Econ.* 9, 79–94. doi: 10.1146/annurev-resource-100516-053419

Guarini, A. R., Lourenco, D. A. L., Brito, L. F., Sargolzaei, M., Baes, C. F., Miglior, F., et al. (2018). Genetics and genomics of reproductive disorders in Canadian Holstein cattle. *J. Dairy Sci.* 102, 1341–1353. doi: 10.3168/jds.2018-15038

Guy, S. Z., Hermesch, S., and Thomson, P. C. (2012). Selection of pigs for improved coping with diseases and environmental challenges: resistance or tolerance? *Front. Genet.* 3:281. doi: 10.3389/fgene.2012.00281

Hadinia, S. H., Carneiro, P. R. O., Korver, D. R., and Zuidhof, M. J. (2019). Energy partitioning by broiler breeder hens in conventional daily-restricted feeding and precision feeding systems. *Poultry Sci.* 98, 6721–6732. doi: 10.3382/ps/pez387

Häggman, J., and Juga, J. (2013). Genetic parameters for hoof disorders and feet and leg conformation traits in Finnish Holstein cows. *J. Dairy Sci.* 5, 3319–3325. doi: 10.3168/jds.2012-6334

Halachmi, I., Guarino, M., Bewley, J., and Pastell, M. (2019). Smart animal agriculture: application of real-time sensors to improve animal well-being and production. *Annu. Rev. Anim. Biosci.* 7, 403–424. doi: 10.1146/annurev-animal-020518-114851

Halachmi, I., Klopèiè, M., Polak, P., Roberts, D. J., and Bewley, J. M. (2013). Automatic assessment of dairy cattle body condition score using thermal imaging. *Comp. Elect. Agric.* 99, 34–40. doi: 10.1016/j.compag.2013.08.012

Hamilton, A. W., Davison, C., Tachtatzis, C., Andonovic, I., Michie, C., Ferguson, H. J., et al. (2019). Identification of the rumination in cattle using support vector machines with motion-sensitive bolus sensors. *Sensors* 19:1165. doi: 10.3390/s19051165

Hansen, M. F., Smith, M. L., Smith, L. N., Salter, M. G., Baxter, E. M., Farish, M., et al. (2018). Towards on-farm pig face recognition using convolutional neural networks. *Comp. Ind.* 98, 143–152. doi: 10.1016/j.compind.2018.02.016

Hansen, P. J. (2020). Prospects for gene introgression or gene editing as a strategy for reduction of the impact of heat stress on production and reproduction in cattle. *Theriogenology* 15, 190–202. doi: 10.1016/j.theriogenology.2020.05.010

Harris-Bridge, G., Young, L., Handel, I., Farish, M., Mason, C., Mitchell, M. A., et al. (2018). The use of infrared thermography for detecting digital dermatitis in dairy cattle: what is the best measure of temperature and foot location to use? *Vet. J.* 237, 26–33. doi: 10.1016/j.tvjl.2018.05.008

Haskell, M. J., Simm, G., and Turner, S. P. (2014). Genetic selection for temperament traits in dairy and beef cattle. *Front. Genet.* 5:368. doi: 10.3389/fgene.2014.00368

Heikenfeld, J. (2016). Bioanalytical devices: technological leap for sweat sensing. *Nature* 529, 475–476. doi: 10.1038/529475a

Heinonen, M., Orro, T., Kokkonen, T., Munsterhjelm, C., Peltoniemi, O., and Valros, A. (2010). Tail biting induces a strong acute phase response and tail-end inflammation in finishing pigs. *Vet. J.* 184, 303–307. doi: 10.1016/j.tvjl.2009.02.021

Hellbrügge, B., Tölle, K. H., Bennewitz, J., Henze, C., Presuhn, U., and Krieter, J. (2008a). Genetic aspects regarding piglet losses and the maternal behaviour of sows. Part 1. Genetic analysis of piglet mortality and fertility traits in pigs. *Animal* 2, 1273–1280. doi: 10.1017/S1751731108002504

Hellbrügge, B., Tölle, K. H., Bennewitz, J., Henze, C., Presuhn, U., and Krieter, J. (2008b). Genetic aspects regarding piglet losses and the maternal behaviour of sows. Part 2. Genetic relationship between maternal behaviour in sows and piglet mortality. *Animal* 2, 1281–1288. doi: 10.1017/S1751731108002516

Heringstad, B., Egger-Danner, C., Charfeddine, N., Pryce, J. E., Stock, K. F., Kofler, J., et al. (2018). Invited review: genetics and claw health: opportunities to enhance claw health by genetic selection. *J. Dairy Sci.* 101, 4801–4821. doi: 10.3168/jds.2017-13531

Hess, M. K., Rowe, S. J., Van Stijn, T. C., Henry, H. M., Hickey, S. M., Brauning, R., et al. (2020). A restriction enzyme reduced representation sequencing approach for low-cost, high-throughput metagenome profiling. *PLoS One* 15:e0219882. doi: 10.1371/journal.pone.0219882

Hessing, M. J. C., Hagelsø, A. M., van Beek, J. A. M., Wiepkema, R. P., Schouten, W. G. P., and Krukow, R. (1993). Individual behavioural characteristics in pigs. *Appl. Anim. Behav. Sci.* 37, 285–295. doi: 10.1016/0168-1591(93)90118-9

Hocquette, J. F., Capel, C., David, V., Guémené, D., Bidanel, J., Ponsart, C., et al. (2012). Objectives and applications of phenotyping network set-up for livestock. *Anim. Sci. J.* 83, 517–528. doi: 10.1111/j.1740-0929.2012.01015.x

Hoque, M. A., and Suzuki, K. (2009). Genetics of residual feed intake in cattle and pigs: a review. *Asian Austral. J. Anim. Sci.* 22, 747–755. doi: 10.5713/ajas.2009.80467

Houle, D., Govindaraju, D. R., and Omholt, S. (2010). Phenomics: the next challenge. *Nat. Rev. Genet.* 11, 855–866. doi: 10.1038/nrg2897

Howie, J. A., Avendano, S., Tolkamp, B. J., and Kyriazakis, I. (2011). Genetic parameters of feeding behavior traits and their relationship with live performance traits in modern broiler lines. *Poult. Sci.* 90, 1197–1205. doi: 10.3382/ps.2010-1313

Howie, J. A., Tolkamp, B. J., Avendano, S., and Kyriazakis, I. (2009). The structure of feeding behavior in commercial broiler lines selected for different growth rates. *Poult. Sci.* 88, 1143–1150. doi: 10.3382/ps.2008-2441

Hu, L., Ma, Y., Liu, L., Kang, L., Brito, L. F., Wang, D., et al. (2019). Detection of functional polymorphisms in the hsp70 gene and association with cold stress response in Inner-Mongolia Sanhe cattle. *Cell Stress Chaperone* 24, 409–418. doi: 10.1007/s12192-019-00973-5

Huzzey, J. M., Nydam, D. V., Grant, R. J., and Overton, T. R. (2011). Associations of prepartum plasma cortisol, haptoglobin, fecal cortisol metabolites, and nonesterified fatty acids with postpartum health status in Holstein dairy cows. *J. Dairy Sci.* 94, 5878–5889. doi: 10.3168/jds.2010-3391

Iyasere, O. S., Edwards, S. A., Bateson, M., Mitchell, M., and Guy, J. H. (2017). Validation of an intramuscularly-implanted microchip and a surface infrared thermometer to estimate core body temperature in broiler chickens exposed to heat stress. *Comput. Electron. Agric.* 33, 1–8. doi: 10.1016/j.compag.2016.12.010

Jacobs, J. A., and Siegford, J. M. (2012). Invited review: the impact of automatic milking systems on dairy cow management, behavior, health, and welfare. *J. Dairy Sci.* 95, 2227–2247. doi: 10.3168/jds.2011-4943

Jamrozik, J., Koeck, A., Kistemaker, G. J., and Miglior, F. (2016). Multiple-trait estimates of genetic parameters for metabolic disease traits, fertility disorders, and their predictors in Canadian Holsteins. *J. Dairy Sci.* 99, 1990–1998. doi: 10.3168/jds.2015-10505

Jamrozik, J., and Miller, S. P. (2014). Genetic evaluation of calving ease in Canadian Simmentals using birth weight and gestation length as correlated traits. *Livest. Sci.* 162, 42–49. doi: 10.1016/j.livsci.2014.01.027

Jayaraman, B., and Nyachoti, C. M. (2017). Husbandry practices and gut health outcomes in weaned piglets: a review. *Anim. Nutr.* 3, 205–211. doi: 10.1016/j.aninu.2017.06.002

Jensen, A. B., Palme, R., and Forkman, B. (2006). Effect of brooders on feather pecking and cannibalism in domestic fowl (*Gallus gallus* domesticus). *Appl. Animal Behav. Sci.* 99, 287–300. doi: 10.1016/j.applanim.2005.10.017

Jensen, P., Buitenhuis, B., Kjaer, J., Zanella, A., Mormède, P., and Pizzari, T. (2008). Genetics and genomics of animal behaviour and welfare-Challenges and possibilities. *Appl. Anim. Behav. Sci.* 113, 383–403. doi: 10.1016/j.applanim.2008.01.012

Jia, W., Bandodkar, A. J., Valdés-Ramírez, G., Windmiller, J. R., Yang, Z., Ramírez, J., et al. (2013). Electrochemical tattoo biosensors for real-time noninvasive lactate monitoring in human perspiration. *Anal. Chem.* 85, 6553–6560. doi: 10.1021/ac401573r

Jirkof, P., Rudeck, J., and Lewejohann, L. (2019). Assessing affective state in laboratory rodents to promote animal welfare—what is the progress in applied refinement research? *Animals* 9:1026. doi: 10.3390/ani9121026

Johnson, A. K., and Marchant-Forde, J. N. (2009). "Welfare of pigs in the farrowing environment," in *The Welfare of Pigs*, ed. J. N. Marchant-Forde (Cham: Springer), 141–178.

Johnson, J. S. (2018). Heat stress: impact on livestock well-being and productivity and mitigation strategies to alleviate the negative effects. *Anim. Prod. Sci.* 58, 1404–1413. doi: 10.1071/AN17725

Johnson, J. S., Martin, K. L., Pohler, K. G., and Stewart, K. R. (2016). Effects of rapid temperature fluctuations prior to breeding on reproductive efficiency in replacement gilts. *J. Therm. Biol.* 61, 29–37. doi: 10.1016/j.jtherbio.2016.08.003

Johnson, J. S., and Shade, K. A. (2017). Characterizing body temperature and activity changes at the onset of estrus in replacement gilts. *Livest. Sci.* 199, 22–24. doi: 10.1016/j.livsci.2017.03.004

Johnston, D., Kenny, D. A., McGee, M., Waters, S. M., Kelly, A. K., and Earley, B. (2016). Electronic feeding behavioural data as indicators of health status in dairy calves. *Irish J. Agric. Food Res.* 55, 159–168. doi: 10.1515/ijafr-2016-0016

Jones, R. B., Beuving, G., and Blokhuis, H. J. (1988). Tonic immobility and heterophil/ lymphocyte responses of the domestic fowl to corticosterone infusion. *Phys. Behav.* 42, 249–253. doi: 10.1016/0031-9384(88)90078-9

Jorquera-Chavez, M., Fuentes, S., Dunshea, F. R., Warner, R. D., Poblete, T., and Jongman, E. C. (2019). Modelling and validation of computer vision techniques to assess heart rate, eye temperature, ear-base temperature and respiration rate in cattle. *Animals* 9:1089. doi: 10.3390/ani9121089

Kapell, D. N. R. G., Hill, W. G., Neeteson, A. M., McAdam, J., Koerhuis, A. N. M., and Avendaño, S. (2012). Twenty-five years of selection for improved leg health in purebred broiler lines and underlying genetic parameters. *Poult. Sci.* 91, 3023–3043. doi: 10.3382/ps.2012-02578

Kapell, D. N. R. G., Hocking, P. M., Glover, P. K., Kremer, V. D., and Avendaño, S. (2017). Genetic basis of leg health and its relationship with body weight in purebred turkey lines. *Poult. Sci.* 96, 1553–1562. doi: 10.3382/ps/pew479

Kaplan, R. M., Burke, J. M., Terrill, T. H., Miller, J. E., Getz, W. R., Mobini, S., et al. (2004). Validation of the FAMACHA© eye color chart for detecting clinical anemia in sheep and goats on farms in the southern United States. *Vet. Parasitol.* 123, 105–120. doi: 10.1016/j.vetpar.2004.06.005

Karsas, M., Lamb, G., and Green, R. J. (2018). The immunology of mind control – Exploring the relationship between the microbiome and the brain-part 1. *Curr. Allergy Clin. Immunol.* 31, 103–109.

Kashiha, M., Bahr, C., Ott, S., Moons, C. P. H., Niewold, T. A., Ödberg, F. O., et al. (2013). Automatic identification of marked pigs in a pen using image pattern recognition. *Comp. Electron. Agric.* 93, 111–120. doi: 10.1016/j.compag.2013.01.013

Katiyatiya, C. L. F., Bradley, G., and Muchenje, V. (2017). Thermotolerance, health profile and cellular expression of HSP90AB1 in Nguni and Boran cows raised on natural pastures under tropical conditions. *J. Therm. Biol.* 69, 85–94. doi: 10.1016/j.jtherbio.2017.06.009

Keeling, L. J., Rushen, J., and Duncan, I. J. (2011). "Understanding animal welfare," in *Animal Welfare*, 2nd Edn, ed. D. Fraser (Hoboken, NJ: Wiley), 13–26. doi: 10.1079/9781845936594.0013

Keeling, L. J., Wallenbeck, A., Larsen, A., and Holmgren, N. (1996). Scoring tail damage in pigs: an evaluation based on recordings at Swedish slaughterhouses. *Acta Vet. Scand.* 54, 1–6. doi: 10.1186/1751-0147-54-32

Ketterson, E. D., and King, J. R. (1977). Metabolic and behavioral responses to fasting in the white-crowned sparrow (*Zonotrichia leucophrys* gambelii). *Physiol. Zool.* 50, 115–129. doi: 10.1086/physzool.50.2.30152551

Kim, H., Min, Y., and Choi, B. (2018). Monitoring cattle disease with ingestible bio-sensors utilizing LoRaWAN: method and case studies. *J. Korean Inst. Inf. Technol.* 16, 123–134. doi: 10.14801/jkiit.2018.16.4.123

Kim, K. S., Seibert, J. T., Edea, Z., Graves, K. L., Kim, E. S., Keating, A. F., et al. (2018). Characterization of the acute heat stress response in gilts: III. Genome-wide association studies of thermotolerance traits in pigs. *J. Anim. Sci.* 96, 2074–2085. doi: 10.1093/jas/sky131

King, M. T. M., and DeVries, T. J. (2018). Graduate student literature review: detecting health disorders using data from automatic milking systems and associated technologies. *J. Dairy Sci.* 101, 8605–8614. doi: 10.3168/jds.2018-14521

Knap, P. W. (2005). Breeding robust pigs. *Aust. J. Exp. Agric.* 45, 763–773. doi: 10.1071/EA05041

Knap, P. W. (2008). "Robustness," in *Resource Allocation Theory Applied to Farm Animal Production*, ed. W. M. Rauw (Wallingford: CABI), 288–301.

Knízková, I., Kunc, P., Gürdíl, G. A. K., Pinar, Y., and Selví, K. Ç (2007). Applications of infrared thermography in animal production. *J. Fac. Agric.* 22, 329–336.

Knol, E. F., Leenhouwers, J. I., and Van der Lende, T. (2002). Genetic aspects of piglet survival. *Livest. Prod. Sci.* 48, 47–55. doi: 10.1016/S0301-6226(02)00184-187

Köck, A., Ledinek, M., Gruber, L., Steininger, F., Fuerst-Waltl, B., and Egger-Danner, C. (2018). Genetic analysis of efficiency traits in Austrian dairy cattle and their relationships with body condition score and lameness. *J. Dairy Sci.* 101, 445–455. doi: 10.3168/jds.2017-13281

Koeck, A., Jamrozik, J., Schenkel, F. S., Moore, R. K., Lefebvre, D. M., Kelton, D. F., et al. (2014). Genetic analysis of milk β-hydroxybutyrate and its association

with fat-to-protein ratio, body condition score, clinical ketosis, and displaced abomasum in early first lactation of Canadian Holsteins. *J. Dairy Sci.* 97, 7286–7292. doi: 10.3168/jds.2014-8405

Koknaroglu, H., and Akunal, T. (2013). Animal welfare: an animal science approach. *Meat Sci.* 95, 821–827. doi: 10.1016/j.meatsci.2013.04.030

Koltes, J. E., Cole, J. B., Clemmens, R., Dilger, R. N., Kramer, L. M., Lunney, J. K., et al. (2019). A vision for development and utilization of high-throughput phenotyping and big data analytics in livestock. *Front. Genet.* 10:1197. doi: 10.3389/fgene.2019.01197

Kongsro, J. (2014). Estimation of pig weight using a Microsoft Kinect prototype imaging system. *Comput. Electron. Agric.* 109, 32–35. doi: 10.1016/j.compag.2014.08.008

König, S., and May, K. (2019). Invited review: phenotyping strategies and quantitative-genetic background of resistance, tolerance and resilience associated traits in dairy cattle. *Animal* 13, 897–908. doi: 10.1017/S1751731118003208

Kovács, L., Jurkovich, V., Bakony, M., Szenci, O., Póti, P., and TåZsér, J. (2014). Welfare implication of measuring heart rate and heart rate variability in dairy cattle: literature review and conclusions for future research. *Animal* 8, 316–330. doi: 10.1017/S1751731113002140

Kozak, M., Tobalske, B., Martins, C., Bowley, S., Wuerbel, H., and Harlander-Matauschek, A. (2016a). Use of space by domestic chicks housed in complex aviaries. *Appl. Animal Behav. Sci.* 181, 115–121. doi: 10.1016/j.applanim.2016.05.024

Kozak, M., Tobalske, B., Springthorpe, D., Szkotnicki, B., and Harlander-Matauschek, A. (2016b). Development of physical activity levels in laying hens in three-dimensional aviaries. *Appl. Animal Behav. Sci.* 185, 66–72.

Kpodo, K. R., Duttlinger, A. W., and Johnson, J. S. (2019). Effects of pen location on thermoregulation and growth performance in grow-finish pigs during late summer. *Transl. Anim. Sci.* 3:txz033. doi: 10.1093/tas/txz033

Kraimi, N., Dawkins, M., Gebhardt-Henrich, S. G., Velge, P., Rychlik, I., Volf, J., et al. (2019). Influence of the microbiota-gut-brain axis on behavior and welfare in farm animals: a review. *Physiol. Behav.* 210:112658. doi: 10.1016/j.physbeh.2019.112658

Kume, S., Nonaka, K., Oshita, T., and Kozakai, T. (2010). Evaluation of drinking water intake, feed water intake and total water intake in dry and lactating cows fed silages. *Livest. Sci.* 128, 46–51. doi: 10.1016/j.livsci.2009.10.012

Kurilshikov, A., Wijmenga, C., Fu, J., and Zhernakova, A. (2017). Host genetics and gut microbiome: challenges and perspectives. *Trends Immunol.* 38, 633–647. doi: 10.1016/j.it.2017.06.003

Kyle, B. L., Kennedy, A. D., and Small, J. A. (1998). Measurement of vaginal temperature by radiotelemetry for the prediction of estrus in beef cows. *Theriogenology* 49, 1437–1449. doi: 10.1016/S0093-691X(98)00090-9

Laberge, B., and Rousseau, A. N. (2017). Rethinking environment control strategy of confined animal housing systems through precision livestock farming. *Biosyst. Eng.* 155, 96–123. doi: 10.1016/j.biosystemseng.2016.12.005

Lacey, B., Hamrita, T. K., Lacy, M. P., Van Wicklen, G. L., and Czarick, M. (2000). Monitoring deep body temperature responses of broilers using biotelemetry. *J. Appl. Poult. Res.* 9, 6–12. doi: 10.1093/japr/9.1.6

Lambton, S. L., Knowles, T. G., Yorke, C., and Nicol, C. J. (2015). The risk factors affecting the development of vent pecking and cannibalism in free-range and organic laying hens. *Anim. Welfare* 24, 101–111. doi: 10.7120/09627286.24.1.101

Lao, F., Brown-Brandl, T., Stinn, J. P., Liu, K., Teng, G., and Xin, H. (2016). Automatic recognition of lactating sow behaviors through depth image processing. *Comp. Elect. Agric.* 125, 56–62. doi: 10.1016/j.compag.2016.04.026

Larsen, H., Hemsworth, P. H., Cronin, G. M., Gebhardt-Henrich, S. G., Smith, C. L., and Rault, J. L. (2018). Relationship between welfare and individual ranging behaviour in commercial free-range laying hens. *Animal* 12, 2356–2364. doi: 10.1017/S1751731118000022

Lawrence, A. B., Vigors, B., and Sandøe, P. (2019). What is so positive about positive animal welfare?—A critical review of the literature. *Animals* 9:783. doi: 10.3390/ani9100783

Lee, J., Jin, L., Park, D., and Chung, Y. (2016a). Automatic recognition of aggressive behavior in pigs using a kinect depth sensor. *Sensors* 16:631. doi: 10.3390/s16050631

Lee, Y., Bok, J. D., Lee, H. J., Lee, H. G., Kim, D., Lee, I., et al. (2016b). Body temperature monitoring using subcutaneously implanted thermo-loggers from Holstein steers. *Asian Austral. J. Anim. Sci.* 29, 299–306. doi: 10.5713/ajas.15.0353

Leek, B. F. (1983). Clinical diseases of the rumen: a physiologist's view. *Vet. Rec.* 113, 110–114. doi: 10.1136/vr.113.1.10

Lees, A. M., Lees, J. C., Sejian, V., Wallage, A. L., and Gaughan, J. B. (2018). Short communication: using infrared thermography as an in situ measure of core body temperature in lot-fed Angus steers. *Int. J. Biometeorol.* 62, 3–8. doi: 10.1007/s00484-017-1433-y

Leonard, S. M., Xin, H., Brown-Brandl, T. M., and Ramirez, B. C. (2019). Development and application of an image acquisition system for characterizing sow behaviors in farrowing stalls. *Comp. Elect. Agric.* 163:104866. doi: 10.1016/j.compag.2019.104866

Li, L., and Brown, D. J. (2016). Estimation of genetic parameters for lambing ease, birthweight and gestation length in Australian sheep. *Anim. Prod. Sci.* 56, 934–940. doi: 10.1071/AN14129

Liakos, K. G., Busato, P., Moshou, D., Pearson, S., and Bochtis, D. (2018). Machine learning in agriculture: a review. *Sensors* 18:2674. doi: 10.3390/s18082674

Liang, D., Wood, C. L., McQuerry, K. J., Ray, D. L., Clark, J. D., and Bewley, J. M. (2013). Influence of breed, milk production, season, and ambient temperature on dairy cow reticulorumen temperature. *J. Dairy Sci.* 96, 5072–5081. doi: 10.3168/jds.2012-6537

Littlejohn, M. D., Henty, K. M., Tiplady, K., Johnson, T., Harland, C., Lopdell, T., et al. (2014). Functionally reciprocal mutations of the prolactin signalling pathway define hairy and slick cattle. *Nat. Commun.* 5, 1–8. doi: 10.1038/ncomms6861

Liu, Z., Zhang, D., Wang, W., He, X., Peng, F., Wang, L., et al. (2017). A comparative study of the effects of long-term cold exposure, and cold resistance in min pigs and large white pigs. *Acta Agric. Scand. A Anim. Sci.* 67, 34–39. doi: 10.1080/09064702.2018.1431306

Lohölter, M., Rehage, R., Meyer, U., Lebzien, P., Rehage, J., and Dänicke, S. (2013). Evaluation of a device for continuous measurement of rumen pH and temperature considering localization of measurement and dietary concentrate proportion. *Landbauforsch. Volkenrode.* 63, 61–68. doi: 10.3220/LBF-2013-61-68

López Armengol, M. F., Freund, R. P., Giménez, G. N., and Rubio, N. (2017). Effect of extreme severe heat stress on respiratory rate in unshorn and shorn Australian Merino rams from Northern Patagonia. *Braz. J. Vet. Res. Anim. Sci.* 54, 36–47. doi: 10.11606/issn.1678-4456.bjvras.2017.108524

Løvendahl, P., Damgaard, L. H., Nielsen, B. L., Thodberg, K., Su, G., and Rydhmer, L. (2005). Aggressive behaviour of sows at mixing and maternal behaviour are heritable and genetically correlated traits. *Livest. Prod. Sci.* 93, 73–85. doi: 10.1016/j.livprodsci.2004.11.008

Lowe, G., Sutherland, M., Waas, J., Schaefer, A., Cox, N., and Stewart, M. (2019). Infrared thermography—A non-invasive method of measuring respiration rate in calves. *Animals* 9:535. doi: 10.3390/ani9080535

Mallard, B. A., Emam, M., Paibomesai, M., Thompson-Crispi, K., and Wagter-Lesperance, L. (2015). Genetic selection of cattle for improved immunity and health. *Jpn. J. Vet. Res.* 63(Suppl. 1), S37–S44.

Mallikarjunappa, S., Schenkel, F. S., Brito, L. F., Bissonette, N., Miglior, F., Chesnais, J., et al. (2020). Association of genetic polymorphisms related to Johne's disease with estimated breeding values of Holstein sires for milk ELISA test scores. *BMC Vet. Res.* 16:165. doi: 10.1186/s12917-020-02381-9

Manning, J. K., Cronin, G. M., González, L. A., Hall, E. J. S., Merchant, A., and Ingram, L. J. (2017). The effects of global navigation satellite system (GNSS) collars on cattle (*Bos taurus*) behaviour. *Appl. Anim. Behav. Sci.* 187, 154–159. doi: 10.1016/j.applanim.2016.11.013

Manteuffel, C., Hartung, E., Schmidt, M., Hoffmann, G., and Schön, P. C. (2017). Online detection and localisation of piglet crushing using vocalisation analysis and context data. *Comp. Elect. Agric.* 135, 108–114. doi: 10.1016/j.compag.2016.12.017

Manteuffel, G. (2002). Central nervous regulation of the hypothalamic-pituitary-adrenal axis and its impact on fertility, immunity, metabolism and animal welfare-A review. *Arch. Anim. Breed.* 45, 575–595. doi: 10.5194/aab-45-575-2002

Marchant, J. N., Broom, D. M., and Corning, S. (2001). The influence of sow behaviour on piglet mortality due to crushing in an open farrowing system. *Anim. Sci.* 72, 19–28. doi: 10.1017/S135772980005551X

Marchant-Forde, J. N. (2015). The science of animal behavior and welfare: challenges, opportunities, and global perspective. *Front. Vet. Sci.* 2:16. doi: 10.3389/fvets.2015.00016

Marchant-Forde, J. N., Lay, D. C. Jr., McMunn, K. A., Cheng, H. W., Pajor, E. A., et al. (2009). Post-natal piglet husbandry practices and well-being: the effects of alternative techniques delivered separately. *J. Anim. Sci.* 87, 1479–1492. doi: 10.2527/jas.2008-1080

Marie-Etancelin, C., Francois, D., Weisbecker, J.-L., Marcon, D., Moreno-Romieux, C., Bouvier, F., et al. (2019). Detailed genetic analysis of feeding behaviour in Romane lambs and links with residual feed intake. *J. Anim. Breed. Genet.* 136, 174–182. doi: 10.1111/jbg.12392

Martin, P., Barkema, H. W., Brito, L. F., Narayana, S. G., and Miglior, F. (2018). Symposium review: novel strategies to genetically improve mastitis resistance in dairy cattle. *J. Dairy Sci.* 101, 2724–2736. doi: 10.3168/jds.2017-13554

Maselyne, J., Saeys, W., and Van Nuffel, A. (2015). Review: quantifying animal feeding behaviour with a focus on pigs. *Physiol. Behav.* 138, 37–51. doi: 10.1016/j.physbeh.2014.09.012

Mason, G. (2006). "Stereotypic behaviour in captive animals: fundamentals and implications for welfare and beyond," in *Stereotypic Animal Behaviour: Fundamentals and Applications to Welfare*, Second Edn, eds J. Rushen and G. Mason (Wallingford: CABI), 325–356. doi: 10.1079/9780851990040.0325

Mathew, A. G., Cissell, R., and Liamthong, S. (2007). Antibiotic resistance in bacteria associated with food animals: a United States perspective of livestock production. *Foodborne Pathog. Dis.* 4, 115–133. doi: 10.1089/fpd.2006.0066

Mathijs, E. (2004). *Socio-Economic Aspects of Automatic Milking. In Automatic Milking—A Better Understanding*. Wageningen: Academic Publishers, 46–55.

Mattachini, G., Antler, A., Riva, E., Arbel, A., and Provolo, G. (2013). Automated measurement of lying behavior for monitoring the comfort and welfare of lactating dairy cows. *Livest. Sci.* 158, 145–150. doi: 10.1016/j.livsci.2013.10.014

Matthews, S. G., Miller, A. L., Clapp, J., Plötz, T., and Kyriazakis, I. (2016). Early detection of health and welfare compromises through automated detection of behavioural changes in pigs. *Vet. J.* 217, 43–51. doi: 10.1016/j.tvjl.2016.09.005

Mayorga, E. J., Ross, J. W., Keating, A. F., Rhoads, R. P., and Baumgard, L. H. (2020). Biology of heat stress: the nexus between intestinal hyperpermeability and swine reproduction. *Theriogenology* 154, 73–83. doi: 10.1016/j.theriogenology.2020.05.023

McCulloch, S. P. (2013). A critique of FAWC's five freedoms as a framework for the analysis of animal welfare. *J. Agric. Environ. Ethics* 26, 959–975. doi: 10.1007/s10806-012-9434-9437

McLaren, A., Mucha, S., Mrode, R., Coffey, M., and Conington, J. (2016). Genetic parameters of linear conformation type traits and their relationship with milk yield throughout lactation in mixed-breed dairy goats. *J. Dairy Sci.* 99, 5516–5525. doi: 10.3168/jds.2015-10269

Mcloughlin, M. P., Stewart, R., and McElligott, A. G. (2019). Automated bioacoustics: methods in ecology and conservation and their potential for animal welfare monitoring. *J. R. Soc. Interf.* 16:20190225. doi: 10.1098/rsif.2019.0225

McRae, K. M., Baird, H. J., Dodds, K. G., Bixley, M. J., and Clarke, S. M. (2016). Incidence and heritability of ovine pneumonia, and the relationship with production traits in New Zealand sheep. *Small Rumin. Res.* 145, 136–141. doi: 10.1016/j.smallrumres.2016.11.003

Mellor, D. J. (2016). Updating animal welfare thinking: moving beyond the "five freedoms" towards "A lifeworth living.". *Animals* 6:21. doi: 10.3390/ani6030021

Metkar, S. K., and Girigoswami, K. (2019). Diagnostic biosensors in medicine–A review. *Biocatal. Agric. Biotechnol.* 17, 271–283. doi: 10.1016/j.bcab.2018.11.029

Meuwissen, T. H. E., Hayes, B. J., and Goddard, M. E. (2001). Prediction of total genetic value using genome-wide dense marker maps. *Genetics* 157, 1819–1829.

Meuwissen, T., Hayes, B., and Goddard, M. (2016). Genomic selection: a paradigm shift in animal breeding. *Anim. Front.* 6, 6–14. doi: 10.2527/af.2016-0002

Miglior, F., Fleming, A., Malchiodi, F., Brito, L. F., Martin, P., and Baes, C. F. (2017). A 100-year review: identification and genetic selection of economically important traits in dairy cattle. *J. Dairy Sci.* 100, 10251–10271. doi: 10.3168/JDS.2017-12968

Mignon-Grasteau, S., Chantry-Darmon, C., Boscher, M. Y., Sellier, N., Le Bihan-Duval, E., and Bertin, A. (2017). Genetic determinism of fearfulness, general activity and feeding behavior in chickens and its relationship with digestive efficiency. *Behav. Genet.* 47, 114–124. doi: 10.1007/s10519-016-9807-1

Milan, H. F. M., Maia, A. S. C., and Gebremedhin, K. G. (2016). Technical note: device for measuring respiration rate of cattle under field conditions. *J. Anim. Sci.* 94, 5434–5438. doi: 10.2527/jas.2016-0904

Miranda-de la Lama, G. C., Pascual-Alonso, M., Guerrero, A., Alberti, P., Alierta, S., Sans, P., et al. (2013). Influence of social dominance on production, welfare and the quality of meat from beef bulls. *Meat Sci.* 94, 432–437. doi: 10.1016/j.meatsci.2013.03.026

Misztal, I. (2017). Breeding and genetics symposium: resilience and lessons from studies in genetics of heat stress. *J. Anim. Sci.* 95, 1780–1787. doi: 10.2527/jas2016.0953

Moberg, G. P. (2009). "Biological response to stress: implications for animal welfare," in *The Biology of Animal Stress: Basic Principles and Implications for Animal Welfare*, eds G. P. Moberg and J. A. Mench (Wallingford: CABI).

Moberg, G. P., and Mench, J. A. (eds). (2000). *The Biology of Animal Stress: Basic Principles and Implications for Animal Welfare*. Wallingford: CABI.

Mormède, P., Foury, A., Terenina, E., and Knap, P. W. (2011). Breeding for robustness: the role of cortisol. *Animal* 5, 651–657. doi: 10.1017/S1751731110002168

Morota, G., Ventura, R. V., Silva, F. F., Koyama, M., and Fernando, S. C. (2018). Big data analytics and precision animal agriculture symposium: machine learning and data mining advance predictive big data analysis in precision animal agriculture. *J. Anim. Sci.* 96, 1540–1550. doi: 10.1093/jas/sky014

Moser, J., Kriehuber, E., and Trautinger, F. (2012). A simple and rapid quantitative sweat test based on cobalt chloride color change. *Skin Pharm. Physiol.* 25, 150–154. doi: 10.1159/000336922

Mostaço, G. M., Miranda, K. O. D. S., Condotta, I., and Salgado, D. (2015). Determination of piglets' rectal temperature and respiratory rate through skin surface temperature under climatic chamber conditions. *Eng. Agric.* 35, 979–989. doi: 10.1590/1809-4430-Eng.Agric.v35n6p979-989/2015

Mota, R. R., Lopes, P. S., Tempelman, R. J., Silva, F. F., Aguilar, I., Gomes, C. C. G., et al. (2016). Genome-enabled prediction for tick resistance in Hereford and Braford beef cattle via reaction norm models. *J. Anim. Sci.* 94, 1834–1843. doi: 10.2527/jas.2015-0194

Mottram, T., Lowe, J., McGowan, M., and Phillips, N. (2008). Technical note: a wireless telemetric method of monitoring clinical acidosis in dairy cows. *Comp. Elect. Agric.* 64, 45–48. doi: 10.1016/j.compag.2008.05.015

Moura, D. J., Silva, W. T., Naas, I. A., Tolón, Y. A., Lima, K. A. O., and Vale, M. M. (2008). Real time computer stress monitoring of piglets using vocalization analysis. *Comp. Elect. Agric.* 64, 11–18. doi: 10.1016/j.compag.2008.05.008

Mu, C., Yang, Y., and Zhu, W. (2016). Gut microbiota: the brain peacekeeper. *Front. Microbiol.* 7:345. doi: 10.3389/fmicb.2016.00345

Muir, W. M. (1996). Group selection for adaptation to multiple-hen cages: selection program and direct responses. *Poult. Sci.* 75, 447–458. doi: 10.3382/ps.0750447

Muir, W. M. (2003). "Indirect selection for improvement of animal well-being," in *Poultry Genetics, Breeding and Biotechnology*, eds W. M. Muir and S. E. Aggrey (Wallingford: CABI), 247–256.

Muir, W. M. (2005). Incorporation of competitive effects in forest tree or animal breeding programs. *Genetics* 170, 1247–1259. doi: 10.1534/genetics.104.035956

Muir, W. M., Bijma, P., and Schinckel, A. (2013). Multilevel selection with kin and non-kin groups, experimental results with japanese quail (coturnix japonica). *Evolution* 67, 1598–1606. doi: 10.1111/evo.12062

Muir, W. M., Cheng, H. W., and Croney, C. (2014). Methods to address poultry robustness and welfare issues through breeding and associated ethical considerations. *Front. Genet.* 5:407. doi: 10.3389/fgene.2014.00407

Mungroo, N. A., and Neethirajan, S. (2014). Biosensors for the detection of antibiotics in poultry industry-A review. *Biosensors* 4, 472–493. doi: 10.3390/bios4040472

Muns, R., Nuntapaitoon, M., and Tummaruk, P. (2016). Non-infectious causes of pre-weaning mortality in piglets. *Livest. Sci.* 184, 46–57. doi: 10.1016/j.livsci.2015.11.025

Munsterhjelm, C., Heinonen, M., and Valros, A. (2015). Effects of clinical lameness and tail biting lesions on voluntary feed intake in growing pigs. *Livest. Sci.* 181, 210–219. doi: 10.1016/j.livsci.2015.09.003

Nääs, I. A., Garcia, R. G., and Caldara, F. R. (2014). Infrared thermal image for assessing animal health and welfare. *J. Anim. Behav. Biometeorol.* 2, 66–72. doi: 10.14269/2318-1265/jabb.v2n3p66-72

Nalon, E., Conte, S., Maes, D., Tuyttens, F. A. M., and Devillers, N. (2013). Assessment of lameness and claw lesions in sows. *Livest. Sci.* 156, 10–23. doi: 10.1016/j.livsci.2013.06.003

Nasirahmadi, A., Edwards, S. A., and Sturm, B. (2017). Implementation of machine vision for detecting behaviour of cattle and pigs. *Livest. Sci.* 202, 25–38. doi: 10.1016/j.livsci.2017.05.014

Nayeri, S., Sargolzaei, M., and Tulpan, D. (2019). A review of traditional and machine learning methods applied to animal breeding. *Anim. Heal. Res. Rev.* 20, 31–46. doi: 10.1017/S1466252319000148

N'dri, A. L., Mignon-Grasteau, S., Sellier, N., Beaumont, C., and Tixier-Boichard, M. (2007). Interactions between the naked neck gene, sex, and fluctuating ambient temperature on heat tolerance, growth, body composition, meat quality, and sensory analysis of slow growing meat-type broilers. *Livest. Sci.* 110, 33–45. doi: 10.1016/j.livsci.2006.09.025

Neethirajan, S. (2017). Recent advances in wearable sensors for animal health management. *Sens. Bio Sens. Res.* 12, 15–29. doi: 10.1016/j.sbsr.2016.11.004

Neethirajan, S., Tuteja, S. K., Huang, S. T., and Kelton, D. (2017). Recent advancement in biosensors technology for animal and livestock health management. *Biosens. Bioelectron.* 98, 398–407. doi: 10.1016/j.bios.2017.07.015

Nguyen, T. T. T., Bowman, P. J., Haile-Mariam, M., Nieuwhof, G. J., Hayes, B. J., and Pryce, J. E. (2017). Short communication: implementation of a breeding value for heat tolerance in Australian dairy cattle. *J. Dairy Sci.* 100, 7362–7367. doi: 10.3168/jds.2017-12898

Nielsen, B., Su, G., Lund, M. S., and Madsen, P. (2013). Selection for increased number of piglets at d 5 after farrowing has increased litter size and reduced piglet mortality. *J. Anim. Sci.* 91, 2575–2582. doi: 10.2527/jas.2012-5990

Nielsen, H. M., Amer, P. R., and Olesen, I. (2008). "Challenges of including welfare and environmental concerns in the breeding goal," in *Proceedings of the European Association of Animal Production*, Vilnius, 24–27.

Nixon, M., Bohmanova, J., Jamrozik, J., Schaeffer, L. R., Hand, K., and Miglior, F. (2009). Genetic parameters of milking frequency and milk production traits in Canadian Holsteins milked by an automated milking system. *J. Dairy Sci.* 92, 3422–3430. doi: 10.3168/jds.2008-1689

Nkrumah, J. D., Crews, D. H. Jr., Basarab, J. A., Price, M. A., Okine, E. K., Wang, Z., et al. (2007). Genetic and phenotypic relationships of feeding behavior and temperament with performance, feed efficiency, ultrasound, and carcass merit of beef cattle. *J. Anim. Sci.* 85, 2382–2390. doi: 10.2527/jas.2006-657

Nogami, H., Okada, H., Miyamoto, T., Maeda, R., and Itoh, T. (2014). Wearable wireless temperature sensor nodes appressed to base of a calf's tail. *Sens. Mater.* 26, 539–545. doi: 10.18494/sam.2014.1043

Norris, D., Ngambi, J. W., Mabelebele, M., Alabi, O. J., and Benyi, K. (2014). Genetic selection for docility: a review. *J. Anim. Plant Sci.* 24, 13–18.

Norton, T., and Berckmans, D. (2018). "Precision livestock farming: the future of livestock welfare monitoring and management?," in *Animal Welfare in a Changing World*, ed. A. Butterworth (Wallingford: CABI).

Nursita, I. W., and Cholis, N. (2019). Mapping efforts of the advantages of local beef thermotolerance: comparison of sweating rate of Peranakan Ongole cattle and it's cross with *Bos taurus*. *Earth Environ. Sci.* 239:012023. doi: 10.1088/1755-1315/239/1/012023

Nuutinen, J., Alanen, E., Autio, P., Lahtinen, M. R., Harvima, I., and Lahtinen, T. (2003). A closed unventilated chamber for the measurement of transepidermal water loss. *Sci. Res. Technol.* 9, 85–89. doi: 10.1034/j.1600-0846.2003.00025.x

Nyman, A. K., Persson Waller, K., Bennedsgaard, T. W., Larsen, T., and Emanuelson, U. (2014). Associations of udder-health indicators with cow factors and with intramammary infection in dairy cows. *J. Dairy Sci.* 97, 5459–5473. doi: 10.3168/jds.2013-7885

Oczak, M., Ismayilova, G., Costa, A., Viazzi, S., Sonoda, L. T., Fels, M., et al. (2013). Analysis of aggressive behaviours of pigs by automatic video recordings. *Comp. Elect. Agric.* 99, 209–217. doi: 10.1016/j.compag.2013.09.015

Oczak, M., Maschat, K., Berckmans, D., Vranken, E., and Baumgartner, J. (2015). Classification of nest-building behaviour in non-crated farrowing sows on the basis of accelerometer data. *Biosyst. Eng.* 140, 148–158. doi: 10.1016/j.biosystemseng.2015.09.007

Oliveira, D. P., Lourenco, D. A. L., Tsuruta, S., Misztal, I., Santos, D. J. A., De Araújo Neto, F. R., et al. (2018). Reaction norm for yearling weight in beef cattle using single-step genomic evaluation. *J. Anim. Sci.* 96, 27–34. doi: 10.1093/jas/skx006

Oliveira, H. R., Brito, L. F., Lourenco, D. A. L., Silva, F. F., Jamrozik, J., Schaeffer, L. R., et al. (2019a). Invited review: advances and applications of random regression models: from quantitative genetics to genomics. *J. Dairy Sci.* 102, 7664–7683. doi: 10.3168/jds.2019-16265

Oliveira, H. R., Lourenco, D. A. L., Masuda, Y., Misztal, I., Tsuruta, S., Jamrozik, J., et al. (2019b). Single-step genome-wide association for longitudinal traits of Canadian Ayrshire, Holstein, and Jersey dairy cattle. *J. Dairy Sci.* 102, 9995–10011. doi: 10.3168/jds.2019-16821

Olsson, A. S., Würbel, H., and Mench, J. A. (2011). *Behaviour in Animal Welfare*. Wallingford: CABI.

Osei-Amponsah, R., Chauhan, S. S., Leury, B. J., Cheng, L., Cullen, B., Clarke, I. J., et al. (2019). Genetic selection for thermotolerance in ruminants. *Animals* 9:948. doi: 10.3390/ani9110948

Ott, S., Soler, L., Moons, C. P. H., Kashiha, M. A., Bahr, C., Vandermeulen, J., et al. (2014). Different stressors elicit different responses in the salivary biomarkers cortisol, haptoglobin, and chromogranin A in pigs. *Res. Vet. Sci.* 97, 124–128. doi: 10.1016/j.rvsc.2014.06.002

Oviedo-Rondón, E. O., Lascelles, B. D. X., Arellano, C., Mente, P. L., Eusebio-Balcazar, P., Grimes, J. L., et al. (2017). Gait parameters in four strains of turkeys and correlations with bone strength. *Poult. Sci.* 96, 1989–2005. doi: 10.3382/ps/pew502

Palme, R. (2012). Monitoring stress hormone metabolites as a useful, non-invasive tool for welfare assessment in farm animals. *Anim. Welfare* 21, 331–337. doi: 10.7120/09627286.21.3.331

Papadopoulos, E., Gallidis, E., and Ptochos, S. (2012). Anthelmintic resistance in sheep in Europe: a selected review. *Vet. Parasitol.* 189, 85–89. doi: 10.1016/j.vetpar.2012.03.036

Parois, S. P., Duttlinger, A. W., Richert, B. T., Lindemann, S. R., Johnson, J. S., and Marchant-Forde, J. N. (2020). Replacing dietary antibiotics with 0.*20%* L-glutamine in swine nursery diets after weaning and transport: impact on short and long-term welfare markers, behaviors and microbiota. *Front. Vet. Sci.* 7:140. doi: 10.3389/fvets.2020.00140

Pawluski, J., Jego, P., Henry, S., Bruchet, A., Palme, R., Coste, C., et al. (2017). Low plasma cortisol and fecal cortisol metabolite measures as indicators of compromised welfare in domestic horses (*Equus caballus*). *PLoS One* 12:e0182257. doi: 10.1371/journal.pone.0182257

Peixoto, M. G. C. D., Pires, M. F. A., Pereira, M. C., Carvalho, M. R. S., Ribeiro, G. C., Brito, L. F., et al. (2011). Integrando o temperamento às características de importância para o melhoramento de bovinos de leite: resultados de um estudo com fêmeas Guzerá. *Rev. Bras. Zoot.* 40, 26–37.

Phocas, F., Belloc, C., Bidanel, J., Delaby, L., Dourmad, J. Y., Dumont, B., et al. (2016a). Towards the agroecological management of ruminants, pigs and poultry through the development of sustainable breeding programmes: I. Selection goals and criteria. *Animal* 10, 1749–1759. doi: 10.1017/S1751731116000926

Phocas, F., Belloc, C., Bidanel, J., Delaby, L., Dourmad, J. Y., Dumont, B., et al. (2016b). Towards the agroecological management of ruminants, pigs and poultry through the development of sustainable breeding programmes. II. Breeding strategies. *Animal* 10, 1760–1769. doi: 10.1017/S1751731116001051

Piccoli, M. L., Brito, L. F., Braccini, J., Oliveira, H. R., Cardoso, F. F., Roso, V. M., et al. (2020). Comparison of genomic prediction methods for evaluation of adaptation and productive efficiency traits in Braford and Hereford cattle. *Livest. Sci.* 231:103864. doi: 10.1016/j.livsci.2019.103864

Poppe, M., Mulder, H. A., Ducro, B. J., and de Jong, G. (2019). Genetic analysis of udder conformation traits derived from automatic milking system recording in dairy cows. *J. Dairy Sci.* 102, 1386–1396. doi: 10.3168/jds.2018-14838

Porto, S. M. C., Arcidiacono, C., Anguzza, U., and Cascone, G. (2015). The automatic detection of dairy cow feeding and standing behaviours in free-stall barns by a computer vision-based system. *Biosyst. Eng.* 133, 46–55. doi: 10.1016/j.biosystemseng.2015.02.012

Preisinger, R. (2018). Innovative layer genetics to handle global challenges in egg production. *Br. Poult. Sci.* 59, 1–6. doi: 10.1080/00071668.2018.1401828

Pryce, J. E., Parker Gaddis, K. L., Koeck, A., Bastin, C., Abdelsayed, M., Gengler, N., et al. (2016). Invited review: opportunities for genetic improvement of metabolic diseases. *J. Dairy Sci.* 99, 6855–6873. doi: 10.3168/jds.2016-10854

Putz, A. M., Harding, J. C. S., Dyck, M. K., Fortin, F., Plastow, G. S., and Dekkers, J. C. M. (2019). Novel resilience phenotypes using feed intake data from a natural disease challenge model in wean-to-finish pigs. *Front. Genet.* 9:660. doi: 10.3389/fgene.2018.00660

Quintanilla, R., Varona, L., and Noguera, J. L. (2006). Testing genetic determinism in rate of hoof growth in pigs using Bayes factors. *Livest. Sci.* 105, 50–56. doi: 10.1016/j.livsci.2006.04.030

Radcliffe, J. S., Brito, L. F., Reddivari, L., Schmidt, M., Herman, E. M., and Schinckel, A. P. (2019). A swine model of soy protein-induced food allergenicity: implications in human and swine nutrition. *Anim. Front.* 9, 52–59. doi: 10.1093/af/vfz025

Ralph, C. R., and Tilbrook, A. J. (2016). Invited review: the usefulness of measuring glucocorticoids for assessing animal welfare. *J. Anim. Sci.* 94, 457–470. doi: 10.2527/jas2015-9645

Ramos, P. V. B., Silva, F. F., da Silva, L. O. C., Santiago, G. G., Menezes, G. R., de, O., et al. (2020). Genomic evaluation for novel stayability traits in Nellore cattle. *Reprod. Domest. Anim.* 55, 266–273. doi: 10.1111/rda.13612

Rault, J. L., Carter, C. S., Garner, J. P., Marchant-Forde, J. N., Richert, B. T., and Lay, D. C. (2013). Repeated intranasal oxytocin administration in early life dysregulates the HPA axis and alters social behavior. *Physiol. Behav.* 112, 40–48. doi: 10.1016/j.physbeh.2013.02.007

Rauw, W. M., and Gomez-Raya, L. (2015). Genotype by environment interaction and breeding for robustness in livestock. *Front. Genet.* 6:310. doi: 10.3389/fgene.2015.00310

Rauw, W. M., Johnson, A. K., Gomez-Raya, L., and Dekkers, J. C. M. (2017). A hypothesis and review of the relationship between selection for improved production efficiency, coping behavior, and domestication. *Front. Genet.* 8:134. doi: 10.3389/fgene.2017.00134

Rauw, W. M., Kanis, E., Noordhuizen-Stassen, E. N., and Grommers, F. J. (1998). Undesirable side effects of selection for high production efficiency in farm animals: a review. *Livest. Prod. Sci.* 56, 15–33. doi: 10.1016/S0301-6226(98)00147-X

Ravagnolo, O., and Misztal, I. (2002). Effect of heat stress on nonreturn rate in holstein cows: genetic analyses. *J. Dairy Sci.* 85, 3092–3100. doi: 10.3168/jds.S0022-0302(02)74396-8

Reader, J. D., Green, M. J., Kaler, J., Mason, S. A., and Green, L. E. (2011). Effect of mobility score on milk yield and activity in dairy cattle. *J. Dairy Sci.* 94, 5045–5052. doi: 10.3168/jds.2011-4415

Reimert, I., Bolhuis, J. E., Kemp, B., and Rodenburg, T. B. (2013). Indicators of positive and negative emotions and emotional contagion in pigs. *Physiol. Behav.* 109, 42–50. doi: 10.1016/j.physbeh.2012.11.002

Rexroad, C., Vallet, J., Matukumalli, L. K., Reecy, J., Bickhart, D., Blackburn, H., et al. (2019). Genome to phenome: improving animal health, production, and well-being – a new USDA blueprint for animal genome research 2018–2027. *Front. Genet.* 10:327. doi: 10.3389/fgene.2019.00327

Roche, J. R., Friggens, N. C., Kay, J. K., Fisher, M. W., Stafford, K. J., and Berry, D. P. (2009). Body condition score and its association with dairy cow productivity, health, and welfare. *J. Dairy Sci.* 92, 5769–5801. doi: 10.3168/jds.2009-2431

Rodenburg, T. B., Bijma, P., Ellen, E. D., Bergsma, R., De Vries, S., Bolhuis, J. E., et al. (2010). Breeding amiable animals? Improving farm animal welfare by including social effects in breeding programmes. *Anim. Welfare* 19(Suppl. 1), 77–82.

Rodenburg, T. B., Komen, H., Ellen, E. D., Uitdehaag, K. A., and van Arendonk, J. A. M. (2008). Selection method and early-life history affect behavioural development, feather pecking and cannibalism in laying hens: a review. *Appl. Anim. Behav. Sci.* 110, 217–228. doi: 10.1016/j.applanim.2007.09.009

Rodenburg, T. B., and Turner, S. P. (2012). The role of breeding and genetics in the welfare of farm animals. *Anim. Front.* 2, 16–21. doi: 10.2527/af.2012-2044

Rohrer, G. A., Brown-Brandl, T., Rempel, L. A., Schneider, J. F., and Holl, J. (2013). Genetic analysis of behavior traits in swine production. *Livest. Sci.* 157, 28–37. doi: 10.1016/j.livsci.2013.07.002

Rotz, C. A., Coiner, C. U., and Soder, K. J. (2003). Automatic milking systems, farm size, and milk production. *J. Dairy Sci.* 86, 4167–4177. doi: 10.3168/jds.S0022-0302(03)74032-6

Rufener, C., Berezowski, J., Maximiano Sousa, F., Abreu, Y., Asher, L., and Toscano, M. J. (2018). Finding hens in a haystack: consistency of movement patterns within and across individual laying hens maintained in large groups. *Sci. Rep.* 8, 1–10. doi: 10.1038/s41598-018-29962-x

Ruis, M. A. W., Te Brake, J. H. A., Engel, B., Buist, W. G., Blokhuis, H. J., and Koolhaas, J. M. (2001). Adaptation to social isolation acute and long-term stress responses of growing gilts with different coping characteristics. *Physiol. Behav.* 73, 541–551. doi: 10.1016/S0031-9384(01)00548-0

Rushen, J., Butterworth, A., and Swanson, J. C. (2011). Animal behavior and well-being symposium:Farm animal welfare assurance: science and application. *J. Anim. Sci.* 89, 1219–1228. doi: 10.2527/jas.2010-3589

Rutten, C. J., Velthuis, A. G. J., Steeneveld, W., and Hogeveen, H. (2013). Invited review: sensors to support health management on dairy farms. *J. Dairy Sci.* 96, 1928–1952. doi: 10.3168/jds.2012-6107

Saeys, Y., Inza, I., and Larrañaga, P. (2007). A review of feature selection techniques in bioinformatics. *Bioinformation* 23, 2507–2517. doi: 10.1093/bioinformatics/btm344

Santana, M. L., Eler, J. P., Cardoso, F. F., Albuquerque, L. G., and Ferraz, J. B. S. (2013). Phenotypic plasticity of composite beef cattle performance using reaction norms model with unknown covariate. *Animal* 7, 202–210. doi: 10.1017/S1751731112001711

Scharf, B., Wax, L. E., Aiken, G. E., and Spiers, D. E. (2008). Regional differences in sweat rate response of steers to short-term heat stress. *Int. J. Biometeorol.* 52, 725–732. doi: 10.1007/s00484-008-0165-4

Scheffer, M., Bolhuis, J. E., Borsboom, D., Buchman, T. G., Gijzel, S. M. W., Goulson, D., et al. (2018). Quantifying resilience of humans and other animals. *Proc. Natl. Acad. Sci. U.S.A.* 115, 11883–11890. doi: 10.1073/pnas.1810630115

Schmidt, S. E., Neuendorff, D. A., Riley, D. G., Vann, R. C., Willard, S. T., Welsh, T. H., et al. (2014). Genetic parameters of three methods of temperament evaluation of Brahman calves. *J. Anim. Sci.* 92, 3082–3087. doi: 10.2527/jas.2013-7494

Schultz, E. B., Santana, T. E. Z., Silva, F. F., Garcia, A. O., Oliveira, H. R., Rodrigues, M. T., et al. (2020). Genetic parameter estimates for caprine arthritis encephalitis in dairy goats. *J. Dairy Sci.* 103, 6407–6411. doi: 10.3168/jds.2019-17740

Schütz, K. E., Cox, N. R., and Tucker, C. B. (2014). A field study of the behavioral and physiological effects of varying amounts of shade for lactating cows at pasture. *J. Dairy Sci.* 97, 3599–3605. doi: 10.3168/jds.2013-7649

Scott, K. A., Torrey, S., Stewart, T., and Weaver, S. A. (2000). "Pigs selected for high lean growth exhibit increased anxiety response to humans," in *Proc. 30th Ann. Meet. Soc. Neuroci*, New Orleans, LA.

Sellier, N., Guettier, E., and Staub, C. (2014). A review of methods to measure animal body temperature in precision farming. *Am. J. Agric. Sci. Technol.* 2, 74–79. doi: 10.7726/ajast.2014.1008

Serenius, T., and Stalder, K. J. (2006). Selection for sow longevity. *J. Anim. Sci.* 84(Suppl. 1), E166–E171. doi: 10.2527/2006.8413_supplE166x

Sewalen, A., Miglior, F., and Kistemaker, G. J. (2011). Genetic parameters of milking temperaemnt and milking speed in Canadian Holsteins. *J. Dairy Sci.* 94, 512–516. doi: 10.3168/jds.2010-3479

Shen, C., Tong, X., Chen, R., Gao, S., Liu, X., Schinckel, A. P., et al. (2019). Identifying blood-based biomarkers associated with aggression in weaned pigs after mixing. *Appl. Anim. Behav. Sci.* 224:104927. doi: 10.1016/j.applanim.2019.104927

Shepley, E., Berthelot, M., and Vasseur, E. (2017). Validation of the ability of a 3D pedometer to accurately determine the number of steps taken by dairy cows when housed in tie-stalls. *Agriculture* 7:53. doi: 10.3390/agriculture7070053

Siegel, P. B., Barger, K., and Siewerdt, F. (2019). Limb health in broiler breeding: history using genetics to improve welfare. *J. Appl. Poult. Res.* 28, 785–790. doi: 10.3382/japr/pfz052

Sih, A., Bell, A., and Johnson, J. C. (2004). Behavioral syndromes: an ecological and evolutionary overview. *Trends Ecol. Evol.* 19, 372–378. doi: 10.1016/j.tree.2004.04.009

Silva, F. F., Mulder, H. A., Knol, E. F., Lopes, M. S., Guimarães, S. E. F., Lopes, P. S., et al. (2014). Sire evaluation for total number born in pigs using a genomic reaction norms approach. *J. Anim. Sci.* 92, 3825–3834. doi: 10.2527/jas.2013-6486

Silva, M., Exadaktylos, V., Ferrari, S., Guarino, M., Aerts, J. M., and Berckmans, D. (2009). The influence of respiratory disease on the energy envelope dynamics

of pig cough sounds. *Comp. Elect. Agric.* 69, 80–85. doi: 10.1016/j.compag.2009.07.002

Singh, C. V., Kumar, D., and Singh, Y. P. (2001). Potential usefulness of the plumage reducing Naked Neck (Na) gene in poultry production at normal and high ambient temperatures. *World's Poultry Sci. J.* 57, 139–156. doi: 10.1079/WPS20010011

Smulders, D., Verbeke, G., Mormède, P., and Geers, R. (2006). Validation of a behavioral observation tool to assess pig welfare. *Physiol. Behav.* 89, 438–447. doi: 10.1016/j.physbeh.2006.07.002

Spoliansky, R., Edan, Y., Parmet, Y., and Halachmi, I. (2016). Development of automatic body condition scoring using a low-cost 3-dimensional Kinect camera. *J. Dairy Sci.* 99, 7714–7725. doi: 10.3168/jds.2015-10607

Stavrakakis, S., Li, W., Guy, J. H., Morgan, G., Ushaw, G., Johnson, G. R., et al. (2015). Validity of the Microsoft Kinect sensor for assessment of normal walking patterns in pigs. *Comp. Elect. Agric.* 117, 1–7. doi: 10.1016/j.compag.2015.07.003

Stear, M. J., Nikbakht, G., Matthews, L., and Jonsson, N. N. (2012). Breeding for disease resistance in livestock and fish. *CAB Rev. Perspect. Agric. Vet. Sci. Nutr. Nat. Resour.* 7, 1–10. doi: 10.1079/PAVSNNR20127007

Stephens, M. A. C., and Wand, G. (2012). Stress and the HPA axis: role of glucocorticoids in alcohol dependence. *Alcohol Res.* 34, 468–483.

Stewart, M., Webster, J. R., Schaefer, A. L., Cook, N. J., and Scott, S. L. (2005). Infrared thermography as a non-invasive tool to study animal welfare. *Anim. Welfare* 14, 319–325.

Strutzke, S., Fiske, D., Hoffmann, G., Ammon, C., Heuwieser, W., and Amon, T. (2019). Technical note: development of a noninvasive respiration rate sensor for cattle. *J. Dairy Sci.* 102, 690–695. doi: 10.3168/jds.2018-14999

Su, G., Lund, M. S., and Sorensen, D. (2007). Selection for litter size at day five to improve litter size at weaning and piglet survival rate. *J. Anim. Sci.* 85, 1385–1392. doi: 10.2527/jas.2006-631

Sullivan, M. L., Cawdell-Smith, A. J., Mader, T. L., and Gaughan, J. B. (2011). Effect of shade area on performance and welfare of short-fed feedlot cattle. *J. Anim. Sci.* 89, 2911–2925. doi: 10.2527/jas.2010-3152

Suravajhala, P., Kogelman, L. J. A., and Kadarmideen, H. N. (2016). Multi-omic data integration and analysis using systems genomics approaches: methods and applications in animal production, health and welfare. *Genet. Sel. Evol.* 48, 1–14. doi: 10.1186/s12711-016-0217-x

Tajet, H., Andresen, Ø, and Meuwissen, T. H. E. (2006). Estimation of genetic parameters of boar taint; skatole and androstenone and their correlations with sexual maturation. *Acta Vet. Scand.* 48, 1–4. doi: 10.1186/1751-0147-48-S1-S9

Terrasson, G., Llaria, A., Marra, A., and Voaden, S. (2016). Accelerometer based solution for precision livestock farming: geolocation enhancement and animal activity identification. *Mater. Sci. Eng.* 156:012031. doi: 10.1088/1757-899X/138/1/012004

Tetens, J., Heuer, C., Heyer, I., Klein, M. S., Gronwald, W., Junge, W., et al. (2015). Polymorphisms within the APOBR gene are highly associated with milk levels of prognostic ketosis biomarkers in dairy cows. *Physiol. Genomics* 47, 129–137. doi: 10.1152/physiolgenomics.00126.2014

Teunissen, L. P. J., Klewer, J., De Haan, A., De Koning, J. J., and Daanen, H. A. M. (2011). Non-invasive continuous core temperature measurement by zero heat flux. *Physiol. Meas.* 32, 559–570. doi: 10.1088/0967-3334/32/5/005

Thompson, R., Matheson, S. M., Plötz, T., Edwards, S. A., and Kyriazakis, I. (2016). Porcine lie detectors: automatic quantification of posture state and transitions in sows using inertial sensors. *Comp. Elect. Agric.* 127, 521–530. doi: 10.1016/j.compag.2016.07.017

Thomsen, P. T., Munksgaard, L., and Togersen, F. A. (2008). Evaluation of a lameness scoring system for dairy cows. *J. Dairy Sci.* 91, 119–126. doi: 10.3168/jds.2007-0496

Timsit, E., Assié, S., Quiniou, R., Seegers, H., and Bareille, N. (2011). Early detection of bovine respiratory disease in young bulls using reticulo-rumen temperature boluses. *Vet. J.* 190, 136–142. doi: 10.1016/j.tvjl.2010.09.012

Tolkamp, B. J., Allcroft, D. J., Barrio, J. P., Bley, T. A. G., Howie, J. A., Jacobsen, T. B., et al. (2011). The temporal structure of feeding behavior. *Am. J. Physiol. Regul. Integr. Comp. Physiol.* 301, R378–R393. doi: 10.1152/ajpregu.00661.2010

Tomisław, G., Tadeusz, J., Paweł, K., Sylwia, T. S., and Uhl, T. (2019). Recent advancement approach for precision agriculture. *Mech. Mach. Sci.* 7, 2907–2916. doi: 10.1007/978-3-030-20131-9_287

Tong, X., Shen, C., Chen, R., Gao, S., Liu, X., Schinckel, A. P., et al. (2020). Reestablishment of social hierarchies in weaned pigs after mixing. *Animals* 10:36. doi: 10.3390/ani10010036

Traulsen, I., Scheel, C., Auer, W., Burfeind, O., and Krieter, J. (2018). Using acceleration data to automatically detect the onset of farrowing in sows. *Sensors* 18:170. doi: 10.3390/s18010170

Tremblay, M., Hess, J. P., Christenson, B. M., McIntyre, K. K., Smink, B., van der Kamp, A. J., et al. (2016). Factors associated with increased milk production for automatic milking systems. *J. Dairy Sci.* 99, 3824–3837. doi: 10.3168/jds.2015-10152

Tscharke, M., and Banhazi, T. M. (2013). Review of methods to determine weight and size of livestock from images. *Aust. J. Multi. Disc. Eng.* 10, 1–17. doi: 10.7158/14488388.2013.11464860

Tse, C., Barkema, H. W., DeVries, T. J., Rushen, J., and Pajor, E. A. (2017). Effect of transitioning to automatic milking systems on producers' perceptions of farm management and cow health in the Canadian dairy industry. *J. Dairy Sci.* 100, 2404–2414. doi: 10.3168/jds.2016-11521

Tse, C., Barkema, H. W., DeVries, T. J., Rushen, J., and Pajor, E. A. (2018). Impact of automatic milking systems on dairy cattle producers' reports of milking labour management, milk production and milk quality. *Animal* 12, 2649–2656. doi: 10.1017/s1751731118000654

Turner, S. P. (2011). Breeding against harmful social behaviours in pigs and chickens: state of the art and the way forward. *Appl. Anim. Behav. Sci.* 134, 1–9. doi: 10.1016/j.applanim.2011.06.001

Turner, S. P., Camerlink, I., Baxter, E. M., D'Eath, R. B., Desire, S., and Roehe, R. (2018). "Breeding for pig welfare: opportunities and challenges," in *Advances in Pig Welfare*, ed. M. Špinka (Sawston: Woodhead Pub), 399–414. doi: 10.1016/b978-0-08-101012-9.00012-5

Turner, S. P., and Dwyer, C. M. (2007). Welfare assessment in extensive animal production systems: challenges and opportunities. *Anim. Welfare* 16, 189–192.

Tuyttens, F. A. M., de Graaf, S., Heerkens, J. L. T., Jacobs, L., Nalon, E., Ott, S., et al. (2014). Observer bias in animal behaviour research: can we believe what we score, if we score what we believe? *Anim. Behav.* 90, 273–280. doi: 10.1016/j.anbehav.2014.02.007

van der Eijk, J. A. J., Rodenburg, T. B., de Vries, H., Kjaer, J. B., Smidt, H., Naguib, M., et al. (2020). Early-life microbiota transplantation affects behavioural responses, serotonin and immune characteristics in chicken lines divergently selected on feather pecking. *Sci. Rep.* 10, 1–13. doi: 10.1038/s41598-020-59125-w

Van Eenennaam, A. L., and Young, A. E. (2018). Gene editing in livestock: promise, prospects and policy. *CAB Rev. Perspect. Agric. Vet. Sci. Nutr. Nat. Resour.* 13, 1–14. doi: 10.1079/PAVSNNR201813027

Vanderick, S., Troch, T., Gillon, A., Glorieux, G., and Gengler, N. (2014). Genetic parameters for direct and maternal calving ease in Walloon dairy cattle based on linear and threshold models. *J. Anim. Breed. Genet.* 131, 513–521. doi: 10.1111/jbg.12105

Vargas, G., Neves, H. H. R., Cardoso, V., Munari, D. P., and Carvalheiro, R. (2017). Genetic analysis of feet and leg conformation traits in Nelore cattle. *J. Anim. Sci.* 95, 2379–2384. doi: 10.2527/jas2016.1327

Vasseur, E., Rushen, J., Haley, D. B., and de Passillé, A. M. (2012). Sampling cows to assess lying time for on-farm animal welfare assessment. *J. Dairy Sci.* 95, 4968–4977. doi: 10.3168/jds.2011-5176

Ventura, R., Fonseca e Silva, F., Manuel Yáñez, J., and Brito, L. F. (2020). Opportunities and challenges of phenomics applied to livestock and aquaculture breeding in South America. *Anim. Front.* 10, 45–52. doi: 10.1093/af/vfaa008

Verma, S., Bhatia, A., Chug, A., and Singh, A. P. (2020). Recent advancements in multimedia big data computing for IoT applications in precision agriculture: opportunities, issues, and challenges. *Intel. Syst. Ref. Lib.* 163, 391–416. doi: 10.1007/978-981-13-8759-3_15

Vetters, M. D. D., Engle, T. E., Ahola, J. K., and Grandin, T. (2013). Comparison of flight speed and exit score as measurements of temperament in beef cattle. *J. Anim. Sci.* 91, 374–381. doi: 10.2527/jas.2012-5122

Viazzi, S., Bahr, C., Schlageter-Tello, A., Van Hertem, T., Romanini, C. E. B., Pluk, A., et al. (2013). Analysis of individual classification of lameness using automatic measurement of back posture in dairy cattle. *J. Dairy Sci.* 96, 257–266. doi: 10.3168/jds.2012-5806

Vidic, J., Manzano, M., Chang, C. M., and Jaffrezic-Renault, N. (2017). Advanced biosensors for detection of pathogens related to livestock and poultry. *Vet. Res.* 48, 1–22. doi: 10.1186/s13567-017-0418-5

Viviana Santos, L., Brügemann, K., Ebinghaus, A., and König, S. (2018). Genetic parameters for longitudinal behavior and health indicator traits generated in automatic milking systems. *Arch. Anim. Breed.* 61, 161–171. doi: 10.5194/aab-61-161-2018

von Borell, E., Langbein, J., Després, G., Hansen, S., Leterrier, C., Marchant-Forde, J., et al. (2007). Heart rate variability as a measure of autonomic regulation of cardiac activity for assessing stress and welfare in farm animals - A review. *Physiol. Behav.* 92, 293–316. doi: 10.1016/j.physbeh.2007.01.007

Vranken, E., and Berckmans, D. (2017). Precision livestock farming for pigs. *Anim. Front.* 7, 32–37. doi: 10.2527/af.2017.0106

Wallenbeck, A., and Keeling, L. J. (2013). Using data from electronic feeders on visit frequency and feed consumption to indicate tail biting outbreaks in commercial pig production. *J. Anim. Sci.* 91, 2879–2884. doi: 10.2527/jas.2012-5848

Wemelsfelder, F., and Mullan, S. (2014). Applying ethologieal and health indicators to practical animal welfare assessment. *OIE Rev. Sci. Tech.* 33, 111–120. doi: 10.20506/rst.33.1.2259

Weschenfelder, A. V., Torrey, S., Devillers, N., Crowe, T., Bassols, A., Saco, Y., et al. (2012). Effects of trailer design on animal welfare parameters and carcass and meat quality of three Pietrain crosses being transported over a long distance. *J. Anim. Sci.* 90, 3220–3231. doi: 10.2527/jas.2011-4676

Wethal, K. B., and Heringstad, B. (2019). Genetic analyses of novel temperament and milkability traits in Norwegian Red cattle based on data from automatic milking systems. *J. Dairy Sci.* 102, 8221–8233. doi: 10.3168/jds.2019-16625

Wethal, K. B., Svendsen, M., and Heringstad, B. (2020). A genetic study of new udder health indicator traits with data from automatic milking systems. *J. Dairy Sci.* 103, 7188–7198. doi: 10.3168/jds.2020-18343

Williams, M. L., Mac Parthaláin, N., Brewer, P., James, W. P. J., and Rose, M. T. (2016). A novel behavioral model of the pasture-based dairy cow from GPS data using data mining and machine learning techniques. *J. Dairy Sci.* 99, 2063–2075. doi: 10.3168/jds.2015-10254

Woodford, K. B., Brakenrig, M. H., and Pangborn, M. C. (2015). New Zealand case studies of automatic-milking-systems adoption. *Proc. New Zeal. Soc. Anim. Prod.* 75, 127–131.

Woolhouse, M., Ward, M., Van Bunnik, B., and Farrar, J. (2015). Antimicrobial resistance in humans, livestock and the wider environment. *Philos. Trans. R. Soc. B Biol. Sci.* 370:20140083. doi: 10.1098/rstb.2014.0083

World Organization for Animal Health – OIE (2019). *Terrestrial Animal Health Code*. Available at: https://www.oie.int/en/standard-setting/terrestrial-code/access-online/ (accessed May 05, 2020).

Wurtz, K., Camerlink, I., D'Eath, R. B., Fernández, A. P., Norton, T., Steibel, J., et al. (2019). Recording behaviour of indoor-housed farm animals automatically using machine vision technology: a systematic review. *PLoS One* 14:e0226669. doi: 10.1371/journal.pone.0226669

Wurtz, K. E., Siegford, J. M., Bates, R. O., Ernst, C. W., and Steibel, J. P. (2017). Estimation of genetic parameters for lesion scores and growth traits in group-housed pigs. *J. Anim. Sci.* 95, 4310–4317. doi: 10.2527/jas2017.1757

Xu, Q., Wang, Y. C., Liu, R., Brito, L. F., Kang, L., Yu, Y., et al. (2017). Differential gene expression in the peripheral blood of Chinese Sanhe cattle exposed to severe cold stress. *Genet. Mol. Res.* 16:gmr16029593. doi: 10.4238/gmr16029593

Yahav, S., Shinder, D., Tanny, J., and Cohen, S. (2005). Sensible heat loss: the broiler's paradox. *Worlds Poult. Sci. J.* 61, 419–434. doi: 10.1079/wps200453

Zadinová, K., Stupka, R., Stratil, A., Èítek, J., Vehovskı, K., and Urbanová, D. (2016). Boar taint– The effects of selected candidate genes associated with androstenone and skatole levels– A review. *Anim. Sci. Pap. Reports.* 34, 107–128.

Zessin, K. H. (2006). Emerging diseases: a global and biological perspective. *J. Vet. Med. Ser. B Infect. Dis. Vet. Public Heal. B* 53, 7–10. doi: 10.1111/j.1439-0450.2006.01011.x

Zhao, L., Wang, G., Siegel, P., He, C., Wang, H., Zhao, W., et al. (2013). Quantitative genetic background of the host influences gut microbiomes in chickens. *Sci. Rep.* 3:1163. doi: 10.1038/srep01163

Zimmerman, P. H., and Koene, P. (1998). The effect of frustrative nonreward on vocalisations and behaviour in the laying hen, Gallus gallus domesticus. *Behav. Process.* 44, 73–79. doi: 10.1016/S0376-6357(98)00035-7

Zuidhof, M. J. (2018). Lifetime productivity of conventionally and precision-fed broiler breeders. *Poultry Sci.* 97, 3921–3937. doi: 10.3382/ps/pey252

Zumbach, B., Misztal, I., Tsuruta, S., Sanchez, J. P., Azain, M., Herring, W., et al. (2008). Genetic components of heat stress in finishing pigs: parameter estimation. *J. Anim. Sci.* 86, 2076–2081. doi: 10.2527/jas.2007-0282

Conflict of Interest: The authors declare that the research was conducted in the absence of any commercial or financial relationships that could be construed as a potential conflict of interest.

frontiers in Genetics

REVIEW
published: 20 August 2020
doi: 10.3389/fgene.2020.00923

Infrared Spectrometry as a High-Throughput Phenotyping Technology to Predict Complex Traits in Livestock Systems

*Tiago Bresolin and João R. R. Dórea**

Department of Animal and Dairy Sciences, University of Wisconsin-Madison, Madison, WI, United States

High-throughput phenotyping technologies are growing in importance in livestock systems due to their ability to generate real-time, non-invasive, and accurate animal-level information. Collecting such individual-level information can generate novel traits and potentially improve animal selection and management decisions in livestock operations. One of the most relevant tools used in the dairy and beef industry to predict complex traits is infrared spectrometry, which is based on the analysis of the interaction between electromagnetic radiation and matter. The infrared electromagnetic radiation spans an enormous range of wavelengths and frequencies known as the electromagnetic spectrum. The spectrum is divided into different regions, with near- and mid-infrared regions being the main spectral regions used in livestock applications. The advantage of using infrared spectrometry includes speed, non-destructive measurement, and great potential for on-line analysis. This paper aims to review the use of mid- and near-infrared spectrometry techniques as tools to predict complex dairy and beef phenotypes, such as milk composition, feed efficiency, methane emission, fertility, energy balance, health status, and meat quality traits. Although several research studies have used these technologies to predict a wide range of phenotypes, most of them are based on Partial Least Squares (PLS) and did not considered other machine learning (ML) techniques to improve prediction quality. Therefore, we will discuss the role of analytical methods employed on spectral data to improve the predictive ability for complex traits in livestock operations. Furthermore, we will discuss different approaches to reduce data dimensionality and the impact of validation strategies on predictive quality.

Keywords: beef cattle, dairy cattle, near-infrared, novel phenotypes, mid-infrared, spectral information

OPEN ACCESS

Edited by:
Fabyano Fonseca Silva, Universidade Federal de Viçosa, Brazil

Reviewed by:
Wei Shen, Qingdao Agricultural University, China
Clément Grelet, Walloon Agricultural Research Centre, Belgium

***Correspondence:**
João R. R. Dórea
joao.dorea@wisc.edu

Specialty section:
This article was submitted to Livestock Genomics, a section of the journal Frontiers in Genetics

Received: *06 April 2020*
Accepted: *24 July 2020*
Published: *20 August 2020*

Citation:
Bresolin T and Dórea JRR (2020) Infrared Spectrometry as a High-Throughput Phenotyping Technology to Predict Complex Traits in Livestock Systems. Front. Genet. 11:923. doi: 10.3389/fgene.2020.00923

INTRODUCTION

For many years dairy and beef cattle breeding have focused on improving the production and profitability of animals through genetics, nutrition, and management, often at the expense of other relevant traits. To remain competitive and meet the world population increase and global climate changes, farmers need to balance production, profitability, and sustainability. There is an extensive list of key phenotypes that must be measured to achieve the emerging breeding goals for the advance of genomic selection (Boichard and Brochard, 2012) and management decisions in the context of

precision agriculture. However, recording such phenotypes in large-scale or across different herds and countries is a challenge (Gengler et al., 2016). High-throughput phenotyping technologies have grown in importance in livestock systems because of their ability to generate real-time and accurate animal-level information. Several technologies (e.g., sensors, infrared spectrometry, and image analysis, among others) have been used to generate novel complex traits in dairy and beef cattle, with infrared spectrometry being one of the most relevant tools used in livestock to date (De Marchi et al., 2014; Dixit et al., 2017; Bell and Tzimiropoulos, 2018). Infrared spectrometry is based on the interaction between electromagnetic radiation (infrared light) and matter. The modern Fourier transform infrared spectrometers spans an enormous range of infrared spectrum, which is divided into three main regions: NIR, near-infrared (800–2,500 nm or 4,000–12,500 cm^{-1}); MIR, mid-infrared (2,500–25,000 nm or 400–4,000 cm^{-1}); and FAR, far-infrared (25,000–1,000,000 nm or 10–400 cm^{-1}). NIR and MIR are the main regions used in livestock applications (Griffiths and de Hasenth, 2007). This technology is fast, non-invasive, non-destructive, and has great potential for on-line measurement (De Marchi et al., 2014; Dixit et al., 2017).

Infrared spectrometry, mainly MIR, has been widely used worldwide to predict the concentration of protein, casein, fat, lactose, and urea of milk through regular recording schemes (De Marchi et al., 2014). When cows are milked 2–3 times daily, this biological sample can be more deeply interrogated to generate novel complex traits, which are usually expensive and difficult to be measure on a large scale (e.g., individual milk fatty acids, proteins, feed intake, methane emission, fertility, energy balance, health status, and others). The majority of milk constituents synthesized in the mammary gland are based on the by-products from the digestion of the nutrients ingested in a given day (McParland and Berry, 2016). Therefore, changes in milk composition profile on that day or in the following days can be used as a biomarker for complex phenotypes related to metabolism. Within the beef industry, NIR technology has been shown to be a valuable and cost-effective technology to assess several meat quality attributes (e.g., tenderness, fat content, color, among others) at the same time without any or minimal sample preparation and pretreatment (Prieto et al., 2009a; Dixit et al., 2017; Chapman et al., 2019). Therefore, the NIR technique can be applied directly to the samples, which is an advantage compared to reference methods, and it is also important for the slaughterhouses that can reduce losses with carcass sample assessment and sample preparation. Both technologies (NIR and MIR) have great potential to assess different milk or meat attributes using in-line systems, which could lend deep insights and added efficiencies for both the dairy and beef industries.

Several authors have successfully used infrared spectrometry to predict a range number of traits as reported in previous reviews papers (Prevolnik et al., 2004; Prieto et al., 2009a, 2017; De Marchi et al., 2014; McParland and Berry, 2016; Dixit et al., 2017; Chapman et al., 2019). Although the aforementioned reviews discussed the use of MIR and NIR spectrometry as a tool to predict milk and meat traits, very little attention has been given to analytical methods and validation strategies employed in analyzing such spectral data. Thus, complementary to the previous reviews, the objectives of this review are: to provide a recent update on the use of MIR and NIR techniques as tools to predict several novel complex traits in livestock system, with an emphasis in dairy and beef cattle; and review and discuss the analytical methods employed on spectral data to improve predictive ability, the different approaches used to reduce data dimensionality, and the impact of validation strategies on the prediction quality.

METHODOLOGY

For this review, research articles published in peer-reviewed journals were retrieved from Web of Science using the keywords or the random combination of keywords presented in **Table 1**. Initially, a total of 348 papers published until May 2020 was found. The papers using NIR or MIR were selected based on the phenotype of interest (e.g., milk composition, feed intake, energy balance, methane emission, fertility, health status, and meat quality traits), and from the 348 studies, only 113 were included in this review. Studies using pre-calibrated or pre-trained models, provided by a company or third party, were not considered in this review. The coefficient of determination (R^2) was used as an indicator of prediction quality for continuous variables. Some authors used the correlation coefficient as one of the metrics to report the model prediction quality. As such, the correlation coefficients were converted to R^2 in order to have a single statistical metric for model evaluation. Although we have adopted R^2 as metric to evaluate prediction quality in this review, due to the number of phenotypes and studies, we also recognize that other important metrics, such as Root Mean Squared Error and Mean Absolute Error, must be considered to better evaluate prediction quality, once R^2 could be inflated by one sample or it could be very sensitive to the range of the variable of interest. For discrete distributed traits, the metric for prediction quality, reviewed in the published papers, was the overall accuracy. Thus, only the R^2 or accuracy reported by the author in the validation set (internal or external) were considered in this review paper. The validation strategy employed by each author (i.e., data-splitting, leave-one-out cross, or k-folds cross-validation) was reviewed and it is presented in the tables, along with the information of prediction quality for each respective phenotype. However, some papers reviewed here did not completely describe the validation strategy adopted; therefore, it was not reported in the tables of this review. More information related to

TABLE 1 | Keywords used to retrieve published papers from Web of Science*.

Cattle	Mid or Near-infrared
Dairy	Milk compounds, milk fatty acids, protein, minerals, metabolic status, energy balance, feed efficiency, feed intake, energy intake, methane emission, reproduction, fertility, lameness, blood metabolites
Beef	Meat quality, feed efficiency, feed intake, energy intake, methane emission, metabolic status, energy balance, reproduction, fertility

**Random combination of mid or near-infrared with the target phenotypes for beef and dairy cattle.*

the compiled validation strategies is presented in the section "Validation Strategies."

COMPLEX TRAITS PREDICTED BY INFRARED SPECTROMETRY DATA

Over the past several years, many studies have investigated the effectiveness of NIR and MIR to predict novel complex phenotypes in dairy and beef cattle, as shown in **Figure 1**. Since De Marchi et al. (2014) wrote a review paper on milk MIR spectrometry, there has been an exponential increase in the number of studies using milk MIR spectral data to predict a range of complex traits. Overall, these studies include the direct quantification of compounds present in milk (e.g., milk fatty acids and protein profile) as well as the prediction of traits linked to milk spectra (e.g., health status, feed intake, methane emission, fertility, and energy balance). The use of NIR spectrometry to assess meat chemical composition and quality traits was reviewed for different species including beef, chicken, and pork by many authors (Prevolnik et al., 2004; Prieto et al., 2009a, 2017; Dixit et al., 2017; Chapman et al., 2019). The authors have stated that NIR is capable of measuring meat chemical composition and quality associated traits in different species, including beef cattle. However, the interest in using NIR technology as an alternative to predict novel traits in beef cattle since the first review paper (Prevolnik et al., 2004) has been lower than for using MIR spectrometry, based on the amount of paper using each method compiled for this current review (**Figure 1**). The number of studies developed in the last years using MIR and NIR techniques highlights the growing interest by the scientific community and livestock industry in this topic. Indeed, several novel phenotypes have been recently generated using both MIR and NIR techniques in dairy and beef cattle and they will be covered throughout this review section.

Milk Composition

Beyond the nutritional meaningful for human, milk composition (e.g., protein, fat, lactose, and minerals) has direct implications on the sensory and technological properties of milk products as well as on the economic value of the milk and milk products (Soyeurt et al., 2009; Bastin et al., 2011; Bonfatti et al., 2011; Gengler et al., 2016; Fleming et al., 2017). Thus, over the last few years, efforts have been made by scientists and the dairy industry to quantify milk composition using modern high-throughput phenotyping techniques such as MIR spectrometry. Indeed, milk recording schemes worldwide have used MIR technique to measure total fat, protein, casein, lactose, and urea contents, which is quick and inexpensive when compared with gold standard methods (De Marchi et al., 2014). Given the promising and availability of milk spectra per cow per milking, several studies have reported that the major milk fatty acids (FA) can also be predicted using spectra data (**Tables 2**, **3**).

For FA with less than 16 carbons (C4:0; C6:0; C8:0; C10:0; C12:0; and C14:0) the R^2 reported varied from 0.37 to 0.97 in the validation set (**Table 2**). The feasibility of milk MIR spectra to predict FA with 16 carbons (C16:0 and C16:1) was investigated by several authors. The R^2 observed in the validation sets were between the range of 0.33 and 0.95 (**Table 2**). For the FA with more than 16 carbons (C17:0; C18:0; C18:1 *cis*-9; C18:2 *cis*-9, *trans*-11; C18:2 *cis*-9, *cis*-12; and C18:3 *cis*-9, *cis*-12, *cis*-15) the R^2 reported in the validation set varied from 0.07

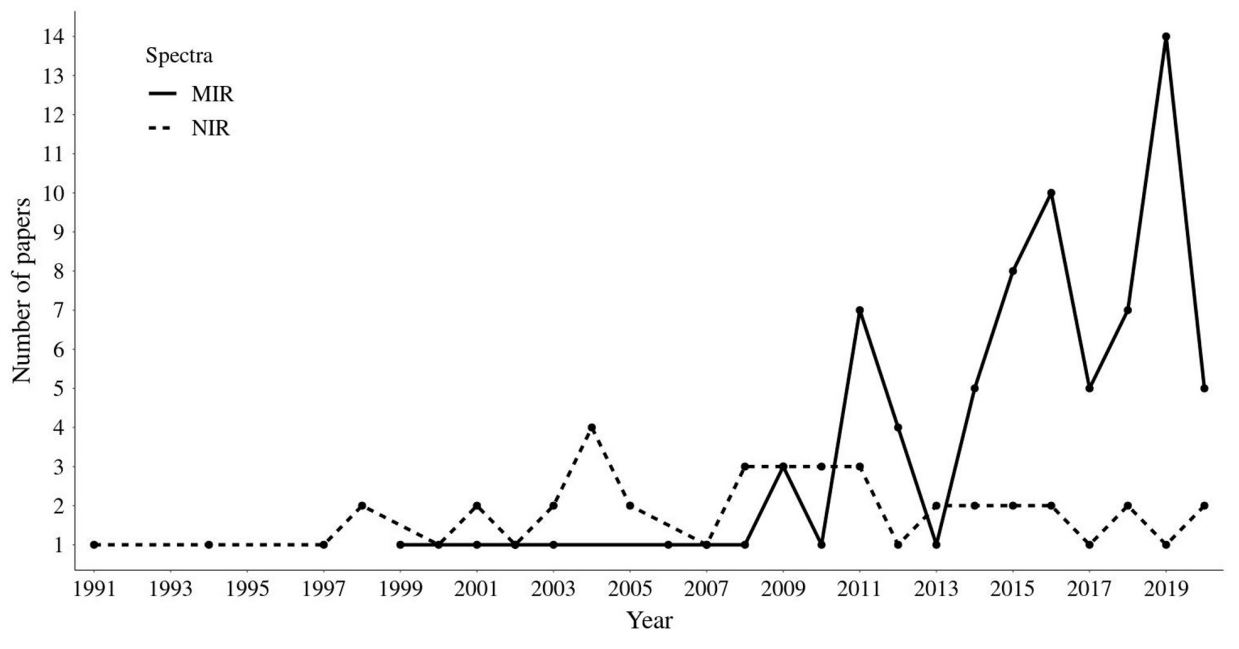

FIGURE 1 | Published papers retrieved from Web of Science based on the combination of keywords presented in **Table 1**. Scientific papers published up to May 2020.

TABLE 2 | Number of samples (N) and coefficient of determination in the validation set for the milk fatty acids predicted from mid-infrared spectrometry using partial least square methodology in dairy cattle.

References	N	Breed	Validation*	C4:0	C6:0	C8:0	C10:0	C12:0	C14:0	C16:0	C16:1
Soyeurt et al. (2006)	49	Mul	CV	0.51	0.52	0.59	0.64	0.74	0.82	0.82	–
Soyeurt et al. (2008)	78	Mul	LOOCV	–	–	–	–	–	0.90	0.84	–
Rutten et al. (2009)	3,622	–	R-Tr/Te	0.91	0.96	0.94	0.92	0.85	0.94	0.94	–
Afseth et al. (2010)	224	Nor	20-F CV	0.72	0.83	0.88	0.89	0.90	0.82	0.65	–
Coppa et al. (2010)	468	–	Tr/Te[b]	0.66	0.88	0.90	0.91	0.89	0.88	0.91	–
De Marchi et al. (2011)[a]	267	Bro	LOOCV	–	–	0.48	0.52	0.52	0.56	0.49	–
Soyeurt et al. (2011)	517	Mul	Tr/Te[b]	0.89	0.95	0.93	0.92	0.92	0.95	0.93	–
Ferrand et al. (2011)	250	Mul	Tr/Te	0.85	0.96	0.96	0.91	0.91	0.93	0.88	–
Eijndhoven et al. (2013)	1,236	Mul	Tr/Te[b]	0.92	0.93	0.92	0.93	0.85	0.95	0.93	–
Ferrand-Calmels et al. (2014)	345	Mul	R-Tr/Te	0.93	0.96	0.97	0.95	0.96	0.95	0.94	–
Lopez-Villalobos et al. (2014)	850	Cro	R-Tr/Te	0.73	0.78	0.81	0.81	0.86	0.77	0.74	0.33
Eskildsen et al. (2014)	890	Mul	10-F CV	–	0.88	0.89	0.91	0.91	0.90	0.91	0.63
Martin et al. (2015)[a]	422	–	20-F CV	0.82	–	–	–	–	0.82	0.66	–
Ferragina et al. (2015)[b]	1,264	Bro	R-Tr/Te[b]	–	–	–	0.67	–	–	0.60	–
Gottardo et al. (2016)	112	Mul	LOOCV	0.92	0.94	0.94	–	0.93	0.93	0.92	–
Bonfatti et al. (2016)	1,040	Sim	10-F CV	–	–	–	0.88	0.90	0.90	0.92	–
Fleming et al. (2017)	1,911	Mul	10-F CV	0.66	0.38	0.37	0.66	0.71	0.80	0.86	0.62
Ho et al. (2020)	240	Hol	10-F CV	0.94	0.94	0.90	0.89	0.90	0.93	0.95	–

*[a]Correlation coefficient (r) transformed to coefficient of determination (R^2). [b]Bayes B methodology employed; multibreed (Mul); Norwegian Red (Nor); Brown Swiss (Bro); Crossbreed (Cro); Simmental (Sim); Holstein (Hol); number of folds (n-F) in the cross-validation, leave-one-out cross-validation (LOOCV), train and test cross-validation defined by splitting the data set randomly (R-Tr/Te) or not (Tr/Te), external or independent validation. *The validation strategy defined as "CV" was assigned for the reviewed paper that did not completely describe the validation method adopted or the authors defined that cross-validation was employed.*

TABLE 3 | Coefficient of determination in the validation set for the milk fatty acids predicted from mid-infrared in dairy cattle*.

References	C17:0	C18:0	C18:1[a]	C18:2[b]	C18:2[c]	C18:3[d]	SFA	MUFA	PUFA
Soyeurt et al. (2006)	–	0.69	–	0.07	0.62	0.14	0.94	0.85	0.39
Soyeurt et al. (2008)	–	0.85	–	–	–	–	–	0.93	
Rutten et al. (2009)	–	0.82	0.92	0.58	0.36	0.45	–	–	–
Afseth et al. (2010)	–	0.48	0.92	0.53	0.49	0.29	0.92	0.94	0.52
Coppa et al. (2010)	0.65	0.80	0.93	0.73	0.34	–	0.95	0.91	0.75
De Marchi et al. (2011)[1]	0.56	0.42	0.50	0.21	–	–	–	–	–
Soyeurt et al. (2011)	0.61	0.88	0.95	0.63	0.71	0.60	0.99	0.97	0.81
Ferrand et al. (2011)	–	0.77	0.91	0.70	0.65	–	0.98	0.92	0.38
Eijndhoven et al. (2013)	–	0.72	–	–	–	–	0.99		
Ferrand-Calmels et al. (2014)	–	0.85	0.97	0.83	0.78	–	1.00	0.98	0.78
Lopez-Villalobos et al. (2014)	0.43	0.60	0.87	0.64	0.66	0.51	0.93	–	0.73
Eskildsen et al. (2014)	0.54	0.82	0.82	0.37	0.65	–	–	–	–
Martin et al. (2015)[1]	–	0.62	0.84	–	–	–	0.77	0.86	–
Ferragina et al. (2015)[2]	–	0.49	–	–	–	–	–	–	–
Gottardo et al. (2016)	–	0.80	–	–	–	–	0.99	0.95	0.71
Bonfatti et al. (2016)	–	0.78	0.90	0.65	–	–	0.97	0.93	0.75
Fleming et al. (2017)	0.53	0.73	0.79	–	0.65	–	0.94	0.84	0.66
Ho et al. (2020)	0.82	0.81	0.72	–	–	–	–	–	–

*[1]Correlation coefficient (r) transformed to coefficient of determination (R^2). [2]Bayes B methodology employed. [a]C18:1 cis9. [b]C18:2 cis9, trans 11. [c]C18:2 cis9, cis12. [d]C18:3 cis9, cis12, cis15. SFA, saturate fatty acids; MUFA, monounsaturated fatty acids; PUFA, and polyunsaturated fatty acids. *The number of samples, breed, and validation strategy are described in **Table 2**.*

to 0.95 (**Table 3**). The sums of saturated and monounsaturated FA were predicted with precision (R^2) higher than 0.80, whereas for the polyunsaturated FA, the R^2 varied from 0.38 to 0.81 in the validation set (**Table 3**). In general, FA with larger proportion (% of total FA) in the milk (e.g., C14:0, C16:0, and C18:1) presented greater R^2 (e.g., C14:0, C16:0, and C18:1), when compared to milk FA of small individual proportion in milk (e.g., C17:0).

Studies have also investigated the effectiveness of using milk spectra data as a potential predictor of total protein, casein,

and whey, as well as the individual caseins and whey proteins (**Table 4**). The R^2 in the validation set for total protein and casein were greater than 0.70, except Sørensen et al. (2003); De Marchi et al. (2009), Rutten et al. (2011), and McDermott et al. (2016) that observed R^2 in a range of 0.25–0.58. The R^2 for total whey varied from 0.42 (McDermott et al., 2016) to 0.69 (Niero et al., 2016) in the validation set. For the individual caseins αS1-CN, αS2-CN, β-CN, and κ-CN R^2 in a range of 0.18 (β-CN; Rutten et al., 2011) to 0.78 (αS1-CN; Ferrand et al., 2012) were reported in the validation set. The α-LA whey protein fraction presented the lowest prediction R^2, varying from 0.06 (Eskildsen et al., 2016) to 0.48 (Ferrand et al., 2012), compared with β-LG where the prediction R^2 were in a range of 0.34 (Eskildsen et al., 2016) to 0.64 (Bonfatti et al., 2011) in the validation set.

The effectiveness of milk spectra data to predict mineral composition in dairy cattle has also been investigated. The prediction quality reported in the validation set for Ca, Mg, Na, and P is presented in **Table 5**. Model performances were satisfactory to predict Ca and P ($R^2 > 0.67$) in Soyeurt et al. (2009); Toffanin et al. (2015), Visentin et al. (2016), and Franzoi et al. (2019). But the same minerals were poorly predicted ($R^2 < 0.55$) by Gottardo et al. (2015); Bonfatti et al. (2016), Malacarne et al. (2018), and Fleming et al. (2019). For K, Mg, and Na the R^2 reported by the authors varied from 0.25 (Malacarne et al., 2018) to 0.75 (Franzoi et al., 2019) in the validation set.

Divergences in the predictability reported might be related to the different gold standard methodologies used in the reference data, population studied, and the sample size (De Marchi et al., 2014). Overall, the R^2 observed in the published papers reviewed here highlight the potential of milk spectra data as a predictor of milk FA, proteins, and minerals. These studies also underline the need for future work using robust analytical data mining techniques and large datasets as a way to improve the model performance for phenotypes that have been inaccurate predicted. The possibility of more frequent predictions of such phenotypes could potentially create discoveries in different areas of animal science, such as genetics/genomics, nutrition, physiology, and reproduction. For example, some authors have demonstrated that milk fatty acids can be good predictors of plasma non-esterified fatty acids concentration (Mann et al., 2016; Dórea et al., 2017), which is an important phenotype associated with negative energy balance in lactating dairy cows. Additionally, such predictions can be used as a powerful tool to improve management decisions on livestock operations.

Feed Intake

Given the economic impact of animal feed costs on farmer's profitability, feed efficiency has been widely discussed as a key phenotype to be included in the selection indexes and for management decisions on livestock operations (Berry and Crowley, 2013; Berry, 2015; Seymour et al., 2019). Selecting animal for feed efficiency is highly attractive, but the practical implementation might be challenging, primarily because individual feed intake records on a large-scale are unavailable to date, and secondly some aspect of production, such as milk output or body weight, and energy sinks including maintenance, need to be accounted to determine individual feed efficiency (Berry and Crowley, 2013; Connor, 2015). Therefore, the use of NIR and MIR spectrometry has been explored as a potential tool to predict traits related to feed efficiency in beef and dairy cattle, as shown in **Tables 6**, **7**. Seven studies evaluated the use of fecal NIR on fecal samples to predict organic or dry matter intake, reporting R^2 ranging from 0.44 (Huntington et al., 2011) to 0.98 (Decruyenaere et al., 2004) in the validation set (**Table 6**). From the studies reviewed, only one study reported the use of feed (grass NIR) to predict dry matter intake, in which the R^2 reported in the validation set was 0.71. It is important to point out that the results have not always been consistent, and few studies have compiled data sets of sufficient size to generate robust and accurate prediction equations. Furthermore, the use of NIR spectrometry on grab fecal and grass samples requires preparation and pretreatment, which is laborious, time-consuming, and may not be applicable on a large-scale.

Due to the difficulties in utilizing fecal or grass samples with NIR to predict intake, the value of milk MIR spectrometry for prediction of feed efficiency has also been evaluated (**Table 7**). As many milk recording schemes globally already use MIR spectrometry to predict protein, fat, casein, lactose, and urea

TABLE 4 | Number of samples (N) and coefficient of determination in the validation set for the major protein content predicted from milk spectra using partial least square methodology in dairy cattle.

References	N	Breed	Validation	Prot	Cas	Whey	α_{S1}-CN	α_{S2}-CN	β-CN	κ-CN	α-LA	β-LG
Luginbühl (2002)	74	–	Tr/Te*	–	0.90	–	–	–	–	–	–	–
Sørensen et al. (2003)[a]	86	Multibreed	–	–	0.53	–	–	–	–	–	–	–
De Marchi et al. (2009)[a]	1,336	Simmental	20-F CV	0.58	0.58	0.53	0.50	0.35	0.32	0.43	0.29	0.55
Bonfatti et al. (2011)	1,517	Simmental	4-F CV	0.78	0.77	0.61	0.66	0.49	0.53	0.49	0.31	0.64
Rutten et al. (2011)	1,800	Holstein	R-Tr/Te	-	0.25	0.53	0.18	0.26	0.19	0.28	0.20	0.56
Ferrand et al. (2012)	193	Multibreed	Tr/Te	0.99	0.88	0.58	0.65	0.71	0.78	0.54	0.48	0.45
Bonfatti et al. (2016)	1,137	Simmental	10-F CV	0.81	0.80	0.53	0.74	0.49	0.58	0.39	0.24	0.48
Eskildsen et al. (2016)	832	Multibreed	Tr/Te	–	–	–	0.66	0.36	0.25	0.71	0.06	0.34
McDermott et al. (2016)[a]	730	Multibreed	4-F CV*	–	0.55	0.42	0.43	0.43	0.45	0.31	0.29	0.48
Niero et al. (2016)	114	Multibreed	LOOCV	0.88	0.88	0.69	–	–	0.60	0.74	0.37	0.47

*Total protein (Prot), total casein (Cas), number of folds (n-F) in the cross-validation, leave-one-out cross-validation (LOOCV), train and test cross-validation defined by splitting the data set randomly (R-Tr/Te) or not (Tr/Te). [a]Correlation coefficient (r) transformed to coefficient of determination (R^2), and *external or independent validation.*

TABLE 5 | Number of samples (N) and coefficient of determination in the validation set for mineral contents using partial least square methodology.

References	N	Breed	Validation*	Ca	K	Mg	Na	P
Soyeurt et al. (2009)	92	Multibreed	LOOCV	0.87	0.36	0.65	0.65	0.85
Gottardo et al. (2015)	208	–	10-F CV[b]	0.55	–	–	–	–
Toffanin et al. (2015)	208	Holstein	LOOCV	0.53[c]	–	–	–	0.70[c]
Bonfatti et al. (2016)	689	Simental	10-F CV	0.48	0.41	0.46	–	0.43
Visentin et al. (2016)	923	Multibreed	R-Tr/Te[b]	0.67	0.69	0.65	0.40	0.68
Malacarne et al. (2018)[a]	153	Holstein	Tr/Te[b]	0.25	0.34	0.26	0.25	0.53
Franzoi et al. (2019)[b]	93	Holstein	CV	0.79	0.55	0.68	0.75	0.87
Fleming et al. (2019)	986	Multibreed	10- FCV	0.25	–	–	–	–

*[a]Bulk milk samples. [b]Backward interval partial least squares (BiPLS), number of folds (n-F) in the cross-validation, leave-one-out cross-validation (LOOCV), train and test cross-validation defined by splitting the data set randomly (R-Tr/Te), external or independent validation. [c]Correlation coefficient (r) transformed to coefficient of determination (R^2). *The validation strategy defined as "CV" was assigned for the reviewed paper that did not completely describe the validation method adopted or the authors defined that cross-validation was employed.*

contents (De Marchi et al., 2014), they can be a useful source of information on large-scale operations. The majority of researchers have aimed to predict dry matter intake, though some have also evaluated predictions for residual feed intake, net energy intake, and effective energy intake. For dry matter intake, the R^2 in the validation set was in a range of 0.29 (Wallén et al., 2018) to 0.77 (Shetty et al., 2017b). The studies evaluating the use of milk spectra to predict effective energy intake reported R^2 varying from 0.49 (McParland et al., 2014) to 0.74 (McParland et al., 2011). McParland et al. (2015) observed R^2 of 0.56 for energy intake in the validation set. McParland et al. (2014) and Shetty et al. (2017b) reported R^2 of 0.36 and 0.46, respectively, to predicted residual feed intake from MIR data in the validation set. The majority of the studies observed that combining MIR data with other animal-level variables, such as milk yield, body weight, and feeding behavior resulted in greater prediction precision and accuracy compared to predictions based only on MIR data. The reviewed studies suggest that milk MIR spectra data is a promising tool to predict indicator traits for feed efficiency in dairy cattle. Such a novel source of information has the potential to bring new insights into management decisions and breeding programs.

TABLE 6 | Number of samples (N), and coefficient of determination in the validation set (R^2) for the prediction of dry matter intake (DMI) and organic matter intake (OMI) traits using grass near-infrared (G-NIR) and fecal near-infrared (F-NIR) spectrometry [§].

References	N	Breed	Spectra	Trait	Validation	R^2
Agnewa et al. (2004)	203	dairy	G-NIR	DMI	7-F CV	0.71
Boval et al. (2004)	88	beef	F-NIR	OMI	3-F CV	0.52
Decruyenaere et al. (2004)	139	dairy	F-NIR	DMI	CV	0.98
Garnsworthy and Unalt (2004)	91	dairy	F-NIR	DMI	R-Tr/Te[a]	0.97
Tran et al. (2010)	1,322	dairy	F-NIR	DMI	Tr/Te[a]	0.58
Huntington et al. (2011)	406	beef	F-NIR	DMI	CV	0.44
Landau et al. (2016)	125	beef	F-NIR	DMI	6-F CV	0.75
Johnson et al. (2017)	408	beef	F-NIR	DMI	CV	0.73

*Number of folds (n-F) in the cross-validation (CV), train and test cross-validation defined by splitting the data set randomly (R-Tr/Te) or not (Tr/Te). [a]External or independent validation. *The validation strategy defined as "CV" was assigned for the reviewed paper that did not completely describe the validation method adopted or the authors defined that cross-validation was employed. [§] All the studies applied partial least square statistical methodology.*

Energy Balance

Dairy cows in early lactation are under high energy demand to meet their requirements for lactation and often energy intake is unable to meet a cow's requirements, leading animals to enter in a period of negative energy balance (Collard et al., 2000; de Vries and Veerkamp, 2000; McParland et al., 2012). Effective and accurate early assessment of a cow's energy balance

TABLE 7 | Number of samples (N) and coefficient of determination (R^2) for dry matter intake (DMI), residual feed efficiency (RFI), effective energy intake (EEI), net energy intake (NEI), and energy intake (EI) traits using milk mid-infrared spectrometry in dairy cattle.

References	N	Breed	Trait	Method	Validation	R^2
McParland et al. (2011)	5,469	Holstein	EEI	PLS	4-F CV*	0.74[a]
McParland et al. (2012)	4,109	Holstein	EEI	PLS	4-F CV*	0.64[a]
McParland et al. (2014)	1,335	Holstein	RFI	PLS	Tr/Te*	0.36[a]
McParland et al. (2014)	1,335	Holstein	EEI	PLS	Tr/Te*	0.49[a]
McParland et al. (2015)	1,270	Holstein	EI	PLS	20-F CV	0.56[a]
Shetty et al. (2017b)	1,044	Multibreed	DMI	PLS	R-Tr/Te*	0.77
Shetty et al. (2017b)	1,044	Multibreed	RFI	PLS	R-Tr/Te*	0.46
Dórea et al. (2018)	1,279	Holstein	DMI	ANN	LOOCV*	0.70
Wallén et al. (2018)	857	Norwegian red	DMI	PLS	5-F CV*	0.29[a]
Wallén et al. (2018)	857	Norwegian red	NEI	PLS	5-F CV*	0.42[a]
Lahart et al. (2019)	1,074	Multibreed	DMI	PLS	LOOCV*	0.64
Smith et al. (2019)	11,941	Holstein	EEI	PLS	4-F CV*	0.52
Grelet et al. (2020)	1,034	Holstein	DMI	SVM	R-Tr/Te	0.66

*Number of folds (n-F) in the cross-validation, leave-one-out cross-validation (LOOCV), partial least square (PLS), artificial neural network (ANN), Support Vector Machine (SVM) train and test cross-validation defined by splitting the data set randomly (R-Tr/Te) or not (Tr/Te). *External or independent validation. [a]Correlation coefficient (r) transformed to coefficient of determination R^2.*

could be useful for management strategies, mitigating the costs associated with detrimental effects of negative energy balance, and future genetic selection (McParland et al., 2012; Grelet et al., 2019). Energy balance has been estimated in dairy cows through alternative methods that are mostly based on the difference between energy intake and energy output or considering the change in body reserves (Coffey et al., 2001; Friggens et al., 2007; Banos and Coffey, 2010). The drawback to these methods is that they require regular measurements of energy intake, body condition score, and body weight, which are expensive to collect on a sufficiently large number of animals, not well suited to assess short-term changes, and vary with intake respectively (McParland et al., 2012). Moving forward to high throughput phenotyping, milk spectra have been used as a potential tool to predict energy balance (**Table 8**). McParland et al. (2011; 2012; 2014; 2015) reported R^2 in a range of 0.29–0.56 in the validation set using evening milk spectra data. A moderate R^2 (0.60) was reported by Smith et al. (2019) to predict energy balance in the validation set, whereas Ho et al. (2020) observed low R^2 (0.48), which according to the authors could be due to the small dataset used when compared with the previous studies. The predictive ability observed by the authors highlights the potential of milk spectra data to predict herd or individual energy status level; however, more efforts are needed to improve the prediction quality. Furthermore, the models used only require milk spectra and yield, which are both routinely generated during milk recording. Therefore, farmers could have access to the individual animal energy status at the time of milking without additional cost.

Methane Emission

Strategies to predict enteric methane emission (CH_4) have been widely explored by different research groups worldwide. Such interest is usually driven by concerns regarding the carbon footprint and lower feed efficiency due to energy losses in CH_4 (Johnson and Johnson, 1995). Mitigating CH4 emissions may improve the livestock systems' sustainability and profitability (Knapp et al., 2014). However, the majority of the classical methods used to quantify CH_4 in the papers reviewed here (i.e., respiration chamber, sulfur hexafluoride tracer, and sniffer systems) are difficult, expensive, or not feasible to carry out on large scale operations (Hammond et al., 2016; Patra, 2016; Negussie et al., 2017). Several indirect measurements (e.g., feed intake, volatile fatty acids, milk FA, body weight, hindgut, feces, among others) have been proposed as a predictor of CH_4 emission, in which milk FA have been stated as a promising CH_4 proxy in dairy cattle (Negussie et al., 2017). Many studies have investigated the correlation between different milk FA, quantified using gas chromatography, and enteric CH_4 production (Chilliard et al., 2009; Dijkstra et al., 2011; van Lingen et al., 2014; Rico et al., 2016). Based on the moderate to high correlations (0.50–0.80) observed by these authors, milk FA can be considered a potential indicator of individual animal enteric CH_4 emissions. Since milk FA can be predicted from milk spectra, as previously discussed in section "Milk Composition," several researchers have investigated the feasibility of using milk spectra data to predict the volume of CH_4 eructed daily by a dairy cow (**Table 9**). Overall, the R^2 reported by the papers reviewed here varied from 0.01 (Wang and Bovenhuis, 2019) to 0.79 (Dehareng et al., 2012) in the validation set. The variation in the predictive ability across studies can be partially explained by the different methods used to determine CH_4 emission (e.g., respiration chambers, sulfur hexafluoride tracer, and sniffer method). Based on the prediction quality presented by some of the authors in experimental settings, milk spectra data has the potential to predict enteric CH_4 emissions (Vanlierde et al., 2015). The validity of spectra data to predict CH_4 emissions under conditions more similar to a commercial herd was only partly confirmed only by Shetty et al. (2017a). In beef cattle, the majority of studies have measured methane emission using classical direct methods, but to the best of our knowledge, no studies have attempted to predict methane emission indirectly using infrared spectrometry data.

Fertility

Although fertility is a non-yield trait, it is the key to overall profitability in cattle farming as poor fertility increases the

TABLE 8 | Number of samples (N) and coefficient of determination (R^2) in the validation for energy balance trait using milk mid-infrared spectrometry in dairy cattle[§].

References	N	Breed	Validation	R^2
McParland et al. (2011)	5,469	Holstein	4-F CV*	0.56[a]
McParland et al. (2012)	4,109	Holstein	4-F CV*	0.29[a]
McParland et al. (2014)	1,335	Holstein	Tr/Te*	0.46[a]
McParland et al. (2015)	1,270	Holstein	20-F CV	0.53[a]
Ho et al. (2019)	240	Holstein	10-F CV	0.48
Smith et al. (2019)	11,941	Holstein	4-F CV*	0.60

*Number of folds (n-F) in the cross-validation, train and test cross-validation defined by splitting the data set randomly (R-Tr/Te) or not (Tr/Te). *External or independent validation. [a]Correlation coefficient (r) transformed to coefficient of determination (R^2). [§]All studies used partial least square methodology.*

TABLE 9 | Number of samples (N) and coefficient of determination in validation set (R^2) for methane emission trait predicted from milk mid-infrared spectra data.

References	N	Breed	Method	Validation	R^2
Dehareng et al. (2012)	60	Holstein	PLS	LOOCV	0.79
Vanlierde et al. (2015)	446	Multibreed	PLS	Tr/Te*	0.23[a]
Vanlierde et al. (2016)	532	Multibreed	PLS	5-F CV	0.70
Shetty et al. (2017a)	2,202	Holstein	PLS	R-Tr/Te*	0.39
Bittante and Cipolat-Gotet (2018)	1,150	Brown Swiss	Bayes B	R-Tr/Te	0.57
Vanlierde et al. (2018)	584	Multibreed	PLS	5-F CV	0.57
van Gastelen et al. (2018)	218	Holstein	PLS	10-F CV	0.49
Wang and Bovenhuis (2019)	801	Holstein	PLS	LOOCV*	0.01

*Partial least square (PLS), multivariate linear regression (MLR), number of folds (n-F) in the cross-validation (CV), leave-one-out cross-validation (LOOCV), train and test cross-validation defined by splitting the data set randomly (R-Tr/Te) or not (Tr/Te). *External validation. [a]Correlation coefficient (r) transformed to coefficient of determination (R^2).*

replacement rate due to involuntary culling, costs related to fertility treatments, and multiple inseminations, which directly affect animal production (Boichard, 1990; Dekkers, 1991; González-Recio et al., 2004; Berry et al., 2014; Pravia et al., 2014; Kaniyamattam et al., 2016). Since fertility traits are difficult and expensive to measure, early indicator or associated traits (e.g., body condition score, body weight, metabolic and endocrine blood traits, and milk composition) can be used either to enhance indirect genetic improvement of fertility or for reproductive management decisions (Berry et al., 2003; Moraes et al., 2007; Friggens et al., 2008; Diskin and Kenny, 2014). Hempstalk et al. (2015) developed a biological-based ML model to predict the likelihood of conception success given the herd- and cow-specific attributes, with particular attention to the use of milk spectral data. The area under the curve reported by the authors in the external validation set varied from 0.49 to 0.60 across different ML algorithms. However, the inclusion of milk spectra, compared with the same model using only non-MIR data (e.g., days in milk, milk yield, number of inseminations, breeding values, among others) in the ML models, did not improve the accuracy of predicting the likelihood of conception to an insemination. The prediction accuracies of pregnancy status using milk spectra data were also assessed by Toledo-Alvarado et al. (2018). The area under the curve across breed had similar patterns averaging 0.61 for Holsteins and 0.64 for Alpine Grey cows in the cross-validation. The authors concluded that pregnant versus open cows post insemination could be discriminated with promising accuracy using milk spectra, parity, and days in milk. Ho et al. (2019) reported that milk spectra from early lactation cow together with other on-farm data (e.g., days in milk, days from calving to insemination, calving age, milk yield, genotypes, among others) could be used to classify cows that conceived at first insemination or did not conceive within the breading season with reasonable accuracy, based on the area under the curve (0.75), in herd-by-herd external validation. Delhez et al. (2020) observed that milk spectra recorded after 150 days of pregnancy was promising to predict the pregnancy status in Holstein, with the area under the curve around 0.76 in cow-independent external validation. More efforts need to be made to investigate the reliability of milk spectra to predict fertility traits since the accuracies observed to date are not high and the number of studies is very low, although recent. Nevertheless, these studies provide new insights into novel phenotypes that can be used indirectly to improve fertility, especially in dairy cattle, which could become an important tool for management decisions on dairy farms.

Health Status

Several metabolic disorders and diseases, such as ketosis, mastitis, milk fever, lameness, displaced abomasum, metritis, retained placenta, and cystic ovaries have important impacts on profitability and animal welfare (Kelton et al., 1998; Friggens et al., 2007; McArt et al., 2015; Jamrozik et al., 2016). To mitigate herd losses, producer-recorded events have been used for management decisions at farmer-level and genetic selection (Jamrozik et al., 2013; Miglior et al., 2014; Luke et al., 2019). However, the bottleneck relies on the difficulty of routinely collecting high-quality direct phenotypes on farms (Egger-Danner et al., 2015). Subclinical hyperketonemia or ketosis is one of the most frequent diseases in dairy cattle and it is characterized by increased concentrations of the ketone bodies acetoacetate, β-hydroxybutyrate (BHB), and acetone in blood, milk, and urine (Hansen, 1999). Additionally, blood metabolites such as glucose, non-esterified fatty acids (NEFA), blood urea nitrogen (BUN), and insulin-like growth factor 1 (IGF-1), and glutamic oxaloacetic transaminase (GOT) might also be used as indicators of metabolic status in dairy cows (Fenwick et al., 2008; Benedet et al., 2019; Grelet et al., 2019). Blood metabolic profile testing is the gold standard for diagnosis, however, it is invasive, logistically challenging, and costly (Luke et al., 2019). MIR spectrometry has been explored as possible high-throughput phenotyping technology to predict BHB concentration in blood or milk, and acetone in milk (**Table 10**). Within the published papers de Roos et al. (2007) and Grelet et al. (2016) predicted the concentration of BHB in milk and the R^2 reported by the authors in the validation was 0.62 and 0.63, respectively. Seven published papers evaluated the use of milk spectra as a predictor of BHB in serum and the R^2 varied from 0.40 (Belay et al., 2017) to 0.70 (Grelet et al., 2019) in the validation set. Although few studies have focused on predicting acetone in milk from milk spectra, the R^2 observed by Hansen (1999) and de Roos et al. (2007) were higher than 0.70, except Grelet et al. (2016) which observed R^2 of 0.67 in the validation set. Heuer et al. (2001) observed a standard error of cross-validation, the prediction quality metric used by the authors, of 0.24 to predict acetone in milk. Likewise, the feasibility of using spectral data to predict glucose, NEFA, BUN, and IGF-1 were also investigated in this review (**Table 10**). The R^2 reported by the authors varied between 0.20 (glucose; Benedet et al., 2019) to 0.61 (IGF-1; Grelet et al., 2019) in the validation set.

Mastitis is the most common and costly contagious disease in dairy cattle characterized as an inflammation of the mammary gland and udder tissue. To the best of our knowledge, only Rienesl et al. (2019) investigated the possibility of using milk spectra to predict mastitis, which reported satisfactory accuracy (0.68) in the validation data set (**Table 11**). Mineur et al. (2017) and Bonfatti et al. (2020) investigated the ability of milk spectra data as a predictor of lameness and the predictions were poor to be employed as an on-farm tool to detect lameness in cows (**Table 11**). Based on the results presented by the reviewed papers, milk spectra might be useful to predict the concentration of BHB in serum or milk, acetone on milk, and mastitis occurrence in dairy cattle. However, more studies using larger and more diverse calibration data sets are needed, especially across countries, to improve the prediction quality before models can be used for on-farm management or genetic selection purposes.

Meat Traits

Meat quality is a complex concept that involves many attributes such as tenderness, juiciness, flavor, marbling, color, and shelf life (Williams, 2008). Meat tenderness is one of the most important attributes affecting consumers' acceptability, followed by fat content and visual attributes (Shackelford et al., 2001; Liu et al., 2003; Williams, 2008). Considering the increasing demands for meat and consumers willing to pay higher prices for

TABLE 10 | Number of samples (N) and coefficient of determination (R^2) in the validation set for β-hydroxybutyrate (BHB), acetone (Ac), non-esterified fatty acids (NEFA), blood urea nitrogen (BUN), glucose (Glu), glutamic oxaloacetic transaminase (GOT), and insuline-like growth factor 1 (IGF-1) using milk mid-infrared spectrometry in dairy cattle.

References	N	Breed	Sample	Trait	Method	Validation*	R^2
Hansen (1999)	310	–	Milk	Ac	PLS	Tr/Te	0.81
Heuer et al. (2001)	180	–	Milk	Ac	PLS	LOOCV	0.24[b]
de Roos et al. (2007)	1,080	Holstein	Milk	Ac	PLS	CV	0.72[c]
de Roos et al. (2007)	1,080	Holstein	Milk	BHB	PLS	CV	0.62[c]
Grelet et al. (2016)	224	Holstein	Milk	Ac	PLS	R-Tr/Te[a]	0.67
Grelet et al. (2016)	434	Holstein	Milk	BHB	PLS	R-Tr/Te[a]	0.63
Belay et al. (2017)	1,914	Holstein	Blood	BHB	PLS	R-Tr/Te[a]	0.40
Pralle et al. (2018)	3,629	Holstein	Blood	BHB	ANN	R-Tr/Te[a]	0.56
Bonfatti et al. (2019)	1,910	Multibreed	Blood	BHB	PLS	R-Tr/Te[a]	0.52
Benedet et al. (2019)	295	Multibreed	Blood	BHB	PLS	3-F CV	0.63
Benedet et al. (2019)	294	Multibreed	Blood	NEFA	PLS	3-F CV	0.52
Benedet et al. (2019)	294	Multibreed	Blood	BUN	PLS	3-F CV	0.58
Benedet et al. (2019)	294	Multibreed	Blood	Glu	PLS	3-F CV	0.20
Benedet et al. (2019)	294	Multibreed	Blood	GOT	PLS	3-F CV	0.24
Grelet et al. (2019)	205	Holstein	Blood	BHB	PLS	4-F CV	0.70
Grelet et al. (2019)	234	Holstein	Blood	NEFA	PLS	4-F CV	0.39
Grelet et al. (2019)	387	Holstein	Blood	IGF-1	PLS	4-F CV	0.61
Grelet et al. (2019)	380	Holstein	Blood	Glu	PLS	4-F CV	0.44
Luke et al. (2019)	878	Holstein	Blood	BHB	PLS	R-Tr/Te[a]	0.60
Luke et al. (2019)	878	Holstein	Blood	NEFA	PLS	R-Tr/Te[a]	0.45
Luke et al. (2019)	878	Holstein	Blood	BUN	PLS	R-Tr/Te[a]	0.35
Müller et al. (2019)	585	Holstein	Blood	BHB	PLS	CV	0.42

*Partial least square (PLS), artificial neural network (ANN), train and test cross-validation defined by splitting the data set randomly (R-Tr/Te), number of folds (n-F) in the cross-validation (CV), leave-one-out cross-validation (LOOCV). [a]External or independent validation. [b]Standard error in the cross-validation as accuracy metric. [c]Correlation coefficient (r) transformed to coefficient of determination (R^2). *The validation strategy defined as "CV" was assigned for the reviewed paper that did not completely describe the validation method adopted or the authors defined that cross-validation was employed.*

TABLE 11 | Number of samples (N), accuracy (Acc), sensitive (Sen), and specificity (Spe) in the validation set for mastitis (Mas) and lameness (Lam) traits using milk mid-infrared spectrometry using partial least square in dairy cattle.

Reference	N	Breed	Trait	Validation	Acc (%)	Sen (%)	Spe (%)
Mineur et al. (2017)	9,811	Multibreed	Lam	R-Tr/Te	–	60	62
Rienesl et al. (2019)	2,340	Multibreed	Mas	R-Tr/Te*	68	57	79
Bonfatti et al. (2020)	3,771	Multibreed	Lam	10-F CV	62	57	62

*Train and test cross-validation defined by splitting the data set randomly (R-Tr/Te), number of folds (n-F) in the cross-validation (CV), and *external or independent validation.*

certified, high-quality meat products, there is a growing interest by the beef meat chain to accurately assess meat quality traits (Andrés et al., 2008; Prieto et al., 2008). To date, meat quality traits have been measured using physical methods, which are time-consuming, expensive, destructive (depreciating the value of the carcass), and unsuitable to perform individually in large-scale (Su et al., 2018; Chapman et al., 2019). To satisfy the requirements of the modern meat industry, NIR spectrometry has been stated as an alternative tool for high throughput phenotyping meat quality traits because it is considered an accurate, fast, non-invasive and non-destructive technique with great potential for in-line application (Prevolnik et al., 2004; Prieto et al., 2009a; Chapman et al., 2019). The feasibility and robustness of NIR technique to predict meat quality traits in cattle have been investigated by several researchers (**Tables 12–14**). Here our focus will be on meat tenderness, intramuscular fat content, meat color, and cooking loss traits, since such attributes impact consumers' satisfaction. Meat quality traits can be measured using different methodologies, but in our review, such traits were summarized regardless of the methodology applied. The R^2 observed in the reviewed papers for meat tenderness varied from 0.12 (De Marchi et al., 2007) to 0.81 (Prieto et al., 2014) in the validation set (**Table 12**). The R^2 for intramuscular fat content varied from 0.02 (Magalhães et al., 2018) to 0.99 (Su et al., 2014) in the validation set (**Table 13**). For color traits (L*, a*, and b*), the R^2 in the validation set (**Table 14**) were in a range of 0.16 (Magalhães et al., 2018) to 0.93 (Zhang et al., 2015). The R^2 observed for cooking losses varied from 0.001 (Prieto et al., 2008) to 0.61 (Zhang et al., 2015) in the validation set (**Table 14**). Overall, NIR spectrometry has shown great potential to assess meat quality traits within different breeds. Furthermore, meat quality traits can be generated directly on the raw beef under

TABLE 12 | Number of samples (N) and coefficient of determination (R^2) in the validation set for meat tenderness trait predicted from near-infrared spectrometry in cattle.

References	N	Breed	Method	Validation*	R^2
Mitsumoto et al. (1991)	11	Japanese Black	MLR	–	0.67[b]
Hildrum et al. (1994)	10	Norwegian	PCR	CV	0.29[b]
Byrne et al. (1998)	70	–	PLS	CV	0.37[b]
Park et al. (1998)	119	–	PLS	Tr/Te	0.63
Rødbotten et al. (2000)	79	Norwegian Red	PLS	LOOCV	0.36[b]
Rødbotten et al. (2001)	48	Norwegian	PLS	CV	0.72[b]
Venel et al. (2001)	67	–	PLS	LOOCV	0.31[b]
Leroy et al. (2003)	189	Belgian White Blue	PLS	CV	0.25
Liu et al. (2003)	22	Multibreed	PLS	LOOCV	0.48
Shackelford et al. (2005)	146	Multibreed	MLR	Tr/Te	0.22
De Marchi et al. (2007)	148	Piamontese	PLS	4-FCV	0.12
Andrés et al. (2008)	112	Maronesa	PLS	LOOCV	0.53
Ripoll et al. (2008)	190	Multibreed	PLS	R-Tr/Te	0.74
Prieto et al. (2008)	67	-	PLS	LOOCV	0.17
Prieto et al. (2009b)	194	Crossbred	PLS	LOOCV	0.31
Rosenvold et al. (2009)	381	Hereford	PLS	R-Tr/Te	0.58
Cecchinato et al. (2009)	1,298	Piamontese	PLS	Tr/Te	0.50
Yancey et al. (2010)	40	Multibreed	PLS	LOOCV	0.28[b]
Cecchinato et al. (2011)	1,208	Piamontese	PLS	R-Tr/Te	0.21
De Marchi et al. (2013)	336	Multibreed	PLS	8-FCV	0.34
De Marchi (2013)	81	Crossbred	PLS	LOOCV	0.13
Prieto et al. (2014)	63	Crossbred	PLS	LOOCV	0.81
Zhang et al. (2015)	162	Yak	PLS	R-Tr/Te	0.43
Magalhães et al. (2018)	644	Nelore	PLS	LOOCV	0.40
Su et al. (2018)	442	Multibreed	PLS	R-Tr/Te[a]	0.60
Qiao et al. (2015)	234	-	SVM	Tr/Te	0.20
Wyrwisz et al. (2019)	89	Holstein	PLS	TR/Te	0.62
Savoia et al. (2020)	1,166	Piamontese	Bayes B	LOOCV[a]	0.16
Cafferky et al. (2020)	595	Multibreed	PLS	LOOCV	0.22

*Mulitple linear regression (MLR), principal components regression (PCR), partial least square (PLS), support vector machine (SVM), number of folds (n-F) in the cross-validation (CV), leave-one-out cross-validation (LOOCV), train and test cross-validation defined by splitting the data set randomly (R-Tr/Te) or not (Tr/Te). [a]External or independent validation. [b]Correlation coefficient (r) transformed to coefficient of determination (R^2). *The validation strategy defined as "CV" was assigned for the reviewed paper that did not completely describe the validation method adopted or the authors defined that cross-validation was employed.*

slaughterhouses conditions as the NIR technique may not require sample pre-preparation. Nevertheless, further research needs to be conducted to validate the models across breeds and use modern data mining approaches to improve prediction quality.

TABLE 13 | Number of samples (N) and coefficient of determination (R^2) in the validation set for intramuscular fat content predicted from near-infrared spectrometry in cattle.

References	N	Breed	Method	Validation*	R^2
Mitsumoto et al. (1991)	11	Japanese Black	MLR	–	0.92[2]
Sanderson et al. (1997)	72	British Friesian	PLS	4-FCV	0.95
Rødbotten et al. (2000)	79	Norwegian Red	PLS	LOOCV	0.58[b]
Cozzolino and Murray (2002)	100	–	PLS	4-FCV	0.86
Cozzolino et al. (2002)	78	Hereford	PLS	4-FCV	0.92
Prevolnik et al. (2005)	34	Multibreed	PLS	CV	0.93
Ripoll et al. (2008)	190	Multibreed	PLS	R-Tr/Te[a]	0.76
Prieto et al. (2011)	194	Multibreed	PLS	LOOCV	0.43
Cecchinato et al. (2012)	148	Piamontese	PLS	4-FCV	0.82
Prieto et al. (2014)	63	Crossbred	PLS	LOOCV	0.86
Su et al. (2014)	182	Multibreed	PLS	R-Tr/Te[a]	0.99
Dixit et al. (2016)	108	–	PLS	Tr/Te	0.82
Magalhães et al. (2018)	644	Nelore	PLS	LOOCV	0.02

*Mulitple linear regression (MLR), partial least square (PLS), number of folds (n-F) in the cross-validation (CV), leave-one-out cross-validation (LOOCV), train and test cross-validation set defined by splitting the data randomly (R-Tr/Te) or not (Tr/Te). [a]External or independent validation. [b]Correlation coefficient (r) transformed to coefficient of determination (R^2). *The validation strategy defined as "CV" was assigned for the reviewed paper that did not completely describe the validation method adopted or the authors defined that cross-validation was employed.*

DATA MINING

Frequently, the main goal of using infrared spectrometry technology in the livestock industry is the development of predictive models to determine the content of specific compounds present in products such as milk, meat, and feedstuffs. However, many compounds present in such products are highly correlated with phenotypes that are difficult to measure in commercial and research settings, such as feed intake, methane emission, energy balance, methane emission, fertility, metabolic diseases, and meat quality traits, as previously discussed. In this context, several research studies have attempted to develop predictive models to predict such complex phenotypes for management decisions or breeding purposes. However, we have noted that factors such as the analytical method chosen to develop the predictive models and the cross-validation strategy used to evaluate the analytical approaches are not deeply discussed in the research studies involving livestock data. If not utilized properly, those two factors can result in (a) poor predictions due to the lack of ability of certain models to capture complex relationships between explanatory and response variables and (b) overoptimistic prediction quality due to high data dependency occurring between training and validation dataset. To developed robust predictive models using spectral data the following three steps should be followed: (1) spectra pretreatment, to remove noise or non-informative wavenumbers, (2) model training (or algorithm training), in which analytical techniques are used to assess the set of coefficients, number of latent variables, or hyperparameters, and (3) model validation, in which an independent dataset is used to evaluate the predictive ability of

TABLE 14 | Number of samples (N) and coefficient of determination (R^2) in the validation set for L* (R^2_{L*}), a* (R^2_{a*}), and b* (R^2_{b*}) meat color, and cooking losses (R^2_{CL}) traits predicted from near-infrared spectrometry in cattle.

References	N	Breed	Method	Validation[§]	R^2_{L*}	R^2_{a*}	R^2_{b*}	R^2_{CL}
Mitsumoto et al. (1991)	11	Japanese black	MLR	CV	–	–	–	0.59[b]
Leroy et al. (2003)	189	Belgian White Blue	PLS	CV	0.83	0.39	0.75	0.25
Liu et al. (2003)	113	Multibreed	PLS	LOOCV	0.55	0.90	0.78	–
De Marchi et al. (2007)	148	Piamontese	PLS	4-FCV	–	–	–	0.15
Andrés et al. (2008)	109	Maronesa	PLS	LOOCV	0.80	0.23	0.27	0.02
Prieto et al. (2008)	67	–	PLS	LOOCV	0.87	0.71	0.90	0.001
Prieto et al. (2009b)	194	Crossbred	PLS	LOOCV	0.83	0.76	0.84	0.23
Cecchinato et al. (2009)	1,298	Piamontese	PLS	CV	0.65	0.69	0.81	0.50
Cecchinato et al. (2011)	1,208	Piamontese	PLS	R-Tr/Te	0.64	0.68	0.44	0.04
De Marchi et al. (2013)	336	Multibreed	PLS	8-FCV	0.70	0.73	0.60	0.38
De Marchi (2013)	81	Crossbred	PLS	LOOCV	0.41	0.58	0.57	0.31
Prieto et al. (2014)	63	Crossbred	PLS	LOOCV	0.80	0.71	0.77	–
Zhang et al. (2015)	162	Yak	PLS	R-Tr/Te	0.74	0.81	0.93	0.61
Qiao et al. (2015)	234	–	SVM	Tr/Te	0.80	0.64	0.54	–
Magalhães et al. (2018)	644	Nelore	PLS	LOOCV	0.16	0.17	0.45	–
Su et al. (2018)	442	Multibreed	PLS	R-Tr/Te[a]	0.61	0.64	0.38	0.56
Wyrwisz et al. (2019)	89	Holstein	PLS	Tr/Te	0.33	0.57	0.61	0.47
Savoia et al. (2020)	1,166	Piamontese	Bayes B	LOOCV[a]	0.84	0.55	0.63	0.16

Mulitple linear regression (MLR), partial least square (PLS), support vector machine (SVM), number of folds (n-F) in the cross-validation (CV), leave-one-out cross-validation (LOOCV), train and test cross-validation set defined by splitting the data randomly (R-Tr/Te) or not (Tr/Te). [a]External or independent validation. [2]Correlation coefficient (r) transformed to coefficient of determination (R^2). [§]The validation strategy defined as "CV" was assigned for the reviewed paper that did not completely describe the validation method adopted or the authors defined that cross-validation was employed.

the model developed using the training dataset. These three main steps will be discussed throughout this review section.

Spectra Preprocessing

Infrared spectra data comprise signals related to compounds present in the biological sample as well as non-informative signals coming from background, high-frequency noise, baseline shift, and overlapping bands (Rinnan et al., 2009a). Therefore, preprocessing spectral data is a common and crucial strategy that helps to mitigate such undesirable signals present in the raw data, maximizing the relationship between the infrared spectrum and the target phenotype (Rinnan et al., 2009a; De Marchi et al., 2014; McParland and Berry, 2016). Furthermore, preprocessing the spectra data prior to fit the calibration model is used in attempting to obtain robust prediction models and to restrict the insertion of bias into the model. However, applying unsuitable or a high stringent preprocessing strategy might remove important information from the biological sample (Rinnan et al., 2009a). Spectra preprocessing are commonly performed using mathematical pretreatment techniques or variable selection approach. The main mathematical pretreatment techniques used in the reviewed papers to mitigate signal noise can be divided into two groups, scatter-correction methods (e.g., multiplicative scatter correction, standard normal variate, and orthogonal scatter correction) and spectral derivatives (e.g., Savitzky-Golay polynomial derivative). Multiplicative scatter correction (MSC) is used to remove physical effects including particle size and surface blaze from the spectra, which do not carry any chemical or physical information, by correcting differences in the baseline and the trend (Martens et al., 1983). Standard normal variate (SNV) aims to remove the multiplicative effects of scatter and particle size, giving the sample a unit standard deviation (Barnes et al., 1989). Orthogonal scatter correction (OSC) eliminates the parts linearly unrelated (orthogonal) to the response variable (Wold et al., 1998). Savitzky-Golay (SG) first derivative is used to improve the spectra resolution by eliminating constant baseline, whereas the second derivative eliminates both baseline and linear trend (Savitzky and Golay, 1964). More details and theory overview about the mathematical pretreatment techniques employed on NIR and MIR spectra can be found in Rinnan et al. (2009a,b). From the 113 published papers reviewed here, researchers have used spectra data without pretreatment (50), SG first derivative (28), SG second derivative (10), MSC (7), SNV (5), and OSC (2). Eleven authors did not report if some mathematical pretreatment was applied to the spectra data. Several authors also used the combination of more than one pretreatment strategy (e.g., SG first derivative + MSC; SG second derivative + SNV; and SG first derivative + SG second derivative + MSC). Some authors have reported an increase in the prediction quality using pretreated spectra data (Heuer et al., 2001; Rødbotten et al., 2001; Soyeurt et al., 2011; De Marchi et al., 2011), whereas others have observed that the pretreatment failed to improve prediction accuracies (McParland et al., 2011; Cecchinato et al., 2012; Dehareng et al., 2012; Shetty et al., 2017a; Cafferky et al., 2020).

Analytical methods commonly employed on spectra data are suitable to reduce the full-spectrum to a few latent variables or perform some type of regularization (e.g., ridge and lasso). However, even performing such dimensionality reduction, they may also be penalized by noise or non-informative wavenumbers. Furthermore, the number of wavenumbers in

infrared spectrometry datasets usually outnumbers the sample size. For example, a dataset containing 30 samples with their respective spectra data (1,060 wavenumbers). Note that the number of parameters p (1,060 wavenumbers) is greater than the number of observations n (30 samples). In such situations, the use of least squares is not appropriate since it will yield a set of coefficient estimates that result in a perfect fit to the data and the residuals will be zero (James et al., 2013). This phenomenon is a concern in data analysis because such perfect fit will potentially lead to overfitting the data (Hastie et al., 2009). Variable selection, therefore, is an important strategy used prior to the model calibration to reduce the data dimensionality by selecting a subset of relevant features from the original space to improve the model robustness and reduce the model complexity (Koljonen et al., 2008; Rinnan et al., 2009a). Although several authors removed the water noise wavenumbers, here we are only taking into account studies that performed variable selection based on a mathematical or statistical approach. Thus, only nine out of 113 published papers reviewed here performed variable selection prior to the calibration model. Variable selection was employed using a genetic algorithm (GA), uninformative variable elimination (UVE), variable importance for projection (VIP), and coefficient of variation (CV) combined with Markov Blanket (MB) techniques by 4, 3, 2, and 1 studies, respectively. Briefly, GA is an algorithm based on the biological evolution theory and natural selection and the main idea is to find within the set of predictor variables the ones that best fitted the model. The best predictor variables need to show high "fitness" and probability to "survive" to be included in the subsequent variable sets used for model refit. An iterative process is performed until the GA has selected the best predictor variable set or the best combination of them (Leardi et al., 1992). UVE approach adds artificial noise predictor variables, multiplied by a constant close to zero in order to eliminate any possible interaction with the original variables, to the reference dataset before fitting the model. The wavenumbers (original variables) that play a less important role in the model (based on the root mean square error, for example) than the random variables are considered uninformative and eliminated from the dataset before the procedure is repeated. The iterative process is performed until the stop criterion is reached (Centner and Massart, 1996). Using the VIP technique, one calculates a coefficient v that represents the importance or influence of each predictor variable on the response variable. Thus, predictor variables with a $v <$ user-defined threshold u ($v < 1$, for example) are less relevant to fit the model and can be eliminated (Wold et al., 1993). CV is a well-known standardized measure of dispersion and it is used to eliminate wavenumbers that lack variability between samples. The MB notion is widely used in Bayesian Network and is defined as: for a node (target variable), its MB is the minimal set of parents, children, and spouses (wavenumbers) that best represents the node (Pearl, 1988). Studies that performed variable selection prior to the calibration step have reported an improvement in the quality of the predictions for different phenotypes and analytical approaches (Wu et al., 2009, 2012; Gottardo et al., 2015, 2016; Niero et al., 2016; Dórea et al., 2018). Although the authors have observed that spectra pretreatment and variable selection improved the predictions accuracies, there is no consensus in the literature regarding which situations such techniques will effectively result in better prediction ability, especially using larger datasets. Therefore, the effect of spectra data pretreatment and variable selection on the prediction quality should be more deeply investigated. Furthermore, as pointed out by De Marchi et al. (2014) and observed in the published papers reviewed here, the authors usually report only the precision and accuracy for the best model, while information regarding other models is not shown and discussed for full comparison.

Calibration Models

From the 113 published papers retrieved from Web of Science, Partial Least Squares (PLS) was the most used statistical approach (101 papers) for the development of predictive equations, when compared to other machine learning (ML) methods. The simple implementation makes PLS a well-established and widely used methodology to generate novel complex traits from infrared spectrometry data in different fields. PLS is a dimension reduction technique suitable when the number of predictors is greater than the number of observations (e.g., infrared spectra data) as well as when strong collinearity exists between predictor variables, i.e., some wavenumbers can be rewritten as a linear function of others (Martens and Naes, 1987). Briefly, PLS maximizes the covariance between the predictor variables and the response variable resulting in a small set of components (latent variables), commonly called factors, that are used to predict target phenotypes in a new dataset (Martens and Jensen, 1982; Martens and Naes, 1987). Multiple linear regression (MLR) has also been used (Mitsumoto et al., 1991; Shackelford et al., 2005) or compared to other methodology (Pralle et al., 2018; Müller et al., 2019) to predict complex phenotypes using spectra data. MLR solves a number of simultaneous equations exploring the linear relationship between several explanatory variables (i.e., wavenumbers) and the continuous response variable (Hastie et al., 2009). Despite the power of such statistical method, Pralle et al. (2018) did not observe improvement in the prediction quality. In contrast, Müller et al. (2019) reported improvement when MLR was implemented compared with other methodologies such as PLS. In addition, the bottleneck of MLR methodology is that its implementation will often face the problem that the number of parameters is greater than the number of samples (Hastie et al., 2009). The PLS method to date has succeeded in predicting some complex traits with high accuracies, whereas for other traits, the prediction quality was poor, as previously reported in section "Complex Traits Predicted by Infrared Spectrometry Data." This fact highlights the need for more research studies evaluating other analytical strategies able to deal with missing data, non-linear relationships between response and explanatory variables, and high-dimensional data to improve the prediction quality of complex phenotypes. Recently, Bayesian and ML techniques have been implemented to predict a range of phenotypes in livestock; however, it is at a small proportion compared with the number of studies using PLS. Bayesian models have been developed for high-dimensional regression and they are widely used in the context of genomic prediction (Meuwissen et al., 2001). In addition to

the possibility of assigning prior information for the marker effects, here substituted by the wavenumbers' effects, Bayesian methods are also able to perform estimate shrinkage and variable selection. For genomic prediction, Bayesian methods may have greater predictive power than dimension-reduction methods (Meuwissen et al., 2001; de los Campos et al., 2013). Ferragina et al. (2015) reported that Bayes B approach, which is one of the many Bayesian methods available, outperformed PLS methods for predicting milk components and technological properties using infrared spectral data and Bayes B was able to select a small subset of important wavenumbers. Based on Ferragina et al. (2015) finds, Bittante and Cipolat-Gotet (2018); Toledo-Alvarado et al. (2018), and Savoia et al. (2020) also used Bayes B methodology to predict complex phenotypes using spectra data. ML techniques such as Support Vector Machine (SVM) and Artificial Neural Networks (ANN) have been tested as an alternative to the traditional PLS method, because of their ability to search in a high-dimensional space of predictor variables for features that best describe the response variable, with the ability to self-learn. Additionally, such methods can better model the complex relationships (e.g., non-linear and interactions) between the input variables and the response outcome, which could improve the prediction quality (Gianola et al., 2011). Indeed, the authors that used SVM or ANN approaches have reported an increase in prediction quality compared with PLS method (Hempstalk et al., 2015; Qiao et al., 2015; Dórea et al., 2018; Pralle et al., 2018; Grelet et al., 2020). Although ML methodologies are suitable to be implemented in the high-dimensional space of predictor variables, this approach tends to easily overfit, in general because of small datasets and noisy data (Hempstalk et al., 2015). Overfitting is a recurrent issue in ML methods, such as in ANN, and it is clearly identified by high prediction accuracy in the training dataset but very poor in the validation dataset. For such methods, it is very important to perform unbiased validation strategy, therefore ensuring maximum possible data independency between training and validation would be ideal to unbiased predictions (Roberts et al., 2017). Additionally, ML techniques often require an extensive search for hyperparameters (e.g., number of neurons, number of layers, learning rate, among others) before training the algorithms to perform final prediction (Bengio, 2012). Such search is critical in order to define the network architecture, which may detrimentally affect prediction quality if not appropriate (Bengio, 2012). Based on the comparisons between traditional (PLS) and advanced analytical methods (Bayesian and ML) found in the reviewed papers, the use of advanced techniques resulted in improved prediction accuracy for some complex phenotypes. However, the prediction quality is influenced by many factors, including the trait to be predicted (e.g., qualitative or quantitative), the quality of the reference data (observed data) set, the spectra quality, the spectra preprocessing, the sample size used to develop the prediction equations, and the validation strategies used for model development and validation (Karoui et al., 2010; Rutten et al., 2010; Ferragina et al., 2015; Bonfatti et al., 2017; Dórea et al., 2018). In addition, directly predicted traits (e.g., milk fat) usually has a significant signal in the spectra data, whereas indirectly predicted traits (e.g., feed efficiency and methane emission) the signal in the spectra is associated to complex traits through compounds found in the scanned products (milk or meat, for example) (Ferragina et al., 2015). The number of research studies implementing alternative methods to predict complex traits in livestock systems is small and, therefore, more investigation using a different analytical approach, sample size, data pretreatment, and variable selection, is important to shed light on the predictive analytics of complex phenotypes.

Validation Strategies

Infrared spectrometry data (MIR and NIR) have been stated as an important source of information to generate many novel complex phenotypes in dairy and beef cattle (Prevolnik et al., 2004; De Marchi et al., 2014; McParland and Berry, 2016; Gengler et al., 2016; Chapman et al., 2019). To predict such phenotypes, robust models or equations must be developed using a training dataset that represents the population variability. The approval that ensures prediction quality of the developed models is given through their performance when implemented in a validation dataset, ideally, an external dataset not previously utilized for model development. However, defining the external validation dataset is a non-trivial task in some cases, since the dependency between training and validation sets needs to be reduced as much as possible. The main reason for reducing such dependence between training and validation sets is the need to approximate prediction quality from model validation to real-life implementation, in which very little dependency between training and validation set will occur. In this review, we considered as an external validation set, all datasets in which some level of dependency between training and validation set was broken. For example, research trials using multiple herds where one herd or trial was removed from the dataset to validate the model. Although this is the desired validation strategy, in some situations, it is difficult to define an external validation set due to the hierarchical structure of the dataset. In such case or when datasets are small, internal validation is usually performed, which was the most used strategy in the papers reviewed here (67 out of 113). In this review, we considered internal validation the studies in which hierarchical structure in the dataset (e.g., country, herd, dietary effect, etc.) was not considered for data split strategies (holdout, leave-one-out, k-fold). Therefore, to create the training and internal validation datasets the reviewed studies used one of the data-splitting techniques: holdout (22 studies), leave-one-out cross-validation (20 studies), and k-fold cross-validation (25 studies). An example of each validation strategy technique used for model validation is depicted in **Figure 2**.

Briefly, in the holdout strategy (**Figure 2A**), given that animals are sourced in different herds, about 80% of the dataset is randomly used in the model training and the remaining 20% is used for model validation (Stone, 1974; Picard and Berk, 1990). When holdout is adopted, the test error rate can be highly variable depending on which sample is assigned in the training and validation set (Hastie et al., 2009). Leave-one-out cross-validation is an alternative to the holdout approach and involves splitting the dataset into two parts in which $N - 1$ observations are used to train the model and a single sample N is used to validate the model (**Figure 2B**). The splitting is iterated

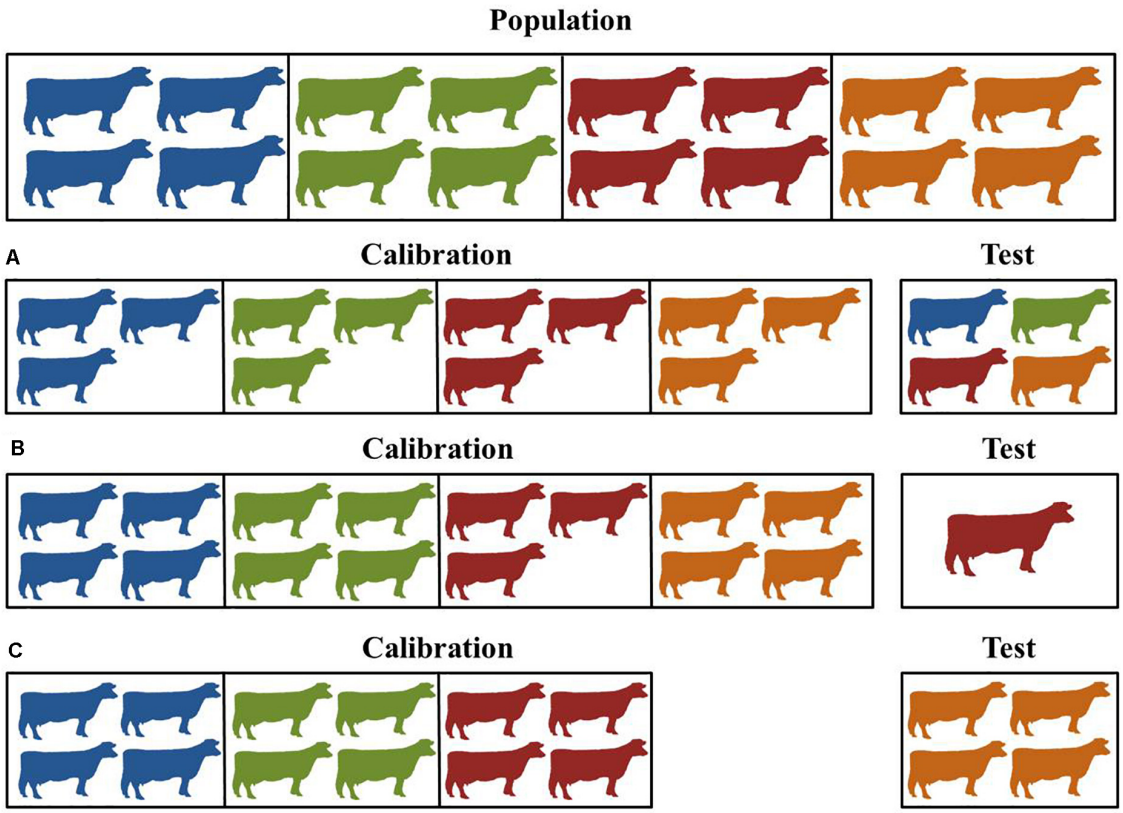

FIGURE 2 | Example of validation strategies employed in the publish papers retrieved from Web of Science. **(A)** split-data or k-fold cross-validation, **(B)** leave-one-out cross-validations, and **(C)** leave-one-group-out cross-validation. Colors represent animals from different herds.

N times until all the observations were used in the validation and the model performance is averaged across the *N* validation sets. Thus, the test error in leave-one-out cross-validation is highly variable compared to holdout, because the training dataset contains almost the same number of observations (*N* – *1*) as the entire dataset (Hastie et al., 2009). Leave-one-out is commonly used when the sample size is small and there is concern about the limited size of the calibration set (Gianola and Schön, 2016). The idea of leave-one-out cross-validation technique can also be adapted to perform leave-one-herd-out (e.g., group, farm, trial, year, among others), which can be a good strategy to reduce data dependence between training and validation dataset (**Figure 2C**). The k-fold cross-validation is performed by dividing the entire dataset into k disjoint sets of approximately equal size, usually randomly, in which *k* – *1* sets are used in the training and one set is used to validate the model. Such process is repeated *k* times until all *k* sets were used in the validation and the model performance is averaged across all *k* validation sets (Stone, 1974; Hastie et al., 2009). This process can be repeated many times, wherein each iteration different samples are assigned in both training and validation sets. Due to the larger validation dataset assigned in k-fold cross-validation as well as the test error averaged across the *k* different subsets, the test error is less sensitive to the partition of the dataset than in the leave-one-out cross-validation (Hastie et al., 2009). The drawback of the three procedures adopted to split the dataset, except for the leave-one-herd-out strategy, is that animals from the same herd or multiple records from the same animal will be present on the training and validation set, creating dependence between them.

Studies comparing different validation strategies using spectra data confirmed the hypothesis that prediction quality was inflated according to the split-data strategy employed to externally validate the model (Shetty et al., 2017b; Dórea et al., 2018; Lahart et al., 2019; Luke et al., 2019; Smith et al., 2019; Wang and Bovenhuis, 2019). Therefore, evaluating the fitted model using only internal validation is not recommended. The performance of the model fitting will be better than it should be, resulting in greater model precision and accuracy than if a true external validation is used, but the prediction accuracies in the external validation set are more realistic and quite often observed in practice. Several authors (32 out of the 112 papers reviewed here) reported that an independent dataset was used to externally validate the model's performance. However, by reviewing the papers from the 32 studies only seventeen fully performed external model validation. In those studies, the authors validated the models' performance using an external/independent dataset, which an entire farm, herd, trial, year, study, region, dataset, or batch was removed from the training dataset. The remaining studies (15) only assigned records by animal, individual records,

or lactations either randomly or not from the entire dataset to external validate the model. Such strategy does not produce a good independent dataset to test the model against real-life implementation because animals from the same herd or group can be present on the training and validation set. Fourteen out of 112 papers did not report if model performance was evaluated, only stated that cross-validation was employed, or the procedure was not clearly described. Therefore, it is a good practice to use external validation (if large sample size is available), based on data from a different farm, herd, trial, year, region, or batch, before full deployment of such predictive models.

CONCLUDING REMARKS

Important advances have been made in the nutrition, reproduction, management, and molecular breeding techniques of beef and dairy cattle in recent years. However, efficient and precise phenotyping remains a bottleneck and, therefore, modern high-throughput techniques should be developed, improved, and applied to take full advantage of the advancements performed in the different animal knowledge fields. Of the techniques currently available, this review summarized the applications of MIR and NIR spectrometry as a novel high-throughput phenotyping technique to generate complex phenotypes in dairy and beef cattle. Furthermore, it presented an overview, status update, and insights into the use of such techniques and the data mining strategies employed to predict the phenotypes of interest. The majority of studies compiled have demonstrated the capability and power of MIR and NIR technique to generate complex traits such as feed efficiency, methane emissions, energy balance, health, and meat quality from different biological samples routinely accessed, without additional cost and at the animal-level. Therefore, these phenotypes would be widely explored in dairy and beef cattle for on-farm decision-making, management, and breeding purpose. MIR and NIR spectrometry has important advantages compared to gold standard methods such as speed, low cost, non-invasive, non-destructive, and potential for in-line application; however, for the implementation of these high-throughput techniques into livestock operations, numerous issues regarding the modeling methodology must be considered. Few studies have used a large dataset as well as machine learning or Bayesian techniques to develop the calibrations models. Therefore, larger datasets and modern data mining approaches should be investigated to improve predictive ability and to confirm the existing calibration models.

AUTHOR CONTRIBUTIONS

TB and JD equally contributed direct and intellectual to the work and approved it for publication. Both authors contributed to the article and approved the submitted version.

REFERENCES

Afseth, N. K., Martens, H., Randby, S., Gidskehaug, L., Narum, B., Jørgensen, K., et al. (2010). Predicting the fatty acid composition of milk: a comparison of two fourier transform infrared sampling techniques. *Appl. Spectrosc.* 64, 700–707. doi: 10.1366/000370210791666200

Agnewa, R. E., Park, R. S., Maynea, C. S., and Laidlaw, A. S. (2004). Potential of near infrared spectroscopy to predict the voluntary intake of grazed grass. *Anim. Feed. Sci. Technol.* 115, 169–178. doi: 10.1016/J.ANIFEEDSCI.2004.01.009

Andrés, S., Silva, A., Soares-Pereira, A. L., Martins, C., Bruno-Soares, A. M., and Murray, I. (2008). The use of visible and near infrared reflectance spectroscopy to predict beef *M. longissimus thoracis et lumborum* quality attributes. *Meat Sci.* 78, 217–224. doi: 10.1016/j.meatsci.2007.06.019

Banos, G., and Coffey, M. P. (2010). Genetic association between body energy measured throughout lactation and fertility in dairy cattle. *Animal* 4, 189–199. doi: 10.1017/S1751731109991182

Barnes, R. J., Dhanoa, M. S., and Lister, S. J. (1989). Standard normal variate transformation and detrending of near-infrared diffuse reflectance spectra. *Appl. Spectrosc.* 43, 772–777. doi: 10.1366/0003702894202201

Bastin, C., Gengler, N., and Soyeurt, H. (2011). Phenotypic and genetic variability of production traits and milk fatty acid contents across days in milk for Walloon Holstein first-parity cows. *J. Dairy Sci.* 94, 4152–4163. doi: 10.3168/jds.2010-4108

Belay, T. K., Dagnachew, B. S., Kowalski, Z. M., and Ådnøy, T. (2017). An attempt at predicting blood β-hydroxybutyrate from Fourier-transform mid-infrared spectra of milk using multivariate mixed models in Polish dairy cattle. *J. Dairy Sci.* 100, 6312–6326. doi: 10.3168/jds.2016-12252

Bell, M. J., and Tzimiropoulos, G. (2018). Novel monitoring systems to obtain dairy cattle phenotypes associated with sustainable production. *Front. Sustain. Food Syst.* 2:31. doi: 10.3389/fsufs.2018.00031

Benedet, A., Manuelian, C. L., Zidi, A., Penasa, M., and De Marchi, M. (2019). Invited review: β-hydroxybutyrate concentration in blood and milk and its associations with cow performance. *Animal* 13, 1676–1689. doi: 10.1017/S175173111900034X

Bengio, Y. (2012). "Practical recommendations for gradient-based training of deep architectures," in *Neural Networks: Tricks of the Trade*, eds G. Montavon, G. B. Orr, and K.-R. Müller (Heidelberg: Springer), 437–478. doi: 10.1007/978-3-642-35289-8_26

Berry, D. P. (2015). Breeding the dairy cow of the future: What do we need? *Anim. Prod. Sci.* 55, 823–837. doi: 10.1071/AN14835

Berry, D. P., Buckley, F., Dillon, P., Evans, R. D., Rath, M., and Veerkamp, R. F. (2003). Genetic relationships among body condition score, body weight, milk yield, and fertility in dairy cows. *J. Dairy Sci.* 86, 2193–2204. doi: 10.3168/jds.S0022-0302(03)73809-0

Berry, D. P., and Crowley, J. J. (2013). Cell biology symposium: genetics of feed efficiency in dairy and beef cattle. *J. Anim. Sci.* 91, 1594–1613. doi: 10.2527/jas.2012-5862

Berry, D. P., Wall, E., and Pryce, J. E. (2014). Genetics and genomics of reproductive performance in dairy and beef cattle. *Animal* 8, 105–121. doi: 10.1017/S1751731114000743

Bittante, G., and Cipolat-Gotet, C. (2018). Direct and indirect predictions of enteric methane daily production, yield, and intensity per unit of milk and cheese, from fatty acids and milk Fourier-transform infrared spectra. *J. Dairy Sci.* 101, 7219–7235. doi: 10.3168/jds.2017-14289

Boichard, D. (1990). Estimation of the economic value of conception rate in dairy cattle. *Livest. Prod. Sci.* 24, 187–204. doi: 10.1016/0301-6226(90)90001-M

Boichard, D., and Brochard, M. (2012). New phenotypes for new breeding goals in dairy cattle. *Animal* 6, 544–550. doi: 10.1017/S1751731112000018

Bonfatti, V., Degano, L., Menegoz, A., and Carnier, P. (2016). Short communication: mid-infrared spectroscopy prediction of fine milk composition and technological properties in Italian Simmental. *J. Dairy Sci.* 99, 8216–8221. doi: 10.3168/jds.2016-10953

Bonfatti, V., Di Martino, G., and Carnier, P. (2011). Effectiveness of mid-infrared spectroscopy for the prediction of detailed protein composition and contents of protein genetic variants of individual milk of Simmental cows. *J. Dairy Sci.* 94, 5776–5785. doi: 10.3168/JDS.2011-4401

Bonfatti, V., Ho, P. N., and Pryce, J. E. (2020). Usefulness of milk mid-infrared spectroscopy for predicting lameness score in dairy cows. *J. Dairy Sci.* 103, 2534–2544. doi: 10.3168/jds.2019-17551

Bonfatti, V., Tiezzi, F., Miglior, F., and Carnier, P. (2017). Comparison of Bayesian regression models and partial least squares regression for the development of infrared prediction equations. *J. Dairy Sci.* 100, 7306–7319. doi: 10.3168/jds.2016-12203

Bonfatti, V., Turner, S.-A., Kuhn-Sherlock, B., Luke, T. D. W., Ho, P. N., Phyn, C. V. C., et al. (2019). Prediction of blood β-hydroxybutyrate content and occurrence of hyperketonemia in early-lactation, pasture-grazed dairy cows using milk infrared spectra. *J. Dairy Sci.* 102, 6466–6476. doi: 10.3168/jds.2018-15988

Boval, M., Coates, D. B., Lecomte, P., Decruyenaere, V., and Archimède, H. (2004). Faecal near infrared reflectance spectroscopy (NIRS) to assess chemical composition, in vivo digestibility and intake of tropical grass by Creole cattle. *Anim. Feed. Sci. Technol.* 114, 19–29. doi: 10.1016/j.anifeedsci.2003.12.009

Byrne, C. E., Downey, G., Troy, D. J., and Buckley, D. J. (1998). Non-destructive prediction of selected quality attributes of beef by near-infrared reflectance spectroscopy between 750 and 1098 nm. *Meat Sci.* 49, 399–409. doi: 10.1016/S0309-1740(98)00005-9

Cafferky, J., Sweeney, T., Allen, P., Sahar, A., Downey, G., Cromie, A. R., et al. (2020). Investigating the use of visible and near infrared spectroscopy to predict sensory and texture attributes of beef *M. longissimus thoracis et lumborum*. *Meat Sci.* 159:107915. doi: 10.1016/j.meatsci.2019.107915

Cecchinato, A., De Marchi, M., Boukha, A., Ribeca, C., and Carnier, P. (2009). Genetic correlations between measures of beef quality traits and their predictions by near- infrared spectroscopy in the Piemontese cattle breed. *Ital. J. Anim. Sci.* 8, 51–53. doi: 10.4081/ijas.2009.s2.51

Cecchinato, A., De Marchi, M., Penasa, M., Albera, A., and Bittante, G. (2011). Near-infrared reflectance spectroscopy predictions as indicator traits in breeding programs for enhanced beef quality. *J. Anim. Sci.* 89, 2687–2695. doi: 10.2527/jas.2010-3740

Cecchinato, A., De Marchi, M., Penasa, M., Casellas, J., Schiavon, S., and Bittante, G. (2012). Genetic analysis of beef fatty acid composition predicted by near-infrared spectroscopy. *J. Anim. Sci.* 90, 429–438. doi: 10.2527/jas.2011-4150

Centner, V., and Massart, D.-L. (1996). Elimination of uninformative variables for multivariate calibration. *Anal. Chem.* 68, 3851–3858. doi: 10.1021/ac960321m

Chapman, J., Elbourne, A., Truong, V. K., and Cozzolino, D. (2019). Shining light into meat - a review on the recent advances in in vivo and carcass applications of near infrared spectroscopy. *Int. J. Food Sci. Technol.* doi: 10.1111/ijfs.14367

Chilliard, Y., Martin, C., Rouel, J., and Doreau, M. (2009). Milk fatty acids in dairy cows fed whole crude linseed, extruded linseed, or linseed oil, and their relationship with methane output. *J. Dairy Sci.* 92, 5199–5211. doi: 10.3168/jds.2009-2375

Coffey, M. P., Emmans, G. C., and Brotherstone, S. (2001). Genetic evaluation of dairy bulls for energy balance traits using random regression. *Anim. Sci.* 73, 29–40. doi: 10.1017/S1357729800058021

Collard, B. L., Boettcher, P. J., Dekkers, J. C. M., Petitclerc, D., and Schaeffer, L. R. (2000). Relationships between energy balance and health traits of dairy cattle in early lactation. *J. Dairy Sci.* 83, 2683–2690. doi: 10.3168/jds.S0022-0302(00)75162-9

Connor, E. E. (2015). Invited review: improving feed efficiency in dairy production: challenges and possibilities. *Animal* 9, 395–408. doi: 10.1017/S1751731114002997

Coppa, M., Ferlay, A., Leroux, C., Jestin, M., Chilliard, Y., Martin, B., et al. (2010). Prediction of milk fatty acid composition by near infrared reflectance spectroscopy. *Int. Dairy J.* 20, 182–189. doi: 10.1016/j.idairyj.2009.11.003

Cozzolino, D., De Mattos, D., and Vaz Martins, D. (2002). Visible/near infrared reflectance spectroscopy for predicting composition and tracing system of production of beef muscle. *Anim. Sci.* 74, 477–484. doi: 10.1017/S1357729800052632

Cozzolino, D., and Murray, I. (2002). Effect of sample presentation and animal muscle species on the analysis of meat by near infrared reflectance spectroscopy. *J. Near Infrared Spec.* 10, 37–44. doi: 10.1255/jnirs.319

de los Campos, G., Hickey, J. M., Pong-Wong, R., Daetwyler, H. D., and Calus, M. P. L. (2013). Whole genome regression and prediction methods applied to plant and animal breeding. *Genetics* 193, 327–345. doi: 10.1534/genetics.112.143313

De Marchi, M. (2013). On-line prediction of beef quality traits using near infrared spectroscopy. *Meat Sci.* 94, 455–460. doi: 10.1016/j.meatsci.2013.03.003

De Marchi, M., Berzaghi, P., Boukha, A., Mirisola, M., and Galol, L. (2007). Use of near infrared spectroscopy for assessment of beef quality traits. *Ital. J. Anim. Sci.* 6, 421–423. doi: 10.4081/ijas.2007.1s.421

De Marchi, M., Bonfatti, V., Cecchinato, A., Di Martino, G., and Carnier, P. (2009). Prediction of protein composition of individual cow milk using mid-infrared spectroscopy. *Ital. J. Anim. Sci.* 8, 399–401. doi: 10.4081/ijas.2009.s2.399

De Marchi, M., Penasa, M., Cecchinato, A., and Bittante, G. (2013). The relevance of different near infrared technologies and sample treatments for predicting meat quality traits in commercial beef cuts. *Meat Sci.* 93, 329–335. doi: 10.1016/j.meatsci.2012.09.013

De Marchi, M., Penasa, M., Cecchinato, A., Mele, M., Secchiari, P., and Bittante, G. (2011). Effectiveness of mid-infrared spectroscopy to predict fatty acid composition of Brown Swiss bovine milk. *Animal* 5, 1653–1658. doi: 10.1017/S1751731111000747

De Marchi, M., Toffanin, V., Cassandro, M., and Penasa, M. (2014). Invited review: mid-infrared spectroscopy as phenotyping tool for milk traits. *J. Dairy Sci.* 97, 1171–1186. doi: 10.3168/jds.2013-6799

de Roos, A. P. W., van den Bijgaart, H. J. C. M., Hørlyk, J., and Jong, G. (2007). Screening for Subclinical ketosis in dairy cattle by fourier transform infrared spectrometry. *J. Dairy Sci.* 90, 1761–1766. doi: 10.3168/jds.2006-203

de Vries, M. J., and Veerkamp, R. F. (2000). Energy balance of dairy cattle in relation to milk production variables and fertility. *J. Dairy Sci.* 83, 62–69. doi: 10.3168/jds.s0022-0302(00)74856-9

Decruyenaere, V., Visser, M., de Stilmant, D., Clément, C., and Sinnaeve, G. (2004). Faecal near infrared reflectance spectroscopy for ruminant feed intake prediction. *Grassl. Sci.* 9, 1034–1036.

Dehareng, F., Delfosse, C., Froidmont, E., and Soyeurt, H. (2012). Potential use of milk mid-infrared spectra to predict individual methane emission of dairy cows. *Animal* 6, 1694–1701. doi: 10.1017/S1751731112000456

Dekkers, J. C. M. (1991). Estimation of economic values for dairy cattle breeding goals: bias due to sub-optimal management policies. *Livest. Prod. Sci.* 29, 131–149. doi: 10.1016/0301-6226(91)90062-U

Delhez, P., Ho, P. N., Gengler, N., Soyeurt, H., and Pryce, J. E. (2020). Diagnosing the pregnancy status of dairy cows: How useful is milk mid-infrared spectroscopy? *J. Dairy Sci.* 103, 3264–3274. doi: 10.3168/jds.2019-17473

Dijkstra, J., van Zijderveld, S. M., Apajalahti, J. A., Bannink, A., Gerrits, W. J. J., Newbold, J. R., et al. (2011). Relationships between methane production and milk fatty acid profiles in dairy cattle. *Anim. Feed Sci. Technol.* 166-167, 590–595. doi: 10.1016/j.anifeedsci.2011.04.042

Diskin, M. G., and Kenny, D. A. (2014). Optimising reproductive performance of beef cows and replacement heifers. *Animal* 8, 27–39. doi: 10.1017/S175173111400086X

Dixit, Y., Casado-Gavalda, M. P., Cama-Moncunill, R., Cama-Moncunill, X., Cullena, P. J., and Sullivan, C. (2016). Prediction of beef fat contente simultaneously under static and motion conditions using near infrared spectroscopy. *J. Near Infrared Spec.* 24, 353–361. doi: 10.1255/jnirs.1221

Dixit, Y., Casado-Gavalda, M. P., Cama-Moncunill, R., Cullen, P. J., and Sullivan, C. (2017). Challenges in model development for meat composition using multipoint nir spectroscopy from at-line to in-line monitoring. *J. Food Sci.* 81, 1557–1562. doi: 10.1111/1750-3841.13770

Dórea, J. R. R., French, E. A., and Armentano, L. E. (2017). Use of milk fatty acids to estimate plasma nonesterified fatty acid concentrations as an indicator of animal energy balance. *J. Dairy Sci.* 100, 6164–6176. doi: 10.3168/jds.2016-12466

Dórea, J. R. R., Rosa, G. J. M., Weld, K. A., and Armentano, L. E. (2018). Mining data from milk infrared spectroscopy to improve feed intake predictions in lactating dairy cows. *J. Dairy Sci.* 101, 5878–5889. doi: 10.3168/jds.2017-13997

Egger-Danner, C., Cole, J. B., Pryce, J. E., Gengler, N., Heringstad, B., Bradley, A., et al. (2015). Invited review: overview of new traits and phenotyping strategies in dairy cattle with a focus on functional traits. *Animal* 9, 191–207. doi: 10.1017/s1751731114002614

Eijndhoven, M. H. T. M.-V., Soyeurt, H., Dehareng, F., and Calus, M. P. L. (2013). Validation of fatty acid predictions in milk using mid-infrared spectrometry across cattle breeds. *Animal* 7, 348–354. doi: 10.1017/S1751731112001218

Eskildsen, C. E., Rasmussen, M. A., Engelsen, S. B., Larsen, L. B., Poulsen, N. A., and Skov, T. (2014). Quantification of individual fatty acids in bovine milk by

infrared spectroscopy and chemometrics: understanding predictions of highly collinear reference variables. *J. Dairy Sci.* 97, 7940–7951. doi: 10.3168/jds.2014-8337

Eskildsen, C. E., Skov, T., Hansen, M. S., Larsen, L. B., and Poulsen, N. A. (2016). Quantification of bovine milk protein composition and coagulation properties using infrared spectroscopy and chemometrics: a result of collinearity among reference variables. *J. Dairy Sci.* 99, 8178–8186. doi: 10.3168/jds.2015-10840

Fenwick, M. A., Llewellyn, S., Fitzpatrick, R., Kenny, D. A., Murphy, J. J., Patton, J., et al. (2008). Negative energy balance in dairy cows is associated with specific changes in IGF-binding protein expression in the oviduct. *Reproduction* 135, 63–75. doi: 10.1530/REP-07-0243

Ferragina, A., de los Campos, G., Vazquez, A. I., Cecchinato, A., and Bittante, G. (2015). Bayesian regression models outperform partial least squares methods for predicting milk components and technological properties using infrared spectral data. *J. Dairy Sci.* 98, 8133–8151. doi: 10.3168/jds.2014-9143

Ferrand, M., Huquet, B., Barbey, S., Barillet, F., Faucon, F., Larroque, H., et al. (2011). Determination of fatty acid profile in cow's milk using mid-infrared spectrometry: interest of applying a variable selection by genetic algorithms before a PLS regression. *Chemometr. Intell. Lab.* 106, 183–189. doi: 10.1016/j.chemolab.2010.05.004

Ferrand, M., Miranda, G., Larroque, H., Leray, O., Guisnel, S., Lahalle, F., et al. (2012). Determination of protein composition in milk by mid-infrared spectrometry. *ICAR Tech. Ser.* 16, 41–45.

Ferrand-Calmels, M., Palhière, I., Brochard, M., Leray, O., Astruc, J. M., Aurel, M. R., et al. (2014). Prediction of fatty acid profiles in cow, ewe, and goat milk by mid-infrared spectrometry. *J. Dairy Sci.* 97, 17–35. doi: 10.3168/jds.2013-6648

Fleming, A., Schenkel, F., Ali, R., Corredig, M., Carta, S., Gregu, C., et al. (2019). Phenotypic investigation of fine milk components in bovine milk and their prediction using mid-infrared spectroscopy. *Can. J. Anim. Sci.* 99, 218–227. doi: 10.1139/cjas-2018-0058

Fleming, A., Schenkel, F. S., Chen, J., Malchiodi, F., Bonfatti, V., Ali, R. A., et al. (2017). Prediction of milk fatty acid content with mid-infrared spectroscopy in Canadian dairy cattle using differently distributed model development sets. *J. Dairy Sci.* 100, 5073–5081. doi: 10.3168/jds.2016-12102

Franzoi, M., Niero, G., Visentin, G., Penasa, M., Cassandro, M., and De Marchi, M. (2019). Variation of detailed protein composition of cow milk predicted from a large database of mid-infrared spectra. *Animals* 9:176. doi: 10.3390/ani9040176

Friggens, N. C., Bjerring, M., Ridder, C., Højsgaard, S., and Larsen, T. (2008). Improved detection of reproductive status in dairy cows using milk progesterone measurements. *Reprod. Domest. Anim.* 43, 113–121. doi: 10.1111/j.1439-0531.2008.01150.x

Friggens, N. C., Ridder, C., and Løvendahl, P. (2007). On the use of milk composition measures to predict the energy balance of dairy cows. *J. Dairy Sci.* 90, 5453–5467. doi: 10.3168/jds.2006-821

Garnsworthy, P. C., and Unalt, Y. (2004). Estimation of dry-matter intake and digestibility in group-fed dairy cows using near infrared reflectance spectroscopy. *Anim. Sci.* 79, 327–334. doi: 10.1017/S1357729800090184

Gengler, N., Soyeurt, H., Dehareng, F., Bastin, C., Colinet, F., Hammami, H., et al. (2016). Capitalizing on fine milk composition for breeding and management of dairy cows. *J. Dairy Sci.* 99, 4071–4079. doi: 10.3168/jds.2015-10140

Gianola, D., Okut, H., Weigel, K. A., and Rosa, G. J. M. (2011). Predicting complex quantitative traits with Bayesian neural networks: a case study with Jersey cows and wheat. *BMC Genet.* 12:87. doi: 10.1186/1471-2156-12-87

Gianola, D., and Schön, C.-C. (2016). Cross-validation without doing cross-validation in genome-enabled prediction. *G3* 6, 3107–3128. doi: 10.1534/g3.116.033381

González-Recio, O., Pérez-Cabal, M. A., and Alenda, R. (2004). Economic value of female fertility and its relationship with profit in Spanish dairy cattle. *J. Dairy Sci.* 87, 3053–3061. doi: 10.3168/jds.S0022-0302(04)73438-4

Gottardo, P., De Marchi, M., Cassandro, M., and Penasa, M. (2015). Technical note: improving the accuracy of mid-infrared prediction models by selecting the most informative wavelengths. *J. Dairy Sci.* 98, 4168–4173. doi: 10.3168/jds.2014-8752

Gottardo, P., Penasa, M., Lopez-Villalobos, N., and De Marchi, M. (2016). Variable selection procedures before partial least squares regression enhance the accuracy of milk fatty acid composition predicted by mid-infrared spectroscopy. *J. Dairy Sci.* 99, 7782–7790. doi: 10.3168/jds.2016-10849

Grelet, C., Bastin, C., Gelé, M., Davière, J.-B., Johan, M., Werner, A., et al. (2016). Development of Fourier transform mid-infrared calibrations to predict acetone, β-hydroxybutyrate, and citrate contents in bovine milk through a European dairy network. *J. Dairy Sci.* 99, 4816–4825. doi: 10.3168/jds.2015-10477

Grelet, C., Froidmont, E., Foldager, L., Salavati, M., Hostens, M., Ferris, C. P., et al. (2020). Potential of milk mid-infrared spectra to predict nitrogen use efficiency of individual dairy cows in early lactation. *J. Dairy Sci.* 103, 4435–4445. doi: 10.3168/jds.2019-17910

Grelet, C., Vanlierde, A., Hostens, M., Foldager, L., Salavati, M., Ingvartsen, K. L., et al. (2019). Potential of milk mid-IR spectra to predict metabolic status of cows through blood components and an innovative clustering approach. *Animal* 13, 649–658. doi: 10.1017/S1751731118001751

Griffiths, P. R., and de Hasenth, J. A. (2007). *Fourier Transform Spectrometry*, 2nd Edn. Hoboken, NJ: John Wiley and Sons Inc.

Hammond, K., Crompton, L. A., Bannink, A., Dijkstra, J., Yanez-Ruiz, D. R., O'Kiely, P., et al. (2016). Review of current in vivo measurement techniques for quantifying enteric methane emission from ruminants. *Anim. Feed Sci. Technol.* 219, 13–30. doi: 10.1016/j.anifeedsci.2016.05.018

Hansen, P. W. (1999). Screening of dairy cows for ketosis by use of infrared spectroscopy and multivariate calibration. *J. Dairy Sci.* 82, 2005–2010. doi: 10.3168/jds.S0022-0302(99)75437-8

Hastie, T., Tibshirani, R., and Friedman, J. (2009). *The Elements of Statistical Learning*, 2 Edn. New York, NY: Springer.

Hempstalk, K., McParland, S., and Berry, D. P. (2015). Machine learning algorithms for the prediction of conception success to a given insemination in lactating dairy cows. *J. Dairy Sci.* 98, 5262–5273. doi: 10.3168/jds.2014-8984

Heuer, C., Luinge, H. J., Lutz, E. T. G., Schukken, Y. H., van der Maas, J. H., Wilmink, H., et al. (2001). Determination of acetone in cow milk by fourier transform infrared spectroscopy for the detection of subclinical ketosis. *J. Dairy Sci.* 84, 575–582. doi: 10.3168/JDS.S0022-0302(01)74510-9

Hildrum, K. I., Nilsen, B. N., Mielnik, M., and Naes, T. (1994). Prediction of sensory characteristics of beef by near-infrared spectroscopy. *Meat Sci.* 38, 67–80. doi: 10.1016/0309-1740(94)90096-5

Ho, P. N., Bonfatti, V., Luke, T. D. W., and Pryce, J. E. (2019). Classifying the fertility of dairy cows using milk mid-infrared spectroscopy. *J. Dairy Sci.* 102, 10460–10470. doi: 10.3168/jds.2019-16412

Ho, P. N., Marett, L. C., Wales, W. J., Axford, M., Oakes, E. M., and Pryce, J. E. (2020). Predicting milk fatty acids and energy balance of dairy cows in Australia using milk mid-infrared spectroscopy. *Anim. Prod. Sci.* 60, 164–168. doi: 10.1071/AN18532

Huntington, G. B., Leonard, E. S., and Burns, J. C. (2011). Technical note: use of near-infrared reflectance spectroscopy to predict intake and digestibility in bulls and steers. *J. Anim. Sci.* 89, 1163–1166. doi: 10.2527/jas.2010-3376

James, G., Written, D., Hastie, T., and Tibshirani, R. (2013). *An Introduction to Statistical Learning with Applications in R*. New York, NY: Springer.

Jamrozik, J., Koeck, A., Kistemaker, G. J., and Miglior, F. (2016). Multiple-trait estimates of genetic parameters for metabolic disease traits, fertility disorders, and their predictors in Canadian Holsteins. *J. Dairy Sci.* 99, 1990–1998. doi: 10.3168/jds.2015-10505

Jamrozik, J., Koeck, A., Miglior, F., Kistemaker, G., Schenkel, F., Kelton, D., et al. (2013). Genetic and genomic evaluation of mastitis resistance in Canada. *Interbull Bull.* 47, 43–51.

Johnson, J. R., Carstens, G. E., Prince, S. D., Ominski, K. H., Wittenberg, K. M., Undi, M., et al. (2017). Application of fecal near-infrared reflectance spectroscopy profiling for the prediction of diet nutritional characteristics and voluntary intake in beef cattle. *J. Dairy Sci.* 95, 447–454. doi: 10.2527/jas2016.0845

Johnson, K. A., and Johnson, D. E. (1995). Methane emissions from cattle. *J. Anim. Sci.* 73, 2483–2492. doi: 10.2527/1995.7382483x

Kaniyamattam, K., Elzo, M. A., Cole, J. B., and De Vries, A. (2016). Stochastic dynamic simulation modeling including multitrait genetics to estimate genetic, technical, and financial consequences of dairy farm reproduction and selection strategies. *J. Dairy Sci.* 99, 8187–8202. doi: 10.3168/jds.2016-11136

Karoui, R., Downey, G., and Blecker, C. (2010). Mid-infrared spectroscopy coupled with chemometrics: a tool for the analysis of intact food systems and the exploration of their molecular structure quality relationships - A review. *Chem. Rev.* 110, 6144–6168. doi: 10.1021/cr100090k

Kelton, D. F., Lissemore, K. D., and Martin, R. E. (1998). Recommendations for recording and calculating the incidence of selected clinical diseases of dairy cattle. *J. Dairy Sci.* 81, 2502–2509. doi: 10.3168/JDS.S0022-0302(98)70142-0

Knapp, J. R., Laur, G. L., Vadas, P. A., Weiss, W. P., and Tricarico, J. M. (2014). Invited review: enteric methane in dairy cattle production: quantifying the opportunities and impact of reducing emissions. *J. Dairy Sci.* 97, 3231–3261. doi: 10.3168/jds.2013-7234

Koljonen, J., Nordling, T. E. M., and Alander, J. T. (2008). A review of genetic algorithms in near infrared spectroscopy and chemometrics: past and future. *J. Near Infrared Spectrosc.* 16, 189–197. doi: 10.1255/jnirs.778

Lahart, B., McParland, S., Kennedy, E., Boland, T. M., Condon, T., Williams, M., et al. (2019). Predicting the dry matter intake of grazing dairy cows using infrared reflectance spectroscopy analysis. *J. Dairy Sci.* 102, 8907–8918. doi: 10.3168/jds.2019-16363

Landau, S. Y., Dvash, L., Roudman, M., Muklada, H., Barkai, D., Yehuda, Y., et al. (2016). Faecal near-IR spectroscopy to determine the nutritional value of diets consumed by beef cattle in east Mediterranean rangelands. *Animal* 10, 192–202. doi: 10.1017/S175173111500169X

Leardi, R., Boggia, R., and Terrile, M. (1992). Genetic algorithms as a strategy for feature selection. *J. Chemom.* 6, 267–281. doi: 10.1002/cem.1180060506

Leroy, B., Lambotte, S., Dotreppe, O., Lecocq, H., Istasse, L., and Clinquart, A. (2003). Prediction of technological and organoleptic properties of beef *Longissimus thoracis* from near-infrared reflectance and transmission spectra. *Meat Sci.* 66, 45–54. doi: 10.1016/S0309-1740(03)00002-0

Liu, Y., Lyon, B. G., Windham, W. R., Realini, C. E., Pringle, T. D. D., and Duckett, S. (2003). Prediction of color, texture, and sensory characteristics of beef steaks by visible and near infrared reflectance spectroscopy. A feasibility study. *Meat Sci.* 65, 1107–1115. doi: 10.1016/S0309-1740(02)00328-5

Lopez-Villalobos, N., Spelman, R. J., Melis, J., Davis, S. R., Berry, S. D., Lehnert, K., et al. (2014). Estimation of genetic and crossbreeding parameters of fatty acid concentrations in milk fat predicted by mid-infrared spectroscopy in New Zealand dairy cattle. *J. Dairy Res.* 81, 340–349. doi: 10.1017/S0022029914000272

Luginbühl, W. (2002). Evaluation of designed calibration samples for casein calibration in Fourier transform infrared analysis of milk. *LWT Food Sci. Technol.* 35, 554–558. doi: 10.1006/FSTL.2002.0902

Luke, T. D. W., Rochfort, S., Wales, W. J., Bonfatti, V., Marett, L., and Pryce, J. E. (2019). Metabolic profiling of early-lactation dairy cows using milk mid-infrared spectra. *J. Dairy Sci.* 102, 1747–1760. doi: 10.3168/jds.2018-15103

Magalhães, A. F. B., Teixeira, G. H. A., Ríos, A. C. H., Silva, D. B. S., Mota, L. F. M., Muniz, M. M. M., et al. (2018). Prediction of meat quality traits in Nelore cattle by near-infrared reflectance spectroscopy. *J. Anim. Sci.* 96, 4229–4237. doi: 10.1093/jas/sky284

Malacarne, M., Visentin, G., Summer, A., Cassandro, M., Penasa, M., Bolzoni, G., et al. (2018). Investigation on the effectiveness of mid-infrared spectroscopy to predict detailed mineral composition of bulk milk. *J. Dairy Res.* 85, 83–86. doi: 10.1017/S0022029917000826

Mann, S., Nydam, D. V., Lock, A. L., Overton, T. R., and McArt, J. A. A. (2016). Short communication: association of milk fatty acids with early lactation hyperketonemia and elevated concentration of nonesterified fatty acids. *J. Dairy Sci.* 99, 5851–5857. doi: 10.3168/jds.2016-10920

Martens, H., and Jensen, S. A. (1982). "Partial least squares regression: a new two-stage NIR calibration method," in *Proceedings of the 7th World Cereal and Bread Congress*, Amsterdam, 607–647.

Martens, H., Jensen, S. A., and Geladi, P. (1983). "Multivariate linearity transformations for near infrared reflectance spectroscopy," in *Nordic Symposium on Applied Statistics*, ed. O. H. J. Christie (Stokkand: Stokkand Forlag), 205–234.

Martens, H., and Naes, T. (1987). *Multivariate Calibration by Data Compression*. Chichester: John Wiley & Sons.

Martin, A. D., Afseth, N. K., Kohler, A., Randby, Å., Eknæs, M., Waldmann, A., et al. (2015). The relationship between fatty acid profiles in milk identified by Fourier transform infrared spectroscopy and onset of luteal activity in Norwegian dairy cattle. *J. Dairy Sci.* 98, 5374–5384. doi: 10.3168/jds.2015-9343

McArt, J. A. A., Nydam, D. V., and Overton, M. W. (2015). Hyperketonemia in early lactation dairy cattle: a deterministic estimate of component and total cost per case. *J. Dairy Sci.* 98, 2043–2054. doi: 10.3168/jds.2014-8740

McDermott, A., Visentin, G., De Marchi, M., Berry, D. P., Fenelon, M. A., O'Connor, P. M., et al. (2016). Prediction of individual milk proteins including free amino acids in bovine milk using mid-infrared spectroscopy and their correlations with milk processing characteristics. *J. Dairy Sci.* 99, 3171–3182. doi: 10.3168/jds.2015-9747

McParland, S., Banos, G., McCarthy, B., Lewis, E., Coffey, M. P., O'Neill, B., et al. (2012). Validation of mid-infrared spectrometry in milk for predicting body energy status in Holstein-Friesian cows. *J. Dairy Sci.* 95, 7225–7235. doi: 10.3168/jds.2012-5406

McParland, S., Banos, G., Wall, E., Coffey, M. P., Soyeurt, H., Veerkamp, R. F., et al. (2011). The use of mid-infrared spectrometry to predict body energy status of Holstein cows. *J. Dairy Sci.* 94, 3651–3661. doi: 10.3168/jds.2010-3965

McParland, S., and Berry, D. P. (2016). The potential of Fourier transform infrared spectroscopy of milk samples to predict energy intake and efficiency in dairy cows. *J. Dairy Sci.* 99, 4056–4070. doi: 10.3168/jds.2015-10051

McParland, S., Kennedy, E., Lewis, E., Moore, S. G., McCarthy, B., O'Donovan, M., et al. (2015). Genetic parameters of dairy cow energy intake and body energy status predicted using mid-infrared spectrometry of milk. *J. Dairy Sci.* 98, 1310–1320. doi: 10.3168/jds.2014-8892

McParland, S., Lewis, E., Kennedy, E., Moore, S. G., McCarthy, B., O'Donovan, M., et al. (2014). Mid-infrared spectrometry of milk as a predictor of energy intake and efficiency in lactating dairy cows. *J. Dairy Sci.* 97, 5863–5871. doi: 10.3168/jds.2014-8214

Meuwissen, T. H. E., Hayes, B. J., and Goddard, M. E. (2001). Prediction of total genetic value using genome-wide dense marker maps. *Genetics* 157, 1819–1829.

Miglior, F., Koeck, A., Jamrozik, J., Schenkel, F. S., Kelton, D. F., Kistemaker, G. J., et al. (2014). Index for mastitis resistance and use of BHBA for evaluation of health traits in Canadian Holsteins. *Interbull Bull.* 48, 73–78.

Mineur, A. Köck, A., Grelet, C., Gengler, N., Egger-Danner, C., and Sölkner, J. (2017). First results in the use of milk mid-infrared spectra in the detection of lameness in Austrian dairy cows. *Agric. Conspec. Sci.* 82, 163–166.

Mitsumoto, M., Maeda, S., Mitsuhashi, T., and Ozawa, S. (1991). Near-infrared spectroscopy determination of physical and chemical characteristics in beef cuts. *J. Food Sci.* 56, 1493–1496. doi: 10.1111/j.1365-2621.1991.tb08623.x

Moraes, J. C. F., Miguel, J. C., and Souza, C. J. H. (2007). Body condition score to predict the postpartum fertility of crossbred beef cows. *Pesq. Agropec. Bras.* 42, 741–746. doi: 10.1590/S0100-204X2007000500018

Müller, U., Kessera, J., Kochb, C., Helfrichc, H.-P., and Rietzd, C. (2019). Monitoring predictive and informative indicators of the energy status of dairy cows during early lactation in the context of monthly milk recordings using mid-infrared spectroscopy. *Livest. Sci.* 221, 6–14. doi: 10.1016/j.livsci.2018.12.020

Negussie, E., de Haas, Y., Dehareng, F., Dewhurst, R. J., Dijkstra, J., Gengler, N., et al. (2017). Invited review: large-scale indirect measurements for enteric methane emissions in dairy cattle: a review of proxies and their potential for use in management and breeding decisions. *J. Dairy Sci.* 100, 2433–2453. doi: 10.3168/jds.2016-12030

Niero, G., Penasa, M., Gottardo, P., Cassandro, M., and De Marchi, M. (2016). Short communication: selecting the most informative mid-infrared spectra wavenumbers to improve the accuracy of prediction models for detailed milk protein content. *J. Dairy Sci.* 99, 1853–1858. doi: 10.3168/jds.2015-10318

Park, B., Chen, Y. R., Hruschka, W. R., Shackelford, S. D., and Koohmaraie, M. (1998). Near-infrared reflectance analysis for predicting beef longissimus tenderness. *J. Anim. Sci.* 76, 2115–2120. doi: 10.2527/1998.7682115x

Patra, A. K. (2016). Recent advances in measurement and dietary mitigation of enteric methane emissions in ruminants. *Front. Vet. Sci.* 3:39. doi: 10.3389/fvets.2016.00039

Pearl, J. (1988). *Probabilistic Reasoning in Intelligent Systems: Networks of Plausible Inference*. San Mateo, CA: Morgan Kaufmann.

Picard, R. R., and Berk, K. N. (1990). Data splitting. *Am. Stat.* 44, 140–147. doi: 10.1080/00031305.1990

Pralle, R. S., Weigel, K. W., and White, H. M. (2018). Predicting blood β-hydroxybutyrate using milk Fourier transform infrared spectrum, milk composition, and producer-reported variables with multiple linear regression, partial least squares regression, and artificial neural network. *J. Dairy Sci.* 101, 4378–4387. doi: 10.3168/jds.2017-14076

Pravia, M. I., Ravagnolo, O., Urioste, J. I., and Garrick, D. J. (2014). Identification of breeding objectives using a bioeconomic model for a beef cattle production system in Uruguay. *Livest. Sci.* 160, 21–28. doi: 10.1016/j.livsci.2013.12.006

Prevolnik, M., Èandek-Potokar, M., Škorjanc, D., Velikonja-Bolta, Š., Škrlep, M., Žnidaršiè, T., et al. (2005). Predicting intramuscular fat content in pork and beef by near infrared spectroscopy. *Near Infrared Spectrosc.* 13, 77–85. doi: 10.1255/jnirs.460

Prevolnik, M., Candek-Potokar, M., and Skorjank, D. (2004). Ability of NIR spectroscopy to predict chemical composition and quality - a review. *Czech J. Anim. Sci.* 49, 500–510. doi: 10.17221/4337-CJAS

Prieto, N., Andrés, S., Giráldez, F. J., Mantecón, A. R., and Lavín, P. (2008). Ability of near infrared reflectance spectroscopy (NIRS) to estimate physical parameters of adult steers (oxen) and young cattle meat samples. *Meat Sci.* 79, 692–699. doi: 10.1016/J.MEATSCI.2007.10.035

Prieto, N., López-Campos, Ó., Aalhus, J. L., Dugan, M. E. R., Juárez, M., and Uttaro, B. (2014). Use of near infrared spectroscopy for estimating meat chemical composition, quality traits and fatty acid content from cattle fed sunflower or flaxseed. *Meat Sci.* 98, 279–288. doi: 10.1016/j.meatsci.2014.06.005

Prieto, N., Pawluczyk, O., Dugan, M. E. R., and Aalhus, J. L. (2017). A review of the principles and applications of near-infrared spectroscopy to characterize meat, fat, and meat products. *Appl. Spectrosc.* 71, 1403–1426. doi: 10.1177/0003702817709299

Prieto, N., Roehe, R., Lavín, P., Batten, G., and Andrés, S. (2009a). Application of near infrared reflectance spectroscopy to predict meat and meat products quality: a review. *Meat Sci.* 83, 175–186. doi: 10.1016/j.meatsci.2009.04.016

Prieto, N., Ross, D. W., Navajas, E. A., Nute, G. R., Richardson, R. I., and Hyslop, J. J. (2009b). On-line application of visible and near infrared reflectance spectroscopy to predict chemical-physical and sensory characteristics of beef quality. *Meat Sci.* 83, 96–103. doi: 10.1016/j.meatsci.2009.04.005

Prieto, N., Ross, D. W., Navajas, E. A., Richardson, R. I., Hyslop, J. J., Simm, G., et al. (2011). Online prediction of fatty acid profiles in crossbred Limousin and Aberdeen Angus beef cattle using near infrared reflectance spectroscopy. *Animal* 5, 155–165. doi: 10.1017/S1751731110001618

Qiao, T., Ren, J., Craigie, C., Zabalza, J., Maltin, C., and Marshalla, S. (2015). Quantitative prediction of beef quality using visible and nir spectroscopy with large data samples under industry conditions. *J. Appl. Spectrosc.* 82, 137–144. doi: 10.1007/s10812-015-0076-1

Rico, D. E., Chouinard, P. Y., Hassanat, F., Benchaar, C., and Gervais, R. (2016). Prediction of enteric methane emissions from Holstein dairy cows fed various forage sources. *Animal* 10, 203–211. doi: 10.1017/S1751731115001949

Rienesl, L., Khayatzadeh, N., Köck, A., Dale, L., Werner, A., Grelet, C., et al. (2019). Mastitis detection from milk mid- infrared (mir) spectroscopy in dairy cows. *Acta Univ. Agric. Silvic. Mendel. Brun.* 67, 1221–1226. doi: 10.11118/actaun201967051221

Rinnan, A., van den Berg, F., and Engelsen, S. B. (2009a). Review of the most common pre-processing techniques for near-infrared spectra. *TrAC Trend Anal. Chem.* 28, 1201–1222. doi: 10.1016/j.trac.2009.07.007

Rinnan, Å., Nørgaard, L., van den Berg, F., Thygesen, J., Bro, R., and Engelsen, S. B. (2009b). "Data Pre-processing," in *Infrared Spectroscopy for Food Quality Analysis and Control*, ed. D.-W. Sun (New York, NY: Academic Press), 29–50.

Ripoll, G., Albertí, P., Panea, B., Olleta, J. L., and Sañudo, C. (2008). Near-infrared reflectance spectroscopy for predicting chemical, instrumental and sensory quality of beef. *Meat Sci.* 80, 697–702. doi: 10.1016/j.meatsci.2008.03.009

Roberts, D. R., Bahn, V., Ciuti, S., Boyce, M. S., Elith, J., Guillera-Arroita, G., et al. (2017). Crossvalidation strategies for data with temporal, spatial, hierarchical, or phylogenetic structure. *Ecography* 40, 913–929. doi: 10.1111/ecog.02881

Rødbotten, R., Mevik, B.-H., and Hildrum, K. I. (2001). Prediction and classification of tenderness in beef from non-invasive diode array detected NIR spectra. *J. Near Infrared Spectrosc.* 9, 199–210. doi: 10.1255/jnirs.306

Rødbotten, R., Nilsen, B. N., and Hildrum, K. I. (2000). Prediction of beef quality attributes from early post mortem near infrared reflectance spectra. *Food Chem.* 69, 427–436. doi: 10.1016/S0308-8146(00)00059-5

Rosenvold, K., Micklander, E., Hansen, P. W., Burling-Claridge, R., Challies, M., Devine, C., et al. (2009). Temporal, biochemical and structural factors that influence beef quality measurement using near infrared spectroscopy. *Meat Sci.* 82, 379–388. doi: 10.1016/j.meatsci.2009.02.010

Rutten, M. J. M., Bovenhuis, H., Heck, J. M. L., and van Arendonk, J. A. M. (2011). Predicting bovine milk protein composition based on Fourier transform infrared spectra. *J. Dairy Sci.* 94, 5683–5690. doi: 10.3168/jds.2011-4520

Rutten, M. J. M., Bovenhuis, H., Hettinga, K. A., van Valenberg, H. J. F., and van Arendonk, J. A. M. (2009). Predicting bovine milk fat composition using infrared spectroscopy based on milk samples collected in winter and summer. *J. Dairy Sci.* 92, 6202–6209. doi: 10.3168/jds.2009-2456

Rutten, M. J. M., Bovenhuis, H., and van Arendonk, J. A. M. (2010). The effect of the number of observations used for Fourier transform infrared model calibration for bovine milk fat composition on the estimated genetic parameters of the predicted data. *J. Dairy Sci.* 93, 4872–4882. doi: 10.3168/jds.2010-3157

Sanderson, R., Lister, S. J., Dhanoa, M. S., Barnes, R. J., and Thomas, C. (1997). Use of near infrared reflectance spectroscopy to predict and compare the composition of carcass samples from young steers. *Anim. Sci.* 65, 45–54. doi: 10.1017/S1357729800016283

Savitzky, A., and Golay, M. J. E. (1964). Smoothing and differentiation of data by simplified least squares procedures. *Anal. Chem.* 36, 1627–1639. doi: 10.1021/ac60214a047

Savoia, S., Albera, A., Brugiapaglia, A., Stasio, L. D., Ferragina, A., Cecchinato, A., et al. (2020). Prediction of meat quality traits in the abattoir using portable and hand-held near-infrared spectrometers. *Meat Sci.* 161:108017. doi: 10.1016/j.meatsci.2019.108017

Seymour, D. J., Cánovas, A., Baes, C. F., Chud, T. C. S., Osborne, V. R., Cant, J. P., et al. (2019). Invited review: determination of large-scale individual dry matter intake phenotypes in dairy cattle. *J. Dairy Sci.* 102, 7655–7663. doi: 10.3168/jds.2019-16454

Shackelford, S. D., Wheeler, T. L., and Koohmaraie, M. (2005). On-line classification of US Select beef carcasses for longissimus tenderness using visible and near-infrared reflectance spectroscopy. *Meat Sci.* 69, 409–415. doi: 10.1016/J.MEATSCI.2004.08.011

Shackelford, S. D., Wheeler, T. L., Meade, M. K., Reagan, J. O., Byrnes, B. L., and Koohmaraie, M. (2001). Consumer impressions of tender select beef. *J. Anim. Sci.* 79, 2605–2614. doi: 10.2527/2001.79102605x

Shetty, N., Difford, G., Lassen, J., Løvendahl, P., and Buitenhuis, A. J. (2017a). Predicting methane emissions of lactating Danish Holstein cows using Fourier transform mid-infrared spectroscopy of milk. *J. Dairy Sci.* 100, 9052–9060. doi: 10.3168/jds.2017-13014

Shetty, N., Løvendahl, P., Lund, M. S., and Buitenhuis, A. J. (2017b). Prediction and validation of residual feed intake and dry matter intake in Danish lactating dairy cows using mid-infrared spectroscopy of milk. *J. Dairy Sci.* 100, 253–264. doi: 10.3168/jds.2016-11609

Smith, S. L., Denholm, S. J., Coffey, M. P., and Wall, E. (2019). Energy profiling of dairy cows from routine milk mid-infrared analysis. *J. Dairy Sci.* 102, 11169–11179. doi: 10.3168/jds.2018-16112

Sørensen, L. K., Lund, M., and Juul, B. (2003). Accuracy of Fourier transform infrared spectrometry in determination of casein in dairy cows' milk. *J. Dairy Res.* 70, 445–452. doi: 10.1017/S0022029903006435

Soyeurt, H., Bruwier, D., Romnee, J. M., Gengler, N., Bertozzi, C., Veselko, D., et al. (2009). Potential estimation of major mineral contents in cow milk using mid-infrared spectrometry. *J. Dairy Sci.* 92, 2444–2454. doi: 10.3168/jds.2008-1734

Soyeurt, H., Dardenne, P., Dehareng, F., Lognay, G., Veselko, D., Marlier, M., et al. (2006). Estimating fatty acid content in cow milk using mid-infrared spectrometry. *J. Dairy Sci.* 89, 3690–3695. doi: 10.3168/jds.S0022-0302(06)72409-2

Soyeurt, H., Dehareng, F., Gengler, N., McParland, S., Wall, E., Berry, D. P., et al. (2011). Mid-infrared prediction of bovine milk fatty acids across multiple breeds, production systems, and countries. *J. Dairy Sci.* 94, 1657–1667. doi: 10.3168/jds.2010-3408

Soyeurt, H., Dehareng, F., Mayeres, P., Bertozzi, C., and Gengler, N. (2008). Variation of Δ^9-desaturase activity in dairy cattle. *J. Dairy Sci.* 9, 13211–13224. doi: 10.3168/jds.2007-0518

Stone, M. (1974). Cross-validatory choice and assessment of statistical predictions. *J. R. Stat. Soc. B.* 36, 111–147.

Su, H., Sha, K., Zhang, L., Zhang, Q., Xu, Y., Zhang, R., et al. (2014). Development of near infrared reflectance spectroscopy to predict chemical composition with a wide range of variability in beef. *Meat Sci.* 98, 110–114. doi: 10.1016/j.meatsci.2013.12.019

Su, H., Zhang, S., Li, H., Xie, P., and Sun, B. (2018). Using near-infrared reflectance spectroscopy to predict physical parameters of beef. *Spectrosc. Lett.* 51, 163–168. doi: 10.1080/00387010.2018.1442355

Toffanin, V., De Marchi, M., Lopez-Villalobos, N., and Cassandro, M. (2015). Effectiveness of mid-infrared spectroscopy for prediction of the contents of calcium and phosphorus, and titratable acidity of milk and their relationship with milk quality and coagulation properties. *Int. Dairy J.* 41, 68–73. doi: 10.1016/j.idairyj.2014.10.002

Toledo-Alvarado, H., Vazquez, A. I., de los Campos, G., Tempelman, R. J., Bittante, G., and Cecchinato, A. (2018). Diagnosing pregnancy status using infrared spectra and milk composition in dairy cows. *J. Dairy Sci.* 101, 2496–2505. doi: 10.3168/JDS.2017-13647

Tran, H., Salgado, P., Tillard, E., Dardenne, P., Nguyen, X. T., and Lecomte, P. (2010). "Global" and "local" predictions of dairy diet nutritional quality using near infrared reflectance spectroscopy. *J. Dairy Sci.* 93, 4961–4975. doi: 10.3168/jds.2008-1893

van Gastelen, S., Mollenhorst, H., Antunes-Fernandes, E. C., Hettinga, K. A., van Burgsteden, G. G., Dijkstra, J., et al. (2018). Predicting enteric methane emission of dairy cows with milk Fourier-transform infrared spectra and gas chromatography–based milk fatty acid profiles. *J. Dairy Sci.* 101, 5582–5598. doi: 10.3168/jds.2017-13052

van Lingen, H. J., Crompton, L. A., Hendriks, W. H., Reynolds, C. K., and Dijkstra, J. (2014). Meta-analysis of relationships between enteric methane yield and milk fatty acid profile in dairy cattle. *J. Dairy Sci.* 97, 7115–7132. doi: 10.3168/jds.2014-8268

Vanlierde, A., Soyeurt, H., Gengler, N., Colinet, F. G., Froidmont, E., and Kreuzer, M. (2018). Short communication: development of an equation for estimating methane emissions of dairy cows from milk Fourier transform mid-infrared spectra by using reference data obtained exclusively from respiration chambers. *J. Dairy Sci.* 101, 7618–7624. doi: 10.3168/jds.2018-14472

Vanlierde, A., Vanrobays, M.-L., Dehareng, F., Froidmont, E., Soyeurt, H., and McParland, S. (2015). Hot topic: innovative lactation-stage-dependent prediction of methane emissions from milk mid-infrared spectra. *J. Dairy Sci.* 98, 5740–5747. doi: 10.3168/jds.2014-8436

Vanlierde, A., Vanrobays, M.-L., Gengler, N., Dardenne, P., Froidmont, E., and Soyeurt, H. (2016). Milk mid-infrared spectra enable prediction of lactation-stage- dependent methane emissions of dairy cattle within routine population-scale milk recording schemes. *Anim. Prod. Sci.* 56, 258–264. doi: 10.1071/AN15590

Venel, C., Mullen, A. M., Downey, G., and Troy, D. J. (2001). Prediction of tenderness and other quality attributes of beef by near infrared reflectance spectroscopy between 750 and 1100 nm; further studies. *J. Near Infrared Spectrosc.* 9, 185–198. doi: 10.1255/jnirs.305

Visentin, G., Penasa, M., Gottardo, P., Cassandro, M., and De Marchi, M. (2016). Predictive ability of mid-infrared spectroscopy for major mineral composition and coagulation traits of bovine milk by using the uninformative variable selection algorithm. *J. Dairy Sci.* 99, 8137–8145. doi: 10.3168/jds.2016-11053

Wallén, S. E., Prestløkken, E., Meuwissen, T. H. E., McParland, S., and Berry, D. P. (2018). Milk mid-infrared spectral data as a tool to predict feed intake in lactating Norwegian Red dairy cows. *J. Dairy Sci.* 101, 6232–6243. doi: 10.3168/jds.2017-13874

Wang, Q., and Bovenhuis, H. (2019). Validation strategy can result in an overoptimistic view of the ability of milk infrared spectra to predict methane emission of dairy cattle. *J. Dairy Sci.* 102, 6288–6295. doi: 10.3168/jds.2018-15684

Williams, J. L. (2008). "Genetic control of meat quality traits," in *Meat biotechnology*, ed. F. Toldrá (New York, NY: Springer), 21–61.

Wold, S., Antti, H., Lindgren, F., and Ohman, J. (1998). Orthogonal signal correction of near-infrared spectra. *Chemometr. Intell. Lab. Syst.* 44, 175–186. doi: 10.1016/S0169-7439(98)00109-9

Wold, S., Johansson, A., and Cochi, M. (1993). *PLS-Partial Least Squares Projections to Latent Structures*. Leiden: ESCOM Science Publishers.

Wu, D., Chen, X., Shi, P., Wang, S., Feng, F., and He, Y. (2009). Determination of α-linolenic acid and linoleic acid in edible oils using near-infrared spectroscopy improved by wavelet transform and uninformative variable elimination. *Anal. Chim. Acta* 634, 166–171. doi: 10.1016/j.aca.2008.12.024

Wu, D., Nie, P., He, Y., and Bao, Y. (2012). Determination of calcium content in powdered milk using near and mid-infrared spectroscopy with variable selection and chemometrics. *Food Bioprocess Technol.* 5, 1402–1410. doi: 10.1007/s11947-010-0492-4

Wyrwisz, J., Moczkowska, M., Kurek, M. A., Karp, S., Atanasov, A. G., and Wierzbicka, A. (2019). Evaluation of WBSF, color, cooking loss of *Longissimus lumborum* muscle with fiber optic near-infrared spectroscopy (FT-NIR), depending on aging time. *Molecules* 24:757. doi: 10.3390/molecules24040757

Yancey, J. W. S., Apple, J. K., Meullenet, J.-F., and Sawyer, J. T. (2010). Consumer responses for tenderness and overall impression can be predicted by visible and near-infrared spectroscopy, Meullenet–Owens razor shear, and Warner–Bratzler shear force. *Meat Sci.* 85, 487–492. doi: 10.1016/j.meatsci.2010.02.020

Zhang, L., Sun, B., Xie, P., Li, H., Su, H., Sha, K., et al. (2015). Using near infrared spectroscopy to predict the physical traits of Bos grunniens meat. *LWT Food Sci Technol.* 64, 602–608. doi: 10.1016/j.lwt.2015.06.022

Conflict of Interest: The authors declare that the research was conducted in the absence of any commercial or financial relationships that could be construed as a potential conflict of interest.

frontiers in Genetics

ERRATUM
published: 07 December 2020
doi: 10.3389/fgene.2020.628196

Erratum: Infrared Spectrometry as a High-Throughput Phenotyping Technology to Predict Complex Traits in Livestock Systems

*Frontiers Production Office**

Frontiers Media SA, Lausanne, Switzerland

OPEN ACCESS

Approved by:
Frontiers Editorial Office, Frontiers Media SA, Switzerland

***Correspondence:**
Frontiers Production Office
production.office@frontiersin.org

Specialty section:
This article was submitted to Livestock Genomics, a section of the journal Frontiers in Genetics

Received: *11 November 2020*
Accepted: *11 November 2020*
Published: *07 December 2020*

Citation:
Frontiers Production Office (2020) Erratum: Infrared Spectrometry as a High-Throughput Phenotyping Technology to Predict Complex Traits in Livestock Systems. Front. Genet. 11:628196. doi: 10.3389/fgene.2020.628196

Keywords: beef cattle, dairy cattle, near-infrared, novel phenotypes, mid-infrared, spectral information

An Erratum on

Infrared Spectrometry as a High-Throughput Phenotyping Technology to Predict Complex Traits in Livestock Systems
by Bresolin, T., and Dórea, J. R. R. (2020). Front. Genet. 11:923. doi: 10.3389/fgene.2020.00923

Due to a production error, an incorrect reference citation "Vanlierde et al. (2016)" was inserted in Table 5. It should be "Visentin et al. (2016)." The corrected **Table 5** appears below.

The publisher apologizes for this mistake. The original article has been updated.

REFERENCES

Visentin, G., Penasa, M., Gottardo, P., Cassandro, M., and De Marchi, M. (2016). Predictive ability of mid-infrared spectroscopy for major mineral com-position and coagulation traits of bovine milk by using the uninformative variable selection algorithm. *J. Dairy Sci.* 99, 8137–8145. doi: 10.3168/jds.2016-11053

TABLE 5 | Number of samples (N) and coefficient of determination in the validation set for mineral contents using partial least square methodology.

References	N	Breed	Validation*	Ca	K	Mg	Na	P
Soyeurt et al. (2009)	92	Multibreed	LOOCV	0.87	0.36	0.65	0.65	0.85
Gottardo et al. (2015)	208	–	10-F CV[b]	0.55	–	–	–	–
Toffanin et al. (2015)	208	Holstein	LOOCV	0.53[c]	–	–	–	0.70[c]
Bonfatti et al. (2016)	689	Simental	10-F CV	0.48	0.41	0.46	–	0.43
Visentin et al. (2016)	923	Multibreed	R-Tr/Te[b]	0.67	0.69	0.65	0.40	0.68
Malacarne et al. (2018)[a]	153	Holstein	Tr/Te[b]	0.25	0.34	0.26	0.25	0.53
Franzoi et al. (2019)[b]	93	Holstein	CV	0.79	0.55	0.68	0.75	0.87
Fleming et al. (2019)	986	Multibreed	10- FCV	0.25	–	–	–	–

*[a]Bulk milk samples. [b]Backward interval partial least squares (BiPLS), number of folds (n-F) in the cross-validation, leave-one-out cross-validation (LOOCV), train and test cross-validation defined by splitting the data set randomly (R-Tr/Te), external or independent validation. [c]Correlation coefficient (r) transformed to coefficient of determination (R2). *The validation strategy defined as "CV" was assigned for the reviewed paper that did not completely describe the validation method adopted or the authors defined that cross-validation was employed.*

frontiers in Genetics

ORIGINAL RESEARCH
published: 29 September 2020
doi: 10.3389/fgene.2020.563393

Integration of Wet-Lab Measures, Milk Infrared Spectra, and Genomics to Improve Difficult-to-Measure Traits in Dairy Cattle Populations

Alessio Cecchinato[1], Hugo Toledo-Alvarado[2], Sara Pegolo[1], Attilio Rossoni[3], Enrico Santus[3], Christian Maltecca[4], Giovanni Bittante[1] and Francesco Tiezzi[4]*

[1] Department of Agronomy, Food, Natural Resources, Animals and Environment, University of Padova, Padua, Italy, [2] Department of Genetics and Biostatistics, National Autonomous University of Mexico, Mexico City, Mexico, [3] Italian Brown Breeders Association, Bussolengo, Italy, [4] Department of Animal Science, North Carolina State University, Raleigh, NC, United States

OPEN ACCESS

Edited by:
Fabyano Fonseca Silva, Universidade Federal de Viçosa, Brazil

Reviewed by:
Rodrigo Reis Mota, University of Liège, Belgium
Kathryn Tiplady, Livestock Improvement Corporation, New Zealand
Tesfaye Kebede Belay, Norwegian University of Life Sciences, Norway

***Correspondence:**
Alessio Cecchinato
alessio.cecchinato@unipd.it

Specialty section:
This article was submitted to Livestock Genomics, a section of the journal Frontiers in Genetics

Received: *18 May 2020*
Accepted: *31 August 2020*
Published: *29 September 2020*

Citation:
Cecchinato A, Toledo-Alvarado H, Pegolo S, Rossoni A, Santus E, Maltecca C, Bittante G and Tiezzi F (2020) Integration of Wet-Lab Measures, Milk Infrared Spectra, and Genomics to Improve Difficult-to-Measure Traits in Dairy Cattle Populations. Front. Genet. 11:563393. doi: 10.3389/fgene.2020.563393

The objective of this study was to evaluate the contribution of Fourier-transformed infrared spectroscopy (FTIR) data for dairy cattle breeding through two different approaches: (i) estimating the genetic parameters for 30 measured milk traits and their FTIR predictions and investigating the additive genetic correlation between them and (ii) evaluating the effectiveness of FTIR-derived phenotyping to replicate a candidate bull's progeny testing or breeding value prediction at birth. Records were available from 1,123 cows phenotyped using gold standard laboratory methodologies (LAB data). This included phenotypes related to fine milk composition and milk technological characteristics, milk acidity, and milk protein fractions. The dataset used to generate FTIR predictions comprised 729,202 test-day records from 51,059 Brown Swiss cows (FIELD data). A first approach consisted of estimating genetic parameters for phenotypes available from LAB and FIELD datasets. To do so, a set of bivariate animal models were run, and genetic correlations between LAB and FIELD phenotypes were estimated using FIELD information obtained at the population level. Heritability estimates were generally higher for FIELD predictions than for the corresponding LAB measures. The additive genetic correlations (r_a) between LAB and FIELD phenotypes had different magnitudes across traits but were generally strong. Overall, these results demonstrated the potential of using FIELD information as indicator traits for the indirect genetic improvement of LAB measures. In the second approach, we included genotype information for 1,011 cows from the LAB dataset, 1,493 cows from the FIELD dataset, 181 sires with daughters in both LAB and FIELD datasets, and 540 sires with daughters in the FIELD dataset only. Predictions were obtained using the single-step GBLUP method. A four fold cross-validation was used to assess the predictive ability of the different models, assessed as the ability to predict masked LAB records from daughters of progeny testing bulls. The correlation between observed and predicted LAB measures in validation was averaged over the four training-validation sets. Different sets of phenotypic information were used sequentially in cross-validation schemes: (i) LAB cows from the training set; (ii) FIELD cows from the training set; and (iii) FIELD cows from the validation set. Models that included FIELD records showed an improvement for

the majority of traits. This study suggests that breeding programs for difficult-to-measure traits could be implemented using FTIR information. While these programs should use progeny testing, acceptable values of accuracy can be achieved also for bulls without phenotyped progeny. Robust calibration equations are, deemed as essential.

Keywords: high-throughput phenotyping, Fourier-transformed infrared spectroscopy, genetic parameters, genomic predictions, dairy cattle, single-step GBLUP

INTRODUCTION

In the omics- era, an emerging field of research is represented by phenomics, which is the study of phenotypes on a genome-wide scale (Bilder et al., 2009; Houle et al., 2010). In animal breeding, the advance in high-throughput genomics has increased the need for simple, fast, accurate, and high-throughput phenotyping technologies. Fourier-transformed infrared spectroscopy (FTIR), including part of near- and mid-infrared (NIR and MIR) electromagnetic radiations, is a versatile and cost-effective analytical tool to collect individual data for monitoring traditional and novel milk traits in dairy cattle (Boichard and Brochard, 2012). For many years, milk composition traits such as fat and protein content, as well as lactose, urea, and casein content, have been routinely estimated by FTIR spectroscopy (Barbano and Clark, 1989). More recently, infrared technology has also been proposed as an alternative method for the quantification of difficult- or expensive-to-measure milk phenotypes including protein fractions, fatty acids, and minerals as well as milk coagulation properties (MCP), cheese yield, and curd nutrient recoveries (Soyeurt et al., 2006a,b, 2011; Ferragina et al., 2013; Cecchinato et al., 2015; Sanchez et al., 2018). In addition, FTIR data has been shown to be a potentially valuable tool for predicting health and reproductive phenotypes (Belay et al., 2017; Toledo-Alvarado et al., 2018), as well as residual feed intake, dry matter intake (DMI), and methane emissions (Bittante and Cipolat-Gotet, 2018; Dórea et al., 2018).

Within the animal breeding context, studies have shown the potential for using FTIR predictions as indicator traits of novel phenotypes like MPC, fatty acid profiles, and other milk components (Cecchinato et al., 2009; Rutten et al., 2011; Bonfatti et al., 2017). Multi-trait prediction allows simultaneous use of information from relatives and from different traits (Henderson and Quaas, 1976). It has been demonstrated that, using different databases, breeds, and traits, the effectiveness of FTIR calibrations to provide novel phenotypes exploitable in indirect selective breeding relies on the magnitude of heritability of FTIR predictions, and the additive genetic correlation between predictions and the measured traits (i.e., gold standard/breeding targets). Although the predictive ability of FTIR data is moderate for some traits, the genetic response achievable using FTIR predictions as indicator traits may be equal to or slightly lower than the response achievable from direct measurements of traits are utilized (Cecchinato et al., 2009; Rutten et al., 2010).

Besides the infrared technology, genome-wide prediction using the single-step approach has also been recognized as an important tool to predict phenotypes (Lee et al., 2008; Aguilar et al., 2010). The key principle for all these applications is the simultaneous estimation of all genome-wide marker effects based on a reference population with known phenotypes. Within this framework, the accuracy of prediction might also benefit from the added value of including genomic information in multi-trait prediction models, which have been shown to have better performances compared to single-trait models (Calus and Veerkamp, 2011; Guo et al., 2014; Karaman et al., 2018). While dairy cattle genetic improvement has historically hinged on progeny testing, genomic selection has made available high-accuracy breeding value predictions for candidate bulls at birth. This could mean that the traditional progeny testing is no longer required, provided that these early breeding value predictions are reliable. In this context, we hypothesized that multi-trait genomic prediction models applied to indicator traits estimated from routinely collected FTIR data, and their corresponding gold-standard measured traits could represent a viable option to evaluate the contribution of FTIR data collection for dairy cattle breeding. Cross-validation could be used to test the predictive ability of models that include or do not include FTIR-predicted phenotypes, to replicate a candidate bulls' progeny testing or prediction of breeding value at birth.

Therefore, the overall objective of this study was to test the value of FTIR predictions from field data (FIELD) for the genetic improvement of difficult-to-measure traits in dairy cattle. Steps to address this objective were (i) to infer (co)variance components, heritabilities, and additive genetic correlations between 30 LAB-measured and FIELD-predicted phenotypes, divergent in terms of biological meaning, variability, and heritability, related to fine milk composition and milk technological characteristics [traditional MCP, curd firming (CF) traits, cheese yields and recoveries of nutrients, milk acidity and milk protein fractions] and (ii) to use bivariate single-step GBLUP for evaluating the predictive ability of FTIR-derived phenotyping for these traits by using different phenotyping and genotyping strategies.

MATERIALS AND METHODS

Ethics Statement

This study did not require any specific ethics permit. The cows sampled belonged to commercial private herds and were not experimentally manipulated. Milk samples were collected during routine milk recording coordinated by technicians from the Breeders Federations of Trento Province (FPA, Trento, Italy) and of Alto Adige/Südtirol (Associazione Provinciale delle Organizzazioni Zootecniche Altotesine/Vereinigung der Südtiroler Tierzuchtverbände, Bolzano/Bozen, Italy).

Data Structure

In this study, we used two sets of data collected on Brown Swiss cows: (i) a LAB dataset in which laboratory measurements and spectra data for phenotypes related to milk quality and cheese-making were available to develop calibration equations and (ii) a FIELD-FTIR dataset for testing field prediction at the population level. A subset of the FIELD-FTIR dataset including only first lactation records was used for estimating (co)variance components ($FIELD_{lact1}$); the whole database was instead used for the genomic analyses (FIELD). The data structure is summarized in **Table 1**.

LAB Dataset

The LAB data were part of the Cowability/Cowplus projects. Individual milk samples from 1,200 Brown Swiss cows from 85 herds located in the Alpine province of Trento (Italy) were collected. Details of the animals used in this study and characteristics of the area are reported in Mele et al. (2016). Data on the cows, herds, and single test-day milk yield were provided by the Superbrown Consortium of Bolzano and Trento (Italy), and pedigree information was supplied by the Italian Brown Swiss Cattle Breeders Association (Verona, Italy).

FTIR Spectra Data

Individual milk samples were analyzed using a MilkoScan FT6000 (Foss Electric, Hillerød, Denmark). The spectrum covers from the short-wavelength infrared (SWIR, also known as NIR or IR-B), through the medium-wavelength infrared (MWIR, also known as MIR), to the long-wavelength infrared (LWIR, or LIR) regions with 1,060 spectral points from wavenumber 5,010 to 925 cm^{-1}, which correspond to wavelengths ranging from 1.99 to 10.81 μm and frequencies ranging from 150.19 to 27.73 THz. Spectra were expressed as absorbance calculated as log(1/transmittance). Two spectral acquisitions were carried out for each sample (collected during the evening milking), and the results were averaged before data analysis (Ferragina et al., 2015).

Phenotypes

Traditional Milk Coagulation Properties

Measures of MCP were obtained using two different instruments: a Formagraph (Foss Electric A/S) and an Optigraph (Ysebaert SA, Frépillon, France) according to Cecchinato et al. (2013). Briefly, milk samples (10 mL) were heated to 35°C and 200 μL of a rennet solution (Hansen Standard 160, with 80 ± 5% chymosin and 20 ± 5% pepsin; 160 international milk clotting units/mL; Pacovis Amrein AG, Bern, Switzerland), diluted to 1.6% (wt/vol) in distilled water, was added at the beginning of the analysis. The time of analysis was extended up to 90 min after rennet addition. Rennet coagulation time (RCT) was defined as the time (min) from the addition of enzyme to the beginning of coagulation, k_{20} (min) was defined as the interval from RCT to the time at which a curd firmness of 20 mm was obtained, and a_{30} and a_{45} (mm) were measurements of curd firmness at 30 and 45 min after rennet addition, respectively.

TABLE 1 | Summary of data structure for laboratory (LAB) measures, after editing, and Fourier transform infrared predictions (FIELD).

Item	LAB	$FIELD_{lact1}$ [1]	FIELD[2]
Animals	1,123	39,833	51,059
Records	1,123	235,372	729,202
Herds	83	2,494	2,607
Animals in the pedigree	6,526	97,933	136,332
Number of generations	5	5	13
Sires	266	1,210	1,835
Dams	1,044	29,716	38,449

[1] $FIELD_{lact1}$ = dataset limited to cows belonging to first lactation. [2] FIELD = whole dataset.

Modeling the Curd Firmness

A set of parameters of CF at time t (CF_t) was estimated, and details are described in Bittante et al. (2015). Estimated parameters included rennet coagulation time (RCT_{eq}, min), estimated from the CF_t equation; potential asymptotical curd firmness (CF_P, mm), representing the maximum potential curd firmness after infinite time in the absence of syneresis; curd-firming rate constant (k_{CF}, %/min), which is a measure of the rate of CF; syneresis rate constant (k_{SR}, %/min); maximum curd firmness (CF_{max}, mm); and time to CF_{max} (t_{max}, min).

Milk Acidity

The milk pH was measured using a Crison Basic 25 electrode (Crison, Barcelona, Spain).

Cheese Yields and Curd Nutrient Recoveries

To assess cheese-making properties, milk samples were processed according to all the steps of the cheese-making practice used in artisanal commercial dairies for producing a traditional whole milk cheese described by Bittante et al. (2014). Briefly, 1,500 mL of milk was heated to 35°C in a stainless steel microvat, supplemented with thermophilic starter culture, and mixed with rennet. The resulting curd from each vat was double-cut and heated for 30 min to 55°C, drained, shaped in wheels, pressed, salted, and weighed. The whey was drained from the curd, weighted, and analyzed for fat, protein, lactose, and total solid content using FT2 (Foss Electric A/S, Hillerød, Denmark). Three cheese yield (CY) traits were calculated expressing the weight (wt) of fresh curd ($\%CY_{CURD}$), of curd DM ($\%CY_{SOLIDS}$), and of water retained in the curd ($\%CY_{WATER}$) as a percentage of the weight of milk processed. Four recovery (REC) traits were calculated as proportions of nutrients and energy of the milk retained in the curd (REC_{SOLIDS}, REC_{FAT}, $REC_{PROTEIN}$, and REC_{ENERGY} calculated as the % ratio between the nutrient in curd and the corresponding nutrient in processed milk). The energy within the curd was calculated as the difference between energy in the milk and in the whey (NRC, 2001).

Milk Proteins

Concentrations of the major casein (CN) fractions (α_{S1}–CN, α_{S2}–CN, β-CN, and κ-CN) and whey proteins, β-lactoglobulin (β-LG), and alpha-lactalbumin (α-LA) were determined using a validated reversed phase high-performance liquid chromatography (RP-HPLC) method (Bonfatti et al., 2008). Each

protein fraction was expressed as a percentage of the milk total nitrogen (N) content.

Data Editing

Only records with spectra and measured phenotypes available were kept. After data editing and removing observations outside three standard deviations, the final number of records and phenotypes used in subsequent analyses varied from 770 to 1,120 depending on the trait as reported in **Table 2**.

Field Data

Spectra Data

The FIELD data for our study were provided by the Breeders Federations of Trento Province (FPA, Trento, Italy) and

TABLE 2 | Descriptive statistics for laboratory (LAB) measures and Fourier transform infrared predictions (FIELD) for the investigated traits.

Trait[1]	LAB			$FIELD_{lact1}$[2]			FIELD[3]		
	N	Mean	*SD*	*N*	Mean	*SD*	*N*	Mean	*SD*
Traditional MCP									
RCT, min	1,096	19.8	5.38	232,660	20.47	4.76	712,420	19.98	4.81
k_{20}, min	1,073	5.34	2.43	232,775	5.59	1.68	710,826	5.59	1.66
a_{30}, mm	1,051	29.29	10.97	232,702	27.3	8.53	713,759	27.92	8.59
a_{45}, mm	1,096	33.28	8.00	232,869	33.31	4.06	714,254	32.78	4.03
Curd firming									
RCT_{eq}, min	1,093	20.62	5.41	233,828	21.23	5.17	718,385	20.86	5.18
CF_p, mm	1,105	49.89	9.43	234,065	49.21	5.95	723,632	49.37	6.14
k_{CF}, % × min^{-1}	1,104	12.83	3.91	233,641	12.12	2.61	721,173	12.84	2.70
k_{SR}, % × min^{-1}	1,102	1.21	0.43	233,568	1.14	0.23	721,261	1.21	0.25
C_{max}, mm	1,105	37.23	7.03	234,106	37.04	4.53	723,364	36.80	4.68
t_{max}, min	1,071	40.34	9.85	233,779	42.76	8.74	720,164	41.17	8.88
Optigraph									
RCT, min	787	18.88	4.11	232,856	18.77	3.29	712,568	18.80	3.35
k_{20}, min	770	8.04	2.62	232,628	8.09	2.15	709,025	8.41	2.09
a_{30}, mm	782	26.6	10.6	232,561	25.91	8.34	713,482	25.54	8.31
a_{45}, mm	786	41.03	11.04	232,783	40	8.67	713,992	39.65	8.63
Acidity									
pH	1,112	6.64	0.08	232,772	6.63	0.07	715,433	6.65	0.06
Cheese yields, %									
CY_{CURD}	1,120	15.04	1.9	234,247	14.92	1.64	722,328	14.95	1.65
CY_{SOLIDS}	1,101	7.19	0.9	233,860	7.11	0.84	719,915	7.13	0.86
CY_{WATER}	1,112	7.80	1.29	234,317	7.9	1.03	724,431	7.77	1.04
Recoveries, %									
$REC_{PROTEIN}$	1,112	78.09	2.44	233,940	78.81	2.18	720,358	78.25	2.28
REC_{FAT}	1,083	89.97	3.27	233,818	89.39	2.92	716,200	89.48	2.95
REC_{SOLIDS}	1,115	52.00	3.55	233,973	51.21	3.07	721,441	51.66	3.18
REC_{ENERGY}	1,101	67.25	3.28	233,630	66.58	2.89	719,822	67.05	3.00
N fractions, % total N									
Caseins	1,097	77.97	1.2	233,395	78.25	1.41	700,206	77.88	1.36
β-CN	1,098	32.12	2.42	233,861	32.86	1.60	721,345	32.22	1.69
κ-CN	1,087	9.53	1.33	234,358	9.26	1.50	713,219	9.44	1.49
α_{S1}-CN	1,096	25.71	1.69	235,058	25.80	0.71	724,579	25.72	0.75
α_{S2}-CN	1,091	9.17	1.05	234,457	9.12	0.58	723,390	9.15	0.59
Whey proteins	1,094	11.06	1.61	234,276	11.08	1.16	722,788	10.99	1.18
β-LG	1,091	8.70	1.47	234,252	8.71	1.33	721,472	8.63	1.36
α-LA	1,097	2.37	0.49	232,535	2.38	0.46	713,999	2.34	0.46

[1]RCT = rennet coagulation time; k_{20} = curd firming rate as the time to a curd firmness of 20 mm; $a_{30(45)}$ = curd firmness at 30 (45) min from rennet addition; RCT_{eq} = rennet coagulation time estimated using the equation; CF_P = asymptotic potential curd firmness; k_{CF} = curd firming instant rate constant; k_{SR} = syneresis instant rate constant; CF_{max} = maximum curd firmness achieved within 45 min; t_{max} = time at achievement of CF_{max}; $\%CY_{CURD}$ = weight of fresh curd as percentage of weight of milk processed; $\%CY_{SOLIDS}$ = weight of curd solids as percentage of weight of milk processed; $\%CY_{WATER}$ = weight of water curd as percentage of weight of milk processed; $REC_{PROTEIN}$ = protein of the curd as percentage of the protein of the milk processed; REC_{FAT} = fat of the curd as percentage of the fat of the milk processed; REC_{SOLIDS} = solids of the curd as percentage of the solids of the milk processed; REC_{ENERGY} = energy of the curd as percentage of energy of the milk processed; true protein nitrogen (N) and milk N fractions are expressed as percentage of total milk N; β-CN (β-casein), κ-CN (κ-casein), αs_1-CN (αs_1-casein), αs_2- CN (αs_2-casein); caseins: Σ(β-CN+κ-CN+ αs_1-CN+αs_2-CN); β-LG (β-lactoglobulin), α-LA (α-lactalbumin), whey proteins: Σ(β-LG+ α-LA). [2]$FIELD_{lact1}$ = dataset limited to cows belonging to first lactation. [3]FIELD = whole dataset.

of Alto Adige/Südtirol (Associazione Provinciale delle Organizzazioni Zootecniche Altotesine/Vereinigung der Südtiroler Tierzuchtverbände, Bolzano/Bozen, Italy) as part of the Cowability/Cowplus projects. All milk samples were analyzed using a MilkoScan FT6000 (Foss Electric, Hillerød, Denmark). Spectra characteristics, in terms of wavelengths and way of expression (absorbance), were the same as for the LAB data. Spectra were collected between 2010 and 2017.

Spectra Editing

A preliminary analysis was carried out to identify the outlier spectra based on the Mahalanobis distance from the first five principal component scores. The probability level for the chi-squared distribution of a sample's Mahalanobis distance was calculated from the incomplete gamma function with five degrees of freedom (Toledo-Alvarado et al., 2018). Samples with $P < 0.01$ were removed from the dataset. To overcome spectral variations, the absorbance values for every wavelength were centered to a null mean and standardized to a unit sample variance within year periods. Records without parity number, date of calving, animal ID, or pedigree information were also removed. If a cow had predictions from both LAB and FIELD datasets, the FIELD prediction records of that specific cow were deleted. This latter editing step was performed for the following reasons: (i) to avoid an overestimation of additive genetic correlations; (ii) to force the connection between LAB and FIELD data only through the additive genetic effect; and (iii) to avoid EBV inflation for cows with both LAB and FIELD records.

To detect outliers among the predicted phenotypes, a mixed model was fitted for each trait including the fixed non-genetic effects of (i) the stage of lactation (12 monthly classes), (ii) the combined effect of herd (∼2,460 levels), year of the test day (2010–2017), and two seasons of calving (April to September and October to March) (∼22,200 levels). The permanent environmental effects (∼39,600) and animal additive genetic effects were included as random terms.

The residuals of phenotypes outside 3 standard deviations were considered as outliers.

Genotypes

The pool of genotyped individuals consisted of (i) 1,011 LAB cows genotyped with the Illumina BovineSNP50 v.2 BeadChip (Illumina, Inc., San Diego, CA, United States; 54,000 SNPs); (ii) 1,463 FIELD cows which were genotyped with the BovineLD v2.0 BeadChip (Illumina, Inc., San Diego, CA, United States; 7,931 SNPs); (iii) 181 sires with both LAB and FIELD daughters genotyped with the Illumina BovineSNP50 v.2 BeadChip or the Illumina Bovine HD BeadChip (Illumina, Inc., San Diego, CA, United States; 777,000 SNPs); and (iv) 540 sires with FIELD daughters only genotyped as (v). The software FImpute (Sargolzaei et al., 2014) was used for imputation and all individuals were imputed to the BovineSNP50 v.2 BeadChip panel. A total number of 3,195 genotyped individuals were available for this study.

Marker editing was performed using the preGSf90 software (Misztal et al., 2002). Markers were excluded where the call rate was below 95%, the minor allele frequency was below 5%, and/or there was significant deviation from the Hardy–Weinberg equilibrium ($P < 10^{-6}$). SNPs mapped to the sex chromosomes or with unknown position on the genome were also removed. After editing, the number of markers available for analyses was 37,093.

Statistical Analyses

Calibration Equations

Separate models were fitted for each trait considered. We used a Bayesian model (BayesB model) implemented in BGLR (de los Campos and Perez-Rodriguez, 2014), as previously described by Ferragina et al. (2015). Phenotypes in LAB (i.e., the calibration dataset) were regressed on standardized spectra covariates using the linear model:

$$y_i = \beta_0 + \sum_{j=1}^{1,060} x_{ij}\beta_j + \varepsilon_i,$$

where β_0 is an intercept, $\{x_{ij}\}$ are standardized FTIR spectra-derived wavelength data($j = 1, \cdots 1, 060$), $_{\beta_j}$ are the effects of each of the wavelengths, and ε_i are model residuals assumed to be independent and identically distributed, with normal distribution centered at zero and variance σ^2_ε. Models were applied with 100,000 iterations and 20,000 chains discarded as burn in. The editing and analysis were conducted using R software (R Core Team, 2018). To evaluate predictive performance, the coefficient of correlation for the calibration model developed on LAB measures and used for FIELD predictions was calculated for each trait (r_{C_LAB}). The calibration equations obtained with this procedure in LAB data were then applied to the spectral population data (FIELD) in order to obtain FIELD predictions for all traits of concerns.

Genetic Analyses: (Co)Variance Components Estimation Between Measured (LAB) and Predicted (FIELD) Phenotypes

The (co)variance components were estimated using REMLF90 and AIREMLF90 (Misztal et al., 2002), considering LAB measures and FIELD predictions as distinct traits. The connection between the two datasets was guaranteed by 266 sires, 1,044 dams, 94 sires of sires, and 372 sires of dams in common between LAB and FIELD datasets (**Table 1**). To save time and improve convergence of models, for this first approach, the FIELD dataset has been limited to cows belonging to first lactation ($FIELD_{lact1}$).

The program was run until a convergence criterion of 1^{e-10} was reached.

The model for LAB-measures was

$$y = Xb + Z_a a + e, \quad (1)$$

where **y** is the vector of observations for traits of concern; **b,** **a,** and **e** correspond to the vector of fixed non-genetic effects,

random animal additive genetic effects, and random residual effects, respectively; **X** and $\mathbf{Z}_a$ are the incidence matrices relating each observation in **y** to **b** and **a**. The non-genetic fixed effects included in the model were (i) the DIM of each cow within parity (60 levels) and (ii) herd-test day (83 levels). The random terms were animal additive genetic effects and residual effects. The pedigree file included all phenotyped animals and their ancestors (∼6,500 animals).

$$\text{Heritability was computed as } h^2 = \frac{\sigma_a^2}{\sigma_a^2 + \sigma_e^2}$$

where σ_a^2 and σ_e^2 are the additive genetic and residual variances, respectively.

The model for FIELD$_{lact1}$ records was

$$y = Xb + Z_a a + Z_{pe} pe + e, \quad (2)$$

where **y** is the vector of observations for the traits of concern; b, a, pe, and e correspond to the vector of fixed non-genetic effects, random animal additive genetic effects, random permanent environmental effects, and random residuals effects, respectively; **X**, $\mathbf{Z}_a$, and $\mathbf{Z}_{pe}$ are the incidence matrices relating each observation in y, a, b, and pe, respectively. The fixed non-genetic effects were (i) the stage of lactation (12 monthly classes) and (ii) the combined effect of herd (∼2,460 levels), year of the test-day (2010–2017), and season of calving (April to September and October to March) (∼22,200 levels). The random terms were permanent environmental effects (∼39,600), animal additive genetic effects, and residual effects. The pedigree file included all phenotyped animals and their ancestors (∼97,900 animals). Only first lactation records were utilized to avoid convergence problems. The residuals were considered uncorrelated across the two traits (LAB and FIELD$_{lact1}$ predictions).

$$\text{Heritability was computed as } h^2 = \frac{\sigma_a^2}{\sigma_a^2 + \sigma_{pe}^2 + \sigma_e^2}$$

where σ_a^2, σ_{pe}^2 , and σ_e^2 are the additive genetic, permanent environmental, and residual variances, respectively.

For each trait, the additive genetic correlation between LAB and FIELD$_{lact1}$ was estimated from the variance–covariance matrix of the random additive genetic effect as $r_a = \frac{\sigma_{a1,a2}}{\sigma_{a1} \times \sigma_{a2}}$ where $\sigma_{a1,a2}$ is the additive genetic covariance between two traits, and σ_{a1} and σ_{a2} are the additive genetic standard deviations for traits 1 and 2, respectively.

Predictive Ability Estimated Using Genomic and Infrared Information

In order to assess the ability of FIELD data to predict LAB records as phenotypes of interest, a fourfold cross-validation was used. In this setting, the LAB phenotype is considered as the breeding goal while the FIELD record is its correlated trait. The models employed for both LAB and FIELD data were the same as for the variance component estimation, except for the stage of lactation effect in the FIELD dataset that was replaced with a stage of lactation by parity effect (5 parity classes, 72 levels in total), since the whole FIELD dataset was used (not restricting the records to first lactation).

Sires with both LAB and FIELD daughters were randomly assigned to four groups, evenly sized based on the number of LAB cows for each sire. Details on the number of records and cows in each set are reported in **Supplementary Table S1**. Cross-validation was performed using alternatively 3 groups for training (denoted with the suffix "t") and one group for validation (denoted with the suffix "v"), for the scenarios that only included the training sets.

The cross-validation considered different training sets, either using LAB or FIELD data alone or combined: (i) model "LAB.t" included phenotypes available are from LAB cows that were daughters of the sires in the training set; (ii) model "FIELD.t" included phenotypes available from FIELD cows that were daughters of the sires in the training set; (iii) model "LAB.t + FIELD.t" included phenotypes from LAB and FIELD cows that were daughters of the sires in the training set; (iv) model "FIELD.t + FIELD.v" included phenotypes available are from all FIELD cows (no alternate masking of phenotypes was performed here); and (v) model "LAB.t + FIELD.t + FIELD.v" included phenotypes available from LAB cows that were daughters of the sires from the training set and all FIELD cows. Model "LAB.t" assesses the predictive ability when FIELD records are not collected, i.e., no use of FTIR data. Model "FIELD.t" evaluates the impact of FIELD phenotyping the daughters of the bulls in the reference population, with no LAB phenotypes included in the genetic evaluation. Model "LAB.t + FIELD.t" evaluates the impact of including FIELD phenotypes for the daughters of the bulls in the progeny test. In model "FIELD.t + FIELD.v," progeny testing bulls have daughters phenotyped with FTIR data while in model "LAB.t + FIELD.t + FIELD.v," the progeny testing bulls have daughters phenotyped with LAB data as well.

Accuracy of prediction was quantified as

$$acc_x = cor(y_{val,x}^{LAB}, (G)EBV_{val,x}^{LAB})$$

where acc_x is the accuracy in the validation set x (x = 1,2,3,4), $y_{val,x}^{LAB}$ are the masked LAB records from cows in validation set x, $(G)EBV_{val,x}^{LAB}$ is the estimated genomic breeding value for LAB cows in validation set x, and *cor* refers to the Pearson correlation. Estimated genomic breeding values were calculated using the program BLUPf90 (Misztal et al., 2002) that combines pedigree-derived and SNP-derived genomic relationship matrices (Legarra et al., 2009). All 3,195 genotypes available for this study were included in the analysis.

For this part of the study, we did not use the variance components estimated in the previous step, but we tested different genetic correlation (covariance) values in order to find those that better maximized prediction accuracy. Firstly, estimates of variance components were obtained from single-trait models (**Supplementary Table S2**). Single-trait models were used in order to remove the inflation in the estimates due to genetic covariances. Then, different values of genetic correlation between LAB and FIELD phenotypes ranging from 0.1 to 1, with 0.1 step increases, were generated. Each prediction run

was then repeated for the values of covariance generated by each value of assumed genetic correlation. This allowed the exploration of the predictive ability over all the potential values of genetic correlation.

RESULTS AND DISCUSSION

Descriptive Statistics

Descriptive statistics for all investigated LAB-measured and FIELD-predicted traits are summarized in **Table 2**. Extensive description and discussion of the results for the LAB dataset have been reported in previous works, including the differences between MCP measured with FRM and OPT (Cecchinato et al., 2013; Bittante et al., 2015; Pegolo et al., 2018). Generally, we observed consistency between the mean values from LAB, $FIELD_{lact1}$, and FIELD datasets for all the investigated traits. We only observed a slight loss of variability for all the FTIR-predicted phenotypes as demonstrated by the lower standard deviations, compared to for the observed traits.

Variance Components and Heritability of Measured and Predicted Traits

Coagulation Traits and Milk Acidity

Variance components and heritability estimates from LAB and $FIELD_{lact1}$ datasets for coagulation traits and milk acidity are reported in **Table 3** and **Figure 1**. The coefficient of correlation for the calibration models developed on LAB measures (r_{C_LAB}) and used for FIELD predictions, and the additive genetic correlation (r_a) between LAB and FIELD traits are reported in **Table 3** and **Figure 2**. As previously reported, in order to guarantee convergence of animal models, these analyses have been restricted to a dataset with only first lactation records of FIELD data. Generally, a decrease in both genetic and residual variances was observed in $FIELD_{lact1}$ with respect to LAB data. A similar pattern was reported in other studies (Bonfatti et al., 2017). In particular, residual variances for LAB traits were 1.3–6 times greater than residual plus permanent environmental variances in $FIELD_{lact1}$. In the case of LAB parameters obtained from mechanical lacto-dynamographs (traditional MCP and Curd firming model), this difference increases particularly for traits recorded at increasing time intervals from milk gelation. This is caused by the decreasing repeatability of the measures recorded by the instrument with the progress of the textural test. Therefore, heritability estimates were comparable between datasets for traits recorded earlier (e.g., RCT, k_{CF}), whereas heritability estimates decreased for later measured LAB traits, but not for FTIR predicted $FIELD_{lact1}$ traits (a_{30}, a_{45}, CF_P, CF_{max}). Optigraph, yielding an optical prediction and not a mechanical measurement, does not show the same decrease in repeatability and heritability, for traits describing the later part of CF pattern. Generally, heritability estimates of measured and predicted traits were comparable to other studies (Cecchinato et al., 2009; Bonfatti et al., 2017).

TABLE 3 | Estimates of variance components and heritability of measured LAB traits, coefficient of correlation of the calibration model used for infrared prediction (r_{C_LAB}) developed on LAB measures and used for FIELD predictions, estimates of variance components and heritability of Fourier transform infrared $FIELD_{lact1}$ predictions, and additive genetic correlation (r_a) between LAB and FIELD traits for the coagulation and acidity traits.

Traits[1]	LAB					r_{C_LAB}	$FIELD_{lact1}$[2]					r_a		
	σ^2_a	σ^2_e	σ^2_p	h^2	SE		σ^2_a	σ^2_{pe}	σ^2_e	σ^2_p	h^2	SE	Est	SE
Traditional MCP														
RCT, min	7.155	14.967	22.122	0.323	0.098	0.858	5.911	2.091	8.901	16.904	0.350	0.003	0.892	0.081
k_{20}, min	1.160	4.552	5.712	0.203	0.089	0.682	0.751	0.303	1.095	2.149	0.350	0.010	0.780	0.031
a_{30}, mm	15.998	93.280	109.278	0.146	0.080	0.722	21.905	8.288	28.067	58.260	0.376	0.011	0.836	0.026
a_{45}, mm	4.592	47.238	51.830	0.089	0.067	0.586	3.499	1.480	6.158	11.137	0.314	0.010	0.787	0.042
Curd firming														
RCT_{eq}, min	6.648	15.588	22.236	0.299	0.098	0.853	6.057	2.301	10.469	18.827	0.322	0.010	0.863	0.018
CF_p, mm	10.389	58.367	68.756	0.151	0.076	0.742	8.010	2.681	14.418	25.110	0.319	0.010	0.835	0.027
k_{CF}, % × min^{-1}	3.678	8.720	12.398	0.297	0.095	0.656	1.676	0.702	2.974	5.352	0.313	0.010	0.683	0.038
k_{SR}, % × min^{-1}	0.035	0.115	0.150	0.233	0.088	0.571	0.012	0.005	0.027	0.044	0.270	0.009	0.602	0.052
C_{max}, mm	5.786	32.505	38.291	0.151	0.076	0.742	4.888	1.852	7.733	14.474	0.338	0.011	0.847	0.025
t_{max}, min	21.794	54.064	75.858	0.287	0.097	0.774	18.862	7.647	29.049	55.558	0.340	0.011	0.783	0.028
Optigraph														
RCT, min	3.426	9.261	12.687	0.270	0.111	0.837	2.783	0.978	4.095	7.856	0.354	0.010	0.904	0.134
k_{20}, min	1.629	4.441	6.070	0.268	0.119	0.809	1.426	0.466	1.567	3.460	0.412	0.011	0.919	0.012
a_{30}, mm	26.076	76.993	103.069	0.253	0.115	0.760	20.611	8.158	28.236	57.005	0.362	0.003	0.802	0.016
a_{45}, mm	47.194	64.650	111.844	0.422	0.131	0.743	19.957	7.373	28.803	56.133	0.356	0.010	0.799	0.024
Acidity														
pH	0.001	0.002	0.003	0.201	0.081	0.752	0.001	0.000	0.002	0.003	0.205	0.007	0.756	0.035

[1] RCT = rennet coagulation time; k_{20} = curd firming rate as the time to a curd firmness of 20 mm; $a_{30(45)}$ = curd firmness at 30 (45) min from rennet addition; RCT_{eq} = rennet coagulation time estimated using the equation; CF_P = asymptotic potential curd firmness; k_{CF} = curd firming instant rate constant; k_{SR} = syneresis instant rate constant; CF_{max} = maximum curd firmness achieved within 45 min; t_{max} = time at achievement of CF_{max}. [2] $FIELD_{lact1}$ = dataset limited to cows belonging to first lactation.

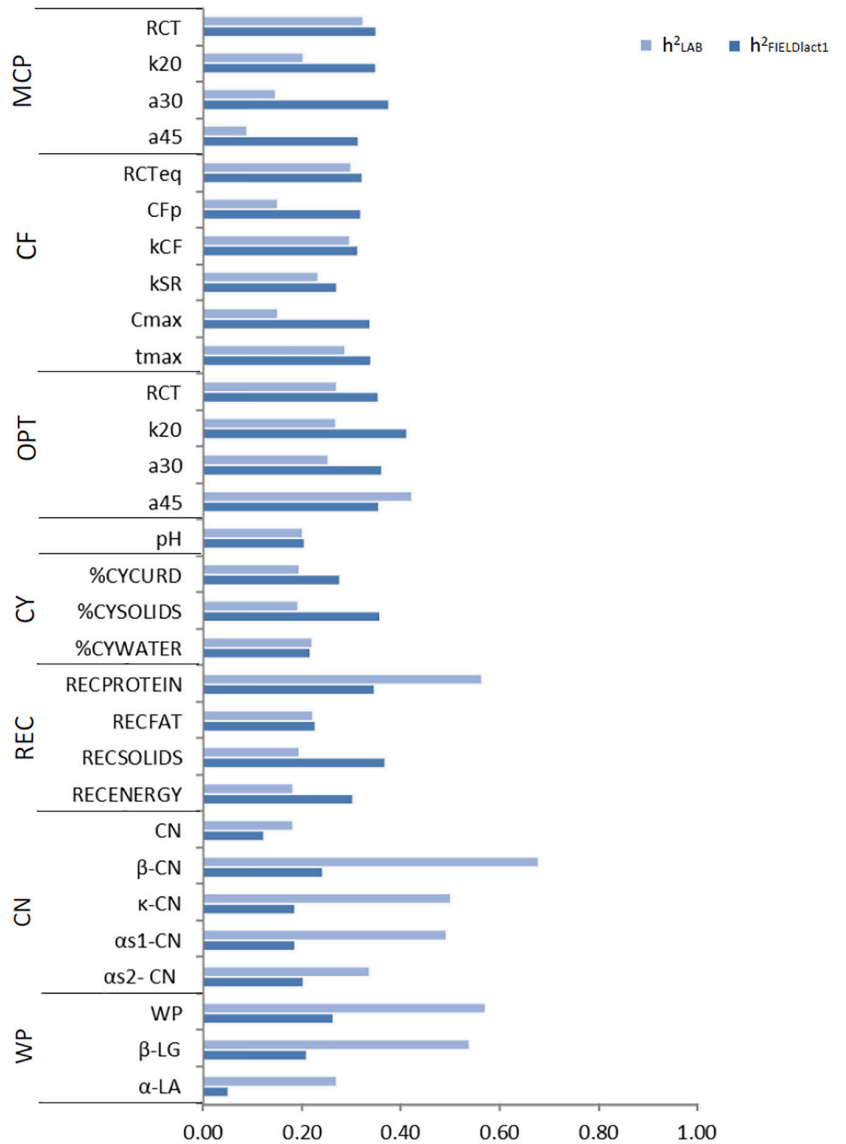

FIGURE 1 | Estimates of heritability for LAB measures and FTIR predictions of the investigated traits using LAB and $FIELD_{lact1}$ data. MCP = milk coagulation properties; RCT = rennet coagulation time; k_{20} = curd firming (CF) rate as the time to a curd firmness of 20 mm; $a_{30(45)}$ = curd firmness at 30 (45) min from rennet addition; RCT_{eq} = rennet coagulation time estimated using the equation; CF_P = asymptotic potential curd firmness; k_{CF} = curd firming instant rate constant; k_{SR} = syneresis instant rate constant; CF_{max} = maximum curd firmness achieved within 45 min; t_{max} = time at achievement of CF_{max}; OPT = Optigraph; CY = cheese yield; $\%CY_{CURD}$ = weight of fresh curd as percentage of weight of milk processed; $\%CY_{SOLIDS}$ = weight of curd solids as percentage of weight of milk processed; $\%CY_{WATER}$ = weight of water curd as percentage of weight of milk processed; REC = recoveries; $REC_{PROTEIN}$ = protein of the curd as percentage of the protein of the milk processed; REC_{FAT} = fat of the curd as percentage of the fat of the milk processed; REC_{SOLIDS} = solids of the curd as percentage of the solids of the milk processed; REC_{ENERGY} = energy of the curd as percentage of energy of the milk processed. [1]True protein nitrogen (N) and milk N fractions are expressed as percentage of total milk N; β-CN (β-casein), κ-CN (κ-casein), αs_1-CN (αs_1-casein), αs_2-CN (αs_2-casein); caseins (CN): Σ(β-CN+κ-CN+ αs_1-CN+αs_2-CN); β-LG (β-lactoglobulin), α-LA (α-lactalbumin), whey proteins (WP): Σ(β-LG+ α-LA).

Cheese-making traits. Variance components and heritability estimates of LAB and $FIELD_{lact1}$ for cheese yield and recovery traits are reported in **Table 4** and **Figure 1**. In addition, the r_{C_LAB} developed on LAB data and the r_a between LAB and FIELD traits are reported in **Table 4** and **Figure 2**. For CY traits, genetic variances were larger in $FIELD_{lact1}$ for CY_{CURD} (∼1.2-fold) and CY_{SOLIDS} (∼1.6-fold) and smaller for CY_{WATER} (∼1.2-fold). For all these traits, a ∼1.5-fold reduction was observed in residual plus permanent environmental variances. For CY_{CURD} and CY_{WATER}, heritability estimates were comparable between the two datasets, while the heritability estimate of CY_{SOLIDS} was almost double in $FIELD_{lact1}$ (0.358), compared to LAB (0.192). Variance components for REC traits had different behaviors: $REC_{PROTEIN}$ and REC_{FAT} had smaller genetic variances for

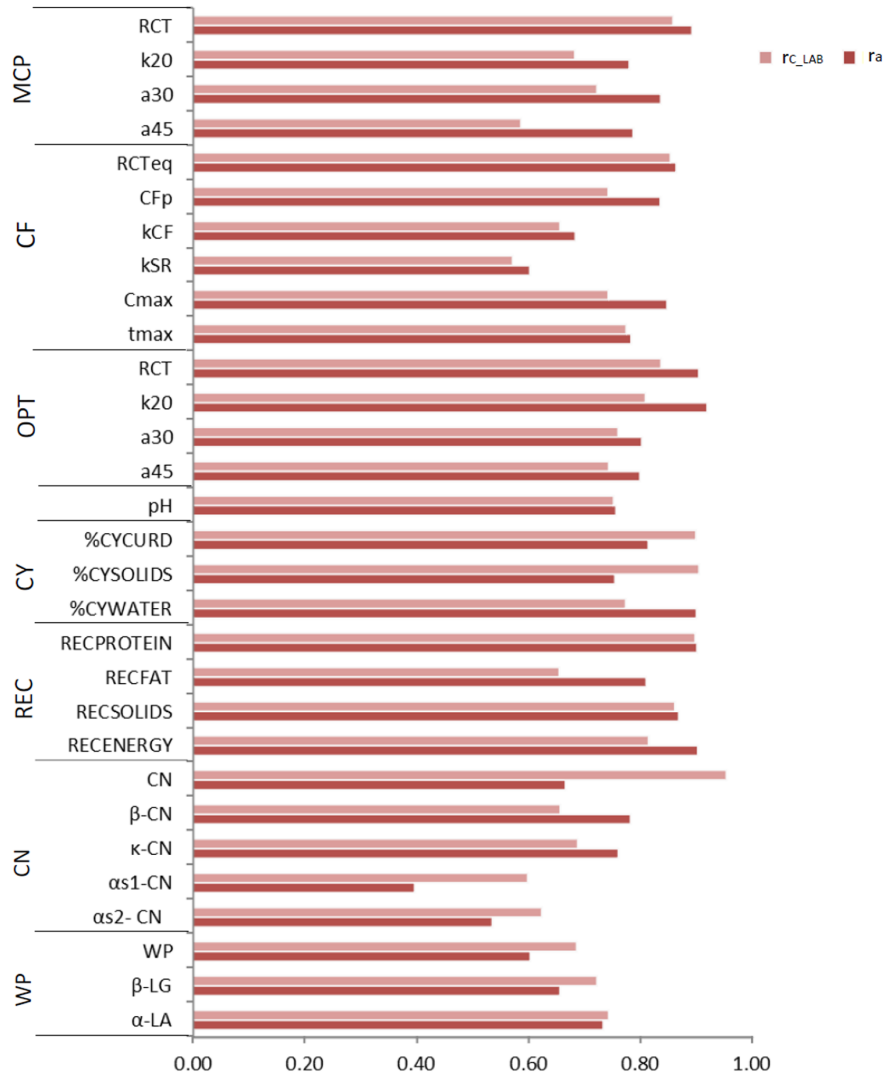

FIGURE 2 | Coefficient of correlation of the calibration models used for infrared prediction (r_{C_LAB}) and additive genetic correlations (r_a) between LAB measures and FTIR predictions of the investigated traits using LAB and $FIELD_{lact1}$ data. MCP = milk coagulation properties; RCT = rennet coagulation time; k_{20} = curd firming (CF) rate as the time to a curd firmness of 20 mm; $a_{30(45)}$ = curd firmness at 30 (45) min from rennet addition; RCT_{eq} = rennet coagulation time estimated using the equation; CF_P = asymptotic potential curd firmness; k_{CF} = curd firming instant rate constant; k_{SR} = syneresis instant rate constant; CF_{max} = maximum curd firmness achieved within 45 min; t_{max} = time at achievement of CF_{max}; OPT = Optigraph; CY = cheese yield; $\%CY_{CURD}$ = weight of fresh curd as percentage of weight of milk processed; $\%CY_{SOLIDS}$ = weight of curd solids as percentage of weight of milk processed; $\%CY_{WATER}$ = weight of water curd as percentage of weight of milk processed; REC = recoveries; $REC_{PROTEIN}$ = protein of the curd as percentage of the protein of the milk processed; REC_{FAT} = fat of the curd as percentage of the fat of the milk processed; REC_{SOLIDS} = solids of the curd as percentage of the solids of the milk processed; REC_{ENERGY} = energy of the curd as percentage of energy of the milk processed. [1]True protein nitrogen (N) and milk N fractions are expressed as percentage of total milk N; β-CN (β-casein), κ-CN (κ-casein), αs_1-CN (αs_1-casein), αs_2- CN (αs_2-casein); caseins (CN): Σ(β-CN+κ-CN+ αs_1-CN+αs_2-CN); β-LG (β-lactoglobulin), α-LA (α-lactalbumin), whey proteins (WP): Σ(β-LG+ α-LA).

$FIELD_{lact1}$ compared to LAB traits (∼1.6- and 1.2-fold, respectively), while REC_{SOLIDS} and REC_{ENERGY} had larger genetic variances in $FIELD_{lact1}$, compared to LAB (∼1.3-fold). On the other hand, we observed a reduction in residual variance for all traits except $REC_{PROTEIN}$ which had a slightly higher value in $FIELD_{lact1}$, compared to the LAB trait. Accordingly, heritability estimates for REC traits were comparable or higher in $FIELD_{lact1}$, with the exception of $REC_{PROTEIN}$ which had a lower value in $FIELD_{lact1}$ (0.247 vs. 0.563).

Milk Protein Fractions

Genetic parameters of milk protein fractions are also presented in **Table 4** and **Figure 1**. In the case of milk proteins, heritability estimates of LAB traits were comparable to previous studies (Schopen et al., 2009). FTIR-predicted milk proteins showed a marked decrease in genetic variance, compared to LAB measures (especially α_{S1}-CN, from 0.873 to 0.065), while residual variances were larger for total CN, κ-CN, total whey, β-LG, and α-LA, smaller for α_{S1}-CN and α_{S2}-CN, and comparable for β-CN.

TABLE 4 | Estimates (Est, with standard error reported as SE) of variance components and heritability of measured LAB traits, coefficient of correlation of the calibration model used for infrared prediction (r_{C_LAB}) developed on LAB measures and used for predictions using FIELD spectra, estimates of variance components and heritability of Fourier transform infrared $FIELD_{lact1}$ predictions, and additive genetic correlation (r_a) between LAB and FIELD for the cheese yield, curd nutrient recovery traits, and protein fractions.

Traits[1]	LAB					r_{C_LAB}	$FIELD_{lact1}$[2]					r_a		
	σ^2_a	σ^2_e	σ^2_p	h^2	SE		σ^2_a	σ^2_{pe}	σ^2_e	σ^2_p	h^2	SE	Est	SE
Cheese yields, %														
$\%CY_{CURD}$	0.408	1.687	2.094	0.195	0.079	0.899	0.495	0.218	1.075	1.788	0.277	0.010	0.814	0.028
$\%CY_{SOLIDS}$	0.105	0.443	0.548	0.192	0.080	0.905	0.170	0.066	0.240	0.477	0.358	0.011	0.754	0.034
$\%CY_{WATER}$	0.192	0.681	0.874	0.220	0.086	0.773	0.158	0.093	0.480	0.731	0.216	0.009	0.900	0.017
Recoveries, %														
$REC_{PROTEIN}$	2.302	1.783	4.084	0.563	0.116	0.897	1.437	0.507	2.203	4.147	0.347	0.010	0.901	0.010
REC_{FAT}	1.633	5.718	7.351	0.222	0.088	0.655	1.395	0.538	4.212	6.145	0.227	0.009	0.810	0.030
REC_{SOLIDS}	1.707	7.071	8.778	0.194	0.081	0.861	2.283	0.792	3.124	6.200	0.368	0.011	0.868	0.019
REC_{ENERGY}	1.539	6.933	8.472	0.182	0.081	0.814	2.027	0.703	3.963	6.693	0.303	0.004	0.902	0.010
N fractions, % total N														
Caseins	0.133	0.589	0.722	0.182	0.086	0.953	0.174	0.031	1.211	1.416	0.123	0.006	0.665	0.059
β-CN	3.199	1.492	4.690	0.678	0.104	0.656	0.519	0.180	1.450	2.148	0.242	0.009	0.782	0.020
κ-CN	0.765	0.752	1.516	0.501	0.106	0.687	0.300	0.170	1.145	1.615	0.186	0.008	0.760	0.029
αs1-CN	0.873	0.901	1.774	0.492	0.108	0.598	0.065	0.028	0.259	0.352	0.186	0.008	0.396	0.058
αs_2-CN	0.240	0.466	0.706	0.337	0.104	0.623	0.056	0.033	0.187	0.276	0.203	0.009	0.535	0.058
Whey proteins	0.852	0.631	1.482	0.571	0.852	0.686	0.295	0.124	0.701	1.120	0.264	0.090	0.603	0.112
β-LG	0.635	0.537	1.712	0.538	0.103	0.722	0.289	0.117	0.976	1.382	0.209	0.008	0.656	0.034
α-LA	0.026	0.069	0.095	0.270	0.099	0.743	0.006	0.002	0.120	0.127	0.051	0.002	0.733	0.037

[1] *$\%CY_{CURD}$ = weight of fresh curd as percentage of weight of milk processed; $\%CY_{SOLIDS}$ = weight of curd solids as percentage of weight of milk processed; $\%CY_{WATER}$ = weight of water curd as percentage of weight of milk processed; $REC_{PROTEIN}$ = protein of the curd as percentage of the protein of the milk processed; REC_{FAT} = fat of the curd as percentage of the fat of the milk processed; REC_{SOLIDS} = solids of the curd as percentage of the solids of the milk processed; REC_{ENERGY} = energy of the curd as percentage of energy of the milk processed; true protein nitrogen (N) and milk N fractions are expressed as percentage of total milk N; β-CN (β-casein), κ-CN (κ-casein), αs_1-CN (αs_1-casein), αs_2-CN (αs_2-casein); caseins: Σ(β-CN+κ-CN+ αs_1-CN+αs_2-CN); β-LG (β-lactoglobulin), α-LA (α-lactalbumin), whey proteins: Σ(β-LG+ α-LA).* [2] *$FIELD_{lact1}$ = dataset limited to cows belonging to first lactation.*

Heritability estimates were lower in $FIELD_{lact1}$ for all protein traits, ranging from high-moderate (ranging from 0.182 to 0.678) to moderate-low (ranging from 0.051 to 0.264; **Figure 1**). These results were in accordance with previous studies, showing a decrease in the estimated genetic variance and heritabilities for predicted milk proteins compared to measured traits (Rutten et al., 2011; Bonfatti et al., 2017), and are essentially due to the low r_{C_LAB} values obtained for these traits.

Reliability of Calibrations and Genetic Correlation Between Measured and Predicted Traits

To assess the reliability of calibration equations in the animal breeding context, we estimated, besides the r_{C_LAB}, the r_a between LAB and $FIELD_{lact1}$ traits as an indicator of the potential of FTIR calibrations to provide novel phenotypes for indirect selective breeding. Results are displayed in **Figure 2**. The r_{C_LAB} ranged from 0.571 (k_{SR}) to 0.953 (total CN). In general, estimates of r_a for milk coagulation and cheese-making traits were high (>0.75), except for k_{CF} and k_{SR} which displayed moderate-high estimates (>0.60). On the other hand, only two milk proteins showed r_a smaller than 0.6: α_{S1}-CN (0.396) and α_{S2}-CN (0.535). These two traits were those with the lowest r_{C_LAB} among all traits tested (**Table 4**: 0.598 and 0.623, respectively). This means that expected genetic gain using these two predicted milk proteins would be moderately lower, compared to that achievable for the other traits. These results were in accordance with Bonfatti et al. (2017) which found high r_a for milk protein content but lower r_a for percentage traits (0.58, on average). On the other hand, Rutten et al. (2011) reported greater r_a values compared to those in our study (0.62–0.97), which might be ascribed to differences in population (breed, size) and/or in the analytical technique used for milk protein investigation (capillary electrophoresis vs. HPLC). The reliability of calibration r_{C_LAB} was associated with the decrease in genetic variance between LAB and $FIELD_{lact1}$ traits (R^2 = 0.45). In particular, lower r_{C_LAB} corresponded to larger decrease in genetic variance (**Figure 3A**). A weaker relationship was observed between r_{C_LAB} and the decrease in residual variance (R^2 = 0.09, data not reported in Figures). A positive relationship (R^2 = 0.26) was observed between r_{C_LAB} and r_a: a higher reliability of the calibration model corresponded to a higher additive genetic correlation between the LAB-measures and $FIELD_{lact1}$ predictions (**Figure 3B**). Beyond this correlation, it is worth noting from **Figure 2** that 22 out of 30 investigated traits presented genetic correlations greater than the reliability of calibration ($r_a > r_{C\_LAB}$). So, even calibrations with a relatively small predictive ability could be exploited in selective breeding, if their r_a between measured and predicted traits is sufficiently high.

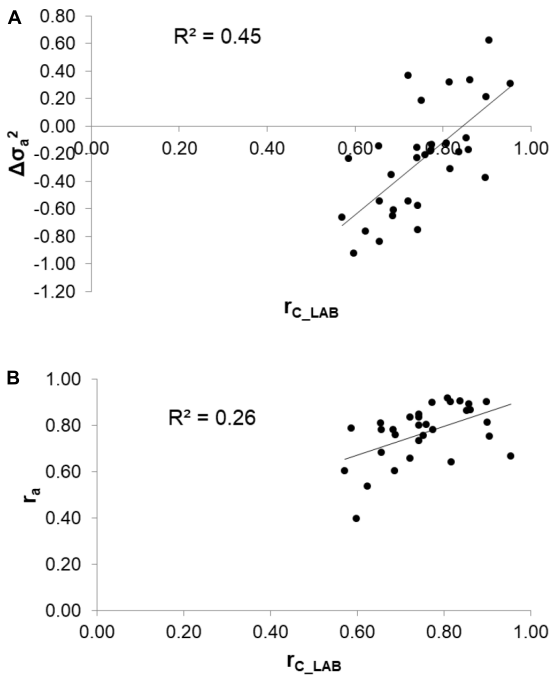

FIGURE 3 | Relationships between the coefficient of correlation of calibration models (r_{C_LAB}) used for infrared prediction and **(A)** the change in additive genetic variance ($\Delta\sigma_a^2$) and **(B)** the additive genetic correlation (r_a) between LAB measures and FTIR predictions.

Single-Step GBLUP Prediction Accuracy by Cross-Validation

Table 5 and **Supplementary Figure S1** report the results for the cross-validation performed in order to compare different phenotyping strategies. The cross-validation mimicked the progeny testing scheme, where the LAB phenotypes of testing sires were predicted based on LAB phenotypes from daughters of proven bulls and FIELD information from daughters of proven and progeny testing bulls. Results are presented as the average of the prediction accuracy for the fourfold of sires. For the scenarios that included FIELD information, results in **Table 5** show the largest predictive ability obtained within the range of genetic correlation values tested, which is also reported in **Table 5**. The change in prediction accuracy for each trait over the values of genetic correlation is reported in **Supplementary Figure S1**.

Prediction With LAB Information

In the LAB.t scenario, daughters of progeny testing bulls are not phenotyped and FIELD information is not included and the genetic evaluation is based on a single-trait model. The predictive ability for the different traits followed, to a large extent, the trait heritability (**Figure 1**). Among MCP traits, RCT showed the highest accuracy (0.118), with the other traits showing almost null values. For CF traits, only RCT_{eq}, k_{CF}, and t_{max} showed values of accuracy above 0.10. CF_p and C_{max} showed null values, which is in agreement with the low (∼0.1) heritability estimates. Optigraph traits showed a different trend, with RCT reporting the strongest prediction accuracy (0.168) but not the largest heritability. Prediction accuracies were below 0.1 for all CY traits, for which heritability estimates barely reached the value of 0.2. Prediction accuracy was largest for $REC_{PROTEIN}$ among recovery traits, and its heritability estimate was the largest in the group (∼0.55). A similar scenario was found among casein fractions, where whey proteins, β-LG, and β-CN showed one of the strongest prediction accuracies (0.208, 0.187, and 0.153, respectively) and the largest heritability (above 0.50). Surprisingly, α_{S1}-CN showed a strong predictive ability (0.165), yet not the largest heritability estimate (∼0.50). Prediction with only LAB information can be considered unreliable from a genetic evaluation standpoint, given the limited size of the dataset and the relative cost needed to acquire each single record. However, this scenario was included as a reference for the other, more reliable, models.

Prediction When LAB and FIELD Information Is Included

The LAB.t+FIELD.t scenario mimics a genetic evaluation where both LAB and FIELD information of proven bulls is included. The comparison with the LAB.t scenario proves the value of including FIELD.t information, which highlights the importance of the construction of FTIR calibration equations and the collection of data at the population level on daughters of proven bulls. Still, the genetic merit of bulls can be predicted at birth under this scenario. The genetic evaluation leverages a bivariate model. Overall, prediction accuracy showed a strong increase, compared to the previous scenario. The largest increases in prediction accuracy were observed for curd firming traits, with MCP k_{20}, a_{30}, and a_{45} having prediction accuracies of 0.208, 0.190, and 0.181, respectively (compared to null accuracies in LAB.t); Optigraph a_{30} prediction accuracy increased from 0.037 to 0.242; and CF_p increased from 0.038 to 0.235. Among protein composition traits, κ-CN increased from 0.051 to 0.330, while α_{S1}-CN did not increase (being the only trait not showing any increase). For all the abovementioned traits that showed an increase, the optimal value of genetic correlation appeared to be 0.9, which corroborates the relevance of FIELD information for accurately predicting LAB breeding values and phenotypes. The values of correlation for the calibration model used for infrared prediction (r_{C_LAB}) and additive genetic correlations (r_a) estimated from the data were large for these traits but not the largest found.

The LAB.t+FIELD.t+FIELD.v scenario mimicked a genetic evaluation based on a progeny testing scheme, which implies the collection of FTIR spectra information on the daughters of progeny testing bulls (FIELD.v). Here, genetic merit of bulls cannot be estimated at birth but collection of FIELD phenotypes is needed as in traditional progeny testing. As compared to a previously discussed scenario, the advantage of the FIELD.v data seemed marginal, showing a maximum of 1.2-fold increase and often a decrease in prediction accuracy. Traits that benefited the most were OPT k_{20} (from 0.250 to 0.302), CY_{WATER} (from 0.203 to 0.242), and casein proportion (from 0.198 to 0.230). Traits that did not show an increase were α_{S2}-CN, whey proteins, α-LA, and β-LG.

TABLE 5 | Best-performing model in terms of accuracy (acc) for each of the scenarios studied. The values in bold indicate the best performing scenario (in terms of accuracy) for each trait.

Trait[2]	LAB.t[1]	LAB.t + FIELD.t		LAB.t + FIELD.t + FIELD.v		FIELD.t		FIELD.t + FIELD.v	
	acc	r_a	acc	r_a	Acc	r_a	acc	r_a	acc
Traditional MCP									
RCT, min	0.118	0.9	0.285	**0.9**	**0.322**	0.9	0.285	0.9	0.321
k_{20}, min	0.016	0.9	0.208	1.0	0.227	0.9	0.212	**0.4**	**0.233**
a_{30}, mm	0.032	0.9	0.190	0.9	0.212	0.8	0.193	**0.9**	**0.215**
a_{45}, mm	0.027	0.9	0.181	0.9	0.192	0.9	0.184	**0.9**	**0.196**
Curd firming									
RCT_{eq}, min	0.102	0.9	0.286	**0.9**	**0.319**	0.9	0.286	0.9	0.312
CF_p, mm	0.038	0.9	0.235	0.9	0.258	0.9	0.236	**0.9**	**0.262**
k_{CF}, % × min^{-1}	0.104	0.7	0.217	0.8	0.236	0.1	0.200	**1.0**	**0.249**
k_{SR}, % × min^{-1}	0.093	0.6	0.189	0.6	0.204	0.2	0.176	**0.2**	**0.216**
C_{max}, mm	0.038	0.9	0.224	0.9	0.249	0.9	0.225	**0.9**	**0.258**
t_{max}, min	0.112	0.9	0.233	**0.9**	**0.269**	0.9	0.223	0.9	0.265
Optigraph									
RCT, min	0.168	0.9	0.283	0.9	0.315	0.8	0.283	**0.8**	**0.316**
k_{20}, min	0.053	1	0.250	**1.0**	**0.302**	0.9	0.248	1.0	0.296
a_{30}, mm	0.037	0.9	0.242	0.9	0.262	0.9	0.257	**0.9**	**0.274**
a_{45}, mm	0.060	0.9	0.331	**0.9**	**0.350**	0.9	0.325	0.9	0.346
Acidity									
pH	0.113	0.7	0.221	0.6	0.225	0.3	0.227	**0.3**	**0.236**
Cheese yields, %									
CY_{CURD}	0.070	0.9	0.296	**0.9**	**0.317**	0.8	0.298	0.9	0.315
CY_{SOLIDS}	0.088	0.9	0.348	**0.9**	**0.362**	0.9	0.343	0.9	0.331
CY_{WATER}	0.076	0.9	0.203	0.9	0.242	0.9	0.198	**0.9**	**0.249**
Recoveries, %									
$REC_{PROTEIN}$	0.147	1	0.340	**1**	**0.365**	1	0.329	1	0.362
REC_{FAT}	0.078	0.9	0.192	**0.9**	**0.193**	0.9	0.192	0.9	0.182
REC_{SOLIDS}	0.071	0.9	0.376	**0.9**	**0.377**	0.8	0.376	0.9	0.345
REC_{ENERGY}	0.103	0.9	0.343	**0.9**	**0.358**	0.9	0.343	0.9	0.334
N fractions, % total milk N									
Caseins	0.036	0.9	0.198	**1**	**0.230**	0.9	0.200	1	0.204
β-CN	0.153	0.9	0.297	**0.9**	**0.308**	0.2	0.287	0.9	0.284
κ-CN	0.051	1	0.307	**1**	**0.330**	1	0.296	0.9	0.280
α_{S1}-CN	**0.165**	0.1	0.164	0.1	0.165	0.8	0.055	0.8	0.061
α_{S2}-CN	0.099	**0.6**	**0.170**	0.6	0.159	0.5	0.146	0.6	0.123
Whey proteins	0.208	0.7	0.243	0.5	0.238	0.9	0.206	**0.9**	**0.244**
β-LG	0.187	0.5	0.224	0.5	0.224	0.9	0.206	**0.9**	**0.254**
α-LA	0.054	0.9	0.140	0.9	0.137	0.5	0.133	**1**	**0.154**

[1] The value of genetic correlation was implicitly considered equal to 0 in the LAB.t scenario. [2] RCT = rennet coagulation time; k_{20} = curd firming rate as the time to a curd firmness of 20 mm; $a_{30(45)}$ = curd firmness at 30 (45) min from rennet addition; RCT_{eq} = rennet coagulation time estimated using the equation; CF_P = asymptotic potential curd firmness; k_{CF} = curd firming instant rate constant; k_{SR} = syneresis instant rate constant; CF_{max} = maximum curd firmness achieved within 45 min; t_{max} = time at achievement of CF_{max}; $\%CY_{CURD}$ = weight of fresh curd as percentage of weight of milk processed; $\%CY_{SOLIDS}$ = weight of curd solids as percentage of weight of milk processed; $\%CY_{WATER}$ = weight of water curd as percentage of weight of milk processed; $REC_{PROTEIN}$ = protein of the curd as percentage of the protein of the milk processed; REC_{FAT} = fat of the curd as percentage of the fat of the milk processed; REC_{SOLIDS} = solids of the curd as percentage of the solids of the milk processed; REC_{ENERGY} = energy of the curd as percentage of energy of the milk processed. [1] True protein nitrogen (N) and milk N fractions are expressed as percentage of total milk N; β-CN (β-casein), κ-CN (κ-casein), αs_1-CN (αs_1-casein), αs_2-CN (αs_2-casein); caseins: Σ(β-CN+κ-CN+ αs_1-CN+αs_2-CN); β-LG (β-lactoglobulin), α-LA (α-lactalbumin), and whey proteins: Σ(β-LG+ α-LA).

Prediction When LAB Information Is Not Included

Scenarios FIELD.t and FIELD.t+FIELD.v mimic a breeding scheme where LAB information is not included in the genetic evaluations. Still, LAB information is used to obtain FTIR phenotype prediction equations. The underlying model is a bivariate model that produces LAB breeding values, although LAB records are not included. Comparing the LAB.t+FIELD.t scenario to the FIELD.t scenario allows the evaluation of the contribution of LAB information when FIELD information is recorded on the daughters of proven bulls. Here, differences were negligible, except for α_{S1}-CN that showed a dramatic decrease

from 0.165 to 0.055 when LAB information was removed. This is due to the low quality of the calibration model used for FTIR predictions (r_{C_LAB} = 0.60 and r_a = 0.40). The comparison of the LAB.t+FIELD.t+FIELD.v scenario to the FIELD.t+FIELD.v allows us to further prove the value of LAB phenotypes when FIELD information is also recorded in daughters of progeny testing bulls. Again, changes were negligible for most traits, confirming the low relevance of LAB information when solid FTIR calibration equations are used. The relevance of FIELD.v information is assessed in the comparison of FIELD.t and FIELD.t+FIELD.v, when LAB information is absent. While the increase was negligible in the presence of LAB information (maximum of 1.2-fold increase in accuracy), in this case the fold increase reached 1.25 with several traits being about 1.1. This supports the hypothesis that progeny testing could be beneficial for most traits, but probably the gain in accuracy would not match the cost of delaying the candidate bull's evaluation. It should be considered that generation interval can be dramatically reduced when FIELD.v information is omitted, compromising prediction accuracy, but probably not sufficiently to justify progeny testing cost.

Best Performing Scenario in Terms of Prediction Accuracy

With the exception of α_{S1}-CN, which showed a poor FTIR calibration equation, all traits showed an advantage in the inclusion of FIELD information, supporting the need for well-constructed calibration equations that allow us to obtain predicted phenotypes at the population level. Furthermore, an increase in prediction accuracy was found with the inclusion of FIELD.v information rather than just FIELD.t, either with or without the presence of LAB.t phenotypes. Scenarios that included all FIELD information outperformed scenarios that just included FIELD.t, with the exception of α_{S2}-CN. This would lead to further speculation on the need for conducting progeny testing for new bulls, but the gain in accuracy of prediction is probably not translated into gain in genetic progress due to increased generation interval. It should also be noted that for some traits, i.e., k_{20}, k_{CF}, k_{SR}, βCN, pH, α_{S1}-CN, and α-LA (not necessarily those with low FTIR prediction accuracy), the trend of prediction accuracy over the values of assumed genetic correlation was sometimes null if not negative.

Despite the large number of traits involved, this study does not allow us to declare a breakeven value for any genetic parameter that would serve to predict the value of FIELD vs. LAB information. The only trait that did not benefit from FIELD information happened to be α_{S1}-CN, for which the quality of the FTIR calibration equation was particularly low, followed by the low FIELD heritability and low genetic correlation with LAB measures. All other traits benefited from the inclusion of FIELD information and the accuracy gained with FIELD information greatly depended on the genetic correlation between LAB and FIELD traits. Nonetheless, it was not possible to declare a breakeven value of genetic correlation which deemed the use of FIELD information advantageous. Breakeven values of genetic correlations for indicator traits were found to be 0.5 by Calus and Veerkamp (2011), who studied genomic selection performance under multi-trait scenarios, and 0.7–0.8 by Mulder and Bijma (2007) who studied the impact of genotype by environment interactions in breeding programs. Given that this study based on field data, there could be more factors affecting the value of indicator traits in genomic prediction. Further research is needed in order to explore all potential contributions.

CONCLUSION

The present study reported two approaches for assessing the contribution of FTIR calibration equations at the population level for dairy cattle breeding. With the first approach, results indicate that FIELD predictions can be used in breeding programs for the genetic improvement of difficult-to-measure traits and that indirect selection for FIELD predictions will provide satisfactory responses. With the second approach, for the first time we highlighted the utility of FTIR predictions for breeding purposes using real data to simulate different genetic evaluation scenarios, where FTIR-derived phenotypic information is dosed into (single-step) GBLUP to predict wet-lab measured performance of daughters of progeny testing bulls. Collection of FIELD measures for progeny testing bulls appears to be advantageous for increasing the predictive ability for most of the traits studied, but the increase in generation interval due to progeny testing does not justify the increase in prediction accuracy. LAB information from proven bulls' daughters could be included in the genetic evaluations without a detrimental effect. As there is no evidence of a clear advantage to including FIELD information for progeny testing bulls, progeny testing schemes could be replaced by the construction of robust calibration equations together with more vast collection of FIELD measures on daughters of proven bulls.

In general, the increase in predictive ability observed with the inclusion of FIELD information is very favorable and reaches moderate values for 12 traits. While further research is needed in the modeling of FTIR-predicted data, results are promising. Once calibration equations are developed, the cost of collecting FIELD is virtually null, provided that routine spectra acquisition within milk recording schemes is performed and available for breeders. Yet, the cost of developing robust calibration equations should be factored into the total cost of implementing (genomic) selection that includes FIELD data. Thus, an economic analysis should be performed before progressing its use in breeding programs for difficult-to-measure traits.

DATA AVAILABILITY STATEMENT

The raw data supporting the conclusions of this article will be made available by the authors, without undue reservation.

AUTHOR CONTRIBUTIONS

AC conceived the study, contributed to set up the objectives of this study, drafted the first version of the manuscript, and supervised the project. HT-A performed the statistical analysis together with FT. SP contributed to the critical interpretation of

the results and to manuscript drafting. GB and CM contributed to the critical revision of the manuscript. FT conceived the study with AC, contributed to the critical interpretation of the results, and to manuscript drafting. All authors have read and approved the final manuscript.

ACKNOWLEDGMENTS

The authors wish to thank Italian Brown Swiss Cattle Breeders Association (ANARB, Verona, Italy), the Associazione Provinciale delle Organizzazioni Zootecniche Altoatesine/Vereinigung der Südtiroler Tierzuchtverbände, and the Federazione Latterie Alto Adige/Sennereiver-band Südtirol (Bolzano/Bozen, Italy) for providing the data.

SUPPLEMENTARY MATERIAL

The Supplementary Material for this article can be found online at: https://www.frontiersin.org/articles/10.3389/fgene.2020.563393/full#supplementary-material

REFERENCES

Aguilar, I., Misztal, I., Johnson, D. L., Legarra, A., Tsuruta, S., and Lawlor, T. J. (2010). Hot topic: A unified approach to utilize phenotypic, full pedigree, and genomic information for genetic evaluation of Holstein final score. *J. Dairy Sci.* 93, 743–752. doi: 10.3168/jds.2009-2730

Barbano, D. M., and Clark, J. L. (1989). Infrared milk analysis — challenges for the future. *J. Dairy Sci.* 72, 1627–1636. doi: 10.3168/jds.S0022-0302(89)79275-4

Belay, T. K., Svendsen, M., Kowalski, Z. M., and Ådnøy, T. (2017). Genetic parameters of blood β-hydroxybutyrate predicted from milk infrared spectra and clinical ketosis, and their associations with milk production traits in Norwegian Red cows. *J. Dairy Sci.* 100, 6298–6311. doi: 10.3168/jds.2016-12458

Bilder, R. M., Sabb, F. W., Cannon, T. D., London, E. D., Jentsch, J. D., Parker, D. S., et al. (2009). Phenomics: the systematic study of phenotypes on a genome-wide scale. *Neuroscience* 164, 30–42. doi: 10.1016/j.neuroscience.2009.01.027

Bittante, G., and Cipolat-Gotet, C. (2018). Direct and indirect predictions of enteric methane daily production, yield, and intensity per unit of milk and cheese, from fatty acids and milk Fourier-transform infrared spectra. *J. Dairy Sci.* 101, 7219–7235. doi: 10.3168/jds.2017-14289

Bittante, G., Cipolat-Gotet, C., Malchiodi, F., Sturaro, E., Tagliapietra, F., Schiavon, S., et al. (2015). Effect of dairy farming system, herd, season, parity, and days in milk on modeling of the coagulation, curd firming, and syneresis of bovine milk. *J. Dairy Sci.* 98, 2759–2774. doi: 10.3168/jds.2014-8909

Bittante, G., Ferragina, A., Cipolat-Gotet, C., and Cecchinato, A. (2014). Comparison between genetic parameters of cheese yield and nutrient recovery or whey loss traits measured from individual model cheese-making methods or predicted from unprocessed bovine milk samples using Fourier-transform infrared spectroscopy. *J. Dairy Sci.* 97, 6560–6572.

Boichard, D., and Brochard, M. (2012). New phenotypes for new breeding goals in dairy cattle. *Animal* 6:18. doi: 10.1017/S1751731112000018

Bonfatti, V., Grigoletto, L., Cecchinato, A., Gallo, L., and Carnier, P. (2008). Validation of a new reversed-phase high-performance liquid chromatography method for separation and quantification of bovine milk protein genetic variants. *J. Chromatogr. A* 1195, 101–106. doi: 10.1016/j.chroma.2008.04.075

Bonfatti, V., Vicario, D., Degano, L., Lugo, A., and Carnier, P. (2017). Comparison between direct and indirect methods for exploiting Fourier transform spectral information in estimation of breeding values for fine composition and technological properties of milk. *J. Dairy Sci.* 100, 2057–2067. doi: 10.3168/JDS.2016-11951

Calus, M. P. L., and Veerkamp, R. F. (2011). Accuracy of multi-trait genomic selection using different methods. *Genet. Sel. Evol.* 43:26. doi: 10.1186/1297-9686-43-26

Cecchinato, A., Albera, A., Cipolat-Gotet, C., Ferragina, A., and Bittante, G. (2015). Genetic parameters of cheese yield and curd nutrient recovery or whey loss traits predicted using Fourier-transform infrared spectroscopy of samples collected during milk recording on Holstein, Brown Swiss, and Simmental dairy cows. *J. Dairy Sci.* 98, 4914–4927. doi: 10.3168/jds.2014-8599

Cecchinato, A., Cipolat-Gotet, C., Casellas, J., Penasa, M., Rossoni, A., and Bittante, G. (2013). Genetic analysis of rennet coagulation time, curd-firming rate, and curd firmness assessed over an extended testing period using mechanical and near-infrared instruments. *J. Dairy Sci.* 96, 50–62. doi: 10.3168/jds.2012-5784

Cecchinato, A., de Marchi, M., Gallo, L., Bittante, G., and Carnier, P. (2009). Mid-infrared spectroscopy predictions as indicator traits in breeding programs for enhanced coagulation properties of milk. *J. Dairy Sci.* 92, 5304–5313. doi: 10.3168/jds.2009-2246

de los Campos, G., and Perez-Rodriguez, P. (2014). Genome-wide regression and prediction with the BGLR statistical package. *Genetics* 198, 483–495. doi: 10.1534/genetics.114.164442

Dórea, J. R. R., Rosa, G. J. M., Weld, K. A., and Armentano, L. E. (2018). Mining data from milk infrared spectroscopy to improve feed intake predictions in lactating dairy cows. *J. Dairy Sci.* 101, 5878–5889. doi: 10.3168/jds.2017-13997

Ferragina, A., Cipolat-Gotet, C., Cecchinato, A., and Bittante, G. (2013). The use of Fourier-transform infrared spectroscopy to predict cheese yield and nutrient recovery or whey loss traits from unprocessed bovine milk samples. *J. Dairy Sci.* 96, 7980–7990. doi: 10.3168/jds.2013-7036

Ferragina, A., de los Campos, G., Vazquez, A. I, Cecchinato, A., and Bittante, G. (2015). Bayesian regression models outperform partial least squares methods for predicting milk components and technological properties using infrared spectral data. *J. Dairy Sci.* 98, 8133–8151. doi: 10.3168/jds.2014-9143

Guo, G., Zhao, F., Wang, Y., Zhang, Y., Du, L., and Su, G. (2014). Comparison of single-trait and multiple-trait genomic prediction models. *BMC Genet.* 15:30. doi: 10.1186/1471-2156-15-30

Henderson, C. R., and Quaas, R. L. (1976). Multiple trait evaluation using relatives' records. *J. Anim. Sci.* 43, 1188–1197. doi: 10.2527/jas1976.4361188x

Houle, D., Govindaraju, D. R., and Omholt, S. (2010). Phenomics: the next challenge. *Nat. Rev. Genet.* 11, 855–866. doi: 10.1038/nrg2897

Karaman, E., Lund, M. S., Anche, M. T., Janss, L., and Su, G. (2018). Genomic prediction using multi-trait weighted GBLUP accounting for heterogeneous variances and covariances across the genome. *G3 Genes Genomes Genet.* 8, 3549–3558. doi: 10.1534/g3.118.200673

Lee, S. H., van der Werf, J. H. J., Hayes, B. J., Goddard, M. E., and Visscher, P. M. (2008). Predicting unobserved phenotypes for complex traits from whole-genome SNP data. *PLoS Genet.* 4:e1000231. doi: 10.1371/journal.pgen.1000231

Legarra, A., Aguilar, I., and Misztal, I. (2009). A relationship matrix including full pedigree and genomic information. *J. Dairy Sci.* 92, 4656–4663. doi: 10.3168/jds.2009-2061

Mele, M., Macciotta, N. P. P., Cecchinato, A., Conte, G., Schiavon, S., and Bittante, G. (2016). Multivariate factor analysis of detailed milk fatty acid profile: effects of dairy system, feeding, herd, parity, and stage of lactation. *J. Dairy Sci.* 99, 9820–9833.

Misztal, I., Tsuruta, S., Strabel, T., Auvray, B., Druet, T., and Lee, D. H. (2002). "BLUPF90 and related programs (BGF90), Commun. No. 28-07," in *Proceedings of the 7th World Congress on Genetics Applied to Livestock Production*, Montpellier.

Mulder, H. A., and Bijma, P. (2007). Effects of genotype x environment interaction on genetic gain in breeding programs. *J. Anim. Sci.* 83, 49–61. doi: 10.2527/2005.83149x

NRC (2001). *Nutrient Requirements of Dairy Cattle Subcommittee on Dairy Cattle Nutrition. Committee on Animal Nutrition Board on Agriculture and Natural Resources National Research Council*. Washington, DC: National Academy Press.

Pegolo, S., Mach, N., Ramayo-Caldas, Y., Schiavon, S., Bittante, G., and Cecchinato, A. (2018). Integration of GWAS, pathway and network analyses reveals novel mechanistic insights into the synthesis of milk

proteins in dairy cows. *Sci. Rep.* 8:566. doi: 10.1038/s41598-017-18916-4

R Core Team (2018). *R: The R Project for Statistical Computing*. Vienna: R Core Team.

Rutten, M. J. M., Bovenhuis, H., Heck, J. M. L., and van Arendonk, J. A. M. (2011). Predicting bovine milk protein composition based on Fourier transform infrared spectra. *J. Dairy Sci.* 94, 5683–5690. doi: 10.3168/JDS.2011-4520

Rutten, M. J. M., Bovenhuis, H., and van Arendonk, J. A. M. (2010). The effect of the number of observations used for Fourier transform infrared model calibration for bovine milk fat composition on the estimated genetic parameters of the predicted data. *J. Dairy Sci.* 93, 4872–4882.

Sanchez, M. P., El Jabri, M., Minéry, S., Wolf, V., Beuvier, E., Laithier, C., et al. (2018). Genetic parameters for cheese-making properties and milk composition predicted from mid-infrared spectra in a large data set of Montbéliarde cows. *J. Dairy Sci.* 101, 10048–10061. doi: 10.3168/jds.2018-14878

Sargolzaei, M., Chesnais, J. P., and Schenkel, F. S. (2014). A new approach for efficient genotype imputation using information from relatives. *BMC Genom.* 15:478. doi: 10.1186/1471-2164-15-478

Schopen, G. C. B., Heck, J. M. L., Bovenhuis, H., Visker, M. H. P. W., van Valenberg, H. J. F., and van Arendonk, J. A. M. (2009). Genetic parameters for major milk proteins in Dutch Holstein-Friesians. *J. Dairy Sci.* 92, 1182–1191. doi: 10.3168/jds.2008-1281

Soyeurt, H., Dardenne, P., Dehareng, F., Lognay, G., Veselko, D., Marlier, M., et al. (2006a). Estimating fatty acid content in cow milk using mid-infrared spectrometry. *J. Dairy Sci.* 89, 3690–3695. doi: 10.3168/jds.S0022-0302(06)72409-2

Soyeurt, H., Dardenne, P., Gillon, A., Croquet, C., Vanderick, S., Mayeres, P., et al. (2006b). variation in fatty acid contents of milk and milk fat within and across breeds. *J. Dairy Sci.* 89, 4858–4865. doi: 10.3168/JDS.S0022-0302(06)72534-6

Soyeurt, H., Dehareng, F., Gengler, N., McParland, S., Wall, E., Berry, D. P., et al. (2011). Mid-infrared prediction of bovine milk fatty acids across multiple breeds, production systems, and countries. *J. Dairy Sci.* 94, 1657–1667. doi: 10.3168/jds.2010-3408

Toledo-Alvarado, H., Vazquez, A. I., de Los Campos, G., Tempelman, R. J., Bittante, G., and Cecchinato, A. (2018). Diagnosing pregnancy status using infrared spectra and milk composition in dairy cows. *J. Dairy Sci.* 101, 2496–2505. doi: 10.3168/jds.2017-13647

Conflict of Interest: The authors declare that the research was conducted in the absence of any commercial or financial relationships that could be construed as a potential conflict of interest.

frontiers in Veterinary Science

REVIEW
published: 21 October 2020
doi: 10.3389/fvets.2020.551269

Image Analysis and Computer Vision Applications in Animal Sciences: An Overview

Arthur Francisco Araújo Fernandes[1], João Ricardo Rebouças Dórea[1] and Guilherme Jordão de Magalhães Rosa[1,2]*

[1] Department of Animal and Dairy Sciences, University of Wisconsin-Madison, Madison, WI, United States, [2] Department of Biostatistics and Medical Informatics, University of Wisconsin-Madison, Madison, WI, United States

Computer Vision, Digital Image Processing, and Digital Image Analysis can be viewed as an amalgam of terms that very often are used to describe similar processes. Most of this confusion arises because these are interconnected fields that emerged with the development of digital image acquisition. Thus, there is a need to understand the connection between these fields, how a digital image is formed, and the differences regarding the many sensors available, each best suited for different applications. From the advent of the charge-coupled devices demarking the birth of digital imaging, the field has advanced quite fast. Sensors have evolved from grayscale to color with increasingly higher resolution and better performance. Also, many other sensors have appeared, such as infrared cameras, stereo imaging, time of flight sensors, satellite, and hyperspectral imaging. There are also images generated by other signals, such as sound (ultrasound scanners and sonars) and radiation (standard x-ray and computed tomography), which are widely used to produce medical images. In animal and veterinary sciences, these sensors have been used in many applications, mostly under experimental conditions and with just some applications yet developed on commercial farms. Such applications can range from the assessment of beef cuts composition to live animal identification, tracking, behavior monitoring, and measurement of phenotypes of interest, such as body weight, condition score, and gait. Computer vision systems (CVS) have the potential to be used in precision livestock farming and high-throughput phenotyping applications. We believe that the constant measurement of traits through CVS can reduce management costs and optimize decision-making in livestock operations, in addition to opening new possibilities in selective breeding. Applications of CSV are currently a growing research area and there are already commercial products available. However, there are still challenges that demand research for the successful development of autonomous solutions capable of delivering critical information. This review intends to present significant developments that have been made in CVS applications in animal and veterinary sciences and to highlight areas in which further research is still needed before full deployment of CVS in breeding programs and commercial farms.

Keywords: computer vision, sensors, imaging, phenotyping, automation, livestock, precision livestock, high-throughput phenotyping

OPEN ACCESS

Edited by:
Peter Dovc,
University of Ljubljana, Slovenia

Reviewed by:
Ute Knierim,
University of Kassel, Germany
Johannes Baumgartner,
University of Veterinary Medicine Vienna, Austria

****Correspondence:***
Arthur Francisco Araújo Fernandes
afernandes2@wisc.edu

Specialty section:
This article was submitted to Livestock Genomics, a section of the journal Frontiers in Veterinary Science

Received: *28 April 2020*
Accepted: *15 September 2020*
Published: *21 October 2020*

Citation:
Fernandes AFA, Dórea JRR and Rosa GJM (2020) Image Analysis and Computer Vision Applications in Animal Sciences: An Overview. Front. Vet. Sci. 7:551269. doi: 10.3389/fvets.2020.551269

INTRODUCTION

Sighted animals, including humans, experience vision in a way that seems natural and automatic. Early in life, and quite often from the moment of birth, animals use their vision system to navigate the world around them, and to identify and interact with other animals, as well as their surrounding environment. Therefore, the vision system of an animal is constantly being trained and adapted so that it can be used for several tasks. For instance, in humans, this system works with the luminous signal being captured by the eye and transferred via the optic nerve to the brain, where it is processed and interpreted (1). This complex vision system can adapt to different light conditions autonomously while allowing us to focus on objects and to have a 3-dimensional representation of the world. But what would be vision for a computer and how can computer vision impact animal breeding and production? This review is divided into three sections. The first section provides a brief introduction to image analysis and computer vision, describing current developments and algorithms of interest. The second section describes common types of sensors available and their functionality. The third presents a historical view on applications in animal sciences, followed by examples and areas of current interest. The review closes with a discussion on areas that are currently of great importance for the improvement of computer vision system (CVS) applications in livestock improvement and production.

OVERVIEW OF STRATEGIES TO WORK WITH DIGITAL IMAGES

What Is Digital Image Processing, Image Analysis, and Computer Vision?

Digital Image Processing, Digital Image Analysis, and Computer Vision can be viewed as an amalgam of terms that very often are used to describe similar processes and applications, generating confusion regarding their meaning. Most of the confusion arises because these are interconnected fields that emerged with the development of technologies for digital image acquisition. For the sake of clarity, we can divide and define these three areas as follows.

Digital Image Processing

Digital Image Processing deals with capturing and translating a visual signal into a digital image. As such, it can be viewed as the area that studies the process of obtaining a visual signal of the world and transforming it in order to make it interpretable. It spans from the study of image formation, as a result of the acquisition of light signals by specifically designed sensors, to the interpretation of the image as an array of connected values. Therefore, digital image processing involves the conception, design, development, and enhancement of digital imaging algorithms and programs (2). As such, it is a discipline heavily based on physics and mathematics. The term can also be used to directly address the applications or techniques used for digital image manipulation, ranging from noise reduction, image equalization, image filtering, and other transformations used for preparing images for subsequent steps in an analysis pipeline or for enhancing images aesthetically. A group of techniques of great importance in digital image processing is edge and contour detection. Although there are several methods for edge detection, they all rely on the fact that edges are regions in an image where there is a drastic change in color/intensity along with a particular orientation (2, 3). These techniques are, in general, useful in many applications in image processing, such as image correction and sharpening (i.e., highlight of the edges) and in image analysis, such as identification of complex structures and matching of objects in an image with specific templates.

Digital Image Analysis

Digital image analysis, or just digital imaging, on the other hand, corresponds to the process of extracting meaningful information from an image (2). This information can be descriptive statistics from the image, ranging from global image metrics, such as color/brightness histograms and distribution, block statistics from regions/windows across the images, such as intensity, moments (mean, variance), and integral images, to the identification of more complex structures in the image. Such information extracted from the image analysis can be used then as input for imaging processing techniques, such as image sharpening (4), thresholding (5), smoothing and edge/contour enhancement (6). On the other hand, image processing techniques can also be applied prior to image analysis techniques. An example is the use of edge detection techniques in the process of identification of structures, such as lines and circles in an image (3). Another is for image segmentation, i.e., to divide an image into different regions, which can be simple image binarization (a division of the image into two regions, such as background and foreground) or multiple regions, such as different objects present in an image. There are several methods of image segmentation, but basically, they can be classified into methods that perform a global clustering of image pixels according to some criteria independent of spatial information (e.g., k-means clustering), and methods that account for more information, such as spatial, texture, color, edges, and shape, such as energy-based (graph-cuts) methods (7, 8).

Computer Vision

Computer Vision can be defined as the field that aims to describe the world through images by interpreting, reconstructing, and extracting properties from images, such as shapes, textures, densities, and distances (9). CVSs are also known as machine vision systems, visual image systems, or just image systems. Therefore, Computer Vision is essentially the development of artificial systems to handle visual problems of interest, and for such, it uses image processing and analysis techniques. Along with image analysis and processing, other areas such as Machine Learning and Pattern Recognition are also highly interconnected with Computer Vision.

Pattern Recognition is a field that studies not only images but also other signals, such as sound and texts. As the name suggests, it is an area dedicated to the study of patterns that may appear in any given signal. In the context of imaging, pattern recognition is generally studied within image analysis as

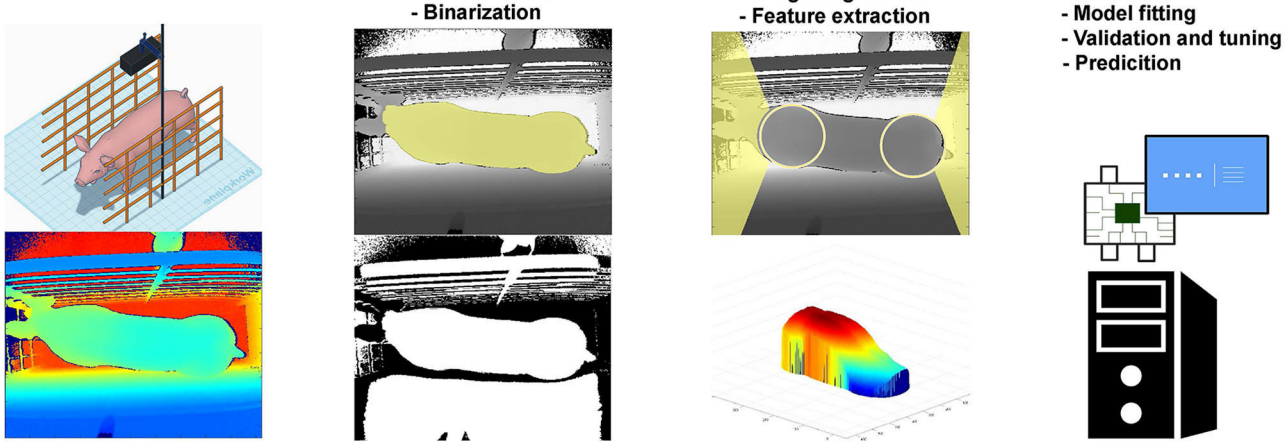

FIGURE 1 | Example of a computer vision system framework. **(A)** Image acquisition; **(B)** Image Processing; **(C)** Image Analysis; **(D)** Data Analysis.

the development of mathematical methods for the identification of simple geometrical structures such as lines and circles (3, 10) or key-point features that can be jointly used to identify more complex objects or patterns (11, 12). Machine Learning is also a broader field that is concerned with the development and application of algorithms for extracting information from the most diverse data sets (13), and several machine learning algorithms have been developed or adapted specifically for solving computer vision problems.

An example of CVS is presented in **Figure 1**, where a 3D camera is used to capture images from pigs [adapted from (14)]. In a standard pipeline, after these images have been captured, they are processed (**Figure 1B**) using common imaging processing techniques such as image thresholding and binarization. Using the processed image, features of interest are identified, such as the pig head and tail (**Figure 1C**), and are removed together with the image background. From the resultant image of the pigs back, several measures were taken (e.g., volume, area, height, and length). These measures leverage important information from the images evaluated and can be used then for the development and evaluation of predictive models (**Figure 1D**), such as prediction of body weight.

Image Formation

An important aspect of digital imaging is how the image itself is acquired since there are sensors better suited for different applications. Before images could be processed and analyzed in computers, there was the need to develop sensors able to recognize, measure, and digitalize luminous signals. It was in the 1970s, with the advent of the charge-coupled devices (CCD) sensors (15), that digital imaging was developed, and the interest in CVS appeared. Basically, in digital image formation, luminous signals are captured by the sensor, coded, and stored in arrays of data that can be interpreted and manipulated in computational algorithms (9). Thus, for a computer, an image is nothing more than numerical values in a structured array of data that codifies light and colors for each point in the image (**Figure 2**). This array can be a single matrix, where the values inside the matrix correspond to black or white (binary image) or different shades of gray (grayscale image). Also, it can be an array of 3 matrices in the case of color images (i.e., intensities of red, green, and blue, on the RGB color space) or even multiple matrices for hyperspectral images. Therefore, mathematical manipulations and statistics of an image were among the first studies developed in digital image analysis and processing.

Another turning point in the history of computer vision was the advent of personal digital cameras in the 1990s, reducing the costs and popularizing the process of capturing and analyzing digital images (16, 17). Since then, several applications of digital photography have appeared. This popularization of digital cameras is directly connected to the increasing volume of data (photos and videos) generated over the last few years in many fields due to the increasing number of computer vision applications to solve the most diverse problems. This increased interest in computer vision and related areas can be illustrated by the increasing number of publications in the last decade (**Figure 3**).

Some areas of recent interest in computer vision are object sensing, mapping, recognition, motion tracking, navigation, image segmentation, and scene interpretation. However, while humans and animals do most of these actions intuitively, the majority of the vision tasks are considered as difficult problems in computer science, and the algorithms available are prone to errors (9). Thus, many successful CVSs are the result of multidisciplinary approaches tailored for specific cases, for example, interactive segmentation (8), face detection based on image features (18), and machine learning methods for object detection and recognition, such as optical recognition (19) and image classification, such as classification of regions and cells of histopathological images (20).

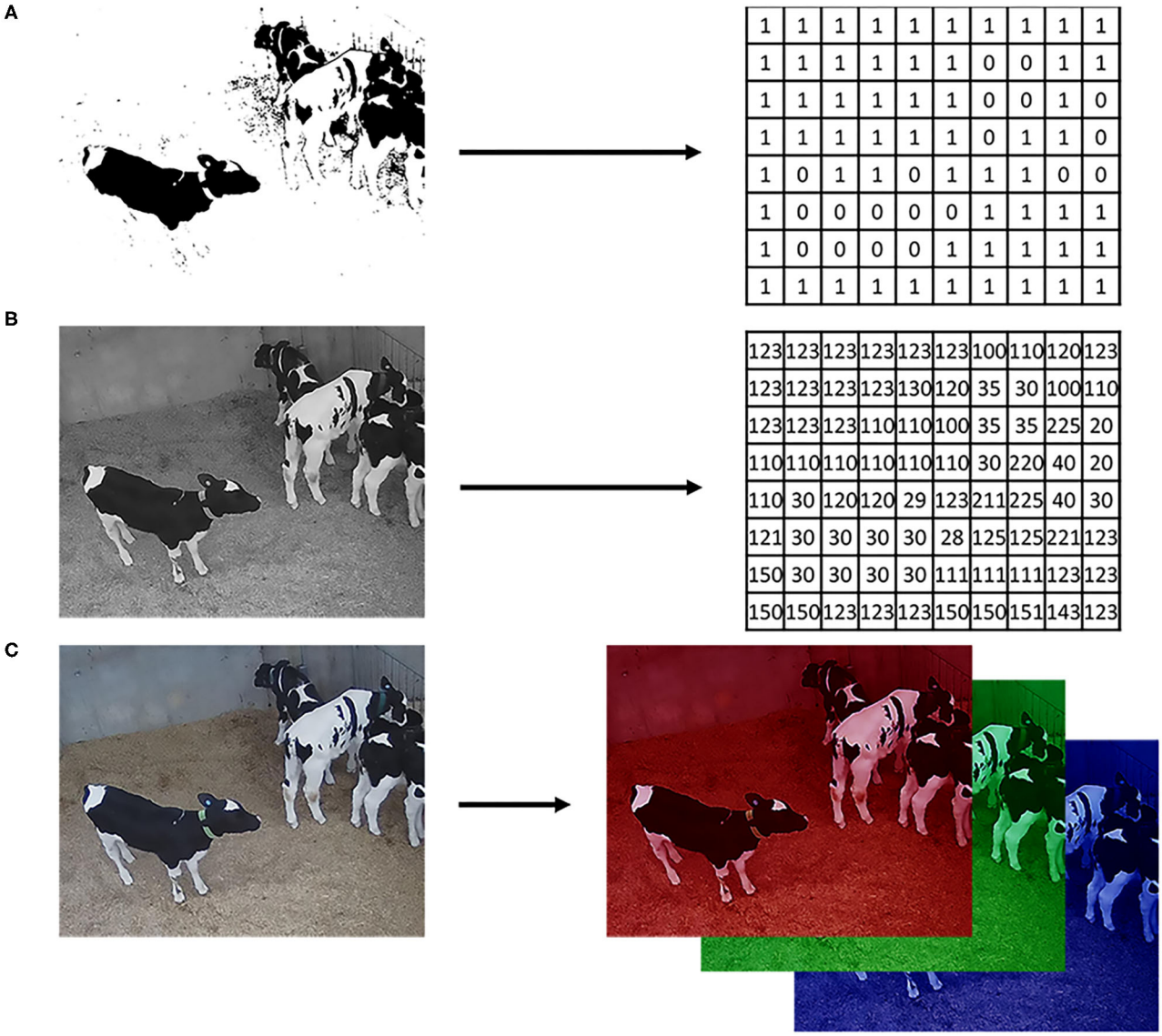

FIGURE 2 | Digital image representation. **(A)** Logical image with values 1 for white and 0 for black; **(B)** Grayscale image in the 24-bits depth format (values ranging from 0 to 255); **(C)** Color image on the RGB color space where each matrix is a 24-bits depth image, one for each color layer.

Among the machine learning techniques used in computer vision, it is worth mentioning deep learning algorithms, which have recently been successfully used in diverse computer vision applications. These algorithms are an extension of traditional artificial neural networks (ANN), and they achieve great power and flexibility by learning more abstract representations of the inputs as a nested hierarchy of concepts (21). These nested concepts, or hidden layers, generate very complex models with many parameters that were possible to be trained only with the advent of very large datasets, data augmentation techniques, and advancements in ANN, such as the development of learning optimization via stochastic gradient descent, new activation functions such as rectified linear unit (ReLU), regularization techniques, and efficient use of graphics processing unit (GPU) (21, 22).

Metrics for Model Comparison and Assessing Predictive Ability

As there are CVS developed for many different tasks and using a wide range of methods and models, there will be also many ways to compare competing approaches for different applications. In the following, we discuss some of these comparison methods by splitting them according to the class of the variable being predicted. For the scope of this study, we will split the predicted variable into two classes: (1) a variable that we deem associated/correlated to the image, and (2) the image per see (or even parts of the image).

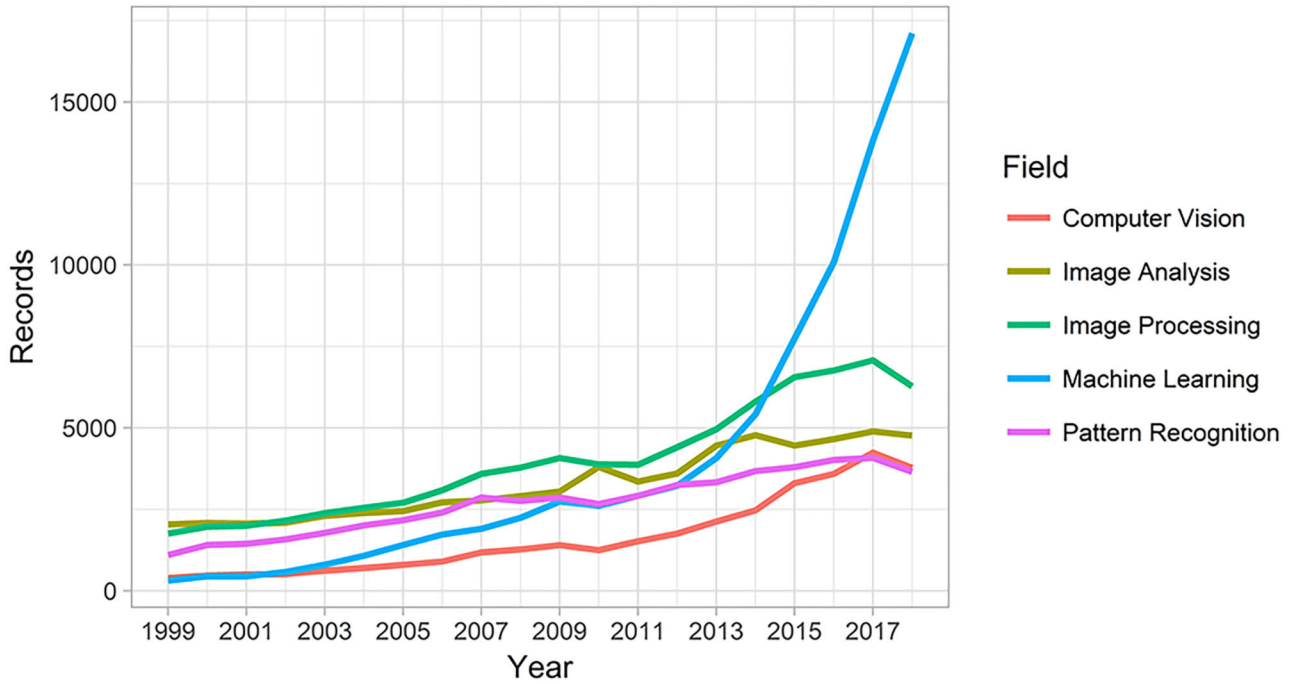

FIGURE 3 | Count of publications hits in "Web of Science" for computer vision, image analysis, image processing, machine learning and pattern recognition.

In some applications, the interest will be to predict a variable by using information extracted from the images. These variables of interest can be a categorical variable such as animal species, behavior classes, and scores (e.g., leg score, body conditioning score), or a continuous variable such as body area, height, and weight.

For categorical variables, the simplest case assumes only two states (e.g., health/disease, moving/standing, among others), and the general scenario allows for multiple classes to be evaluated at the same time (e.g., behaviors such as laying, drinking, eating, walking, etc.). The metrics used to evaluate the predictive methods, in this case, are going to assess the frequency of two types of error: false positive (a.k.a. nuisance alarm) and false negative (a.k.a. missing alarm) errors and the most basic assessment tools are via tables of errors, or confusion matrix as below:

	y = 0	**y = 1**
$\hat{y} = 0$	TP	FP
$\hat{y} = 1$	FN	TN

Here, y corresponds to the true category or ground truth (e.g., $y = 1$ for disease and $y = 0$ for healthy), which can be a manual measurement or derived from a gold standard method, and $\hat{y}$ corresponds to the predicted class. The combination of each value of y and $\hat{y}$ gives either a true positive (TP), true negative (TN), false negative (FN), or false positive (FP). From the confusion matrix and the TP, TN, FN, and FP counts for any given experiment, several metrics can be derived, such as: sensitivity (recall or true positive ratio) $= \frac{TP}{TP+FN}$; false positive rate (FPR), also known as, false discovery rate (FDR) $= \frac{FP}{TP+FP}$; precision $= \frac{TP}{TP+FP}$; specificity $= \frac{TN}{TN+FP}$; and accuracy $= \frac{TP+TN}{TP+FP+TN+FN}$. However, when evaluating classification methods sometimes it is interesting to evaluate many threshold values used to classify $\hat{y}$ as one class or another. This evaluation is often done using receiver operating characteristic (ROC) curves, which measures the tradeoff between sensitivity and FDR, or 1- specificity (which yields the same value). Another metric is the precision-recall (PR) curve which is useful to evaluate the trade-off between precision and recall as the threshold value varies, i.e., the trade-off between the fraction of the detection that is actually true positives (i.e., precision) and the fraction of true positives that are detected (i.e., sensitivity) (13). Also, PR curves are especially interesting when we have situations with unbalanced data. In these situations, a ROC curve may present a misleading high area under the curve (AUC), for a model that is only predicting every data point as from the class that has more true values (**Figure 4**). For both curves, the quality of competing methods is often summarized by the AUC for which higher area means better fitting, with an area of one meaning a perfect fit.

For applications where the variable of interest is continuous, the predictive ability is typically evaluated using the Pearson product-moment correlation coefficient (r) between the input (y) and the predicted output ($\hat{y}$):

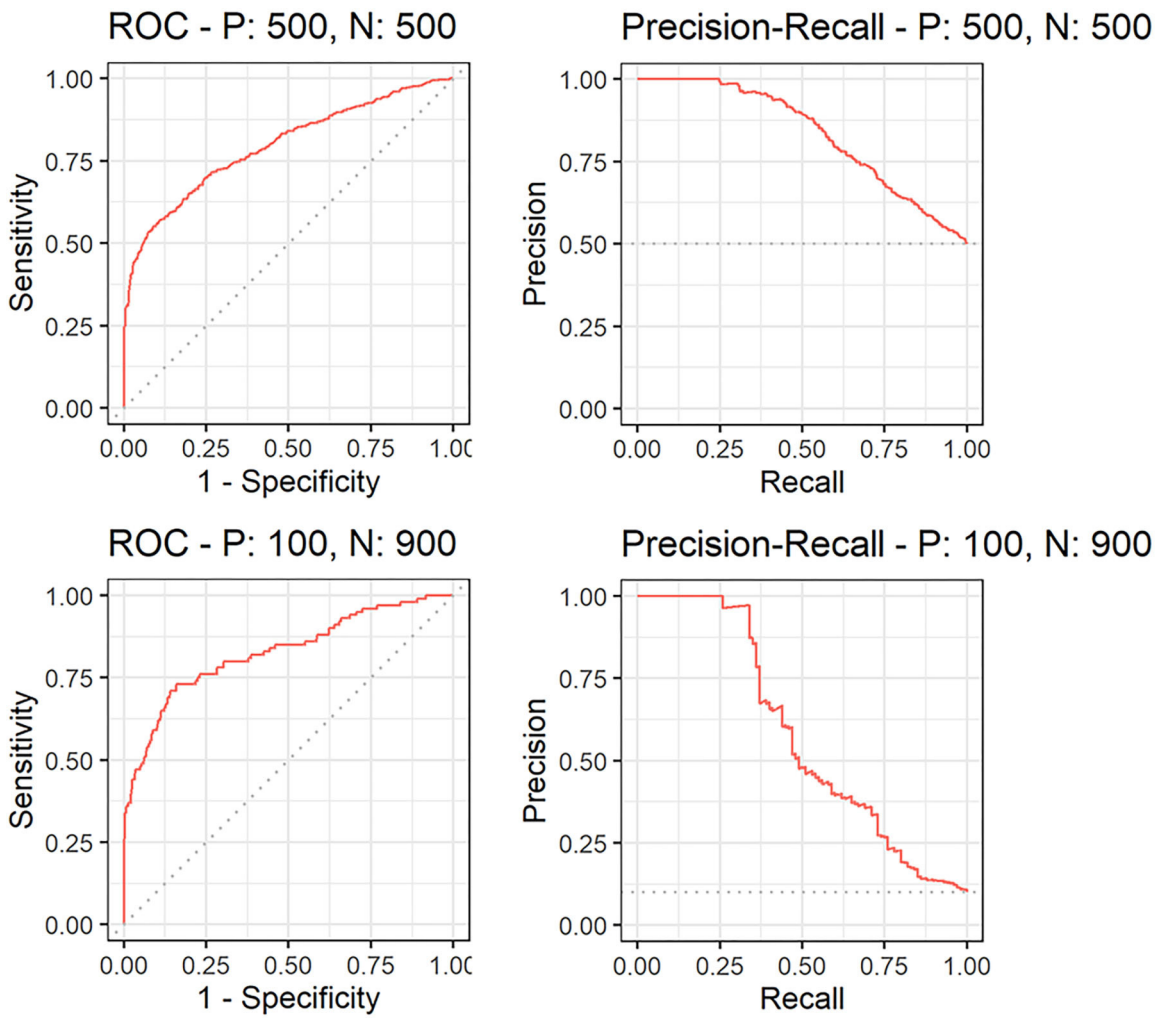

FIGURE 4 | Comparison of receiver operator curves (ROC) and precision-recall curves for a balanced [with 500 positive (P) and 500 negative (N) labels] and unbalanced (with 100 P and 1102 900 N) datasets.

$$\mathrm{r} == \frac{cov(y, \hat{y})}{\sigma_y \sigma_{\hat{y}}}$$

where $cov(y, \hat{y})$ is the covariance, and σ_y and $\sigma_{\hat{y}}$ are the square root of the input and output variances. Alternatively, instead of the predictive correlation r, its square is often reported. Both r and r^2 measure the linear relationship between y and $\hat{y}$, and the closer to 1 the better. However, they are not measurements of prediction accuracy, as they do not take prediction bias into account. In this context, another measure often reported is the predictive error, or rather, the mean absolute predictive error (MAE or MAPE), which is a direct measure of how much the predictions deviate from the true values and can be defined as:

$$MAE = mean(|y - \hat{y}|)$$

Because MAE can be influenced by the scale, when comparing between different studies it is often better to use a scale independent measure (23), such as the mean absolute scaled error (MASE), which can be defined as:

$$MASE = mean(\left|\frac{y - \hat{y}}{mean(y)}\right|)$$

In applications where the variable of interest can be the whole images or parts of the image, such as identification of objects within the image, the predictive ability can be evaluated via the pixel-wise accuracy, i.e., the ratio of pixels correctly predicted vs. the total number of pixels. However, this measure of prediction quality will tend to be high for most of the applications as the majority of the pixels within large objects will be correctly predicted. Another interesting measure in this scenario is the Jaccard index, a.k.a. Intersection over Union (IoU), which is the ratio of the intersection between the ground truth (A) and the predicted area ($\hat{A}$) by the union of these areas:

$$IoU_{(A,\,\hat{A})} = \frac{\left|A \cap \hat{A}\right|}{\left|A \cup \hat{A}\right|}$$

Thus, IoU is a measure of similarity between the two areas, and values closer to 1 indicate more similarity, meaning a better fit of the predictive method (24).

As a final note on this topic, it is important to evaluate the generalization performance of the candidate methods, in other words, their predictive capability on independent data set. This evaluation will provide insight into the variability of the predictive error as well as potential overfitting (a situation when a method performs very well on the training data but not so on the independent dataset). This independent dataset, or validation set, is ideally a dataset collected in another moment from different animals. But most of the time if the data is large enough it can be a reserved portion of the original data. Another interesting technique is cross-validation, where the data is divided into multiple subsets, and each time one of the subsets is reserved for validation while the others are used for training. Thus, in a k-fold cross-validation, the dataset is divided into k subsets, and if $k = n$ (number of data points) the approach is called a leave-one-out cross-validation. For a more in-depth reading on model assessment and selection, the reader can refer to Chapter 7 of Hastie et al. (25).

SENSORS USED FOR IMAGING IN ANIMAL AND VETERINARY SCIENCES

Currently, the most used image sensor devices are standard digital cameras and/or surveillance cameras that capture electromagnetic waves within the visible light spectra to generate digital images (color or grayscale). However, there are also other technologies that have been used for more specific applications, such as devices that are based on infra-red, ultrasound, and ionizing radiation. Moreover, some technologies can generate more complex arrays of images such as three-dimensional (3D) and hyperspectral images. They are, however, in general, more expensive than standard digital cameras. Nonetheless, each different imaging technology can be used for specific applications.

Images on the Visible Light Spectrum

Cameras for standard digital imaging work with signals within the visible light range, and they generally have a CCD or a complementary metal-oxide-semiconductor (CMOS) sensor. Both sensors have a similar function, which is to capture light and convert it into a digital image, however, they have some important differences. On one hand, CCD sensors are charged passively by the light source, and the information captured in each pixel is processed sequentially. CMOS sensors, on the other hand, have active pixels with a transistor for each pixel so that the information from each pixel is translated to the image independently and generally asynchronously to the digital image (26). These differences in sensor architecture lead to differences in sensor prices and capabilities. Even though the industry is in constant development, CCD sensors, in general, have a higher dynamic range and produce more uniform images, while CMOS sensors are cheaper, energy efficient, and more responsive.

Infrared Radiation

Infrared radiation (IR) has a wavelength longer than the visible light, and according to the International Organization for Standardization (ISO) it can be divided into near-infrared (NIR), mid-infrared (MIR), and far-infrared (FIR). This division has been based on the specific wavelength thresholds of 0.78–3, 3–50, and 50–1,000 μm for NIR, MIR, and FIR, respectively. There are many different applications of IR in imaging, and for the purpose of this review, the most significant ones are in 3D imaging, spectroscopy, night vision, and thermal imaging (also known as Thermography). For all these applications, there are different IR sensors specific to capture radiation within NIR, MIR, or FIR ranges. In most of the night vision cameras, the sensors rely on an emitter, which emits IR on the NIR wavelength to actively illuminate the scene. On the other hand, thermal imaging uses the principle that all objects produce radiant heat (emitted, transmitted, and/or reflected), thus there is no need for an emitter since the sensors are capable of capturing the heat signal in the MIR or FIR range (27). The sensors for thermal imaging can be divided into two groups, cooled or uncooled focal plane array. The main difference is that the cooled sensors generally produce better images and less variable measurements, at the cost of being heavier, less portable, and expensive.

In animal, veterinary, and wildlife applications, both night vision and thermal cameras have been used mostly for monitoring animals (livestock or wildlife) at night or dim light situations, either alone or in association with standard digital image sensors (28). Such applications can be dated to the use of military night vision scopes for observation of nighttime animal behavior in the 70s (29). However, thermal cameras also have applications in diagnostic imaging to detect small changes in the body's surface temperature (30), which can be due to stress, fever, inflammation, and ischemia. Nevertheless, proper use of thermal imaging for diagnostic purposes still requires correct calibration of the device, adequate location, and correct positioning of the animal and camera (27, 30).

3D Imaging

Many different sensors and techniques are used for measurement of the distance of objects to the camera, acquisition, and formation of 3D images. In livestock, these sensors can be used, for example, for measurement of animal volume, surface, and gait, among other traits. From the several technologies developed for 3D imaging, we will focus on optical applications (i.e., applications that use radiation on visible and near-visible light) used in 3D cameras, also known as depth sensors. These techniques can be further divided into passive, such as *stereo imaging* and *structure from motion*, or active, such as *structured light* and *time of flight* (31).

In *stereo imaging*, two or more cameras are used, and principles of epipolar geometry are applied in order to calculate the distance (z) of a point P to the cameras (32). In a simplified stereoscopic triangulation (**Figure 5**) using two similar cameras with the same focal length f, the differences of the projections

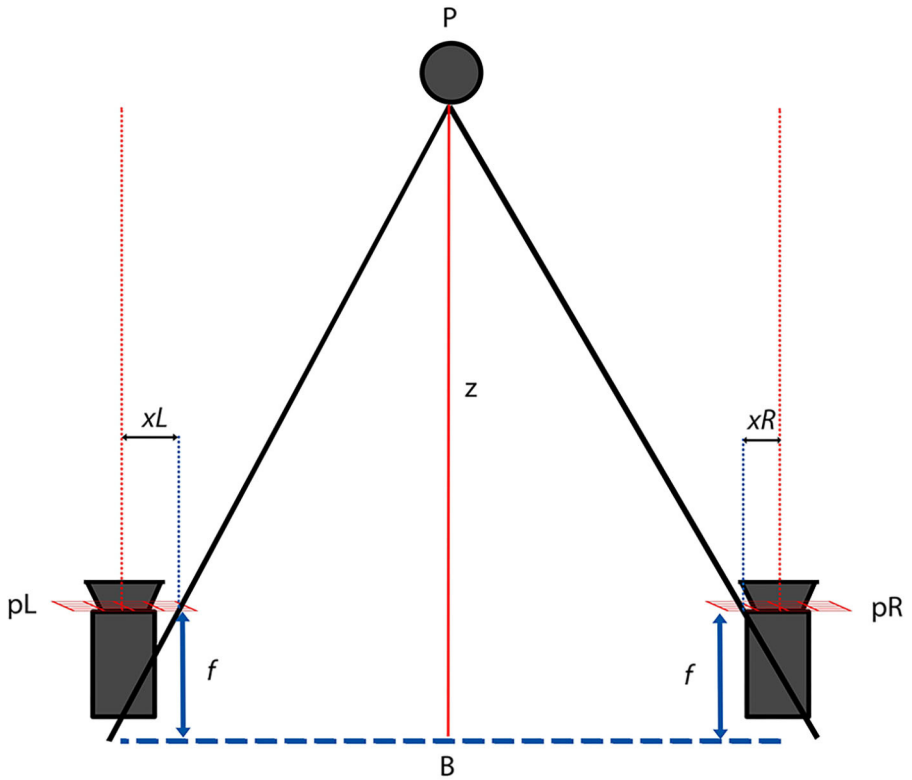

FIGURE 5 | Epipolar triangulation used on a rectified stereo imaging system with two similar cameras. P is the point of interest; xL and xR its projection on the camera planes pL and pR; f is the camera focal length and B the baseline plane.

(x_L and x_R) of point P on the planes of the cameras is the disparity between the images. That disparity can be used then to calculate the distance of point P to the baseline plane, where B is the distance between cameras.

Similarly, in *structure from motion*, a disparity map can be created between the images from a single moving camera, in which case the distance between the points where each image was captured by the camera can be used as the distance between "cameras." The main difficulty of such a strategy is that it needs the object of interest to be practically motionless.

Structured light, also known as *coded light* refers to the use of active emission of known light patterns for which the illuminated surface will present structural distortions in the shade/light patterns according to irregularities in the surface, angle, and distance to the emitter (**Figure 6**). Therefore, similarly to *stereo imaging*, the distortions in the emitted patterns provide unique correspondence for triangulation with the camera. The emitter can vary from a punctual laser, a blade scanner, multiple shadow patterns that split the scene into areas of interest, or even the use of complex multi-laser patterns that create a spatial neighborhood (31, 32).

Time of flight (ToF) and *Light Detection and Ranging* (LiDAR) cameras are based on signal modulation and ranging, similar to other technologies such as *Sound Navigation Ranging* (SONAR) and *Radio Detection and Ranging* (RADAR) (32). These techniques measure the distance between the sensor and a target object by detecting the time difference from the signal emitted by a transmitter, reflected on a target object, and captured back by a receiver (**Figure 7**). Even though the principle is simple, there is a great implementation challenge due to the speed of light, interference with natural light, dispersion, and absorption of the light. Modern ToF cameras generally consist of a transmitter array that emits a modulated IR or NIR light (to reduce environmental interference) and a receiver array that captures the reflected signal and calculates the signal phase/time lag for each pixel (31). Recently, in order to improve the transmitter performance, devices equipped with micro-electro-mechanical system (MEMS) mirrors have received great interest from the scientific and industry community (33).

Lastly, there are also hybrid 3D cameras that combine RGB sensors with depth sensors based on one or more of the technologies described above. Examples include cameras based on active stereoscopy, which combine stereo imaging from multiple cameras with structured light to improve the depth estimation. **Table 1** shows some of the current 3D cameras available and their technical specifications.

Other Imaging Technologies of Importance

There are many other imaging related technologies of importance in animal and veterinary sciences, such as spectral and hyperspectral imaging, ultrasound, x-ray, computed

FIGURE 6 | Example of a structured light system based on linear shadow pattern. **(A)** The scene with natural illumination. **(B)** The same scene now under the structured light projected by the emitter.

tomography, and satellite images. In the following, we briefly describe some of these technologies.

Spectroscopy, spectral imaging, and more recently hyperspectral imaging have been adopted extensively for evaluation of meat attributes and chemical characteristics as well for quantification of milk protein and fat content (34, 35). These technologies are mostly composed of sensors equipped with a NIR emitter, and are based on the principle that different compounds will absorb the radiation differently in each wavelength, thus generating a "signature" (36). In Spectroscopy, for each wavelength measured inside the range, a punctual value of absorbance is generated. Meanwhile, a spectral image is a matrix with a value of absorbance for each pixel, and a hyperspectral image corresponds to a cube of several matrices (one for each wavelength) providing both spectral and spatial information.

Several medical diagnostic imaging technologies have also been employed for many applications with animals such as evaluation of muscle and fat composition, and bone mineralization in live animals and carcasses (37–39). Some worth noting technologies include ultrasound (US), dual-energy x-ray absorptiometry (DXA), computed tomography (CT), and magnetic resonance (MR). All these technologies are appealing since they make possible the generation of images for the evaluation of the body composition. From these technologies, only US is currently used in farm conditions due to many factors such as price, portability, and no anesthesia required. Nonetheless, it still requires a trained operator.

APPLICATIONS OF COMPUTER VISION SYSTEMS IN ANIMAL AND VETERINARY SCIENCES

Before the advent of CVS, many applications required the use of the trained eye for visual classification of traits in live animals, such as animal behavior, body condition score, carcass fat deposition, meat marbling, or classification of eggshell quality. There are also methods that use the aid of lenses, such as microscopes, for evaluation of cell morphology in a blood smear or spermatozoid motility and defects. Moreover, other signals such as ultrasound, infrared, and x-rays are widely used to produce images for diagnostic purposes. However, most of the methods currently used for the measurement of traits of interest need expert personnel requiring the training of evaluators from time to time to maintain good measurement quality. Also, most of such measuring processes are time demanding, stressful to the animals, and costly for the farmer, making it prohibitive due to animal welfare and economic reasons. Therefore, there is an interest in developing automatic, indirect methods for monitoring livestock and measuring traits of interest. For such tasks, CVS generally uses algorithms and principles of pattern recognition, image analysis, and processing in order to tackle the most diverse problems. The framework presented in **Figure 1** can be seen as a CVS pipeline, with a fixed sensor capturing the information that is presented by the world or actively exploring the world and adjusting its perception (field of view, exposure, among others). The development of automated CVS can enable high-throughput phenotyping in livestock, and the data generated by such systems can be then used for many different applications, from the development of smart farm management tools to advancing breeding programs.

In the following, we present selected applications of CVS as an answer to the need for such automated, non-invasive methods for the measurement of carcass and meat traits, live animals' identification, tracking, monitoring, and phenotyping using different sensors.

Carcass and Meat Traits

Probably one of the first applications of a CVS was in meat sciences, with the earliest reported studies found in the 1980s (40–42). In these studies, the system was composed of a camera, light source, digitizer, and computer unit. The CVS needed an operator to position beef meat cuts on a surface at a known distance and angle from the camera, and to trigger the image acquisition. Thus, the meat cuts were all positioned in the same manner with constant background and illumination. At that time, the interest was to predict the cut content of lean meat and fat, and to compare the results from the CVS to trained United States Department of Agriculture (USDA) meat graders.

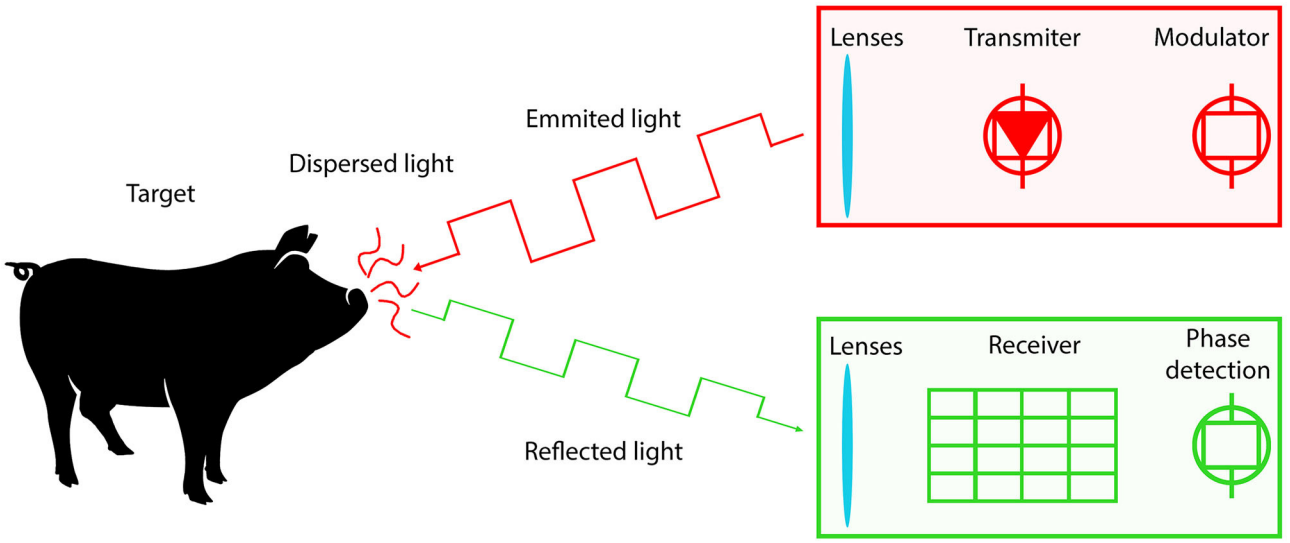

FIGURE 7 | Principle of time of flight (ToF) 3D cameras (depth sensors).

TABLE 1 | Comparison of 3D cameras and their technical specifications.

Device	Manufacturer	Sensors	Technology	Range (m)	Environment	FPS	FOV (V×H)	Resolution (pixels)
Kinect V1[a]	Microsoft	3D (IR emitter + IR camera) Color	Structured Light	0.8– 4	Indoor	30 30	45° × 58°	480 × 640
Kinect V2[a]	Microsoft	3D (IR emitter + IR camera) Color	Time of flight	0.5–4.5	Indoor	30 30	60° × 70° 54° × 84°	424 × 515 1080 × 1920
Kinect Azure	Microsoft	3D-N (IR emitter + IR camera) 3D-W (IR emitter + IR camera) Color	Time of flight Time of flight	0.5–5.5 0.3–2.8	Indoor	30 30	65° × 75° 120° × 120° 59° × 90°	576 × 640 1024 × 1024 2160 × 3840
Xtion[a]	Asus	3D	Time of flight	0.8–3.5	Indoor	30	45° × 58°	480 × 640
Xtion Pro Live	Asus	3D Color	Time of flight	0.8–3.5	Indoor	30 30	45° × 58°	480 × 640 1024 × 1280
Xtion 2	Asus	3D Color	Time of flight	0.8–3.5	Indoor	30 15	52° × 74° 60° × 75°	480 × 640 1944 × 2592
Intel SR305	Intel	3D (IR emitter + IR camera) Color	Structured light	0.2–1.5	Indoor	60 30	54° × 70° 42° × 68°	480 × 640 1080 × 1920
Intel D415	Intel	3D (IR emitter + IR camera) Color	Active Stereo	0.2–10	indoor/outdoor	90 30	40° × 65° 43° × 70°	720 × 1280 1080 × 1920
Intel D435	Intel	3D (IR emitter + IR camera) Color	Active Stereo	0.1–10	indoor/outdoor	90 30	58° × 87° 43° × 70°	720 × 1280 1080 × 1920
Intel L515	Intel	3D (IR emitter + MEMS[b]) Color	LIDAR	0.2–9.0	Indoor	30 30	55° × 70° 43° × 70°	768 × 1024 1080 × 1920
Structure[a]	Occipital	3D (IR emitter + IR camera)	Structured Light	0.8–4.0	Indoor	30	43° × 57°	480 × 640
Structure II	Occipital	3D (IR emitter + IR camera) Ultra-wide monochrome	Active Stereo	0.3–5.0	indoor/outdoor	54 100	46° × 59° 160°Diag	960 × 1280 480 × 640
Structure Core	Occipital	3D (IR emitter + IR camera) Color	Active Stereo	0.3–10	indoor/outdoor	54 100	46° × 59° 85°Diag	960 × 1280 480 × 640

[a]*Out of production/Discontinued;* [b]*Micro-electro-mechanical system mirror.*

In these studies, multiple linear regressions fitting variables extracted from the CVS were compared to models that included manual measurements and USDA graded variables. Even though the system was not fully automated, the prediction equations developed with the variables measured by the system presented slightly better results than the prediction equations developed with variables measured by trained graders. The best linear model for prediction of lean meat weight developed with the variables

TABLE 2 | Examples of computer vision applications in meat sciences (studies highlighted in bold were with live animals).

	Applications	Image signal	References
Cattle and Small Ruminants	Carcass	3D; US; VL	(41, 43, 44)
	Fat (kg and%)	US, VL	(41, 43, 45)
	Lean meat (kg and %)	VL	(41, 42, 45)
	Tenderness	VL	(45, 46)
Fishery	Fat Pigmentation	IR; VL	(47)
	Sorting	HS	(48)
	Freshness	VL; HS; 3D	(49, 50)
Poultry	Classification	HS; VL	(51)
	Brest weight	3D	(52)
	Egg shell classification	VL	(53)
Pork	Carcass	US; VL; CT; 3D	(37, 39, 54–56)
	Classification	HS; VL	(51)
	Quality	HS; IR; VL	(57)

CT, Computed Tomography; 3D, 3-dimensional; HS, Hyperspectral; IR, Infrared; US, Ultrasound; VL, Visible Light.

extracted from the CVS achieved R^2 from 0.93 to 0.95 against 0.84–0.94 from the model that included USDA graded covariates (41, 42).

Since these earlier studies, there has been an increasing interest in the use of computer vision for prediction of the most diverse meat quality traits, not only for beef but also for fish, poultry, and pork (**Table 2**). There are applications focused on imaging technologies for determination of not only meat crude protein and fat content but also more refined chemical characteristics like fatty acids profile, freshness (50, 57), as well as prediction of meat quality, palatability, tenderness, and other traits normally evaluated by a panel of trained experts (45, 46, 51) or even automatic sorting and weighing cuts and viscera which is normally performed manually (48, 52). Again, different devices and imaging technologies have been used, with several predictive approaches evaluated. However, independently of the imaging device used, such applications pipelines generally involve several steps such as: (1) Sample preparation with standardization of meat cut used, presentation, background and light conditions; (2) Device calibration (when needed), collection and processing of the images; (3) Direct measurement of attributes of interest using a gold standard methodology (i.e., chemical analysis); and (4) Model fitting, which corresponds to the prediction of the gold standard using the image features as predictors. It is interesting to note that the image processing in step 2 can involve several sub-steps such as histogram equalization, background removal, and image smoothing. Also, in the case of hyperspectral images the processing involves selection of wavelengths and/or reduction of dimensionality using techniques such as Fourier transformation (58) and principal components, for an in-depth review of applications of hyperspectral imaging see Xiong et al. (34). It is also worth noting, that there is no standard model of choice for step 4 since in the literature several predictive approaches have been evaluated. These predictive approaches could be statistical models such as linear and partial least square regression to machine learning methods, such as support vector machines, random forests, and artificial neural networks.

Monitoring and Phenotyping of Live Animals

Differently from carcass and meat cuts that can be easily positioned for image acquisition under a well-controlled light source and even background, several obstacles arise when working with live animals. As an example, in farm conditions, the illumination can change throughout the day even inside a barn due to sun position, clouds, and seasons. Moreover, there will be differences between artificial light sources from one farm/barn to another, as they may use different types of lamps with different voltage and positioning. The background is also going to be different in each location, and it is prone to changes over time for a given location. Examples of differences in the background are floor surface material for animals in a barn and vegetation for free-range animals. Therefore, the diversity of situations is probably one of the biggest challenges in implementing a CVS that are robust enough to perform satisfactorily across different farm conditions.

Nevertheless, many efforts have been made over the years to develop CVS for monitoring and phenotyping livestock, poultry, and fish as well. In the current study, we do not intend to deliver an extensive review on the matter as there are already reviews on technology applications for poultry (59, 60), machine vision for detection of cattle and pig behavior (61), and computer vision applications for fisheries (62). Nonetheless, in the following, a broader view is presented regarding applications developed for traits of interest in animal and veterinary sciences, providing examples from earlier works to the current trends while highlighting challenges, advances that have been made, and areas of current interest. **Table 3** shows a summary of selected applications, presenting the traits of interest and the kind of imaging sensor used.

Evaluation of Body Composition, Meat, and Carcass Traits in Live Animals

In section Carcass and Meat Traits we saw that CVS had been successfully used for prediction of traits such as lean meat and fat content from carcass and meat cuts. Nevertheless, the same predictive performance has not been observed initially for the evaluation of meat and carcass traits in live animals.

Initial attempts for the prediction of carcass composition on swine have been performed by Doeschl-Wilson et al. (54) where a CVS achieved a predictive R^2 of 0.31 and 0.19 for fat and of 0.04 and 0.18 for lean meat on the foreloin and hindloin regions, respectively. In the search for improvement of performance on the prediction of carcass and meat traits on live animals, researchers have focused on the use of medical imaging devices for such tasks. In recent studies using medical imaging devices, ultrasound measurements presented positive and moderate correlations of 0.6 and 0.56 with the carcass measurements of lean meat and fat depths, while CT presented low to moderate correlations of 0.48–0.67 for fat and high correlations of 0.91–0.94 for lean meat (37, 39). Moreover, these

TABLE 3 | Examples of computer vision applications in live animals.

	Applications	Image signal	References
Cattle and small ruminants	Mastitis	IR	(63–66)
	Digital dermatitis	IR	(67, 68)
	Body temperature	TR	(69–71)
	Gait and body measurements	3D	(44, 72)
	Weight	3D	(44, 73)
	Coat and conformation	VL	(74)
	Body condition	VL; TR; 3D	(75–78)
Fishery	Tracking	3D	(79)
	Shape	VL	(80)
	Weight	VL	(81)
Poultry	Behavior	VL; 3D	(82–84)
	Shape	3D	(84)
Dog	Behavior	3D	(85)
Pork	Tracking	VL; 3D	(86–90)
	Behavior	VL; 3D	(91–94)
	Weight	VL; 3D	(14, 95–97)
	Gait and body measurements	3D	(14, 97–99)

3D, 3-dimensional; TR, Thermography; VL, Visible Light.

technologies have several drawbacks regarding animal handling and cost, as explained previously. In order to tackle these limitations, some recent works developed CVS based on 3D cameras for non-contact automated estimation of muscle score (55) and of fat and lean muscle content (56) on live pigs. Alsahaf et al. (55) developed a system that extracted morphometric features from the images of moving pigs for prediction of muscle scores between 1 and 5. With a gradient boosted classifier, they achieved classification accuracy between 0.3 and 0.58, and MAE of 0.65, showing that most of the errors where between neighboring classes. Meanwhile, Fernandes et al. (56) evaluated not only features extracted from the images, but also deep learning methods that do not require image processing, with the deep learning approaches achieving better results. Their results present an improvement over previous studies with cross-validation predictive MAE, and R^2 for lean muscle depth of 3.33 mm and 0.50, respectively, and of 0.84 mm and 0.45 for fat depth. Nevertheless, these R^2 presented are still low showing and there is room for improvement on the predictions of lean muscle and fat.

Animal Tracking and Behavior Analysis Using CCD or CMOS Cameras

Some of the most desired applications of CVS for live animals correspond to animal identification, tracking, and monitoring, ultimately identifying changes in their daily behavior. Animal identification can refer to the identification of an animal when there is only one animal in the image to more complex scenarios where there are multiple animals in the image or the identification of different individual animals in a single or multiple images matching their identification. Meanwhile, tracking involves the continuous identification of the animal across frames in a video feed or across images from different locations as the animals are moved from one location to the other. Regarding behavior, animals tend to synchronize their behavior within a group, and conspicuous deviations may be caused by environmental stress, management problems, or disease, although individual behavioral differences need to be taken into account. Therefore, there is a constant effort to understand behavioral changes and their relationship with other traits of interests, such as animal health status and growth. Closer evaluations of animal behavior and health are normally conducted by trained evaluators at specific time points, such as the time of transferring animals from one location to another (e.g., from nursery to grow-out farms) or around vaccinations. This is because managers and workers have limited time to spend in observing a group of animals. Also, with the current trend of an increasing size of livestock operations, there is also an increase in the animal/manager ratio. Thus, a basic use of CVS for evaluation of animal behavior can be the acquisition and storage of images and videos that can be assessed later or remotely by the farmers. This improves animal management since there is no need for the evaluator to be physically present, which otherwise can cause behavioral changes on the animals. Also, the evaluator can loop across images, and replay them, improving the quality of the evaluation. Nonetheless, this kind of system is not optimum since the evaluator would still need to check all the images. Therefore, there are efforts in the literature that attempt to develop CVS that can automatically classify animal behavior and alert the manager in real time regarding important changes.

Initial works with pigs demonstrated the applicability of a CVS to identify the animal position and to track its movement (86, 87). These works showed that the image processing algorithms available at the time could segment a single pig from the background under specific conditions. The conditions were: (1) camera positioned to get the top view of the animal, and (2) dark background for a white pig. The method developed by Tillett et al. (86) estimated a point distribution of landmarks on the pig contour for a sequence of frames (13–30 frames) and was able to model small changes in the animal's posture. However, only seven sequences where evaluated and it was prone to miss the animal if the changes in position were abrupt from one frame to another. On the other hand, Lind et al. (87) used a more robust segmentation approach based on the generation of a background matrix for image subtraction and consequently animal segmentation. Even though this method cannot identify animal posture, it was efficient for use in a real-time application and efficiently tracked differences in animal activity. In their study, the developed CVS was able to track the distance traveled and the walking behavior (path) identifying differences between a pig that received apomorphine or not. Similar approaches based on traditional imaging thresholding and frame by frame comparisons were also used with broilers for the identification of flock behavior over time (82) and at different feeders (83).

Animal tracking and activity-related traits are still of great interest, with the identification and tracking of multiple animals and their interactions as one of the biggest issues. In order

to overcome this challenge, a successful approach in pigs was to identify the animals by ellipsis fitting on the animal area and recognition of patterns printed on their backs (88). By using this simple approach, researchers were able to track and identify multiple animals with an accuracy of 88.7%, enabling the characterization and evaluation of simple activity status as active or non-active with high correlation (mean of 0.9) with evaluations made by a human observer (88, 100). However, this identification and tracking approach cannot be used for animals with darker skin or in commercial farms that have animals with different skin colors since the method was developed for white pigs on a dark floor background and using a surveillance camera. Another challenge in the use of patterns printed on the animal's skin for identification in commercial settings is the higher stocking density and pen size. In an attempt to solve the issue of multiple animal tracking, Matthews et al. (89) developed an approach using multiple 3D cameras to track multiple pigs in a pen and record their behavior, achieving an overall tracking accuracy of 0.89. In a more recent study, a deep learning approach has been tested for identification and tracking of multiple pigs using standard digital cameras, achieving a precision of 0.91 and recall rate of 0.67 on a test data set of pigs under challenging floor and lightening conditions (90). Even though these are promising results, these systems are prone to lose animal tracking over time, without a current solution on how to get back to the correct tracking of each animal. Thus, there is still the need for a reliable CVS capable of identification and tracking of individual animals in farm conditions.

In order to identify more behaviors, like feeding and drinking, manual segmentation of the captured image in regions of interest (ROI) have proved effective (91). The basic concept is to identify not only the animals but also objects, such as the water source and feeders, and track how animals interact with those objects. Using this technique associated with a transfer function model, with a single input and single output, Kashiha et al. (91) were able to identify pig drinking behavior with an R^2 of 0.92 on a single dataset with 40 pigs divided in 4 pens. Machine learning techniques have proven efficient for the identification of animal posture such as standing, lying, or sitting (85, 93). In their study, Barnard et al. (85) achieved a mean accuracy of 0.91 when using a structural support vector machine to classify dog postures from depth images. In another study, Lao et al. (93) defined a classification tree for identification of several sow behaviors using videos from 3D cameras with high (99%) accuracy for lying, sitting, and drinking behaviors and lower for kneeling (78%) and shifting (64%). Machine learning techniques have also shown to be powerful for the identification of social interactions among animals, such as mounting and aggressive behavior (92, 94). Viazzi et al. (92) achieved a mean accuracy of 0.88 when using linear discriminant analysis for classifying aggressive behavior in pigs, while Chen et al. (94) achieved an accuracy of 0.97 on the validation set using a convolution neural network and long short-term memory approach. Even though there was an improvement in accuracy in the latter study, it did not include an automated strategy for the identification of individual animals. Thus, current methods can be used for the identification of behavior changes on group level, but not on individual level. Another aspect that must be highlighted here is that the methods discussed above are supervised learning approaches, and as such, they need a dataset of labeled images (ground truth) for the training step. In order to produce those training datasets, manual classification of the images by a human observer is needed, thus the model will be at most as good as the human observer who evaluated the images in the first place. One way to improve the gold standard used in such methods is by the development and adoption of well-defined methodologies for the measurement and record of traits of interest, followed by regular training and testing of the human evaluators to increase intra and inter-evaluator reliability. Another approach that can also be used is crowdsourcing the development of the dataset. With crowdsourcing, the manual classification of the images can be done by several evaluators and using majority vote, so reducing the impact of individual evaluators' subjectivity (101). Another approach that has shown improvement of the predictive accuracy is the use of multi-model prediction, also known as model assemble methods. One of the most basic assemble would be the use of the average predicted value from multiple models (102). The combination of crowdsourcing the dataset development with the use of multiple model classifiers has allowed an increase in accuracy for applications in medical image analysis, with an artificial intelligence system outperforming trained evaluators (103).

Identification of Mastitis and Digital Dermatitis by Thermography

So far, most of the computer vision applications presented have used standard CCD or CMOS cameras. As previously discussed in section Images on the Visible Light Spectrum, there are also other sensors of interest, such as thermal and depth cameras. Thermal imaging cameras are commonly used in veterinary sciences as a diagnostic tool in clinical examination. The images can be used to identify differences in external/skin temperature that can be related to inflammatory process, infection, necrosis, stress, and overall health. In research, infrared thermography (IRT) has been used to identify mastitis in dairy cattle and sheep (63, 64), and for digital dermatitis in sheep (68), showing the capability to classify healthy and clinically sick animals. Moreover, in a controlled study Metzner et al. (65) observed that IRT was capable of detecting an increase in udder temperature ∼10 h after inoculation with *E. coli*. Nevertheless, these were clinical trial studies with a limited number of animals, thus there is still the need to evaluate IRT under more general farm conditions. Zaninelli et al. (66) evaluated the use of IRT for udder health using data from more than 300 cows from three farms. In their study, even though the images were collected manually, the imaging processing was automated using a classical image threshold for measurement of udder temperature. In this initial step toward automation of udder health evaluation, a threshold model was developed for the classification of udder health in two categories, achieving an area under the curve (AUC) around 0.8. In another study, 149 cows from eight farms were clinically evaluated for digital dermatitis, and IRT was evaluated as a non-invasive field diagnostic tool for dairy cattle (67). In their study, an AUC of 0.84 for the receiver operating characteristic (ROC) curve was observed for classification on the

temperature difference from the front and rear feet, showing promises of IRT as an on-farm tool. However, the authors pointed out that images were collected manually and that in 11% of the cows' data had to be removed due to excessive dirt. Also, there are still many complications related to IRT measurement variation and repeatability. In some studies, it was observed that animal skin/surface temperature can vary according to external factors, such as environmental temperature, wind speed, or other factors, such as operator and camera positioning, and body region evaluated (69–71). Thus, IRT applications have been challenging, and they are still generally based on semi-automated CVS, so that additional effort should be placed on developing methods for automation and improvement of measurements for on farm conditions.

Evaluation of Animal Surface and Related Traits Using 3D Cameras

The interest in the use of 3D cameras is due to the capability of measuring traits in the 3-dimensional space such as animal, body position, gait, and volume. Also, for some applications, there is an improvement of image processing since, within 3D images, there is less noise due to light and background conditions and it is easier to use the distance to the camera as a threshold. Regarding the uses of depth sensors, there are many examples of successful applications including tracking of fish within a tank (79), identification of landmarks on animal shape with consecutive modeling of gait (72, 99), body condition score (78), sickness detection (84), and the estimation of many other body measurements that will be discussed below.

Studies in gait analysis usually demanded intense manual labeling of video frames by a human observer and/or an expensive system of plate markers to be positioned on the animal body and multiple cameras (98). However, with the introduction of time of flight technology and more accessible 3D cameras, CVS with a single or two sensors were capable of efficiently estimate walking kinematics in pigs in a cost-effective framework with prediction accuracy comparable to the state of the art of kinematics systems ($R^2 = 0.99$) (99).

Spoliansky et al. (78) developed an automated CVS based on 3D cameras for the evaluation of dairy cows' body condition score (BCS). In this study, top view images were collected from cows at the moment they were leaving the milking parlor. These images were then automatically processed with removal of background, rotation, and centralization of the cow, holes filled, and normalization. Several image features were extracted from the processed images and used for the development of multiple linear regression models via stepwise regression. Even though the variables extracted did not present a high correlation with BCS, the developed model achieved an average R^2 of 0.68, which is comparable or better than previous studies based on manual processing of the images using either standard digital images (75, 76) or thermal cameras (77).

In chickens, 3D sensors have also been used to identify small modifications in the animal surface that is related to head and tail positioning (84). In this study, in which animals were challenged with the Newcastle disease virus, it was possible to identify alterations in the animal shape and behavior 6 days after the inoculation.

Other applications in which depth sensors are showing promising results are for estimation of animal body measurements (heights, widths, area, and volume as examples) and body weight (44, 96, 97). In one study, a CVS based on depth image could extract additional information on the animal volume, achieving an R^2 of 0.99 (96) under experimental conditions. In another study (97), depth cameras were evaluated for estimation of body measurements on pigs in farm conditions, achieving high R^2 (0.77–0.93) between the manual measurement and the measures estimated from the images. Nevertheless, these previous studies used some level of manual handling of the images and they did not evaluate model performance using an independent set of animals or a cross-validation approach. This hampers the evaluation of how generalizable the prediction models are, that is, how these CVS based on 3D cameras would perform in practice. Another drawback of these previous studies is the lack of automation for application in farm conditions, where it would be extremely difficult to manually process the images.

Automated Prediction of Individual Body Measurements

Automated non-contact prediction of body weight and body measurements is a long-desired application for many animal production systems. Kashiha et al. (95) developed a CVS for automated prediction of BW in pigs under experimental conditions achieving good prediction ($R^2 = 0.97$) for body weight using surveillance cameras. However, as stated by the authors, this previous method was still restricted by background and light conditions, along with animal coat color. Recently, Fernandes et al. (14) developed an automated CVS based on depth camera for real-time video processing and prediction of body weight in live pigs. They worked with videos collected under farm conditions using multiple linear regression models with features extracted from the images as predictor variables, achieving high predictive accuracy evaluated with cross-validation ($R^2 = 0.92$). An adaptation of their CVS was also evaluated for prediction of body weight in beef cattle from depth images (73) achieving high R^2 (0.79–0.91) with an artificial neural network approach. In both works, the images were collected from animals partially restrained and there was only one animal in the camera field of view so that future developments with the CVS on barn conditions would be necessary for better evaluation.

There are also many attempts to develop CVS for automated prediction of body weight and body measurements in fish, where the main challenges are related to fish body positioning and segmentation, and external factors such as light and background conditions. To tackle these issues, one study in halibut developed a CVS based on multi-scale body contour matching and completion using a double local threshold model with body shape priors (80). The final model developed was able to estimate the fish body with an average intersection over union (IoU) of 95.6%. In another study in Nile tilapia, Fernandes et al. (81) used a deep learning approach for fish body segmentation from images under different lighting and background conditions.

The approach was able to distinguish fish from the background with a validation IoU of 99%, and for the fish body from fins and background of 0.91%. In their study, the final fish body area was then used for prediction of fish body weight, achieving a predictive R^2 of 0.96. Nevertheless, in this study, the fish were removed from the water, while in the previous one images from the top view of fish in a shallow water area were used. Hence, it is still necessary to develop CVSs that can evaluate fish underwater inside production cages. This adds more challenges, such as interference and occlusion due to different water transparency.

Perspectives of CVS for High-Throughput Phenotyping

CVS together with other sensor technologies are at the forefront of precision livestock farming, with some systems already been implemented in farm applications (104). Such systems have the potential to enable high-throughput phenotyping (HTP), which can be defined as the measurement of a single or many different traits of interest at multiple times during the animal life. HTP applications promise the generation of large amounts of data that will improve the accuracy of current methods and open a myriad of opportunities to advance breeding programs and livestock production (105). Nevertheless, for their implementation on breeding programs, there is the need to develop automated and robust CVS that are capable of collecting, processing, analyzing, and transmitting individual animal data. For this to happen, several key resources and tools must be developed such as improvement of rural broadbands, data integration, data mining, and novel predictive tools among others (106). A specific strategy used to circumvent the issue of individual animal identification is by using other technologies such as RFID tags, associated with the CVS (72). Nevertheless, there is still room for more progress in the use of image analysis for animal identification. Recent developments in machine learning algorithms for image analysis such as deep learning have shown promising results in other areas such as human face recognition, disease detection, and classification, among others (22). Generally, these algorithms demand very large datasets to be trained such as the Microsoft Common Objects in Context (COCO) (107). Nonetheless, with techniques such as transfer learning of pre-trained models, we expect that deep learning may play an important role in the future development of CVS applications for animal production.

Animal phenotyping, or rather, the measurement of traits of interest, has long been a constant and important practice in animal management and also for the development of breeding programs for different animal production systems. In this manuscript, we discussed CVS as an interesting tool for the collection of such phenotypes without direct interaction with the animals. Thus, in the last decade, several efforts have been made toward the measurement of group-level traits, such as group growth, activity, drinking and feeding behavior, and animal spatial distribution among others with most of the successful applications based on standard digital cameras implementing classic image analysis and machine learning algorithms. Nevertheless, most of the works in the literature deals with a small group of animals, with just a few works evaluating CVS in farm environments (14, 66, 67, 97) or under challenging light and background conditions (80, 81, 90) with the application of more sophisticated machine learning algorithms.

Nevertheless, there are already some examples of how CVS can be leveraged by breeding programs. In a study by Moore et al. (108), data from 17,765 image carcass records of prime cuts and carcass weight of commercial beef slaughter was used to predict genetic parameters in beef cattle. The authors concluded that by leveraging the information from the CVS it was possible to yield more accurate genetic parameters due to the higher volume of data. In another study, Nye et al. (74) developed a web scraper and an image segmentation algorithm to extract images and information from breeding programs catalogs. The information retrieved was used in a subsequent step to predict genetic parameters related to coat pigmentation and conformation traits in dairy cattle. The authors demonstrated that, for dairy cattle, approximately only 50 images were required to train their semi-supervised machine learning approach.

CONCLUDING REMARKS

The idea of developing CVSs for automatic monitoring and measuring traits of interest in animals is not new. Early developments in digital image analysis and computer vision have shown the potential of the use of images to evaluate animal behavior, gait, body weight, and other traits in experimental conditions, with some more recent studies evaluating also on-farm applications. Also, there are studies showing that different imaging technologies can be better suited for specific applications, such as IRT for identification of mastitis and digital dermatitis in dairy cattle, or spectral and hyperspectral imaging in food sciences. However, there is also a great number of attempts to develop CVS based on more accessible technologies such as standard digital cameras and 3D cameras.

Applications of CVS in animal and veterinary sciences are currently a growing research area. Even though there are already some commercial products for monitoring groups of live animals, or slaughtered animals at the abattoir, there are still several challenges that demand intense research for the successful development and deployment of practical solutions. Current challenges involve the development and implementation of reliable CVS for the autonomous acquisition of data regarding single or multiple traits in farm conditions, as there are still few studies that evaluated these CVS using validation data sets, including different animals in the same farm or across multiple farms. Another area of importance is individual animal identification and tracking since most of the currently developed methods are still prone to error. There is also the need for the development of methods to connect the increasing number of devices used for different applications. This may enable the implementation of more sophisticated predictive algorithms based on multiple inputs and multiple outputs (joint prediction of multiple traits). Finally, there is the need for the development of applications for the delivery of the information generated

by the CVS to connected systems thus generating valuable information to farmers and managers. This is the focus of areas such as big data and internet of things which, even though are not the focus of this review, these areas are going to be indispensable for the further development of CVS animal breeding programs and production systems.

AUTHOR CONTRIBUTIONS

AF, JD, and GR contributed to the conception and design of the review. AF wrote the first draft of the manuscript. All authors contributed to manuscript revision, read, and approved the submitted version.

FUNDING

The authors thank the financial support from the Coordination for the Improvement of High Education Personnel (CAPES), Brazil ordinance (49/2013), the Wisconsin Agriculture Experiment Station Hatch grant (142-AAC7939), and United States Department of Agriculture (USDA).

REFERENCES

1. Gregory RL. *Eye and Brain : The psychology of seeing*. Third. New York: McGraw-Hill (1978). Available online at: https://sofamphoto.files.wordpress.com/2014/09/eye-brain-gregory.pdf (accessed August 24, 2017).
2. Burger W, Burge MJ. *Digital image processing: An Algorithmic Introduction Using Java*. 2nd ed. London: Springer London (2005). p. 811.
3. Atherton TJ, Kerbyson DJ. Size invariant circle detection. *Image Vis Comput*. (1999) 17:795–803. doi: 10.1016/S0262-8856(98)00160-7
4. Kheradmand A, Milanfar P. Non-linear structure-aware image sharpening with difference of smoothing operators. *Front ICT*. (2015) 2:22. doi: 10.3389/fict.2015.00022
5. Rosin PL, Ioannidis E. Evaluation of global image thresholding for change detection. *Pattern Recognit Lett*. (2003) 24:2345–56. doi: 10.1016/S0167-8655(03)00060-6
6. Polesel A, Ramponi G, Mathews VJ. Image enhancement via adaptive unsharp masking. *IEEE Trans Image Process*. (2000) 9:505–10. doi: 10.1109/83.826787
7. Nakagomi K, Shimizu A, Kobatake H, Yakami M, Fujimoto K, Togashi K. Multi-shape graph cuts with neighbor prior constraints and its application to lung segmentation from a chest CT volume. *Med Image Anal*. (2013) 17:62–77. doi: 10.1016/j.media.2012.08.002
8. Tang M, Gorelick L, Veksler O, Boykov Y. GrabCut in one cut. In: *Proceedings of "International Conference on Computer Vision" (ICCV)* (Sydney), 8. (2013). Available online at: http://www.csd.uwo.ca/\simyuri/Papers/iccv13_one_cut.pdf (accessed March 8, 2017).
9. Szelisk R. Computer vision : algorithms applications. In: Gries D, Schneider FB. London: Springer-Verlag (2011). doi: 10.1007/978-1-84882-935-0
10. Hough PVC. Method and Means For Recognizing Complex Patterns (1962). Available online at: https://www.osti.gov/scitech/biblio/4746348 (accessed April 17, 2017).
11. Bay H, Tuytelaars T, Van Gool L. SURF: Speeded Up Robust Features. In: *European Conference on Computer Vision* (Berlin, Heidelberg: Springer) (2006). p. 404–417. doi: 10.1007/11744023_32
12. Leutenegger S, Chli M, Siegwart RY. BRISK: binary robust invariant scalable keypoints. In: *International Conference on Computer Vision* (Barcelona: IEEE). (2011). p. 2548–55. doi: 10.1109/ICCV.2011.6126542
13. Murphy KP. *Machine Learning: A Probabilistic Perspective*. Cambridge, Massachusetts: MIT Press (2012). Available at: http://mitpress.mit.edu (accessed June 18, 2019).
14. Fernandes AFA, Dórea JRR, Fitzgerald R, Herring W, Rosa GJM. A novel automated system to acquire biometric and morphological measurements and predict body weight of pigs via 3D computer vision. *J Anim Sci*. (2019) 97:496–508. doi: 10.1093/jas/sky418
15. Boyle WS, Smith GE. Buried channel charge coupled devices. 9. (1973). Available online at: https://patents.google.com/patent/US3792322 (accessed May 17, 2019]
16. Lister M. (1995). *The photographic image in digital culture*. London: Routledge
17. van Dijck J. Digital photography: communication, identity, memory. *Vis Commun*. (2008) 7:57–76. doi: 10.1177/1470357207084865
18. Viola P, Jones MJ. Robust Real-Time Face Detection. *Int J Comput Vis*. (2004) 57:137–54. doi: 10.1023/B:VISI.0000013087.49260.fb
19. LeCun Y, Bottou L, Bengio Y, Haffner P. Gradient-based learning applied to document recognition. *Proc IEEE*. (1998) 86:2278–324. doi: 10.1109/5.726791
20. Litjens G, Sánchez CI, Timofeeva N, Hermsen M, Nagtegaal I, Kovacs I, et al. Deep learning as a tool for increased accuracy and efficiency of histopathological diagnosis. *Sci Rep*. (2016) 6:26286. doi: 10.1038/srep26286
21. Goodfellow I, Bengio Y, Courville A. *Deep Learning*. Cambridge, MS: MIT Press (2016).
22. LeCun Y, Bengio Y, Hinton G. Deep learning. *Nature*. (2015) 521:436–44. doi: 10.1038/nature14539
23. Hyndman RJ, Koehler AB. Another look at measures of forecast accuracy. *Int J Forecast*. (2006) 22:679–88. doi: 10.1016/j.ijforecast.2006.03.001
24. Aggarwal CC. (2015). *Data Mining: The Textbook*. New York, NY: Springer. doi: 10.1007/978-3-319-14142-8
25. Hastie T, Tibshirani R, Friedman J. *The Elements of Statistical Learning. Second Edition*. New York, NY: Springer New York (2009). doi: 10.1007/978-0-387-84858-7
26. Helmers H, Schellenberg M. CMOS vs. CCD sensors in speckle interferometry. *Opt Laser Technol*. (2003) 35:587–95. doi: 10.1016/S0030-3992(03)00078-1
27. Ring F, Jung A, Zuber J. *Infrared Imaging A Casebook in Clinical Medicine*. Bristol-UK: IOP Publishing. (2015). doi: 10.1088/978-0-7503-1143-4
28. Lavers C, Franks K, Floyd M, Plowman A. Application of remote thermal imaging and night vision technology to improve endangered wildlife resource management with minimal animal distress and hazard to humans. *J Phys Conf Ser*. (2005) 15:207–12. doi: 10.1088/1742-6596/15/1/035
29. Swanson GA, Sargeant AB. Observation of nighttime feeding behavior of ducks. *J Wildl Manage*. (1972) 36:959–61. doi: 10.2307/3799457
30. McManus C, Tanure CB, Peripolli V, Seixas L, Fischer V, Gabbi AM, et al. Infrared thermography in animal production: an overview. *Comput Electron Agric*. (2016) 123:10–6. doi: 10.1016/j.compag.2016.01.027
31. Zanuttigh P, Mutto CD, Minto L, Marin G, Dominio F, Cortelazzo GM. *Time-of-Flight and Structured Light Depth Cameras: Technology and Applications*. Cham: Springer International Publishing (2016). p. 355. doi: 10.1007/978-3-319-30973-6
32. Giancola S, Valenti M, Sala R. A survey on 3D cameras: metrological comparison of time-of-flight, structured-light and active stereoscopy technologies. In: *SpringerBriefs in Computer Science* (Cham: Springer) (2018). p. 90. doi: 10.1007/978-3-319-91761-0
33. Yoo HW, Druml N, Brunner D, Schwarzl C, Thurner T, Hennecke M, et al. MEMS-based lidar for autonomous driving. *Elektrot Informat*. (2018) 135:408–15. doi: 10.1007/s00502-018-0635-2
34. Xiong Z, Sun D-W, Zeng X-A, Xie A. Recent developments of hyperspectral imaging systems and their applications in detecting quality attributes of red meats: a review. *J Food Eng*. (2014) 132:1–13. doi: 10.1016/j.jfoodeng.2014.02.004
35. Tao F, Ngadi M. Recent advances in rapid and nondestructive determination of fat content and fatty acids composition of muscle foods. *Crit Rev Food Sci Nutr*. (2018) 58:1565–93. doi: 10.1080/10408398.2016.1261332

36. Ozaki Y, McClure WF, Christy AA (editors). *Near-Infrared Spectroscopy in Food Science and Technology*. Hoboken, NJ: JohnWiley & Sons, Inc. (2007). p. 11–46. doi: 10.1002/0470047704
37. Font-i-Furnols M, Carabús A, Pomar C, Gispert M. Estimation of carcass composition and cut composition from computed tomography images of live growing pigs of different genotypes. *Animal.* (2015) 9:166–78. doi: 10.1017/S1751731114002237
38. Scholz AM, Bünger L, Kongsro J, Baulain U, Mitchell AD. Non-invasive methods for the determination of body and carcass composition in livestock: dual-energy X-ray absorptiometry, computed tomography, magnetic resonance imaging and ultrasound: invited review. *Animal.* (2015) 9:1250–64. doi: 10.1017/S1751731115000336
39. Lucas D, Brun A, Gispert M, Carabús A, Soler J, Tibau J, et al. Relationship between pig carcass characteristics measured in live pigs or carcasses with Piglog, Fat-o-Meat'er and computed tomography. *Livest Sci.* (2017) 197:88–95. doi: 10.1016/J.LIVSCI.2017.01.010
40. Lin SSP. *Automated Pattern Recognition of Beef.* (1978). Available online at: http://krex.k-state.edu/dspace/bitstream/handle/2097/13198/LD2668R41978L54.pdf?sequence=1 (accessed August 29, 2017).
41. Cross HR, Gilliland DA, Durland PR, Seideman S. Beef carcass evaluation by use of a video image analysis system. *J Anim Sci.* (1983) 57:908–17. doi: 10.2527/jas1983.574908x
42. Wassenberg RL, Allen DM, Kemp KE. Video image analysis prediction of total kilograms and percent primal lean and fat yield of beef carcasses. *J Anim Sci.* (1986) 62:1609–16. doi: 10.2527/jas1986.6261609x
43. Teixeira A, Joy M, Delfa R. In vivo estimation of goat carcass composition and body fat partition by real-time ultrasonography. *J Anim Sci.* (2008) 86:2369–76. doi: 10.2527/jas.2007-0367
44. Gomes RA, Monteiro GR, Assis GJF, Busato KC, Ladeira MM, Chizzotti ML. Technical note: estimating body weight and body composition of beef cattle trough digital image analysis. *J Anim Sci.* (2016) 94:5414–22. doi: 10.2527/jas.2016-0797
45. Nunes J, Piquerez M, Pujadas L, Armstrong E, Fernández A, Lecumberry F. Beef quality parameters estimation using ultrasound and color images. *BMC Bioinformatics.* (2015) 16 (Suppl. 4):S6. doi: 10.1186/1471-2105-16-S4-S6
46. Jackman P, Sun D-W, Allen P, Brandon K, White A-M. Correlation of consumer assessment of longissimus dorsi beef palatability with image colour, marbling and surface texture features. *Meat Sci.* (2010) 84:564568. doi: 10.1016/j.meatsci.2009.10.013
47. Folkestad A, Wold JP, Rørvik, K.-A., Tschudi J, Haugholt KH, Kolstad K, et al. Rapid and non-invasive measurements of fat and pigment concentrations in live and slaughtered Atlantic salmon (*Salmo salar* L.). *Aquaculture.* (2008) 280:129–35. doi: 10.1016/j.aquaculture.2008.04.037
48. Paluchowski LA, Misimi E, Grimsmo L, Randeberg LL. Towards automated sorting of Atlantic cod (Gadus morhua) roe, milt, and liver - Spectral characterization and classification using visible and near-infrared hyperspectral imaging. *Food Control.* (2016) 62:337–45. doi: 10.1016/j.foodcont.2015.11.004
49. Sture Ø, Øye ER, Skavhaug A, Mathiassen JR. A 3D machine vision system for quality grading of Atlantic salmon. *Comput Electron Agric.* (2016) 123:142–8. doi: 10.1016/j.compag.2016.02.020
50. Khoshnoudi-Nia S, Moosavi-Nasab M. Prediction of various freshness indicators in fish fillets by one multispectral imaging system. *Sci Rep.* (2019) 9:14704. doi: 10.1038/s41598-019-51264-z
51. Zapotoczny P, Szczypiński PM, Daszkiewicz T. Evaluation of the quality of cold meats by computer-assisted image analysis. *LWT - Food Sci Technol.* (2016) 67:37–49. doi: 10.1016/j.lwt.2015.11.042
52. Adamczak L, Chmiel M, Florowski T, Pietrzak D, Witkowski M, Barczak T. The use of 3D scanning to determine the weight of the chicken breast. *Comput Electron Agric.* (2018) 155:394–9. doi: 10.1016/j.compag.2018.10.039
53. Guanjun B, Mimi J, Yi X, Shibo C, Qinghua Y. Cracked egg recognition based on machine vision. *Comput Electron Agric.* (2019) 158:159–66. doi: 10.1016/j.compag.2019.01.005
54. Doeschl-Wilson AB, Green DM, Fisher AV, Carroll SM, Schofield CP, Whittemore CT. The relationship between body dimensions of living pigs and their carcass composition. *Meat Sci.* (2005) 70:229–40. doi: 10.1016/j.meatsci.2005.01.010
55. Alsahaf A, Azzopardi G, Ducro B, Hanenberg E, Veerkamp RF, Petkov N. Estimation of muscle scores of live pigs using a kinect camera. *IEEE Access.* (2019) 7:52238–45. doi: 10.1109/ACCESS.2019.2910986
56. Fernandes AFA, Dórea JRR, Valente BD, Fitzgerald R, Herring W, Rosa GJM. Comparison of data analytics strategies in computer vision systems to predict pig body composition traits from 3D images. *J Anim Sci.* (2020) 98:1–9. doi: 10.1093/jas/skaa250
57. Wang X, Zhao M, Ju R, Song Q, Hua D, Wang C, et al. Visualizing quantitatively the freshness of intact fresh pork using acousto-optical tunable filter-based visible/near-infrared spectral imagery. *Comput Electron Agric.* (2013) 99:41–53. doi: 10.1016/j.compag.2013.08.025
58. Ostermeier GC, Sargeant GA, Yandell BS, Parrish JJ. measurement of bovine sperm nuclear shape using fourier harmonic amplitudes. *J Androl.* (2001) 22:584–94. doi: 10.1002/J.1939-4640.2001.TB02218.X
59. Sassi N, Ben, Averós X, Estevez I. Technology and poultry welfare. *Animals.* (2016) 6:62–83. doi: 10.3390/ani6100062
60. Li N, Ren Z, Li D, Zeng L. Review: automated techniques for monitoring the behaviour and welfare of broilers and laying hens: towards the goal of precision livestock farming. *Animal.* (2019) 14:617–25. doi: 10.1017/S1751731119002155
61. Nasirahmadi A, Edwards SA, Sturm B. Implementation of machine vision for detecting behaviour of cattle and pigs. *Livest Sci.* (2017) 202:25–38. doi: 10.1016/j.livsci.2017.05.014
62. Saberioon M, Gholizadeh A, Cisar P, Pautsina A, Urban J. Application of machine vision systems in aquaculture with emphasis on fish: state-of-the-art and key issues. *Rev Aquac.* (2017) 9:369–87. doi: 10.1111/raq.12143
63. Hovinen M, Siivonen J, Taponen S, Hänninen L, Pastell M, Aisla A-M, et al. Detection of clinical mastitis with the help of a thermal camera. *J Dairy Sci.* (2008) 91:4592–8. doi: 10.3168/jds.2008-1218
64. Martins RFS, do Prado Paim T, de Abreu Cardoso C, Stéfano Lima Dallago B, de Melo CB, Louvandini H, et al. Mastitis detection in sheep by infrared thermography. *Res Vet Sci.* (2013) 94:722–4. doi: 10.1016/j.rvsc.2012.10.021
65. Metzner M, Sauter-Louis C, Seemueller A, Petzl W, Zerbe H. Infrared thermography of the udder after experimentally induced Escherichia coli mastitis in cows. *Vet J.* (2015) 204:360–2. doi: 10.1016/J.TVJL.2015.04.013
66. Zaninelli M, Redaelli V, Luzi F, Bronzo V, Mitchell M, Dell'Orto V, et al. First evaluation of infrared thermography as a tool for the monitoring of udder health status in farms of dairy cows. *Sensors.* (2018) 18:862. doi: 10.3390/s18030862
67. Alsaaod M, Syring C, Dietrich J, Doherr MG, Gujan T, Steiner A. A field trial of infrared thermography as a non-invasive diagnostic tool for early detection of digital dermatitis in dairy cows. *Vet J.* (2014) 199:281–5. doi: 10.1016/j.tvjl.2013.11.028
68. Byrne DT, Berry DP, Esmonde H, McGovern F, Creighton P, McHugh N. Infrared thermography as a tool to detect hoof lesions in sheep. *Transl Anim Sci.* (2019) 3:577–88. doi: 10.1093/tas/txy132
69. Byrne DT, Berry DP, Esmonde H, McHugh N. Temporal, spatial, inter-, and intra-cow repeatability of thermal imaging. *J Anim Sci.* (2017) 95:970–9. doi: 10.2527/jas2016.1005
70. Yang C, Li G, Zhang X, Gu X. Udder skin surface temperature variation pre- and post-milking in dairy cows as determined by infrared thermography. *J Dairy Res.* (2018) 85:201–3. doi: 10.1017/S0022029918000213
71. Scoley GE, Gordon AW, Morrison SJ. Use of thermal imaging in dairy calves: exploring the repeatability and accuracy of measures taken from different anatomical regions1. *Transl Anim Sci.* (2019) 3:564–76. doi: 10.1093/tas/txy126
72. Salau J, Haas JH, Junge W, Thaller G. Automated calculation of udder depth and rear leg angle in Holstein-Friesian cows using a multi-Kinect cow scanning system. *Biosyst Eng.* (2017) 160:154–69. doi: 10.1016/j.biosystemseng.2017.06.006
73. Cominotte A, Fernandes AFA, Dorea JRR, Rosa GJM, Ladeira MM, van Cleef EHCB, et al. Automated computer vision system to predict body weight and average daily gain in beef cattle during growing and finishing phases. *Livest Sci.* (2020) 232:103904–14. doi: 10.1016/j.livsci.2019.103904
74. Nye J, Zingaretti LM, Pérez-Enciso M. Estimating conformational traits in dairy cattle with deepaps: a two-step deep learning automated

phenotyping and segmentation approach. *Front Genet.* (2020) 11:513. doi: 10.3389/fgene.2020.00513
75. Bewley JM, Peacock AM, Lewis O, Boyce RE, Roberts DJ, Coffey MP, et al. Potential for estimation of body condition scores in dairy cattle from digital images. *J Dairy Sci.* (2008) 91:3439–53. doi: 10.3168/jds.2007-0836
76. Bercovich A, Edan Y, Alchanatis V, Moallem U, Parmet Y, Honig H, et al. Development of an automatic cow body condition scoring using body shape signature and Fourier descriptors. *J Dairy Sci.* (2013) 96:8047–59. doi: 10.3168/jds.2013-6568
77. Halachmi I, Klopči,č M, Polak P, Roberts DJ, Bewley JM. Automatic assessment of dairy cattle body condition score using thermal imaging. *Comput Electron Agric.* (2013) 99:35–40. doi: 10.1016/j.compag.2013.08.012
78. Spoliansky R, Edan Y, Parmet Y, Halachmi I. Development of automatic body condition scoring using a low-cost 3-dimensional Kinect camera. *J Dairy Sci.* (2016) 99:7714–25. doi: 10.3168/jds.2015-10607
79. Saberioon MM, Cisar P. Automated multiple fish tracking in three-Dimension using a Structured Light Sensor. *Comput Electron Agric.* (2016) 121:215–21. doi: 10.1016/j.compag.2015.12.014
80. Wang G, Hwang J-N, Wallace F, Rose C. Multi-scale fish segmentation refinement and missing shape recovery. *IEEE Access.* (2019) 7:52836–45. doi: 10.1109/ACCESS.2019.2912612
81. Fernandes AFA, Turra EM, de Alvarenga ÉR, Passafaro TL, Lopes FB, Alves GFO, et al. Deep Learning image segmentation for extraction of fish body measurements and prediction of body weight and carcass traits in Nile tilapia. *Comput Electron Agric.* (2020) 170:105274. doi: 10.1016/j.compag.2020.105274
82. Kashiha M, Pluk A, Bahr C, Vranken E, Berckmans D. Development of an early warning system forabroiler house using computer vision. *Biosyst Eng.* (2013) 116:36–45. doi: 10.1016/j.biosystemseng.2013.06.004
83. Neves DP, Mehdizadeh SA, Tscharke M, Nääs I, de A, Banhazi TM. Detection of flock movement and behaviour of broiler chickens at different feeders using image analysis. *Inf Process Agric.* (2015) 2:177–82. doi: 10.1016/j.inpa.2015.08.002
84. Okinda C, Lu M, Liu L, Nyalala I, Muneri C, Wang J, et al. A machine vision system for early detection and prediction of sick birds: a broiler chicken model. *Biosyst Eng.* (2019) 188:229–42. doi: 10.1016/j.biosystemseng.2019.09.015
85. Barnard S, Calderara S, Pistocchi S, Cucchiara R, Podaliri-Vulpiani M, Messori S, et al. Quick, accurate, smart: 3d computer vision technology helps assessing confined animals' behaviour. *PLoS ONE.* (2016) 11:e0158748. doi: 10.1371/journal.pone.0158748
86. Tillett RD, Onyango CM, Marchant JA. Using model-based image processing to track animal movements. *Comput Electron Agric.* (1997) 17:249–61. doi: 10.1016/S0168-1699(96)01308-7
87. Lind NM, Vinther M, Hemmingsen RP, Hansen AK. Validation of a digital video tracking system for recording pig locomotor behaviour. *J Neurosci Methods.* (2005) 143:123–32. doi: 10.1016/j.jneumeth.2004.09.019
88. Kashiha MA, Bahr C, Ott S, Moons CPH, Niewold TA, Ödberg FO, et al. Automatic identification of marked pigs in a pen using image pattern recognition. *Comput Electron Agric.* (2013) 93:111–20. doi: 10.1016/j.compag.2013.01.013
89. Matthews SG, Miller AL, PlÖtz T, Kyriazakis I. Automated tracking to measure behavioural changes in pigs for health and welfare monitoring. *Sci Rep.* (2017) 7:17582. doi: 10.1038/s41598-017-17451-6
90. Psota ET, Mittek M, Pérez LC, Schmidt T, Mote B. Multi-pig part detection and association with a fully-convolutional network. *Sensors.* (2019) 19:852. doi: 10.3390/s19040852
91. Kashiha MA, Bahr C, Haredasht SA, Ott S, Moons CPH, Niewold TA, et al. The automatic monitoring of pigs water use by cameras. *Comput Electron Agric.* (2013) 90:164–9. doi: 10.1016/j.compag.2012.09.015
92. Viazzi S, Ismayilova G, Oczak M, Sonoda LT, Fels M, Guarino M, et al. Image feature extraction for classification of aggressive interactions among pigs. *Comput Electron Agric.* (2014) 104:57–62. doi: 10.1016/j.compag.2014.03.010
93. Lao F, Brown-Brandl T, Stinn JP, Liu K, Teng G, Xin H. Automatic recognition of lactating sow behaviors through depth image processing. *Comput Electron Agric.* (2016) 125:56–62. doi: 10.1016/j.compag.2016.04.026
94. Chen C, Zhu W, Steibel J, Siegford J, Wurtz K, Han J, et al. Recognition of aggressive episodes of pigs based on convolutional neural network and long short-term memory. *Comput Electron Agric.* (2020) 169:105166. doi: 10.1016/j.compag.2019.105166
95. Kashiha MA, Bahr C, Ott S, Moons CPH, Niewold TA, Ödberg FO, et al. Automatic weight estimation of individual pigs using image analysis. *Comput Electron Agric.* (2014) 107:38–44. doi: 10.1016/j.compag.2014.06.003
96. Kongsro J. Estimation of pig weight using a Microsoft Kinect prototype imaging system. *Comput Electron Agric.* (2014) 109:32–5. doi: 10.1016/j.compag.2014.08.008
97. Pezzuolo A, Guarino M, Sartori L, González LA, Marinello F. On-barn pig weight estimation based on body measurements by a Kinect v1 depth camera. *Comput Electron Agric.* (2018) 148:29–36. doi: 10.1016/J.COMPAG.2018.03.003
98. Stavrakakis S, Guy JH, Warlow OME, Johnson GR, Edwards SA. Walking kinematics of growing pigs associated with differences in musculoskeletal conformation, subjective gait score and osteochondrosis. *Livest Sci.* (2014) 165:104–13. doi: 10.1016/j.livsci.2014.04.008
99. Stavrakakis S, Li W, Guy JH, Morgan G, Ushaw G, Johnson GR, et al. Validity of the Microsoft Kinect sensor for assessment of normal walking patterns in pigs. *Comput Electron Agric.* (2015) 117:1–7. doi: 10.1016/j.compag.2015.07.003
100. Ott S, Moons CPH, Kashiha MA, Bahr C, Tuyttens FAM, Berckmans D, et al. Automated video analysis of pig activity at pen level highly correlates to human observations of behavioural activities. *Livest Sci.* (2014) 160:132–7. doi: 10.1016/j.livsci.2013.12.011
101. Arganda-Carreras I, Turaga SC, Berger DR, Cireşan D, Giusti A, Gambardella LM, et al. Crowdsourcing the creation of image segmentation algorithms for connectomics. *Front Neuroanat.* (2015) 9:142. doi: 10.3389/fnana.2015.00142
102. Burnham KP, Anderson DR (editors). *Model Selection and Multimodel Inference – A Pratical Information – Theoretic Approach*. New York, NY: Springer New York (2004). p. 149–203. doi: 10.1007/b97636
103. McKinney SM, Sieniek M, Godbole V, Godwin J, Antropova N, Ashrafian H, et al. International evaluation of an AI system for breast cancer screening. *Nature.* (2020) 577:89–94. doi: 10.1038/s41586-019-1799-6
104. Berckmans D. General introduction to precision livestock farming. *Anim Front.* (2017) 7:6. doi: 10.2527/af.2017.0102
105. Rosa GJM, Dorea JRR, Fernandes AFA, Passafaro TL. 227 Leveraging on high-throughput phenotyping technologies to optimize livestock genetic improvement and husbandry. *J Anim Sci.* (2019) 97:55. doi: 10.1093/jas/skz258.111
106. Koltes JE, Cole JB, Clemmens R, Dilger RN, Kramer LM, Lunney JK, et al. A vision for development and utilization of high-throughput phenotyping and big data analytics in livestock. *Front Genet.* (2019) 10:1197. doi: 10.3389/fgene.2019.01197
107. Lin, T.-Y., Maire M, Belongie S, Bourdev L, Girshick R, Hays J, et al. (2015). *Microsoft COCO: Common Objects in Context. arXiv*. Available online at: https://arxiv.org/abs/1405.0312 (accessed December 5, 2018).
108. Moore KL, Mrode R, Coffey MP. Genetic parameters of Visual Image Analysis primal cut carcass traits of commercial prime beef slaughter animals. *Animal.* (2017) 11:1653–9. doi: 10.1017/S1751731117000489

Conflict of Interest: The authors declare that the research was conducted in the absence of any commercial or financial relationships that could be construed as a potential conflict of interest.

frontiers in Genetics

ORIGINAL RESEARCH
published: 23 October 2020
doi: 10.3389/fgene.2020.593804

Genomic Analysis of IgG Antibody Response to Common Pathogens in Commercial Sows in Health-Challenged Herds

*Leticia P. Sanglard[1], PigGen Canada, Benny E. Mote[2], Philip Willson[3], John C. S. Harding[4], Graham S. Plastow[5], Jack C. M. Dekkers[1] and Nick V. L. Serão[1]**

[1] Department of Animal Science, Iowa State University, Ames, IA, United States, [2] Department of Animal Science, University of Nebraska–Lincoln, Lincoln, NE, United States, [3] Canadian Centre for Health and Safety in Agriculture, University of Saskatchewan, Saskatoon, SK, Canada, [4] Department of Large Animal Clinical Sciences, University of Saskatchewan, Saskatoon, SK, Canada, [5] Department of Agricultural, Food and Nutritional Science, University of Alberta, Edmonton, AB, Canada

OPEN ACCESS

Edited by:
Fabyano Fonseca Silva, Universidade Federal de Viçosa, Brazil

Reviewed by:
Russell Fraser, University of Prince Edward Island, Canada
Laura Caldwell Miller, National Animal Disease Center (USDA ARS), United States

***Correspondence:**
Nick V. L. Serão
serao@iastate.edu

Specialty section:
This article was submitted to Livestock Genomics, a section of the journal Frontiers in Genetics

Received: *11 August 2020*
Accepted: *25 September 2020*
Published: *23 October 2020*

Citation:
Sanglard LP, PigGen Canada, Mote BE, Willson P, Harding JCS, Plastow GS, Dekkers JCM and Serão NVL (2020) Genomic Analysis of IgG Antibody Response to Common Pathogens in Commercial Sows in Health-Challenged Herds. Front. Genet. 11:593804. doi: 10.3389/fgene.2020.593804

Losses due to infectious diseases are one of the main factors affecting productivity in the swine industry, motivating the investigation of disease resilience-related traits for genetic selection. However, these traits are not expected to be expressed in the nucleus herds, where selection is performed. One alternative is to use information from the commercial level to identify and select nucleus animals genetically superior for coping with pathogen challenges. In this study, we analyzed the genetic basis of antibody (Ab) response to common infectious pathogens in health-challenged commercial swine herds as potential indicator traits for disease resilience, including Ab response to influenza A virus of swine (IAV), *Mycoplasma hyopneumoniae* (MH), porcine circovirus (PCV2), and *Actinobacillus pleuropneumoniae* (APP; different serotypes). Ab response was measured in blood at entry into gilt rearing, post-acclimation (∼40 days after entering the commercial herd), and parities 1 and 2. Heritability estimates for Ab response to IAV, MH, and PCV2 ranged from 0 to 0.76. Ab response to APP ranged from 0 to 0.40. The genetic correlation (r_G) of Ab response to IAV with MH, PCV2, PRRSV, and APP_{mean} (average Ab responses for all serotypes of APP) were positive (>0.29) at entry. APP_{mean} was negatively correlated with PCV2 and MH at entry and parity 2 but positively correlated with MH at post-acclimation and parity 1. Genomic regions associated with Ab response to different APP serotypes were identified on 13 chromosomes. The region on chromosome 14 (2 Mb) was associated with several serotypes of APP, explaining up to 4.3% of the genetic variance of Ab to APP7 at entry. In general, genomic prediction accuracies for Ab response were low to moderate, except average Ab response to all infectious pathogens evaluated. These results suggest that genetic selection of Ab response in commercial sows is possible, but with variable success depending on the trait and the time-point of collection. Future work is needed to determine genetic correlations of Ab response with disease resilience, reproductive performance, and other production traits.

Keywords: antibody response, genetic correlation, GWAS, heritability, infectious pathogens

INTRODUCTION

Infectious diseases are well known to cause productivity losses in the swine industry (Lee et al., 2012; Lewis et al., 2007), motivating the investigation of traits related to disease resilience for genetic selection. It has been shown that there is genetic variation in total antibody (Ab) response to swine pathogens, such as porcine reproductive and respiratory syndrome (PRRS) virus (PRRSV) (Serão et al., 2014; Hess et al., 2018; Abella et al., 2019). Selection of more resilient animals could decrease the losses caused by the decreased performance of animals exposed to pathogens.

A common limitation for genetic selection of improved host response to infectious pathogens is that these traits are not expected to be expressed in the nucleus, where selection is performed, because of high biosecurity (Faust et al., 1993). Disease traits are usually expressed at the commercial level, such as during the acclimation or introduction period of gilts into a commercial herd, when they are exposed to several pathogens (Serão et al., 2016). Therefore, one alternative would be to identify genetically superior animals in their ability to overcome the pathogen challenge at the commercial level and use this information to select animals at the nucleus level.

The interest for improved performance in the presence of a wide range of infectious pathogens has led to several studies showing genetic variation for resilience-related traits in livestock (Clapperton et al., 2009; Engle et al., 2014; Serão et al., 2014). More specifically, it has been shown that host genetics plays a role in differences in Ab response in swine (Flori et al., 2011). For instance, pigs selected for a higher immune response after 8 generations presented higher Ab response to various antigens and grew faster than pigs with a lower immune response (Mallard et al., 1998). For PRRSV, the major viral pathogen impacting swine production, moderate to high heritability (h^2 = 0.38–0.46) has been reported for Ab response to this disease in commercial gilts (Serão et al., 2016; Sanglard et al., 2020). Dunkelberger et al. (2017) reported a high h^2 for PRRS viral load (0.61) but not for porcine circovirus type 2 (PCV2; 0.09). In their study, pigs were vaccinated to PRRSV and co-infected with field strains of both viruses. However, other common pathogens, such as influenza A virus of swine (IAV), *Mycoplasma hyopneumoniae* (MH), and *Actinobacillus pleuropneumoniae* (APP) are also involved in the porcine respiratory disease complex (Thacker et al., 1999, 2001; Bates et al., 2009), which is one of the main causes of economic losses in the swine industry. Nonetheless, host-genomic studies of animals exposed to these pathogens are not available in the literature.

Studies have shown that genomic selection using estimates of marker effects on crossbred animals from the commercial level is a good alternative to increase response to selection and, consequently, the performance of commercial animals (Dekkers, 2007). Serão et al. (2016) and Sanglard et al. (2020) showed that Ab response to PRRSV associated with genomic information collected at the commercial level can be used to predict breeding values for Ab response to PRRSV with moderate to high accuracy in crossbred sows. Moderate accuracy of prediction of breeding values for Ab response has also been reported for Newcastle disease and avian influenza virus in chickens (Liu et al., 2014). These results support the possibility of using Ab response for selection for resilience in commercial animals. However, genomic analyses of many common infectious pathogens in pigs are lacking in the literature. Therefore, the objective of this study was to investigate the genetic basis of Ab response to common infectious pathogens in swine production in replacement gilts during acclimation raised in commercial farms [same population as described in Serão et al. (2016)] by (1) estimation of co-variance components of Ab response; (2) identification of quantitative trait loci (QTL) for Ab response; and (3) assessment of the genomic prediction accuracies for Ab response. In order to maximize the robustness and relevance of results to the field, the data collected in this study was by design highly variable, representing data from 23 commercial farms across Canada, with different gilt acclimation and vaccination protocols.

MATERIALS AND METHODS

All procedures for the experiment were performed according to the Canadian Council on Animal Care (2020) base on the Guide to the Care and Use of Experimental Animals, vol. 1, Olfert ED, Cross BM (Ottawa, ON, Canada).

Animals

The datasets used in this study were provided by a consortium of pig breeding companies (genetic suppliers) that operate in Canada (PigGen Canada)[1]. The data included 2,848 commercial F1 (Landrace × Large White) replacement gilts sourced from 17 high-health multipliers from seven breeding companies, all members of PigGen Canada. Replacement gilts were introduced to 23 commercial farms with historical occurrences of natural disease challenges, following the standard acclimation procedures of each farm, including each farm's routine vaccination protocols, in contemporary groups (CG) of 10 to 63 animals (27 ± 15 animals per CG), with a total of 107 CG. The summarized information of the vaccination protocols provided by each farm is provided in **Table 1**. Time of vaccination differed between farms and occurred during entry to the commercial level, during quarantine, during acclimation, in mid-lactation, after weaning, or at alternate parities. Records on administration and dates of vaccination were not available. There were also no records on whether animals were naturally infected with any of those pathogens. A full description of the dataset can be found in Serão et al. (2016).

Abbreviations: Ab, antibody; AGP, accuracy of genomic prediction; APP, *Actinobacillus pleuropneumoniae*; CG, contemporary groups; GC, gene call; GRM, genomic relationship matrix; GWAS, genome-wide association studies; h^2, heritability; IAV, influenza A virus of swine; MH, *Mycoplasma hyopneumoniae*; P1, parity 1; P2, parity 2; PCV2, porcine circovirus type 2; PRRS, porcine reproductive and respiratory syndrome; PRRSV, PRRS virus; QTL, quantitative trait loci; r_g, genetic correlation; SCD, seroconverted datasets; SSC, chromosomes; TGVM, total genetic variance explained by the markers.

[1] http://www.piggencanada.org/

TABLE 1 | Counts and reported vaccination protocols[1] for contemporary groups (CG) by genetic supplier (GS).

GS	MH	CH	CG (n)	N	Qt	PRRSV Vx	IAV Vx	MH Vx
1	1	1	4	134	Yes	Yes	Yes	Yes
		2	3	99	Yes	Yes	Yes	No
	2	3	6	121	Yes	No	No	Yes
	3	4	5	110	Yes	Yes	Yes	Yes
2	4	5	9	120	No	Yes	No	Yes
	5	6	5	90	No	Yes	Yes	Yes
		7	4	47	Yes	No	No	No
	6	8	4	83	Yes	No	No	Yes
3	7	9	9	417	Yes	Yes	Yes	Yes
	8	10	3	120	Yes	No	Yes	Yes
4	9	11	4	133	Yes	No	Yes	Yes
		12	5	92	Yes	No	No	Yes
	10	13	5	150	Yes	No	Yes	Yes
5	11	14	3	101	Yes	Yes	Yes	Yes
		15	4	97	No	No	No	Yes
	12	16	5	131	No	Yes	Yes	Yes
	13	17	4	120	Yes	Yes	Yes	Yes
6	14	18	7	174	No	Yes	Yes	Yes
		19	2	50	No	Yes	Yes	No
	15	20	3	75	No	Yes	Yes	Yes
		21	3	74	Yes	Yes	Yes	Yes
7	16	22	4	159	Yes	No	No	No
	17	23	4	151	Yes	No	No	Yes

[1]*Pathogens potentially vaccinated for at each CG; GS, recoded ID for genetic supplier; MH, recoded ID for multiplier herd; CH, recoded ID for commercial herd; CG (n), number of contemporary groups; N, number of gilts per CG; Qt, quarantine, PRRSV Vx, CG vaccinated to Porcine Reproductive Respiratory Syndrome Virus; IAV Vx, CG vaccinated to Influenza A Virus; MH Vx, CG vaccinated to Mycoplasma hyopneumoniae.*

Phenotypic Data

Blood samples were collected from all replacement gilts at four time-points: when entering the commercial herd (Entry), after the acclimation period (Post-acclimation), and during parity 1 (P1), and parity 2 (P2). The average time (± standard deviation) between Entry and Post-acclimation sampling was 40.8 ± 16.3 days, ranging from 29 to 88 days. Sample collection for P1 and P2 occurred between farrowing and weaning, but the exact date of collection was not available. Animals were not deliberately infected with any of the pathogens in the study; therefore, the level of exposure (if present) to these antigens was unknown and was likely variable, which further supports this study as a model for evaluating the overall genetic basis of response to pathogens in commercial swine populations.

Antibody response to PRRSV, IAV, MH, PCV2, and 8 serotypes of APP (APP1, 2, 3, 5, 7, 10, 12, and 13) were measured as sample-to-positive (S/P; PRRSV, MH, PCV2, and APP) or sample-to-negative (S/N; for IAV only) ratios. Antibody measurements were performed using ELISA (IDEXX PRRS X3, IDEXX Laboratories Inc., Westbrook, United States) for PRRSV, LC-LPS ELISA, developed by the Groupe de Recherche sur les Maladies Infectieuses en Production Animale (GREMIP; Université de Montréal, Montreal, Canada) for all serotypes of APP, IDEXX ELISA for MH; IDEXX Influenza A virus Ab test kit® for IAV, and INgezim CIRCO IgG® for PCV2. All analyses were performed at GREMIP. Since antibody response to IAV was the only pathogen measured in the opposite direction (S/N instead of S/P), we recalculate this measurement as S/P for analyses to facilitate the interpretation of the results. Two summaries of Ab response traits were also created: (1) APP_{mean}, as the mean of S/P for all APP serotype; and (2) MEAN, as the mean of standardized Ab response (S/P ratio divided by the standard deviation) to all infectious pathogens, to summarize the overall Ab response.

Following Serão et al. (2016), five seroconverted datasets (SCD) were created for each time point (Entry, Post-acclimation, P1, and P2) and each pathogen (IAV, MH, PCV2, and APP) based on ≥0, ≥25, ≥50, ≥75, and 100% of seroconverted animals within a CG. For seroconversion, the following diagnostic thresholds were used: S/P ≥ 0.4 (MH, APP, and PRRSV), S/N ≤ 0.6 (IAV), and S/P > 0 (PCV2). Each pathogen at each time with a proportion of positive animals was considered a separate trait. The numbers of animals and mean Ab responses for each dataset are presented in **Table 2**. Datasets with less than 500 animals were not analyzed.

Genotypic Data

A total of 316 animals were genotyped with the Illumina PorcineSNP BeadChip (Illumina Inc., San Diego, United States) at Delta Genomics (Livestock Gentec, Edmonton, Canada), of which 48, 1710, and 1857 were genotyped using versions 60 K v.2, 60 K v.2B, and 80 K, respectively (Illumina Inc., San Diego, United States). These versions include 62163, 61565, and 68528 single-nucleotide polymorphisms (SNP), respectively. A total of 42145 SNP was common to all three versions, and 38191 SNP that passed quality controls were used for the genomic analyses, based on gene call (GC) score >0.5, animal call rate of 80%, and genotype call rate of 99.48%. GC scores measure the quality of the genotyping call for each genotyped SNP within an animal. Of the 3516 genotyped animals, 668 were parents of the gilts and did not have Ab response phenotypes. Still, we kept their genotype information in the dataset to make use of their genomic relationships. A full description of the genotypic data can be found in Serão et al. (2016).

Genetic Parameters

An animal model with a genomic relationship matrix (GRM) from the first method described by VanRaden (2008) was used to estimate co-variance parameters using the following model:

$$y_{ij} = \mu + CG_i + u_{ij} + e_{ij}$$

where y_{ij} is the phenotype of the j^{th} individual of the i^{th} CG; $\mu$is the intercept; $CG_i$is the effect of the i^{th} level of the fixed effect of CG; $u_{ij}$is the breeding value of the j^{th} individual of the i^{th} CG, with$u \sim N(0, GRM\sigma_u^2)$, where $\boldsymbol{GRM}$ is the genomic relationships matrix based on 38191 SNP and 3516 individuals, with SNP genotypes coded as 0/1/2 and averaged and centered within multiplier herd; and e_{ij} is the random residual effect, with$e \sim N(0, I\sigma_e^2)$, where $\boldsymbol{I}$ is the identity matrix. The $\boldsymbol{GRM}$

TABLE 2 | Number of individuals and mean of antibody response across pathogens[1], time points, and seropositive (%) datasets.

Traits[2]	%[3,4]	Entry		Post-acclimation		Parity 1		Parity 2	
		N[4] (positive)	Mean (SD)	N[5] (positive)	Mean (SD)	N[5] (positive)	Mean (SD)	N[5] (positive)	Mean (SD)
IAV	0	2478 (0.49)	0.65 (0.34)	2354 (0.68)	0.51 (0.32)	1968 (0.82)	0.37 (0.29)	1280 (0.88)	0.30 (0.24)
	25	1537 (0.76)	0.47 (0.28)	1907 (0.83)	0.41 (0.26)	1814 (0.88)	0.33 (0.24)	1220 (0.92)	0.27 (0.2)
	50	1351 (0.82)	0.43 (0.26)	1786 (0.86)	0.40 (0.25)	1693 (0.92)	0.30 (0.21)	1220 (0.92)	0.27 (0.2)
	75	877 (0.90)	0.37 (0.22)	1463 (0.90)	0.37 (0.24)	1543 (0.94)	0.28 (0.2)	1132 (0.94)	0.26 (0.19)
MH	0	2479 (0.37)	0.50 (0.62)	2355 (0.65)	0.87 (0.73)	1969 (0.78)	0.97 (0.65)	1280 (0.77)	1.02 (0.67)
	25	1147 (0.76)	0.95 (0.64)	1927 (0.78)	1.04 (0.70)	1684 (0.90)	1.12 (0.58)	1081 (0.90)	1.18 (0.60)
	50	935 (0.84)	1.07 (0.63)	1643 (0.85)	1.15 (0.69)	1637 (0.92)	1.14 (0.57)	1023 (0.93)	1.22 (0.58)
	75	656 (0.94)	1.29 (0.59)	1074 (0.96)	1.41 (0.64)	1410 (0.95)	1.22 (0.55)	946 (0.95)	1.26 (0.56)
	100	–		564 (1.00)	1.73 (0.56)	622 (1.00)	1.49 (0.52)	503 (1.00)	1.48 (0.51)
PCV2	0	2387 (0.84)	2967 (7823)	2329 (0.94)	9121 (26210)	1912 (0.94)	5239 (22556)	1257 (0.97)	2461 (9776)
	25	2346 (0.85)	3017 (7881)	2292 (0.95)	9268 (26395)	1912 (0.94)	5239 (22556)	1257 (0.97)	2461 (9776)
	50	2052 (0.91)	3403 (8347)	2202 (0.97)	9636 (26865)	1861 (0.96)	5374 (22847)	1257 (0.97)	2461 (9776)
	75	1782 (0.95)	3847 (8866)	2094 (0.99)	10056 (27458)	1772 (0.97)	5619 (23387)	1239 (0.98)	2492 (9843)
	100	955 (1.00)	5471 (11596)	1760 (1.00)	11703 (29639)	1221 (1.00)	7592 (27725)	908 (1.00)	3140 (11375)
PRRS	0	2454 (0.03)	0.07 (0.24)	2342 (0.81)	1.19 (0.72)	2022 (0.61)	0.94 (0.9)	1378 (0.56)	0.78 (0.79)
	25	–	–	2053 (0.93)	1.36 (0.61)	1713 (0.69)	1.05 (0.9)	984 (0.72)	0.98 (0.8)
	50	–	–	1886 (0.95)	1.4 (0.57)	1020 (0.80)	1.25 (0.93)	549 (0.84)	1.18 (0.81)
	75	–	–	808 (0.98)	1.45 (0.53)	–	–	–	–
APP1	0	2478 (0.06)	0.25 (0.17)	2354 (0.08)	0.29 (0.17)	1969 (0.05)	0.26 (0.08)	1280 (0.03)	0.25 (0.06)
APP2	0	2479 (0.04)	0.23 (0.08)	2354 (0.09)	0.27 (0.09)	1968 (0.11)	0.26 (0.11)	1280 (0.13)	0.25 (0.12)
APP3	0	2478 (0.01)	0.26 (0.05)	2354 (0.03)	0.28 (0.06)	1968 (0.14)	0.32 (0.15)	1280 (0.15)	0.31 (0.16)
APP5	0	2477 (0.02)	0.22 (0.06)	2354 (0.02)	0.24 (0.06)	1968 (0.04)	0.24 (0.08)	1280 (0.04)	0.23 (0.08)
APP7	0	2479 (0.01)	0.16 (0.04)	2354 (0.01)	0.17 (0.05)	1968 (0.10)	0.23 (0.16)	1280 (0.12)	0.24 (0.18)
APP10	0	2478 (< 0.01)	0.19 (0.05)	2354 (< 0.01)	0.2 (0.05)	1968 (0.02)	0.23 (0.08)	1280 (0.03)	0.22 (0.07)
APP12	0	2478 (0.03)	0.21 (0.08)	2354 (0.03)	0.24 (0.09)	1968 (0.21)	0.32 (0.19)	1280 (0.18)	0.31 (0.19)
APP13	0	2478 (0.01)	0.23 (0.05)	2354 (0.01)	0.24 (0.05)	1967 (0.04)	0.25 (0.09)	1281 (0.04)	0.26 (0.08)
APP_{mean}	0	2479 (0.04)	0.22 (0.04)	2354 (0.04)	0.24 (0.05)	1969 (0.12)	0.26 (0.07)	1281 (0.05)	0.26 (0.09)
MEAN	0	2505	2.57 (0.59)	2364	2.68 (0.49)	2020	1.96 (0.52)	2048	2.49 (1.05)

[1]Antibody response to Porcine Reproductive and Respiratory Syndrome is not being shown as it has been previously published by Serão et al. (2016). [2]Traits: IAV, antibody response to influenza A virus; MH, antibody response to Mycoplasma hyopneumoniae; PCV2, antibody response to porcine circovirus type 2; APP, antibody response to Actinobacillus pleuropneumoniae from different serotypes (represented by the different numbers; APP_{mean}, mean of antibody response to all serotypes of APP; MEAN, mean of standardized antibody response to all infectious pathogens. [3]Minimum percentage of seropositive animals within a contemporary group (% seroconverted data). [4]% seroconverted data were used when the total number of animals were >500. [5]N, Total number of animals (proportion of positive animals based on the diagnostic thresholds of: SIV ≤ 0.6; MH, APP, and PRRS ≥ 0.4; PCV2 > 0).

was created separately for pigs from each breeding company, and relationships between breeding companies were assumed to be zero. The fixed effect of *CG* was included in the model to account for environmental effects due to the farms and other possible environmental effects confounded within the farms (i.e., the timing of PRRSV exposure, if occurred), and not for comparisons between CG.

Bivariate analyses were performed between Ab response to two pathogens within a time-point, and between two time-points for the same pathogen. Co-variance components were estimated for each of the %SCD and were used to estimate heritabilities (h^2) and genetic correlations(r_G). The same fixed and random effects as used for the univariate model were also used for the bivariate analyses.

Genome-Wide Association Studies (GWAS)

Genome-wide association studies (GWAS) were performed using Bayesian variable selection methods (Habier et al., 2011) using GenSel 4.4 (Fernando and Garrick, 2009). The model used in these analyses included an intercept, the fixed effect of *CG*, and the random allele substitution effects of SNP. First, a BayesC0 analysis, a method that fits all SNPs simultaneously in the model, assuming each variance across SNPs, was performed to estimate the variance components for subsequent analyses. Then, BayesCπ was used to estimate the proportion of SNP with zero effect (π). The estimate of π was 0.99 for all datasets. The final GWAS were based on the BayesB method, with π equal to 0.99. One-Mb SNP windows that explained at least 1% of total genetic variance explained by the markers (TGVM) and that had a posterior probability of inclusion (PPI) greater than 0.7 (Garrick and Fernando, 2013) were considered significantly associated with the trait analyzed. The order of the SNP was based on the *Sus scrofa* 11.1 assembly. Candidate genes within 1-Mb in each direction of the identified SNP were identified using Ensembl BioMart (Kinsella et al., 2011).

Genomic Prediction

Genomic prediction was performed using BayesC0, BayesB, and BayesC (Habier et al., 2011). Analyses were performed for each trait and for each %SCD using the same models as described for GWAS in GenSel 4.4 (Fernando and Garrick, 2009).

Seven-fold cross-validation was used, in which data from six breeding companies were used for training and data from the remaining breeding company for validation. This was repeated seven times until all breeding companies were used once for validation. Thus, the relationships between folds (i.e., between genetic backgrounds) were decreased and those within folds were increased. These analyses were performed for each dataset. Accuracy of genomic prediction (AGP) was defined as the correlation between genomic estimated breeding values and phenotypes adjusted for estimates of fixed effects divided by the square root of the estimate of h^2 using the whole dataset. For the seven-fold cross-validation, the accuracy was weighted by the number of individuals in the validation dataset.

RESULTS

Phenotypic Data

The proportion of positive animals in each dataset is shown in **Table 2**. For IAV, MH, and PRRSV, most (i.e., >50%) of the CG had at least one seropositive animal after Post-acclimation and during P1 and P2, while for PCV2, most of the CG were seropositive at entry. Animals came from a high-biosecurity level (multiplier herd) and entered commercial farms where they were mixed with other pigs on the farm and had contact with diverse pathogens. Therefore, the lower proportion of seropositive animals at entry was expected. However, while for PRRSV the higher proportion of CG with at least one seropositive animal occurred at Post-acclimation, for IAV, MH, and PCV2, the proportion of CG with at least one seropositive animal was higher at P1 and P2. For APP, the proportion of CG with at least one seropositive animal was low at all time-points (0 to 21% of CG). There is little information on the actual prevalence of APP infection in the literature; however, a prevalence of 11% for pigs showing pleuritis in Canada has been reported (Amory et al., 2007), which may reflect the low incidence of this pathogen across these farms. There was also evidence of co-exposure during different time-points of the study (**Figure 1**). At entry, co-exposure (natural infection or vaccination) with IAV, MH, and PCV2 was the most common (47.9%). After the acclimation period, PRRSV became more prevalent in the co-exposure and 71.8% of CG were seropositive for IAV, MH, PCV2, and PRRSV. This co-exposure persisted to P1 (76.0%) and P2 (64.9%). If we consider only the CG with all the animals seroconverted (i.e., 100% SCD), PCV2 only or co-exposure with PCV2 and PRRSV were the most common (≥16.8%) at all time-points.

Genetic Parameters

Heritability estimates (h^2) for each trait for each dataset are presented in **Table 3**. For IAV, MH, and PCV2, h^2 estimates for these traits were low to moderate, ranging from $<0.01 \pm 0.05$ (PCV2 at P1) to 0.76 ± 0.07 (PCV2 at entry, 100% SCD). In general, h^2 estimates numerically increased for datasets with a higher proportion of seropositive animals. This trend was more evident at entry. In contrast, APP serotypes had overall greater h^2 estimates; APP10 showed the highest average h^2 estimate (∼0.25), peaking at P2 ($h^2 = 0.38 \pm 0.08$), while APP2 had overall the lowest estimate (∼0.06). Among all traits analyzed, APP_{mean} had the highest average h^2 estimate, ranging from 0.29 ± 0.06 at P1 to 0.55 ± 0.07 at P2. For overall Ab response (MEAN), h^2 estimates ranged from low (0.08 ± 0.05; P2) to moderate (0.39 ± 0.5; post-acclimation). Overall, results indicate that selection for Ab response to some of these infectious pathogens is possible, depending on the time of collection.

Estimates of additive genetic variance (σ_u^2) are presented in **Figure 2**. Similar to the h^2 estimates for IAV, MH, and PCV2, estimates of σ_u^2 numerically increased as the proportion of positive animals increased in the dataset (**Figure 2A**). For APP, the estimate of σ_u^2 was numerically higher during P2. On average, APP2 had the lowest estimates of σ_u^2 and APP_{mean}, the highest (**Figure 2B**).

Estimates of phenotypic and genetic correlations are shown in **Figure 3**. For all time-points, phenotypic correlations (**Figure 3**; upper diagonal) were generally low. The low phenotypic correlation associated with a low genetic correlation may indicate a low environmental correlation as well. Cases of low phenotypic correlation associated with a moderate to high genetic correlation may indicate a negative environmental correlation. Due to the low h^2 of Ab response to the pathogens studied, we are reporting r_G estimates for the %SCD that had the highest h^2 within each time-point and for APP_{mean}. Estimates for each serotype of APP are available in **Supplementary Figure 1**. In summary, among APP, estimates of r_G were positive and moderate to high, ranging from 0.20 ± 0.19 to 0.99 ± 0.05. Between IAV and APP, estimates of r_G were negative at entry and post-acclimation. For the %SCD (**Figure 3**; lower diagonal), estimates of r_G of IAV with MH, PCV2, and PRRSV were consistently moderate to high and positive at all time-points, except for IAV and PCV2 at entry. Between IAV and APP_{mean}, the estimate of r_G was moderate and negative at entry and post-acclimation but not at P2 (positive and low). Between PCV2 and PRRSV, the estimate of r_G was low to moderate and negative at all time-points. The estimate of r_G between APP_{mean} and PRRSV was positive at all time-points. Overall, $r_G$estimates of APP_{mean} with all pathogens were consistent across time-points but among the other pathogens they were more variable, suggesting that genetic changes in one Ab trait may result in complex correlated responses to selection.

Estimates of r_G between time-points for a given pathogen are presented in **Table 4**. All estimates were positive and generally moderate to high for all traits, especially between consecutive time-points. APP1 showed the highest estimates of r_G between time points, ranging from 0.71 ± 0.17 between entry and P1 to 0.99 ± 0.08 between P1 and P2. On average, APP_{mean} had the highest estimate of r_G (0.77) compared to IAV (0.60), MH (0.62), PCV2 (0.51), and MEAN (0.61). Overall, these results indicate that selection for increased Ab response at one time-point would increase Ab response at all time-points.

Genome-Wide Association Studies (GWAS)

Genomic regions that explained at least 1% of TGVM and that had a PPI > 0.7 are presented in **Table 5**. Within each

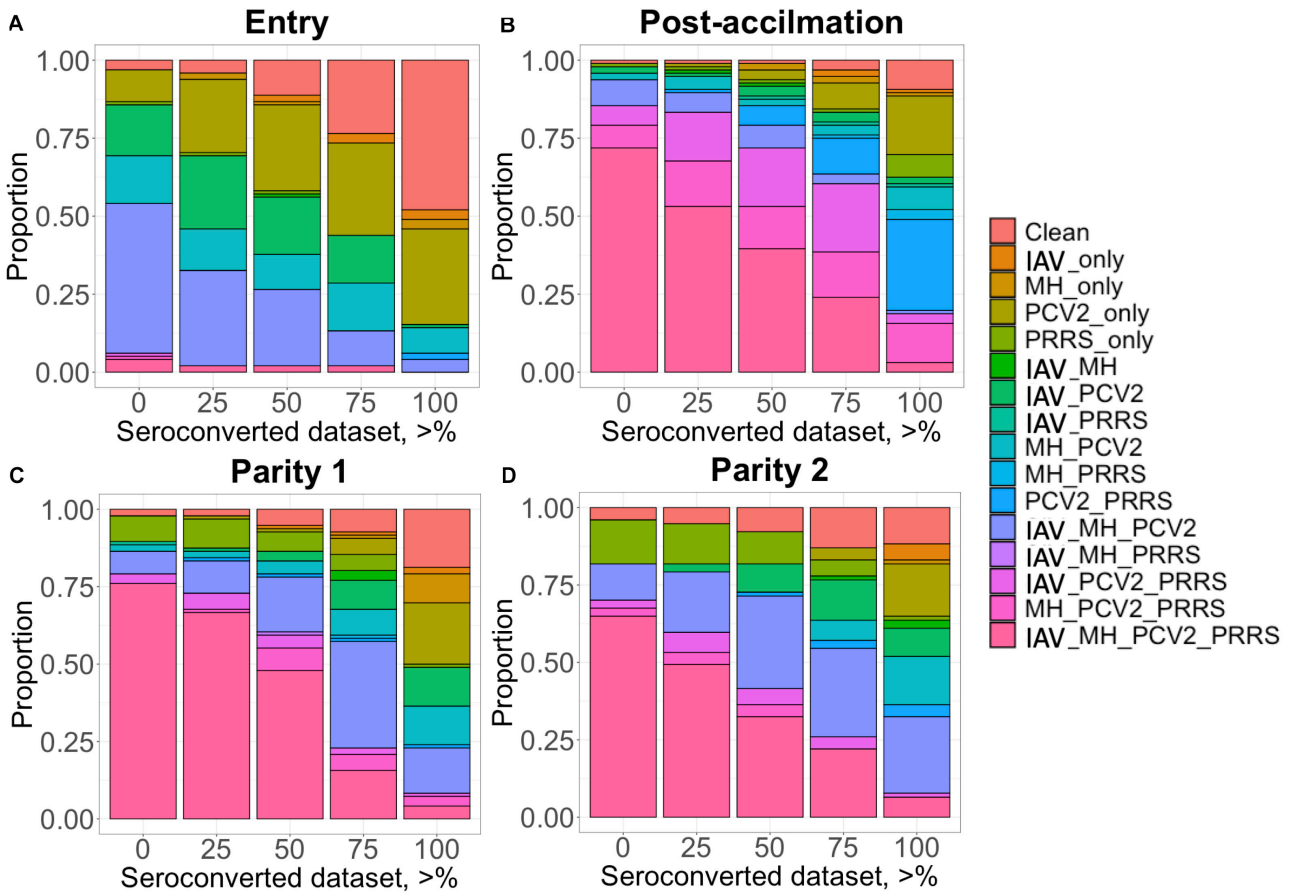

FIGURE 1 | Proportion (*y*-axis) of contemporary group (CG) considered seropositive when a minimum percentage of individuals within this CG is positive (*x*-axis) for each time point: **(A)** Entry; **(B)** post-acclimation; **(C)** at Parity 1, and **(D)** at Parity 2. The colors represent the status of the individuals: clean, when free of any infectious diseases; IAV, influenza A virus; MH, *Mycoplasma hyopneumoniae;* PCV2, porcine circovirus type 2; and PRRS, Porcine Reproductive and Respiratory Syndrome; and all possible combinations of these infectious diseases.

analysis window, we selected the SNP that explained most of the TGVM and fitted the SNP individually in a total of 1-Mb window to estimate the genetic variance explained by that specific SNP (**Supplementary Table 1**). Several QTL were identified for APP serotypes, with most of them at entry and post-acclimation. Many of the identified regions described below included several candidate genes. For APP3 at entry, we identified 4 QTL on *Sus scrofa* chromosomes (SSC) 8, 9, 12, and 14 (2 Mb). The same QTL on SSC 14 was identified at post-acclimation. For APP5 at entry, 6 QTL on SSC 1, 4, 6, 9, and 13 and for at post-acclimation 5 QTL were located on SSC 2, 14, 6, and 8. For APP7 at post-acclimation, 2 QTL were identified on SSC 6 and 14. For APP 10 at entry, 1 QTL was identified on SSC 16. For APP13 at entry, there were 2 QTL on SSC 1 and 9; at post-acclimation, 2 QTL on SSC 14 and 16; and at P2, 2 QTL on SSC 6 and 7. For APP_{mean}, there was 1 QTL on SSC 6 at entry; 3 QTL on SSC 7, 11, and 19 at post-acclimation; and 2 QTL at P2 on SSC 6 and 12. No QTL was identified for the other traits. The region on SSC14 (2 Mb) was associated with four different serotypes at entry and post-acclimation, suggesting that this is a key pleiotropic region associated with Ab response to APP.

Genomic Prediction Accuracies

Genomic prediction results are presented in **Figure 4** for MH, IAV, and PCV2, using BayesB. AGP for IAV were low at all time points and all %SCD, except for 0% SCD at P1, ranging from −0.16 (post-acclimation) to 0.42 (P1). For MH, AGP were also low, ranging from −0.09 (post-acclimation) to 0.28 (P2). In contrast, PCV2 had the highest AGP among all pathogens at entry and post-acclimation, reaching 0.60 and 0.64, respectively. For PCV2 at P2, AGP were very low and negative, ranging from −0.55 (0% SCD) to −0.40 (100% SCD). Among methods evaluated, BayesB and BayesC had slightly higher accuracy than BayesC0. All results are compiled in **Supplementary Table 2**.

For all APP, AGP were low at all time-points (**Figure 5**). At each point, average AGP for APP using BayesB were 0.04 at entry, and 0.10 at post-acclimation, P1, and P2. Among the APP, APP7 showed the highest AGP (up to 0.31 at post-acclimation) and APP10, the lowest (up to −0.09 at entry). For APP_{mean}, AGP ranged from 0.10 (P1 and P2) to 0.16 (post-acclimation).

TABLE 3 | Heritability estimates[1] of antibody response to common infectious pathogens[2] in pigs by time-point.

Traits[3]	%[4]	Entry	Post-accl[5]	Parity 1	Parity 2
IAV	0	0.07 (0.04)	0.05 (0.04)	0.02 (0.04)	0.15 (0.07)
	25	0.11 (0.06)	0.08 (0.05)	< 0.01 (0.04)	0.14 (0.07)
	50	0.18 (0.07)	0.10 (0.05)	0.05 (0.05)	0.14 (0.07)
	75	0.46 (0.10)	0.09 (0.05)	0.07 (0.05)	0.01 (0.05)
MH	0	0.19 (0.05)	0.15 (0.04)	0.17 (0.05)	0.10 (0.06)
	25	0.27 (0.08)	0.18 (0.05)	0.19 (0.05)	0.12 (0.07)
	50	0.27 (0.09)	0.19 (0.06)	0.21 (0.06)	0.11 (0.07)
	75	0.31 (0.11)	0.20 (0.07)	0.19 (0.06)	0.13 (0.07)
	100	0.31 (0.17)	0.21 (0.10)	0.12 (0.10)	0.14 (0.11)
PCV2	0	0.10 (0.04)	0.13 (0.05)	< 0.01 (0.04)	0.02 (0.03)
	25	0.10 (0.04)	0.13 (0.05)	< 0.01 (0.04)	0.02 (0.03)
	50	0.11 (0.05)	0.13 (0.05)	< 0.01 (0.04)	0.02 (0.03)
	75	0.15 (0.06)	0.13 (0.05)	< 0.01 (0.04)	0.02 (0.03)
	100	0.76 (0.07)	0.02 (0.04)	< 0.01 (0.05)	0.02 (0.04)
APP1	0	0.29 (0.05)	0.16 (0.04)	0.14 (0.05)	0.30 (0.07)
APP2	0	0.13 (0.04)	0.11 (0.04)	< 0.01 (0.04)	0.01 (0.05)
APP3	0	0.25 (0.04)	0.27 (0.05)	0.10 (0.04)	0.14 (0.06)
APP5	0	0.22 (0.04)	0.30 (0.05)	0.03 (0.04)	0.10 (0.06)
APP7	0	0.10 (0.04)	0.40 (0.05)	< 0.01 (0.01)	0.25 (0.07)
APP10	0	0.21 (0.04)	0.24 (0.05)	0.17 (0.05)	0.38 (0.08)
APP12	0	0.22 (0.04)	0.27 (0.05)	0.22 (0.05)	0.19 (0.07)
APP13	0	0.25 (0.04)	0.24 (0.05)	0.15 (0.05)	0.31 (0.07)
APP_{mean}	0	0.37 (0.05)	0.38 (0.05)	0.29 (0.06)	0.55 (0.07)
MEAN	0	0.32 (0.05)	0.39 (0.05)	0.14 (0.05)	0.08 (0.05)

[1]Standard error (SE) within parenthesis. [2]Antibody response to Porcine Reproductive and Respiratory Syndrome is not being showed as it has been previously published by Serão et al. (2016). [3]Traits: IAV, antibody response to influenza A virus; M, antibody response to Mycoplasma hyopneumoniae; PCV2, antibody response to porcine circovirus type 2; APP, antibody response to Actinobacillus pleuropneumoniae from different serotypes (represented by the different numbers; APP_{mean}, mean of antibody response to all serotypes of APP; MEAN, mean of standardized antibody response to all infectious pathogens. [4]Minimum percentage of seropositive animals within a contemporary group. [5]Post-accl, post-acclimation.

When analyzing all serology traits together, the AGP for MEAN were moderate to high (**Figure 5**), ranging from 0.45 (post-acclimation) to 1.05 (P1). Overall, these results indicate that genomic prediction for Ab response is possible, but results vary among traits and time-points.

DISCUSSION

In this study, we performed genetic and genomic analyses of Ab response to common infectious pathogens in pigs (IAV, MH, PCV2, and APP) that, along with PRRSV, have been identified as the main agents causing porcine respiratory disease complex, which causes considerable economic losses in the swine industry (Thacker et al., 2001). Few studies are available in the literature regarding the genetic basis of Ab response to these pathogens, especially for IAV and APP. Genetic parameters, GWAS, and genomic prediction accuracies for PRRSV using the same population from this study have been previously reported (Serão et al., 2016). Therefore, in this study, we focused on the relationship between Ab response to PRRSV with Ab response to all other pathogens. It is important to notice that none of the animals in this experiment were artificially inoculated with any of these pathogens. Also, different types of vaccination were used in some of the farms included in this study. However, limited information was available for these, including confirmation on whether these protocols were used for the animals in this study. However, using modified live vaccines is expected to generate similar humoral immune responses to wild-type infection [example for PRRSV (Montaner-Tarbes et al., 2019)]. For the %SCD, the increase in the proportion of seroconverted animals was confounded with a decrease in sample size, and the latter has been previously shown to result in decreased AGP for Ab response to PRRSV in this population (Serão et al., 2016). Moreover, the exact day of blood sample collection for Ab response measurement is uncertain but was confounded with CG. Therefore, the effect of CG should adjust for this effect in this dataset. Other factors, such as diet, management, season, and others, were also confounded in the study. However, differences in diets are not expected to affect Ab response to pathogens and most likely would not affect the conclusions (Pujols et al., 2016; Schweer et al., 2018; Colpoys et al., 2020). Nonetheless, these potential effects were captured by including the fixed effect of CG in the model. Despite these limitations of this study, this work provides genomic analyses, including estimates of h^2 and r_G, and identified regions with the potential to be used for genomic selection for an improved immune response to pathogens in commercial gilts and sows. With the increased pressure by society for animal welfare, the industry has been motivated to investigate resilience traits. Antibody response to specific diseases could reflect the overall immune status of the individual, and although not all pathogens stimulate the similar humoral immune response, it is an important trait to be investigated. Our hypothesis is that selection for an improved Ab response to pathogens is followed by selection for better immune defense of the organism when the animal is facing diseases and, consequently, lesser disturbance of the performance in healthy challenging environments (i.e., more resilience).

Summarizing, although there were some limitations on the study, such as the lack of confirmation of whether animals were vaccinated and/or naturally infected, the existence of several confounding factors (e.g., diet, management, and others), and the lack of information on how long after the exposure the Ab was collected, the advantages prevailed over the disadvantages. The applicability of these results in commercial settings, the possibility of using crossbred performance for selection, identifying novel traits for selection of resilience in pigs, and the use of relevant pathogens common in the swine production are valuable to the pig industry.

Genetic Parameters

To the best of our knowledge, this is the first study reporting genetic parameters for Ab response to MH, PCV2, and APP in gilts and sows. Estimates of h^2 were low to moderate for all Ab responses analyzed. Estimates of h^2 for Ab response to IAV were, in general, low, except at entry (0.46), when 75% of the animals within a CG were positive. Previously,

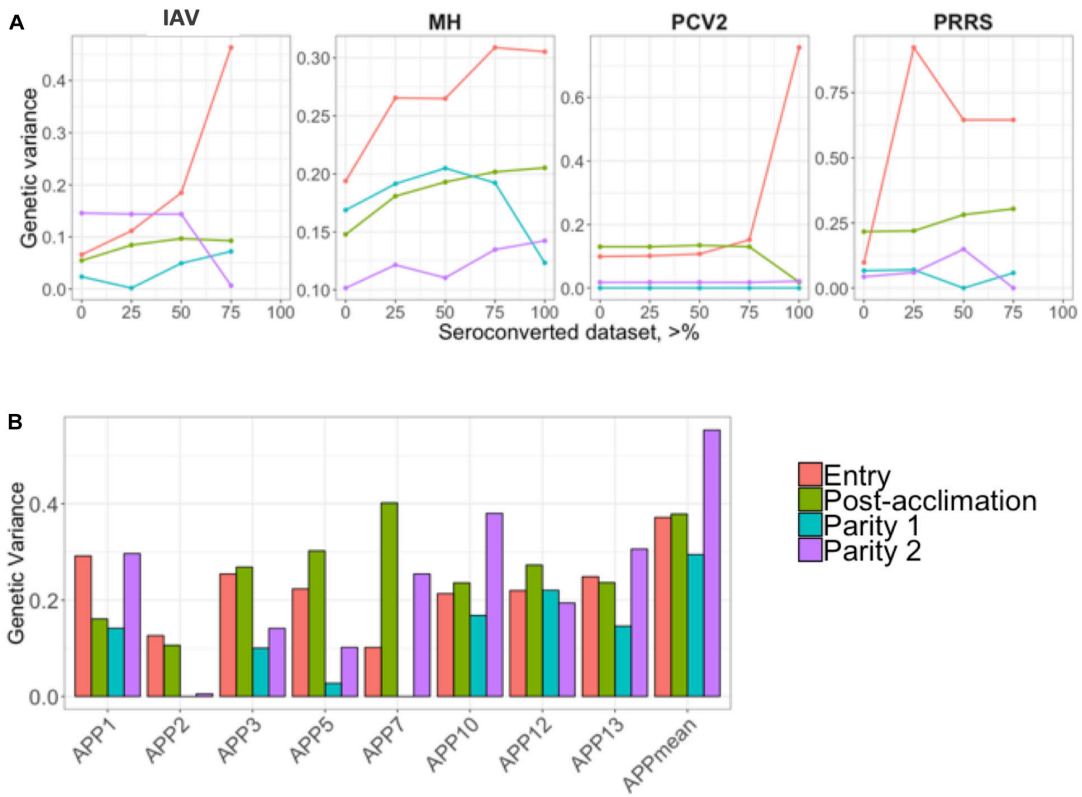

FIGURE 2 | (A) Genetic variances for the seroconverted data for influenza A virus (IAV), *Mycoplasma hyopneumoniae* (MH), porcine circovirus type 2 (PCV2), and Porcine Reproductive and Respiratory Syndrome (PRRS); and **(B)** for *Actinobacillus pleuropneumoniae* (APP). The *y*-axis represents the genetic variances, and the *x*-axis represents the minimum % of positive animals within a contemporary group **(A)** or APP **(B)**. APP_{mean} represents the average of all serotypes of APP analyzed as the phenotype. The colors represent the different time-points of antibody response collection.

an estimate of h^2 for Ab response to IAV of 0.37 has been reported in F1 (Landrace × Large White) piglets (∼76 days old) after vaccination (two doses) to IAV (Zanella et al., 2015). It is important to note, however, that our data were collected across multiple CGs. Thus, multiple confounding effects could explain the lower estimates in our study, such as the fact that not all animals in our study were positive to IAV. Our data is further complicated by the uncertain exposure of the animals, i.e., whether they were naturally infected or vaccinated, the number of vaccination doses received, and the age of the animals when Ab response was measured.

Among all individual pathogens evaluated in our study, MH, in general, presented the highest h^2 of Ab response. Okamura et al. (2012) reported an h^2 estimate of 0.23 for lesion score of mycoplasma pneumonia measured in slaughtered pigs that were experimentally inoculated with MH. In their study, 59% of the animals were considered positive based on lung lesions (Okamura et al., 2012). Their results are similar to ours, where we obtained an average estimate of h^2 of 0.20 for the 50% seroconverted dataset. In another study, also analyzing the score of mycoplasma pneumonia of swine based on lung lesions in slaughtered pigs after vaccination at 6 and 8 weeks of age, the estimate of h^2 was 0.09 (Sato et al., 2016). These two results are not directly comparable with ours since the animals were experimentally infected and the phenotype analyzed was not the same. However, these are, to the best of our knowledge, the only reports on the genetic basis of MH in pigs available in the literature.

For PCV2, h^2 estimates were low at all time-points, except for CG for which all animals were seropositive at entry. Although not analyzing the same trait, Dunkelberger et al. (2017) reported an h^2 estimate of 0.09 for viral load of PCV2 after co-natural infection and vaccination to PRRSV, where 100% was experimentally infected with both pathogens. On the other hand, Walker et al. (2018) reported a high h^2 of 0.64 for PCV2 viral load, with a major QTL located on the MHC class II region. In addition, Bates et al. (2009) reported an estimate of 0.16 for clinical score for PCV2. Although we obtained a very high h^2 estimate for PCV2 Ab response at entry including CG where all animals had seroconverted for PCV2, these results suggested that response to PCV2 is highly influenced by the environment and less determined by host genetics. Thus, in order to use PCV2 Ab response for genetic selection, all animals must be seroconverted when Ab response data is collected.

For APP, estimates of h^2 were low to moderate, ranging from <0.01 (APP2 and APP7 at P2) to 0.40 (APP7 at post-acclimation). In general, APP13 showed higher h^2 estimates (average of 0.25). Although all APP serotypes can cause the same disease, some

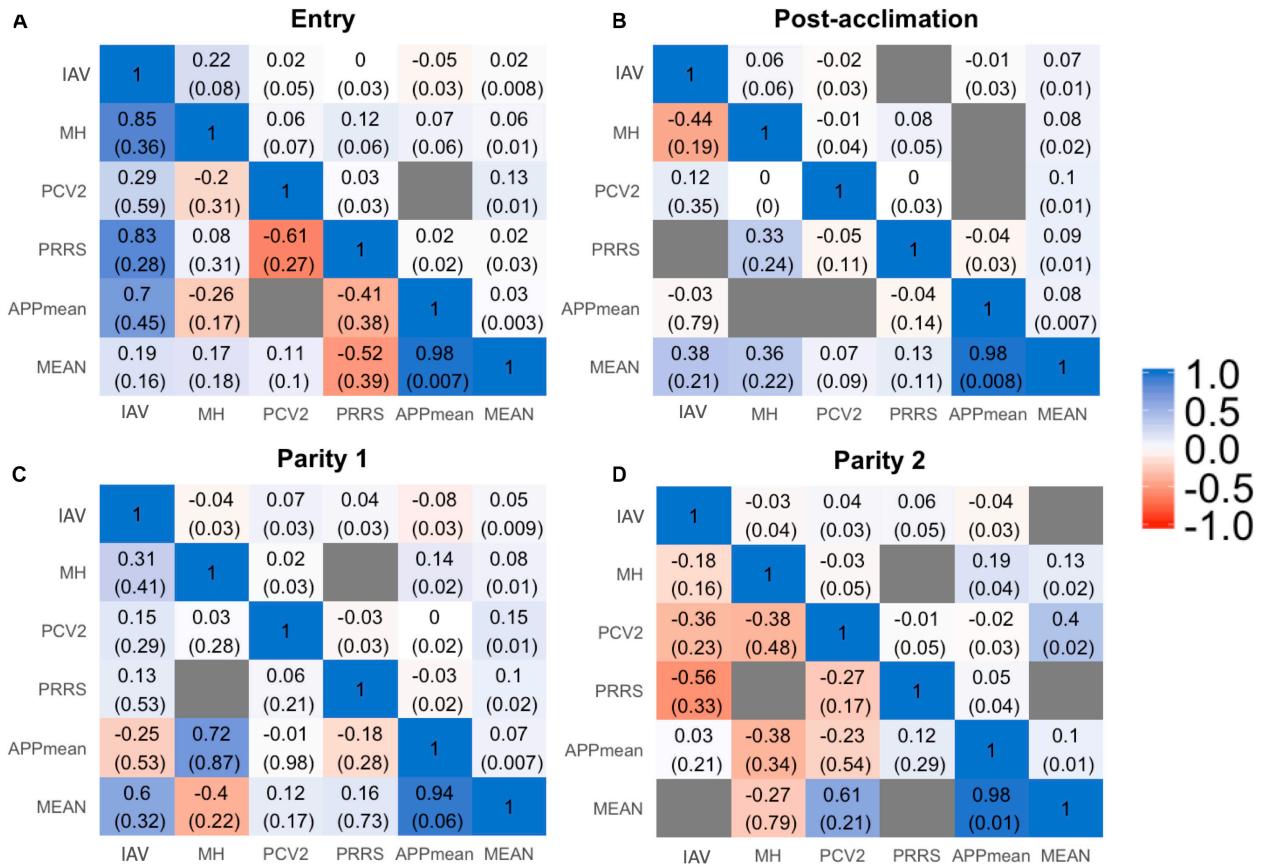

FIGURE 3 | Genetic (lower triangular) and phenotypic (upper triangular) correlation between all the traits influenza A virus (IAV), porcine circovirus type 2 (PCV2), *Mycoplasma hyopneumoniae* (MH), porcine respiratory and reproductive syndrome (PRRS), average of all *Actinobacillus pleuropneumoniae* (APP_{mean}), and overall mean of antibody response for all diseases (MEAN) at entry **(A)**, post-acclimation **(B),** Parity 1 **(C)**, and Parity 2 **(D)**. The seroconverted dataset with higher heritability within each time-point was used for these analyses. The blue color corresponds to positive correlation, the red color to negative correlation, and the gray color when the model did not converge.

TABLE 4 | Estimates[1] of genetic correlations within antibody response to common infectious pathogens in pigs between time-points[2].

Traits[3]	Entry vs. Post-accl[2]	Entry vs. P1[2]	Entry vs. P2[2]	Post-accl vs. P1[2]	Post-accl vs. P2[2]	P1 vs. P2[2]
IAV	0.75 (0.29)	0.94 (0.94)	<0.01 (0.44)	0.73 (0.36)	0.65 (0.45)	0.82 (0.43)
MH	0.68 (0.14)	0.48 (0.18)	0.19 (0.30)	0.55 (0.18)	0.63 (0.28)	1 (0.14)
PCV2	0.04 (0.28)	NC[4]	NC[4]	0.79 (0.49)	0.92 (0.5)	0.96 (1.91)
APP1	0.96 (0.07)	0.71 (0.17)	0.82 (0.13)	0.91 (0.17)	0.99 (0.12)	0.99 (0.08)
APP2	0.90 (0.22)	NC[4]	NC[4]	NC[4]	NC[4]	NC[4]
APP3	0.95 (0.06)	0.55 (0.20)	0.54 (0.19)	0.61 (0.19)	0.64 (0.16)	0.85 (0.25)
APP5	0.74 (0.08)	0.86 (0.20)	0.87 (0.20)	0.8 (0.22)	0.93 (0.15)	0.69 (0.50)
APP7	0.97 (0.08)	0.67 (0.39)	0.62 (0.26)	0.95 (0.31)	0.33 (0.16)	0.84 (0.34)
APP10	1.00 (0.07)	0.53 (0.16)	0.64 (0.14)	0.63 (0.14)	0.85 (0.11)	0.92 (0.11)
APP12	0.97 (0.05)	0.66 (0.17)	0.08 (0.23)	0.44 (0.16)	0.29 (0.2)	0.81 (0.17)
APP13	0.96 (0.07)	0.16 (0.18)	0.59 (0.14)	0.46 (0.17)	0.81 (0.12)	0.95 (0.12)
APP_{mean}	0.99 (0.04)	0.57 (0.11)	0.64 (0.09)	0.70 (0.10)	0.77 (0.07)	0.97 (0.05)
MEAN	0.91 (0.05)	0.73 (0.15)	0.52 (0.23)	0.77 (0.13)	0.32 (0.22)	0.41 (0.30)

[1]Standard error (SE) within parenthesis. [2]Post-accl, post-acclimation; P1, Parity 1; P2, Parity 2. [3]Traits: IAV, antibody response to influenza A virus; M, antibody response to Mycoplasma hyopneumoniae; PCV2, antibody response to porcine circovirus type 2; APP, antibody response to Actinobacillus pleuropneumoniae from different serotypes (represented by the different numbers; APP_{mean}, mean of antibody response to all serotypes of APP; MEAN, mean of standardized antibody response to all infectious pathogens. [4]NC, model did not converge.

TABLE 5 | Percentage of total genetic variance explained for by markers (% TGVM) within a 1-Mb window for Ab response traits with significant QTLs using a threshold of 1% TGVM and posterior probability of inclusion (PPI) of 0.70.

Traits[1]	Time-point	SSC[2]	Position (Mb)	Number of SNPs	% TGVM	PPI
APP3	Entry	8	32	19	2.5	0.86
		14	2	12	1.9	0.88
		9	121	14	1.9	0.82
		12	47	11	1.2	0.72
APP3	Post-acclimation	14	2	12	3.9	0.96
APP5	Entry	9	6	37	1.7	0.93
		13	30	13	1.6	0.74
		1	58	24	1.5	0.72
		6	97	26	1.5	0.82
		4	63	21	1.3	0.75
		1	108	14	1.3	0.70
APP5	Post-acclimation	2	129	21	2.0	0.84
		14	2	12	1.9	0.86
		6	137	15	1.5	0.82
		8	125	15	1.4	0.86
		8	11	26	1.4	0.72
APP7	Post-acclimation	6	157	8	8.8	0.94
		14	2	12	4.3	0.95
APP10	Entry	16	68	23	3.1	0.77
APP13	Entry	1	58	24	5.7	0.89
		9	121	14	3.5	0.92
APP13	Post-acclimation	14	2	12	2.0	0.74
		16	73	22	1.7	0.70
APP13	Parity 2	6	81	23	1.8	0.74
		7	92	26	1.6	0.77
APP_{mean}	Entry	6	79	20	3.5	0.84
APP_{mean}	Post-acclimation	X	113	12	6.2	0.99
		11	61	20	4.6	0.95
		7	74	16	3.0	0.72
APP_{mean}	Parity 2	6	93	13	2.7	0.80
		12	2	20	2.2	0.77

[1] Traits, antibody response to APP, Actinobacillus pleuropneumoniae from different serotypes (represented by the different numbers); APP_{mean}, mean of antibody response to all serotypes of APP. [2] SSC, Sus scrofa chromosome.

serotypes may be more virulent than others (Bossé et al., 2002) and cross-protection between serotypes is limited (Haesebrouck et al., 1997). The incidence of APP seroconversion was very low for all APP serotypes, which may explain the low h^2 of APP Ab response. Averaging the Ab response, overall APP serotypes resulted in a substantial increase in estimates of σ_u^2 and h^2, which may occur because of the variation in Ab response from each individual to each serotype. Similar to APP_{mean}, the h^2 estimate for overall MEAN was also higher than estimates of h^2 for Ab response to individual pathogens, especially at entry and post-acclimation. The higher h^2 for the overall Ab response across pathogens (MEAN) indicates that selection for this trait in sows under healthy challenge may be more successful than selection for Ab response for specific pathogens.

In general, an increase in the proportion of positive individuals in the dataset for IAV, MH, and PCV2 increased the estimate of σ_u^2 for Ab response, as expected (Bishop and Woolliams, 2010), and in an increase in the estimate of h^2. Similarly, the estimate of σ_u^2 of Ab response to APP was higher at P1 and P2 (except for APP2 and APP5), which were also the time-points with higher proportions of positive animals. Similar results were previously reported for PRRSV using samples from this same study (Serão et al., 2016). The low to high h^2 estimates indicate a great variation in the practicability of the use of Ab response traits in commercial swine populations for genetic selection purposes. Altogether, these results indicate that, in order to obtain high genetic variation for Ab response to common infectious pathogens in commercial sows, exposure to these pathogens must happen, via either vaccination and/or natural infection.

It is well known that the infection of an individual by immunosuppressive pathogens, such as PPRSV, weakens its immune system, favoring the entry or multiplication of a second pathogen. For instance, studies have shown that co-infection between some of these agents frequently intensifies the clinical signs of the diseases (Thacker et al., 2001; Dunkelberger et al., 2017). In this study, Ab response to IAV had positive moderate to high estimates of r_G with Ab response to MH and PRRSV at entry, when the proportion of positives for IAV, PCV2, and MH was higher. At post-acclimation, this relationship became negative, coinciding with the increase in the number of positives for PRRSV. A previous study has shown low interactions between MH and IAV (Thacker et al., 2001) such that co-infection with these two pathogens did not intensify the clinical signs from the other. IAV seems to be easily eliminated from the organism by neutralizing antibodies, and there is little or no interference with the activation of the immune system to fight against other pathogens (Holzer et al., 2019). However, the introduction of PRRSV caused a change in the direction of the r_G between Ab response to MH and PRRSV. Conversely, the estimate of the r_G between PRRSV and PCV2 was consistently negative. In commercial settings, co-infection with these two pathogens is common (Engle et al., 2014). Dunkelberger et al. (2017) reported a $r_G$of 0.27 (0.08) between PRRSV and PCV2 viral load in pigs that were PRRSV-vaccinated and co-infected with both pathogens, but a near-zero r_G in non-PRRSV vaccinated pigs [r_G = 0.04 (0.09)]. However, our estimates for r_G for Ab response to PCV2 and PRRSV were negative, suggesting that the immune response to one pathogen is compromised by co-infection with the other pathogen. PCV2 natural infection tends to inhibit innate immune response, which is the initial response to fight against PRRSV infection (Montaner-Tarbes et al., 2019). If infection by one pathogen weakens the immune response to another pathogen, this may cause a negative r_G of Ab responses to both pathogens. These results indicate that selecting for increased Ab response to PCV2 could result in a small reduction in Ab response to PRRSV.

At entry, the estimate of r_G of APP_{mean} was moderate to high positive with IAV and moderate negative with MH. To the best of our knowledge, no reports have shown an association between APP infection and predisposition of viral or bacterial infections, although an increase in the incidence of pleuropneumonia has been associated with

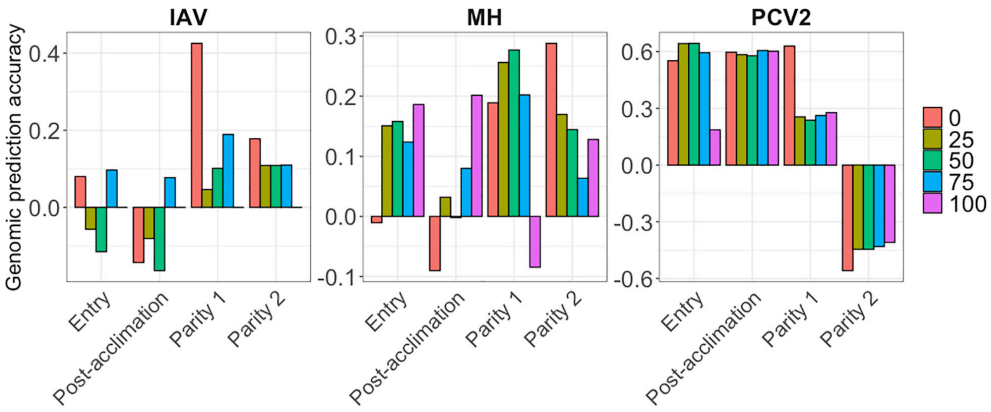

FIGURE 4 | Genomic prediction accuracies (*y*-axis) for the seroconverted data for influenza A virus (IAV), *Mycoplasma hyopneumoniae* (MH), and porcine circovirus type 2 (PCV2) using BayesB. The *x*-axis represents the different time-points of data collection. The colors correspond to the minimum % of seropositive animals within a contemporary group.

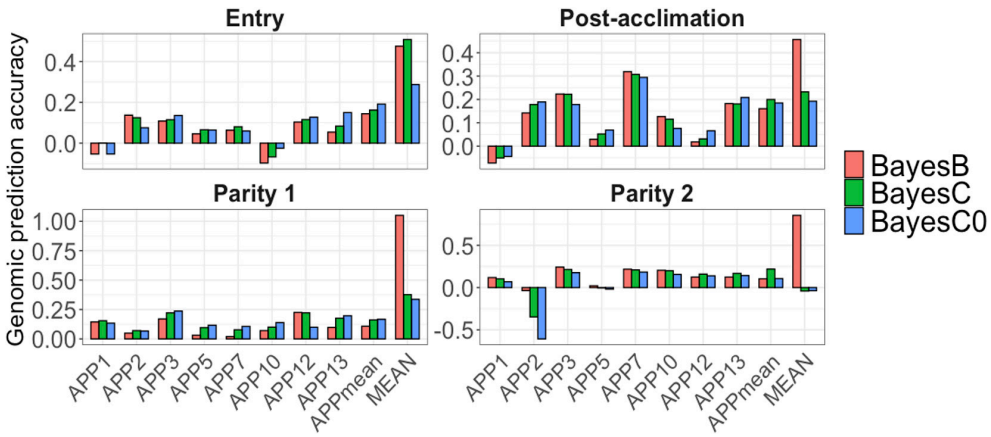

FIGURE 5 | Genomic prediction accuracies (*y*-axis) for *Actinobacillus pleuropneumoniae* (APP1, 2, 3, 5, 7, 10, 12, and 13), average of all serotypes of APP (APP_{mean}), and average of antibody responses for all diseases (MEAN). The *x*-axis represents the different time-points of data collection. The colors correspond to the Bayesian method used. Note the different scales of *y*-axis for each time-point to enhance visualization.

increased environmental stress (Bossé et al., 2002). APP is rapidly eliminated by the innate immune response with little interference in the response to other pathogens (Sato et al., 2016), which may explain the positive r_G between APP_{mean} and MH found in our study. The r_G estimate of MEAN with APP_{mean} was positive and high at all time points, which may be because the serotypes of APP composed most of the Ab responses used to calculate MEAN, in addition to Ab responses to different APP serotypes showing high positive r_G with each other. This r_G was also positive (although sometimes low) with IAV and PCV2. The r_G of MEAN with PRRSV at entry, and with MH at P1 and P2 were negative, indicating that selection for MEAN is possible but should be done with care. Genetic selection over total Ab response is expected to have a correlated response with antibody response to individual pathogens. Thus, it can affect the genetic capacity of the organism to deal with these pathogens, which should be taken in consideration when selecting for immune response-related traits.

The results discussed above were obtained using the 100% SCD for MH, IAV, and PCV2, which had the highest h^2 estimates for Ab response to each pathogen within a time-point. We also evaluated the r_G and r_P for the 0% SCD, which had low h^2 and r_G and obtained an overall similar direction, but lower estimates and greater SE (**Supplementary Figure 1**).

Altogether, these results suggest that genetic progress for direct selection on Ab response traits depends on several factors, such as timing, level of co-exposure, and the number of seroconverted animals. The different extent in innate vs. humoral immune response may also have an effect on the genetic parameters of this traits (Flori et al., 2011; Mangino et al., 2017) as they are related to each other, and one can limit or stimulate the action of the other. Nonetheless, we observed substantial genetic variation for Ab response in this dataset, indicating that the use of specific time-points with a high proportion of seroconverted animals could be an efficient strategy to improve Ab response in commercial sows.

Genome-Wide Association Studies (GWAS)

Several QTL were identified for Ab response to APP at different time-points but not for other infectious pathogens in pigs. APP is highly contagious and can cause pleuropneumonia in pigs. The existence of many APP serotypes can limit its prevention and effective cure (Liu et al., 2017). The difference in virulence of different serotypes is caused mainly by the presence of different toxins and amounts of lipopolysaccharides (LPS) on the surface of the microorganism (Bossé et al., 2002). Therefore, identifying genomic regions associated with Ab response to serotypes of APP could help the use of this trait in selection purposes and a better understanding of the genetic component. Although it has been reported that cross-protection between the APP is limited, the QTL on SSC 14 for 4 of the serotypes suggests the presence of a pleotropic gene in this region. This QTL on SSC 14 at 2 Mb was found to be associated with Ab response to serotypes 3, 5, 7, and 13, especially at post-acclimation, mainly by two SNP, ALGA0074334 and H3GA0038333. This region contains the spleen associated tyrosine kinase (*SYK*) gene which has been associated with surface immunoglobulin (Ig)M complexes and appears to stimulate the signaling cascade in B lymphocytes via an antigen receptor (Müller et al., 1994; Seow et al., 2002). APP antigen stimulates the Ab-mediated immune response, which is produced by B lymphocytes (Appleyard et al., 2002). Interestingly, this same region has also been associated with total number of piglets born in Yorkshire (Do et al., 2018), indicating that selection for Ab response to APP may be associated with indirect selection for resilience in sows, measured as the capacity of maintaining reproductive performance in a disease-challenge environment.

For APP3 at entry, another 3 QTL were identified on SSC 8 (32 Mb), 9 (121 Mb), and 12 (47 Mb). On SSC 8, the ubiquitin C-terminal hydrolase L1 (*UCHL1*) gene has been reported to affect the ovulation rate in the pig (He et al., 2017). A potential candidate gene in the region on SSC 9 (121 Mb) is sterol O-acyltransferase 1 (*SOAT1*), which has been shown to be upregulated in pigs infected with APP7 in comparison to healthy animals (Reiner et al., 2014a). The QTL identified for APP3 at entry in the region on SSC 12 (47 Mb) has previously been associated with survival and clinical signs after challenge with APP7 in an F2 swine population (Reiner et al., 2014b). This region harbors the vitronectin (*VTN*) and fucosyltransferase 2 (*FUT2*) genes, which were less expressed in the liver of healthy animals compared to pigs infected with APP (Skovgaard et al., 2010).

For APP5 at entry, the regions on SSC 9 (6 Mb), 13 (30 Mb), and 4 (63 Mb) include genes that were previously found to be down- (tripartite motif-containing 55, *TRIM55*) and upregulated (diacylglycerol O-acyltransferase 2, *DGAT2*; and uroplakin 1B, *UPK1B*) in pigs infected with APP7 (Reiner et al., 2014a). In addition, *UPK1B* is part of the innate immune system and has been associated with urinary tract infection by gram-negative bacteria in humans (Ertan et al., 2010). Furthermore, the region on SSC 13 (30 Mb) includes several immune genes associated with chemokines, such as the c–c motif chemokine receptor 9 (*CCR9*), c–x–c motif chemokine receptor 6 (*CXCR6*), c–c motif chemokine receptor 2 (*CCR2*) and 5 (*CCR5*), and c–c motif chemokine receptor-like 2 (*CCRL2*). These genes are most related to cytokine–cytokine receptor interactions. Of those, *CCRL2* has recently been implicated in the regulation of reproductive functions in pigs (Gudelska et al., 2020). The region on SSC 4 (63 Mb) has also previously been associated with number of piglets mummified in a large White population (Wu et al., 2019). The region on SSC 8 (125 Mb) contains the secreted phosphoprotein 1 (*SPP1*) gene, which was less expressed in the liver of healthy animals compared to pigs infected with APP (Skovgaard et al., 2010).

For APP5 at post-acclimation, besides the region on SSC 14 (2 Mb), the region on SSC 2 (129 Mb) has been previously associated with APP natural infection in swine (Tsai et al., 2011). This region includes the CD molecule (*CD14*) gene, which along with lymphocyte antigen 96 (*MD2*) and toll-like receptor 4 (*TLR4*), mediates the innate immune response to bacterial LPS, leading to NF-κB activation, cytokine secretion, and the inflammatory response (Tsai et al., 2011). LPS is one of the main virulence factors of APP, making *CD14* a potential candidate gene (Reiner et al., 2014b). Besides the QTL for APP7 at post-acclimation on SSC 14 (2 Mb), another QTL on SSC 6 (157 Mb) was identified, where the transmembrane protein 59 (*TMEM59*) is located. This gene encodes for a protein that has been shown to regulate autophagy in response to *Staphylococcus aureus* infection.

For APP13 at P2, the region on SSC 6 (81 Mb) contains several complement genes, such as the complement C1q (*C1Q*) A chain (*C1QA*), C1Q B chain (*C1QB*), and C1Q C chain (*C1QC*). Complement activation is one of the mechanisms of defense stimulated by APP (Bossé et al., 2002), making these genes potential candidates associated with Ab response to this pathogen. The region on SSC 7 (92 Mb) has also been associated with teat number in swine, an important reproductive trait in pigs (Ding et al., 2009). For APP_{mean}, 2 of the QTL identified at post-acclimation, on SSC X (113 Mb) and 11 (61 Mb), have previously been associated with IgG2 and eosinophil counts, respectively, in Meishan vs. Pietrain pigs infected with *Sarcocystis* sp. (Reiner et al., 2007). The region on SSC 12 (2 Mb) has previously been associated with the sonographic score (based on reflections of high-frequency sound waves) of APP in Hampshire vs. Landrace pigs after challenge with APP7 (Reiner et al., 2014b). The region on SSC 7 (74 Mb) harbors the T-cell receptor alpha locus (*TCRA*), interferon-stimulated transcription factor 3 gamma (*IRF9*), and ribonuclease RNase A family 4 (*ANG*) genes, which have previously been associated with APP natural infection (Skovgaard et al., 2010). Summarizing, most of the candidate genes associated with APP seems to be associated with NF-Kb activation and the complement system. Interestingly, NF-Kb is increased during PRRSV infection (Guo et al., 2017), which can be an important factor during co-infection with these two pathogens. Furthermore, the complement system is part of the innate immune response that influences an acquired immune response (Dempsey et al., 1996), and thus, genes regulating this system may be involved in the genetic control of the antibody response to APP.

Interestingly, several of the regions identified for APP are associated with reproductive traits in pigs, such as number of pigs born, ovulation rate, and number of teats, indicating that the identified QTL for APP could be used for the improvement of resilience in commercial sows. The lack of QTL for the trait MEAN can be due to the dilution effect of some traits having major QTL and others not. Nonetheless, our results suggest that a larger part of the genetic variation for most infectious pathogens explained by several QTL with small effects.

Genomic Prediction Accuracies

Several studies have exploited the use of immune-related traits, such as viral load, level of cytokines, and clinical signs to infectious diseases, for the selection of individuals with a better immune response (Wieland et al., 2004; Kaiser et al., 2005; Thompson-Crispi et al., 2014). However, few studies have focused on the acquired immune response. Serão et al. (2016), using part of the data used in the current study, suggested that Ab response to PRRSV after acclimation can be predicted across populations using SNP. They reported greater AGP when using SNP within the two major QTL for Ab response to PRRSV on SSC7 (30 and 130 Mb) compared to the rest of the genome. Sanglard et al. (2020) observed greater AGP for Ab response to PRRSV than in Serão et al. (2016) in PRRSV-vaccinated gilts from the same population. Ab response to Newcastle disease and avian influenza in chickens was studied by Liu et al. (2014), who reported moderate prediction accuracy for these traits. In our study, AGP ranged from very low to high, depending on the pathogen and time-point.

In general, BayesB is expected to have higher accuracy than BayesC0 in the presence major QTL since BayesB gives more emphasis to QTL with higher effect and shrinks the effect of the other SNP toward zero (Fernando and Garrick, 2013). This pattern was observed for some traits in our study, as we observed a higher accuracy with BayesB for APP10 at entry and APP3 at post-acclimation, both with identified major QTL. Nonetheless, not all traits followed this pattern. For example, we observed cases where no QTL was identified but still, BayesB performed better (such as for IAV, MH, PCV2, and MEAN) or a QTL was identified but BayesC0 performed better (such as APP_{mean}). The performance of BayesC and BayesC0 relative to other methods depends on the actual distribution of the marker effects (Fernando and Garrick, 2013), which is unknown for the novel traits evaluated in this study.

For Ab response to IAV, the low AGP are in accordance with the fact that no QTL were identified for this trait across all time-points, and its low h^2 estimates. For Ab response to MH at entry and post-acclimation, AGP were higher when using 100% SCD. This is in contrast to results by Serão et al. (2016) for Ab response to PRRSV, where lower AGP were observed with increasing %SCD. However, Serão et al. (2016) indicated that this may have been caused by a major reduction in the dataset analyzed with 100% SCD compared to 0% SCD (when AGP was the highest). In our study, however, the major reduction in the size of the dataset from 0% (2,355) to 100% SCD (564) did not seem to negatively impact the results. At P2, the AGP decreased as the %SCD increased (and the number of animals decreased), more similar to what was observed by Serão et al. (2016). For Ab response to PCV2, the AGP were moderate to high. This must have happened because of the very low h^2 estimates for these traits since the division of the correlation between GEBV and adjusted phenotypes by the square root of the h^2 is part of the calculation of AGP. In fact, the average correlations were quite low for PCV2, ranging from −0.04 (75% SCD) to −0.05 (0% SCD). Therefore, the high AGP found for PCV2 has little implication for selection purposes.

For all APP, although some QTL were identified for most serotypes, the AGP were low, including for APP_{mean}, indicating a limitation for the use of this trait for selection purposes. Similar to h^2, the low number of positive animals for APP may limit the genetic expression of these traits among the animals in this dataset; therefore, studies involving Ab response to vaccination or natural infection to APP should not be excluded from future works.

The AGP for MEAN were higher than for the other traits, especially at entry and post-acclimation. Although no major QTL was identified for these traits, the overall sum of small QTL effects captured by the markers suggests that genomic prediction can be used to identify animals with overall better acquired immune response to the pathogens included in this study. This may happen because the SNPs spread along the genome are capturing QTLs with small effects, resulting in overall greater accuracy, even in the absence of major QTLs. This corroborates that selection on the overall mean of Ab response to common pathogens may be more efficient than selection on Ab response to individual pathogens. These results suggest that the genomic predictive ability of most of these traits is limited, but some of them (i.e., MEAN) have the potential to be further explored.

CONCLUSION

For the first time, the genetic basis of Ab response to a range of pathogens in pigs was explored in commercial sows. Differences in the Ab response exist for different pathogens; however, this trait may be still a proxy for resilience in commercial sows. Our results revealed that these traits have low intermediate heritabilities, with exception of APP_{mean} and MEAN. In addition, important genomic regions were identified for some APP serotypes. Most of the Ab response traits had low to moderate genomic predictive ability, especially when no QTL were identified. However, MEAN had moderate to high genomic prediction accuracies. These results suggest that genetic progress by selection on Ab response to these pathogens is possible but may be slow and that selection on the average Ab response to common pathogens in pigs may be an alternative strategy. The use of specific sample collection time-points can result in higher heritabilities, as well as datasets with a higher proportion of seroconverted animals, to increase the genetic variance. Some disadvantages such as the lack of confirmation of whether animals were vaccinated and/or infected with these pathogens, the existence of several confounding factors (e.g., diet,

management, and others), and the lack of information on how long after the exposure the blood was collected and the course the pathogen could limit the interpretation of the results obtained. However, this variability is a strength for the application of these results in commercial settings, as the ability to test for infection with all of these pathogens may not be realistic. Other advantages of this study include the possibility of using crossbred performance for selection, the identification of novel traits for selection of resilience in pigs, the use of commercial populations reared in true commercial conditions, and the use of relevant pathogens that are easy to be measured. New studies including commercial performance, such as reproductive performance, are needed to better understand the relationship between Ab response to these pathogens and commercially important traits in the swine production.

MEMBERS OF THE PigGen CANADA CONSORTIUM

They participated in project and protocol development and implementation, coordinated the sources of sows and collection of associated data, and contributed to the project through regular discussions during execution of the gilt acclimation project: Mr. D. Vandenbroek and Mr. B. DeVries, Alliance Genetics Canada, St. Thomas, ON, Canada; Dr. N. Dion and Ms. S. Blanchette, AlphaGene, Saint-Hyacinthe, QC, Canada; Dr. T. Rathje, DNA Genetics, Columbus, NE, United States; Mr. M. Duggan, FastGenetics, Saskatoon, SK, Canada; Dr. R. Kemp, Genesus, London, ON, Canada; Dr. P. Charagu, Hypor, Regina, SK, Canada; and Dr. P. Mathur, Topigs Norsvin, Helvoirt, Netherlands.

DATA AVAILABILITY STATEMENT

The data that support the findings of this study are not publicly available. Data may be available from authors upon request and authorization from the company that generated the data.

ETHICS STATEMENT

The animal study was reviewed and approved by the Canadian Council on Animal Care (2020).

AUTHOR CONTRIBUTIONS

LS performed the data analyses, interpreted the results, and drafted the manuscript. PC, JH, SB, GP, and JD developed the research project. BM coordinated the data collection. PW coordinated the database. LS, JD, and NS conceived the statistical analyses. LS and NS prepared the first draft of the manuscript. All authors contributed to the final manuscript, and read and approved the final manuscript.

FUNDING

This study was funded by PigGen Canada, Genome Canada, and the Canadian Swine Health Board. The financial support of the Iowa Pork Producers Association was appreciated.

ACKNOWLEDGMENTS

Special thanks are given to the late Dr. Stephen Bishop for his scientific contributions to this work.

SUPPLEMENTARY MATERIAL

The Supplementary Material for this article can be found online at: https://www.frontiersin.org/articles/10.3389/fgene.2020.593804/full#supplementary-material

Supplementary Figure 1 | Genetic (lower triangular) and phenotypic (upper triangular) correlation between all traits: influenza A virus (IAV), porcine circovirus type 2 (PCV2), *Mycoplasma hyopneumoniae* (MH), *Actinobacillus pleuropneumoniae* (APP), and porcine respiratory and reproductive syndrome (PRRS) at Entry (A), Post-acclimation (B), Parity 1 (C), and Parity 2 (D). The values between parenthesis correspond to the standard error of the correlation. The blue color corresponds to positive correlation, the red to negative correlation, and the gray indicate the lack of convergence of the model.

Supplementary Table 1 | Percentage of total genetic variance explained for by markers (% TGVM) within a 1-Mb window for traits with significant QTLs using a threshold of 1% TGVM and posterior probability of inclusion (PPI) of 0.70 (before SNP selection). The SNP explaining most of the TGVM within a window was selected and the % TGVM explained by the SNP (% TGVM-SNP) was also estimated (after SNP selection).

Supplementary Table 2 | Accuracies of genomic prediction.

REFERENCES

Abella, G., Novell, E., Tarancon, V., Varona, L., Pena, R. N., Estany, J., et al. (2019). Identification of resilient sows in porcine reproductive and respiratory syndrome virus-infected farms. *J. Anim. Sci.* 97, 3228–3236. doi: 10.1093/jas/skz192

Amory, J., Mackenzie, A., Eckersall, P., Stear, M., and Pearce, G. (2007). Influence of rearing conditions and respiratory disease on haptoglobin levels in the pig at slaughter. *Vet. Sci.* 83, 428–435. doi: 10.1016/j.rvsc.2007.01.012

Appleyard, G. D., Furesz, S. E., and Wilkie, B. N. (2002). Blood lymphocyte subsets in pigs vaccinated and challenged with *Actinobacillus pleuropneumoniae*. *Vet. Immunol. Immunopathol.* 86, 221–228. doi: 10.1016/S0165-2427(02)00002-8

Bates, J., Moreno, R., Doster, A. R., and Johnson, R. K. (2009). *Selection for Immune Responses to Porcine Circovirus (PCV2) to Decrease Incidence of Porcine Circovirus Associated Disease (PCVAD)*. Available online at: http://digitalcommons.unl.edu/coopext_swine/231 (accessed April 13, 2010).

Bishop, S. C., and Woolliams, J. A. (2010). On the genetic interpretation of disease data. *PLoS One* 5:e8940. doi: 10.1371/journal.pone.0008940

Bossé, J. T., Janson, H., Sheehan, B. J., Beddek, A. J., Rycroft, A. N., Simon Kroll, J., et al. (2002). *Actinobacillus pleuropneumoniae*: pathobiology and pathogenesis of infection. *Microbes Infect.* 4, 225–235. doi: 10.1016/S1286-4579(01)01534-9

Clapperton, M., Diack, A. B., Matika, O., Glass, E. J., Gladney, C. D., Mellencamp, M. A., et al. (2009). Traits associated with innate and adaptive immunity in pigs: heritability and associations with performance under different health status conditions. *Genet. Sel. Evol.* 41:54. doi: 10.1186/1297-9686-41-54

Colpoys, J. D., Curry, S. M., Schweer, W. P., and Gabler, N. K. (2020). Nutrient supplementation effects on pig performance and sickness behavior during a porcine reproductive and respiratory syndrome virus infection. *J. Swine Health Prod.* 28, 79–86.

Dekkers, J. C. M. (2007). Marker-assisted selection for commercial crossbred performance. *J. Anim. Sci.* 85, 2104–2114. doi: 10.2527/jas.2006-683

Dempsey, P. W., Allison, M. E. D., Akkaraju, S., Goodnow, C. C., and Fearon, D. T. (1996). C3d of complement as a molecular adjuvant: bridging innate and acquired immunity. *Science* 271, 348–350. doi: 10.1126/science.271.5247.348

Ding, N., Guo, Y., Knorr, C., Ma, J., Mao, H., Lan, L., et al. (2009). Genome-wide QTL mapping for three traits related to teat number in a White Duroc × Erhualian pig resource population. *BMC Genet.* 10:6. doi: 10.1186/1471-2156-10-6

Do, K., Jung, S., Park, K., Na, C., Park, K., and Park, K. (2018). Effect of single nucleotide polymorphism on the total number of piglets born per parity of three different pig breeds. *Asian Australas. J. Anim. Sci.* 31, 628–635. doi: 10.5713/ajas.17.0028

Dunkelberger, J. R., Serão, N. V. L., Niederwerder, M. C., Kerrigan, M. A., Lunney, J. K., Rowland, R. R. R., et al. (2017). Effect of a major quantitative trait locus for porcine reproductive and respiratory syndrome (PRRS) resistance on response to coinfection with prrs virus and *Porcine circovirus* type 2b (PCV2b) in commercial pigs, with or without prior vaccination for PRRS. *J. Anim. Sci.* 95, 584–598. doi: 10.2527/jas2016.1071

Engle, T. B., Jobman, E. E., Moural, T. W., McKnite, A. M., Bundy, J. W., Barnes, S. Y., et al. (2014). Variation in time and magnitude of immune response and viremia in experimental challenges with *Porcine circovirus* 2b. *BMC Vet. Res.* 10:286. doi: 10.1186/s12917-014-0286-4

Ertan, P., Berdeli, A., Yilmaz, O., Gonulal, D. A., and Yuksel, H. (2010). LY96, UPKIB mutations and TLR4, CD14, MBL polymorphisms in children with urinary tract infection. *Indian J. Pediatr.* 78, 1229–1233. doi: 10.1007/s12098-011-0399-8

Faust, M. A., Robison, O. W., and Tess, M. W. (1993). Genetic and economic analyses of sow replacement rates in the commercial tier of a hierarchical swine breeding structure. *J. Anim. Sci.* 71, 1400–1406. doi: 10.2527/1993.7161400x

Fernando, R. L., and Garrick, D. J. (2009). *GenSel: User Manual for a Portfolio of Genomic Selection Related Analyses*. Ames, IA: Iowa State University.

Fernando, R. L., and Garrick, D. J. (2013). "Bayesian methods applied to GWAS," in *Genome-Wide Association Studies and Genomic Prediction*, Vol. 1019, eds C. Gondro, J. van der Werf, and B. Hayes (Totowa, NJ: Humana Press).

Flori, L., Gao, Y., Oswald, I. P., Lefevre, F., Bouffaud, M., and Mercat, M. (2011). Deciphering the genetic control of innate and adaptive immune responses in pig: a combined genetic and genomic study. *BMC Proc.* 5(Suppl. 4):S32. doi: 10.1186/1753-6561-5-S4-S32

Garrick, D. J., and Fernando, R. L. (2013). Implementing a QTL detection study (GWAS) using genomic prediction methodology. *Methods Mol. Biol.* 1019, 275–298. doi: 10.1007/978-1-62703-447-0-11

Gudelska, M., Dobrzyn, K., Kiezun, M., and Rytelewska, E. (2020). The expression of chemerin and its receptors (CMKLR1, GPR1, CCRL2) in the porcine uterus during the oestrous cycle and early pregnancy and in trophoblasts and conceptuses. *Animal* 14, 2116–2128. doi: 10.1017/S175173112000097X

Guo, H., Chen, M., Duan, D., and Zhang, S. (2017). PRRSV regulates cytokine secretion from PAMs cultured in vitro via activation of MyD88-dependent TLRs signaling pathway. *Int. J. Clin. Exp. Pathol.* 10, 2270–2283.

Habier, D., Fernando, R. L., Kizilkaya, K., and Garrick, D. J. (2011). Extension of the bayesian alphabet for genomic selection. *BMC Bioinformatics* 12:186. doi: 10.1186/1471-2105-12-186

Haesebrouck, F., Chiers, K., Van Overbeke, I., and Ducatelle, R. (1997). *Actinobacillus pleuropneumoniae* infections in pigs: the role of virulence factors in pathogenesis and protection. *Vet. Microbiol.* 58, 239–249. doi: 10.1016/S0378-1135(97)00162-4

He, L. C., Li, P. H., Ma, X., Sui, S. P., Gao, S., Kim, S. W., et al. (2017). Identification of new single nucleotide polymorphisms affecting total number born and candidate genes related to ovulation rate in Chinese Erhualian pigs. *Anim. Genet.* 48, 48–54. doi: 10.1111/age.12492

Hess, A. S., Trible, B. R., Hess, M. K., Rowland, R. R., Lunney, J. K., Plastow, G. S., et al. (2018). Genetic relationships of antibody response, viremia level, and weight gain in pigs experimentally infected with porcine reproductive and respiratory syndrome virus. *J. Anim. Sci.* 96, 3565–3581. doi: 10.1093/jas/sky229

Holzer, B., Martini, V., Edmans, M., and Tchilian, E. (2019). T and B cell immune responses to influenza viruses in pigs. *Front. Immunol.* 10:98. doi: 10.3389/fimmu.2019.00098

Kaiser, P., Poh, T. Y., Rothwell, L., Avery, S., Balu, S., Pathania, U. S., et al. (2005). A genomic analysis of chicken cytokines and chemokines. *J. Interferon Cytokine Res.* 25, 467–484. doi: 10.1089/jir.2005.25.467

Kinsella, R. J., Kähäri, A., Haider, S., Zamora, J., Proctor, G., Spudich, G., et al. (2011). Ensembl BioMarts: a hub for data retrieval across taxonomic space. *Database* 2011:bar030. doi: 10.1093/database/bar030

Lee, Y. M., Alam, M., Choi, B. H., Kim, K. S., and Kim, J. J. (2012). A whole genome association study to detect single nucleotide polymorphisms for blood components (immunity) in a cross between Korean native pig and Yorkshire. *Asian Australas. J. Anim. Sci.* 25, 1674–1680. doi: 10.5713/ajas.2012.12503

Lewis, C. R. G., Ait-Ali, T., Clapperton, M., Archibald, A. L., and Bishop, S. (2007). Genetic perspectives on host responses to porcine reproductive and respiratory syndrome (PRRS). *Viral Immunol.* 20, 343–358. doi: 10.1089/vim.2007.0024

Liu, J., Ma, Q., Yang, F., Zhu, R., Gu, J., Sun, C., et al. (2017). B cell cross-epitope of *Propionibacterium acnes* and *Actinobacillus pleuropneumonia* selected by phage display library can efficiently protect from *Actinobacillus pleuropneumonia* infection. *Vet. Microbiol.* 205, 14–21. doi: 10.1016/j.vetmic.2017.04.026

Liu, T., Qu, H., Luo, C., Li, X., Shu, D., Lund, M. S., et al. (2014). Genomic selection for the improvement of antibody response to newcastle disease and avian influenza virus in chickens. *PLoS One* 9:e112685. doi: 10.1371/journal.pone.0112685

Mallard, B. A., Wilkie, B. N., Kennedy, B. W., Gibson, J., and Quinton, M. (1998). "Immune responsiveness in swine: eight generations of selection for high and low immune response in Yorkshire pigs," in *Proceedings of the 6th World Congress on Genetics Applied to Livestock Production*, Armidale, 257–264.

Mangino, M., Roederer, M., Beddall, M. H., Nestle, F. O., and Spector, T. D. (2017). Innate and adaptive immune traits are differentially affected by genetic and environmental factors. *Nat. Commun.* 8:13850. doi: 10.1038/ncomms13850

Montaner-Tarbes, S., del Portillo, H. A., Montoya, M., and Fraile, L. (2019). Key gaps in the knowledge of the porcine respiratory reproductive syndrome virus (PRRSV). *Front. Vet. Sci.* 6:38. doi: 10.3389/fvets.2019.00038

Müller, B., Cooper, L., and Terhorst, C. (1994). Molecular cloning of the human homologue to the pig protein-tyrosine kinase SYK. *Immunogenetics* 39, 359–362. doi: 10.1007/BF00189234

Okamura, T., Onodera, W., Tayama, T., Kadowaki, H., Kojima-Shibata, C., Suzuki, E., et al. (2012). A genome-wide scan for quantitative trait loci affecting respiratory disease and immune capacity in Landrace pigs. *Anim. Genet.* 43, 721–729. doi: 10.1111/j.1365-2052.2012.02359.x

Pujols, J., Segalés, J., Polo, J., Rodríguez, C., Campbell, J., and Crenshaw, J. (2016). Influence of spray dried porcine plasma in starter diets associated with a conventional vaccination program on wean to finish performance. *Porcine Health Manag.* 2:4. doi: 10.1186/s40813-016-0021-6

Reiner, G., Bertsch, N., Hoeltig, D., Selke, M., Willems, H., Gerlach, G. F., et al. (2014a). Identification of QTL affecting resistance/susceptibility to acute *Actinobacillus pleuropneumoniae* infection in swine. *Mamm. Genome* 25, 180–191. doi: 10.1007/s00335-013-9497-4

Reiner, G., Dreher, F., Drungowski, M., Hoeltig, D., Bertsch, N., Selke, M., et al. (2014b). Pathway deregulation and expression QTLs in response to *Actinobacillus pleuropneumoniae* infection in swine. *Mamm. Genome* 25, 600–617. doi: 10.1007/s00335-014-9536-9

Reiner, G., Kliemt, D., Willems, H., Berge, T., Fischer, R., Köhler, F., et al. (2007). Mapping of quantitative trait loci affecting resistance/susceptibility to *Sarcocystis miescheriana* in swine. *Genomics* 89, 638–646. doi: 10.1016/j.ygeno.2007.01.011

Sanglard, L. P., Fernando, R. L., Gray, K. A., Linhares, D. C. L., Dekkers, J. C. M., Niederwerder, M. C., et al. (2020). Genetic analysis of antibody response to porcine reproductive and respiratory syndrome vaccination as an indicator trait for reproductive performance in commercial sows. *Front. Genet.* 11:1011. doi: 10.3389/fgene.2020.01011

Sato, T., Okamura, T., Kojima-Shibata, C., Kadowaki, H., Suzuki, E., Uenishi, H., et al. (2016). Correlated response of peripheral blood cytokines with selection

for reduced mycoplasma pneumonia of swine lesions in Landrace pigs. *Anim. Sci. J.* 87, 477–483. doi: 10.1111/asj.12462

Schweer, W. P., Patience, J. F., Burrough, E. R., Kerr, B. J., and Gabler, N. K. (2018). Impact of PRRSV infection and dietary soybean meal on ileal amino acid digestibility and endogenous amino acid losses in growing pigs. *J. Anim. Sci.* 96, 1846–1859. doi: 10.1093/jas/sky093

Seow, C. J., Chue, S. C., and Wong, W. S. F. (2002). Piceatannol, a Syk-selective tyrosine kinase inhibitor, attenuated antigen challenge of guinea pig airways in vitro. *Eur. J. Pharmacol.* 443, 189–196. doi: 10.1016/S0014-2999(02)01534-0

Serão, N. V. L., Kemp, R. A., Mote, B. E., Willson, P., Harding, J. C. S., Bishop, S. C., et al. (2016). Genetic and genomic basis of antibody response to porcine reproductive and respiratory syndrome (PRRS) in gilts and sows. *Genet. Sel. Evol.* 48:51. doi: 10.1186/s12711-016-0230-0

Serão, N. V. L., Matika, O., Kemp, R. A., Harding, J. C. S., Bishop, S. C., Plastow, G. S., et al. (2014). Genetic analysis of reproductive traits and antibody response in a PRRS outbreak herd. *J. Anim. Sci.* 92, 2905–2921. doi: 10.2527/jas.2014-7821

Skovgaard, K., Mortensen, S., Boye, M., Hedegaard, J., and Heegaard, P. M. H. (2010). Hepatic gene expression changes in pigs experimentally infected with the lung pathogen *Actinobacillus pleuropneumoniae* as analysed with an innate immunity focused microarray. *Innate Immun.* 16, 343–353. doi: 10.1177/1753425909342730

Thacker, E. L., Halbur, P. G., Ross, R. F., Thanawongnuwech, R., and Thacker, B. J. (1999). *Mycoplasma hyopneumoniae* potentiation of porcine reproductive and respiratory syndrome virus-induced pneumonia. *J. Clin. Microbiol.* 37, 620–627. doi: 10.1177/0363546515605077

Thacker, E. L., Thacker, B. J., and Janke, B. H. (2001). Interaction between *Mycoplasma hyopneumoniae* and swine influenza virus. *J. Clin. Microbiol.* 39, 2525–2530. doi: 10.1128/JCM.39.7.2525-2530.2001

Thompson-Crispi, K. A., Sargolzaei, M., Ventura, R., Abo-Ismail, M., Miglior, F., Schenkel, F., et al. (2014). A genome-wide association study of immune response traits in Canadian Holstein cattle. *BMC Genomics* 15:559. doi: 10.1186/1471-2164-15-559

Tsai, T. H., Chen, S. F., Huang, T. Y., Tzeng, C. F., Chiang, A. S., Kou, Y. R., et al. (2011). Impaired Cd14 and Cd36 expression, bacterial clearance, and Toll-like receptor 4-Myd88 signaling in caveolin-1-deleted macrophages and mice. *Shock* 35, 92–99. doi: 10.1097/SHK.0b013e3181ea45ca

VanRaden, P. M. (2008). Efficient methods to compute genomic predictions. *J. Dairy Sci.* 91, 4414–4423. doi: 10.3168/jds.2007-0980

Walker, L. R., Engle, T. B., Vu, H., Tosky, E. R., Nonneman, D. J., Smith, T. P. L., et al. (2018). Synaptogyrin-2 influences replication of *Porcine circovirus* 2. *PLoS Genet.* 14:e1007750. doi: 10.1371/journal.pgen.1007750

Wieland, S., Thimme, R., Purcell, R. H., and Chisari, F. V. (2004). Genomic analysis of the host response to hepatitis B virus infection. *Proc. Natl. Acad. Sci. U.S.A.* 101, 6669–6674. doi: 10.1073/pnas.0401771101

Wu, P., Wang, K., Zhou, J., Yang, Q., Yang, X., Jiang, A., et al. (2019). A genome wide association study for the number of animals born dead in domestic pigs. *BMC Genet.* 20:4. doi: 10.1186/s12863-018-0692-x

Zanella, R., Gava, D., de Oliveira Peixoto, J., Schaefer, R., Ciacci-zanella, J. R., Biondo, N., et al. (2015). Unravelling the genetic components involved in the immune response of pigs vaccinated against influenza virus. *Virus Res.* 210, 327–336. doi: 10.1016/j.virusres.2015.09.003

Conflict of Interest: The authors declare that the research was conducted in the absence of any commercial or financial relationships that could be construed as a potential conflict of interest.

Advantages of publishing in Frontiers

OPEN ACCESS
Articles are free to read for greatest visibility and readership

FAST PUBLICATION
Around 90 days from submission to decision

HIGH QUALITY PEER-REVIEW
Rigorous, collaborative, and constructive peer-review

TRANSPARENT PEER-REVIEW
Editors and reviewers acknowledged by name on published articles

Frontiers
Avenue du Tribunal-Fédéral 34
1005 Lausanne | Switzerland

Visit us: www.frontiersin.org
Contact us: frontiersin.org/about/contact

REPRODUCIBILITY OF RESEARCH
Support open data and methods to enhance research reproducibility

DIGITAL PUBLISHING
Articles designed for optimal readership across devices

FOLLOW US
@frontiersin

IMPACT METRICS
Advanced article metrics track visibility across digital media

EXTENSIVE PROMOTION
Marketing and promotion of impactful research

LOOP RESEARCH NETWORK
Our network increases your article's readership